NASA Conference Publication 2036

Part II

CTOL Transport Technology - 1978

Proceedings of
a conference held at
Langley Research Center
Hampton, Virginia
February 28 - March 3, 1978

NASA

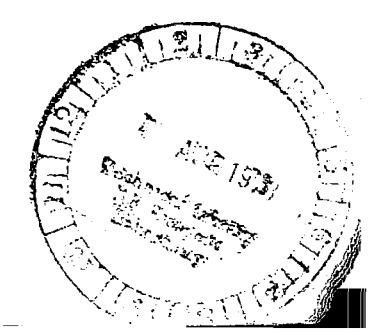

NASA Conference Publication 2036

Part II

CTOL Transport Technology - 1978

Proceedings of
a conference held at
Langley Research Center
Hampton, Virginia
February 28 - March 3, 1978

National Aeronautics
and Space Administration

**Scientific and Technical
Information Office**

1978

PREFACE

The proceedings of the NASA CTOL Transport Technology Conference held at Langley Research Center on February 28 — March 3, 1978, are reported in this NASA Conference Proceedings.

The purpose of the Conference was to provide early dissemination of new technology generated by NASA and specifically associated with advanced conventional take-off and landing (CTOL) transport aircraft. The last such NASA conference in this general area was held in 1971 and was reported in NASA SP-292, entitled "Vehicle Technology for Civil Aviation — The Seventies and Beyond."

The technology reported in this conference resulted from both in-house and contract efforts, including those of the ongoing Aircraft Energy Efficiency (ACEE) Program. The topics covered by session were

I. Propulsion
II. Structures and Materials
III. Laminar Flow Control
IV. Advanced Aerodynamics and Active Controls
V. Operations and Safety
VI. Advanced Systems

The efforts of the members of the Steering Committee, who developed the structure of the Conference and selected and reviewed the papers, are particularly appreciated.

Certain commercial equipment and materials are identified in this paper in order to specify the procedures and configurations adequately. In no case does such identification imply recommendation or endorsement of the product by NASA, nor does it imply that the equipment or materials are necessarily the only ones or the best ones available for the purpose. In many cases equivalent equipment and materials are available and would probably produce equivalent results.

D. William Conner
Conference Chairman

STEERING COMMITTEE

D. William Conner, Chairman
Langley Research Center

Paul G. Johnson
NASA Headquarters

John M. Klineberg
NASA Headquarters

Robert W. Leonard
Langley Research Center

Donald L. Nored
Lewis Research Center

Ronald H. Smith
NASA Headquarters

CONTENTS

Part I*

*Papers 1 to 26 are presented under separate cover.

SESSION V - OPERATIONS AND SAFETY
Chairman: John H. Enders

SESSION VI - ADVANCED SYSTEMS
Chairman: William S. Aiken, Jr.

ADVANCED AERODYNAMICS AND ACTIVE CONTROLS TECHNOLOGY

SESSION INTRODUCTION

William J. Alford, Jr.
NASA Langley Research Center

INTRODUCTION

The purpose of this section is to report on the results, status, and plans of NASA sponsored advanced aerodynamics and active controls technology activities.

Since most of the work underway in these areas is focused on development of subsonic, energy efficient transport aircraft technologies and is sponsored by the Energy Efficient Transport (EET) Element of the Aircraft Energy Efficiency (ACEE) Project (refs. 1 and 2), the material to be presented in this introductory paper is intended to set the stage for the section by providing a synopsis of the EET activities; the titles and authors of the ten section papers; and how the efforts represented by the papers are related to the overall EET plan.

It should be noted that most of the work being reported on has been underway for less than a year and, therefore, in-depth or complete results are not yet available.

ABBREVIATIONS

ACEE	aircraft energy efficiency
ACT	active controls technology
ARC	Ames Research Center
B	Boeing Commercial Airplane Company
DC	Douglas Aircraft Company
DFRC	Dryden Flight Research Center
EET	energy efficient transport
EMS	elastic mode suppression
FLT	flight tests
GA	gust load alleviation

HASCW	high-aspect-ratio supercritical wing
IEM	integrated energy management
L	Lockheed-California Company
L.S.	low speed
LaRC	Langley Research Center
M	maintainable
Max. Ben.	maximum benefit
MFLDN	mixed-flow, long-duct nacelle
MLA	maneuver load alleviation
NASA	National Aeronautics and Space Administration
NLF	natural laminar flow
OAST	Office of Aeronautics and Space Technology
PFC	primary flight control system
R	reliability
RPRV	remotely piloted research vehicle
RSS	relaxed static stability
R&T	research and technology
SCW	supercritical wing
WLA	wing load alleviation
W.T.	wind-tunnel tests
WTE	wing tip extension
WTW	wing tip winglet

ENERGY EFFICIENT TRANSPORT PROJECT

The EET project is one of the elements of the NASA OAST Advanced Civil Aircraft Systems Technology Program (ref. 2) whose objectives are to:

"Expedite industry acceptance and application of advanced aerodynamics and active controls technology in an integrated manner to achieve energy, economic, and aircraft sales benefits."

As illustrated in figure 1, the focus of the EET activities is on advanced subsonic CTOL aircraft of both the near-term derivative category (i.e., B-747, DC-10, and L-1011) and farther-term, new or advanced derivative aircraft (i.e., B-7X7, DC-X-200, and L-RE-1011) category.

A schedule of the EET technology development and evaluation activities is presented in figure 2. The activities consist of NASA-LaRC defined and implemented (with contractor involvement, as appropriate) advanced aerodynamics and active controls efforts and selected concepts contracts with Boeing, Douglas, and Lockheed. These activities, which were initiated in 1976, intensified in 1977 and are expected to continue through fiscal year 1982. Associated research and technology resources are slightly in excess of eighty-five million (then year) dollars.

Advanced Aerodynamics

The advanced aerodynamics activities (fig. 2) focus on three areas: cruise conditions, low-speed conditions, and design methodology.

In the cruise area, high-aspect-ratio supercritical wing airplane models have been designed and are being tested in the Langley 8-foot transonic pressure tunnel to establish a data base for variations in wing characteristics and controls. Analytical and experimental activities are also underway to optimize wing-winglet geometry and to assess wide-body transport applications of winglets. Propulsion/airframe integration experiments are planned to minimize interference effects of below-the-wing pylon-mounted nacelles. Early results of these efforts are presented in reference 3.

Current results and status of the cruise aerodynamics activities are contained in papers 1 and 2 of this section, entitled "NASA Supercritical-Wing Technology" by Dennis W. Bartlett and James C. Patterson, Jr., and "Experimental Results of Winglets on First, Second, and Third Generation Jet Transports" by Stuart G. Flechner and Peter F. Jacobs, respectively. These four authors are aerospace technologists associated with the LaRC Transonic Aerodynamics Branch.

In the low-speed area, efforts are underway to define the high-lift system requirements for high-aspect-ratio supercritical wing configurations and to assess the impact of active controls requirements on high-lift systems. A model has been designed, fabricated, and tested in the Langley V/STOL tunnel. Another model is being designed for fabrication and testing at higher Reynolds numbers in the Ames Research Center (ARC) 12-Foot Tunnel.

Design methodology developments are aimed at expediting three-dimensional, optimum, supercritical wing design capability and mixed-flow-juncture analysis methods. The approach, using computer aided design tools, is to: couple 3-D

boundary layer programs to transonic wing analysis procedures; extend 3-D transonic wing programs to operate in a design mode with either constrained loading or geometry specifications; and to incorporate non-planar capability in the wing programs. There are two papers in this section dealing with advanced transonic flow computational aerodynamics. The first is entitled "Recent Experiences With Three-Dimensional Transonic Potential Flow Calculations" by David A. Caughey of Cornell, Perry A. Newman of LaRC, and Antony Jameson of NYU. This activity was sponsored by NASA in the OAST R&T Base Program (ref. 2). The second paper is entitled "Towards Complete Configurations Using an Embedded Grid Approach" by Charles W. Boppe of Grumman. This and all of the other work being reported on in this section was sponsored by the ACEE/EET Project (ref. 2).

Active Controls

Still referring to figure 2, the active controls technology activities consist of two major developments: integrated analysis and design techniques; and reliable, maintainable flight control systems (ref. 4).

The objective of the integrated analysis and design techniques activity is to evaluate existing analytical and experimental tools for the integrated application of aerodynamics, structures, and controls. The technical approach is to design, under contract (NAS1-14665, with Boeing-Wichita), a high-aspect-ratio supercritical wing incorporating structurally critical gust load alleviation, maneuver load alleviation, and active flutter suppression systems. Three aeroelastic semispan wings including the control systems will be fabricated. One set of two will be flight tested at DFRC utilizing a modified BQM-34E/F "Firebee II" RPRV. The other semispan wing will be tested in the Langley transonic dynamics tunnel. The expected results of this activity will be a comparison and evaluation of the analytical, wind-tunnel, and flight test results including: control system performance, loads, flutter, and unsteady aerodynamic and aeroelastic characteristics. The design methods to be evaluated through test activities are discussed in the last paper of this section, entitled "Active Controls Technology to Maximize Structural Efficiency" by James M. Hoy of Boeing-Seattle and James M. Arnold of Boeing-Wichita.

The principal thrusts of the reliable, maintainable flight controls systems activity are: design of a cost-effective system, using state-of-the-art technology for near-term, non-flight-critical application; and design and evaluation of an advanced, reliable, maintainable system for far-term application. Elements of these activities include: (1) a state-of-the-art assessment by collecting, analyzing, and documenting current airlines avionics systems reliability data, maintenance experience, and operational practices and procedures; (2) development and validation of system evaluation models incorporating control system reliability and performance, aircraft flight safety, airline operations (e.g., route structure, maintenance, delays, etc.) and cost; (3) development and evaluation of two advanced fault-tolerant computer systems: Stanford Research Institute's Software Implemented Fault Tolerance (SIFT) and Charles Stark Draper Laboratory's Fault Tolerant Multiprocessor (FTMP); and (4) studies of fault-tolerant flight control system architectures. Early results of some of these activities are presented in references 5 to 7. Some

current results were given in the oral presentation on fault tolerant computer technology for active controls.

Selected Concepts

To achieve the earlier stated objective of the ACEE/EET Project, a strong NASA/industry partnership is being implemented with the technology focus being that which NASA and the commercial transport industry mutually agree is most relevant for both near-term (current transport derivatives - 1983) and far-term (new aircraft design - 1985+) applications. (See fig. 1.) The three industry participants are Boeing, Douglas, and Lockheed. As indicated in figure 2, selected advanced concepts are being implemented in two phases. Phase I, which is currently underway, is illustrated in figure 2 by the activities listed in the solid rectangles. These activities are primarily developmental in nature lasting through FY-79. Phase II, which is to be initiated this year, is illustrated in figure 2 by the dashed rectangles. These activities are primarily evaluative and demonstrative in nature and are expected to continue through FY-82. Ongoing and planned contractual activities with each company are described below.

Boeing.- In Phase I, there are two contractual activities with Boeing. One of these has a near-term focus (NASA contract NAS1-14741 for selected advanced aerodynamics and active controls technology concepts development on a derivative B-747 aircraft). The tasks include development and analysis, engineering design, and evaluation of wing-tip extensions, wing-tip winglets, wing load alleviation, wind-tunnel testing of these various modifications, choice of a final configuration, and evaluation and recommendations for further work. Some results to date and status of this work are presented in the paper entitled "Application of Winglets and/or Tip Extensions With Active Load Control on the Boeing 747" by Robert L. Allison, Brian R. Perkin, and Richard L. Schoenman of Boeing-Seattle.

The second Boeing contractual activity has a farther term focus (NASA contract NAS1-14742 for selected advanced aerodynamic and active control concepts development). The tasks of this program include: B-747 primary flight control system reliability and maintainability study; integrated energy management; natural laminar flow; high-lift characteristics of high-aspect-ratio supercritical wings; and a maximum benefit of active controls technology planning study. Although a complete status report on these activities is not presented herein, some of the more important considerations related to methods of integrated design to maximize the benefits of active controls are discussed in the paper entitled "Active Controls Technology to Maximize Structural Efficiency" by James M. Hoy of Boeing-Seattle and James M. Arnold of Boeing-Wichita.

Current plans for Phase II include: wind-tunnel testing of the final B-747 configuration selected in Phase I and, possibly, some engineering flight tests; and an in-depth assessment of the integrated application of ACT followed by identification of ACT system design and test requirements.

Douglas.- In Phase I there are also two contracted activities underway with Douglas. The first has a near-term focus (NASA contract NAS1-14743 for selected winglet and mixed-flow long-duct nacelle development for DC-10 derivative aircraft). The tasks include: design and wind-tunnel tests of winglets on a DC-10 wing; and analytical and wind-tunnel investigation of the interference effects of mixed-flow long-duct nacelles on a DC-10 wing. Early results and the status of this work are presented in the paper entitled "Winglet and Long-Duct Nacelle Aerodynamic Development for DC-10 Derivatives" by A. Brian Taylor of Douglas-Long Beach.

The second contractual activity has a farther term focus (NASA contract NAS1-14744 for selected advanced aerodynamic and active control concepts development). The tasks include: wind-tunnel testing of a high-aspect-ratio supercritical wing; definition and study of an optimum wing-winglet combination; definition of a high-lift system for a high-aspect-ratio supercritical wing; and assessment of a low-risk stability augmentation system for current and advanced transports. The status and results of this work are presented in the paper entitled "Advanced Aerodynamics and Active Controls for a Next Generation Transport" by A. Brian Taylor of Douglas-Long Beach.

Current plans for Phase II include: further DC-10 mixed-flow, long-duct nacelle and winglets wind-tunnel testing and flight test demonstrations; further high-aspect-ratio supercritical wing wind-tunnel testing; and in-depth assessment of an active controls transport including the identification of system design and test requirements.

Lockheed.- In Phase I there is a single effort by Lockheed with a near-term focus (NASA contract NAS1-14690 for accelerated development and flight evaluation of active control concepts for subsonic transport aircraft). The tasks include: flight test of a wing load alleviation system on an L-1011 aircraft; addition of 4.5 foot wing-tip extensions and flight tests with a wing load alleviation system; and moving-base simulation testing to develop active stability augmentation permitting a smaller horizontal tail on future L-1011 derivatives. The status and results of this program to date are presented in the paper entitled "Development and Flight Evaluation of Active Controls in the L-1011" by J. F. Johnston and D. M. Urie of Lockheed-California.

Current plans for Phase II call for further development and evaluation of a wing load alleviation system for subsonic commercial transport aircraft.

CONCLUDING REMARKS

Most NASA-sponsored advanced aerodynamics and active controls technology development for CTOL transports is embodied in the ACEE/EET project. The other papers in this section report selected early results of this program. So that their context is clear, this paper has briefly summarized the EET ongoing and planned efforts indicating which are represented by the papers that follow and outlining the nature of the work not reported.

REFERENCES

1. Leonard, Robert W.; and Wagner, Richard D.: Airframe Technology for Energy Efficient Transport Aircraft. [Preprint] 760929, Soc. Automot. Eng., Nov.-Dec. 1976.

2. Alford, W. J.: Energy Efficient Transport. Research and Technology Objectives and Plans. Summary — Fiscal Year 1978 Research and Technology Program. NASA-TM-78623, 1977, p. 22.

3. Bartlett, Dennis W.: Wind-Tunnel Investigation of Several High Aspect-Ratio Supercritical Wing Configurations on a Wide-Body-Type Fuselage. NASA TM X-71996, 1977.

4. Hood, R. V., Jr.: The Aircraft Energy Efficiency Active Controls Technology Program. AIAA 1977 Guidance and Control Conference, Aug. 1977, pp. 279-285.

5. Dade, W. W.; Edwards, R. H.; Katt, G. T.; McClellan, K. L.; and Shomber, H. A.: Flight Control Electronics Reliability/Maintenance Study. NASA CR-145271, 1977.

6. Murray, N. D.: Fault Tolerant Computers for Civil Transport Aircraft. AIAA Paper No. 77-1439, Oct.-Nov. 1977.

7. Advanced Programs Div., Aerospace Corp.: Fault-Tolerant Software Study. NASA CR-145298, 1978.

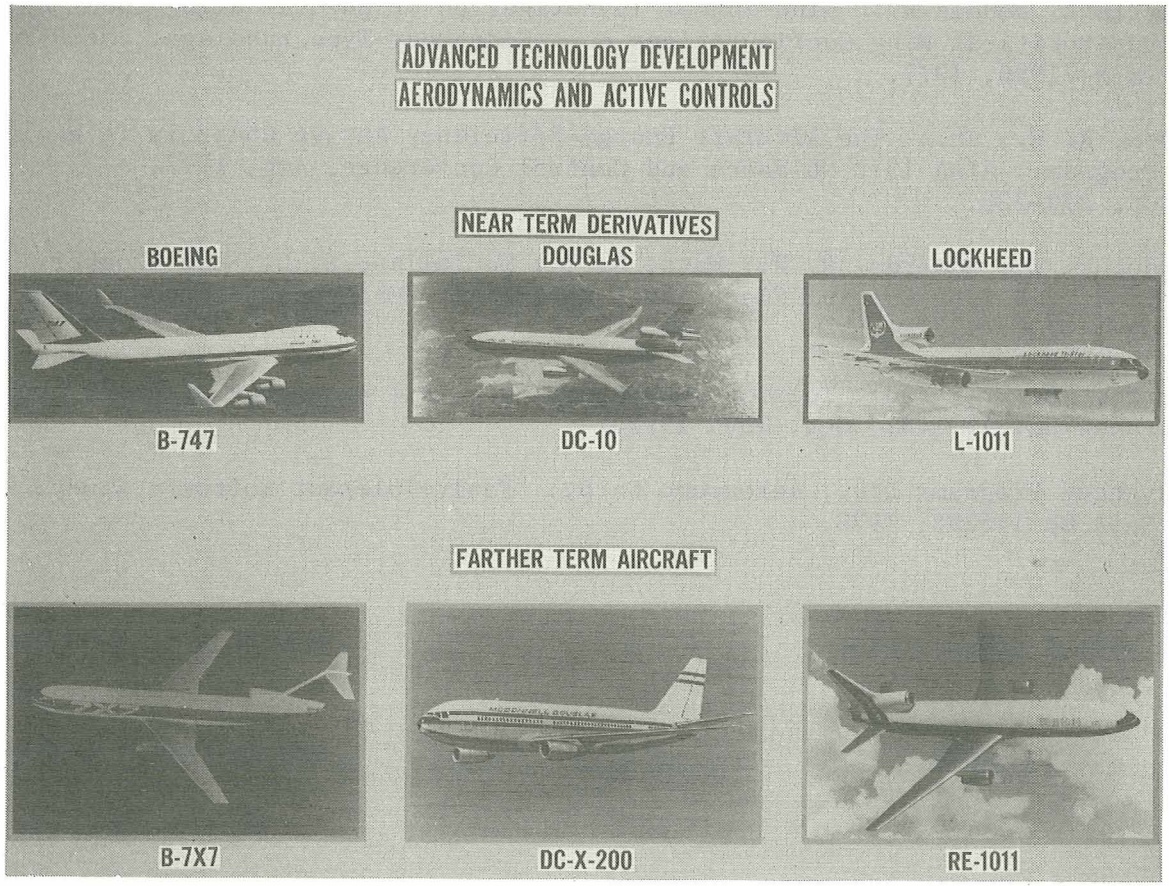

Figure 1.- Energy efficient transport — illustrations of advanced subsonic CTOL aircraft.

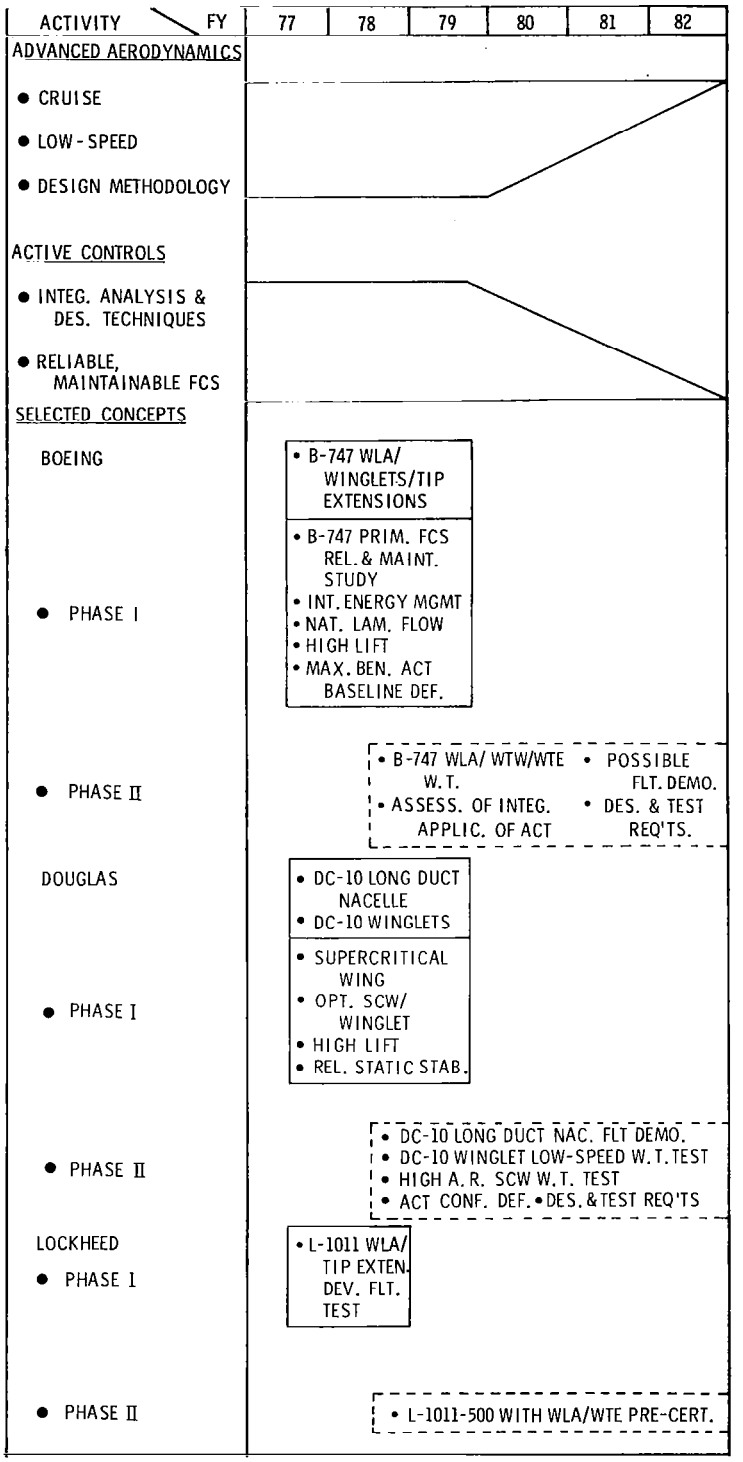

Figure 2.- Energy efficient transport — advanced aerodynamics and active controls technology development and evaluation schedules.

NASA SUPERCRITICAL-WING TECHNOLOGY

Dennis W. Bartlett and James C. Patterson, Jr.
NASA Langley Research Center

This paper, pages 533-552, is deleted and published as NASA TM-78731.

EXPERIMENTAL RESULTS OF WINGLETS ON FIRST, SECOND, AND THIRD GENERATION JET TRANSPORTS

Stuart G. Flechner and Peter F. Jacobs

NASA Langley Research Center

SUMMARY

Winglets are intended to provide substantially greater reductions in drag coefficient, at cruise conditions, than those obtained with a simple wing-tip extension. Extensive experimental investigations have been conducted by NASA to show the effect of winglets on jet transports. This paper presents the results of wind-tunnel investigations of four jet transport configurations representing both narrow and wide-body configurations and also a future advanced aerodynamic configuration. Performance and wing-root bending moment data are presented. In support of a winglet flight research and demonstration program, a comprehensive wind-tunnel investigation was undertaken on one transport configuration to determine the effects of winglets on the aerodynamic characteristics throughout the flight envelope. The investigation was designed to identify any adverse effects due to winglets.

The results of the investigations indicate that winglets improved the cruise lift-to-drag ratio between 4 and 8 percent, depending on the transport configuration. The data also indicate that ratios of relative aerodynamic gain to relative structural weight penalty for winglets are 1.5 to 2.5 times those for wing-tip extensions. The comprehensive investigation has indicated that, over the complete range of flight conditions, winglets produce no adverse effects on buffet onset, lateral-directional stability, and aileron control effectiveness. A winglet flight research and demonstration program has been initiated and results are expected to be available near the end of 1979.

INTRODUCTION

The National Aeronautics and Space Administration has been conducting extensive experimental investigations of the effects of winglets on jet transports. (See refs. 1 to 8.) Winglets, described in detail in reference 1, are intended to provide reductions in drag coefficient, at cruise conditions, substantially greater than those obtained with a simple wing-tip extension.

This paper presents the results of wind-tunnel investigations in the Langley 8-foot transonic pressure tunnel of winglets on four jet transport configurations. Performance and wing-root bending moment data are given for these configurations which represent three generations of jet transports; narrow bodies, wide bodies, and a future advanced aerodynamic concept. In

addition, for one configuration, detailed aerodynamic characteristics are presented at the design condition and also at several off-design conditions. Finally, some milestones in the joint USAF/NASA Winglet Flight Research and Demonstration Program will be presented.

SYMBOLS

The results presented are referred to the stability-axis system for the longitudinal aerodynamic characteristics and to the body-axis system for the lateral-directional aerodynamic characteristics. Force and moment data have been reduced to conventional coefficient form based on the geometry of the basic wing planform for each transport configuration. All measurements and calculations were made in U.S. Customary Units.

AR	aspect ratio
b	wing span
C_B	wing-root bending-moment coefficient, $\frac{\text{Bending moment}}{q_\infty(S/2)(b/2)}$
C_L	lift coefficient, $\frac{\text{Lift}}{q_\infty S}$
C_{l_β}	rate of change of rolling-moment coefficient with sideslip angle (effective dihedral parameter)
$C_{l_{\delta_a}}$	rate of change of rolling-moment coefficient with differential aileron deflection (aileron control effectiveness)
C_n	section normal-force coefficient obtained from integration of pressure measurements
C_{n_β}	rate of change of yawing-moment coefficient with sideslip angle (directional stability parameter)
c	local chord
$\bar{c}$	mean aerodynamic chord of basic configuration
h	span of the upper winglet, measured from the wing chord plane
L/D	lift-to-drag ratio
M_∞	free-stream Mach number
q_∞	free-stream dynamic pressure

R	ratio of merit
S	basic configuration wing planform reference area
SCW	supercritical wing
y	spanwise distance from wing-fuselage juncture, positive outboard
z'	distance along winglet span from chord plane of wing
α	angle of attack
β	angle of sideslip
Δ	incremental value
$\delta_{a,L};\delta_{a,R}$	left and right aileron deflection, positive for trailing edge down
δ_f	flap deflection, positive for trailing edge down
δ_h	horizontal-tail deflection, positive for trailing edge down

Subscripts:

BASIC	reference configuration, model with no wing-tip devices
CRUISE	condition at cruise C_L or cruise M_∞ or both
MAX	condition at maximum bending moment

FUNCTION OF WINGLET

Winglets are small, nearly vertical aerodynamic surfaces which are designed to be mounted at the tips of aircraft wings. (See fig. 1.) Unlike flat end plates, winglets are designed with the same careful attention to airfoil shape and local flow conditions as the wing itself. The primary component of the winglet configurations is a large winglet mounted rearward above the wing tip. The "upper surface" of this airfoil is the inboard surface. For some configurations an additional small winglet, mounted forward, below the wing tip, is necessary. The "upper surface" of the airfoil for this lower winglet is the outboard surface.

The winglets operate in the circulation field around the wing tip. Because of the pressure differential between the wing surfaces at the tip, the air flow tends to move outboard along the wing lower surface, around the tip, and inboard along the wing upper surface. This wing-tip vortex produces cross flows at each winglet. Thus the winglets produce large side forces even at low aircraft angles of attack. Since the side force vectors are

approximately perpendicular to the local flow, the side forces produced by the winglets have forward (thrust) components (fig. 1) which reduce the aircraft induced drag. This is the same principle that enables a sailboat to travel upwind by tacking. For winglets to be fully effective the side forces must be produced as efficiently as possible; therefore, advanced aerodynamic airfoil shapes are used. The side force produced by the winglets, and therefore the thrust produced, is dependent upon the strength of the circulation around the wing tip. Since the circulation strength is a function of the lift loads near the wing tip, winglets are more effective on those aircraft with higher wing loads near the tip.

Theoretical calculations indicate that the aerodynamic benefit would be the same for a given size winglet in either the upper or lower position. Ground clearance of low-wing jet transports limits the span of the lower winglet, and interference with the upper winglet flow limits the chord length of the lower winglet. Thus, from a practical standpoint for low-wing aircraft the lower winglet must be relatively small. As a result, for the jet transports being discussed herein, the contributions of the lower winglet to the reduction of drag were relatively small.

As indicated on figure 1, the winglets tend to straighten the air flow thus slightly reducing the wing-tip vortex strength. However, the trailing vortex hazard still exists. The reduction is an indication of an increase in the aircraft efficiency. Winglets are not designed to improve flight safety for trailing aircraft, but to increase aerodynamic efficiency.

WINGLET EFFECTIVENESS

Configurations

As previously indicated, four jet transport configurations were investigated in the Langley 8-foot transonic pressure tunnel. Photographs of the models are presented in figure 2. First generation jet transports, those with narrow bodies, are represented by the KC-135A. Second generation jet transports, those with wide bodies, are represented by the L-1011 and the DC-10. The third or future generation of jet transports, those with wide bodies and advanced aerodynamic concepts, are represented by a high-aspect-ratio supercritical wing model. This is the "current" (9.8-AR) configuration of reference 9.

Semispan models of the KC-135A and the DC-10 enabled those investigations to be conducted at increased Reynolds numbers, approximately 7 and 5 million, based on mean geometric chords, respectively. Forces and moments were measured by a strain gage balance. The KC-135A fuselage was not attached to the balance but the DC-10 fuselage was attached. The fuselages for the full-span L-1011 and high-aspect-ratio supercritical wing models were represented by bodies of revolution.

The KC-135A and the high-aspect-ratio supercritical wing models did not utilize lower surface winglets. The L-1011 and the DC-10 did utilize the lower surface winglets.

Performance

Figure 3 presents the aerodynamic gain due to winglets for each configuration at its cruise lift coefficient. The aerodynamic gain is represented by the percentage increase in lift-to-drag ratio (L/D) over the basic configurations. At the cruise Mach numbers, indicated by tick marks on the figure, the winglets produced about an 8 percent improvement in L/D for the KC-135A, about a 4 percent improvement for both the L-1011 and DC-10, and about a 6.5 percent improvement for the high-aspect-ratio configuration. Analysis of the data indicated that the KC-135A winglets achieved the greatest performance improvement because the KC-135A has the highest outboard wing loading of those configurations investigated. The KC-135A has an elliptical spanwise load distribution. One characteristic of wide body transports is wing loads over the outboard wing region less than those of an elliptic distribution. This is reflected in reduced winglet performance improvements on the L-1011 and the DC-10. The high-aspect-ratio model was designed for nearly an elliptical spanwise load distribution and therefore the aerodynamic gains with winglets are high, approaching the gains of the KC-135A with winglets. The data shown have not been corrected for full-scale Reynolds number. This correction would result in approximately a one percent increase in lift-to-drag ratio.

It was suggested that the same aerodynamic gains could be obtained simply by increasing the wing span, that is, by adding a wing-tip extension. Therefore as part of each investigation a simple wing-tip extension configuration was also tested. The wing-tip extension for the KC-135A was designed to have the same increase in wing-root bending moment as that due to the winglet at the cruise lift coefficient. This resulted in an increase in the semispan which was equal to 38 percent of the winglet span.

The tip extension configuration for the L-1011 represented a configuration under consideration by the aircraft company. The increase in semispan was approximately 40 percent of the upper winglet span. The DC-10 tip extension represents the change from the Series 10 wing to the Series 30 wing. (The winglet was tested on the Series 10 wing.) The increase in semispan was about 47 percent of the upper winglet span.

The tip extension configuration for the high-aspect-ratio supercritical wing configuration was represented by a higher aspect ratio (11.4) model of reference 9. The increase in semispan was equal to the winglet span.

Figure 3 also presents the aerodynamic gains at cruise lift coefficient for tip extensions. Tip extension performance gains at cruise Mach numbers were about 4 percent for the KC-135A, about 2.5 percent for the L-1011 and the DC-10, and about 7 percent for the high-aspect-ratio supercritical wing configuration. Again, loading near the wing tip affects the gains achieved, but direct comparisons cannot be made because of the different wing-tip extension sizes.

Wing-Root Bending Moments

In the structural design of wings the spanwise variation in bending moments must be considered. Unpublished analysis of wing structures has indicated that structural weight changes are roughly proportional to changes in the wing-root bending moments. Therefore, increases in the maximum wing-root bending moment will be used to approximate structural weight penalties.

Figure 4 presents the percentage increase in wing-root bending moment with winglets or tip extensions over the basic configuration at the maximum wing-root bending moment condition. For uniformity in presenting the data, the maximum wing-root bending moment was considered to occur at the lift coefficient where the plot of pitching-moment coefficient versus lift coefficient becomes nonlinear. The data show that the incremental increase in maximum wing-root bending moment due to tip extensions is always equal to or greater than the incremental increase due to winglets.

The bending moment increments for the KC-135A are lower than those for the other configurations because the KC-135A model wing was designed to aeroelastically deflect the same as the aircraft wing. The other models were rigid representatives of the cruise shape. The aeroelastic deflection reduces the added moments due to the winglets and thus reduces the maximum wing-root bending moment condition.

Relative Merits

To compare the four jet transport configurations with winglets and tip extensions the aerodynamic gain and the structural weight penalty have been considered together in a new term. For this comparison the term ratio of merit has been employed and is defined as the relative aerodynamic gain at cruise lift coefficient, represented by the percentage increase in lift-to-drag ratio over the basic configuration (fig. 3), divided by the relative structural weight penalty at the maximum wing-root bending moment condition, approximated by the percentage increase in wing-root bending moment over the basic configuration (fig. 4). That is,

$$R \approx \frac{\left(\dfrac{\Delta L/D}{(L/D)_{BASIC}}\right)_{CRUISE}}{\left(\dfrac{\Delta C_B}{C_{B,\ BASIC}}\right)_{MAX}}$$

The comparison of the ratios of merit is present in figure 5. As defined by this parameter, winglets are more effective than wing-tip extensions for all the jet transport configurations investigated. (Note the change in scale for the L-1011 and DC-10.) At the cruise Mach number, winglets on the KC-135A provided 2.5 times the improvement of the tip extension in ratio of merit. The winglets on the L-1011 and DC-10 provided improvements at the cruise Mach numbers 1.5 and 2 times those of the tip extensions, respectively. The

winglets on the high-aspect-ratio supercritical wing provided improvement at the cruise Mach number 2 times those of the tip extension.

The ratio of merit for the KC-135A with winglets is greater for two reasons. First, the KC-135A has the highest loading over the outboard wing region resulting in the largest aerodynamic gains from winglets. Secondly, the aeroelastic wing reduced the maximum wing-root bending moments. Aeroelastic wing deflection for the other jet transport models would increase the relative gains for winglets over tip extensions as expressed by the ratio of merit.

DETAILED INVESTIGATIONS

After the benefits obtainable with winglets first became known the U. S. Air Force initiated design studies on the application of the winglet concept, references 10 and 11. (Winglets were also known as vortex diffusers and tip fins.) The potential large fuel savings available by retrofitting winglets to the USAF fleet of large transports has led to a joint USAF/NASA Winglet Flight Research and Demonstration Program. The KC-135A was chosen as the test bed aircraft. Aerodynamically, the KC-135A is an ideal test bed. As previously indicated, the ratios of merit are very high.

In support of this flight program, a comprehensive wind-tunnel investigation was undertaken to determine the aerodynamic characteristics of the KC-135A with winglets throughout the flight envelope. Specifically, the investigation was designed to identify any adverse effects due to winglets. While the results of the investigation are for the KC-135A, the trends indicated are judged to be valid for most large jet transports with winglets.

Wind-Tunnel Models

The comprehensive investigation required four different wind-tunnel model configurations as shown in figure 6. As previously indicated, the semispan model was used to obtain all performance and some loads data. A full-span model with changeable flaps and ailerons was used to obtain the low-speed ($M_\infty = 0.30$) stability and control characteristics. The same fuselage and tail with a pressure instrumented wing was used to obtain high-speed stability and loads data in yaw. The pressure instrumented wing on a tailless body of revolution fuselage was used to obtain stability and loads data at high angles of attack.

Low-Speed Performance

The aerodynamic gain due to winglets at 0.30 Mach number and in a take-off configuration is presented in figure 7. Again, the aerodynamic gain is represented by the percentage increase in lift-to-drag ratio over the basic configuration. The lift coefficient range of interest for low speed performance is substantially higher than the lift coefficient for cruise performance. At these higher lift coefficients the induced drag is a higher percent of the total drag than at the cruise lift coefficient. Since the higher induced drag

indicates the circulation around the wing tip is stronger, the winglet effectiveness is also increased.

Spanwise Load Distribution

Figure 8 presents the effects due to winglets on the spanwise load distribution of the KC-135A and the load distribution along the winglet span. Two lift coefficients, representing the maximum wing-root bending moment condition and the cruise condition, are shown at the cruise Mach number, 0.78. The elliptical spanwise load distribution of the basic KC-135A is shown along with the increase in load near the tip due to the winglet. The effect of the aeroelastic deflection is also shown by the fact that the relative increase in load near the tip due to the winglets is smaller at the high lift coefficient than the increase at the cruise lift coefficient.

Buffet Characteristics

The effect of winglets on the KC-135A buffet characteristics is shown on figure 9. Buffet was considered to occur at the lift coefficient of the initial break in the plot of lift coefficient versus angle of attack. Below the cruise Mach number the lift coefficient for buffet onset is generally higher with winglets on. Above the cruise Mach number there is no significant change in the buffet characteristics.

Lateral-Directional Stability

The effects of winglets on the KC-135A lateral-directional stability is presented in figure 10(a) for high-speed conditions and in figure 10(b) for low-speed conditions. At cruise lift coefficient, winglets increase the high-speed effective dihedral between 10 and 19 percent and increase the directional stability approximately 9 percent. The data presented at the low-speed condition is for a configuration with take-off flaps and moderate differential aileron deflection. Again winglets increase the effective dihedral between 7 and 24 percent and increase the directional stability between 3 and 16 percent. Similar trends were obtained for landing flap conditions and for aileron deflections of 0° and 20°.

Aileron Control Effectiveness

Figure 11 presents the effects of winglets on KC-135A low speed aileron control effectiveness. The data presented in figure 11 is again for the configuration with take-off flaps. The winglets increase the aileron control effectiveness between 3 and 13 percent. Similar trends were also obtained for the landing flap configuration.

FLIGHT RESEARCH AND DEMONSTRATION PROGRAM

As previously mentioned NASA and the USAF are conducting a joint Winglet Flight Research and Demonstration Program using the KC-135A aircraft. An artist's concept of the configuration is shown in figure 12. Final structural

design of the flight hardware is underway. The base-line documentation flights are scheduled to begin during August 1978. The first flight with winglets is anticipated in early 1979 and the flight-test data will be available in the fall of 1979, about three months after the last flight.

SUMMARY OF RESULTS

Wind-tunnel investigations of winglets and tip extensions on model configurations representing three generations of jet transports have been conducted. The data presented indicate the following conclusions:

1. Winglets improved the cruise lift-to-drag ratio between 4 and 8 percent, depending upon the configuration and, in particular, the span load distribution.

2. The ratio of relative aerodynamic gain to relative structural weight penalty for winglets are 1.5 to 2.5 times the ratio for wing-tip extensions.

3. A comprehensive wind-tunnel investigation of winglets on the USAF KC-135A over the complete range of flight conditions has indicated that winglets produce no adverse effects on buffet onset, lateral-directional stability, or aileron control effectiveness.

4. A Winglet Flight Research and Demonstration Program is under way utilizing the KC-135A as the test vehicle. The flight-test results will be available near the end of 1979.

REFERENCES

1. Whitcomb, Richard T.: A Design Approach and Selected Wind-Tunnel Results at High Subsonic Speeds for Wing-Tip Mounted Winglets. NASA TN D-8260, 1976.

2. Flechner, Stuart G.; Jacobs, Peter F.; and Whitcomb, Richard T.: A High Subsonic Speed Wind-Tunnel Investigation of Winglets on a Representative Second-Generation Jet Transport Wing. NASA TN D-8264, 1976.

3. Jacobs, Peter F.; and Flechner, Stuart G.: The Effect of Winglets on the Static Aerodynamic Stability Characteristics of a Representative Second Generation Jet Transport Model. NASA TN D-8267, 1976.

4. Jacobs, Peter F.; Flechner, Stuart G.; and Montoya, Lawrence C.: Effect of Winglets on a First-Generation Jet Transport Wing. I - Longitudinal Aerodynamic Characteristics of a Semispan Model at Subsonic Speeds. NASA TN D-8473, 1977.

5. Montoya, Lawrence C.; Flechner, Stuart G.; and Jacobs, Peter F.: Effect of Winglets on a First-Generation Jet Transport Wing. II - Pressure and Spanwise Load Distributions for a Semispan Model at High Subsonic Speeds. NASA TN D-8474, 1977.

6. Montoya, Lawrence C.; Jacobs, Peter F.; and Flechner, Stuart G.: Effect of Winglets on a First-Generation Jet Transport Wing. III - Pressure and Spanwise Load Distributions for a Semispan Model at Mach 0.30. NASA TN D-8478, 1977.

7. Meyer, Robert R., Jr.: Effect of Winglets on a First-Generation Jet Transport Wing. IV - Stability Characteristics for a Full-Span Model at Mach 0.30. NASA TP-1119, 1978.

8. Jacobs, Peter F.: Effect of Winglets on a First-Generation Jet Transport Wing. V - Stability Characteristics of a Full-Span Wing With a Generalized Fuselage at High Subsonic Speeds. NASA TP-1163, 1978.

9. Bartlett, Dennis W.; and Patterson, James C., Jr.: NASA Supercritical-Wing Technology. NASA TM-78731, 1978.

10. Kulfan, Robert M.; and Howard, Weston M.: Application of Advanced Aerodynamic Concepts to Large Subsonic Transport Airplanes. AFFDL-TR-75-112, U.S. Air Force, Nov. 1975.

11. Ishimitsu, K. K.; VanDevender, N.; Dodson, R.; et al.: Design and Analysis of Winglets for Military Aircraft. AFFDL-TR-76-6, U.S. Air Force, Feb. 1976.

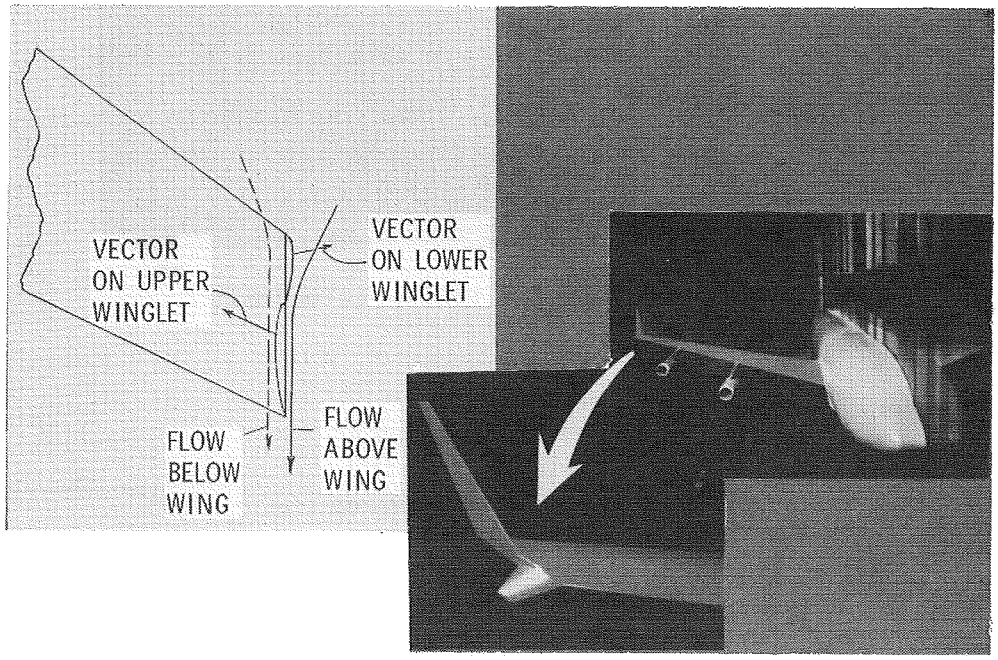

Figure 1.- Aerodynamic effect of winglets.

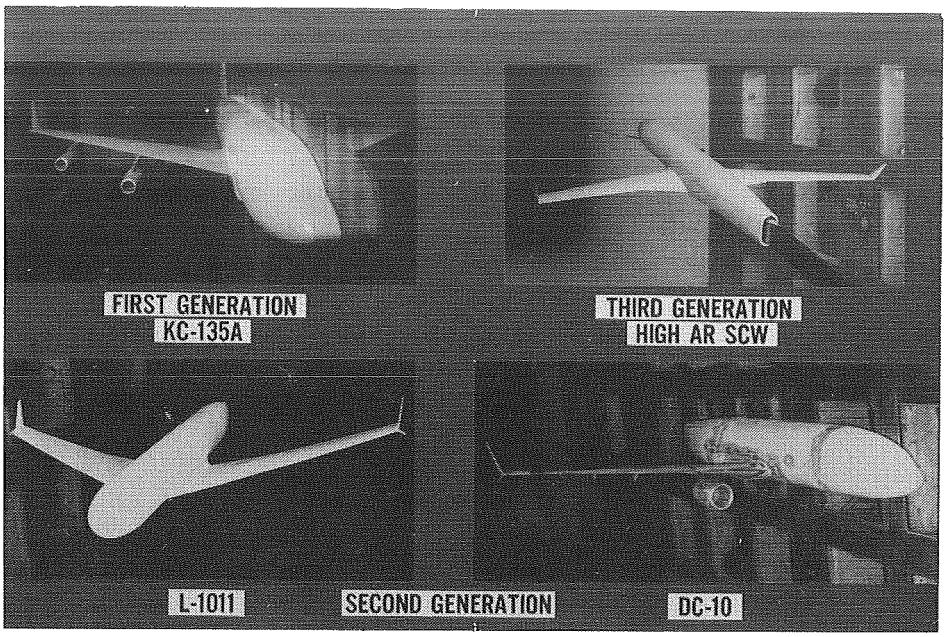

Figure 2.- Winglets on jet transport models.

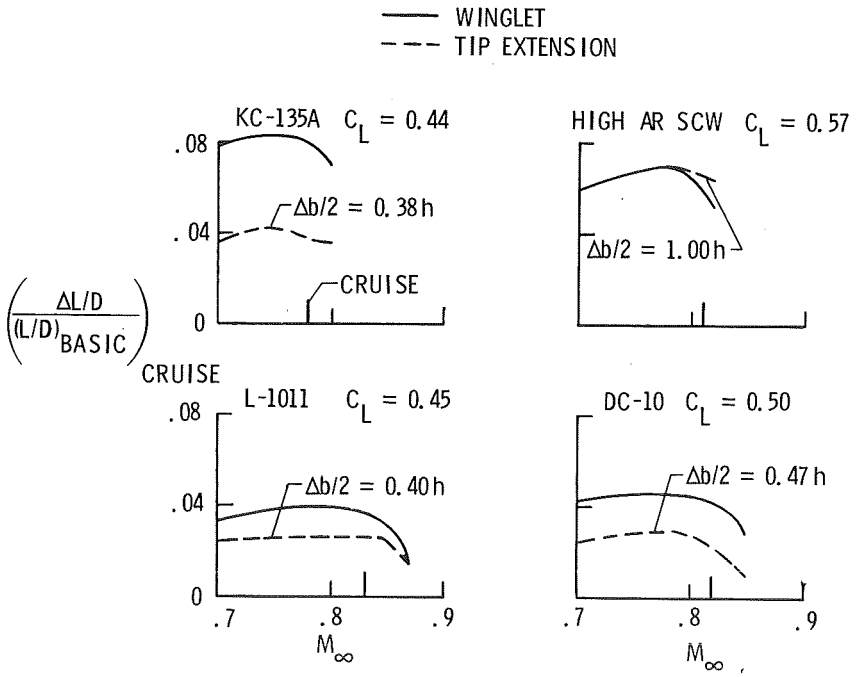

Figure 3.- Winglet and tip extension cruise performance.

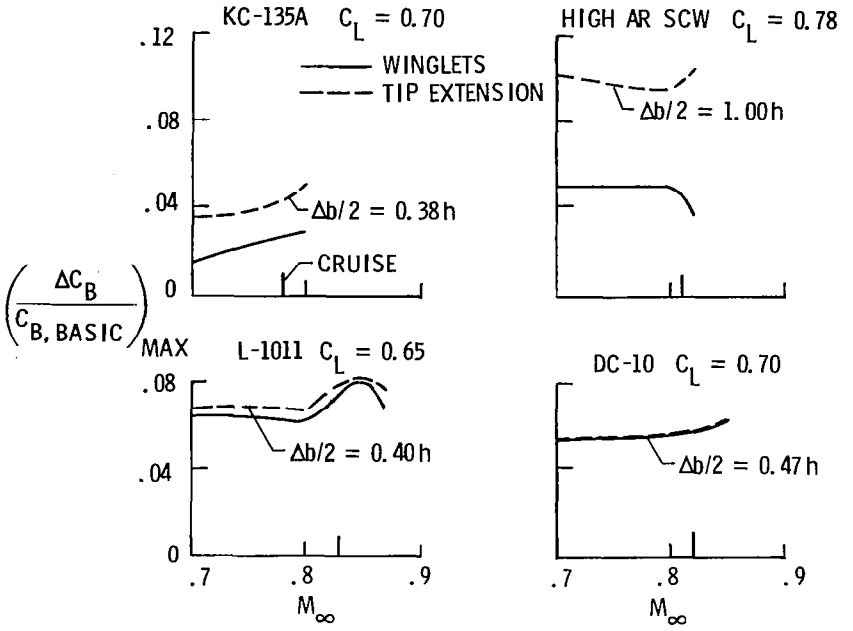

Figure 4.- Wing-root bending moments.

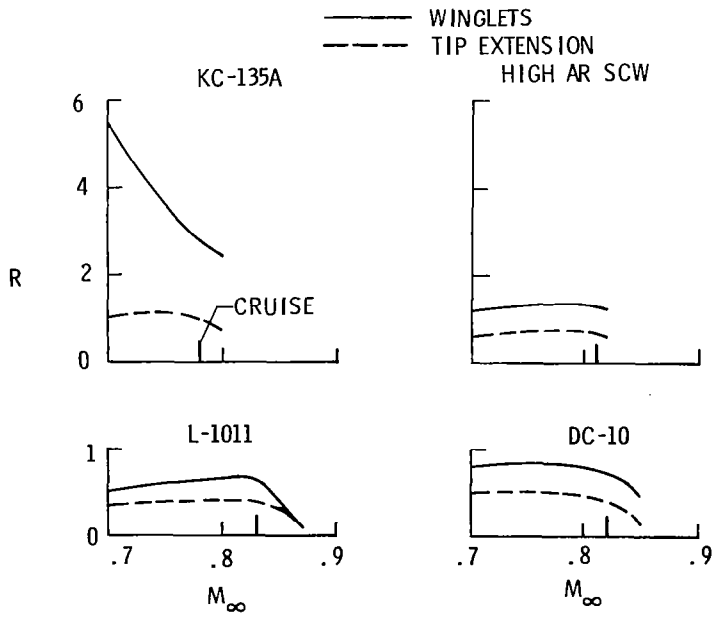

Figure 5.- Comparison of ratios of merit.

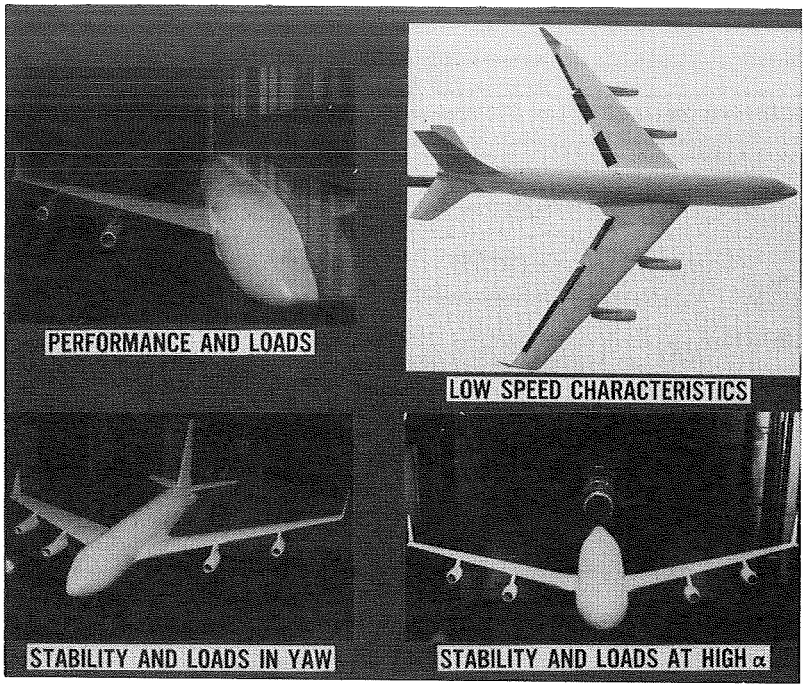

Figure 6.- Winglets on the KC-135A models.

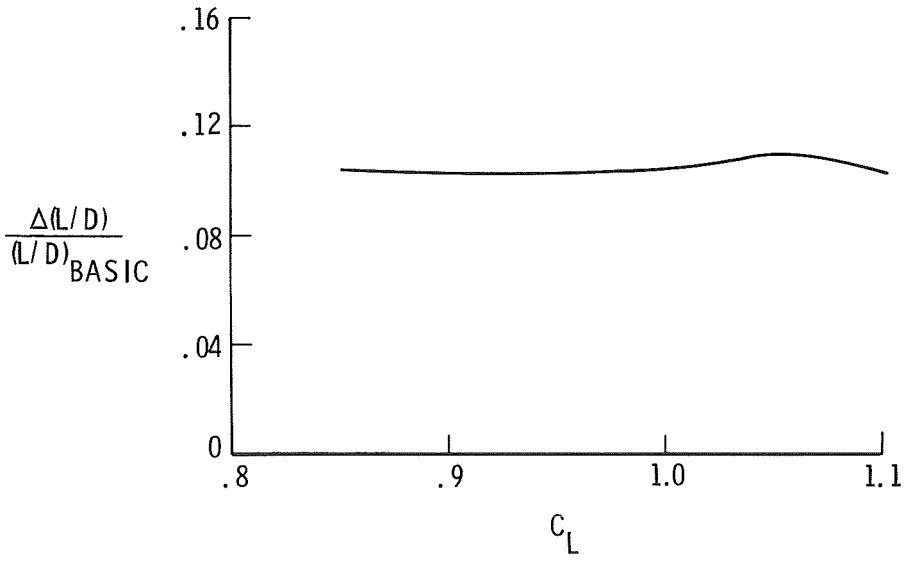

Figure 7.- Low-speed winglet performance. KC-135A semispan model with take-off flaps. $M_\infty = 0.30$.

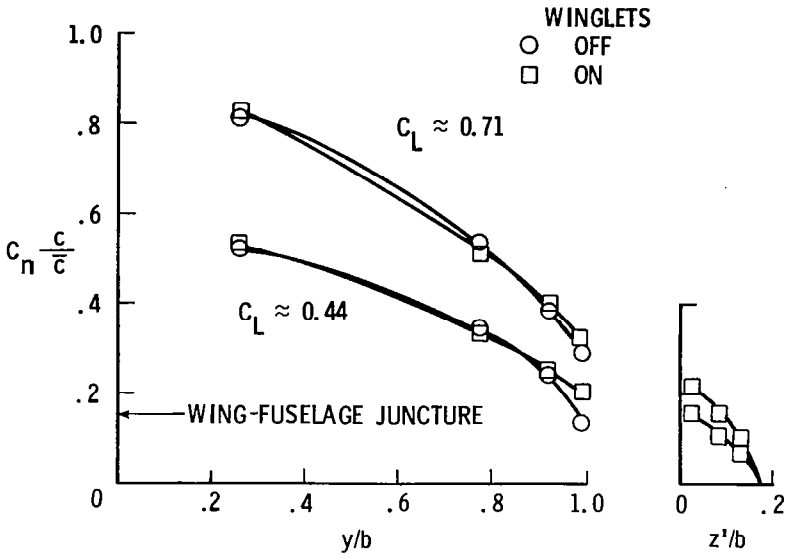

Figure 8.- Effect of winglets on spanwise load distributions. KC-135A semispan model. $M_\infty = 0.78$.

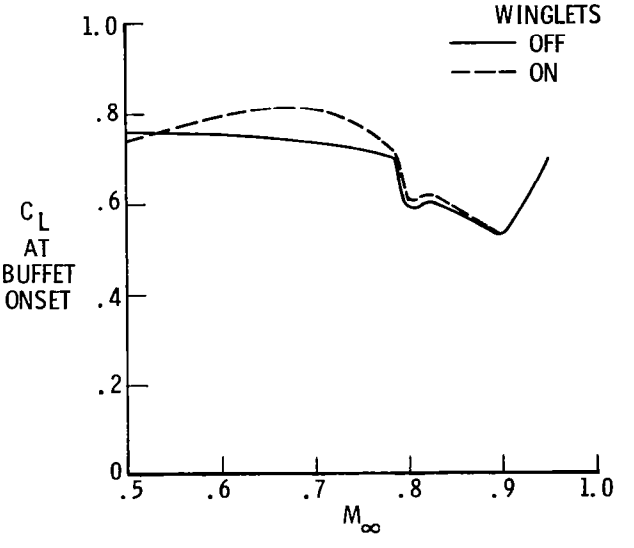

Figure 9.- Effect of winglets on high-speed buffet characteristics. KC-135A full-span tailless model.

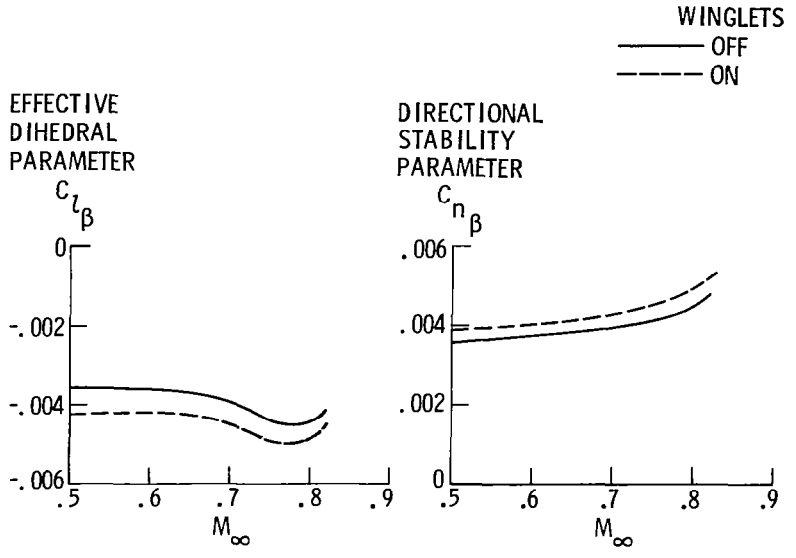

(a) KC-135A full-span, high-speed model. $C_L = 0.44$; $\delta_h = 0^o$.

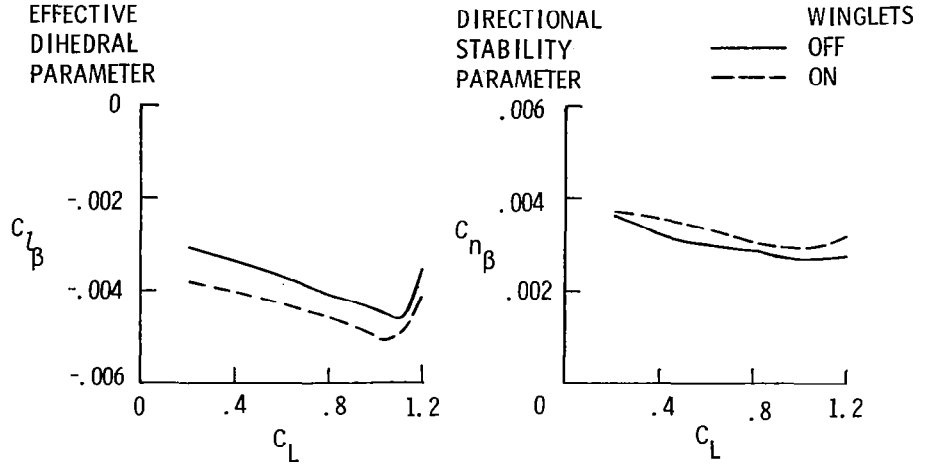

(b) KC-135A full-span, low-speed model. $M_\infty = 0.30$; $\delta_{a,L} = -10^o$; $\delta_{a,R} = 10^o$; $\delta_f = 30^o$; $\delta_h = -10^o$.

Figure 10.- Effect of winglets on lateral-directional stability.

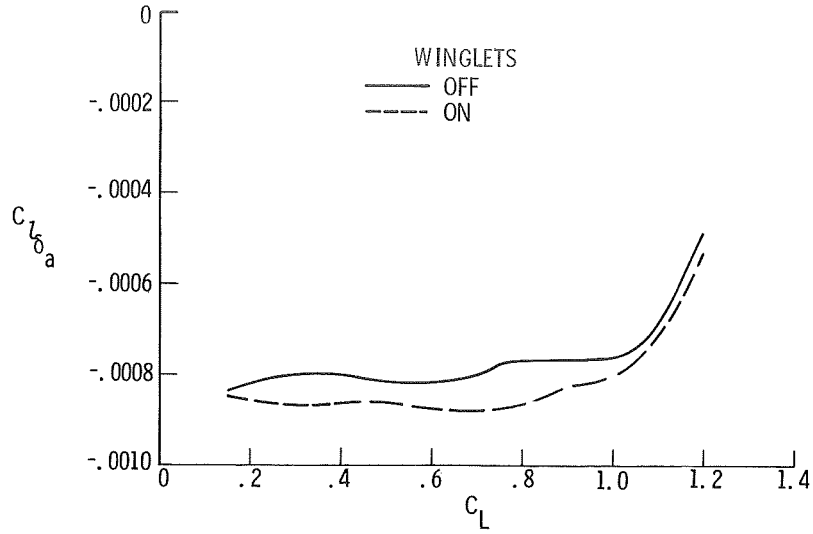

Figure 11.- Effect of winglets on aileron control effectiveness. KC-135A full-span, low-speed model. $M_\infty = 0.30$; $\beta = 0^o$; $\delta_f = 30^o$; $\delta_h = -10^o$.

Figure 12.- USAF KC-135A with NASA winglets.

RECENT EXPERIENCES WITH THREE-DIMENSIONAL TRANSONIC POTENTIAL FLOW CALCULATIONS

David A. Caughey
Cornell University

Perry A. Newman
NASA Langley Research Center

Antony Jameson
New York University

This paper, pages 571-591, is deleted and published as NASA TM-78733.

TOWARDS COMPLETE CONFIGURATIONS USING AN EMBEDDED GRID APPROACH

Charles W. Boppe
Grumman Aerospace Corporation

This paper, pages 593-608, is deleted and published as NASA CR-3030.

WINGLET AND LONG-DUCT NACELLE AERODYNAMIC DEVELOPMENT FOR DC-10 DERIVATIVES*

by

A. Brian Taylor
Douglas Aircraft Company
Long Beach, California

SUMMARY

Two promising advances are under development for application to near-term derivatives of the Douglas DC-10 transport. The winglet, a near-vertical surface at the wing tip, offers substantial cruise drag reduction with less wing root bending moment penalty than a wing-tip extension of the same effectiveness. Wind tunnel tests have confirmed these predictions. The long-duct nacelle also offers substantial drag reduction potential as a result of aerodynamic and propulsion improvements. The aerodynamic design and forthcoming test of the nacelle and pylon installation are described.

INTRODUCTION

The NASA Aircraft Energy Efficiency (ACEE) program has provided a stimulus to industry to accelerate development of technology directed toward energy savings and economic benefits. Under the ACEE Energy Efficient Transport (EET) program, Douglas is pursuing technology developments for potential application to the near-term derivatives of the DC-10 transport. The DC-10 is in extensive and successful use both in the United States and around the world in several versions. By the usual processes of product improvement, development is continuing in a number of areas. These developments are aimed at improvements in product durability, performance, and cost control. The value of the EET program is in the sponsorship of more advanced developments.

Of the advanced improvements possible, the aerodynamic development of winglets and of the long-duct nacelle (LDN) was selected for near-term work.

The function of the winglet is to reduce induced drag. The pictorial concept in figure 1 shows the DC-10 with winglets. The winglet is based on the classical design by Dr. R. T. Whitcomb of NASA Langley (reference 1), and, with his cooperation, has been the subject of considerable study at Douglas. In this form, the winglet consists of a near-vertical upper surface at each wing tip with a smaller lower surface ahead of it. The claimed advantage of a winglet over a wing-tip extension having the same drag reduction is a significantly smaller penalty on wing bending loads and hence a smaller weight penalty.

The purpose of the program is to develop the winglet to a high-potential drag reduction and compare it with wing-tip extensions.

*Including work performed under NASA Contract NAS1-14743

The LDN concept offers significant advantage in cruise efficiency through improvements in propulsive efficiency and the aerodynamics of the installation (reference 2). The work of reference 2 also explored the application of lightweight composite materials and the potential reduction in community noise. The representation in figure 2 shows a DC-10 equipped with the LDN. The LDN carries the outer (fan) duct past to the core nozzle, which incorporates a forced mixer. The advantages offered by this concept include the reduction of scrubbing and interference drag and an improvement in specific fuel consumption due to internal flow mixing.

The EET program concerns itself with the task of integrating the nacelle, pylon, and wing at high speed to achieve an installation with low interference drag.

SYMBOLS AND NOMENCLATURE

Values are given in SI Units and where appropriate also in U.S. Customary Units. Measurements and calculations were made in U.S. Customary Units.

A_c	Channel area, m^2
c	Local chord of wing, used in nondimensional parameter
c_ℓ	Section lift coefficient of local chord
c_R	Root chord of wing at aircraft centerline, used in nondimensional parameter
cc_ℓ/c_R	Nondimensional loading parameter
C_D	Drag coefficient
C_L	Lift coefficient
$C_{L_{W+B}}$	Lift coefficient, wing plus body
C_P	Pressure coefficient
L/D	Lift-to-drag ratio
M	Mach number
Range Factor	Lift-to-drag ratio multiplied by aircraft speed divided by fuel quantity used per unit propulsive thrust
W/δ	Aircraft weight divided by ratio of atmospheric pressure to atmospheric pressure at sea level on a standard day, kg (lb)
x/c_W	Distance from wing leading edge divided by wing chord

Subscripts not identified on previous page

L	Local
o	Freestream

WINGLET

A significant amount of design and analysis has already been performed on winglets for the DC-10. The current program introduces experimental methods to evaluate the aerodynamic potential. The process has the classical elements of design, test, and evaluation. The tests were completed on a 4.7-percent semispan DC-10 model in November 1977 in the NASA Langley 8-foot transonic wind tunnel.

Winglet Design

The basic DC-10 winglet is a Whitcomb design following general design guidelines published in reference 1. Prior to selection of test configurations, analytical studies were made using the Douglas Nonplanar Lifting Surface program (reference 3). Perturbations were made in height, taper ratio, location, upper surface/lower surface combinations, and size.

The analyses from these perturbations substantiated the Whitcomb design. The designs generally utilize a modified NASA GAW airfoil (reference,1), 65 percent wing-tip root chord, one tip chord height and with the winglet trailing edge coincident with the wing trailing edge. A typical design geometry is shown in figure 3. The use of the analysis of reference 3 suggests that there is an increase in winglet performance with forward movement of the upper winglet on the wing-tip chord. The risk in this approach is of interference drag due to the effect of the addition of the peak velocities of the wing and winglet.

Test Configuration

The aircraft configurations were chosen to identify the effect of winglets and of a wing-tip extension. The current DC-10 aircraft versions have been used as a basis, figure 4. The intermediate range DC-10 Series 10, with and without winglets, enables the effect of winglets to be established. This aircraft has a wing span of 47.35 meters (155 feet 4 inches). With the addition of the 3.08-meter (10-foot) span extension that converts the geometry of the Series 10 to that of the long-range Series 30/40, the effect of wing-tip extensions can be determined. With the addition of winglets to the Series 30/40, their effect can be measured and compared to those on the original Series 10.

The winglet configuration alternatives are shown in figure 5. For the Series 10, two chordwise positions were provided. Three winglet incidence angles were provided in each location. The lower winglet was made removable in order to measure effectiveness of the upper winglet with and without the lower winglet. For the Series 30/40, two winglets of different chords were provided to use the best winglet incidence angle from the Series 10 tests. The first winglet chord had the same chordwise proportions as the Series 10 winglet on the Series 10 wing. The second configuration was the Series 10 winglet, which resulted in larger winglet root chord relative to the wing tip chord. The root chord proportion in this case was 0.77.

Experimental Development

Force, moment and pressure data, as well as sufficient flow visualization data to assist in winglet configuration development, were obtained during the initial test. A loss of winglet effectiveness was observed as the Mach number approached cruise values. The reason for this was determined with the aid of oil flow visualization, figure 6. With only the upper winglet installed, the oil flow indicated a flow separation in the winglet root. With the lower winglet also installed, the flow separation transferred itself to the lower surface. The solutions to this difficulty were developed at the tunnel, and comprised wing-winglet juncture tailoring as well as physically moving the lower surface winglet forward to reduce upper and lower winglet interference. In the final winglet configurations little wing-winglet interference is believed present.

Winglet effectiveness is a strong function of the wing span loading without the winglet. A satisfactory correlation of wind tunnel test and flight loadings should indicate that the tunnel test properly simulates the environment for testing winglets and wing-tip extensions for the DC-10 models. Good correlation with flight test, and also with an earlier tunnel test of the DC-10-10 wing, was obtained as shown in the example in figure 7. The basic wing span loading used in the induced drag analysis was also consistent with that of wind tunnel and flight.

The winglet performance predicted from theory does not include viscous effects. It has been found (for example, reference 1) that the largest measured reductions of drag due to adding the winglet are obtained with normal loads on the winglet that are less than suggested as optimum by the theory. Viscous effects reduce the winglet loading potential relative to the analytical inviscid methods. Also, as loading on the winglet increases, viscous drag effects increase and apparently offset improvements in wing-winglet induced drag. It was therefore expected that the wind tunnel development would show the best performance with a winglet offloaded, that is having negative incidence as shown in figure 3. The test data indicated little sensitivity of drag reduction to winglet loading over an incidence range from 0^{o} to -4^{o}. However, a setting of -2^{o} appeared to be the best.

Tests were included to measure the effect of moving the winglet to the forward position on the Series 10 wing shown in figure 5. Oil flow visualization indicated no separation; however, results were inferior to the aft position. The Series 30 winglets previously described were also tested. The larger winglet tested showed a higher level of drag reduction.

Results and Comment

A summary of the principal results at specific cruise lift coefficients of the DC-10 Series 10 and Series 30/40 is shown in table 1. This identifies the reduction in drag coefficient obtained with the winglets installed relative to the wing without the winglets installed. It can be seen that the winglet gain is significant for both models. The Series 30/40 winglet has a slightly smaller gain. This difference is understood, and is due to the relatively washed-out tip extension utilized on the Series 30/40 wing.

Wind tunnel measured performance increments are shown in figure 8. Also shown are two levels of winglet performance estimates using the methods of reference 3. The optimum level of estimated performance occurred at 0 degree upper winglet incidence angle. However, the best test winglet incidence angle was off-loaded by 2 degrees (-2 degrees incidence angle). A second estimate line for the best winglet test configuration is also shown. As shown in the figure, the best winglets for both the Series 10 and Series 30/40 achieved drag reductions somewhat less than the full analytical potential.

However, for the case of reduced winglet incidence, the winglet data agree relatively well with analytical estimates. The measured performance improvement for the wing-tip extension (Series 10 to Series 30/40) also agrees well with the analytical estimate.

A fundamental winglet versus wing-tip extension comparison is shown in figure 9. Measured drag improvements and measured increases in wing-root bending moment for a fixed-lift coefficient of 0.5 are presented. The increase in wing-root bending moment due to a wing-tip device is indicative of the basic wing structural weight penalty for the inclusion of winglets or wing-tip extensions. As indicated, for a fixed value of drag improvement, winglets produce about one-half of the increase in wing-root bending moment as wing-tip extensions. Also, for the same increase in wing-root bending moment, winglets provide approximately twice the drag improvements as wing-tip extensions.

While the results of the high-speed testing are considered a success, the design of the wing and winglet at low speed and high lift requires further work. Furthermore, the characteristics of the entire aircraft with winglet installed remain to be determined.

LONG-DUCT NACELLE

The potential performance improvement offered by the long-duct nacelle on the DC-10 is significant. As a result of the combined improvements in external aerodynamics and internal flow mixing, the potential reduction in fuel burned is 4.5 percent for a typical long range mission. However, it is recognized that this nacelle installation requires at least as careful an aerodynamic design process as that for the current production short duct to avoid erosion of the potential gains. The principal considerations relate to the differences in the configurations, figure 10. The key area of interest to be discussed in this paper is the avoidance of any potential interference drag between nacelle, pylon, and wing due to the lengthening of the fan duct. This lengthening provides the opportunity for mixing of the fan and core flows. In addition, the fan flow is contained within the duct until aft of the core nozzle, reducing scrubbing losses on the core coil and pylon.

The objective of the program is therefore to develop a practical installation for the long-duct nacelle on the DC-10 which maximizes the potential reduction in fuel burned. The nacelle and pylon geometry has been developed analytically, with the evaluation to be based on experimental data. The test will be conducted in May in the Ames 11-foot facility, with a 4.7-percent DC-10 semispan model.

Basis for Design

Allowable configurations are those that retain the current DC-10 pylon primary structure. This approach minimizes changes in nacelle weight and center of gravity, with obvious and direct practical advantages in minimizing development costs and weight growth. Therefore, pylon shape development, to achieve an acceptable cruise configuration, is the primary area of effort.

However, in order to provide a spectrum of data, and as insurance should further improvements in interference drag be justified, a more forward position also will be tested.

High-speed interference drag in nacelle installation results from the effects of excessive velocity additions in the inboard channel formed by the wing nacelle and pylon. Examples of this difficulty are by the Convair 990 (reference 4) and the Douglas DC-8 prototype with long duct nacelle (reference 5).

These past experiences showed an unacceptable drag rise in the original configurations of the nacelle and pylon configurations. The relative shaping and disposition of these components relative to the wing resulted in additions of the flow velocities to an extent that shock wave losses and separation occurred. References 4 and 5 give explanations of the utilization of the area rule principle in solving these problems. The DC-8 prototype experience is summarized in figure 11. The original nacelle and pylon, while achieving the predicted improvements over the preceding short-duct nacelle at moderate Mach numbers, lost performance sharply at the higher Mach numbers desired for cruise. The reasons are reflected in the chart of nacelle pressure coefficients (figure 11), which indicates the strong shock condition. To achieve the desired gain throughout, the nacelle afterbody lines were refined (necessitating redesign of the thrust reverser), and an extended fairing was added to the pylon. This solution was satisfactory and complied with the intention to retain the basic pylon structure that existed.

The procedure described in reference 4 introduces a flow channel analogy by which designs may be evaluated for their interference effects. The flow channel is conventionally bounded by the wing, pylon and nacelle above the horizontal plane of symmetry, and by a suitable plane inboard of the pylon. In the Douglas work for the DC-10, an alternate approach for predicting pressures on the wing and nacelle has been adopted. This approach utilizes the Douglas Three-Dimensional Lifting Neumann program (DTLN). Figure 12 represents data from the two methods for the current DC-10 nacelle. As might be expected, the characteristics of the channel area distribution are consistent with the calculated wing lower surface pressure distribution.

Correlations of DTLN estimates of surface pressures with flight test data indicate that the modeling produces valid predictions in the vicinity of the pylon. A further simplification resulted from comparisons of wing-body-nacelle and wing-nacelle flowfield solutions. These showed little effect of the fuselage on the pressure distributions in the vicinity of the nacelle; therefore, in later analyses the body was eliminated to permit more detailed paneling of the nacelle and pylon.

The baseline LDN configuration employs the existing DC-10 pylon. This would result in the least cost solution if it could be shown not to incur an interference drag. Figure 13 illustrates a comparison of the calculated pressure distributions and channel area distribution for the DC-10 production short-duct and baseline LDN configurations. Both the suction peak under the wing and the subsequent adverse pressure gradient for the baseline are more severe than for the production DC-10. The calculated pressures for the baseline LDN are barely subcritical. The limitations of the Neumann potential flow (with compressibility corrections) method suggest that the baseline LDN configuration could exhibit excess nacelle interference drag.

Even though the wind-tunnel evaluation may show the baseline LDN to be acceptable, a contoured fairing to the pylon does tend to reduce the local Mach number in the channel. Contoured designs have been designed with the aid of the DTLN.

Among the designs considered is that illustrated in figure 14. The contour is applied to the aft fairing of the pylon, thus retaining intact the primary structure. This contour tailors the pressure distributions in the potentially critical regions. Figure 14 shows that the contouring significantly improves the suction areas and adverse pressure gradients on both the wing lower surface and the nacelle afterbody. Figure 13 and 14 wing lower surface pressure coefficients are generally comparable although detailed variations exist due to the use of slightly different panelling distributions. By such contouring, the possibility exists of achieving interference drag as low as or even better than the current production nacelle.

Experimental Program

The test configurations consist of an unpowered flowthrough and a powered current production nacelle and pylon, a number of pylon configurations with an unpowered flowthrough LDN, and an LDN with a powered engine simulator. The power plant represented in the nacelle design is the General Electric CF6-50 Series used on the DC-10 Series 30. It is considered that the results will be representative of the Pratt and Whitney engines used on the DC-10 Series 40.

Overall configuration forces and moments, nacelle normal force, and wing/nacelle/pylon (inboard side only) pressure data will be recorded. Test configurations will be evaluated at cruise Mach number over the range of lift coefficient applicable for cruise conditions. This will require Mach numbers of 0.8 to 0.84 and angles of attack from 1.5 to 3.5 degrees. The relative effect of simulated engine power on the interference drag of the baseline configuration will be recorded. The test will cover fan pressure ratios of 1.0 to approximately 1.6. Flow visualization will be employed, using fluorescent minitufts.

This phase of the long-duct nacelle programs focuses on high-speed development which must be the foundation for a production design. Further development on the installation and determination of characteristics for the aircraft at both high and low speeds will be necessary.

CONCLUDING REMARKS

Douglas, under the Aircraft Energy Efficiency (ACEE)/Energy Efficient Transport (EET) program, is pursuing advanced technology developments toward fuel savings on near-term DC-10 derivatives. Specific major thrusts are development and wind tunnel evaluation of winglets on the DC-10 Series 10 and Series 30/40 configurations and definition of Long-Duct Nacelle (LDN) configurations that will not be severely penalized by interference drag.

For equivalent drag reduction, winglets yield about one half of the increase in wing root bending moment as wing-tip extensions.

Analysis indicates the possibility of LDN and pylon configurations having an interference drag equal to or better than the current CF6-50C configuration. Wind tunnel tests to confirm this are planned.

REFERENCES

1. Whitcomb, Richard T.: A Design Approach and Selected Wind Tunnel Results at High Subsonic Speeds for Wing-Tip Mounted Winglets. NASA TN D-8260, July 1976.

2. Nordstrom, K. E.; March, A. H.; and Sargisson, D. F.: Conceptual Design Study of Advanced Acoustic Composite Nacelles. NASA CR 132703, July 1975.

3. Goldhammer, M. I.: A Lifting Surface Theory for the Analysis of Nonplanar Lifting Systems. AIAA Paper No. 76-16, January 1976.

4. Kutney, John T.; and Piszkin, Stanley P.: Reduction of Drag Rise on the Convair 990 Airplane. J. Aircraft, Volume 1, No. 1, January 1964.

5. Lynch, F. P.: Summary of Results from DC-8 Ship 201 Long-Duct Pod Flight Development Program. Douglas Aircraft Company, Report No. LB 32668, September 1965.

TABLE 1
WINGLET – MEASURED DRAG REDUCTIONS

REDUCTIONS IN DRAG COEFFICIENT, SHOWN FOR TYPICAL CRUISE LIFT COEFFICIENTS

M	BEST SERIES 10 WINGLET $C_L = 0.45$	SERIES 10 TO 30 TIP EXTENSION $C_L = 0.45$	BEST SERIES 30 WINGLET $C_L = 0.50$
0.82	0.0011	0.0009	0.0009
0.74	0.0010	0.0007	0.0010
0.60	0.0011	0.0007	0.0008

Figure 1.- DC-10 with winglets.

Figure 2.- DC-10 with long-duct nacelles.

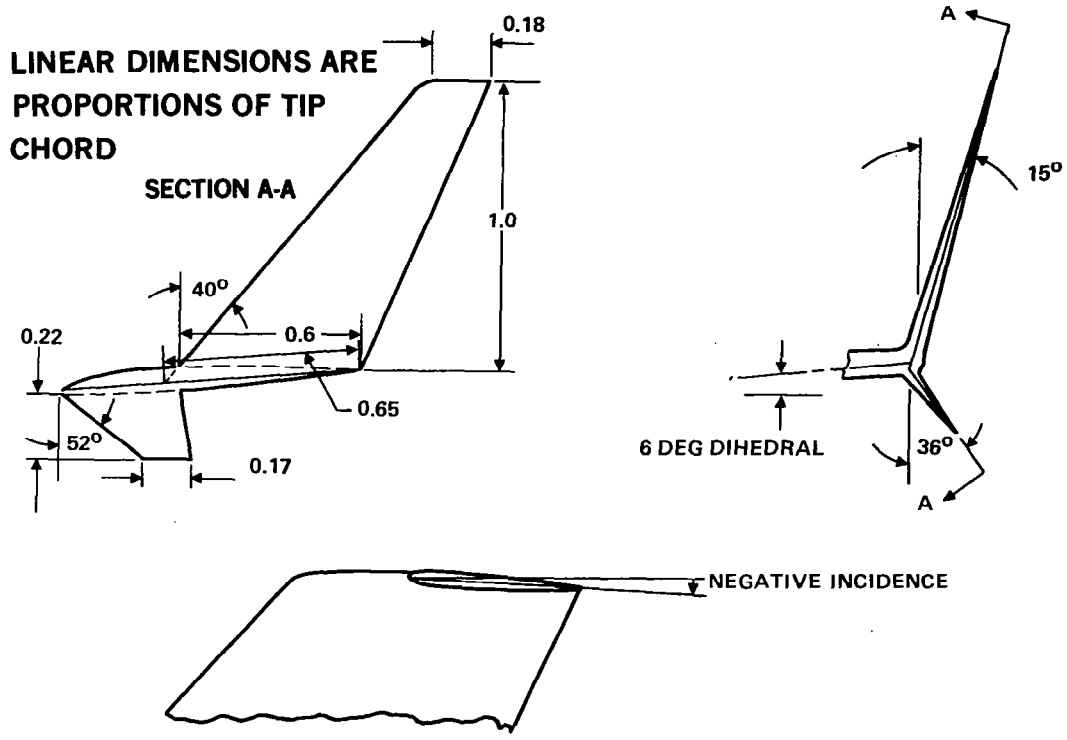

Figure 3.- Winglet - typical geometry.

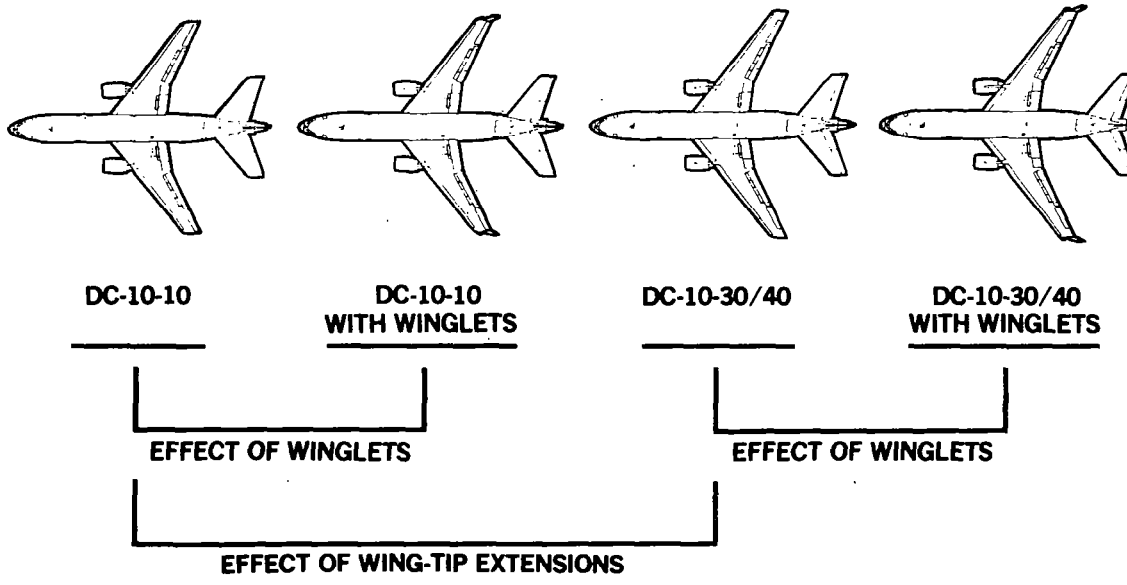

Figure 4.- DC-10 aircraft configurations for evaluation.

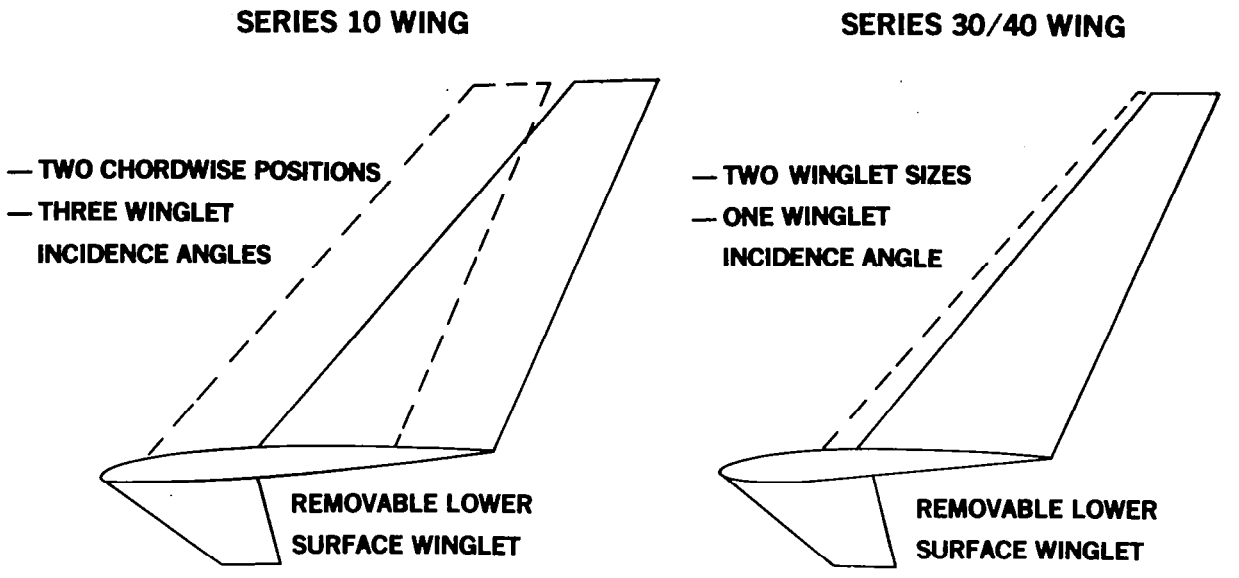

Figure 5.- Winglet test configurations.

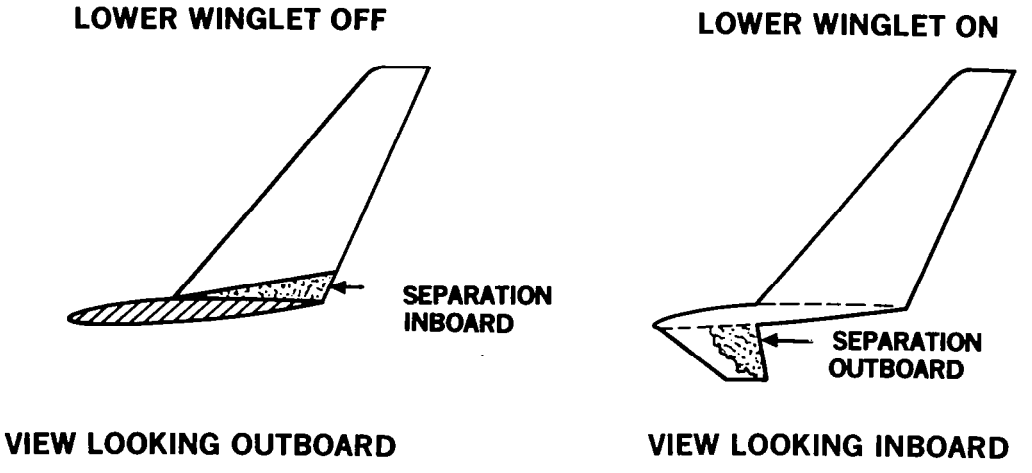

Figure 6.- Initial viscous problems.

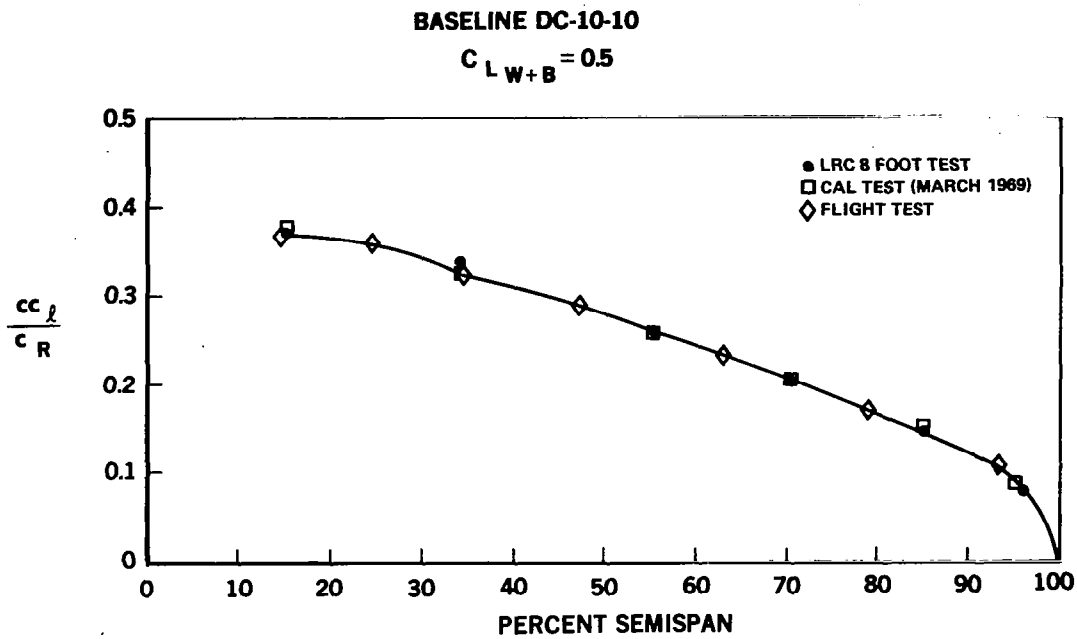

Figure 7.- Wing span loading comparison.

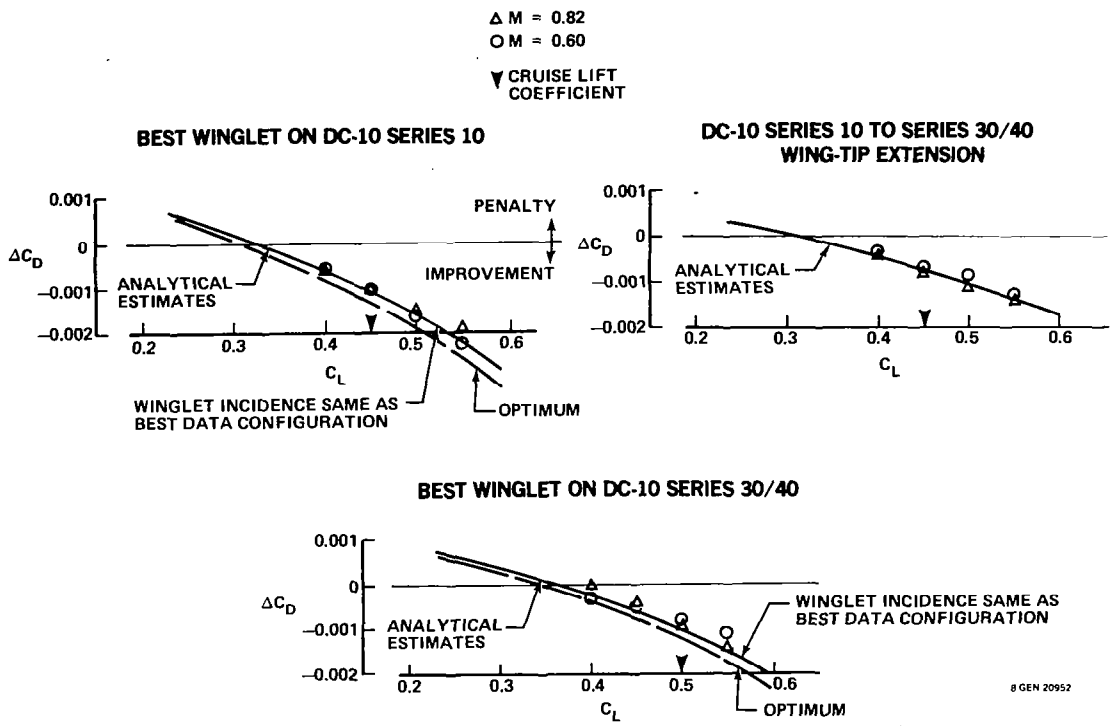

Figure 8.- Incremental cruise drag results.

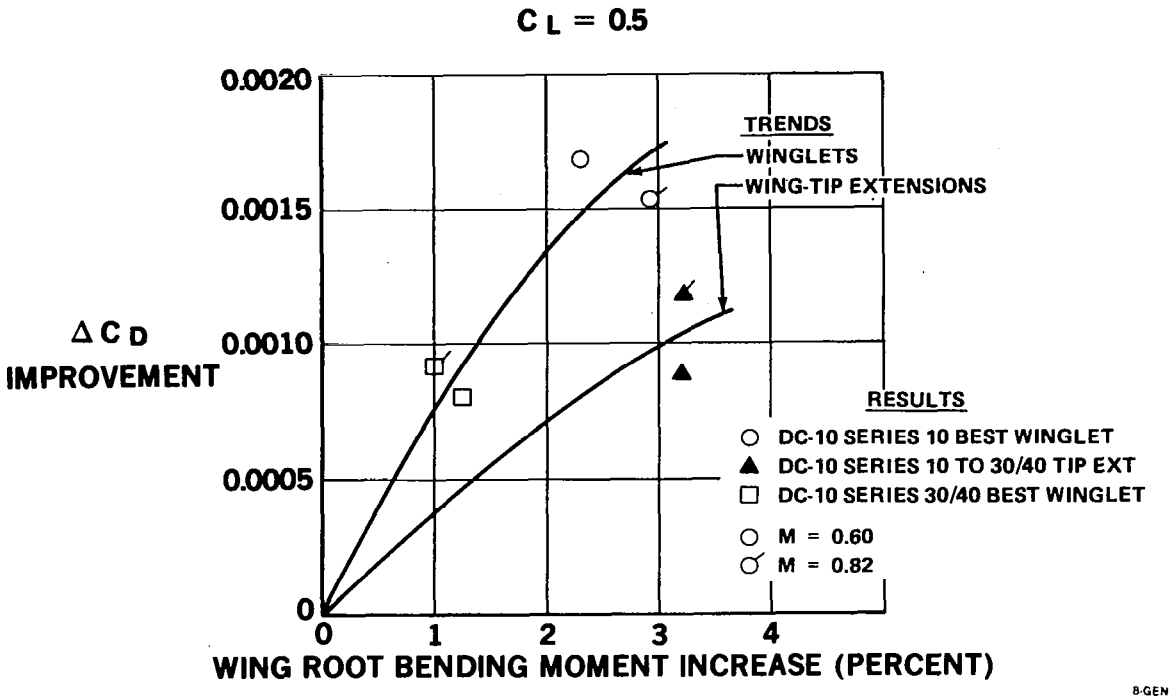

Figure 9.- Measured effects of winglets and a wing tip extension on drag and root bending moment.

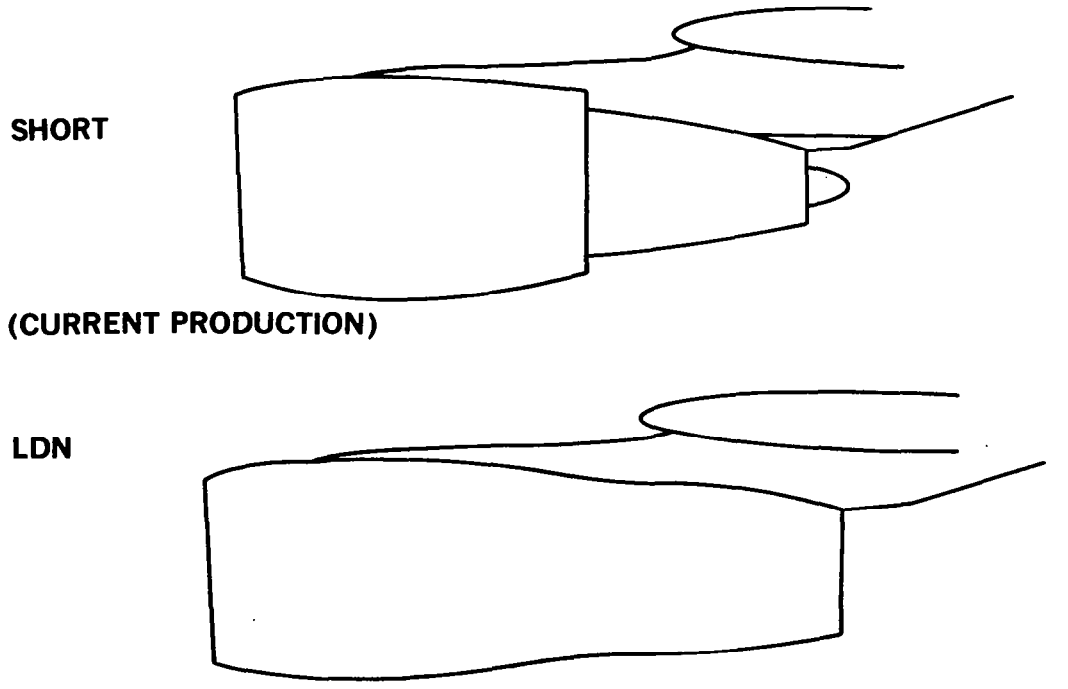

Figure 10.- Comparison of short- and long-duct nacelle shapes.

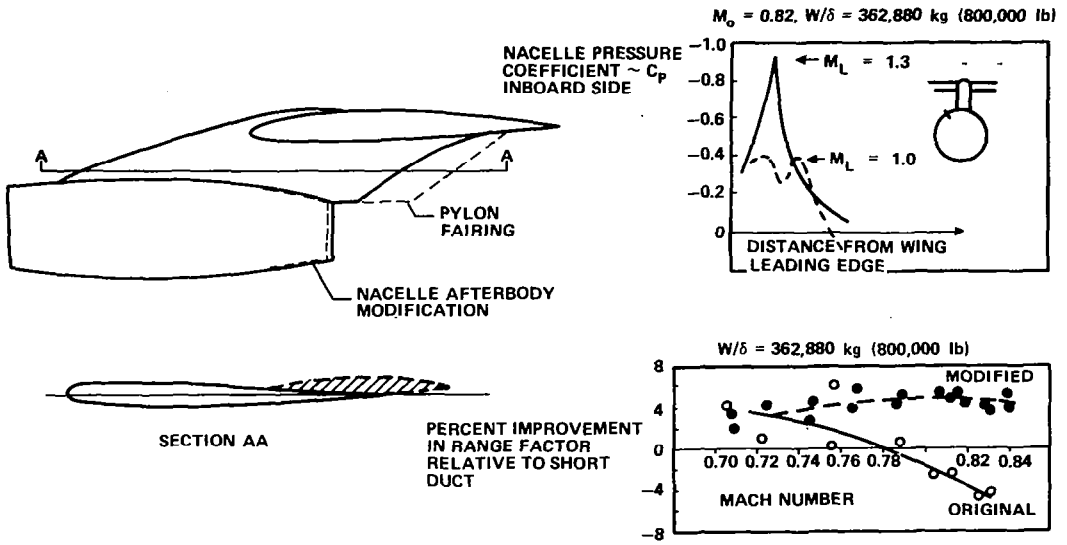

Figure 11.- Prototype DC-8 - effect of nacelle/pylon/wing interference drag.

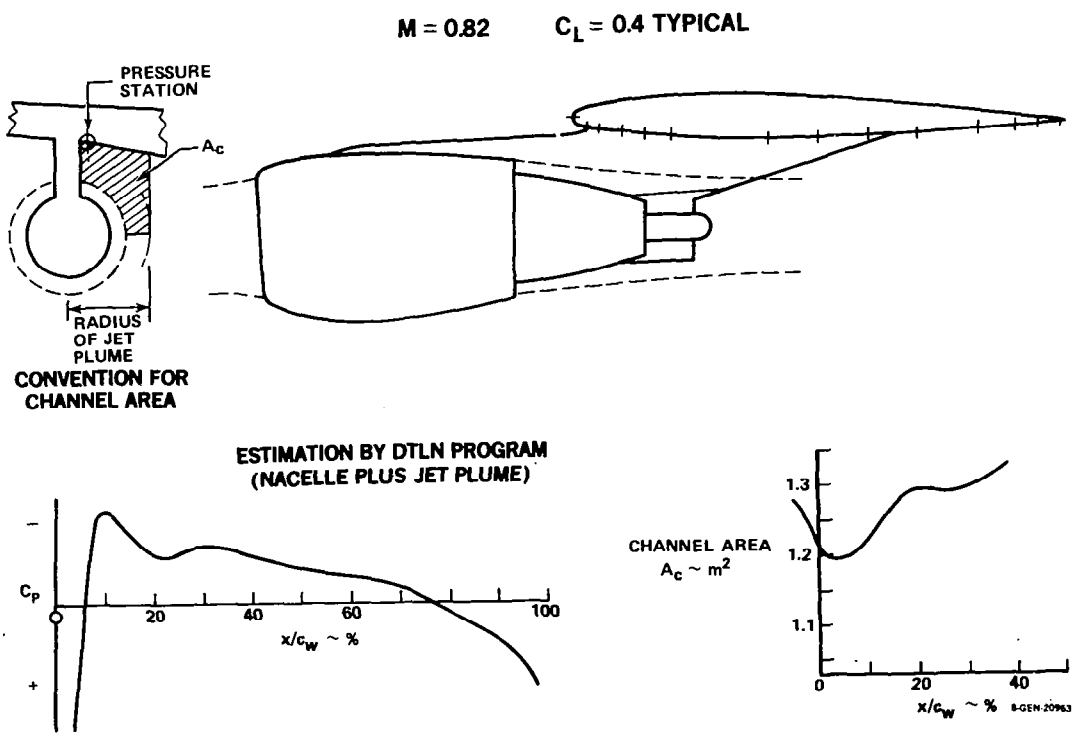

Figure 12.- Flow representations for production nacelle.

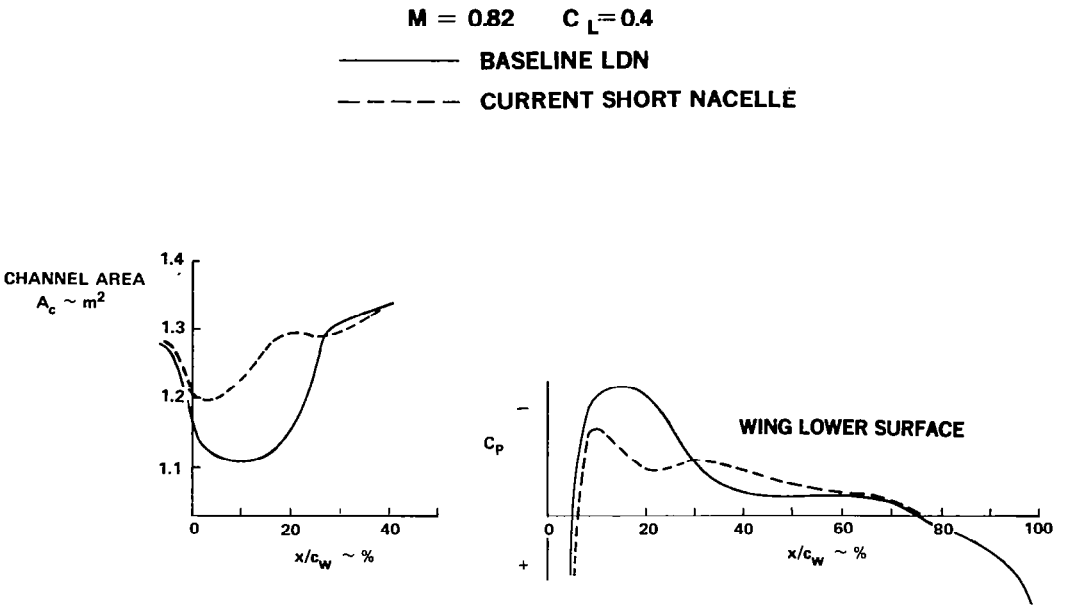

Figure 13.- Flow representations - LDN baseline.

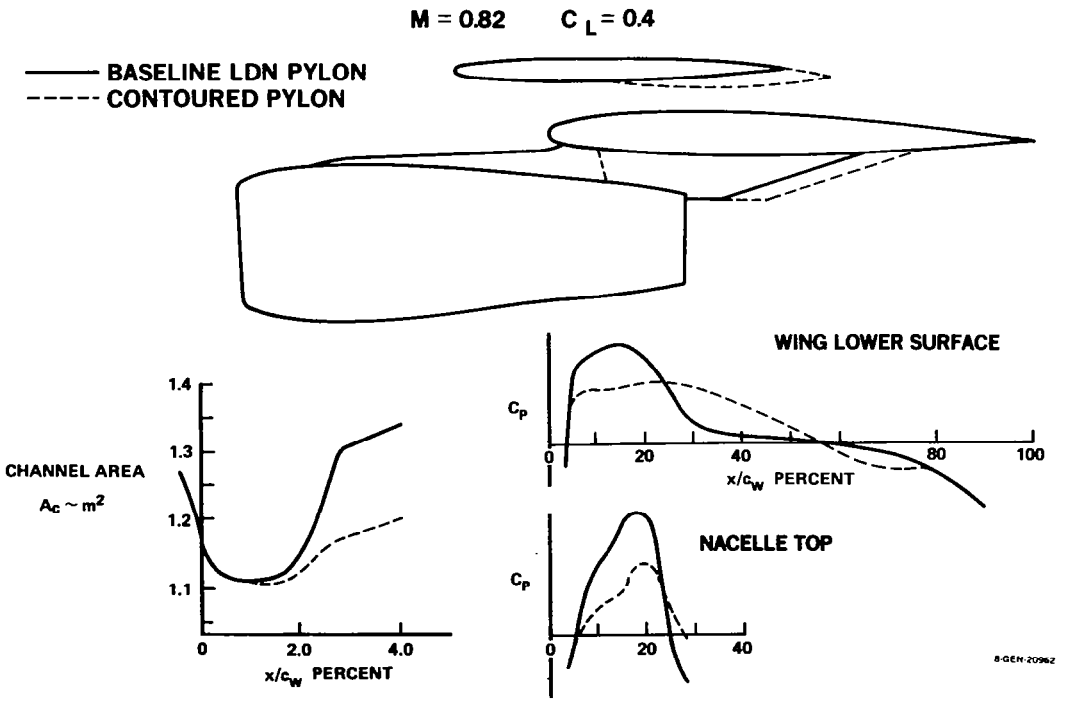

Figure 14.- Flow representations - improved pylon.

APPLICATION OF WINGLETS AND/OR WING TIP EXTENSIONS WITH ACTIVE LOAD CONTROL ON THE BOEING 747 *

Robert L. Allison, Brian R. Perkin and Richard L. Schoenman
Boeing Commercial Airplane Company

SUMMARY

This paper describes and presents early results of a study program to consider the application of wing tip modifications and active control technology to the Boeing 747 airplane for the purpose of improving fuel efficiency. Wing tip extensions, wing tip winglets, and the use of the outboard ailerons for active wing load alleviation are the concepts being considered. Results to date indicate modest performance improvements can be expected. A costs versus benefits approach is being taken to decide which, if any, of the concepts warrant further development and flight test leading to possible incorporation into production airplanes.

INTRODUCTION

As part of the Aircraft Energy Efficiency (ACEE) Energy Efficient Transport (EET) program (refs. 1 and 2), Boeing is investigating applications to the 747 of modified wing tips to improve aerodynamic efficiency, and active ailerons to reduce wing loads. The study configurations are illustrated in figure 1. If determined to be commercially attractive, these concepts, individually or in combination, could have near term application to 747 derivative models. In the long term, the work will provide a technology base for application to new airplane designs. The objective is to improve fuel efficiency.

Improved fuel efficiency can be realized either in terms of fuel saved for fixed range, a range improvement, or an increased payload capability. In the case of wing tip modifications this performance improvement is achieved primarily by increased aerodynamic efficiency in terms of lift over drag (L/D) of the wing. As a rough approximation, the maximum performance benefits accrued from the wing tip modifications would be those resulting from the increase in L/D with no structural weight penalty. The application of Active Control Technology concepts in the form of active wing load alleviation systems can help to eliminate or reduce the structural weight penalties associated with wing tip modifications or with airplane gross weight increases.

This paper presents preliminary estimates of the potential benefits for the 747, a general discussion of the active control concepts, and more specific discussions of the current 747 EET study program. Emphasis is placed on the engineering approach, design requirements and objectives, and constraints on the potential benefits. Only limited results are included.

*Sponsored by NASA under Contract NAS 1-14741

SYMBOLS AND ABBREVIATIONS

Values are given in both SI and U.S. Customary Units. Calculations and measurements were made in U.S. Customary Units.

BM	Bending Moment
BTWT	Boeing Transonic Wind Tunnel
C_L	Lift Coefficient
$\bar{c}$	Mean Aerodynamic Chord
EET	Energy Efficient Transport
FMC	Flutter Mode Control
g	Gravitational Acceleration
GA	Gust Load Alleviation
K	Gain
L/D	Lift to Drag ratio
M	Mach Number
MLC	Maneuver Load Control
OEW	Operating Empty Weight
T	Torsion
UWAL	University of Washington Aeronautical Laboratory
V_e	Equivalent Airspeed
WLA	Wing Load Alleviation
WTE	Wing Tip Extension
WTW	Wing Tip Winglet
δ_A	Aileron Deflection, positive trailing edge down
δ_T	Tab Deflection
η	Wing Spanwise Station, fraction of semispan

Subscripts:

δ_A	Aileron Deflected for MLC
o	Aileron Neutral

POTENTIAL BENEFITS

A thorough assessment of the fuel savings attainable for the study configurations is planned for completion later in the 747 EET program. However, to bring this approach into perspective from the outset, it is worthwhile to determine on a gross basis the approximate magnitude of performance benefits attainable with the concepts being considered.

Using the 747-200B as an example, consider that the wing box weight, excluding the landing gear support beam, represents about 18 percent of the Operating Empty Weight (OEW) of the airplane. Preliminary estimates indicate that a 5 percent reduction in wing box weight is a reasonable goal for a wing load alleviation system utilizing active outboard ailerons. This represents approximately a 1 percent reduction in OEW which can be translated into reduced trip fuel or into increased range or payload. This estimate pertains to the basic wing without the addition of tip extensions or winglets.

Wing load alleviation is more likely to be applied to an existing airplane either to increase the allowable takeoff gross weight or to minimize the additional structural weight associated with wing tip modifications. Consequently, let us now take the example of an improvement which is to be made by increasing the aerodynamic efficiency of the wing by means of wing tip extensions and/or winglets. Assuming for the moment that this could be done with no increase in structural weight, the improvement in L/D could be translated directly into either reduced fuel burned or increased range. Preliminary estimates indicate that the improvements in L/D attainable from wing tip modifications are on the order of 2 to 4 percent for practical configurations. These translate approximately into an increase in range of 75-150 nautical miles assuming maximum takeoff gross weight, or a trip fuel reduction of 2 to 4 percent for fixed range/payload. The trip fuel reductions represent fuel cost savings, based on current fuel prices, in the order of $100,000 to $200,000 per year per airplane for typical 747 operations.

The previous example provides a gross estimate of what the potential performance benefits could be for the 747, assuming the wing load alleviation system allows the tip extensions or winglets to be installed with no change in airplane OEW. However, some increase in airplane OEW may be required, in which case the trip fuel/range/payload benefits would be reduced. There are several limitations on applying the concepts to existing airplanes, some of which are discussed in this paper, which would be less constraining for a new design.

WING LOAD ALLEVIATION CONCEPTS

Wing Load Alleviation concepts can be broken down into two categories, 1) static elastic load alleviation, and 2) structural dynamic load alleviation. The static elastic concepts are concerned with loads due primarily to angle of attack changes resulting from maneuvers or gusts, independent of structural

dynamic effects. The "structural dynamic" concepts are concerned with increasing structural mode damping.

Within these two broad categories, a variety of wing load alleviation systems have been discussed in the literature (e.g., reference 3), with potential benefits indicated in the areas of maneuver and gust load reduction, fatigue, flutter suppression, and ride comfort. The 747 EET program is concentrating on three areas: maneuver load control, gust load alleviation, and flutter mode control defined as follows:

(1) Maneuver Load Control (MLC) is any method of redistributing wing lift during maneuvering flight. Incremental stresses may be reduced by deflecting wing control surfaces symmetrically during a maneuver in a manner that shifts the wing center of lift inboard, thus reducing wing bending moments.

(2) Gust Load Alleviation (GA) is any technique for reducing airframe loads resulting from gust disturbances. It encompasses control of rigid body and/or structural dynamic components of the airplane gust response.

(3) Flutter Mode Control (FMC) is any technique for actively damping flutter modes using aerodynamic control surfaces. It provides potential for weight savings and/or extending flutter placards.

The basic wing box structure of all present Boeing commercial transport aircraft is predominantly sized by maneuver loads. Additional structural material is included where necessary to satisfy gust, flutter and fatigue requirements. The existing 747 wing does not contain appreciable structural material added specifically to meet gust and flutter requirements. However, the situation may be modified by the addition of tip extensions and/or winglets, or by the reduction of strength material in the basic wing if resized to take credit for the MLC and GA systems.

Figure 2 shows a plot of wing structural box weight per unit span as a function of distance along the wing, and shows a wing which is typically designed by maneuver loads. In this particular case, it can be seen that a reduction in the magnitude of the maneuver loads by the use of a maneuver load alleviation system could result in a reduced requirement for structure. The degree to which the implementation of winglets and/or wing tip extensions can be incorporated with minimum structural impact is determined by the reduction in maneuver loads by such a system.

Figure 3 shows a wing which is not only maneuver load critical but is also gust and flutter critical. It can be concluded that for this wing a maneuver load control system would not allow any wing weight reductions since flutter clearance and gust loads requirements are predominant. In this example, a wing load alleviation system utilizing maneuver load control, gust load alleviation and flutter mode control would have to be utilized in order to attain reductions in structural weight.

An understanding of the application of active ailerons to static elastic load alleviation requires consideration of the aerodynamic load distribution over the span of the wing, and the tradeoffs between aerodynamic performance and structural requirements. Generally speaking, maximum lift/drag ratio is accomplished when the load distribution on the wing is near elliptical. However, this is not necessarily the best lift distribution for cruise performance, since wing structural weight also is a factor. The 747 lift distribution tends to be more "triangular" (i.e., lightly loaded outboard) than "elliptical" in order to achieve a reasonable compromise between L/D and structural weight so as to maximize overall performance.

While this lift distribution improves cruise performance, it does not minimize the design loads on the wing which, for the current 747, are determined primarily by a 2.5 g maneuver requirement. To reduce the corresponding wing bending moment, it is possible to modify the lift distribution somewhat between one g cruise and maneuvering flight conditions so as to shift the center of loading farther inboard for maneuvers than for cruise. This already takes place to a certain extent in existing sweptback wings due to aeroelastic effects which tend to twist the tips in a washout direction in maneuvers. Further inboard shifting of the lift distribution in maneuvers can be accomplished by active controls which unload the outboard portions of the wing.

The use of active outboard ailerons to modify the load distribution along the span of the 747 wing is illustrated in figure 4. The solid line shows the lift distribution with ailerons neutral in a steady state 2.5 g pullup. The dashed line shows how the wing loads for the same maneuver are shifted inboard by symmetrically deflecting the ailerons, trailing edge up. Shifting the lift inboard on a sweptback wing also introduces a nose-up pitching moment increment which reduces the downward tail load required for pitch trim in the maneuver. This effect is somewhat analagous to balancing the airplane to a more aft c.g., and requires pitch axis augmentation to maintain the desired stability and control characteristics. Since the direction of the tail lift is opposite that of the wing, reduction of the tail lift allows the 2.5 g limit design maneuver load factor to be achieved with a lower wing lift. It is the combined effect of the inboard shift of the lift distribution and the reduced overall wing lift that reduces the wing bending moments for the structural design maneuver cases. While other surfaces on the wing may be found to be effective in reducing these structural loads, the 747 EET Program is currently considering the use of outboard ailerons only.

A factor to be considered when using ailerons as load alleviation devices is the effectiveness of the surface at high speeds. When used as roll control devices at high dynamic pressure it is possible that a deflection of the outboard aileron will cause the wing to twist sufficiently to reverse the total rolling moment about the airplane centerline from that normally experienced. The speed at which this occurs is known as the aileron roll reversal speed. Because of this phenomenon, many commercial transport airplanes, including the 747, use the inboard aileron and spoilers for roll control at high speed. The outboard aileron is locked out at high speed and is used only for roll control with flaps down. Airplanes which use outboard ailerons for roll control at high speed require additional outer wing torsional material compared to a similar wing with an aileron lockout.

Now consider the surfaces used symmetrically as load relieving devices. Figure 5 shows the spanwise variation of the ratio of wing bending moment with ailerons deflected divided by the wing bending moment with ailerons neutral. The data are representative of a plain aileron at speeds above the aileron roll reversal speed. Results are shown for both a 2.5 g balanced maneuver condition and a constant angle of attack condition. In the 2.5 g balanced maneuver the airplane has been retrimmed after application of the ailerons for load alleviation. For the constant angle of attack condition the airplane has not been retrimmed after aileron application. Aileron roll reversal can be inferred from the constant angle of attack data which show that bending moment is increased at the wing root, although bending moment reductions are still apparent over the rest of the wing. The increased root moments shown in the constant angle of attack data (which give some insight into the effect of activating the aileron in response to a high frequency gust) occur only in an area which is not gust load critical for the 747. The 2.5 g balanced maneuver data show substantial bending moment reduction along the entire wing. Thus an outboard aileron which reverses for roll control can still be used effectively for wing load alleviation when deflected symmetrically.

Shown in figure 6 is a plot of the ratio of wing torsion with ailerons deflected divided by the wing torsion with ailerons neutral. The wing torsion is increased along most of the span. Use of a balance tab on the aileron can reduce this effect and reduce the torsional material needed in the wing for these increased loads. A wing designed with an outboard aileron for high speed roll control will still suffer increased torsion loads when using the surface for maneuver load control because increased control surface deflections are required for load alleviation. To minimize the increased torsion loading it may be advisable to reduce the aileron deflections used for maneuver load control at high speeds by making the available aileron angle a function of airplane speed.

APPLICATION OF ACTIVE AILERONS AND MODIFIED WING TIPS TO THE BOEING 747

Previous discussions have been somewhat general in nature to give some understanding of the phenomena involved. The following discussions will be more specific and relate to those studies which are presently under contract by Boeing from the NASA. Emphasis will be placed on the study approach, design requirements and objectives, and factors constraining the potential performance benefits. Some early results of general interest are also discussed.

747 EET Program Overview

The current 747 EET study program consists of engineering analyses and wind tunnel testing to examine the benefits of applying winglets and/or wing tip extensions to the 747 airplane to improve L/D, and the use of wing load alleviation systems to minimize the structural weight penalties associated with carrying these additional surfaces.

The 747-200B has been selected as the baseline model for the current effort. Pertinent characteristics of this airplane are shown in table I. The specific modifications being considered (figure 1) are as follows:

- Wing tip extensions (WTE)
- Wing tip winglets (WTW)
- Wing load alleviation (WLA) using active outboard ailerons
- A final configuration incorporating WTE and/or WTW with WLA.

The study sequence and general scope of activites are indicated in fig. 7.

The WTE, WTW, and WLA concepts are first being analyzed and evaluated separately so that the costs and benefits associated with each can be identified for reference in selecting the final configuration. Following this selection, the remainder of the analyses and evaluations, leading to a go/no-go recommendation concerning further development and flight test, will be for the final configuration.

One high speed wind tunnel force and pressure test has been conducted, and another is planned, to support development of the winglet and WLA control surface configurations, and to obtain aerodynamic performance, stability and control, and loads data for use in analyses of the concepts. Wind tunnel data from a prior Boeing test of a 1.83 meter (6 foot) tip extension are being used as a basis for the WTE studies. A flutter test is being conducted to support flutter analyses of the winglet configurations.

Study Approach

In evaluating the potential of the concepts for possible fleet implementation, a comprehensive costs versus benefits approach is being taken with some of the more significant airline operational and FAA certification concerns being addressed in addition to the fuel savings and implementation costs. For example, the potential impact of wing span increases on flight line operations and maintenance is being considered, as is the effect of additional systems on dispatch reliability and maintenance costs.

The results of aeroelastic and structural resizing analyses are being included in estimating the performance benefits of the concepts; i.e., the effects of changes in wing twist and the weight changes associated with required

structural modifications will be accounted for in the performance evaluation. By identifying drag and weight increments for the concepts individually and in combination, the relative effectiveness of tip extensions versus winglets can be compared and the weight reduction provided through WLA identified.

In line with this approach, the WLA system functions have been separated into three categories with objectives for each function as follows:

WLA FUNCTION	OBJECTIVE
Maneuver Load Control (MLC)	Bending moment reduction in symmetric maneuvers
Gust Alleviation (GA)	Gust load reduction. Studies of this function will include consideration of: - aileron response to low frequency gusts (e.g., MLC may provide some gust load relief) - damping of first wing bending mode - airplane pitch response
Flutter Mode Control (FMC)	Flutter suppression at speeds above dive speed

The performance benefits and costs (including the effects on system reliability) associated with each of the functions will be considered in selecting the final WLA configuration.

While implementation costs are to be determined for the case of a production line installation for future deliveries, the feasibility of retrofit into existing fleet aircraft will also be explored. Regarding FAA certification, there is some precedent for taking credit for active controls when establishing design loads (e.g., reduction of fin loads with yaw damper operational). The impact on the basic airplane certification of the particular 747 modifications being studied will be considered in the overall assessment.

Design Requirements and Objectives

General - The general design objective is to develop a configuration that will improve fuel efficiency for routine airline operations, will be cost-effective for fleet implementation, and will meet the general design requirements that there shall be no significant adverse impact on safety, handling qualities, or dispatch reliability. Where conflicts arise between the performance/cost objectives and the safety/handling qualities/reliability requirements, priority will be given to the latter.

The added implementation or operational costs, if any, associated with meeting these requirements will be reflected in the cost versus benefit compar-

isons. The intent is to provide a reasonably true indication of the cost savings actually attributable to the configuration modifications, as opposed to apparent performance benefits achieved at the expense of less tangible factors. As an example, part of the wing load alleviation provided by active ailerons in a pullup maneuver results from a reduced tail load, which, in turn, resulted from a nose-up pitching moment increment introduced by the ailerons. Part of the apparent cost savings accruing from the reduced wing load will be offset by the cost of the pitch control augmentation required to retain existing stick force per g characteristics.

Aerodynamic Performance - The aerodynamic performance objective is to develop a configuration that will provide enough performance improvements to warrant fleet installation. There is no single go/no-go criterion which could be applied to all airline situations to determine if a modification is economically attractive. For example, a configuration might not be cost-effective on the basis of trip fuel cost savings, but could nevertheless be quite beneficial on a particular route if it allowed a larger payload. These and other factors will be considered by Boeing in recommending whether or not to proceed to flight test. For purposes of reporting study results, performance for the various study configurations is being compared on the basis of trip fuel savings for fixed payload/range, with no increase in the maximum takeoff weight.

Buffet - The effect of MLC control surface deflection on buffet boundaries must be considered when developing WLA concepts. The outboard aileron reduces lift on the outboard section of the wing, thereby forcing the inboard sections to fly at higher angle of attack for a given wing lift. However, due to the reduced down load on the tail (resulting from the nose-up pitching moment induced by the ailerons) less wing lift is required for a given load factor. Conditions checked to date show that the body (wing root) angle of attack for a given load factor is reduced when the outboard aileron is used for MLC. Hence, a more complete examination, including the effects of changes in section angle of attack due to differences in the aeroelastic twist distribution, must be conducted before reaching a conclusion.

Stability and Control - Wing tip modifications and/or the use of existing control surfaces for wing load alleviation could affect both the longitudinal and lateral/directional stability and control characteristics of the airplane. The requirement being used for the 747 EET is that there should be no significant change in handling qualities or automatic flight control system performance relative to the basic airplane. In general, all of the requirements considered in design and certification of the basic airplane must be reviewed.

There is nothing unique about stability and control analyses for wing tip modifications, although the low speed characteristics of winglets are not well understood at this time. In the case of the WLA system installation, a lateral control surface (outboard aileron) is being used for purposes other than lateral control, and in flight regimes (high speed) where it is locked out at present.

Since aileron deflections introduce pitching moments, the longitudinal control power and stability characteristics are affected. Consequently, pitch augmentation inputs to the elevators have been included in the WLA system configuration. Requirements concerning low speed roll control power and aileron hinge moments are of considerable importance in selecting an aileron tab configuration. The low speed control power requirements are also a prime factor in determining to what extent the MLC system can be employed during flaps down flight.

Structures - The structural criteria for design of the 747 EET are the same as used for all 747 models. These criteria meet or exceed the requirements of FAR Part 25. Included are maneuver and gust criteria for use in structural analysis of aircraft with automatic flight control systems. These criteria account for both normal and failed operations of the flight control systems.

Application of these criteria is considered sufficient for certification of an airplane incorporating a wing load alleviation system for both normal and failed operations of the system. Three operational modes of the wing load alleviation system must be considered: normal operations, passive failures and active failures. It is in the area of failures that most consideration has to be given. Failures can involve system shutdown, jams, hardovers and oscillatory failures. Criteria for the maneuver load control system involve degree of redundancy of the system and whether airplane dispatch can be allowed with a system failed, or if gross weight placards have to be applied. Oscillatory and hardover failures are covered by criteria for automatic flight control systems.

Consideration of the impact on airplane flutter stability due to a wing load alleviation system is necessary. Both the nominal wing load alleviation system and likely failure cases must be considered. The wing load alleviation system must be designed such that there is satisfactory flutter mode damping within the flight envelope with the system on or off or in a failure mode. If a flutter mode suppression system is developed for the 747 EET a basic requirement will be that it will only be used to increase stability of flutter modes above design dive speed to achieve a 20 percent margin of safety. That is, the airplane shall be flutter free to 1.2 times the dive speed with the system active, and it shall be flutter free to the design dive speed with a system failure or malfunction.

The effect of the wing load alleviation system on the fatigue requirements will be evaluated. Fatigue analysis methods will be the same as used on current 747 models but the loads used in the fatigue analysis will be revised to reflect the active control effects.

Selected Results

Wing Tip Modifications - A ground rule for the study which significantly impacts the performance benefits attainable from the wing tip modifications is that the

existing baseline wing jig shape (i.e., the twist distribution of the wing during manufacture) and airfoil sections are to be retained. The aeroelastic twist distribution at cruise, selected to optimize performance for the existing wing, will be modified by the additional loads imposed by the tip extension. As a result, the net performance gains will be less than if the jig twist were reoptimized for the increased span configuration. Figures 8 and 9 illustrate this effect, which is an important difference between studies of tip extensions on existing wings as contrasted with a new wing of increased span and aspect ratio. The "existing structure" curve assumes no additional structural material has been added to accommodate the increased loads. The "resized structure" data points reflect the effects of the additional stiffness resulting when the wing structure was resized without taking credit for wing load alleviation. The added structural weight for the resized structure does not affect the L/D estimate, but would have an adverse effect on performance in terms of range or trip fuel.

Similar effects of non-optimum twist distribution are expected for the winglets. In addition, the parametric trend study of reference 4, based on the work of Dr. Whitcomb (reference 5), points out that greater benefits can be achieved from winglets if the wing/winglet combination is designed as a unit from the start. The 747 tip area is lightly loaded, which tends to limit the effectiveness of the winglet.

A number of winglet configurations had been wind tunnel tested on the 747 prior to the 747 EET program. The geometry of the best of these, designated "Z4", is compared in figure 10 to the geometry of the first winglet tested in the current program, designated "Z9". Chordwise sections illustrating the Z9 winglet camber are shown in figure 11. The geometry changes, relative to the Z4 winglet, were intended to eliminate the reductions in performance benefits due to compressibility effects which had been noted for prior winglets in the cruise Mach number regime.

The cant angle and span for the new winglet (Z9), were the same as for the Z4 but the planforms are different (figure 10). The intent was to spread the load over a longer chord so as to reduce the velocities on the winglet lifting surface, which would be favorable in reducing the Mach number penalties. However, the test data showed excessive forward velocities on both Z4 and Z9.

The first winglet (Z9) test results exhibited a reduction in performance with Mach number similar to the earlier Z4 winglet. Winglet Z9 appeared to be over-cambered near the leading edge in the wing junction region. Winglet Z10 was the result of an attempt to reduce some of this camber (figure 11), and produced a small performance gain at the cruise Mach number.

Wind tunnel test results, expressed in terms of full scale drag improvement, are compared in figure 12. The Mach number effects are clearly evident as well as a generally lower level of benefits with the Z9 and Z10 winglets. Consequently, the winglet design and test effort under the current program is being expanded somewhat to consider additional configurations.

Wing Load Alleviation - The control surfaces currently being considered for the three wing load alleviation functions (MLC, GA, FMC) are indicated in figure 13. The outboard aileron, the primary WLA control surface, is being used for maneuver and gust load alleviation, and possibly also for flutter suppression. The flutter mode control concept and the associated control surfaces have not yet been established. The surfaces indicated for FMC in figure 13 are being considered as potential candidates. The separate FMC surface (aileron segment) would be used only if the existing ailerons were ineffective due, for example, to inadequate resolution or frequency response. The lower rudder is indicated as a candidate because it might be effective in suppressing anti-symmetric flutter modes.

A simplified block diagram depicting the control laws for the maneuver load control (MLC) and gust alleviation (GA) systems is presented in figure 14. The low pass filter in the MLC system has unity steady state gain, whereas the band pass filter for the GA system has zero steady state gain.

The center of gravity acceleration feedback in the MLC control law provides load alleviation in maneuvers and in low frequency (below airplane short period) gusts. The wing acceleration feedback in the GA control law provides damping of the first wing bending vibrational mode, while the pitch rate feedback attenuates the airplane pitch response to gusts. Evaluations of the capability of the systems to alleviate maneuver and gust loads without exciting flutter modes are in progress. Results to date are encouraging.

Aileron Configuration Selection - Trade studies of various aileron/tab configurations ranging from a plain (untabbed) aileron to a 30 percent chord full span balance tab are being conducted. One of the considerations, illustrated in figures 15 and 16, is that the plain aileron is more effective in reducing bending moment but results in higher torsion levels than ailerons with balance tabs. The data shown reflect aileron lift and section pitching moment levels as estimated prior to the recently completed 747 EET wind tunnel testing. To account for the combined effects of bending moment and torsion, preliminary wing resizing studies using the wind tunnel aileron/tab aerodynamic data are in progress. Results to date have shown that the plain aileron is a possible candidate. Further evaluation is necessary before selecting the aileron/tab geometry for the 747 EET final configuration.

CONCLUDING REMARKS

The NASA/Boeing 747 EET program was initiated during May of 1977. Efforts to date have been directed principally at aerodynamic, structural, and WLA system configuration development. Detailed performance estimates and cost versus benefit evaluations are planned for later in the program. However, preliminary estimates indicate that wing tip modifications combined with wing

load alleviation have the potential for providing trip fuel savings on the order of 2 to 4 percent, which is significant on a fleet-wide basis.

As the program progresses there will be an improved understanding of the benefits to be accrued when wing tip extensions and winglets are being applied to an existing airplane, and how these benefits may be different when these devices are being considered for a new airplane design. Criteria being developed during this study relating to structural design and flight control systems will be valuable for future and new advanced airplane designs.

The current program is directed toward determining the feasibility, costs and benefits of the application of wing tip extensions or winglets to the 747 airplane. At the conclusion of this study, a recommendation may be made to proceed into a flight test evaluation.

REFERENCES

1. Klineburg, John M., "Technology for Aircraft Energy Efficiency", paper presented at ASCE International Air Transportation Conference, Washington, D.C., April 4-6, 1977.

2. Leonard, Robert W., and Wagner, Richard D., "Airframe Technology for Energy Efficient Transport Aircraft", presented at SAE 1976 Airplane Engineering and Manufacturing Meeting, San Diego, California, November 29-December 2, 1976; recorded in SAE 1976 Transactions Section 4, Pages 2916-2931, September 23, 1977.

3. The Boeing Company Wichita Division, "B-52 CCV Program Summary", Technical Report AFFDL-TR-74-92, Volume I, March 1975.

4. Heyson, Harry H., et.al., "Theoretical Parametric Study of the Relative Advantages of Winglets and Wing-Tip Extensions", NASA TM X-74003, January, 1977.

5. Whitcomb, Richard T., "A Design Approach and Selected Wind-Tunnel Results at High Subsonic Speeds for Wing-Tip Mounted Winglets", NASA TN D-8260, July, 1976.

TABLE I

CHARACTERISTICS OF 747-200B BASELINE
MODEL FOR 747 EET STUDY PROGRAM*

Maximum Taxi Weight	3,580,000 N (808,000 lb.)
Operating Empty Weight	1,625,000 N (336,000 lb.)
Maximum Payload	712,000 N (160,500 lb.)
Fuel Capacity	1,530,000 N (344,480 lb.)
Wing Span	59.6 m (195.7 ft.)
Wing Aspect Ratio	6.96
Wing Sweep (1/4 Chord)	37.5°

*Note: JT9D-7FW Engines

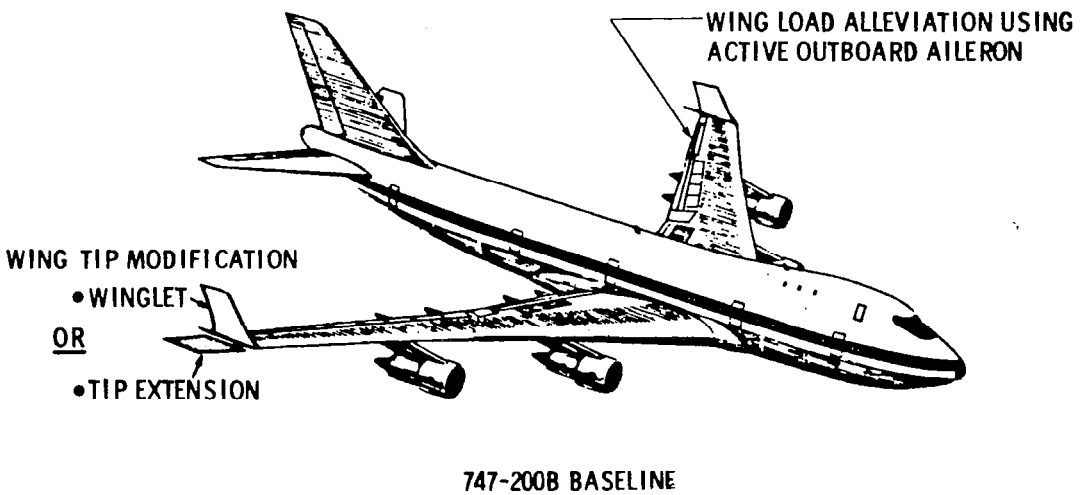

Figure 1.- 747 EET study configurations.

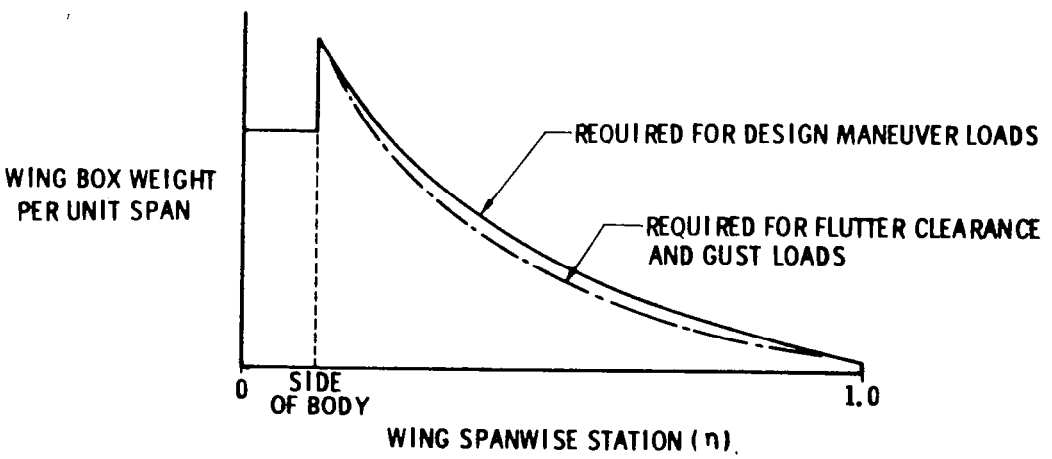

Figure 2.- Typical wing structural box weight distribution for maneuver critical wing.

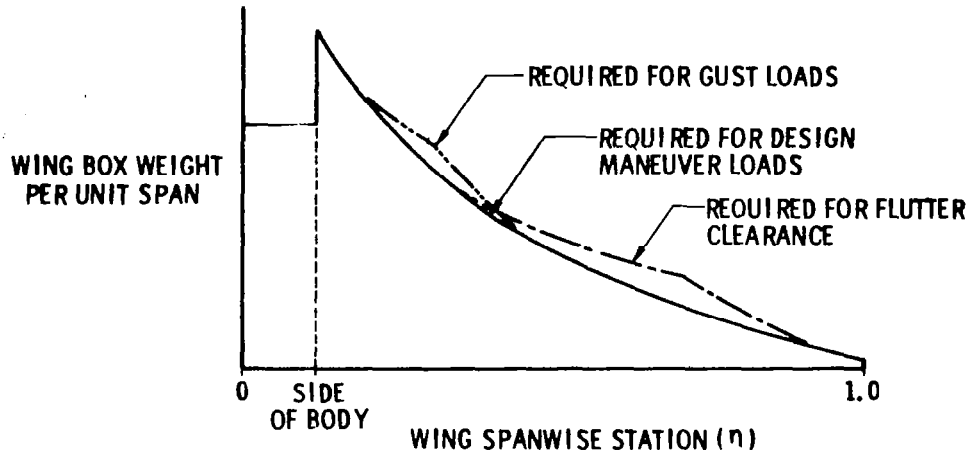

Figure 3.- Typical wing structural box weight distributions for flutter and gust critical wing.

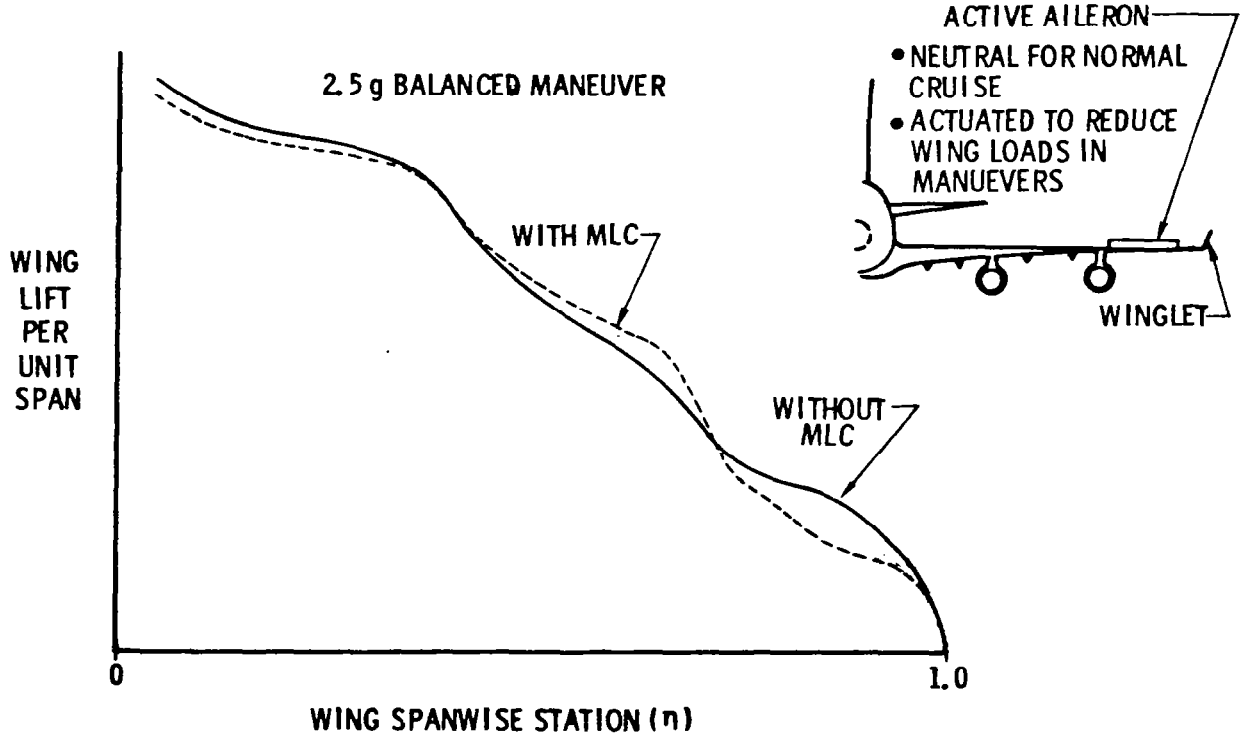

Figure 4.- Maneuver load control concept.

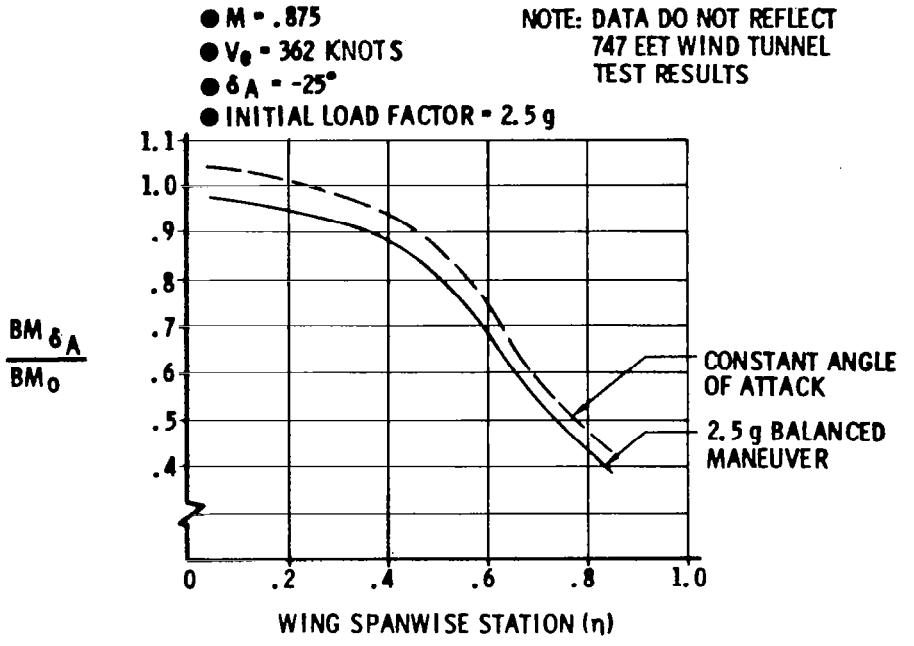

Figure 5.- Effect of plain aileron on wing moment.

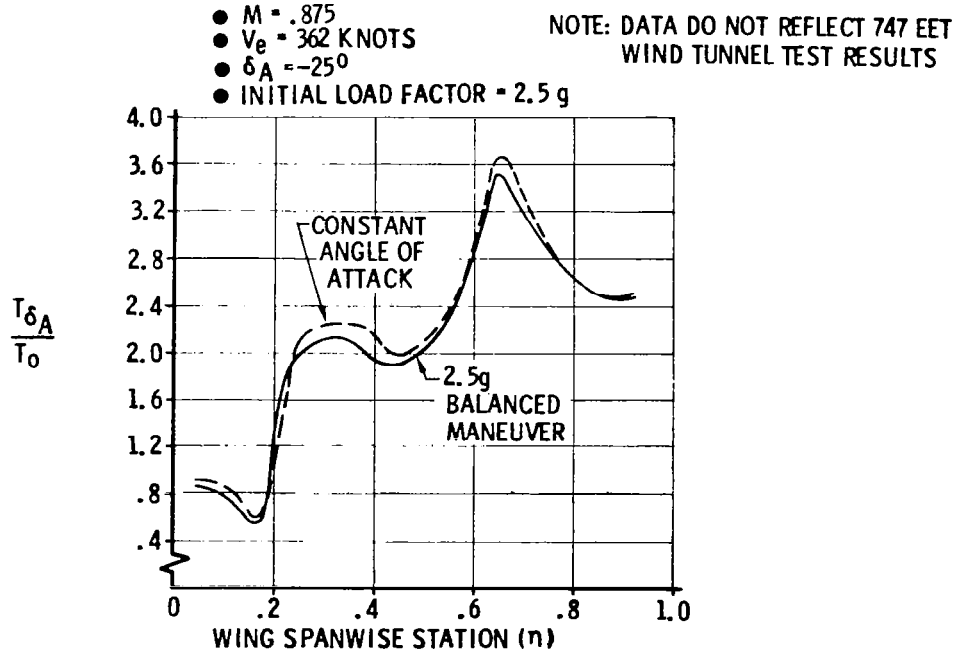

Figure 6.- Effect of plain aileron on wing torsion.

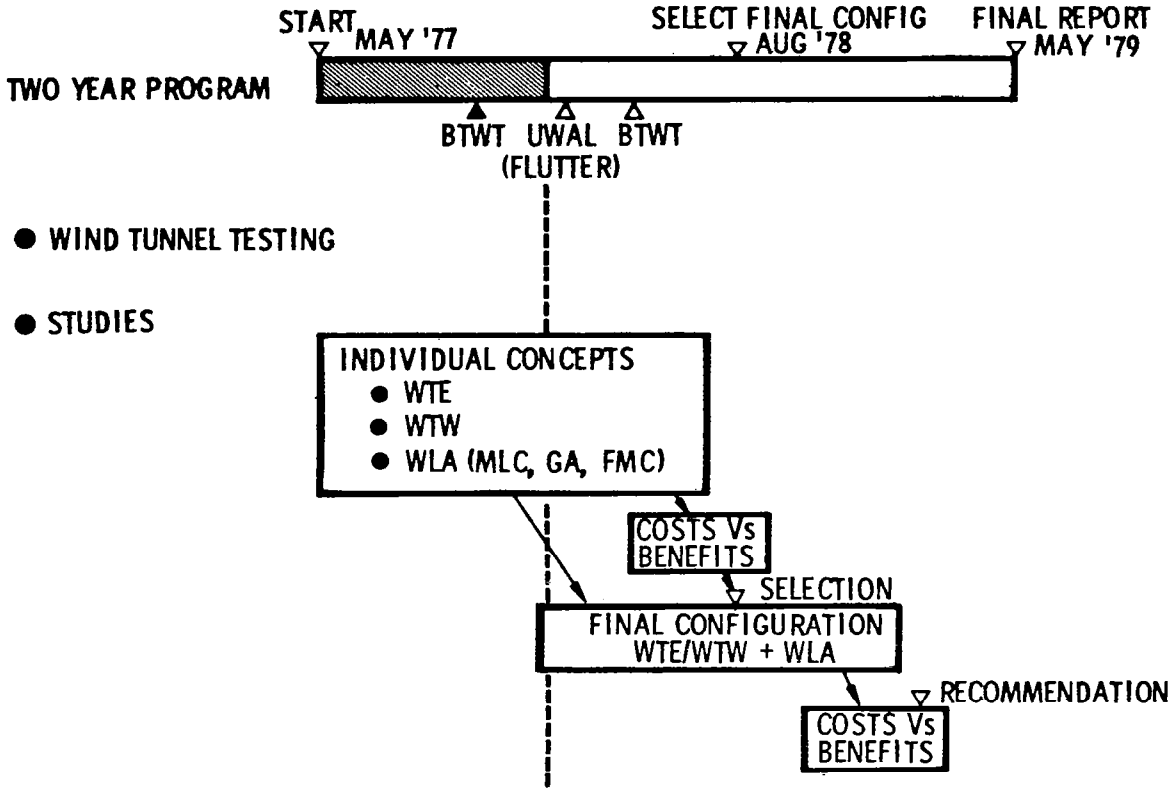

Figure 7.- 747 EET program outline.

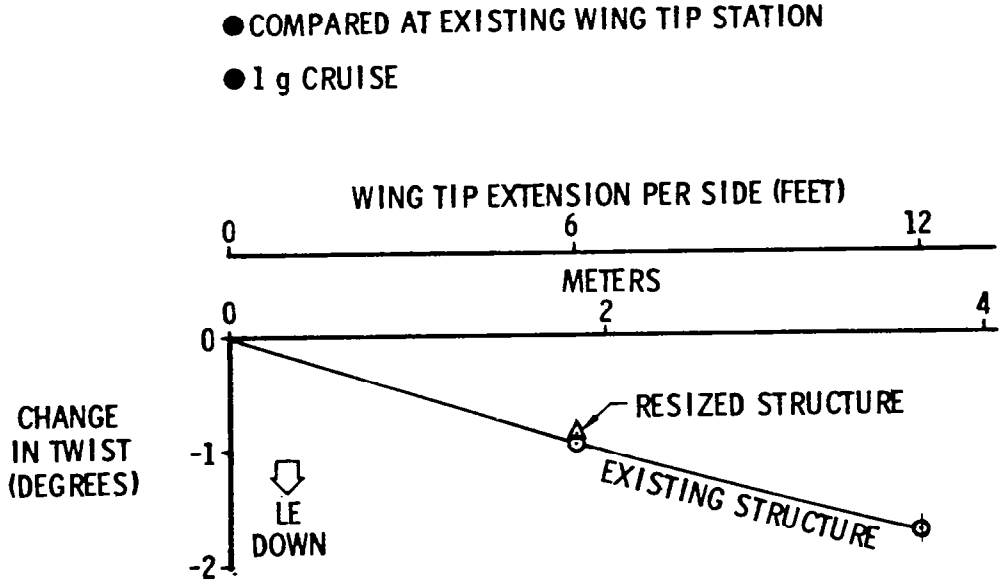

Figure 8.- Effect of tip extensions on aeroelastic twist.

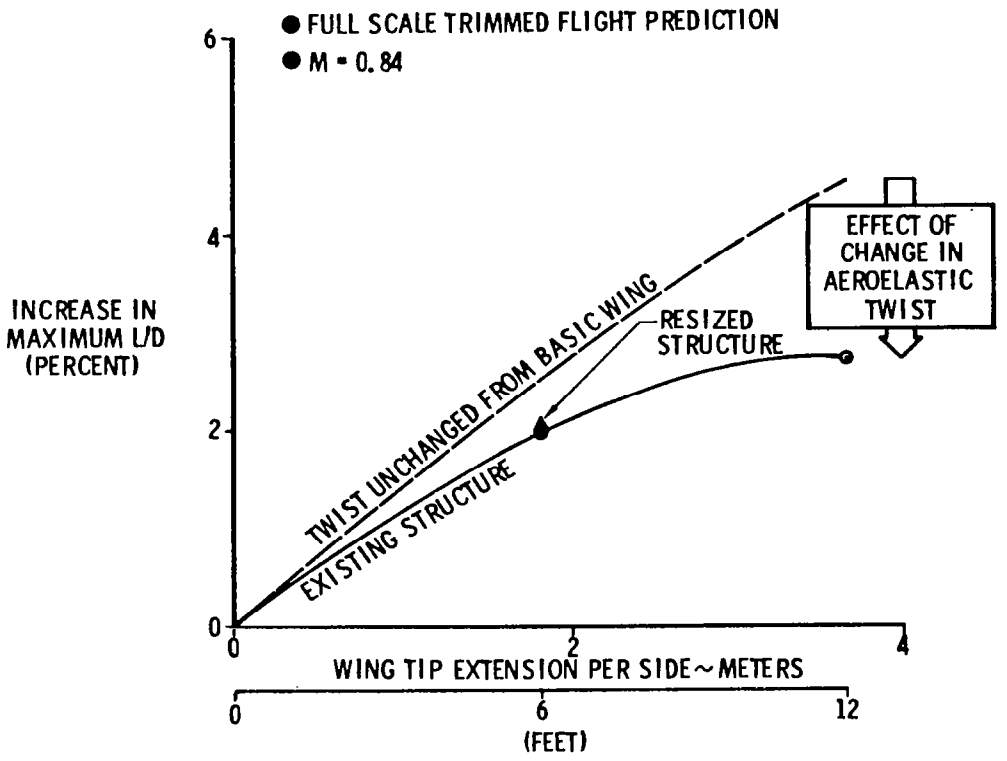

Figure 9.- L/D trends for wing tip extensions.

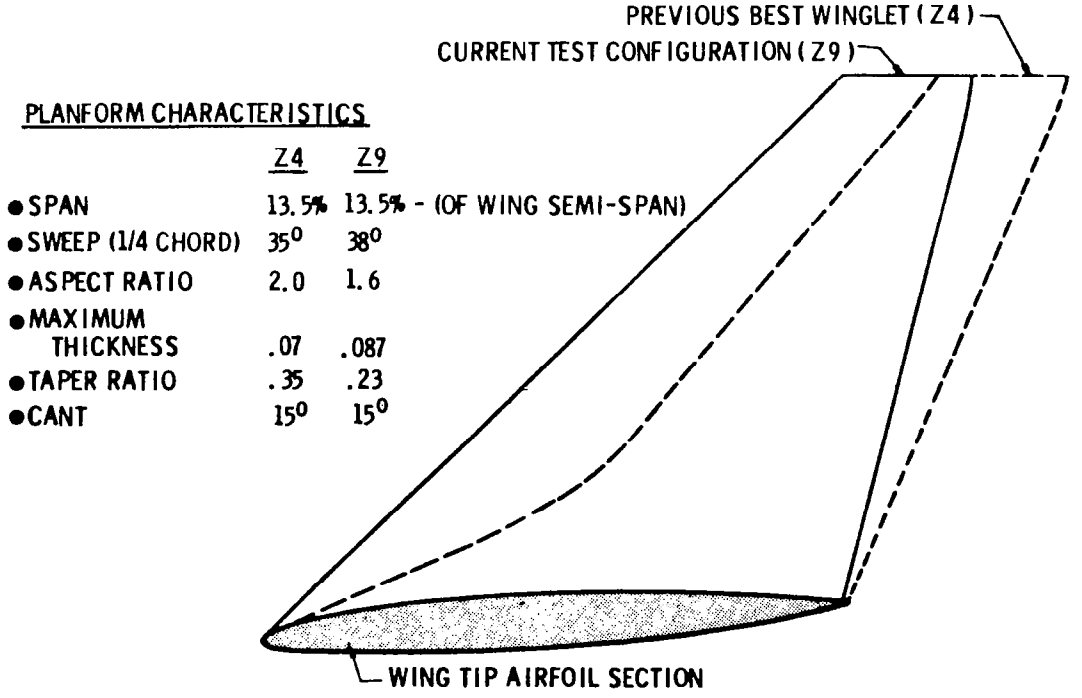

Figure 10.- Winglet geometry comparisons.

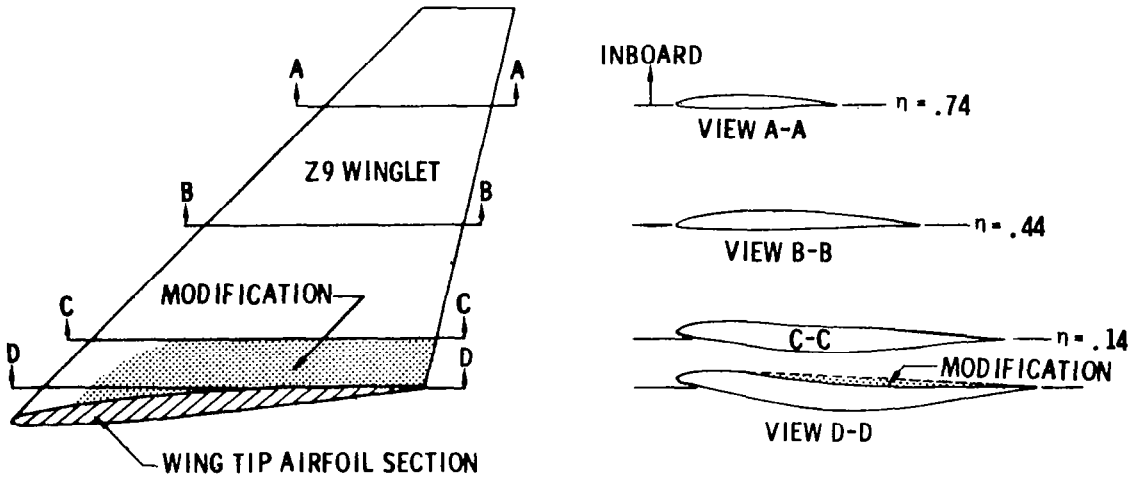

Figure 11.- Winglet cross sections for current test.

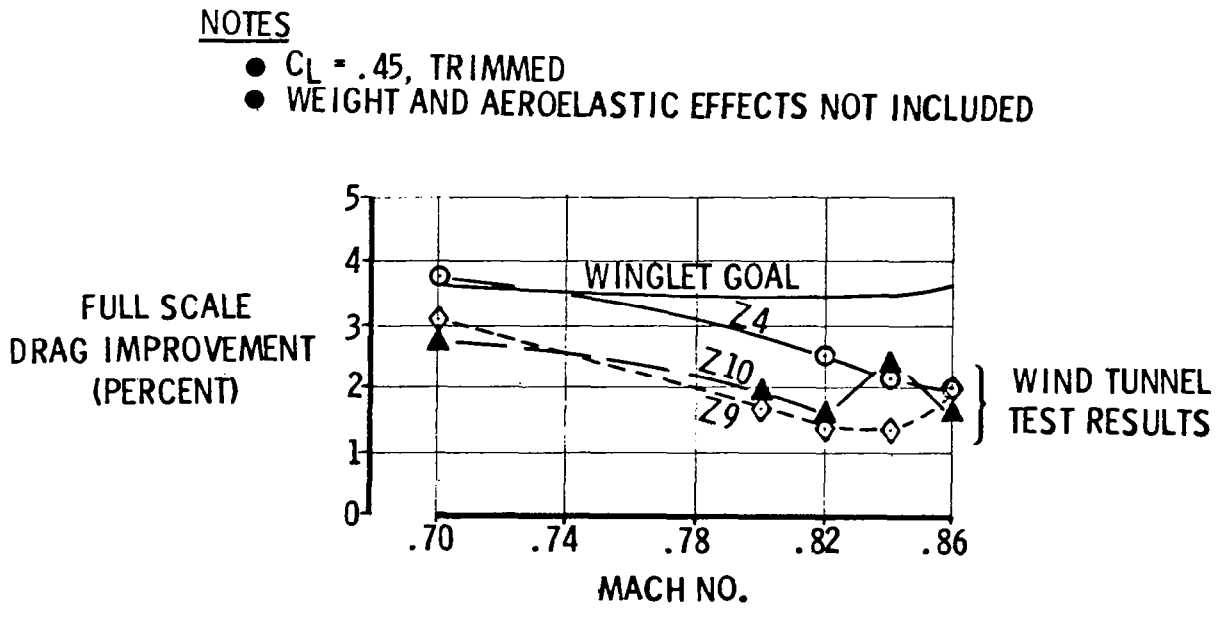

Figure 12.- Winglet drag comparisons.

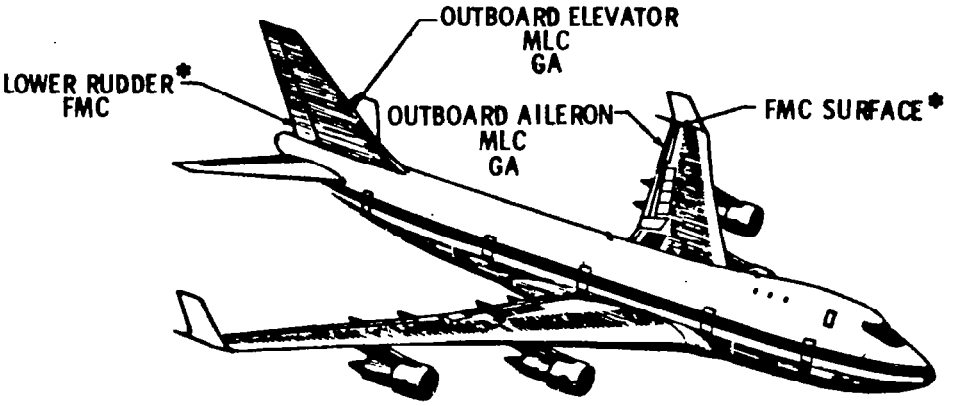

*NOTE: CONTROL SURFACES TO BE USED FOR FMC NOT YET DEFINED

Figure 13.- WLA control surface locations for 747 EET.

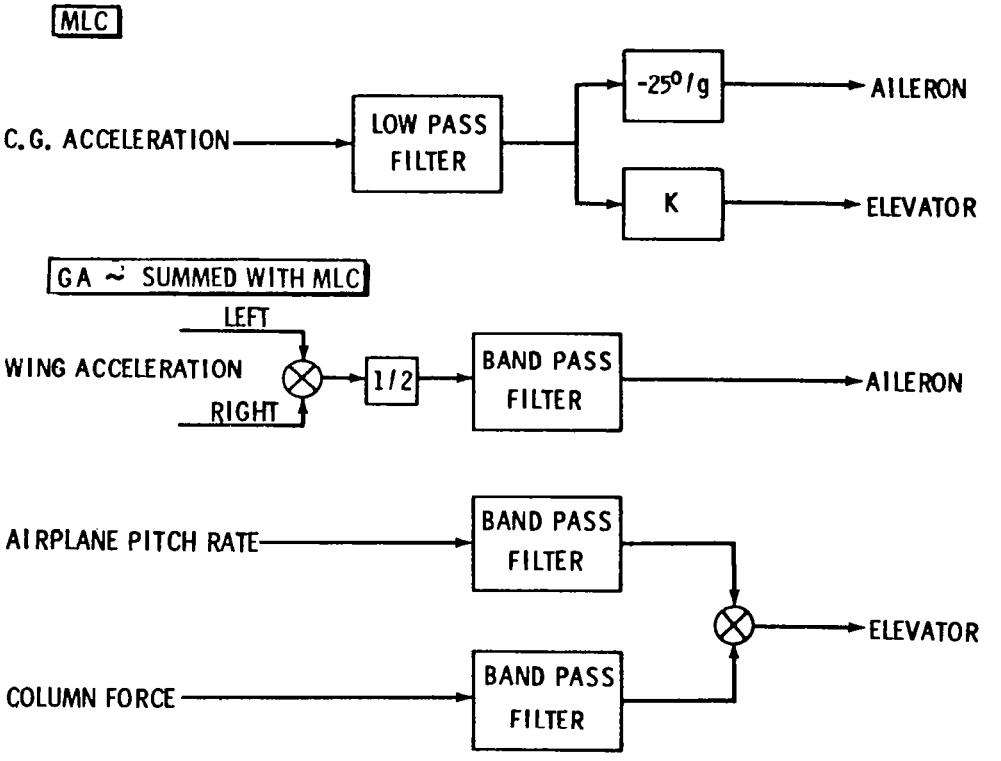

Figure 14.- MLC and GA system control laws.

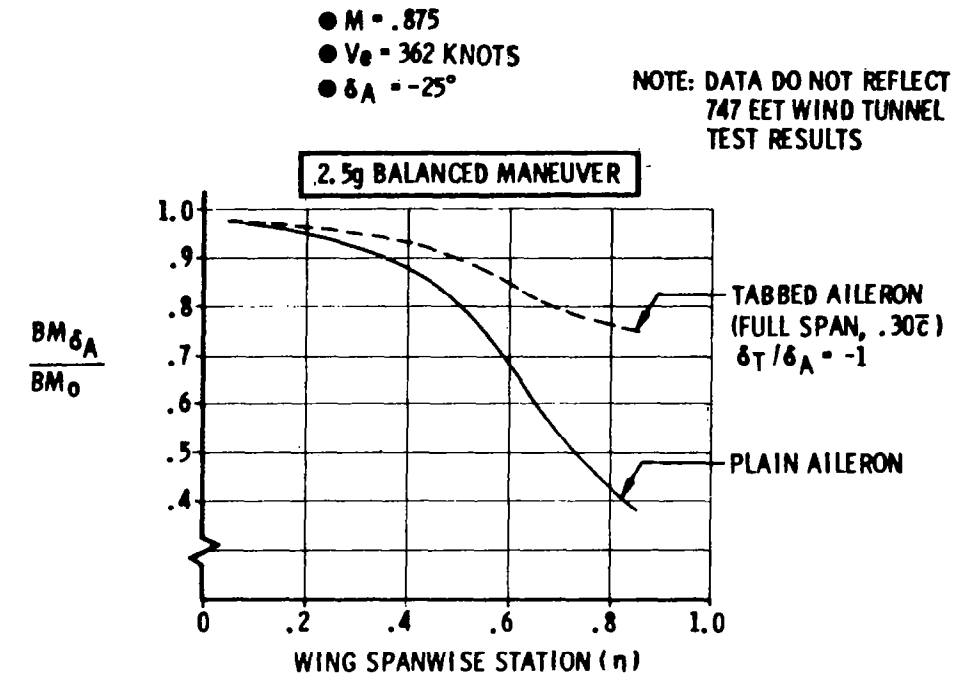

Figure 15.- Bending moment comparisons for plain and tabbed ailerons.

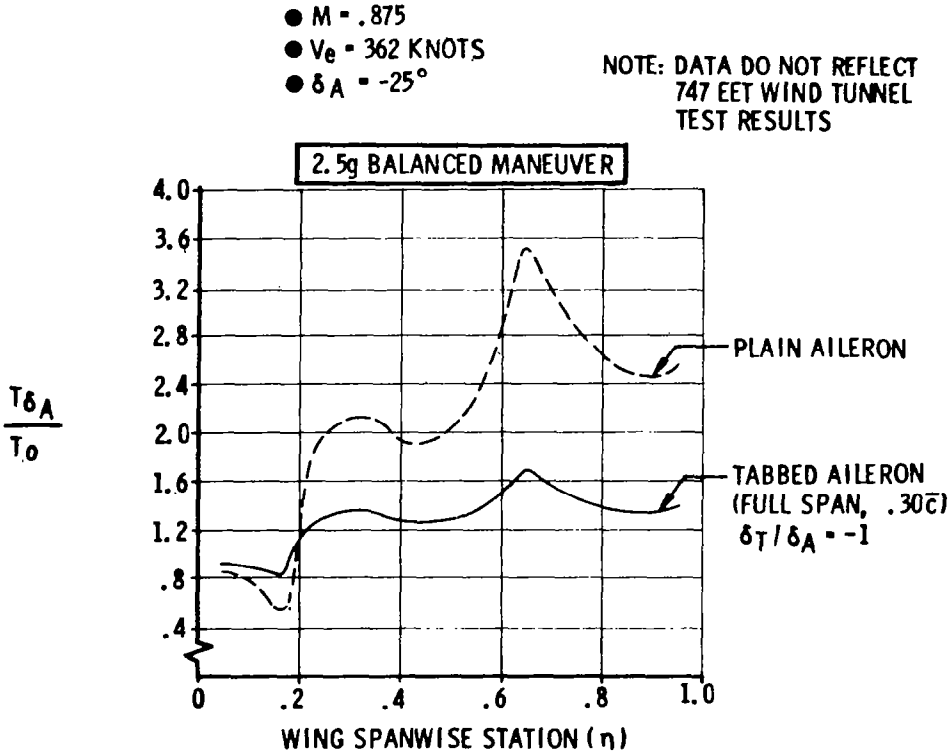

Figure 16.- Torsion comparisons for plain and tabbed ailerons.

DEVELOPMENT AND FLIGHT EVALUATION OF ACTIVE CONTROLS IN THE L-1011

J. F. Johnston and D. M. Urie
Lockheed-California Company

SUMMARY

This paper discusses a cooperative NASA/Lockheed program investigating active controls in the Lockheed L-1011 for increased energy efficiency. The tasks involve (1) active wing load alleviation for extended span, increased aspect ratio, and (2) active stability augmentation with a smaller tail for reduced drag and weight. Tests to date include flight tests of active wing load alleviation on the baseline aircraft and moving-base piloted simulation developing criteria for stability augmentation. Tests with extended span will be accomplished later this year.

Active controls in commercial transports have developed in an evolutionary manner. Some examples are the L-1011 Autoland automatic landing system, and the L-1011 yaw damper permitting a 20% reduction in vertical fin design loads. These developments set up some of the basic principles and techniques for active controls in commercial transports: probability-based analyses for equivalent safety, and definition and mechanization of redundancy requirements. The extensions to wing load alleviation and to relaxed static stability are logical, and the results to date indicate that they are easily accomplishable by use of the proper technologies.

Load Alleviation

The active load alleviation system uses symmetric motions of the outboard ailerons for Maneuver Load Control (MLC) and Elastic Mode Suppression (EMS), and stabilizer motions for Gust Alleviation (GA). The L-1011 is particularly adaptable to wing load alleviation because its outboard ailerons remain effective at high speed. The control laws were derived, after initial explorations of optimal control theory, by use of large-scale maneuver loads, flutter, and gust loads programs. Interactive graphics was an important element of the process.

The active controls computer and hardware were tested in the Vehicle Systems Simulator (VSS) at Lockheed's Rye Canyon research facility and then installed in the house L-1011. The flight tests went smoothly, without any delays caused by the active systems. Open-loop transfer function tests showed excellent test/analysis correlation for the aircraft dynamic response to symmetric aileron and stabilizer drives, and closed-loop transfer function

tests showed the active systems performed as predicted. Wind-up turns and pull-up/push-over maneuvers verified the maneuver load control. Flight tests in turbulence verified the effectiveness of the active controls in reducing gust-induced wing loads.

It was concluded that the use of the large-scale production loads, flutter and gust response programs had produced excellent results in deriving the control laws and predicting airplane response. A corollary conclusion was that the data base built up from ground, flight and wind-tunnel tests was entirely adequate.

Stability Augmentation

The flight dynamics of an L-1011 derivative having a 40% smaller horizontal tail were analyzed using a continuous systems modeling program. These analyses covered the complete flight envelope and identified areas for concentration in flight simulation and augmentation design. Also, these data were studied to determine the applicability of various handling qualities criteria. Criteria for augmentation system design, and unaugmented flying qualities were selected. These criteria utilized current L-1011 flying qualities as a basis.

An augmentation system consisting of a simple pitch rate damper supplemented by a column feed forward for control response tailoring was devised.

Pilot-in-the-loop testing was conducted on a moving base flight simulator. Three pilots flew the small-tail simulation model and a base-line having the current L-1011 tail. Testing was conducted with static margin and air turbulence level as variables.

Results from these piloted simulations show pilot ratings in the acceptable range for an unaugmented small-tail airplane with static margin of 5% even in heavy turbulence. For the small-tail airplane with neutral static stability, the pitch-rate damper augmentation system without feed-forward provides flying qualities as good as those of the unaugmented big-tail airplane at its mid-c.g. condition.

INTRODUCTION

Active controls in commercial transports have developed in an evolutionary manner from flight-path-management systems such as the L-1011 Autoland automatic landing system to load alleviation systems such as the L-1011 yaw damper, which allowed a 20-percent reduction in vertical fin design loads. These developments were important in setting up some of the basic principles

and techniques for active controls in commercial transports: the use of probability-based analyses, and definition and mechanization of redundancy and monitoring requirements.

Both the Autoland and yaw damper active control systems were included in the basic certification of the L-1011 in 1972. Building on this base, research was started in 1974 on use of active controls for wing load alleviation and for stability augmentation. Although the initial objective of the load alleviation was an increase in gross weight using existing wing structure - an increase of 12 percent was found possible - the rising costs of fuel soon made it apparent that load alleviation could best be used to increase the wing span for improved fuel efficiency. The objective of the stability augmentation studies was drag reduction by use of a smaller horizontal tail and reduced stability margin. Studies and wind tunnel tests indicated that the extended span and the smaller tail would each result in a 3 - 3-1/2 percent fuel saving, for a combined saving of 6 - 7 percent.

Both the load alleviation and the stability augmentation studies are now partially funded by NASA's Aircraft Energy Efficiency (ACEE) Program, reference 1, through the Energy Efficient Transport (EET) element, reference 2. The L-1011 was easily adapted to wing load alleviation because its outboard aileron remained effective at high speeds and contained series servo provisions for implementing the control signals. A breadboard load alleviation system was already under test on the full-scale L-1011 Vehicle Systems Simulator (VSS) at Lockheed's Rye Canyon research facility when the joint NASA/Lockheed program began. This program envisages flight verification of the load alleviation system on the baseline L-1011 aircraft and on the airplane with extended span augmented-stability control laws development using moving-base piloted simulation. Both the baseline load alleviation flight tests and the piloted simulated work have been completed successfully. This paper is to present and discuss selected results from these two tasks and it emphasizes the technology involved in their application.

SYMBOLS AND ACRONYMS

ACEE	Aircraft Energy Efficiency
ACS, ACT	Active Control System, Active Control Technology
AS	Augmented Stability
BL	Butt Line
C*	Normalized airplane response time history, $C^* = N_Z + 400q/g$.
CG, c.g.	Center of gravity

SYMBOLS AND ACRONYMS (Cont'd)

EET	Energy Efficient Transport
EHV	Electrohydraulic Valve
EMS	Elastic Mode Suppression
f	Frequency, Hz
FAR	Federal Air Regulations
G,g	Gravity, Damping
GA	Gust (load) Alleviation
GFAM	Graphics Flutter Analysis Method
KEAS	Knots Equivalent Airspeed
M	Mach Number
M_x, M_y	Bending Moment, Torsion Moment
MAC	Mean Aerodynamic Chord
MLC	Maneuver Load Control
n_z	Normal Load Factor
q	Pitch Rate, radians/sec
RE	Reduced Energy
RMS	Root Mean Square
SAS	Stability Augmentation System
V, Vg	Velocity, Gust Velocity
VFS	Visual Flight Simulator
VSS	Vehicle Systems Simulator
δa	Aileron Deflection
ζ	Fraction of Critical Damping
ωd, ωn	Damped and Undamped Natural Frequencies, radians/sec

WING LOAD ALLEVIATION

Basic Criteria

The basic criterion for the use of active controls in commercial transports is:

No Degradation of Safety

A second criterion required for airline schedule reliability is that the system be:

Non-dispatch Critical With One Channel Inoperative

The safety criterion is satisfied by the approach taken in the L-1011 yaw damper design, as illustrated in figure 1, and described more fully in Reference 3. Here the design limit gust load, associated with one occurrence in a 50,000-hour aircraft life, could be reduced from the level F in the figure to the level G - a one-third reduction, in this case - by installing a totally reliable yaw damper. If an extremely conservative assumption were made that the yaw damper was inoperative 3 percent of the time, then the design load would be at the level H, representing the combined probabilities E associated with a 97-percent operative, 3-percent inoperative yaw damper. This conservative design load level H is only slightly higher than the best level G and represents an attractive (approximately one-quarter) reduction from the no-active control (no yaw damper) value F.

From this illustration it may be seen that significant reduction in design loads and structure weight may be obtained with "state-of-the-art" active controls, that is, controls that may be inactive part of the time.

The second criterion, that the aircraft can be dispatched with one channel inoperative, sets the degree of system redundancy. This was selected for the L-1011 yaw damper as a "dual-dual" computer system with triple sensors, figure 2. See also reference 4. This same "dual-dual" system selection has been made for future in-service versions of the L-1011 wing load alleviation and stability augmentation systems.

It is of note that L-1011 service experience shows that the yaw damper has been inactive only about one hour per 100,000 flight hours. This record is three orders of magnitude better than the original design assumption. It suggests that later designs will assume a lower than 3 percent fraction of inoperative time.

System Description

The L-1011 is a triple-turbofan wide body commercial transport having the relatively high fuel efficiency and low noise of the high-bypass-ratio fan engine. An L-1011-500RE (RE for Reduced Energy) configuration is shown in figure 3, where the tip extensions and small tail (relative to the standard L-1011-1) are shown cross-hatched. The augmented-stability work was done with this configuration. The baseline active load alleviation flight tests were done with the standard L-1011-1 having a 2.74m (9 ft) shorter wing span and larger tail plus a longer fuselage than the -500. Its aspect ratio of 6.95 was proportioned for minimum direct operating costs when fuel was about 15 cents per gallon. The L-1011's relatively low design stress, wide-tread gear and outboard engine location all led to a relatively

stiff wing in both bending and torsion, with the result that the outboard ailerons remain effective to the maximum design speed. This characteristic permits use of active wing load alleviation with only minor structural modifications which in turn permits the increased span and aspect ratio appropriate to a design optimized at a higher fuel cost level.

Roll control in the cruise configuration is by means of irreversible inboard and outboard ailerons, each with multiple actuators powered by multiple hydraulic systems. Spoilers add to the roll control in the flaps-down condition. The outboard ailerons of the test airplane, S/N 1001, contain series servos, found unnecessary for roll stabilization, which have been adapted to symmetric motion for active wing load alleviation. The L-1011 Vehicle Systems Simulator (VSS), a full-scale geometric duplication of the L-1011 control systems at Lockheed's Rye Canyon research facility, contains similar aileron series servos.

L-1011 pitch control is by means of a powered stabilizer with geared elevator, the gear ratio varying from zero at high-speed stabilizer angles, to about 3 at low-speed, flaps-down stabilizer angles. The stabilizer is powered by two left-hand and two right-hand actuators, supplied by four different hydraulic systems. An electrohydraulic series servo has been inserted into the series trim linkage to provide active control to the stabilizer. This system is also duplicated on the VSS.

A block diagram of the primary channel of the breadboard active control system (ACS) is shown in figure 4. The secondary channel required to assure fail-passive characteristics is identical except that the stabilizer series servo is not duplicated (the aileron series servos have dual windings). The aileron systems are cross monitored by comparison of corresponding left wing and right wing coil signals, whereas the stabilizer series servo has in-line monitoring by comparison with the output of an analog model of the series servo. In case of excessive signal difference the monitor logic shuts both channels down, and the series servos return to neutral, i.e., they fail passively. The production system will have two dual computer/monitor channels, providing a fail-operational, fail passive sequence.

Inasmuch as the ACS sensors provide currents proportional to acceleration or pitch rate, ground test is performed by inserting calibrated currents to the system. This is called "torquing" the system. Normal operation is checked by torquing both channels equally, and monitor operation by torquing only one channel.

It may be noted that, after initial "burn-in" in the laboratory, the system performed within specification and without any delays during the approximately 150 hours of laboratory and 60 hours of flight tests.

The load alleviation functions provided by the active controls are

Function	Surface	Sensors
Maneuver Load Control (MLC)	Outboard aileron	Wing-tip and body accelerometers
Elastic Mode Suppression (EMS)	Outboard aileron	Wing-tip and body accelerometers
Gust Alleviation (GA)	Stabilizer	Body pitch rate gyros and accelerometers

The maneuver load control is selected at a steady-state value of 8.7 deg/g to offset added bending moments from the extended tips at limit load factor, whereas the elastic mode suppression is chosen to damp the fundamental wing bending mode in the frequency range from 1.2 Hz to 2 Hz. This EMS function is as important as the MLC in controlling loads in turbulence, inasmuch as the wing load power spectrum shows peak contents at low frequency (short period longitudinal mode) and at the wing first bending frequency.

The stabilizer control is used both to offset trim changes due to the symmetric aileron deflections and to reduce airplane pitch response to gusts.

Referring again to the system block diagram shown in figure 4, the body and wingtip accelerometers are oppositely speed-scheduled so as to hold a constant MLC gain and a decreasing EMS gain with increasing airspeed. This scheduling helps to control both gain and phase angles to reduce sensitivity to higher-frequency wing (and fuselage) modes, and was selected in accordance with a design approach that emphasized the importance of flutter- and gust-related interactions with the active controls.

Loads Analysis Techniques

Active controls require an interdisciplinary approach, involving aerodynamics, handling qualities, loads, dynamics and controls expertise. The initial emphasis is on the aerodynamics/handling qualities/loads interactions to define the allowable configuration changes (e.g., extended span, smaller tail) that can lead to performance gains. Where load alleviation is required, the emphasis then shifts to loads/dynamics/controls expertise. Here it has become apparent that the primary responsibility for defining the control laws lies in the loads/dynamics area, in consultation with the avionics and mechanical controls experts. This fact is noted as a departure from past autopilot experience, where the prime responsibility lay with the avionics/controls experts.

The interdisciplinary approach is illustrated in the program flow diagram, figure 5. The tools used in the control law synthesis were

Maneuver Loads Program

Production Design Gust Loads Program

Production Flutter Programs on Computer Graphics

Flutter Optimization Programs

State-Space Models

Optimal Control Programs

Method of Constraints

The first three programs were the primary tools. A brief description of the programs and their uses follows:

Maneuver Loads Program - This is the existing set of L-1011 static aeroelastic loads programs. These programs use analytical representations of aerodynamics, mass (each 251 grid points per side) and stiffness (156 grid points per side) characteristics to perform closed form solutions for the aeroelastic loads at 251 grid points per side. They are updated to reflect measured stiffnesses, aerodynamic load distributions and weights.

Production Design Gust Loads Program - This program, used to determine design gust loads due to vertical gusts, includes analytical representation of two rigid-body modes plus 20 elastic modes and uses unsteady kernel function aerodynamics. A loads analysis of the elastic airplane is performed giving transfer functions, power spectral densities, rms loads for unit rms gust velocity, correlation coefficients, and frequency of exceedance for load quantities over the entire airplane. The program reflects flight test, ground vibration and wind tunnel test results.

Production Flutter Programs on Computer Graphics - An interactive computer graphics system, Graphics Flutter Analysis Methods (GFAM), reference 5, was developed by Lockheed-California Company to complement Lockheed's matrix oriented batch computing system. GFAM is utilized when the problem requires rapid analysis with a high degree of interaction between the engineer and computer. The GFAM L-1011 ACT Synthesis/Flutter Model is a 117 structural degrees of freedom simple beam element representation using unsteady kernel function aerodynamics adjusted for wind tunnel (steady) data. The generalized coordinates include 3 airplane rigid body, one free pitch stabilizer, 35 full airplane vibration modes, 5 simply supported stabilizer modes and 6 unit modes which are associated with the aileron and stabilizer attachment points degrees of freedom.

Program FLUTTER in GFAM computes V-f-g data and plots the data against a reference case which may have been generated in batch. Program FLUTTER VEL. computes the flutter velocity directly.

Flutter Optimization Program - Structural resizing for flutter occurs in two parts. First, the initial structural resizing to satisfy all flutter requirements. Second, the resizing for minimum weight while explicitly satisfying flutter requirements and not violating strength requirements. The engineer performs both resizings in GFAM.

Method of Constraints - Closed loop constraint gain-phase data for each of the flutter and dynamic gust requirements are computed in GFAM using programs FLUTTER FEED and GUST FEED for flutter and gust requirements. From the gain-phase constraint computations, data that best satisfy the objectives of the study are derived. The control law that best fits the constraint gain-phase data is derived with the additional input of realistic mechanization of hardware constraints using program BODE in GFAM. Finally, the closed loop analysis for flutter is performed in GFAM to verify the objectives of the analysis.

State-Space Models - A 40 X 40 state-space (time domain) airplane model was generated in order to perform a quadratic optimization. The model contained 2 rigid and 6 elastic modes, stabilizer control dynamics and unsteady aerodynamics in the time domain based on least square fits of kernel function aerodynamics at selected frequencies. The model was sufficiently accurate to predict handling qualities and loads but insufficient to predict certain flutter modes. A reduced version of the 40 X 40 (i.e., a 12 X 12) state-space model was used to conduct laboratory simulation tests.

Optimal Control Programs - The state-space quadratic optimization procedure utilizes a synthesis algorithm which defines a direct matrix algebra solution of optimal feedback gains. A problem area associated with this application was the excessive number of feedback gains obtained from the full state feedback solution. Current independently funded research is underway to solve the partial state feedback problem.

Alleviation System Tests

The active controls computer was assembled, burned-in and functionally tested in Lockheed's Rye Canyon research facility as described in Reference 6, using the L-1011 Vehicle Systems Simulator (VSS) and Visual Flight Simulator (VFS). The VSS, a full-scale geometrically similar layout of the L-1011 systems, included duplicate series servos, aileron and stabilizer control systems, and L-1011 cockpit controls. Simulated flight was performed by closing the aircraft loop through the VFS. This loop was simulated by a 12 X 12 state space equations set that included three elastic modes. Although the VSS/VFS test results will not be discussed in this paper, it should be noted that these tests developed the final flight test configuration and the pre-flight test system, as well as verifying the specification performance of the active systems. They were a necessary and valuable prerequisite to the flight testing.

The flight tests consisted of:

1. Flutter-type tests to assure that the active controls did not produce any instabilities or noticeable reductions in damping at gains up to twice nominal. These tests were carried to near the limit design speed V_D and Mach number M_D and showed no deterioration in damping even at twice nominal gain.

2. Open- and closed-loop transfer function tests. The open-loop tests, covering response to sinusoidal excitations of the symmetric outboard ailerons and stabilizer separately, checked the analytical description of the airplane and the aerodynamic forces. The excitations covered the range from 0.1 Hz (low speed) or 0.3 Hz (high speed) to about 3 Hz. The speeds ranged from 145 KEAS, flaps down, Mach 0.26, to 378 KEAS, Mach 0.88. Low and high wing fuels were tested. Closed-loop tests checking the performance of the active systems were performed by turning the active systems ON during the sinusoidal excitation. These closed-loop checks were made for 145 KEAS, 345 KEAS and 378 KEAS (Mach numbers 0.26, 0.80 and 0.88, respectively).

3. Maneuver Loads Tests. These consisted of wind-up turns to 1.8 g load factor and push-downs and pull-ups. In addition, the symmetric aileron effectiveness was checked in level flight at 345 KEAS by inserting steady electric signals to hold the outboard ailerons at 5 different steady positions.

4. Gust Loads Tests. With a gust boom installed, gust loads tests were performed at low speed, flaps down, and at cruise speed. Good data were obtained at cruise speed, but the low-speed data were not adequate for meaningful analysis.

Load Alleviation Results and Discussion

Transfer Function Tests - Open-loop transfer function test results and comparisons with predictions for both amplitude and phase, are shown in figures 6 through 12. They represent motions of the wing tips, engine, pilot seat and stabilizer tips, drives by aileron and stabilizer, and speeds of 145 KEAS and 345 KEAS. In all cases the agreement between test and predicted results varied from good to remarkable. These motion predictions were made using the same Graphics Flutter Analysis Methods (GFAM) interactive flutter program that was used for specifying control law phasing. The excellent agreement indicates that the data base and the adequacy of the mathematical description are excellent.

Open-loop loads transfer functions are compared with VGA program predictions in figures 13 through 18. Good test/analysis agreement is shown except that the stabilizer loads were somewhat higher than predicted.

The effects on wing-tip accelerations of closing the loop are shown in figures 19 through 21. They show that the active controls damp the wing bending mode at about 1.6 Hz and have little effect on the higher frequency modes; two engine modes at 2.2 Hz and 2.7 Hz, and fuselage and stabilizer bending modes at 3.5 Hz and 5 Hz.

The wing bending load effects of the active controls are shown in figure 22 for a station at 52 percent semispan. The bending moment at low frequency, 0.3 Hz, was reduced 50 percent, and the wing bending peak at 1.6 Hz was reduced in a manner similar to the wing-tip accelerations at this frequency.

Overall, the transfer function test results confirmed both the mathematical modeling of the airplane and the effectiveness of the active controls.

Maneuver Loads Tests - Typical results for the variation with load factor of wing bending moment, shear and torsion at wing BL 702 (75% semispan) are shown in figures 23 to 25 for the 345-KEAS cruise condition. The bending moments and shears were reduced by the active controls, and the torsion loads were increased, all approximately as predicted.

The symmetric aileron effectiveness per degree is summarized in figure 26, where the incremental bending moment is related to the 1-g bending moment at each span position. The test data, although scattered, give reasonable confirmation to the pre-flight predictions.

Gust Response - The gust response test/analysis correlation was still in process as this paper was being prepared. Some test data were available, however, to show the effect of the active controls. Figure 27 shows cross-spectrum transfer functions of wing bending at BL 286 (31 percent semispan) relative to the measured gust velocity. The solid curve is sight-averaged from overlay plots of the two available ACS-on test runs, and the dashed curve is sight-averaged from overlay plots of the two available ACS-off runs. It may be seen that the active systems provide a substantial wing load reduction in the frequency range below 2 Hz.

STABILITY AUGMENTATION

Criteria

The approach to developing an augmentation system for the small-tail L-1011 active controls derivative airplane was to use the current L-1011 in the manual control mode as the standard of acceptable performance. The small-tail configuration with augmented stability (L-1011-500 RE) was designed such that handling qualities are at least as good as those of the current L-1011. In order to assure this, the following specific criteria were selected.

1. Normalized C* and pitch rate time history response will lie within the envelope of these parameters for the current L-1011. C* is a weighted sum of normal acceleration and pitch rate, $C^* = n_z + 400q/g$

2. Frequency response criteria will assure that oscillatory characteristics compare favorably with current transports.

3. There will be no roots with time to double amplitude less than 55 seconds.

4. There will be at least one pound column force for each six knots speed change away from trim as required by the Federal Aviation Regulations.

The normalized C* step input response time history envelope of the current L-1011 for a wide range of weight and c.g. conditions at a typical cruise flight condition is shown on figure 28. The dotted lines indicate the upper and lower boundaries of this envelope used as a criterion. Figure 29 includes the root locus for the unaugmented current airplane with the big tail as the oscillatory chacteristics which were objectives in the augmentation system.

System Description

The L-1011-500 RE is depicted in figure 3 with the small horizontal tail shown shaded. The small tail has approximately 60% as much exposed area as the current big tail shown in dashed outline. Considering the destabilizing effect of the small tail and stabilizing effect of the extended wing tips, the net inherent stability loss for the L-1011-500 RE compared to the current L-1011 is 5% static margin at low speed conditions and, in cruise, about 3% at M = 0.80 decreasing to no loss at M = 0.90 and above. Corresponding neutral point locations with the small tail are approximately 42% MAC for the landing approach configuration and 38% to 41% MAC in cruise. Comparable L-1011 values are 47% on landing approach and 41.5% MAC in cruise. Ground balance requirements about the main landing gear dictate an L-1011 operational aft c.g. limit of 35% MAC for takeoff and landing, although in-flight c.g. locations aft of this limit are possible for research purposes. Retaining this aft limit for the L-1011-500RE gives the small-tail airplane a static margin varying from 3% to 7% MAC depending on flight conditions.

The design of the augmentation system was based on consideration of the following characteristics of the unaugmented small-tail airplane with the c.g. at the operational aft limit.

1. Results from the piloted flight simulation show generally acceptable handling qualities.

2. Normalized time history characteristics are within selected criteria boundaries.

3. The undamped angular frequency characteristics are considered unacceptably low.

Based on these findings it was concluded that good handling qualities could be achieved with a simple augmentation system which would be highly reliable. This system identified herein as System 1 was conceived as a lagged pitch rate damper to provide the necessary short-period frequency and damping characteristics to suppress turbulence effects. In addition, a washed-out column feed-forward loop was designed to provide the flexibility of adjusting the C* and pitch rate time history characteristics without affecting stability. This loop was used to increase pitch response to control input as in System 2 or to decrease it as in System 3.

The current L-1011 is equipped with Mach trim compensation to give a satisfactory stable stick force gradient with velocity at high speed to comply with FAR part 25 requirements. In this study a new Mach trim system has been defined for the small-tail airplane and its characteristics have been incorporated into the basic airframe speed derivatives. The Avionics Flight Control System of the current L-1011 includes complete automatic pilot modes and it is assumed that a small-tail derivative would also possess this capability. However, no autopilot effects are included in this study although the autopilot would provide a dual channel backup for the pitch stability augmentation system.

Augmentation Design Analysis

Control system analysis was performed using a linearized aerodynamic model. Pitch rate time histories obtained with this model show close agreement with those from digital computer program solutions using the complete flight regime nonlinear aerodynamic simulation model.

Short-period frequency and damping values were sought for the augmented small-tail airplane which would equal or exceed those of the baseline airplane at 25% c.g. Figure 29 shows the effect of c.g. location on characteristic short-period roots of the small-tail L-1011-500RE with the lagged pitch rate damper, system 1, compared with the baseline airplane. These data show that the damping ratio (ζ) of the big-tail airplane is matched while frequency (ω) is increased. It is noteworthy that the augmented system significantly increases the frequency over that of the unaugmented small-tail airplane, and also because of pitch damper lag, suppresses the low frequency instability present for the unaugmented small-tail airplane at 40% c.g. in cruise.

Normalized C* step response time history characteristics of the small-tail L-1011-500 RE with the pitch damper (System 1) are shown as solid lines in figure 28. These data for cruise are well centered between the criteria boundaries. In order to evaluate the importance of C* in the flight simulation, the upper and lower boundaries are matched by activating the washed-out column feed forward loop. It was found that an upper boundary match was facilitated by reducing the pitch damper gain in addition to the column feed forward manipulation; this system is identified as System 2. A lower boundary match was achieved by slightly reducing the stabilizer to column gain; this is identified as System 3.

Because the purpose of this study is to investigate the effects of relaxed static stability, c.g. locations forward of 25% MAC were not included in the flight simulation and were therefore not considered at this stage of the augmentation system development.

Simulation Tests

Flight simulation was conducted on the Lockheed Rye Canyon 4DOF moving base Visual Flight Simulator. An L-1011 cab equipped with televised outside forward visual presentation and cockpit instrumentation including an L-1011 Flight Director was installed on the motion system. Continuous random turbulence of RMS levels up to 2.7m/sec (9 fps) on approach and 3.7m/sec (12 fps) in cruise was simulated using the Dryden spectral form (ref. 7).

Pilots were asked to perform typical flying tasks in varying levels of turbulence at several conditions of static stability. The cruise task consisted of making small altitude and heading changes at M = 0.83 at 10058m (33000 ft.) altitude. The approach task was started 16 km (10 miles) from the runway threshold at 457 m (1500 ft) altitude. Flaps, initially at 10°, were lowered to 26° and then to 33° as gear was extended. An instrument approach was flown using the flight director. Three pilots rated flying qualities using the Cooper-Harper rating scale (ref. 8). Their opinions are presented in composite form on figures 30 through 33.

Simulation Results and Discussion

Figure 30 presents the results of an evaluation of cruise flying qualities for the small-tail L-1011-500 RE with no stability augmentation. In this flight condition turbulence did not significantly affect controllability, but center of gravity location had a marked effect on altitude and pitch attitude control. Pilots commented that because of sluggish response and difficult attitude control, cruise flight at less than 5% MAC static margin with neither stability augmentation nor autopilot would be acceptable only for the brief time period necessary to achieve a more favorable flight condition.

Figure 31 shows comparable evaluation with the stability augmentation engaged. All pilots reported that the augmentation provided a significant improvement in controllability at aft centers of gravity in both levels of air turbulence. There is no clear-cut preference for one system over another, which suggests that the improvement in pitch damping provided by system 1 and present in all systems is more significant than differences in aircraft control response.

Results of an evaluation of approach flying qualities for the L-1011-500RE with no stability augmentation are given in Figure 32. Pilot ratings and comments indicate that aft movement of the c.g. does not appreciably degrade controllability of the small-tail configuration until the c.g. location exceeds 40% MAC. The effect of turbulence on the ratings, however, is pronounced at all c.g. locations, degrading the pilots' ability to control glideslope satisfactorily.

Figure 33 presents pilot ratings of landing approach flying qualities with augmentation. In calm air, because the unaugmented small-tail aircraft was relatively easy to fly, the rating improvement with augmentation was small. In heavy turbulence, a significant improvement was observed at all c.g. locations. The pilots were able to capture and track the glideslope with an acceptable level of work load.

As in the cruise condition, a comparison of the baseline to the L-1011-500RE with augmentation engaged shows the two configurations to be equivalent in calm air but the augmented small-tail L-1011-500 RE is easier to fly in heavy turbulence.

Statistical data showing the effects of air turbulence during cruise on the small-tail airplane with augmentation on and off are compared to the baseline level in figures 34 and 35. Figure 34 shows the effect of reduced tail size on load factor, pitch attitude and pitch rate. There is a slight reduction in normal load factor deviation for the small-tail configuration both with and without augmentation, but the greatest effects are on pitch rate, the feedback variable, and pitch attitude.

Figure 35 summarizes the relative effects of turbulence on primary control system parameters. The column motion required to control the aircraft is significantly less for the augmented small-tail airplane than for the same aircraft without augmentation. This trend is also apparent in the control force implying a reduction in work load. Stabilizer motion is greater for the small-tail aircraft because of the requirement to compensate for reduced inherent damping and control power either by increased pilot activity or by an automatic system. Considering only the small tail, the stabilizer motion is reduced by use of the augmentation system.

CONCLUSIONS

From baseline tests and analysis of an active load alleviation system on the L-1011, it is concluded that

1. Control laws derived using production (large-scale) loads, flutter and gust analysis programs provided satisfactory static and dynamic wing load alleviation without introducing new dynamic problems.

2. The available data base - mass, stiffness and aerodynamics of the L-1011 - built up from previous analyses plus ground, flight and wind-tunnel tests was entirely sufficient, in conjunction with the large-scale analysis programs, for deriving the control laws.

3. The results of the baseline tests and analyses have provided a good base for the next step, the use of active controls with extended tips.

From results of the aft-c.g. simulation study, it is concluded that

4. A simple, reliable pitch augmentation system will restore satisfactory flying qualities to neutrally stable commercial transport aircraft.

5. Flying qualities are generally acceptable for those aircraft with as little as 5% static margin in the event of complete failure of augmentation.

To generalize, it may be concluded that derivative aircraft, benefitting from good data bases and analytical techniques, can make immediate use of active controls for load alleviation and stability augmentation, to the extent of their control system capability.

REFERENCES

1. Povinelli, F. P., Klineberg, J. M., and Kramer, J. J.: Improving Aircraft Energy Efficiency. AIAA Astronautics and Aeronautics, pp. 18-31, February, 1976.

2. Leonard, R. W., and Wagner, R. D.: Airframe Technology for Energy Efficient Transport Aircraft. SAE 1976 Transactions, Section 4, pgs. 2916-2931, Sept. 23, 1977.

3. Hoblit, F. M.: Effect of Yaw Damper on Lateral Gust Loads in Design of the L-1011 Transport. Presented at 37th Meeting of the AGARD Structures and Materials Panel, The Hague, Netherlands, 7-12 October, 1973.

4. Flapper, J. A., and Throndsen, E. O.: L-1011 Flight Control System. AGARDograph AGARD-AG-224, April, 1977.

5. Radovcich, N. A.: Graphics Flutter Analysis Methods - An Interactive Computing System at Lockheed-California Company. Paper No. 8 of NASA SP-390. Presented at Langley Research Center, October 1-2, 1975.

6. Foss, R. L., and Lewolt, J. G.: Use of Active Controls for Fuel Conservation of Commercial Transports, AIAA Paper No. 77-1220, Presented at AIAA Aircraft Systems and Technology Meeting, Seattle, Wash., August 22-24, 1977.

7. MIL-F-8785-B; Military Specification, Flying Qualities of Piloted Airplanes.

8. Cooper, George E.; and Harper, Robert P. Jr.: The Use of Pilot Rating in the Evaluation of Aircraft Handling Qualities. NASA TN D-5153, 1969.

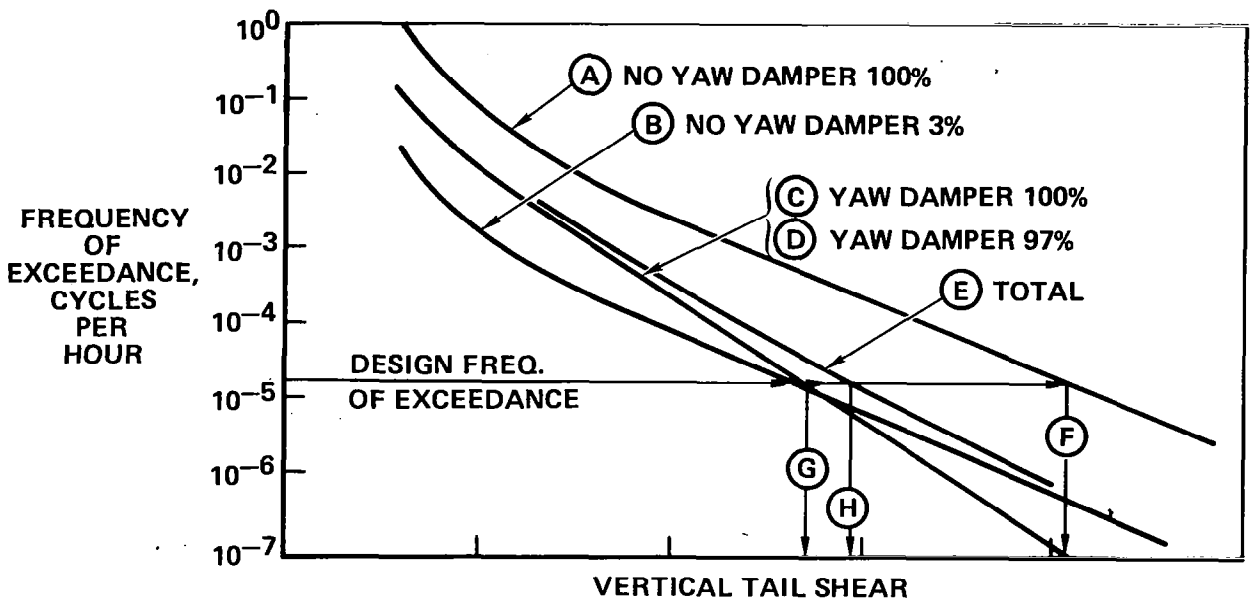

Figure 1.- Probability approach — gust loads.

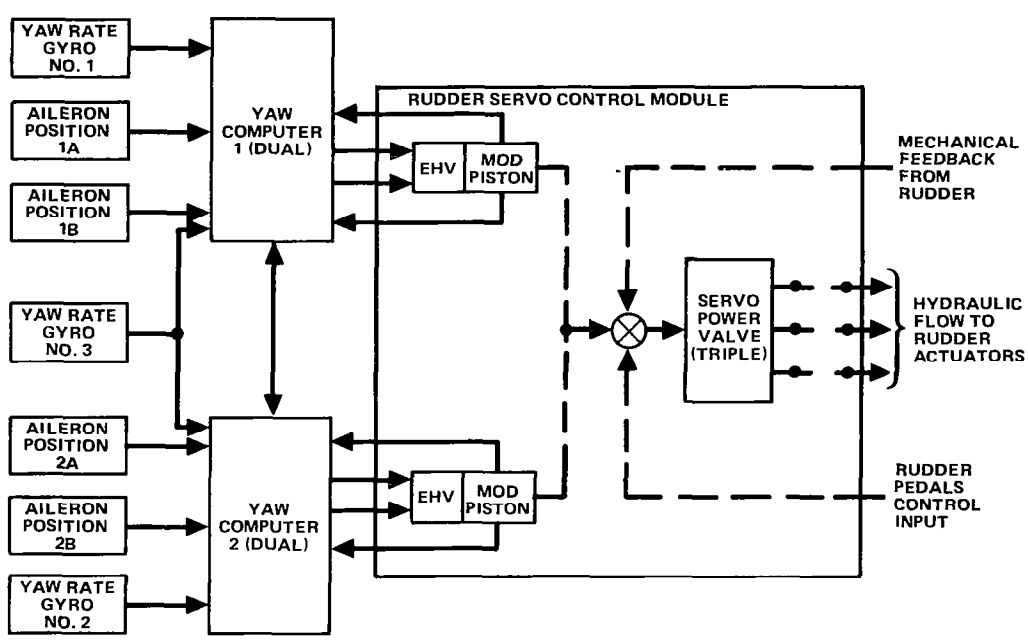

Figure 2.- L-1011 active YAWSAS.

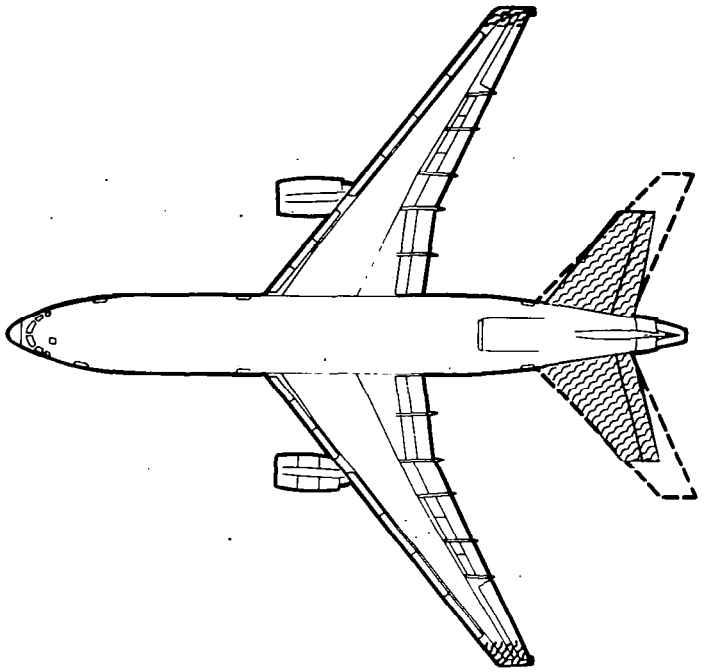

Figure 3.- L-1011-500 RE general arrangement.

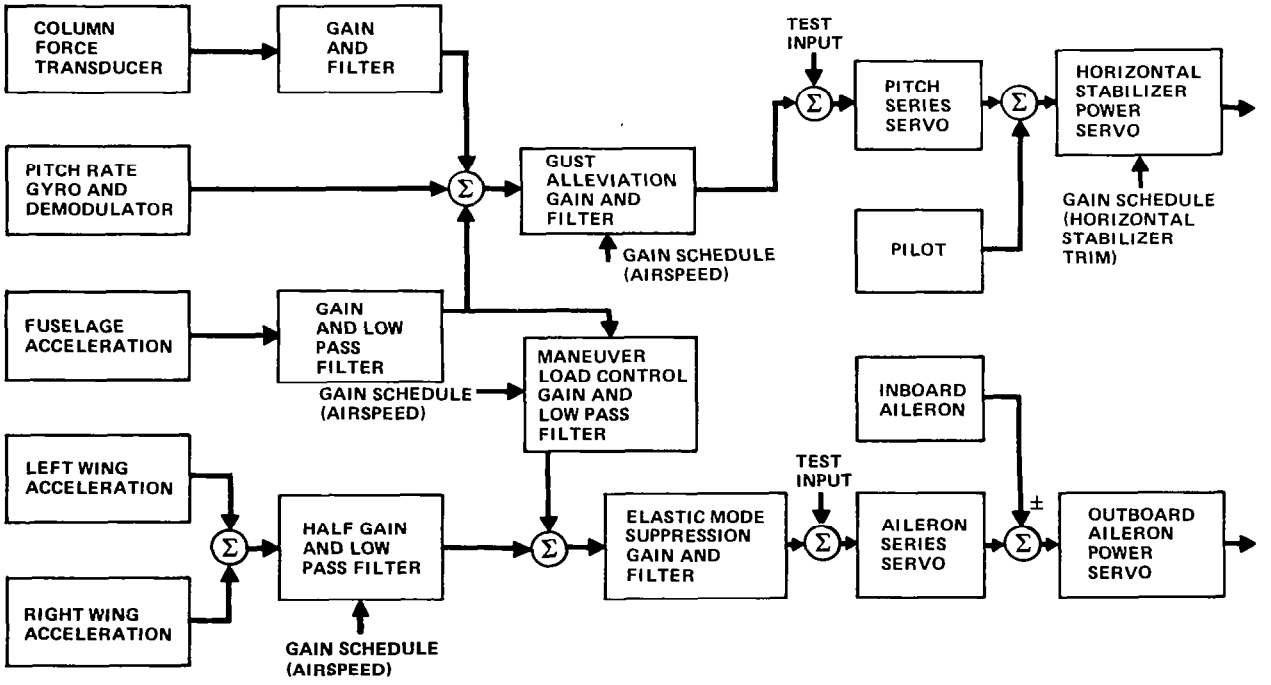

Figure 4.- L-1011 MLC/EMS/GA system block diagram.

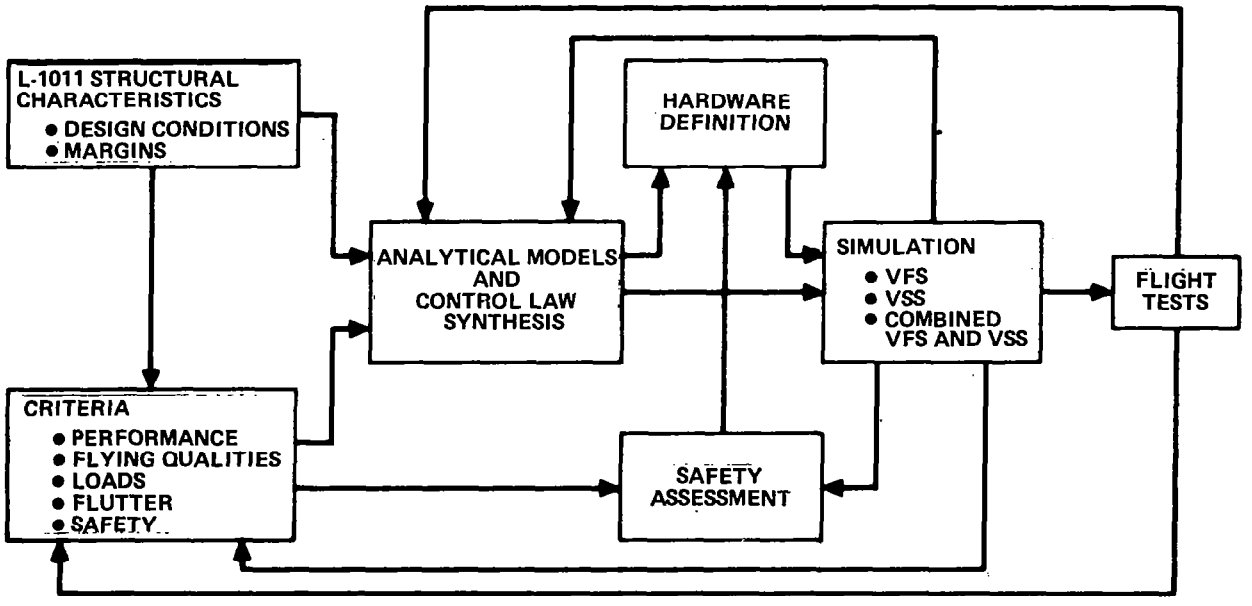

Figure 5.- Program flow diagram.

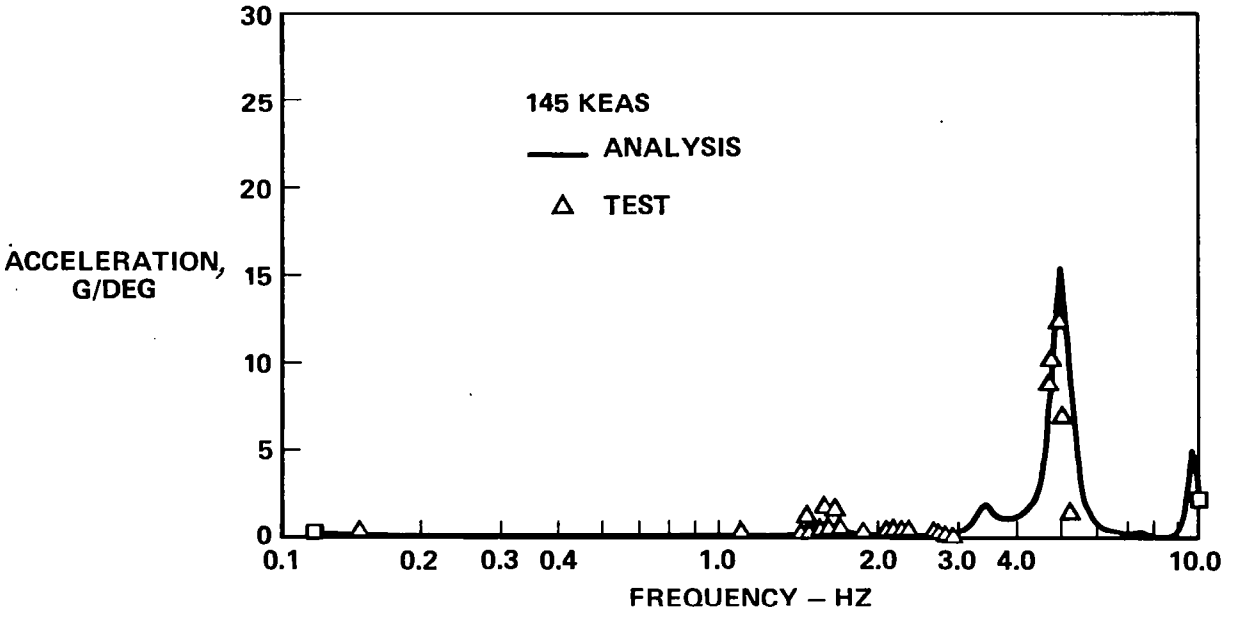

(a) Magnitude.

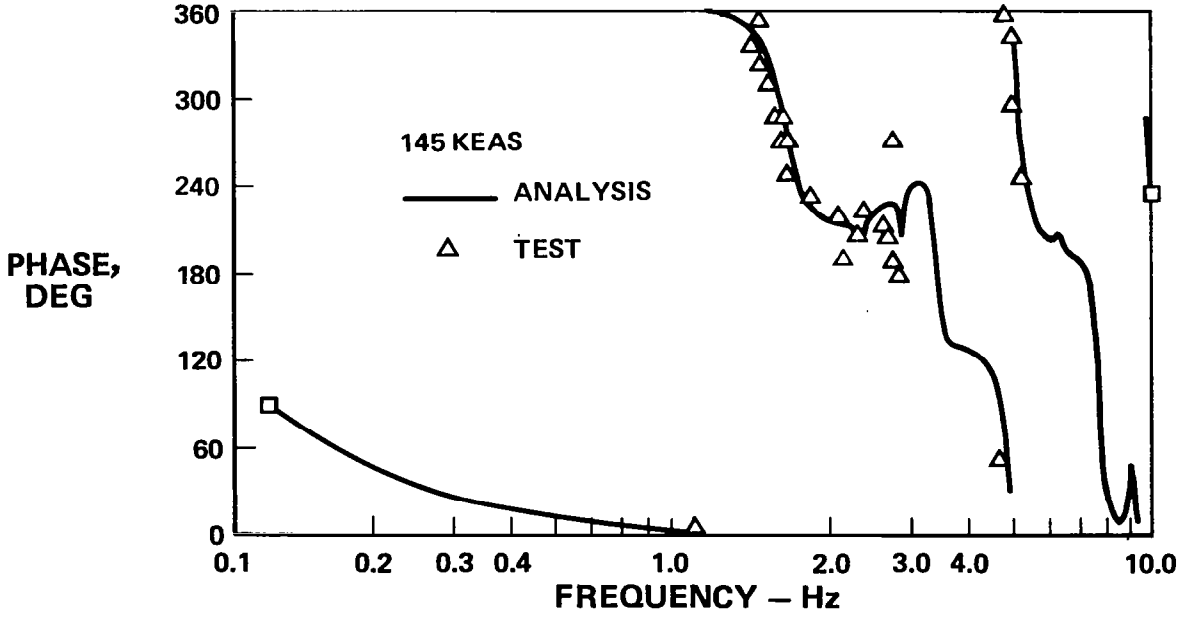

(b) Phase.

Figure 6.- Wing-tip acceleration — stabilizer drive ACS OFF.

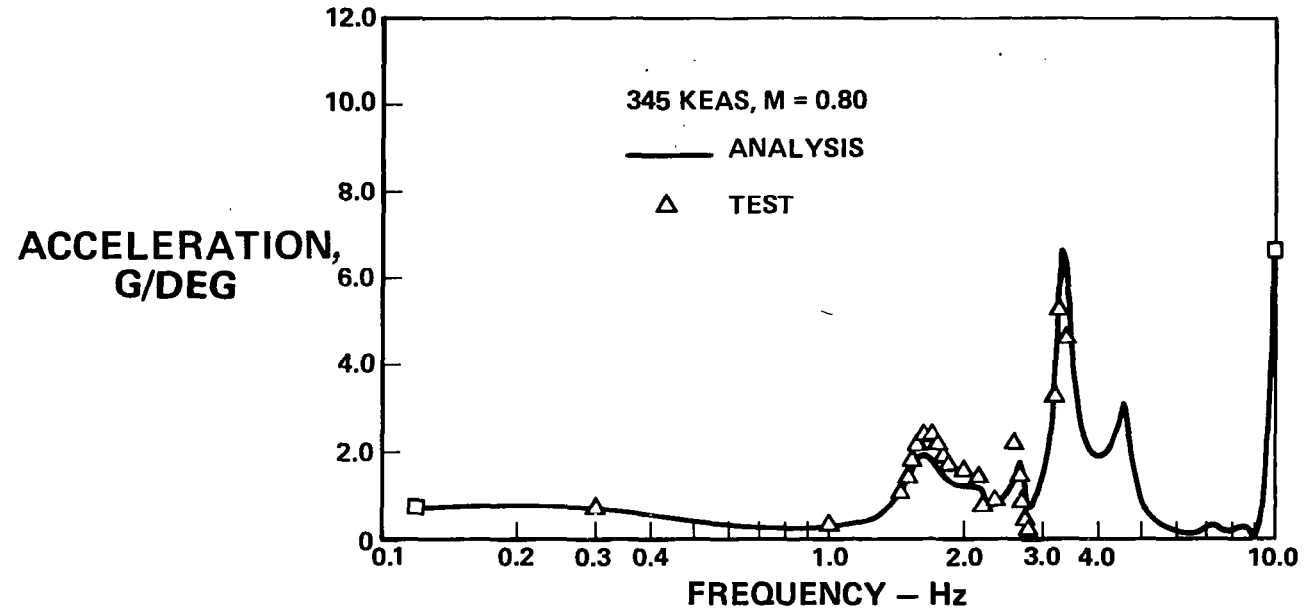

(a) Magnitude.

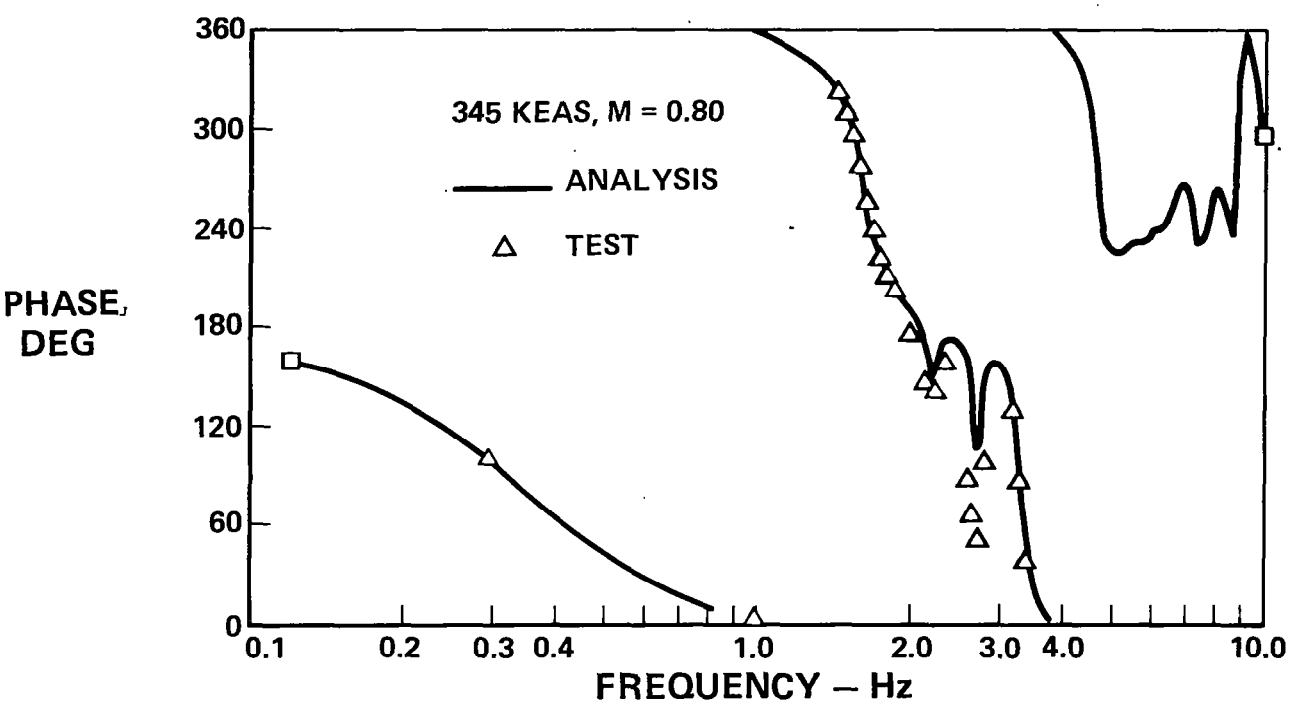

(b) Phase.

Figure 7.- Wing-tip acceleration — stabilizer drive ACS OFF.

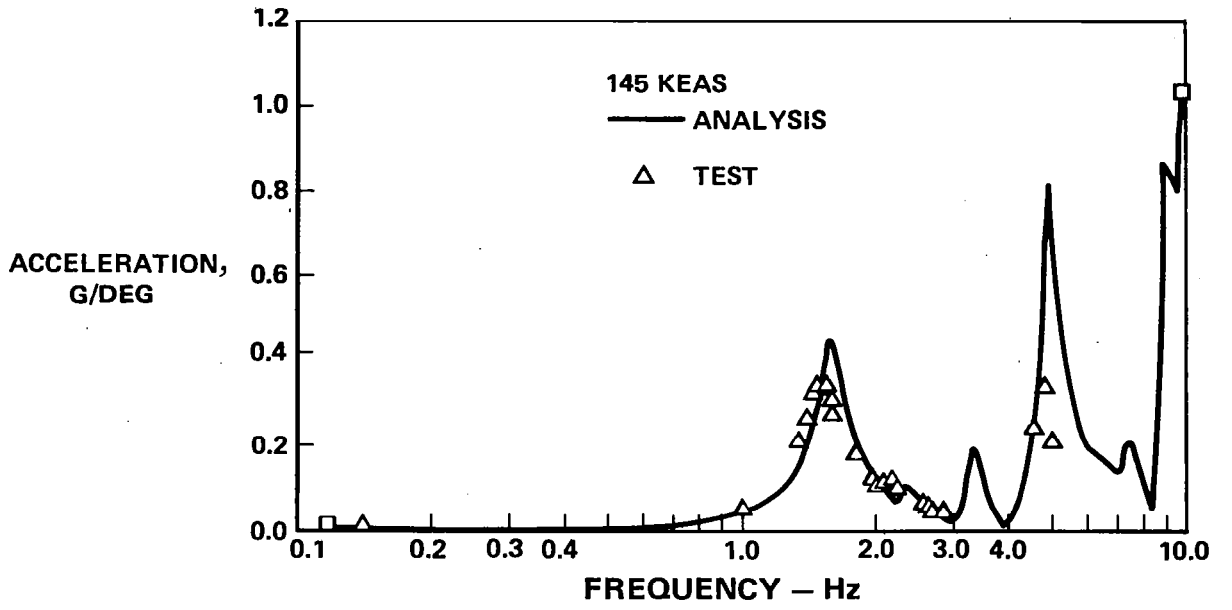

(a) Magnitude.

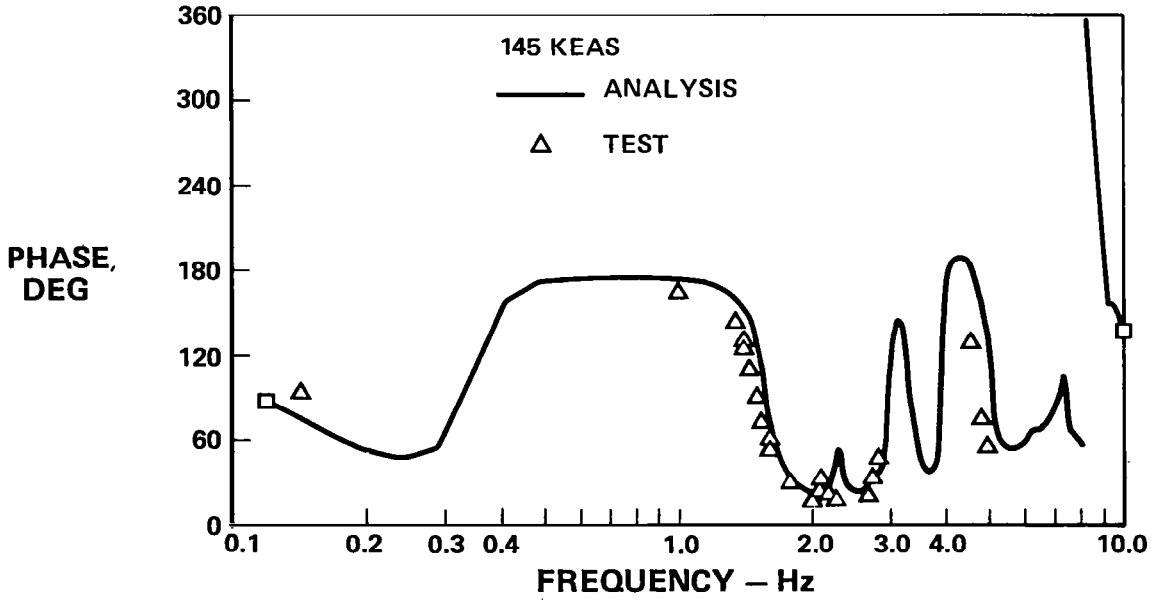

(b) Phase.

Figure 8.- Wing-tip acceleration — aileron drive ACS OFF.

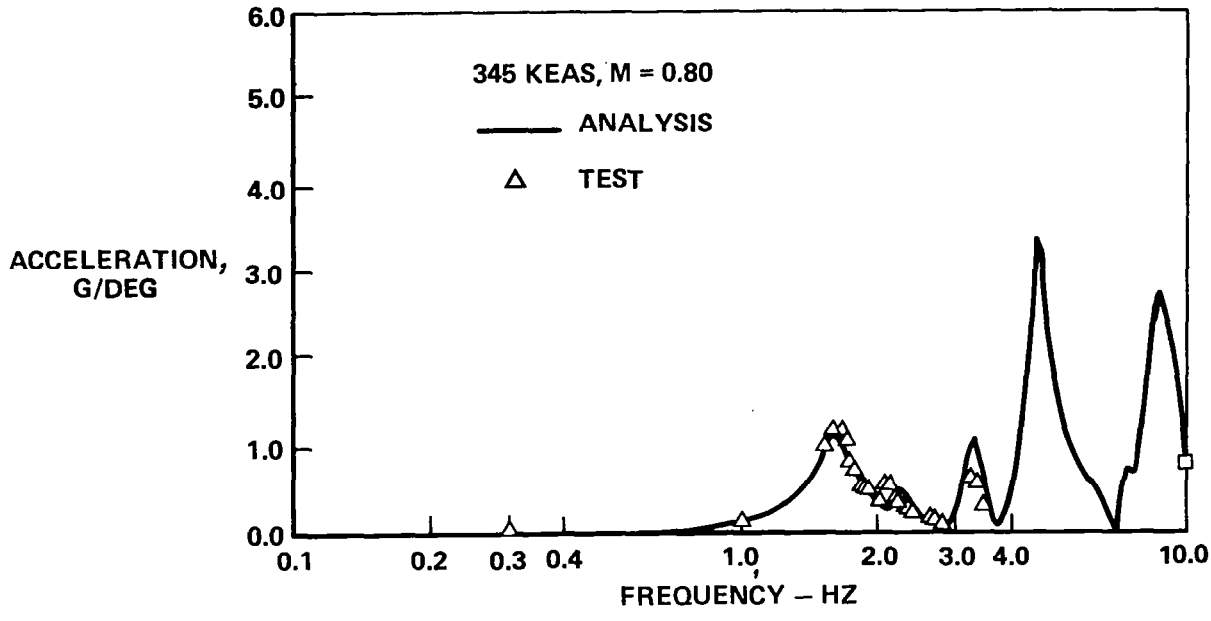

(a) Magnitude.

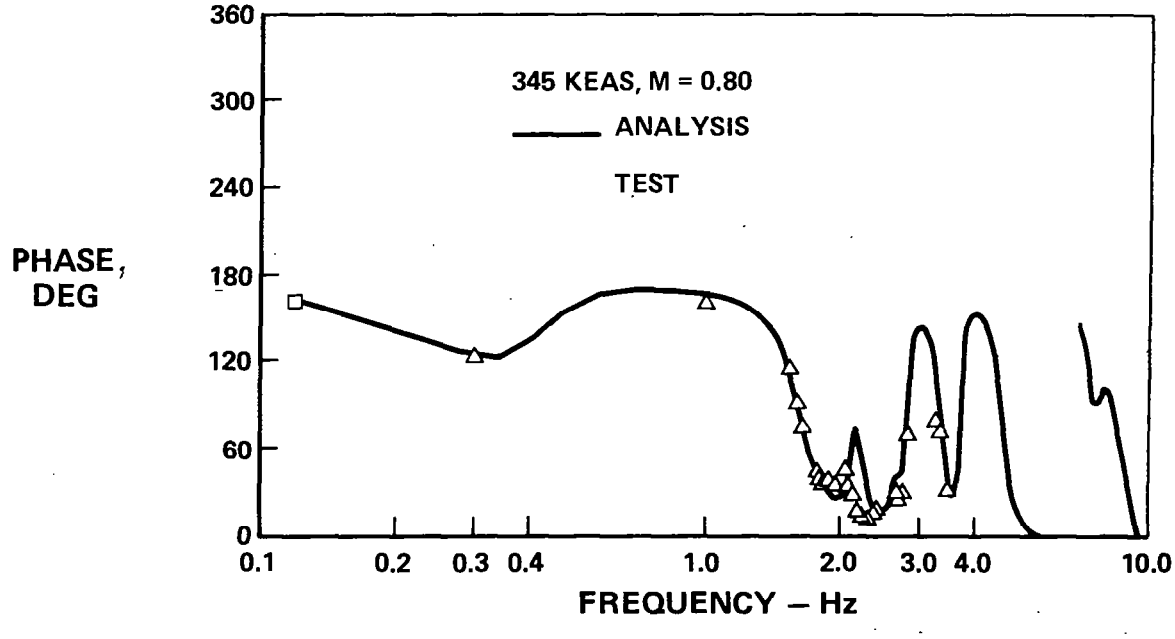

(b) Phase.

Figure 9.- Wing-tip acceleration — aileron drive ACS OFF.

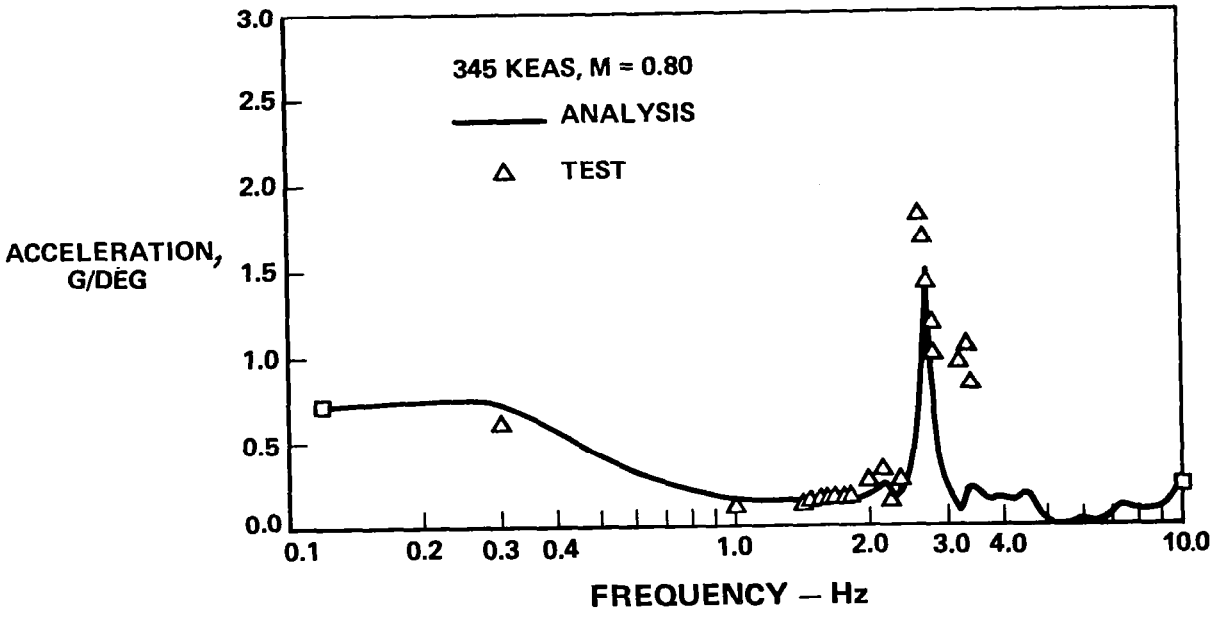

(a) Magnitude.

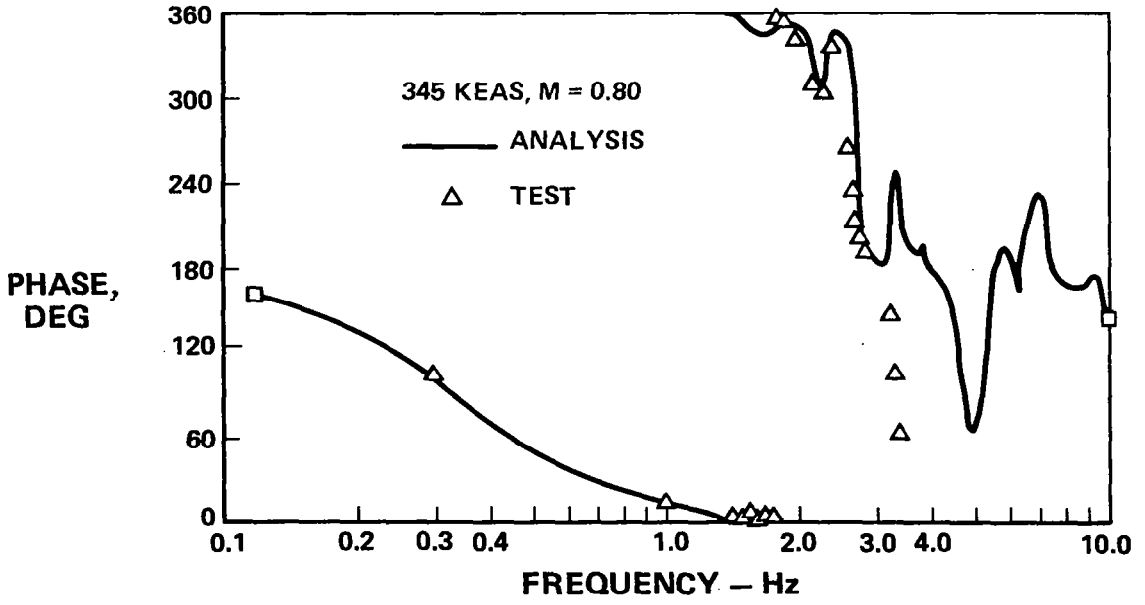

(b) Phase.

Figure 10.- Engine normal acceleration – stabilizer drive ACS OFF.

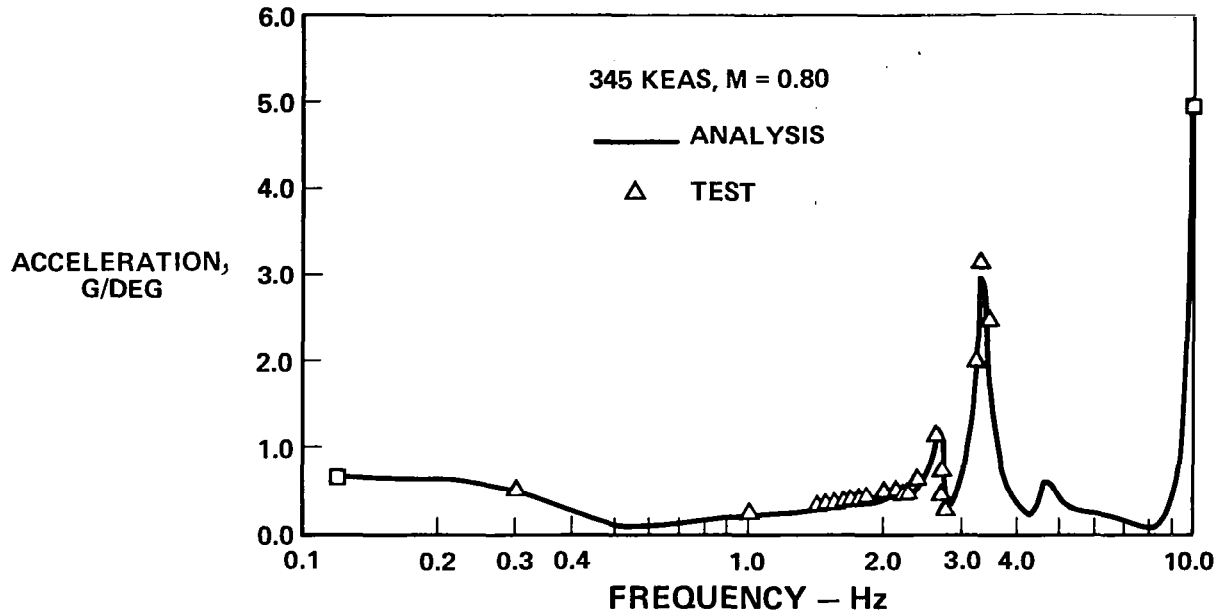

(a) Magnitude.

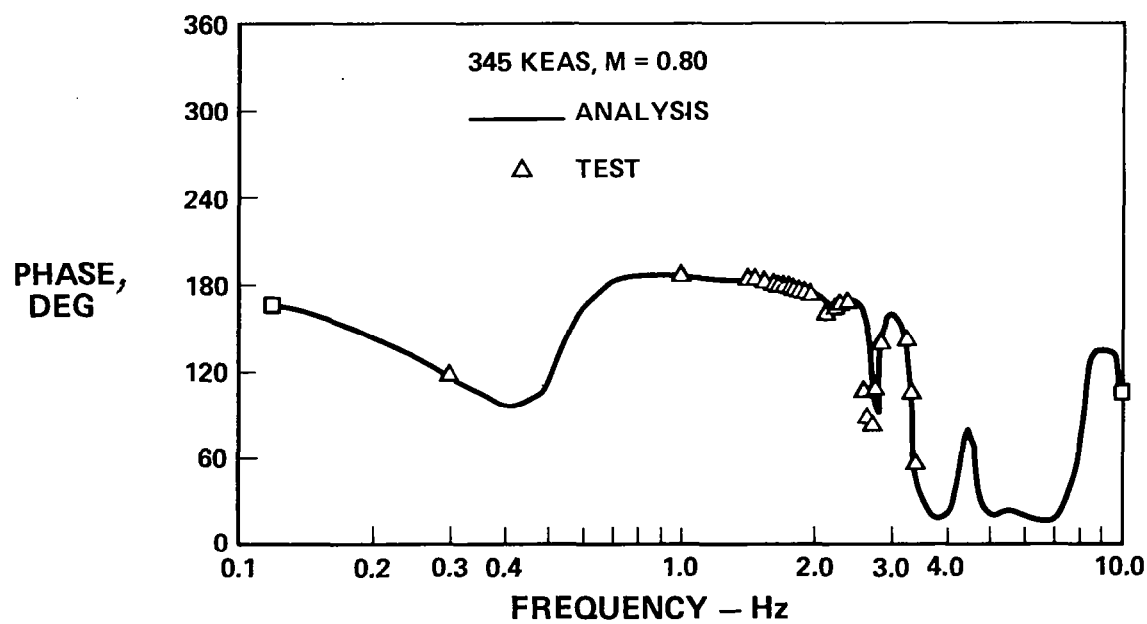

(b) Phase.

Figure 11.- Pilot acceleration — stabilizer drive ACS OFF.

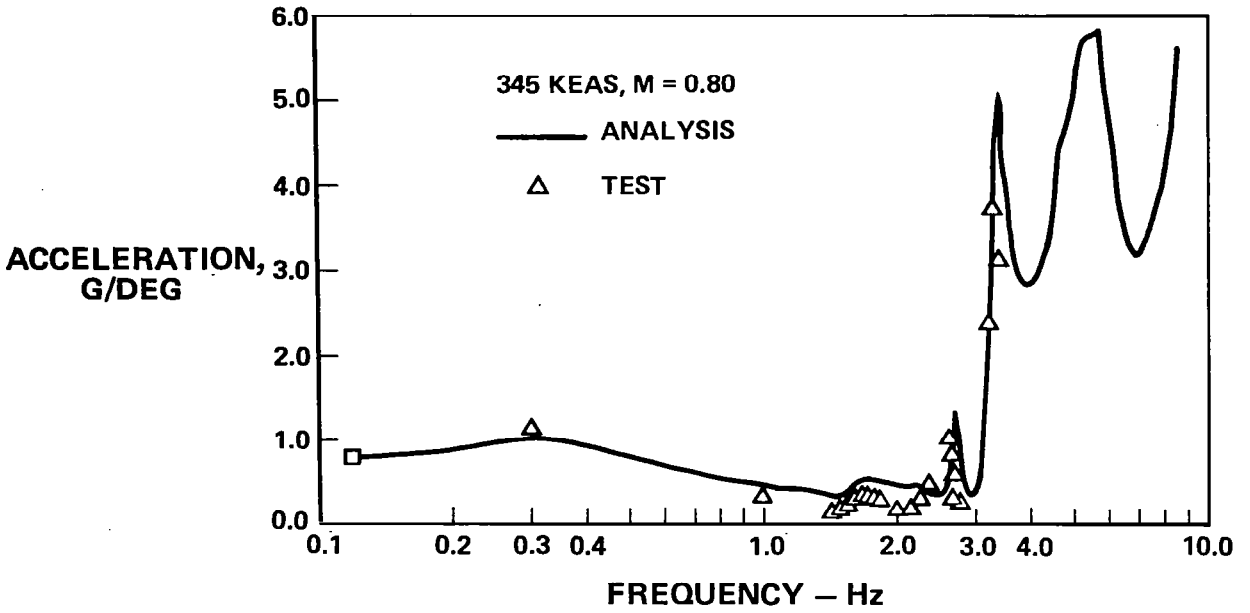

(a) Magnitude.

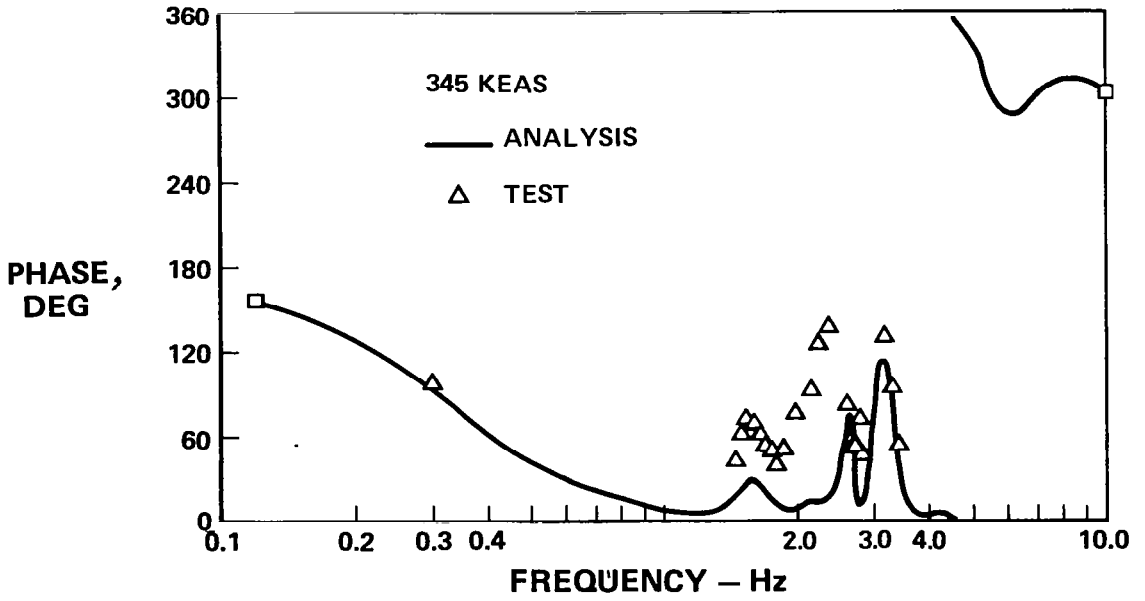

(b) Phase.

Figure 12.- Stabilizer tip acceleration — stabilizer drive ACS OFF.

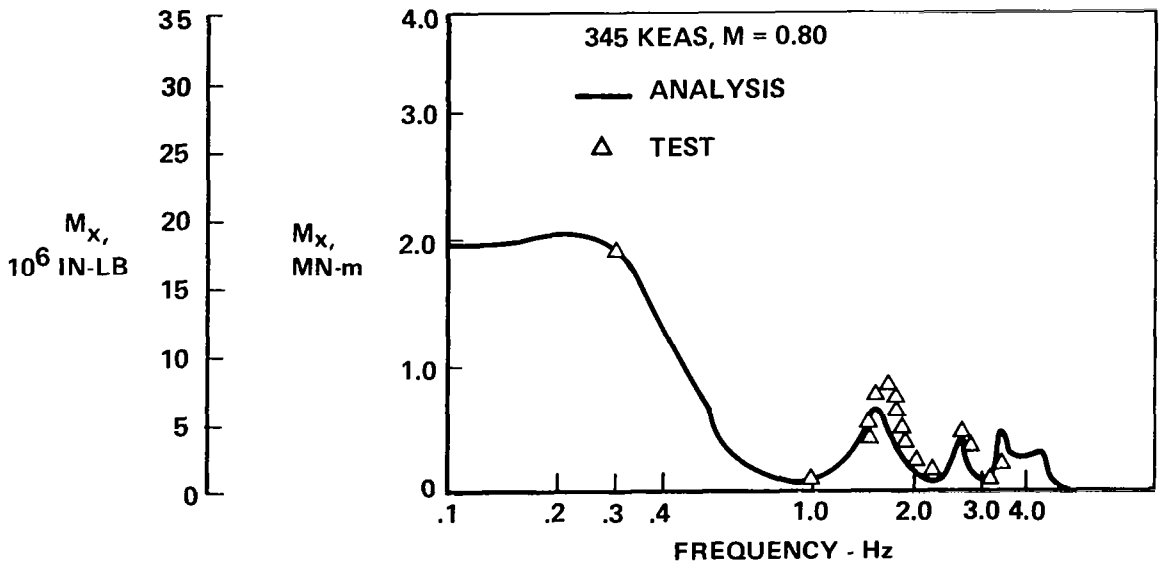

Figure 13.- Wing bending moment at BL 183/degree stabilizer.

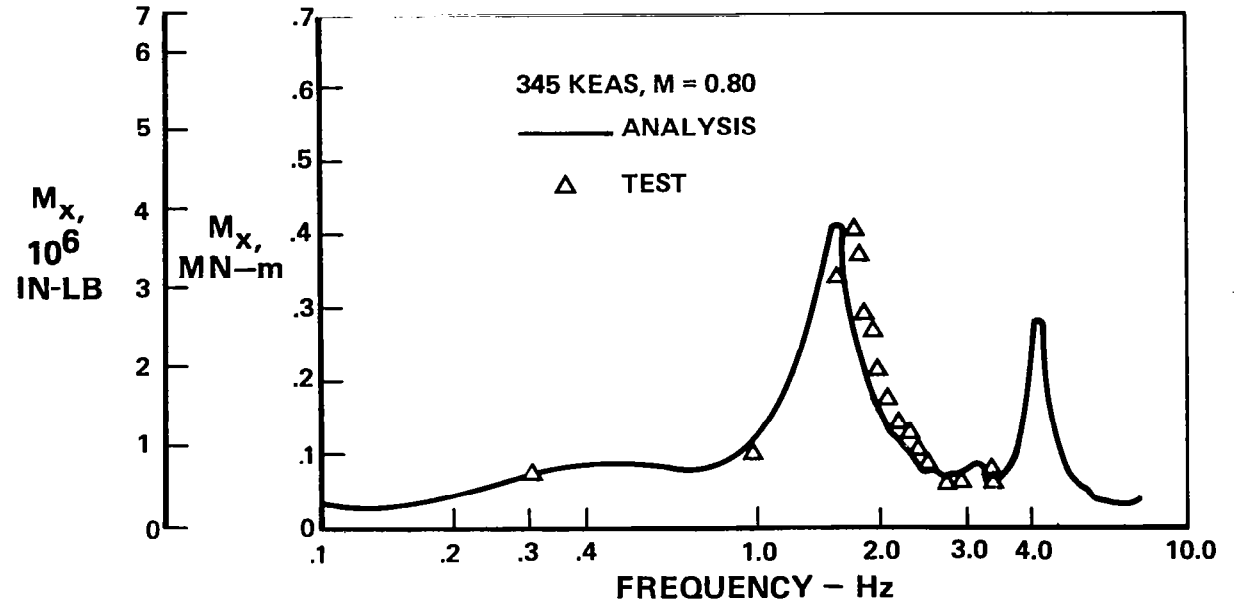

Figure 14.- Wing bending moment at BL 183/degree aileron.

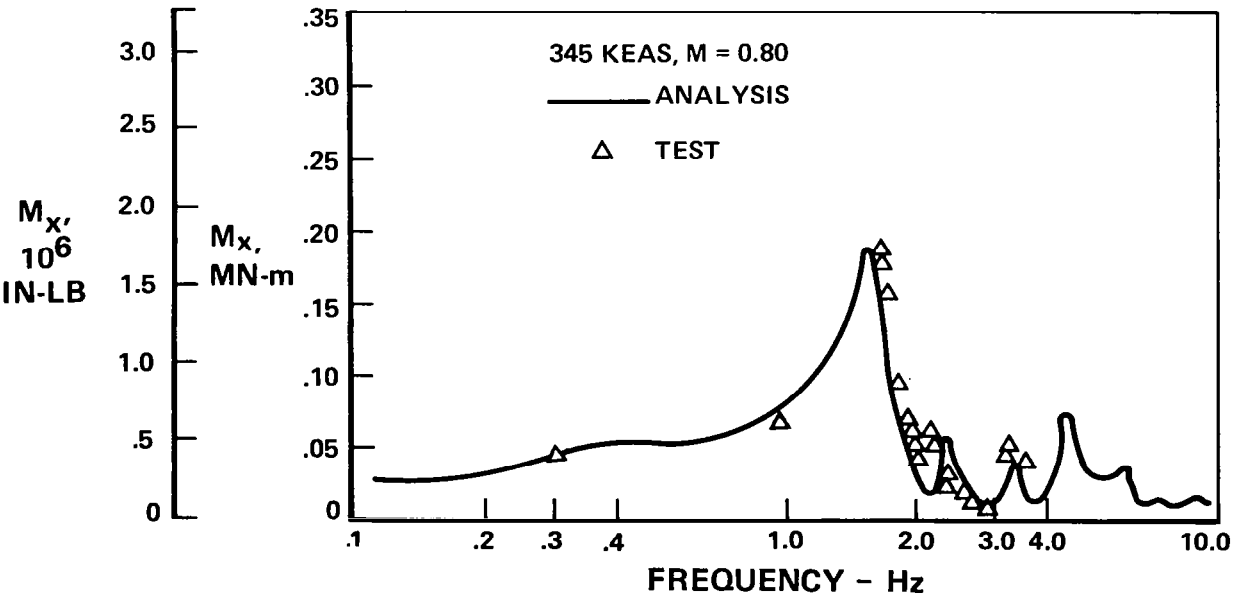

Figure 15.- Wing bending moment at BL 487/degree aileron.

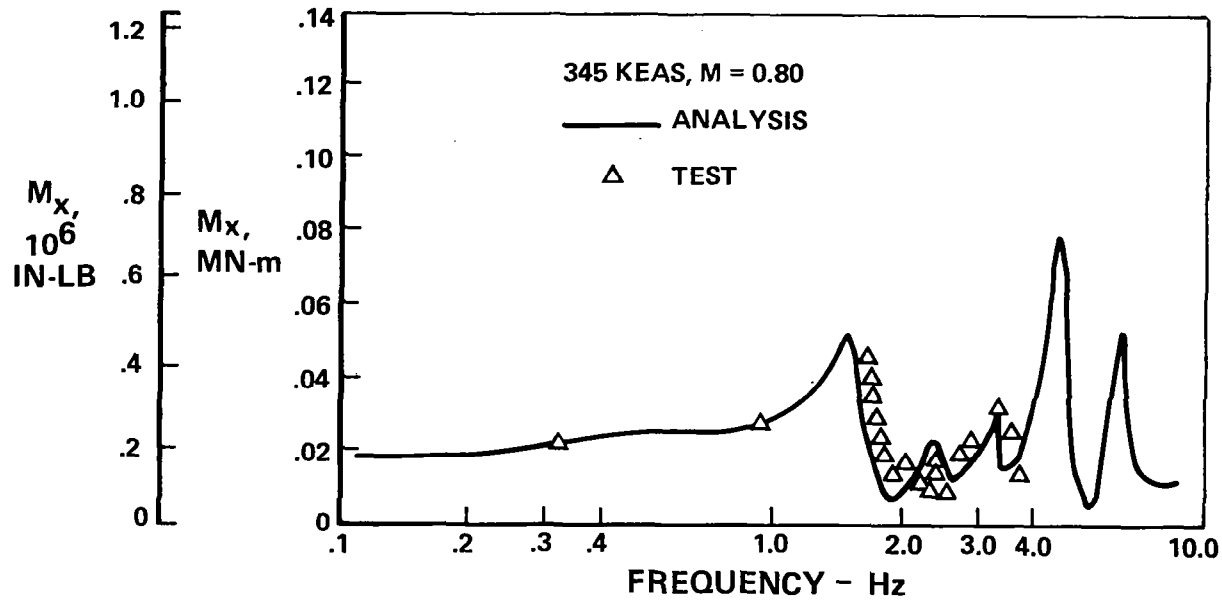

Figure 16.- Wing bending moment at BL 702/degree aileron.

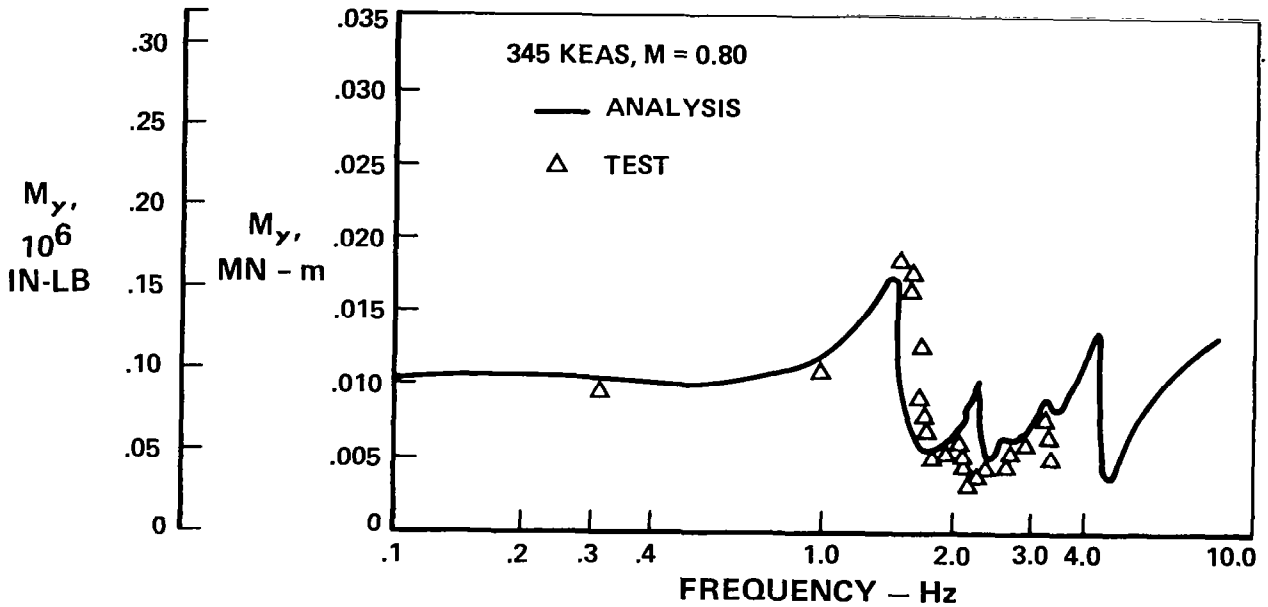

Figure 17.- Wing torsion moment at BL 702/degree aileron.

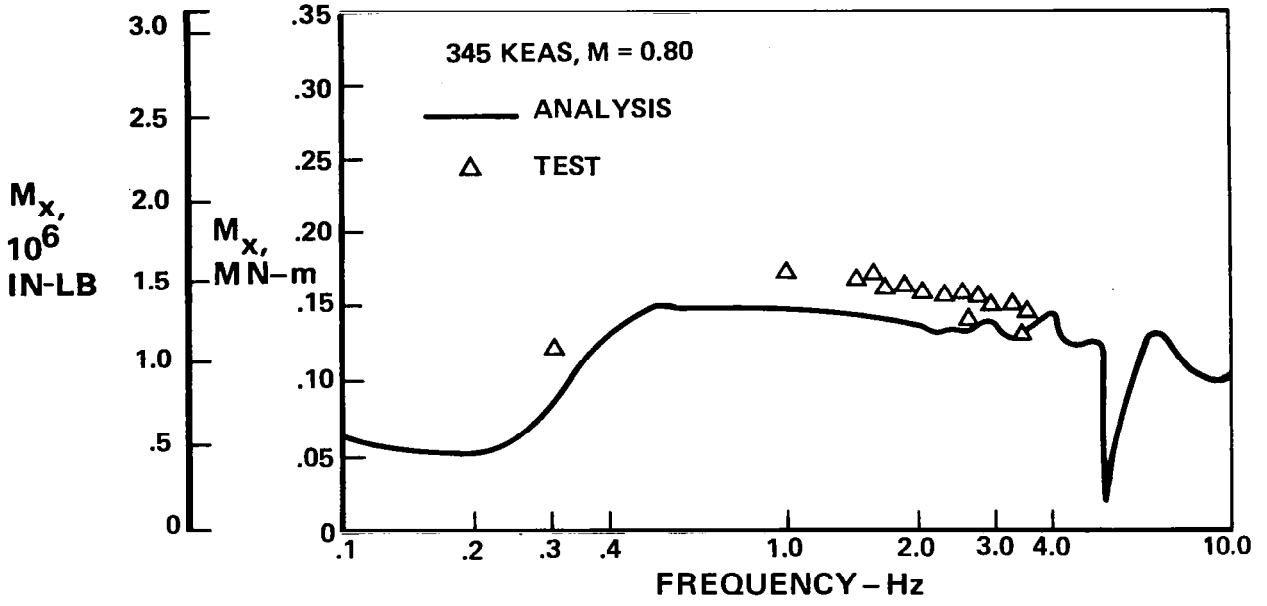

Figure 18.- Horizontal stabilizer bending moment at BL 126/degree stabilizer.

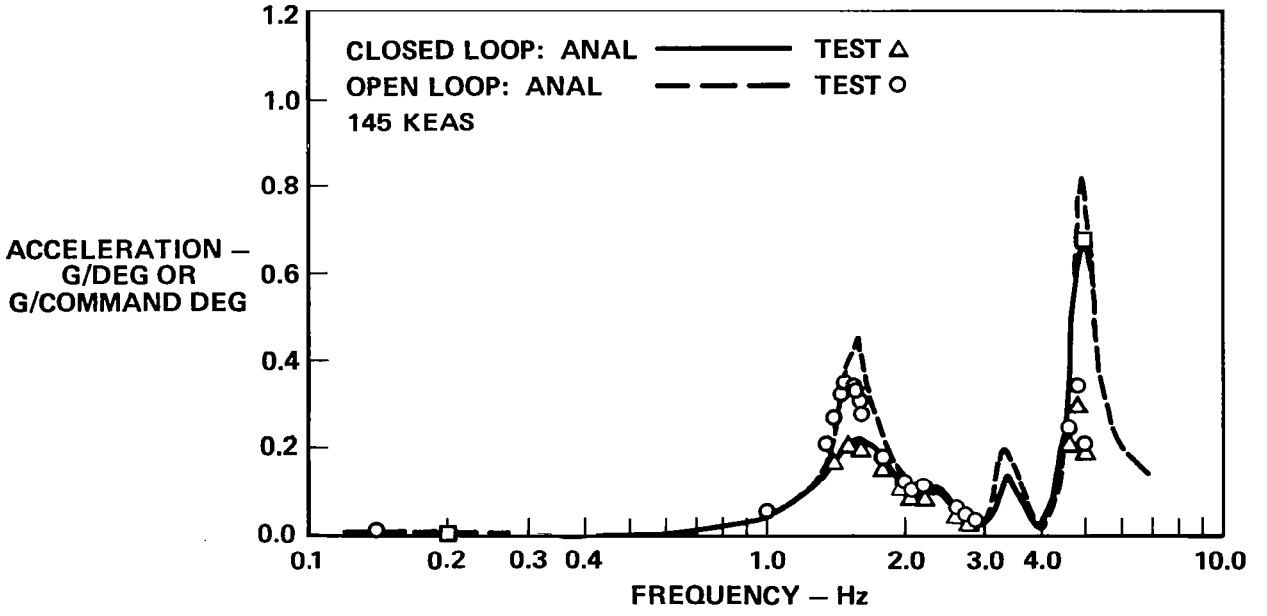

Figure 19.- ACS ON/OFF comparison wing-tip acceleration — aileron drive.

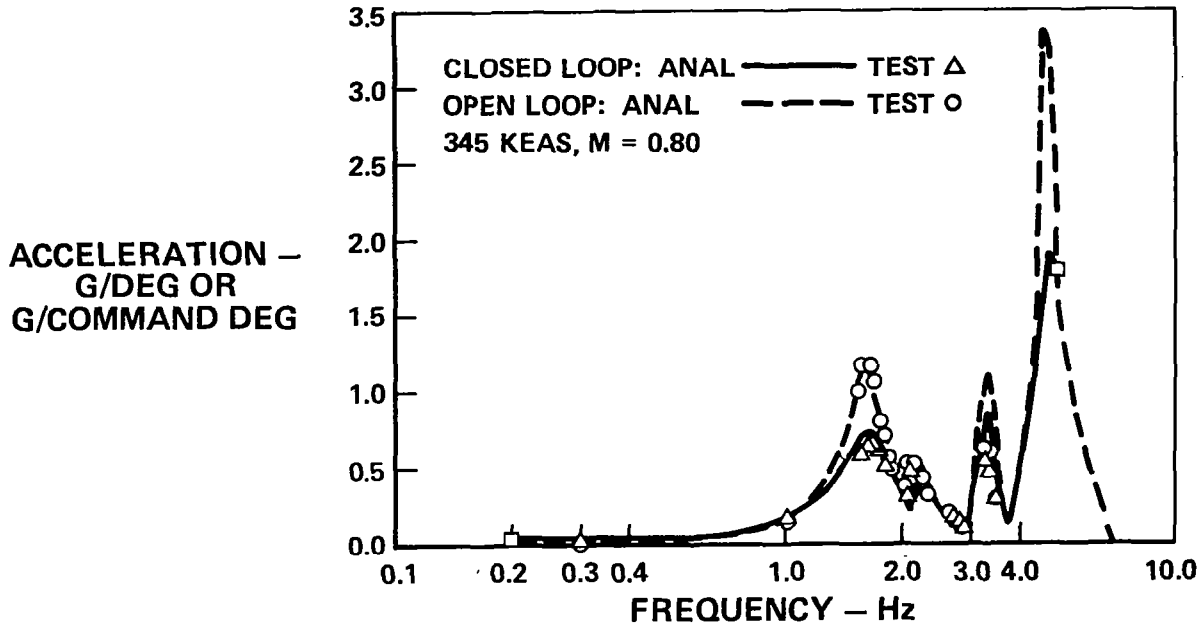

Figure 20.- ACS ON/OFF comparison wing-tip acceleration — aileron drive.

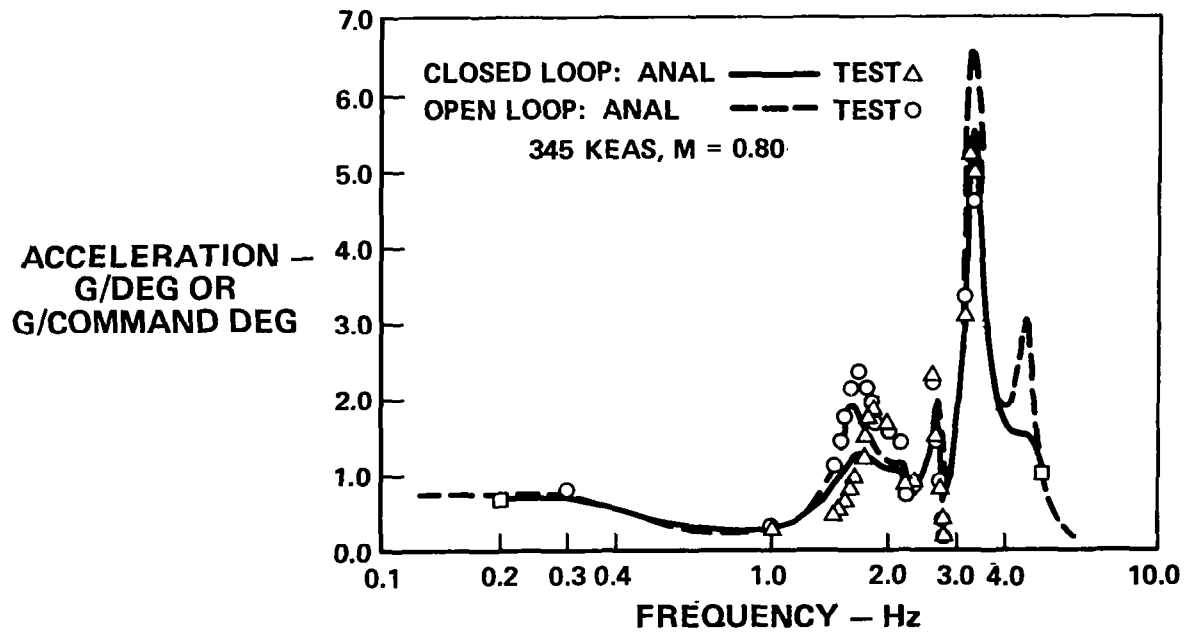

Figure 21.- ACS ON/OFF comparison wing-tip acceleration — stabilizer drive.

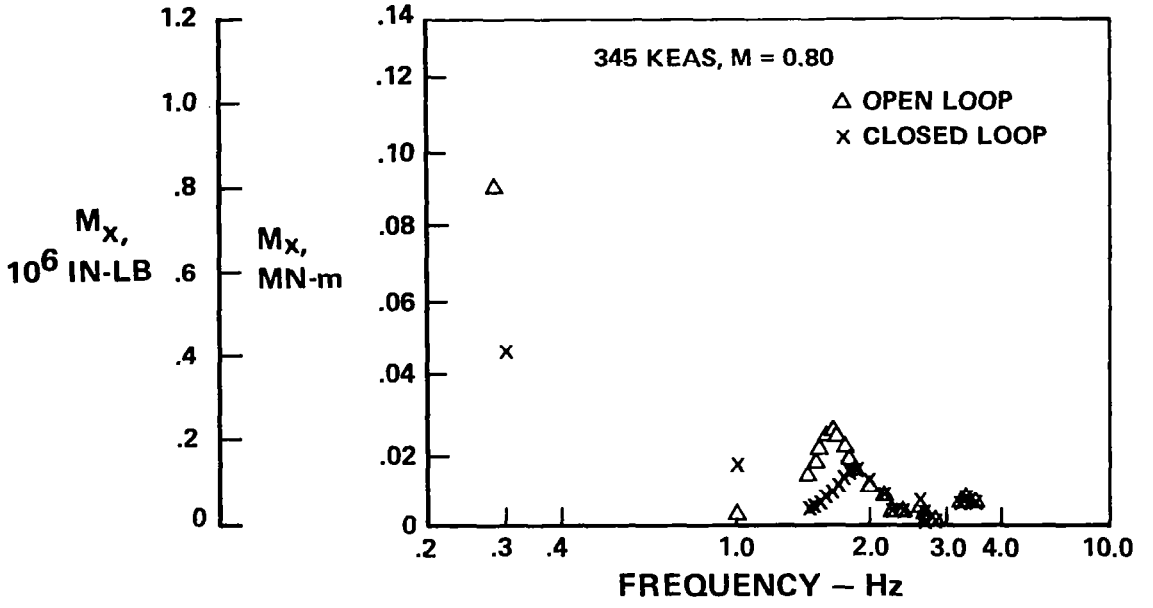

Figure 22.- Wing bending moment at BL 487/volt command stabilizer.

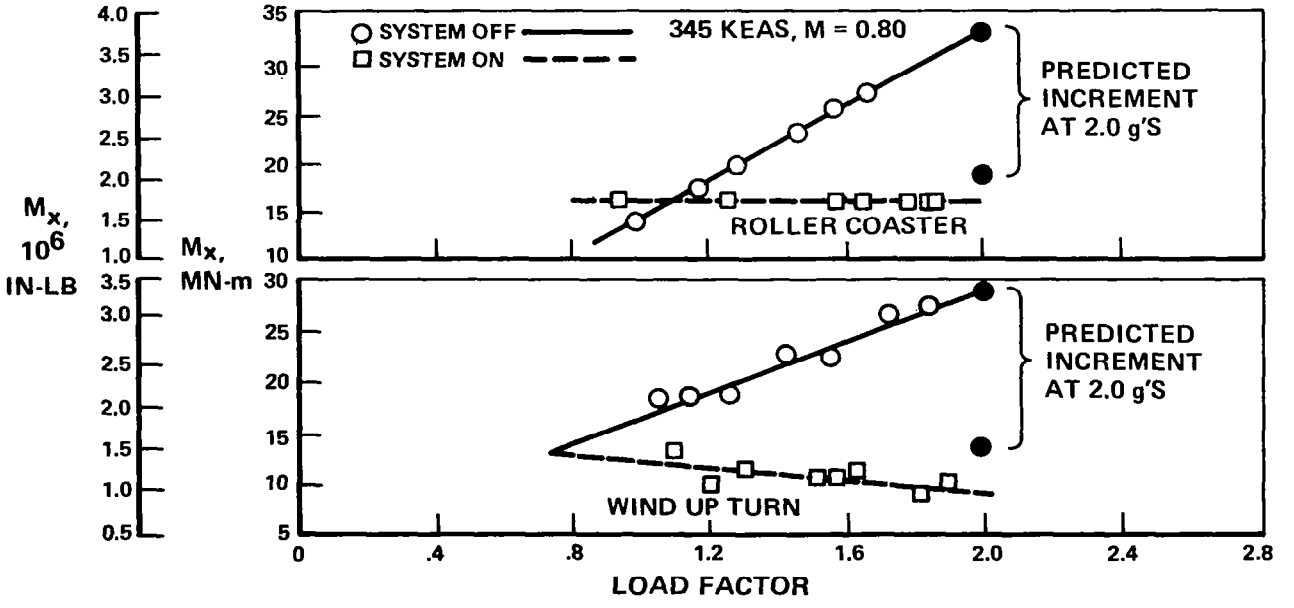

Figure 23.- BL 702 bending moment as function of load factor LC-1M.

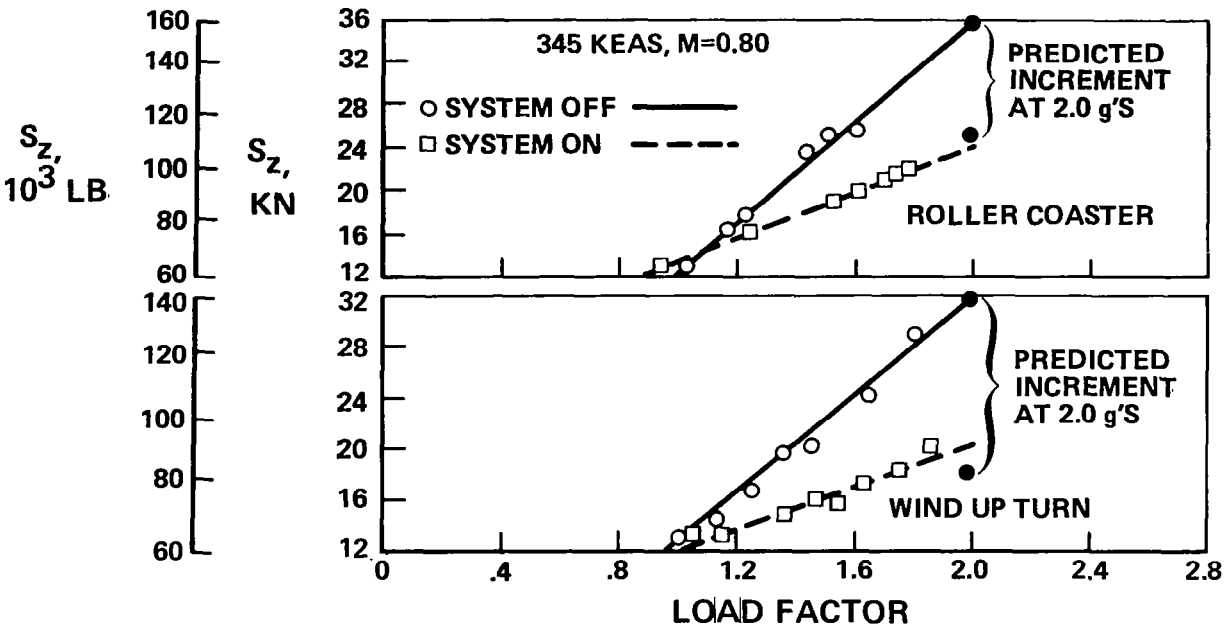

Figure 24.- BL 702 shear as function of load factor LC-1M.

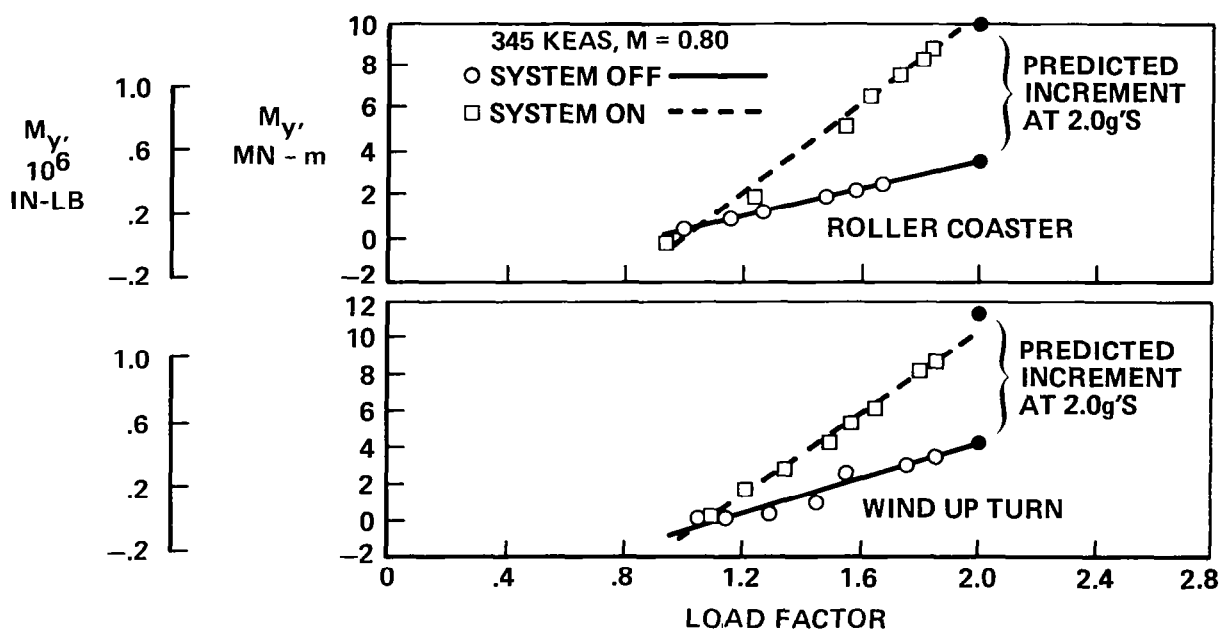

Figure 25.- BL 702 torsion moment as function of load factor LC-1M.

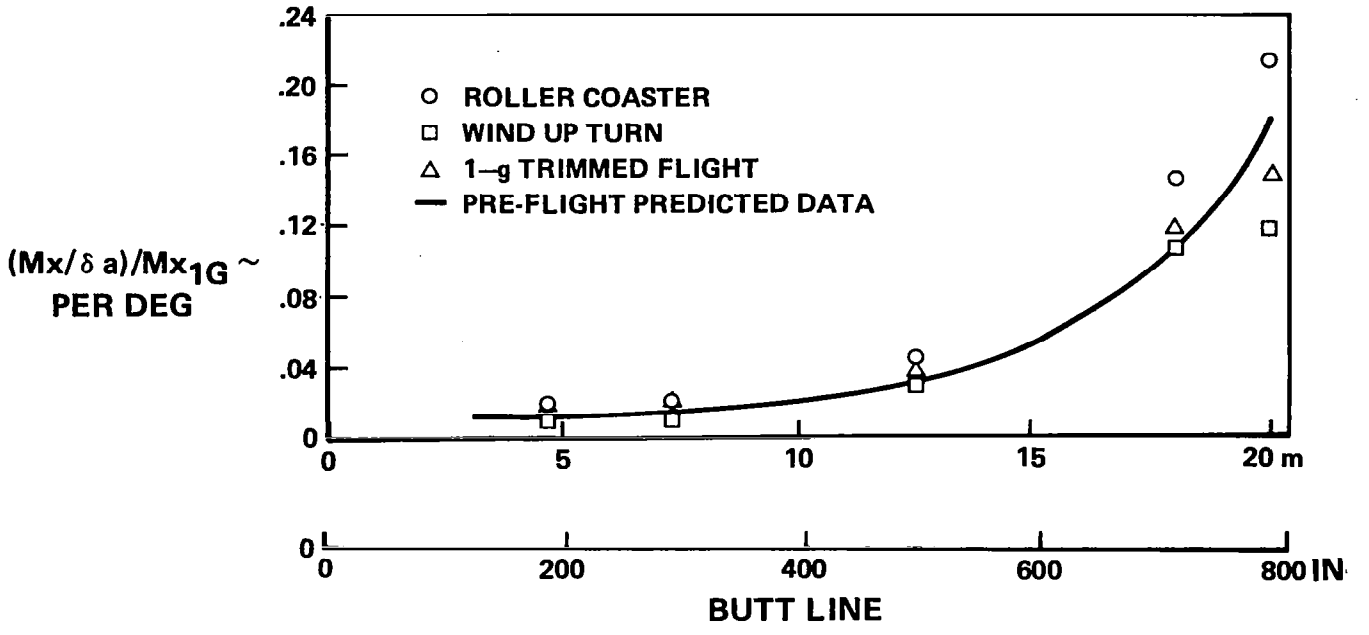

Figure 26.- Relative bending moment.

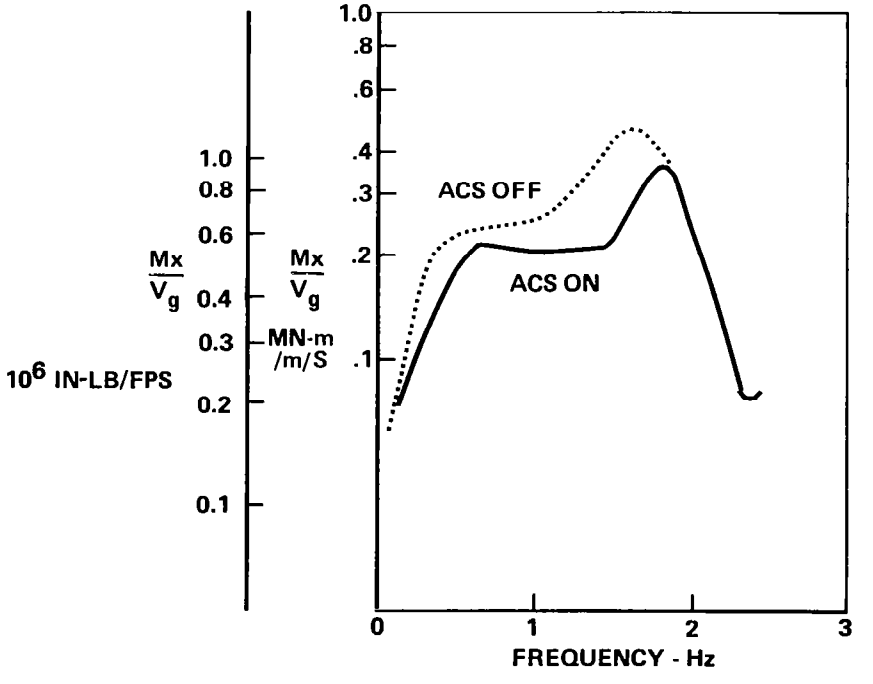

Figure 27.- Wing load in turbulence.

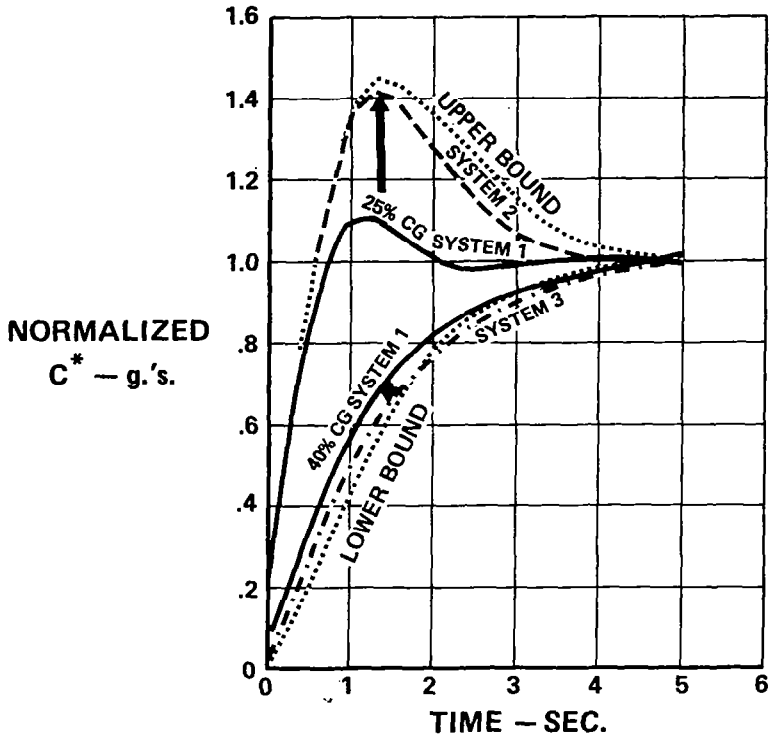

Figure 28.- Effect of feed forward on C* response (cruise).

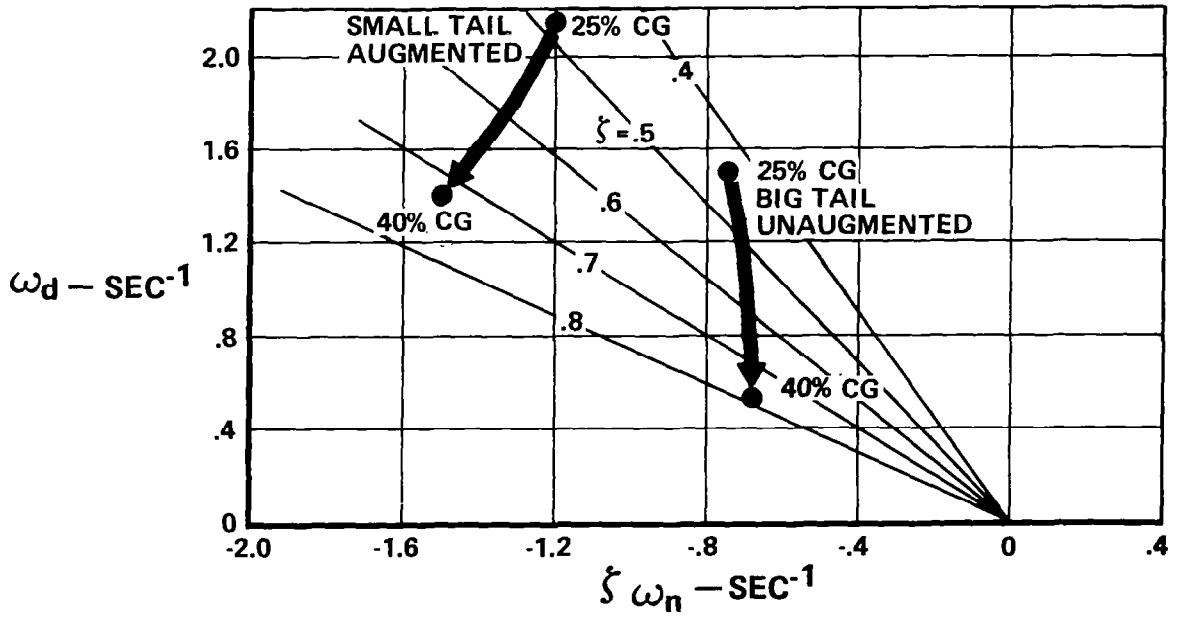

Figure 29.- Root loci — baseline and augmented small tail (cruise).

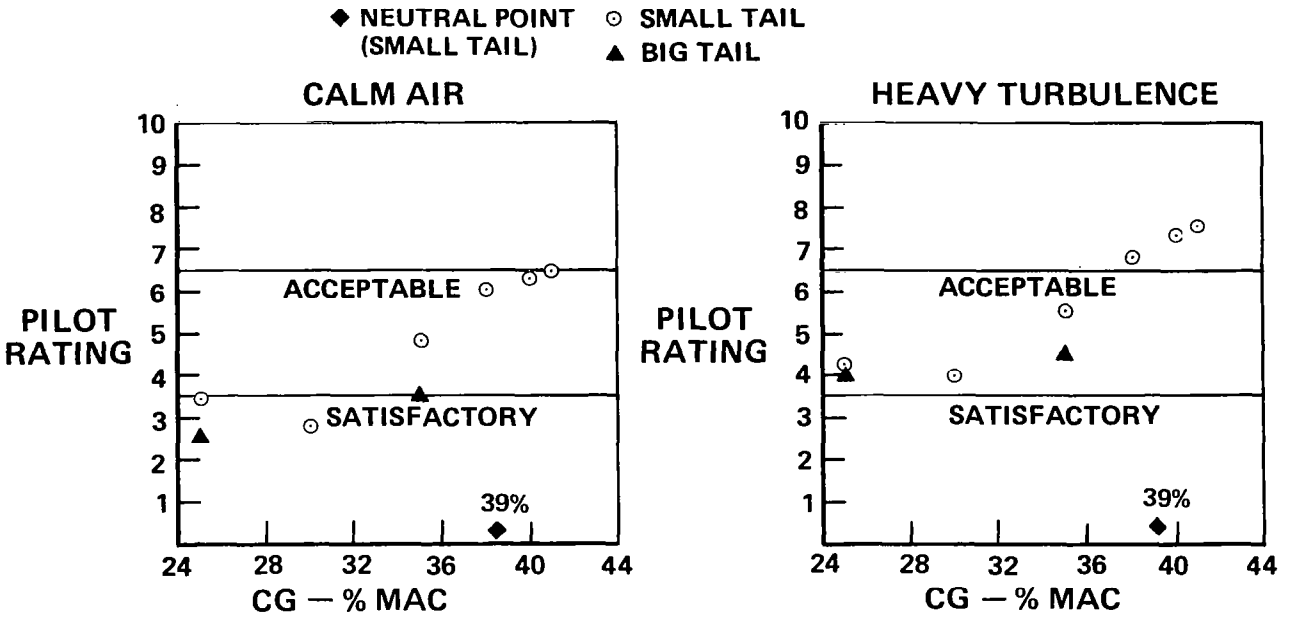

Figure 30.- Unaugmented cruise flying qualities.

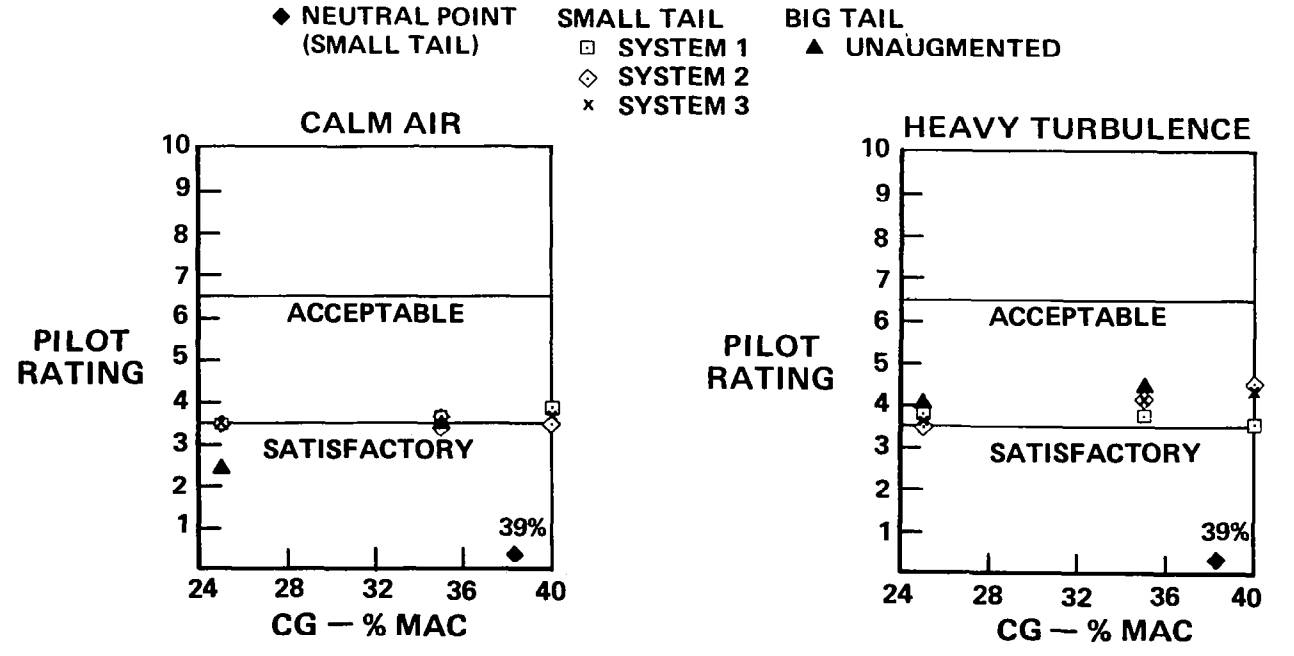

Figure 31.- Augmented cruise flying qualities.

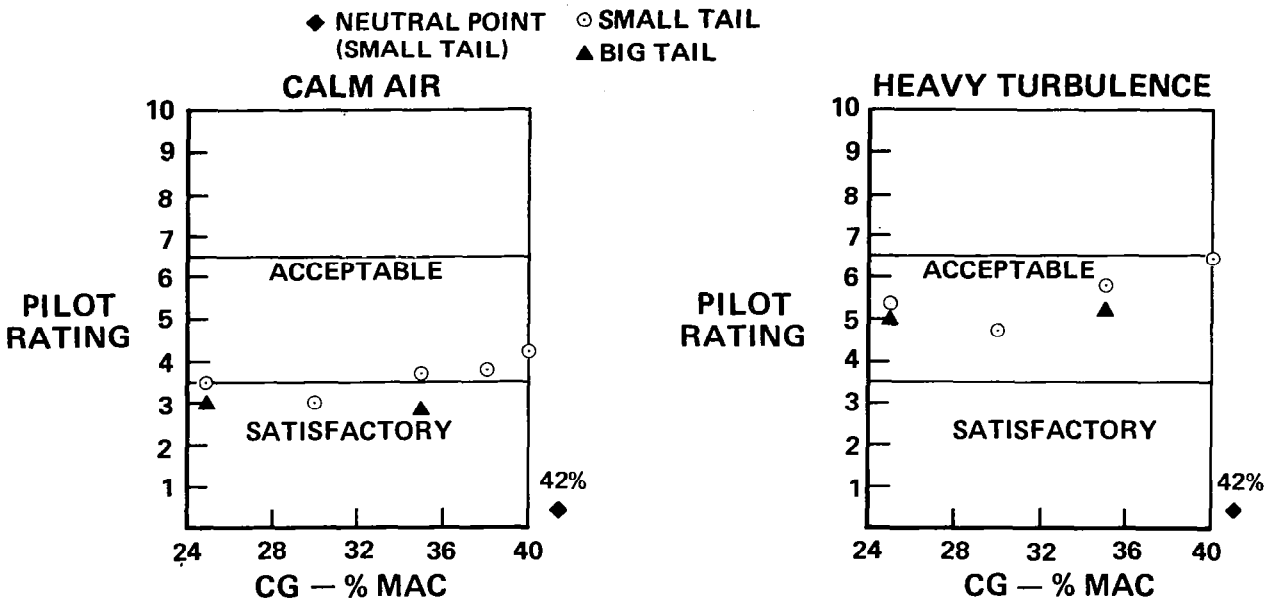

Figure 32.- Unaugmented approach flying qualities.

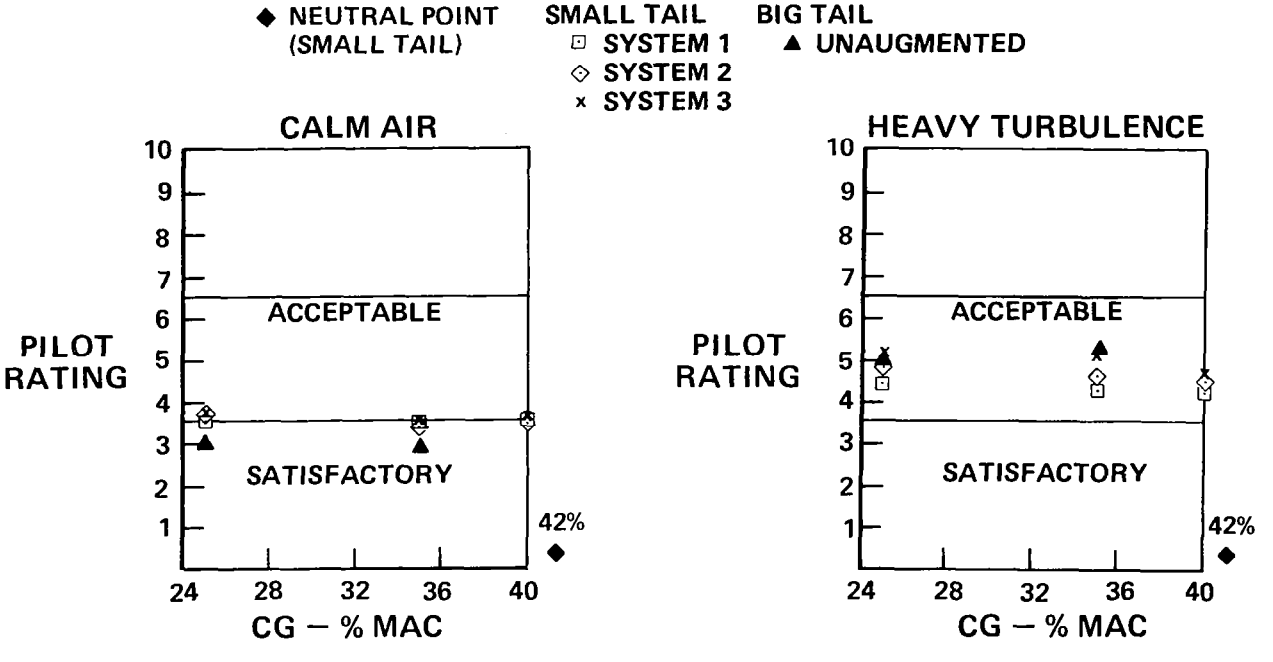

Figure 33.- Augmented approach flying qualities.

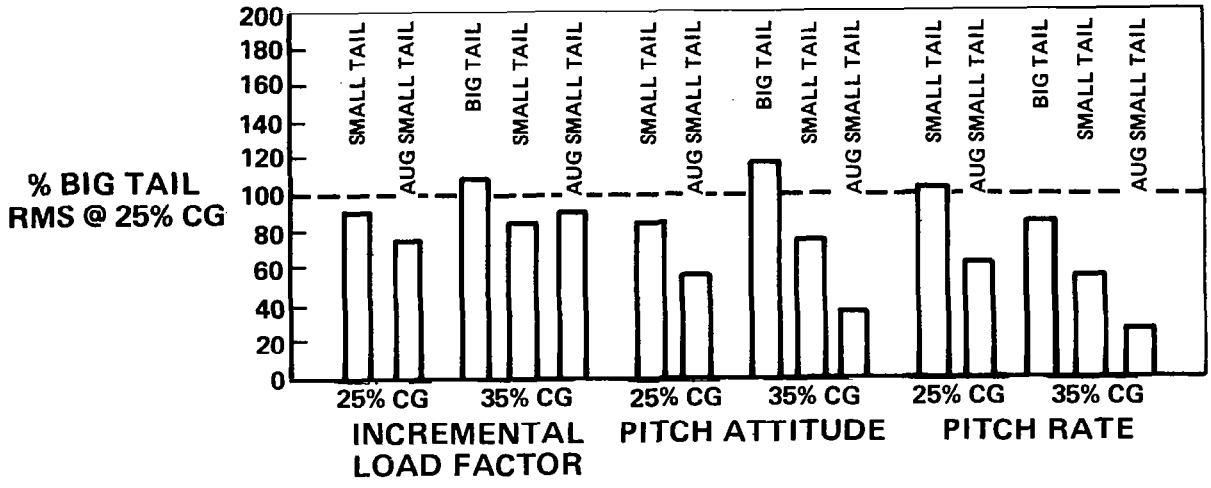

Figure 34.- RMS sirframe response — cruise.

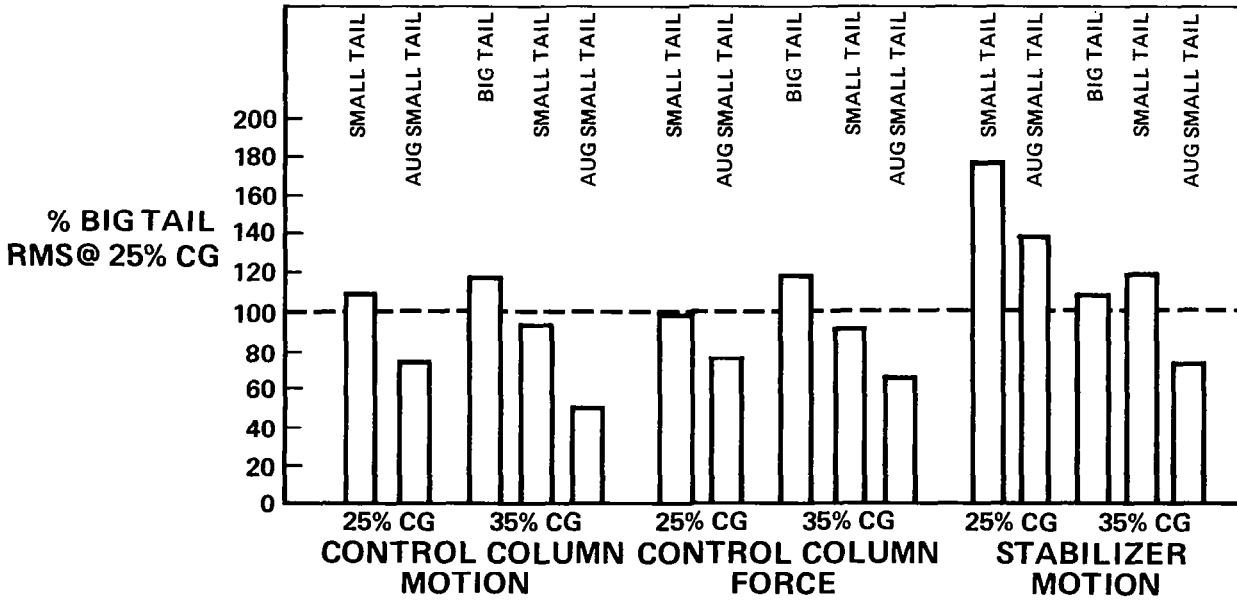

Figure 35.- RMS control activity — cruise.

ADVANCED AERODYNAMICS AND ACTIVE CONTROLS FOR A NEXT GENERATION TRANSPORT*

A. Brian Taylor
Douglas Aircraft Company

SUMMARY

Studies and developments for the Douglas DC-X-200 are described. In aerodynamics, the use of new and flexible tools for the design of supercritical wings is discussed. Trends in the design and performance of high-lift devices are outlined. In the field of active controls, the determination of suitable configurations with regard to flying qualities is described, particularly related to results from a piloted simulation.

INTRODUCTION

By the nature of today's market pressures, the next generation of transports will require a substantial technical advance. At the same time, the introduction of new technology must be guided both by sound economic guidelines and technical acceptance by operators and regulatory bodies. At Douglas, studies for the next generation medium-range transport have focused on the DC-X-200. The DC-X-200, shown in figure 1, is a major derivative of the DC-10, which is an "energy efficient" transport of its generation.

During studies of the DC-X-200, the NASA Aircraft Energy Efficiency (ACEE) program was introduced to accelerate the incorporation of new technology. The ACEE Energy Efficient Transport (EET) program was directed toward the application of advanced aerodynamics and active controls. This effort has been a useful stimulus to development on the DC-X-200 of concepts where promising advances were offered, and where previous cooperative work with NASA had been enjoyed.

The subsequent selection of tasks encompassed the following:

- Aerodynamics: The design and wind tunnel development of high-aspect-ratio supercritical wings. These tasks investigate the cruise speed regime and also high-lift development. Activities combine Douglas and NASA support.

- Configuration Design: The optimized design of a high-aspect-ratio supercritical wing and winglet combination. This work is still in a formative stage and is not discussed further in this paper.

- Active Controls: The determination of criteria, configuration, and flying qualities associated with augmented longitudinal stability of a level likely to be acceptable for the next generation transport; and the design of a practical augmentation system. These activities also combine Douglas and NASA support. In this paper, aspects of the flying qualities investigation will be discussed.

*Including work performed partially under NASA Contract NAS1-14744.

The gains predicted for these concepts can be evaluated in a number of ways. Two simple but effective measures are the improvements in direct operating cost (DOC) and fuel usage. DOC is one measure of the economics of the aircraft to which the particular technology concept contributes. Fuel reductions relate to energy efficiency.

The true quantification of the gains involves a complete aircraft configuration analysis, in which the relationships of all the factors may be represented. Such an analysis is beyond the scope of this paper. Instead, the effects of each concept will be noted independently.

The initially estimated goals for these concepts are shown below:

	Percent Reduction Relative to DC-10 Technology	
Concept	DOC	Fuel Burned
High-Aspect-Ratio Supercritical Wing	4.5	9.0
High-Aspect Ratio	(1.0)	(4.0)
Supercritical Wing	(3.5)	(5.0)
Advanced High-Lift System	1.9	1.5
Augmented Stability	0.5	1.7

The improvements in both DOC and fuel usage for each concept are substantial. Those associated with the high-aspect-ratio supercritical wing are the largest. The estimation is based on the assumption of high-lift system of the conventional standard which will be described later in the paper. An advanced high-lift system, when applied to this wing, results in a fuel reduction which is significant although smaller than that of the basic wing design. The reduction in DOC is important. As an additional benefit, the advanced high-lift system offers improvement in field length and community noise. The augmented stability derives its benefits from a smaller tail and reduced trim drag. The gains shown here reflect a conservative and low-risk design, but nevertheless are attractive. The technology of active controls is emerging, and a full evaluation of the benefits in this application must await the completion of the current study.

The starting point for the cooperative portions of the high-aspect-ratio wing development was a NASA test in May of 1977. This was followed by an intensive Douglas-funded effort for the design of modified wings to be tested in the EET program. These tests will occur throughout 1978. The high-lift design work is also funded by Douglas. The EET program sponsors both evaluation tasks and the wind tunnel tests which will be conducted in 1978.

The stability augmentation system study was initiated with Douglas funds. An extensive piloted simulation program which explored flying qualities has been completed. The augmentation system design is continuing and will be tested in an extensive piloted simulation early in 1978.

SYMBOLS AND NOMENCLATURE

Values are given in SI and U.S. Customary units. Measurement and calculations were made in U.S. Customary units.

$\mathcal{C}_L$	Aircraft centerline
C_L	Lift coefficient
$C_{L_{MAX}}$	Maximum lift coefficient
C_p	Pressure Coefficient
L/D	Lift-to-drag ratio
MAC	Mean aerodynamic chord, used nondimensionally
OWE	Operational empty weight, kg (lb)
PIO	Pilot-induced oscillation
TOFL	Takeoff field length, m (ft)
TOGW	Takeoff gross weight, kg (lb)
$V_{APPROACH}$	Landing approach speed, m/s (KEAS)
VCK	Variable Camber Krueger, a type of leading edge flap
V_{STALL}	Stall speed at a given configuration, m/s (KEAS)
θ/θ_c	Ratio of pitch attitude to pitch attitude commanded (closed loop resonance), expressed in dB

HIGH-ASPECT-RATIO SUPERCRITICAL WING – HIGH-SPEED DEVELOPMENT

The development of the high-aspect-ratio wing for the DC-X-200 has resulted from advances in technology closely applied to aircraft configuration analyses and trade studies. This section will emphasize aspects of the wing design with reference to those configuration considerations which have posed significant problems.

Development and Configuration Considerations

The wing design has utilized both two-dimensional and three-dimensional high Reynolds number data on supercritical wings obtained by Douglas over the past 10 years, as well as data provided by Dr. R. T. Whitcomb's work at NASA Langley (reference 1). However, the wing of the DC-X-200 differs

from today's standard, as typified by the DC-10, not only in its airfoil design, but also in the manner in which the design philosophy and other advanced technologies impact the overall configuration. An example of these interactions and their effects on the wing design can best be shown by the impact of just two of these variables – the requirement for fuel conservation and the incorporation of an advanced high-lift system. The requirement for minimum fuel dictates a configuration where the advantage of the supercritical airfoil is taken out in a wing which is thicker and has a higher aspect ratio than that of today's transports. The higher aspect ratio, in turn, requires that the wing be designed to higher lift coefficients so that the full potential of the aspect ratio can be used. For example, the C_L for optimum cruise for a typical conventional wing with an aspect ratio of 7 is 0.49. For a high aspect ratio of 10.5, typical of the DC-X-200 designs, the optimum C_L is nearly 0.6.

The impact of the advanced high-lift system on this design is the allowance of a smaller wing area. This combination of a relatively small wing spread over a larger span produces the most difficult problems of the wing design and design integration. Integration introduces requirements for structure and the housing of landing gears, which result in the aft extension of the small chord at the fuselage side and in a large inboard trailing edge extension. Two additional features, in themselves favorable to fuel conservation, compound the problem by requiring an aft movement of the landing gear relative to the wing. These features are the wing-mounted, high-bypass-ratio engines and the relaxed static stability. Figure 2 shows a planform comparison of the DC-10 and a DC-X-200 type wing, and indicates the landing gear locations. The landing gear location is approximately 7 percent further aft on the high-aspect-ratio wing. During the early development of the DC-X-200 wing, the size of the inboard trailing edge extension caused an effective loss of sweep over the inboard wing and difficulties at the trailing edge kink.

Wing Design

Because of the sensitivity of wing weight on fuel requirements and direct operating cost, obvious solutions to the design integration problems such as in increased wing area were rejected in favor of a solution which would not jeopardize the economics or fuel efficiency of the aircraft.

With this objective in mind, an extensive study was undertaken to define the configurations to be tested during 1978. In addition to wind tunnel data, the theoretical analyses included considerable use of a Douglas-developed version of the Jameson 3-D transonic method published in reference 2.

Figures 3 and 4 indicate the breadth of configuration analysis contained in the definition of the wings for the EET models. They also indicate the flexibility and design capability of the Douglas-Jameson program. The test configurations are wings W_3, W_4 and W_5. Figure 3 shows the first half of the entire matrix that evolved during the development of the test wing designs. Figure 4 shows the second half. The study baseline was wing W_A, a configuration closely resembling the configurations W_1 and W_2 from a previous cooperative test program. The initial configuration proved to have inadequate transonic performance as a result of the large trailing-edge break and the airfoil sections. Perturbations and variations in twist, planform, and airfoil sections were therefore examined. Some of these perturbations were imposed by aircraft configuration and system studies.

One of the more interesting developments that resulted from the study is the effect of a small leading-edge glove on the inboard shock development. Figure 5 shows isobar plots (lines of constant pressure) provided by the program. Isobars for the wing with no glove illustrate a concentration of

lines representing a shock wave near the midchord. Significant upsweeping of the shock is evident at the root. With the leading-edge glove added, the shock is significantly weakened. Similar effects have recently been verified experimentally by Dr. Whitcomb.

Figure 6 illustrates the improvement in the upper-surface pressure distribution between the initial baseline W_A and the first test wing W_3. The strong aft shock evident in the W_A pressure distribution has been suppressed and its position brought significantly farther forward.

After completion of the design for wing W_3, a more detailed analysis indicated that buffet C_L could be substantially improved with a planform and twist modification. The primary variation in planform was to extend the chord at the outboard trailing-edge break. An upper-surface pressure distribution at 0.8 semispan is compared with that for wing W_3 in figure 7. The Mach number ahead of the shock is suppressed further, and the shock is moved significantly farther forward to allow the boundary layer a better chance to recover to the airfoil trailing edge.

Further performance potential has been indicated for wing W_5. Its airfoils included a reduced leading-edge thickness to address sensitivity to premature drag creep before drag divergence. Furthermore, the test configuration will investigate the effect of increased aft camber. This characteristic tends to improve buffet C_L, provided viscous effects do not cause excessive losses. The test configurations will enable the leading edge of wing W_4 to be combined with the trailing edge of W_5 and vice versa. Hence, the effects of the leading-edge and trailing-edge modifications can be evaluated separately as well as together. The predicted effect of the leading-edge and trailing edge modifications is indicated in figure 8. The reduced leading-edge thickness suppresses the C_p plateau level ahead of the weak shock which exists at approximately 40-percent chord on wing W_4. The increased aft camber increases the C_p plateau level in the aft region.

Figure 9 shows the estimated percent buffet C_L improvements for wings W_4 and W_5 relative to wing W_3. An approximate improvement of 6 percent is shown for W_4, while a 9-percent improvement is indicated for W_5.

Experimental Development

It is important for proper experimental assessment of the higher cambered supercritical airfoils to have a high Reynolds number capability. This need is enhanced by the relatively small chords associated with the high aspect ratio. For this reason, the NASA Ames 11-foot transonic wind tunnel will be used in the development testing.

The test model consists of components of the DC-X-200 design. The model includes the fuselage, nacelle installations, wing configurations, and the tail surfaces. The horizontal stabilizer has variable incidence capability. Pressure instrumentation will be included in the wing.

HIGH-ASPECT-RATIO SUPERCRITICAL WING – HIGH-LIFT DEVELOPMENT

It may seem self-evident that advances in high-lift systems will be justifiable for a new transport, but the choices need careful consideration. Furthermore, their development for supercritical wings is not yet completed. The promise of increased fuel savings, reduced noise characteristics, and improved

economics must be determined in the context of aircraft configuration studies and validated by design analyses, test, and evaluation. These activities have indicated customer requirements and appropriate mechanical systems which appear to satisfy these requirements. The verification process is to design and test a high-lift development model for the configuration which incorporates supercritical airfoil technology, a high-aspect-ratio wing, and augmented longitudinal stability.

The aerodynamic design of the advanced high-lift system for the wind tunnel model has been based on two- and three-dimensional analysis techniques and related experimental results. Combined potential and viscous programs have been utilized to design the high-lift shapes, with the experimental data base as a guide to acceptable pressure peaks and gradients.

Comparison With a Current Wide-Body Transport

Significant low-speed performance gains may be shown for the advanced configuration compared with current wide-bodied transports. These gains result from the increased aspect ratio, supercritical airfoil, and the high-lift system just described. For example, in takeoff lift-to-drag ratios (L/D), there is a 32 percent increase at the respective 1.2 V_{STALL} limit. This is accompanied by a 50-percent increase in $C_{L_{MAX}}$ for the takeoff flap deflections. Such substantial increases in performance result in reduced flyover noise and smaller takeoff field length requirements when compared to existing aircraft.

Because the approach noise condition is often more critical, the improvement in landing performance is even more significant. The design indicates a large increase in approach L/D, figure 10. For a 1.3 V_{STALL} condition the increase in L/D is approximately 44 percent. The $C_{L_{MAX}}$ increase for the advanced configuration is approximately 30 percent larger.

Impact of the High-Lift System Alone

A comparison of the effect of the high-lift systems alone is also of value. For this comparison, aircraft configurations with, respectively, a conventional and an advanced high-lift system have been formulated. The configurations both utilize the aspect ratio, planform, and airfoil of the W_A wing previously described.

The conventional and advanced configurations are shown in figure 11. The conventional system utilizes a circular arc motion trailing-edge vane flap and a leading-edge slat. The inboard and outboard flap systems are separated by a high-speed aileron which is undeflected in the high-lift mode. The selected advanced high-lift components include an inboard and outboard two-segment flap system. A flaperon, which is deflected during takeoff and landing, is located between the inboard and outboard flaps. The leading-edge high-lift device is an inboard and outboard Variable Camber Krueger (VCK). At low speed the lateral control is obtained by an aileron, which extends from the outboard flap to the wing tip, and spoilers. Chordwise sections are shown in figure 12.

For the $C_{L_{MAX}}$ variation with flap deflection, the advanced system indicates a gain of approximately 20 percent for the various flap deflections (figure 13). The improved $C_{L_{MAX}}$ is due to the larger flap extension, the increased high-lift capability of the leading-edge device, and the increments in lift due to the flaperon deflection.

The change in takeoff L/D characteristics between the advanced and conventional high-lift systems is shown in figure 14. The L/D curves presented are determined by the envelope of L/D for various flap deflections which would be used in the takeoff mode. An 11-percent gain in L/D is shown at the largest C_L values. At the maximum C_L value for the conventional high-lift system, an increase in L/D of 23 percent is indicated.

Figure 15 indicates that for landing approach, incorporation of the advanced system increases the approach L/D by some 18 percent, and this figure would result in significant reduction in the critical area of approach noise. A more uniform span load distribution with the deflection of the flaperon and the improved drag characteristics of the advanced high-lift components are two sources of the improvement in L/D characteristics.

The design range for the evaluation aircraft is 5556 km (3000 n mi). At this range, a savings of 0.6 percent of fuel burned is obtained by the configuration incorporating the advanced system relative to the one using the conventional system. More significant, however, is the stage length at which the aircraft is most commonly to be used. The average stage length is expected to be 1389 to 1852 km (750 to 1000 n mi). At these ranges, fuel savings on the order of 1.6 to 1.3 percent, respectively, are indicated.

The results of the sizing comparison are shown in table 1. Takeoff weight, operational empty weight, and wing area are the configuration characteristics represented. The conventional configuration is sized by the approach speed requirement, leading to an initial cruise altitude slightly larger than the mission requirement of 10,363 meters (34,000 feet). The advanced configuration is sized by this requirement. The resulting approach speed is nearly 3 m/s (5 KEAS) less than the mission requirement. The respective wing areas are approximately the same size. However, the advanced configuration has a significantly reduced takeoff field length. Moreover, the improved L/D characteristics will reduce noise levels for both takeoff and landing operations.

Experimental Development

The wind tunnel tests are planned for the Ames 12-foot facility. This tunnel offers the high Reynolds Number capability of nearly 2 million per meter (6 million per foot) which is considered important in developments of this nature. Furthermore, the tunnel offers a Mach number sweep capability.

The configuration selected for test reflects the advanced system with the refined wing planform and airfoil sections previously described, and is illustrated in figure 16. High-lift components will include capability for changes in deflection and position. A low-speed aileron and spoilers are also included in the model components. The wind tunnel model will include pressure instrumentation on the wing and high-lift components.

AUGMENTED LONGITUDINAL STABILITY SYSTEM STUDY

Augmented stability in the DC-X-200 is aimed at matching the known and satisfactory handling qualities of the DC-10, when augmented, and provision of a satisfactory level of handling when unaugmented. In spite of the current rapid progress in active controls, there is much in this field still to be studied and understood. The Douglas EET activity, therefore, covers the design tasks with a thorough and disciplined study.

The study contains three distinct elements. The first is the formulation and verification of the aerodynamic data and flying qualities criteria, the determination of quantitative reliability requirements and the synthesis of the augmentation control laws. The flying qualities and configuration effects have been studied in detail, the study culminating in a piloted simulation in a six-degree-of-motion facility. Only the investigations concerning flying qualities will be discussed in this paper. The second element is the system configuration study consisting of the formulation, analysis, and selection of an architecture and then evaluation of the augmented aircraft. The third element consists of the estimations of the potential fuel savings, the verification of compliance with the proposed safety criteria, and the determination of the impact of relaxed stability on the aircraft certification. The second element is well advanced and will include, later this year, an elaborate simulation and evaluation on the six-degree-of-motion stimulator. The third element also is underway.

Scope of the Flying Qualities Work

The establishment of minimum acceptable levels of stability has been the subject of numerous investigations. A suitable solution requires the development and acceptance of evaluation criteria, a careful definition of the configuration characteristics, the prepararation of a realistic simulation model, and a comprehensive pilot evaluation.

Adequate evaluation needs a comprehensive data base. Very little useful data from wind tunnels are available for this type of configuration. Therefore, aerodynamic data were generated by analytical means and put in the form of linearized small-perturbation equations. These equations have been used primarily for control system design. Full flight-envelope equations were developed for use in the motion-base simulation. The extent of the representation has, it is believed, enabled a thorough exploration of flying qualities on the simulator.

The test was conducted on the Douglas six-degree-of-freedom motion simulator system which supports a complete simulated cockpit and provides realistic motion cues. The cockpit simulator is attached to a base supported by six hydraulic jacks. This configuration, shown in figure 17, has the arrangement developed by the Franklin Institute, with an improved performance unsurpassed by any system for the simulation of transport aircraft motion. Visual simulation for the cockpit is available from a Redifon visual flight attachment.

On the simulator, flying qualities of the unaugmented aircraft were examined through most of the flight envelope. This examination led to emphasis being placed on the cruise flight and landing approach conditions. Five test pilots, experienced in DC-10 and other transport handling evaluations, participated in the experiment.

Flying Qualities Criteria

Criteria for flying qualities must be applied in two cases. The first is the case of the unaugmented vehicle, where total augmentation system failure has occurred. The second case is with the augmentation system in normal operation.

In the first case, acceptable unaugmented qualities are determined by safety considerations. It is usual for these to be given in terms of either Cooper-Harper pilot rating values (reference 3) or the military

flying qualities "levels" (reference 4). Safety considerations for commercial transport aircraft dictate a maximum acceptable pilot rating of 6.5, which corresponds approximately to Level 2 from the military specification. In the second case, the desired flying qualities of the normal augmented aircraft are military Level 1, which corresponds to a pilot rating of 3.5 or better.

At the outset of the work, it was decided that satisfactory (Level 1) flying qualities for the augmented vehicle could be ensured by requiring the augmentation system to provide a match with the proven flying qualities of the DC-10. In addition, other criteria have been considered so as to add confidence in the final characteristics. Chief among these is the "Bandwidth Model" for the pitch tracking task. This criterion was originally developed by Calspan (reference 5) and has been modified and adopted by Douglas for use in transport design work. The Douglas work is reported in reference 6 and the criterion is depicted in figure 18. Briefly, the criterion considers the amount of compensation the pilot must apply to achieve a given level of pitch tracking performance without encountering pilot-induced-oscillation tendencies. The type of aircraft response to be expected from pilot commands is noted in each section of the figure. While this criterion is used for both landing approach and cruise flight conditions, there is slightly less confidence when applied to cruise cases, particularly in the left side of the diagram where few data are yet available to construct the boundaries.

Simulator Tests

The test utilized the large flight envelope data previously developed; thereby simulated flight was permitted through most of the flight envelope as well as flap, slat, and landing gear extension and retraction. Each of the evaluation pilots became familiar with the basic configuration (center of gravity at 25 percent MAC) by performing approaches, landings, go-arounds, climbs to altitude, maneuvers at altitude, descents, and stalls. To gain additional familiarization, the pilots repeated the process for an aft center-of-gravity case (cg at 40 percent MAC). No pilot ratings were taken during this portion of the experiment, but pilot comments were solicited. From the commentary, it was determined that the remainder of the test should concentrate on the landing approach and on the cruise flight condition.

In the formal evaluations, the matrix of test configurations consisted of the 15 possible combinations of five center-of-gravity locations (25, 35, 40, 45, and 50 percent MAC) and three horizontal tail sizes (100, 85, and 70 percent of nominal). Variations in tail size were included in an attempt to identify problems that might be attributed to deficient pitch control at various stability levels. Runs were conducted at each of the two flight conditions with both moderate atmospheric turbulence and smooth air. The description of turbulence here refers to the pilot assessment, which reflects the attenuation of total aircraft motion felt in the cockpit. The actual input turbulence was a level described as "moderate-to-heavy." The intensity of the turbulence is described by a vertical gust component (root mean square) of 2.13 m/s (7 ft/sec) in the landing approach, and 1.52 m/s (5 ft/sec) in the cruise. The turbulence model used is reported in Reference 7.

Some preliminary results are available from the experiment. In general, the landing approach case was critical so most of the analysis has focused in this area. Mean values of pilot ratings (using the Cooper-Harper scale given in figure 18) are shown as a function of static margin in figure 19. These data are for the case of moderate atmospheric turbulence. Although there is considerable scatter in the data, they suggest that the limiting static margin for pilot acceptability is about a negative 4 or 5 percent MAC: i.e., where the mean pilot ratings exceed a value of 6.5. The fact that the mean pilot

ratings in the stable area are poor is attributed to two causes: the presence of moderate turbulence and unsatisfactory lateral-directional characteristics of the simulated aircraft. For the second reason, all the pilot ratings may tend to be slightly higher (worse) than they should be, in which event a minimum static margin of negative 4 or 5 percent MAC may be on the conservative side. Figure 19 provides an indication of the effect of more satisfactory lateral-directional characteristics. This suggests a static margin of negative 8 or 9 percent MAC would be acceptable.

Improved lateral-directional characteristics will be incorporated in a future motion base simulator experiment.

The pilot ratings have been compared with the "Bandwidth Model" previously mentioned and are presented in figure 20. Again, the landing approach case with turbulence is shown. Excellent correlation is apparent, particularly when the poor lateral-directional characteristics are considered. If the pilot ratings were to be reduced (improved) slightly to account for this effect, even better agreement would be achieved. It is estimated that in the region of interest the pilot ratings would be reduced (improved) by approximately one unit due to the improved lateral-directional characteristics. Additional confidence has therefore been furnished for the continued use of this criterion, both for the unaugmented aircraft (Level 2) and the augmented aircraft (Level 1).

CONCLUDING REMARKS

For technology development toward advanced derivatives of the DC-10, Douglas is active in specific fields under the ACEE Energy Efficiency Transport program. These fields are the wind tunnel development at high and low speed of high-aspect-ratio supercritical wing designs, and the design of a longitudinal stability augmentation system. Also included is the design of an optimized wing-winglet combination.

The design work leading to the model development for the high-aspect-ratio supercritical wing has benefitted from the use of new and sophisticated analytical tools which show good agreement with test data. The use of these methods to study a wide range of variables will result in wind-tunnel tests of models much closer to the final configuration.

The determination of acceptable levels of flying quality is a prerequisite for the design in a failure condition of the longitudinal stability augmentation system. In normal operation, the system design will provide a quality similar to a proven high standard, such as the DC-10. Pilot simulator tests have been completed to demonstrate the effects of alternative levels of flying quality, and perhaps more importantly suggest criteria by which these levels may be measured. A further group of tests is planned, which will expand the scope to include control system investigation.

REFERENCES

1. Whitcomb, Richard T.: Review of NASA's Supercritical Wing Airfoils. 9th Congress International Council of Aeronautical Sciences, Haifa, August 1974.

2. Jameson, A.; and Caughey, D. A.: Numerical Calculation of Transonic Flow Past a Swept Wing. New York University DRDA Report C003077-140, May 1977.

3. Cooper, G. E.; and Harper, R. P.: The Use of Pilot Rating in the Evaluation of Aircraft Handling Qualities. NASA TN D-5153, April 1969.

4. Military Specification, Flying Qualities of Piloted Airplanes. MIL-F-8785B (ASG), 7 August 1969.

5. Neal, T. P.; and Smith, R. E.: An In-Flight Investigation to Develop Control System Design Criteria for Fighter Airplanes. AFFDL-TR-70-74, Vol 1, December 1970.

6. Richard, W. W.: Longitudinal Flying Qualities in the Landing Approach. Douglas Aircraft Company, Douglas Paper 6469, May 1976.

7. Barr, N. M.; Gangass, D.; and Schaeffer, D. R.: Wind Models for Flight Simulation and Certification of Landing and Approach Guidance and Control Systems. FAA-RD-74-206, December 1974.

TABLE 1
COMPARISON OF CONFIGURATION USING ADVANCED
OR CONVENTIONAL HIGH-LIFT SYSTEMS

	ADVANCED		CONVENTIONAL	
WING AREA	202.99 m^2	(2,185 FT^2)	205.32 m^2	(2,210 FT^2)
TOGW	137,393 kg	(302,900 LB)	138,073 kg	(304,400 LB)
OWE	81,627 kg	(179,956 LB)	82,135 kg	(181,077 LB)
INITIAL CRUISE ALTITUDE	10,363 m	(34,000 FT)	10,424 m	(34,200 FT)
$V_{APPROACH}$	61.9 m/s	(120.4 KEAS)	64.8 m/s	(126 KEAS)
TOFL	1,768 m	(5,800 FT)	2,179 m	(7,150 FT)

Figure 1.- Douglas DC-X-200 transport.

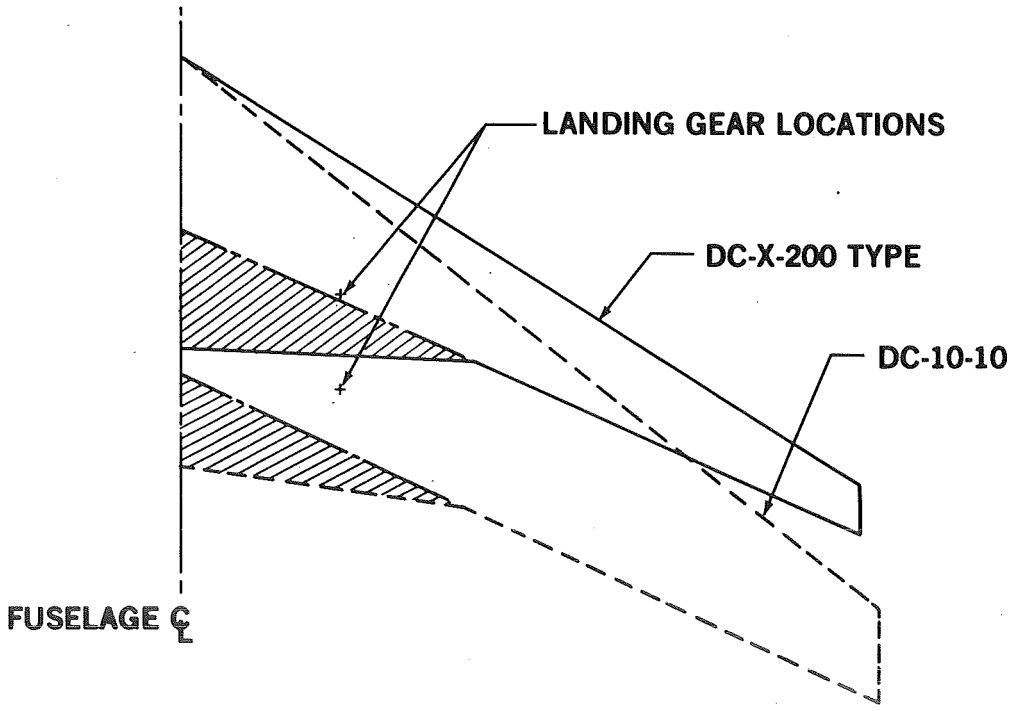

Figure 2.- Planform comparison.

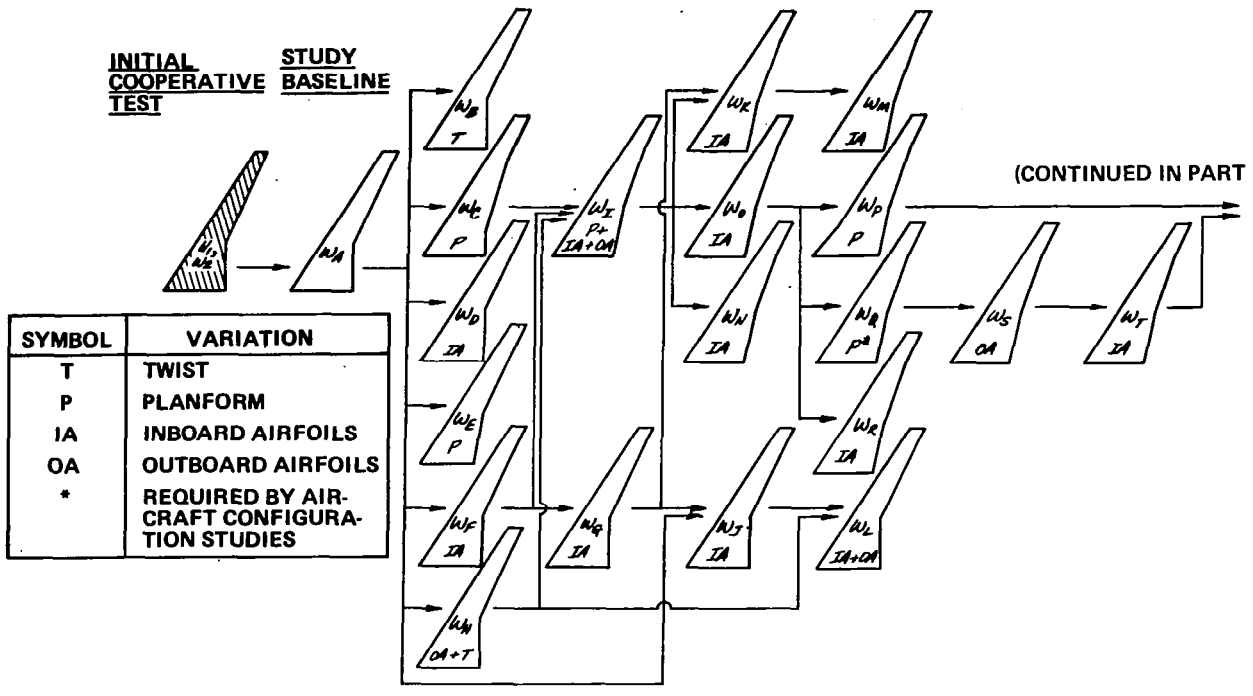

Figure 3.- Wing development matrix (Part 1).

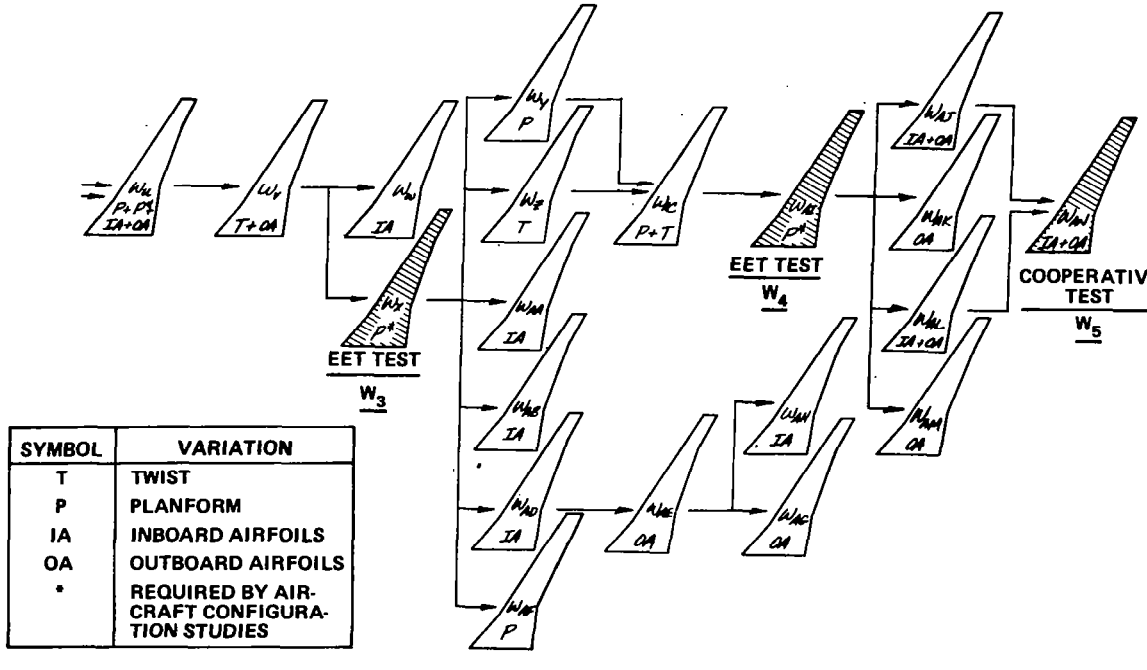

Figure 4.- Wing development matrix (Part 2).

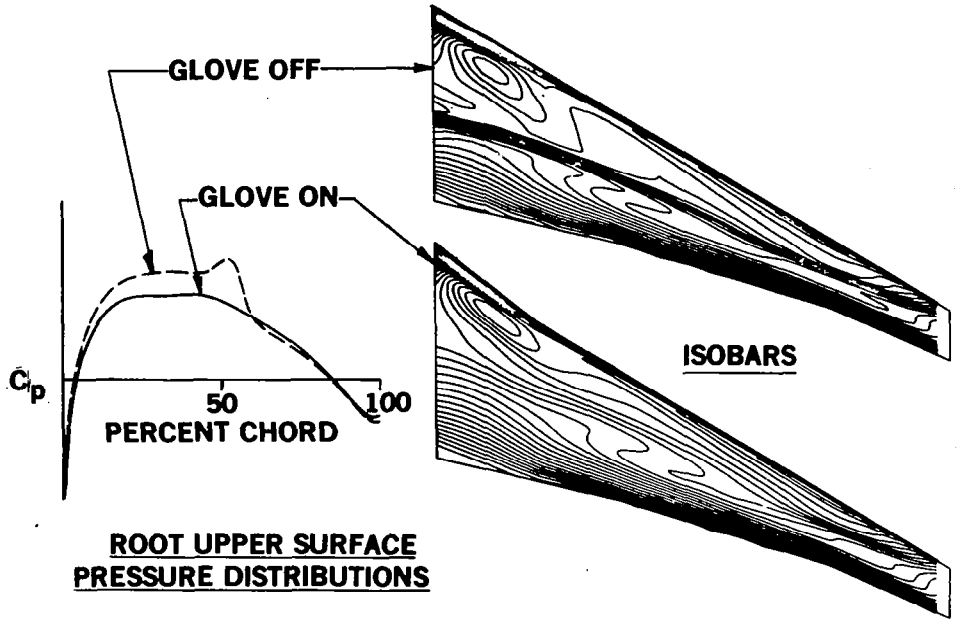

Figure 5.- Effect of inboard leading-edge glove.

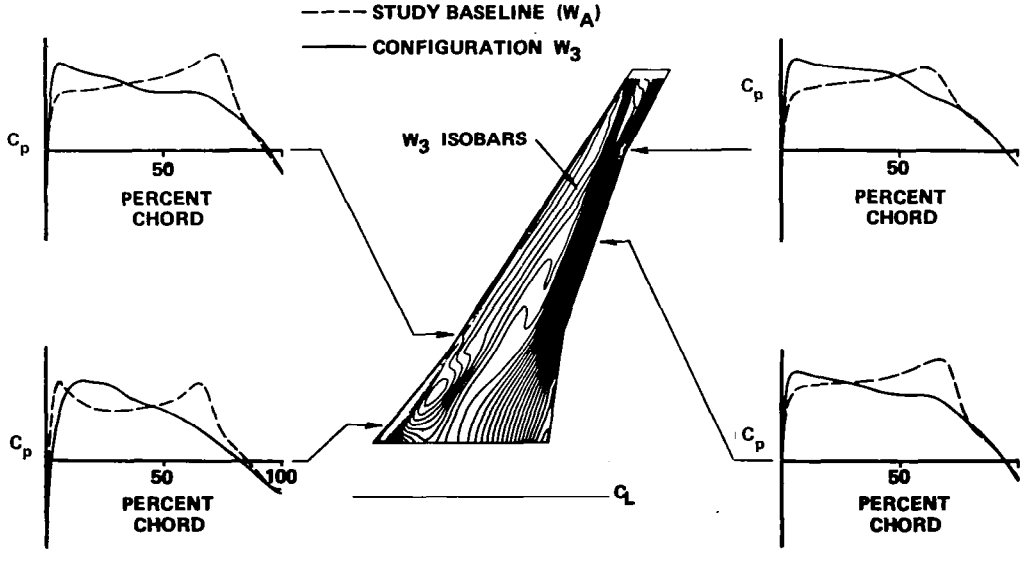

Figure 6.- Comparison of study baseline and configuration W_3 upper baseline pressure distributions.

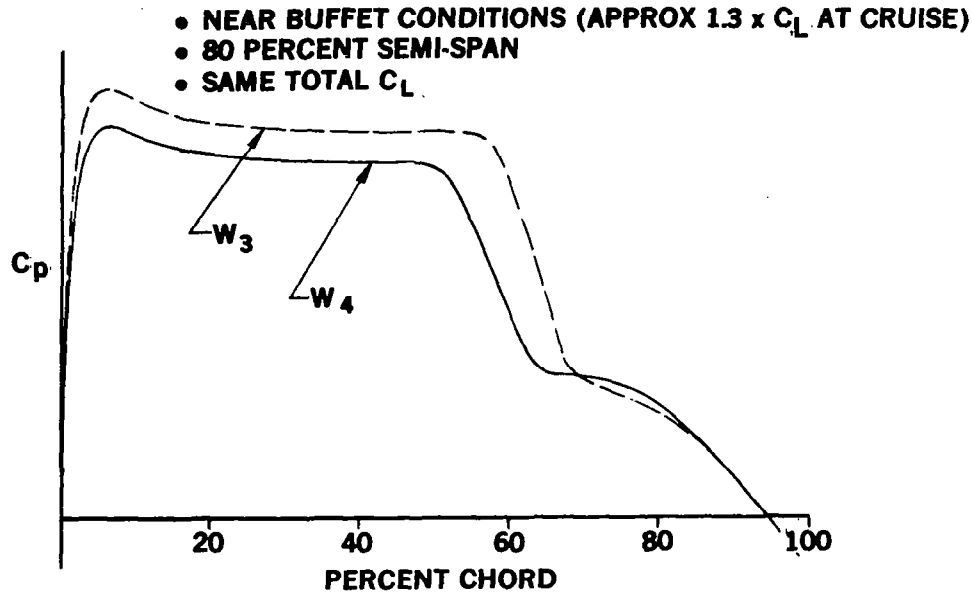

Figure 7.- Comparison of upper-surface chordwise pressure distributions for wings W_3 and W_4.

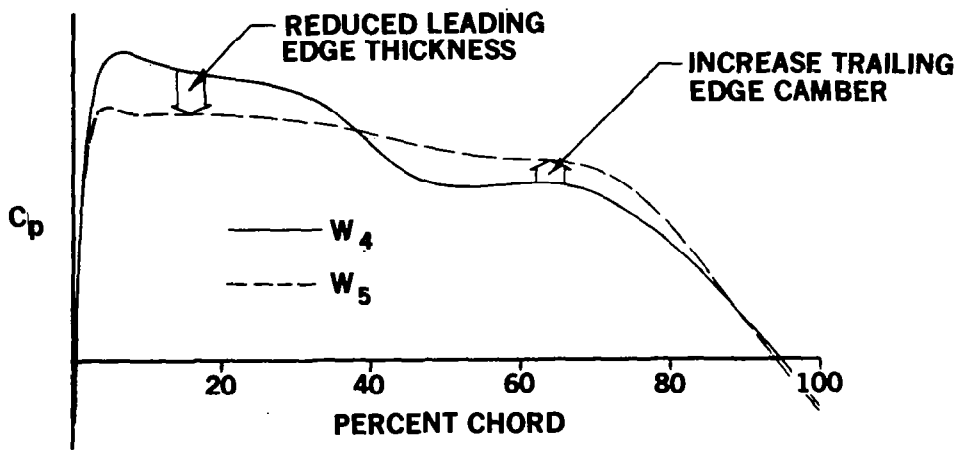

Figure 8.- Comparison of upper-surface chordwise pressure distributions for wings W_4 and W_5.

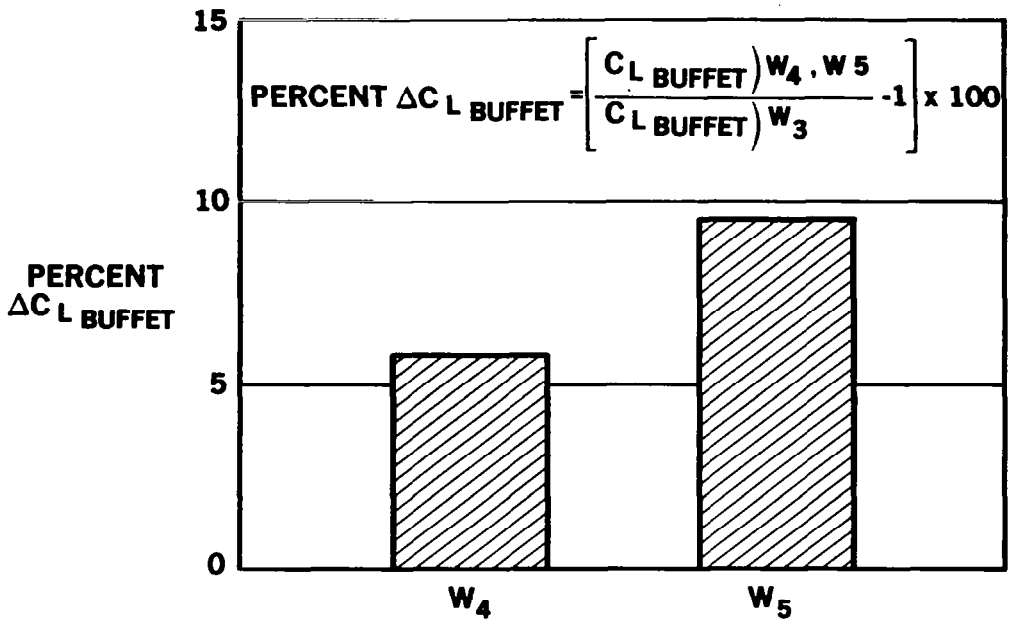

Figure 9.- Estimated $C_{L_{BUFFET}}$ improvement.

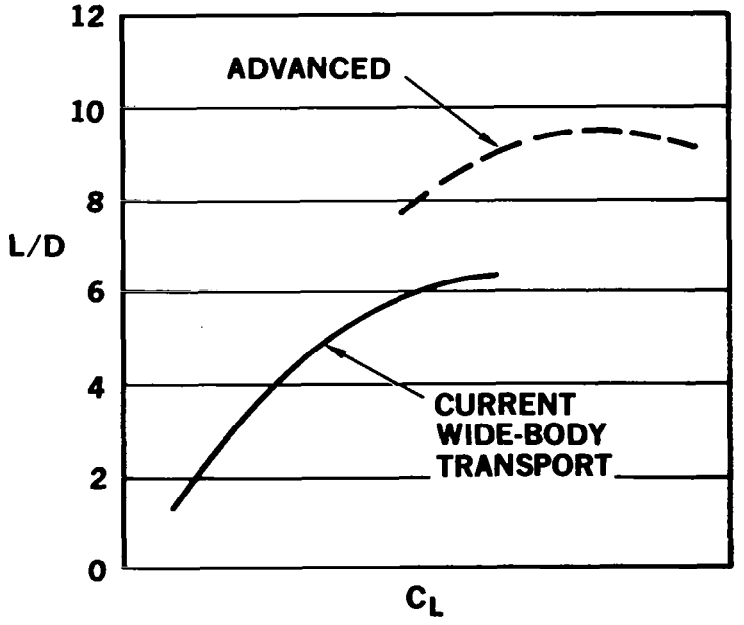

Figure 10.- Comparison of current wide-body and advanced high-aspect-ratio SCW transport landing L/D characteristics.

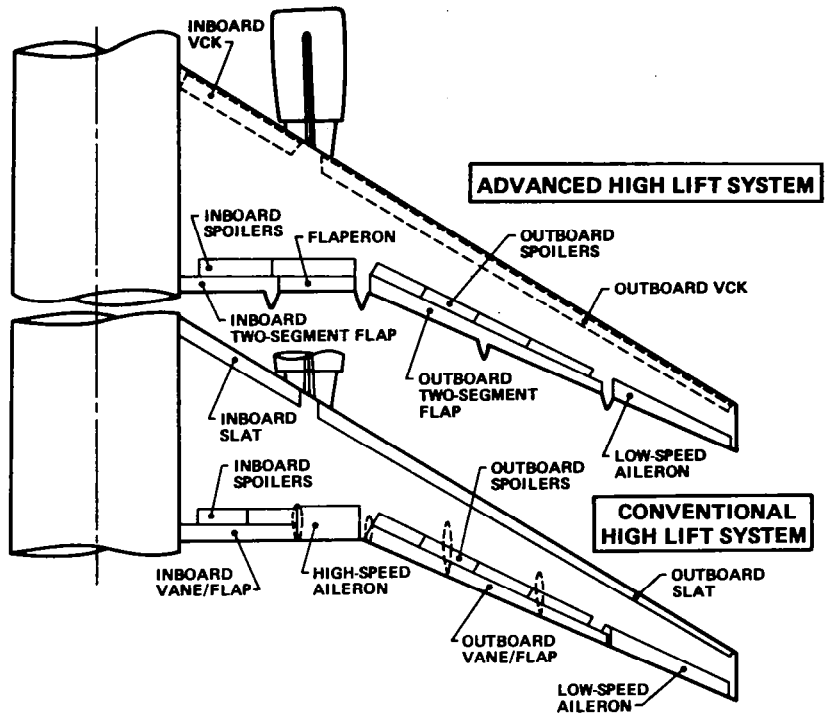

Figure 11.- High-lift system configuration comparison.

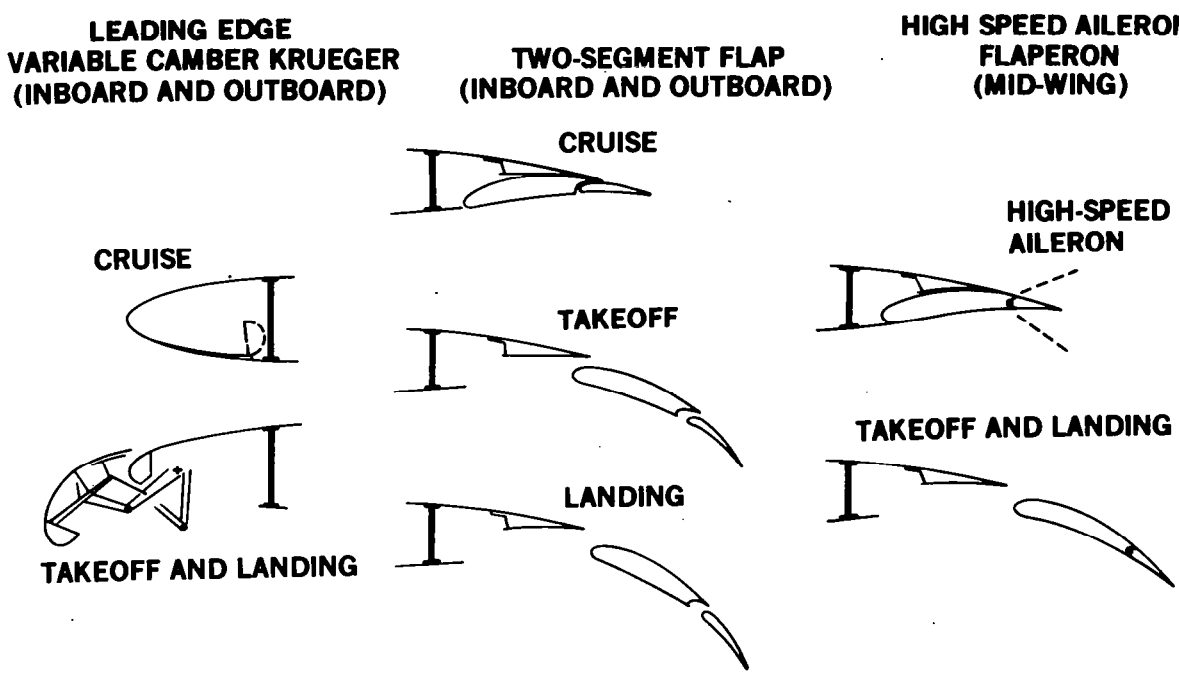

Figure 12.- Advanced high-lift system chordwise sections.

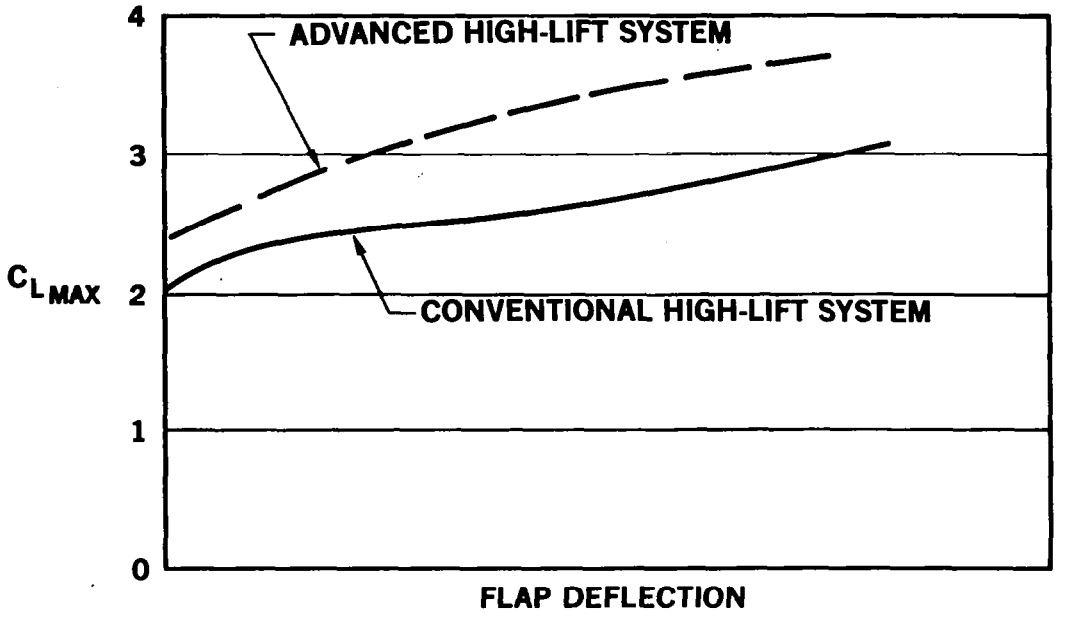

Figure 13.- Comparison of conventional and advanced high-lift system $C_{L_{MAX}}$ characteristics.

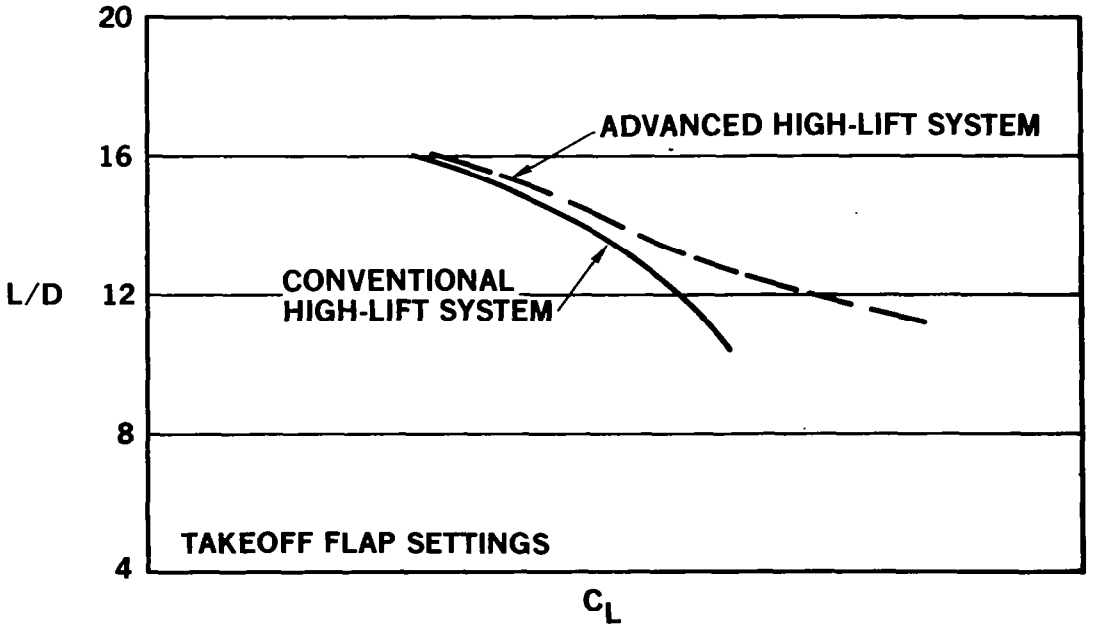

Figure 14.- Comparison of conventional and advanced high-lift system takeoff L/D characteristics.

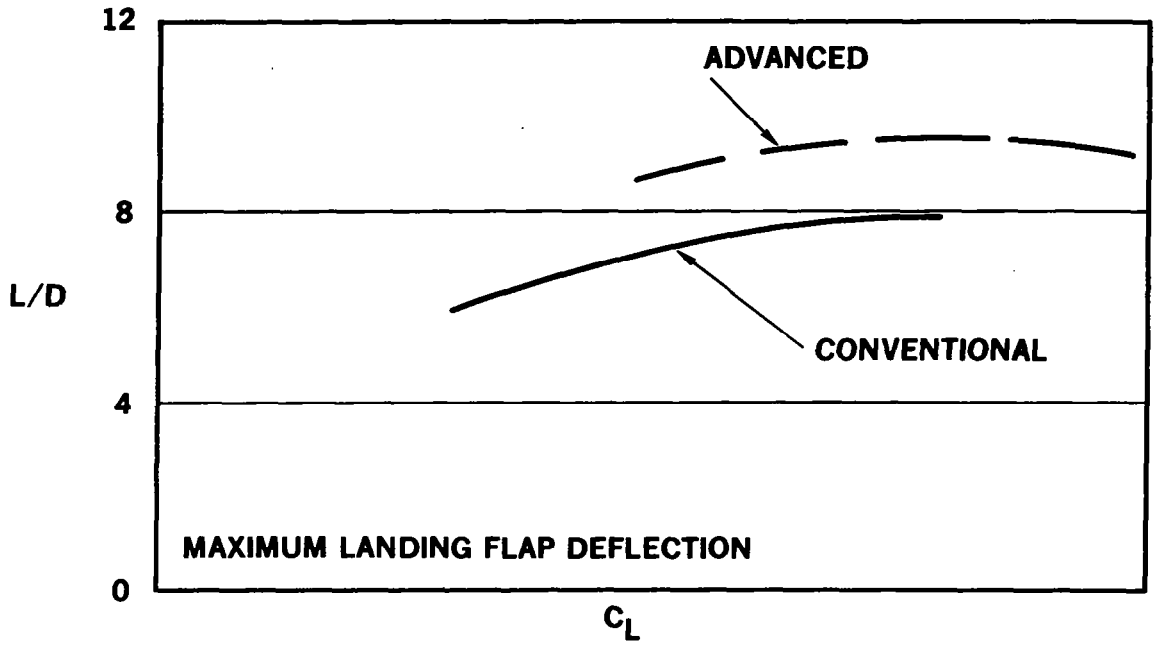

Figure 15.- Comparison of conventional and advanced high-lift system landing approach L/D characteristics.

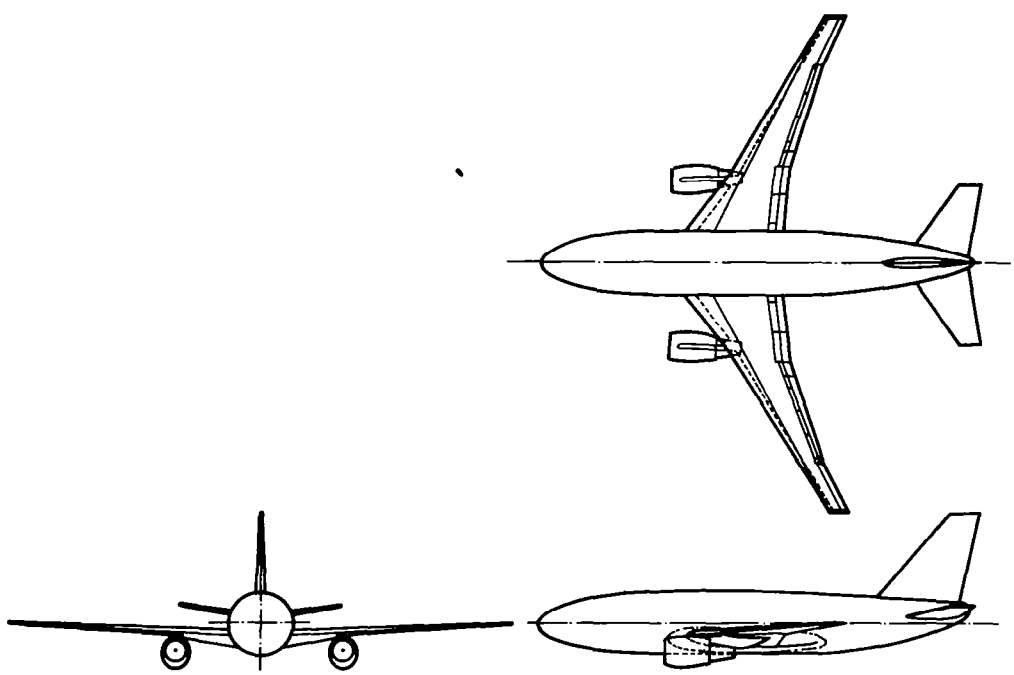

Figure 16.- High-lift, low-speed wind-tunnel model.

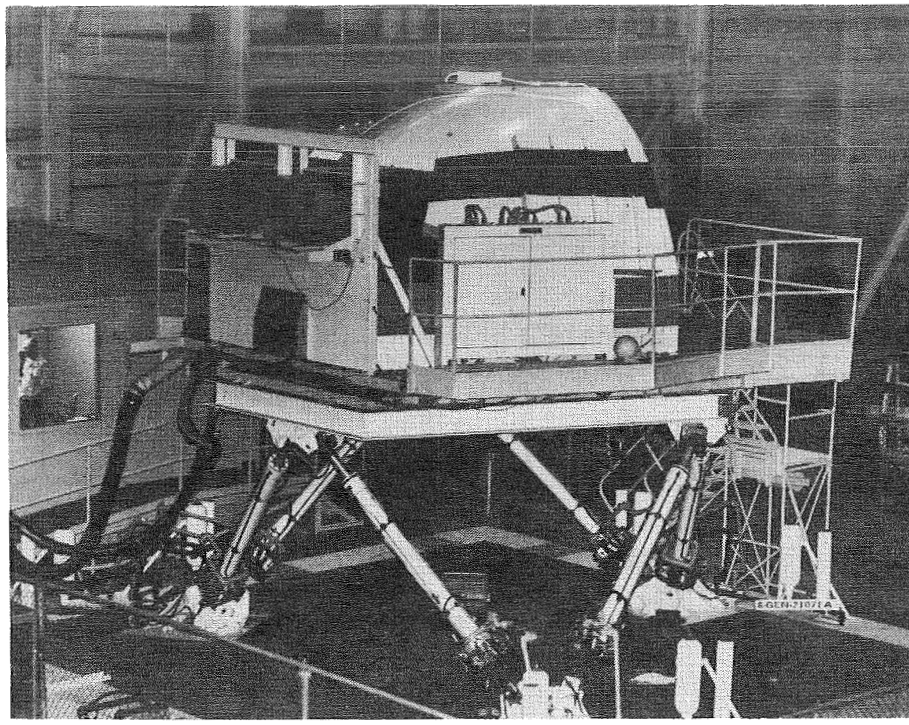

Figure 17.- Douglas six-degree-of-freedom motion simulator.

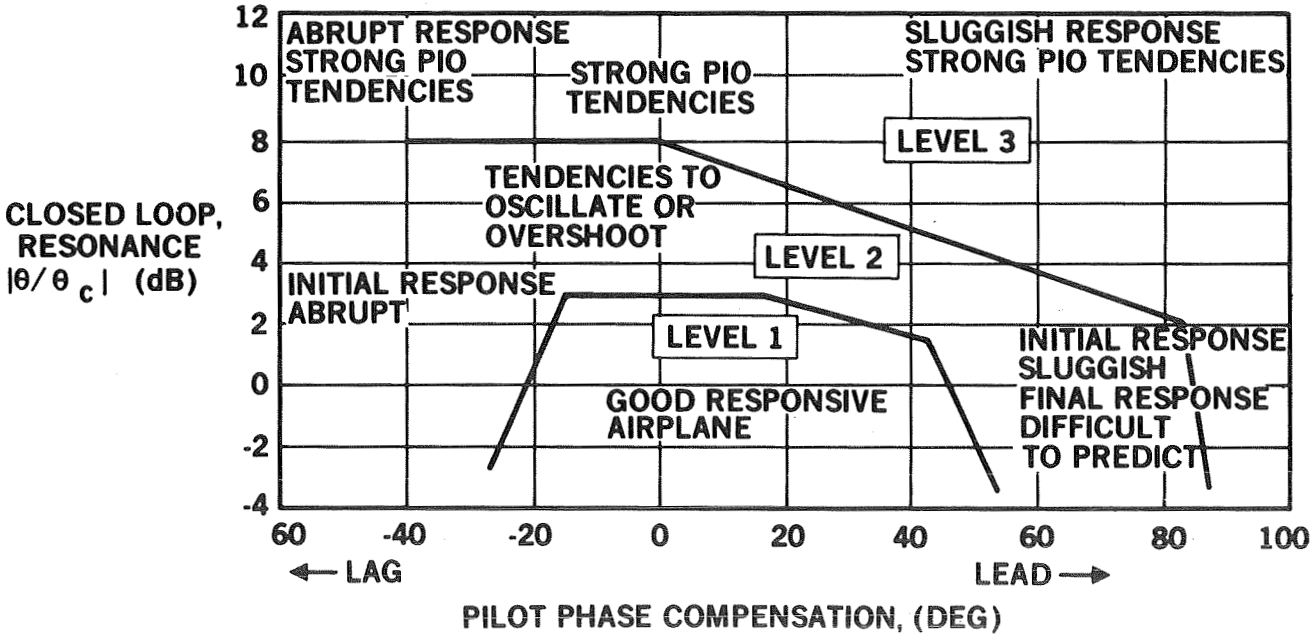

Figure 18.- Pitch tracking criterion.

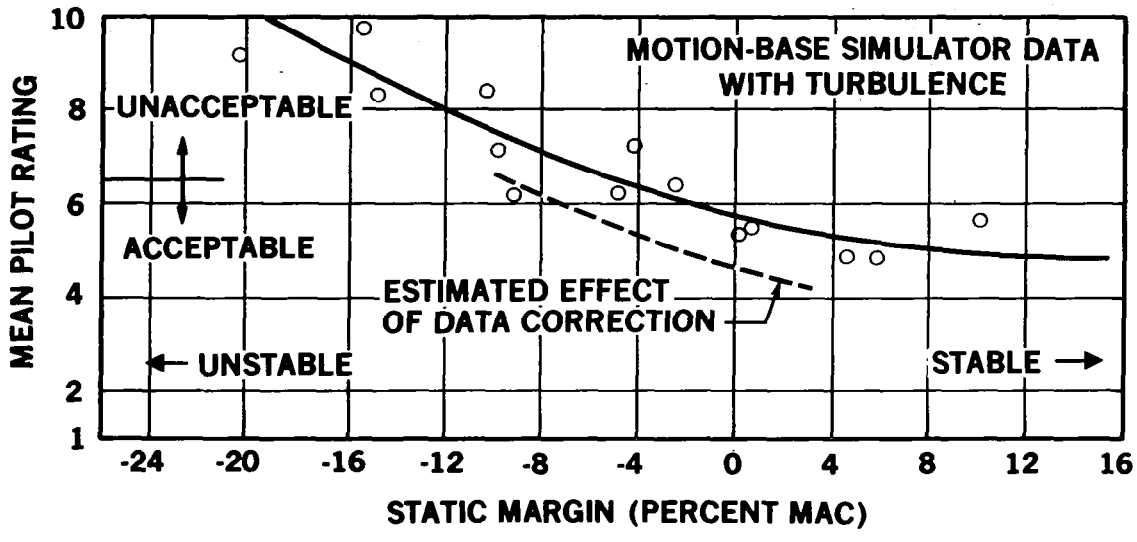

Figure 19.- Pilot acceptance of static instability — landing approach.

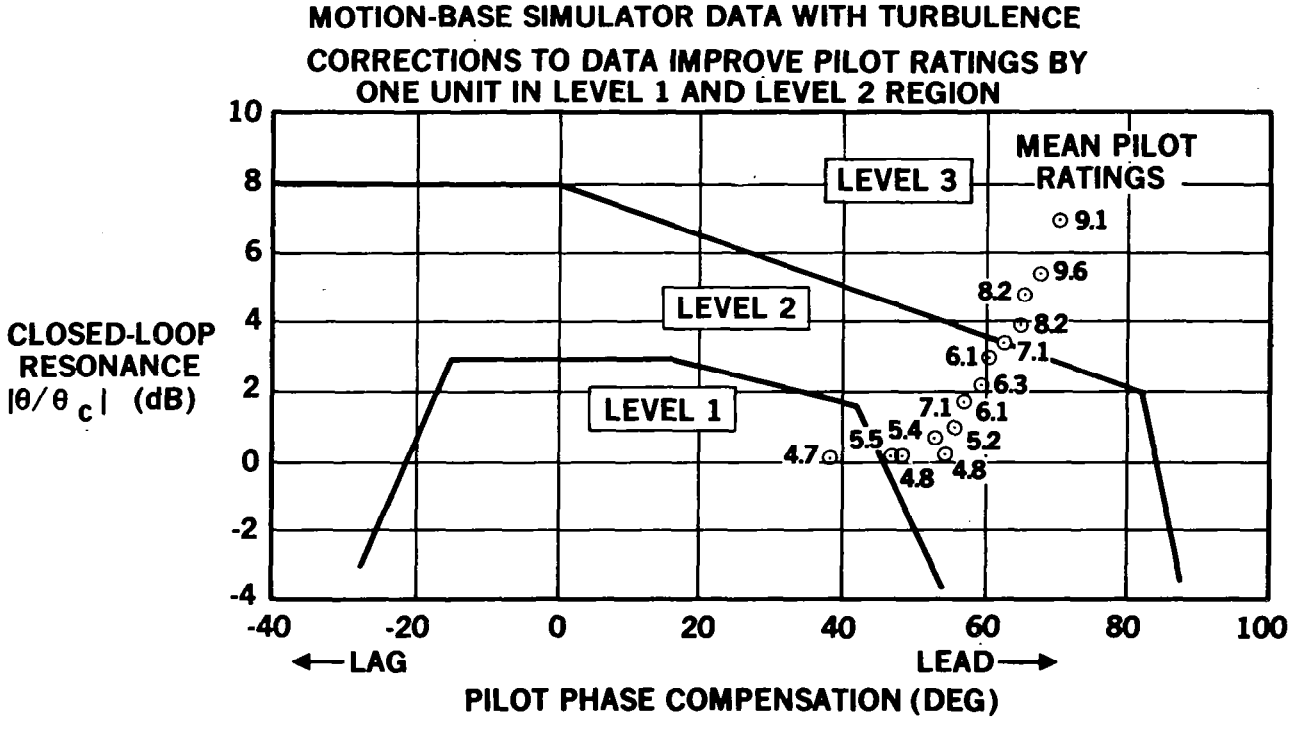

Figure 20.- Landing approach pitch tracking criterion.

ACTIVE CONTROLS TECHNOLOGY TO MAXIMIZE STRUCTURAL EFFICIENCY

James M. Hoy
Boeing Commercial Airplane Company

James M. Arnold
Boeing Wichita Company

ABSTRACT

This paper discusses two programs, being conducted by The Boeing Company, that consider the implication of the dependence on Active Controls Technology (ACT) during the design phase of transport structure: 1) Drones for Aerodynamic and Structural Testing (DAST), and 2) Maximum Benefit of Active Controls Technology (Max Benefit). The purposes of the two programs are compared and then certain aspects of the structural analysis that will be performed on the Max Benefit program are discussed in detail. Critical loading conditions are discussed along with probable ways of alleviating these loads. The paper presents explanations of why fatigue requirements may be critical and can only be partially alleviated. Finally, the significance of certain flutter suppression system criteria are examined.

INTRODUCTION

Although active control technology (ACT) advancements have been increasingly applied to military aircraft, they have not enjoyed the same degree of acceptance in the commercial arena. When they have been applied to commercial transports their use has been limited, usually because of: 1) The need to overcome a problem on a design that has been committed, or 2) The desire to improve an existing transport in the form of a minor model change or a derivative. In both cases the designer and configurator have been constrained by the necessity to make no, or at best, very little, change to the "as-tooled" structure. Reduced structural weight and/or the ability to apply features that would improve aerodynamic performance (i.e., high aspect ratio, engine placement, wing sweep. etc.) with minimum structural weight penalty are the areas of payoff for ACT. Therefore, their full potential has not been exploited. In fact, it seems that a comprehensive evaluation of ACT, when applied during the preliminary design of a commercial transport, has not been completed in an atmosphere that recognizes the effect of Federal Airworthiness Regulations (FAR). Further there are no acceptable operational standards and no detailed examination of the effect of ACT on structural and flight control system design and configuration effects.

Full exploitation of ACT could offer new degrees of freedom for the structural designer, aerodynamist, and configurator. At the same time, the burden of proof will be on the flight control system designer, because his systems

will have to perform to reliability standards approaching those of the structure. The cost of owning these systems must be held in check to preserve economic benefits achieved by lower structural weight and high performance. A much greater degree of design team coordination will be needed to achieve the potential.

Two contracts being performed by Boeing under the Energy Efficient Transport (EET) portion of the NASA Aircraft Energy Efficiency (ACEE) program offer the potential for conducting the detailed examination lacking to date. This paper is limited to the structural investigations involved in those two contracts.

DAST

The feasibility of active controls to improve stability and control, flutter, and ride comfort and to reduce structural loads has been demonstrated in flight as described in references 1 through 5. The next logical step is to integrate active controls into the airplane design cycle. To assist in this step, an integrated wing design with active controls is currently being accomplished by NASA under a contract with the Boeing Wichita Company. The program is designated DAST (Drones for Aerodynamic and Structural Testing) and evaluates an integrated design of a high aspect ratio wing with active controls on a Firebee II drone vehicle. The second advanced research wing (ARW-2) being designed under this program has a supercritical airfoil with an aspect ratio of 10.3.

The primary objectives are to develop the interdisciplinary methodologies required to accomplish an integrated ACT design and to apply these methodologies to the design of a wing maximizing structural efficiency. The DAST vehicle will depend on active controls for maneuver load alleviation, gust load alleviation, and flutter mode suppression. The program will have significant value to the aircraft industry which is just starting to apply some of these advanced control concepts to commercial transports. Further benefits will come when DAST is flown and when flight-measured loads and flutter are correlated with those predicted.

INTEGRATED ACT AIRPLANE DESIGN

The typical conventional aircraft design process is shown in figure 1. Even though the figure reflects active control synthesis for structure or stability and control augmentation, it should be emphasized that in this conventional design process such control functions do not significantly impact the configuration. The first step in developing a new airplane configuration is to establish mission requirements, i.e., payload, range, speed, and takeoff and landing distances. Propulsion, aerodynamics, structures, and weight technologies are then combined to obtain a configuration that meets the mission requirements. Its performance is assessed and the process is iterated until the vehicle meets all of the specified mission performance requirements and satisfies the minimum weight, minimum cost, and other specified criteria.

There are examples of conventional configurations that include modest active control functions, e.g., yaw dampers, ride improvement augmentation, or in the case of the C-5, an airload distribution control system. These active control designs began when the configuration was defined or, in some instances, after the airplane had been built and entered service. With this approach, the active control systems are used to augment the airplane dynamics or extend the airplane's life by minimizing structural fatigue damage, rather than to meet mission performance requirements with a more efficient airplane. If active control technology is not considered from the very outset of the configuration cycle, its full benefit will not be realized. In contrast to the conventional design, the integrated active control design approach capitalizes on the potential of integrating ACT concepts during configuration definition trade studies. With this approach, active controls are included in the design on an equal basis with other major technologies of propulsion, aerodynamics, and structures.

DAST INTEGRATED ACT DESIGN

The integrated DAST design approach emphasizes the structural dynamic benefits of active control and considers only secondarily stability and control benefits. Most aerodynamic parameters were specified and were not optimized as a part of the integrated design process. Table I compares the aerodynamic design parameters that are normally fixed and variable for a conventional transport and the DAST ARW-2 wing. Also, relaxed static stability is being used to minimize trim drag but the horizontal stabilizer and empennage structure are not being optimized.

The DAST integrated design process is similar to the transport design process except the propulsion, fuselage, empennage, and most of the wing parameters were constrained and not allowed to change during the design cycle. Figure 2 shows this design cycle. There are several parameters that are unique to the DAST, as compared to a typical fuel conservative transport. They include wing material, flutter within the flight envelope required, limited amount of power to drive control surfaces, and c.g. control (ballast) used to achieve minimum trim drag.

Structural material selected for the wing was aluminum spar with fiberglass honeycomb skins. The mixed material, selected to provide transport similarity within the drone minimum gage constraints, caused problems in using standard preliminary sizing for steady-state loads and weights. Electrical power to drive the control surfaces was a constraint for the DAST program for which a cost-effectiveness study would be conducted on a transport. To achieve minimum trim drag, wing location and ballast were iterated, as opposed to optimizing the empennage structure and surface sizes.

Several aeroelastic requirements also affected the DAST design. The DAST ARW-2 wing was designed to have a ratio of aerodynamic forces to elastic forces in the same range as a full-scale fuel-conservative transport. The goal was to have the outboard ailerons used for active controls exhibit a loss of effectiveness with increasing dynamic pressure. The primary method used to

meet the ratio of force requirement was to iterate structural stiffness properties through spar spacing and material stiffness. Flutter occurs within the flight envelope without adverse ballasting so the final DAST configuration is similar in flutter to a fuel-conservative transport.

Once the aeroelastic characteristics are satisfied, the active control system synthesis is initiated. Maneuver and gust requirements are imposed at this point in the design cycle. This differs from the conventional design, where the maneuver and gust effects are determined by the aeroelastic analysis. Gust load alleviation, maneuver load alleviation, and flutter suppression concepts are defined and performance is compared to the design gust, maneuver, and flutter requirements. If these requirements are not met with the initial configuration, revisions are made in control surface size, location, or design loads and a second iteration is initiated. This iterative process is repeated until the design loads and flutter requirements are met and the active control system design requirements are determined to be achievable.

ACT DESIGN CYCLE CHARACTERISTICS

Some major characteristics of the integrated ACT design cycle are as follows:

- o A single data base is needed for synthesizing active control functions and predicting ACT benefits such as flutter, loads, and stability and control.
- o Active control systems are added to the design cycle on an equal basis with propulsion, aerodynamics, and structures.
- o The control system synthesis and analyses must produce the aircraft design loads, flutter, and stability and control characteristics.
- o After the active control system is integrated with the aeroelastic model, conventional analysis methods may be used.

The need for a single data base and compatible airplane math models for analysis of stability and control, flutter, structural integrity and ride comfort has been heightened by three factors: the ability to improve performance in each of these areas with active control systems, interaction between ACT functions, and the lack of frequency separation in large airplanes between these areas of concern. This also means that the various performance parameters must be monitored to prevent inadvertent degradation. For the conventional design, these analyses are generally conducted independently, using different data bases and math models. Because of the interaction between ACT functions, the final performance evaluation needs to be with all functions operating simultaneouly even though the synthesis may be accomplished independently.

As shown in figure 2, active control systems are added to the design cycle on an equal basis with propulsion, aerodynamics, and structural dynamics. This approach maximizes the effect of active control technology on the structural design.

MATH MODELS AND ACT DESIGN TECHNIQUES

The math models used for active control system synthesis and analysis must be capable of producing the aircraft design loads, flutter, and stability and control characteristics. It is therefore logical and expedient that the control analyst use the same math model as the loads and flutter analyst. Since the controls engineer normally synthesizes active control systems in the S-plane, it is necessary to formulate the airplane equation in the S-plane.

Selected analytical methods described in reference 6 are useful in aircraft modeling and active control system design. One of the modeling techniques that provides a means of formulating the equations of motion in the S-plane is summarized below.

Unsteady aerodynamic forces acting on the DAST vehicle were computed using numerical methods to satisfy lifting surface theory. The interfacing of the point frequency unsteady aerodynamic coefficients with Laplace transform equations of motion was done with the use of approximating functions. Figure 3 shows a typical aerodynamic coefficient, plotted as s moves up the imaginary axis, and the "best fit" approximating function. The approximating function chosen was a rational polynominal with denominator roots on the left real axis. It can be considered to be a physically reliable frequency interpolating function for the unsteady aerodynamic coefficients. A function was found for each element in the aerodynamic influence matrix. The resulting functions were generalized and included as part of the equations of motion, raising the order of the differential equations once for each denominator root, typically between two and four.

The useful (accurate) range for Laplace arguments is not obvious, although analytic continuity suggests that leaving the imaginary axis (small positive or negative damping) is comparable to interpolating along the imaginary axis. The region near the imaginary axis is of greatest physical interest.

The success of the integrated design process discussed in previous paragraphs is ultimately dependent on the successful synthesis of active control systems. Active control system synthesis is generally accomplished for each function (i.e., flutter suppression, gust load alleviation, maneuver load alleviation, etc.) separately to meet performance requirements. Then the analysis is expanded to evaluate compatibility of the combined functions. System parameters are adjusted, if required, to meet the performance of the individual systems. This cycle is repeated until a system definition that meets the criteria is achieved.

There are some advantages to synthesizing each ACT function to operate independently with the minimum interaction between functions. This approach will produce a less complex system and fewer parameters will require changes as various systems are engaged. A major advantage of independent operation of each function is that redundancy can be made appropriate for each function. Otherwise redundancy of the entire active control system needs to meet the requirements of that function which has the most severe redundancy requirement.

The integrated ACT airplane design requires an interdiscipline of the various technologies of aerodynamics, structural dynamics, and control dynamics. Figure 4 shows the integration of technologies and analysis programs necessary for active control synthesis.

Flexible airframe equations of motion are generated from the vehicle mass, stiffness, and aerodynamic data. The structural coordinates and mode shapes are obtained from the vibration analysis. The equations are formulated in the Laplace domain to be compatible with the standard S-plane control synthesis techniques. Active control system synthesis is accomplished in the S-plane and uses the linear analysis programs shown in figure 4. The three-dimensional gust load analysis is conducted in the frequency domain because it is more efficient. A simulation is used to evaluate flying qualities, nonlinear effects, and failure effects in support of the ACT synthesis. The ACT synthesis cycle is iterated until a system that maximizes structural benefits is obtained. After the ACT system has been defined, the final step is to evaluate performance and define the design requirements.

ACT BENEFITS FOR DAST

High aspect ratio wing designs show potential for improved fuel efficiency through increased lift-to-drag (L/D) ratios. This is achieved by reducing sweep and/or increasing thickness ratio at the cruise Mach number by use of supercritical airfoils and by reducing induced drag by increasing the aspect ratio. However, these benefits are not easily achieved without increasing wing structural weight. Weight penalties come from additional strength necessary to accommodate larger wing design loads due to increases in span and wing lift curve slope. Penalties also come from increased wing stiffness needed to prevent flutter. Integration of maneuver load alleviation (MLA), gust load alleviation (GLA) and flutter suppression system (FSS) active control concepts into such a wing design offers the potential for maximizing the L/D benefits of the high aspect ratio supercritical wing while minimizing structural weight penalties.

The fuel efficient DAST ARW-2 wing, shown in figure 5, was designed to meet the aerodynamic parameters specified in table I by NASA while using active controls to maximize structural efficiency. The wing has a gross area of 3.25 m^2 (35 ft^2) and a span of 5.79 meters (19 feet). A wingtip control surface is used to suppress flutter while this surface is combined with an inboard control surface for maneuver load alleviation. Gust load alleviation utilizes a surface slightly inboard of the wing midspan as illustrated in figure 5.

The wing vertical bending design loads for gust and maneuver are presented in figure 6. The wing maneuver loads are slightly higher than gust loads without active load alleviation. With MLA and GLA the wing is still maneuver load critical except at the tip where it is slightly gust load critical. The combined effect of maneuver and gust load alleviation brings a reduction in DAST ARW-2 loads of approximately 20 percent. As shown in figure 7 the DAST ARW-2 flutter boundary is approximately 17 percent below the design

speed (V_D) for a typical transport. Therefore, the flutter suppression system is required to increase the flutter speed (V_f) approximately 40 percent to meet $1.2V_D$. Initial flutter evaluation with active controls indicates that this amount of improvement in flutter is feasible. If it were not, the structural design would be iterated at increased weight penalty to suppress flutter.

In a transport design where safety is more of a concern, new criteria must be developed to define minimum allowable flutter speed with the flutter suppression system off as well as the usual $1.2V_D$ with the system on. More will be said about this in the last section of this paper.

MAXIMUM BENEFIT OF ACTIVE CONTROLS TECHNOLOGY

Two objectives of the Max Benefit program are to produce a credible assessment of the benefit of ACT on an advanced subsonic commercial transport with ACT integrated into the design process, and to identify technical risk areas and necessary development and test work. The development and test work are needed for reduction of the ACT implementation risks that are excessive by the standards of current commercial practice. The term "benefit of ACT", as used in this program, is a measure of the improvement of airplane fuel use and operational economics.

This program, which has just begun at the Boeing Commercial Airplane Company, is illustrated in figure 8. The major elements of the program are the design of the configuration and ACT system, examination of advanced technology and its application to the synthesis and implementation of the ACT function, and the test and evaluation of the "high risk" elements of a commercially feasible ACT system. The element most significant to this paper is the configuration/ACT system design task.

Figure 9 shows the more significant parts of the configuration task. Since the objective is to identify the benefit due to ACT, the program begins with the selection of a modern conventional (non-ACT) commercial transport and proceeds to design an ACT transport with the same operational characteristics, i.e., passenger/cargo payload, design range, cruise Mach number, etc. The ACT transport is then compared to the conventional transport in terms of fuel use and operational economics.

The credibility of the comparison will depend upon the validity or reality of the reference conventional airplane and the detail and care with which the design and analysis proceed.

The program could be referenced to an existing, in-service, commercial transport; however, it might be argued that any benefit subsequently identified was the result of an outdated reference, i.e., starting point. Therefore, the reference airplane is being selected from recent preliminary designs that incorporate certain technical advances (e.g., advanced airfoil design) but are still conventional with respect to ACT. All technologies (e.g., conventional aluminum skin/stringer structure) will remain fixed throughout the study except as required to incorporate ACT.

A number of configurations will be designed and evaluated. They include synthesis of the appropriate ACT control functions, in the second element of this task, in order to determine how this additional degree of freedom can best be used. The incorporation of ACT in the design process is expected to free the airplane design from a number of constraints that yield the current commercial transport configurations. Changing these constraints will very likely lead to higher aspect ratio wings without the structural penalties that would accompany such design without ACT. Identifying these effects will require careful determination of the airplane structure, weight, and resulting performance. These trades will be used to select a final ACT configuration which will be designed to meet the same mission as the reference conventional airplane. The same mission means that not only the payload (passenger and cargo)/range will be the same, but in addition, the airplane will be designed to operate out of the same length field, with the same noise characteristics, etc.

A very significant aspect of the inclusion of ACT in the design of a commercial transport is the required system reliability, from both a safety and dispatch point of view. In parallel with the configuration trade studies, a series of trades designed to identify the best way to implement the ACT functions will be pursued to identify the definition of the ACT control system that provides those functions necessary for the final ACT configuration.The results of these tasks will then be evaluated from the perspective of fuel requirements and cost of operation. The assessment of the benefits associated with this ACT design will be "strictly" limited to the mission of the reference airplane, but will certainly be indicative of that to be expected on similar design missions. Fully expecting positive results, the work is currently planned to proceed into a test and evaluation phase, which is designed to reduce the risk to a commercially acceptable level. Figure 10 is an illustration of the type of configuration that could result from this study. The principal differences are a higher aspect ratio, a smaller and lighter wing, and a smaller tail.

MAX BENEFITS-STRUCTURAL EVALUATION PLAN

The initial step in this study will reconfigure the reference airplane with reduced longitudinal stability requirements. This will result in a smaller horizontal tail and reduced tail loads. The structural weight saved by this change in empennage and fuselage will be accounted for by conventional loads and weight analysis methods. Subsequent steps will involve changing wing parameters which will result in small, if any, further changes to tail size or loads. For these reasons the major structural analysis effort will be on the wing structure. The following discussions apply to wing only.

Figure 11 shows the structural evaluation procedure. All of the structural analyses start with a math model. These models will be developed jointly by the structure and flight controls engineers. The first and simplest model is the static model which will include aeroelastic effects but no airplane pitch or translations. This model will produce good "steady-state" loads such as maneuver and preliminary gust loads. It will also be possible to use it for a preliminary assessment of fatigue criticality.

The static model will then be upgraded to a quasi-static model by the inclusion of the pitch and vertical translation degrees of freedom and must include the longitudinal control system laws. With this model much better dynamic gust loads will be obtained to be used for both design and fatigue analysis.

Finally the full dynamic model will be developed from the quasi-static model which will include all of the required structural degrees of freedom and final controls laws. This model will be used to determine the final gust loads and it will become the basis of the flutter analysis.

The final output of these analyses will be the structural weight that is required for evaluation of the configuration being studied.

GUST AND MANEUVER DESIGN CONSIDERATIONS

The primary structure design load requirements provide the basis for applying active controls technology for load alleviation. A major portion of a transport airplane wing structure is usually designed by symmetrical balanced maneuvers and gusts. The relative criticality of these two design conditions will influence the choice of load alleviation controls, transducers, and system mechanization. Their relative criticality also depends on the configuration characteristics and the mission requirements. Figure 12 compares maneuver and gust sensitivities as a function of wing loading and airplane lift curve slope. For reference, early versions of the 727 and 747 airplanes are shown on the plot. A high wing loading and low lift curve slope leads to a maneuver-critical airplane. Low wing loading and high lift curve slope leads to a gust-critical airplane.

The lift curve slope is dependent upon Mach number, airfoil type, aspect ratio, and sweep, as shown in figure 13. The comparison between the conventional airfoil and the advanced airfoil is made for wings having the same critical Mach number. This means that the wing with the advanced airfoil can have about 3 degrees less sweep than the wing with the conventional airfoil.

A new airplane configured to take advantage of load alleviation (figure 10) will probably have an advanced airfoil. It will probably have a higher aspect ratio and lower sweep angle relative to current airplanes. The probable range of these parameters is shown by the cross-hatched area of figure 13. These changes will lead to an airplane that is significantly more gust critical than current airplanes, as shown by the cross-hatched area of figure 12. The likely result is that gust load alleviation will have greater benefit than maneuver load alleviation.

A maneuver load alleviation system redistributes the wing lift inboard to reduce the bending moments as shown on the left side of figure 14. One method of achieving this is by deflecting an outboard control surface to reduce the lift outboard. Outboard control surfaces tend to lose their effectiveness as dynamic pressure increases.

Elastic wing twist caused by torque due to control surface deflection results in a redistribution of the wing lift. This change in wing lift counteracts the desired change due to the control surface. Loss of control surface effectiveness is aggravated by increases in either aspect ratio or sweep angle.

Design maneuvers tend to be critical at V_A, the speed at which C_{LMAX} is required to achieve a 2.5g maneuver. At higher speeds, the loads due to the 2.5g maneuver are less, because of aeroelastic washout. Thus, an outboard aileron may have considerable effectiveness at V_A, where it is needed, much less effectiveness at maximum operating speed (V_{MO}) and yet be an efficient maneuver load alleviation device. For configurations with reduced sweep angle 2.5g maneuvers tend to become more critical at V_{MO}, however the outboard control surface also will become more effective so that the same trend will be true.

The loads due to a design gust are unlike maneuver loads in that they increase with speed and are usually critical at V_{MO}. Thus, the same outboard aileron that was effective as a maneuver load alleviation device may be ineffective as a gust load alleviation device.

As shown on the right side of figure 14, the gust load alleviation systems should reduce total load on the wing by dumping lift through some device, such as a mid-span aileron, that is effective at high speed. The system should also pitch the airplane into the gust by the augmented longitudinal stability system. Determination of gust loads on an airplane with such a system operation can be accomplished only by use of the quasi-static or dynamic math models previously described.

DISCUSSION OF FATIGUE EVALUATION

Fatigue cracking is a very slow process and, therefore, it is considered to be an economic rather than a safety problem. For this reason the FAA does not have a fatigue requirement for typical aircraft structure. However the major transport manufacturers have learned that they must carefully check all structures against some fatigue criteria to assure customer safisfaction. Boeing, for instance, requires a low probability of cracking during 20 years normal service. Experience has shown that wing surface material will be critical for fatigue on some transports. This is frequently true of the lower surface and sometimes true for the upper and lower surfaces.

Figure 15 illustrates the fatigue criticality of the wing upper and lower surface of a recent model of the Boeing 747. The curves show weight of the bending material required for static strength and the amount and location of additional fatigue material that was added. This kind of data is configuration sensistive and the fatigue criticality of the configurations to be studied undoubtedly will vary. Four-engined configurations (wing mounted) are more apt to be critical on the upper surface than two- or three-engined configurations. Increasing the design range of a configuration by the addition of more center section fuel will probably reduce the fatigue criticality of both the upper and lower surfaces. Fatigue loads can be only partially alleviated, as

will be shown in the next paragraph, and therefore a configuration that is fatigue critical will have less potential benefit due to ACT than a configuration that is not fatigue critical.

Before approaching the problem of fatigue load alleviation it is important to understand the types of loads that cause fatigue damage.

The total fatigue damage in wing structure can be divided into two parts: (1) ground-air-ground (GAG) damage and (2) ground and flight maneuver and gust damage.

Figure 16 shows the stresses used for fatigue analysis of a highly loaded segment of a wing lower surface of the same model 747 on a typical flight. The GAG cycle is the change in stress from the maximum compression on the ground to the maximum tension in flight that is expected once per flight. The maximum compression is the 1g taxi stress plus an increment for ground dynamics. The maximum tension is the 1g flight stresses plus an increment due to the peak gust or maneuver. For clarity the figure shows only one cycle of alternating load in each flight segment. The analysis uses the correct number of such loads that will result in the total fatigue damage predicted in that flight segment.

Figure 16 also shows that same data with a hypothetical ACT system incorporated. If a 10 percent weight saving were achieved by application of ACT on the strength design the 1g stresses would be 10 percent higher since the 1g loads would be the same. Because there is no simple way to reduce ground dynamic loads, the alternating stresses on the ground would also be 10 percent higher. ACT can reduce inflight maneuver and gust loads as shown but a net increase in the GAG cycle alternating stresses, and therefore in the GAG fatigue damage will result.

Figure 17 shows percent of total fatigue damage done by the GAG cycle on the upper and lower surface of the 747 model referred to previously. Since the weight saving due to ACT could increase the GAG damage, the total damage may exceed the allowable. This would mean that the weight saving for reduced design loads due to ACT would be limited by the fatigue requirement.

It should be emphasized that the above discussion applies only to a configuration that has no fatigue margin. Most configurations have some fatigue margin on the upper surface and many have fatigue margin on the upper and lower surface. On such configurations a much greater weight saving due to ACT would be achieved.

FLUTTER CRITERIA

Flutter is a definite safety concern and strict FAR criteria must be met to assure that the airplane will never encounter it. Some of the configurations being considered, such as higher aspect ratio wings, will have a flutter speed below the required $1.2V_D$. Since the FAR's do not recognize flutter suppression systems (FSS) as a means of clearing flutter new criteria must be established that include FSS and has reasonable probability of acceptance by the FAA.

Flutter modes can be displayed as a plot of stability vs. speed. Most modern jet transports have critical flutter modes that can be characterized by one of the three plots shown on figure 18. Mode 1 is characterized by a rapid reduction in stability as the flutter speed is approached. It is frequently called "hard" flutter and should never be approached in flight. Mode 2 is "soft" flutter that would be considered safe to approach during flight test. Mode 3 is a "hump" mode that is stable but may exhibit unacceptably low damping. Most critical flutter modes on recent jet transports are similar to mode 2 or 3. Sometimes a "tip" mode occurs like mode 1 but these can usually be fixed for a small structural weight penalty. The above suggests the following as reasonable criteria:

1) With the flutter suppression system off the airplane must be shown by analysis to be free from flutter to:

   (a) $1.2V_D$ for modes which have a rapid reduction in damping as the flutter speed is approached and,

   (b) V_D for all other modes.

2) With the flutter suppression system on, the airplane must be shown by analysis to be free from flutter to $1.2V_D$.

3) The airplane must be shown by flight test to be free from flutter or unacceptably low damping to V_D with FSS on and to V_{D2} with FSS off.

V_{D2} is a "system-off" or "after-failure" dive speed that may be below V_D but must be above V_{MO}. V_{D2} would be defined as the highest speed at which damping is still considered acceptable. There would also be a new reduced operational flight envelope with the usual upset margin provided between this envelope and V_{D2}.

The above represents only a "skeleton" for building flutter criteria. Many details such as redundancy, warning systems, and speed tolerances must be addressed.

These criteria would allow flight testing above V_{MO} with FSS off to V_D or until unacceptably low damping occurs. If V_D is attained, consideration should be given to deleting the FSS from the certificated airplanes.

The selection of reasonable FSS criteria is a very important task in the Max Benefits program. It will play a major role in determining the benefits due to the FSS, which may be a significant part of the total benefit of ACT.

CONCLUSIONS

Configuration optimization, including ACT functions, is expected to result in significantly greater benefits than could be achieved by applying the ACT functions to existing airplanes. However, this kind of configuration optimization complicates the design process. Analysis methods used by the aero-

dynamics, flight controls and structures technologies must be integrated. Most of the elements of this integrated design process will be verified during the DAST program. The process will be broadened for the Max Benefit program in order to perform what is believed to be the first credible assessment of the potential of ACT as applied to a new airplane.

Another difference between the ACT functions applied to a new configuration and those applied to an existing airplane is in the application of design load alleviation techniques. Most existing airplanes are maneuver critical whereas a new configuration optimized including ACT functions is expected to be gust critical. Emphasizing gust-load alleviation will probably lead to a more comprehensive control system in terms of transducer inputs, frequency response and actuator rates.

Fatigue is important in structural design because of its potential economic impact. Structural evaluation of the configurations developed during the Max Benefit program will include a fatigue analysis. Many of the configurations will have some of the primary wing structure critical for fatigue. Past experience has shown that the GAG portion of the fatigue damage is frequently a major portion of the total damage. Since this portion cannot be alleviated, those configurations that are fatigue critical will show less benefit from ACT than those that are not.

The present FARs do not consider flutter suppression systems as a method of clearing flutter. A very important task in the early portion of the Max Benefit program will be to establish criteria that allow use of a FSS and ıd yet retains the required level of safety.

Applications of the lessons learned in these two studies should result in significantly improved efficiency of future transports.

REFERENCES

1. AFFDL TR-74-92 Volume I, "B-52 CCV Program Summary", March 1975, The Boeing Company, Wichita Division.
2. AFFDL TR-74-92, Volume II, "B-52CCV Control System Synthesis" Janury 1975 The Boeing Company, Wichita Division
3. AFFDL TR-74-92 Volume III, "B-52 CCV System Design and Aircraft Modification", October 1974, The Boeing Company, Wichita Division.
4. AFFDL TR-74-92 Volume IV, "B-52 CCV Component and Aircraft Ground Test", September 1974, The Boeing Company, Wichita Division.
5. AFFDL TR-74-92 Volume V, "B-52 CCV Control System Flight Test Validation", December 1974, The Boeing Company, Wichita Division.
6. Roger, Kenneth L., "Airplane Math Modeling Methods for Active Control Design", AGARD-CP-228, Structural Aspects of Active Controls, 21 April 1977.

TABLE 1.- AERODYNAMIC WING DESIGN PARAMETER

TYPE OF DESIGN	VARIABLE	FIXED
TRANSPORT -	WING AREA INCIDENCE DIHEDERAL THICKNESS RATIO ASPECT RATIO WING SWEEP TAPER RATIO TAIL AREA	PAYLOAD - RANGE - SPEED TAKEOFF AND LANDING DISTANCE
DAST ARW-2- INTEGRATED ACT	WING AREA INCIDENCE DIHEDERAL	TAPER RATIO ASPECT RATIO WING SWEEP TAPER RATIO TAIL AREA SPEED

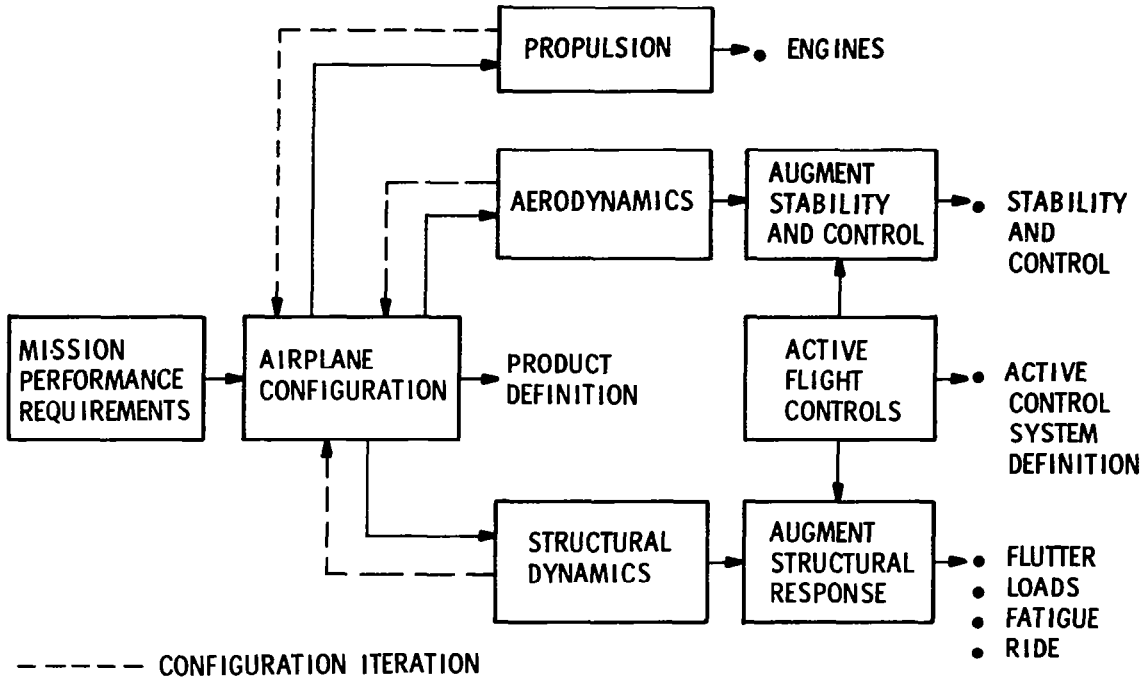

Figure 1.- Conventional aircraft design.

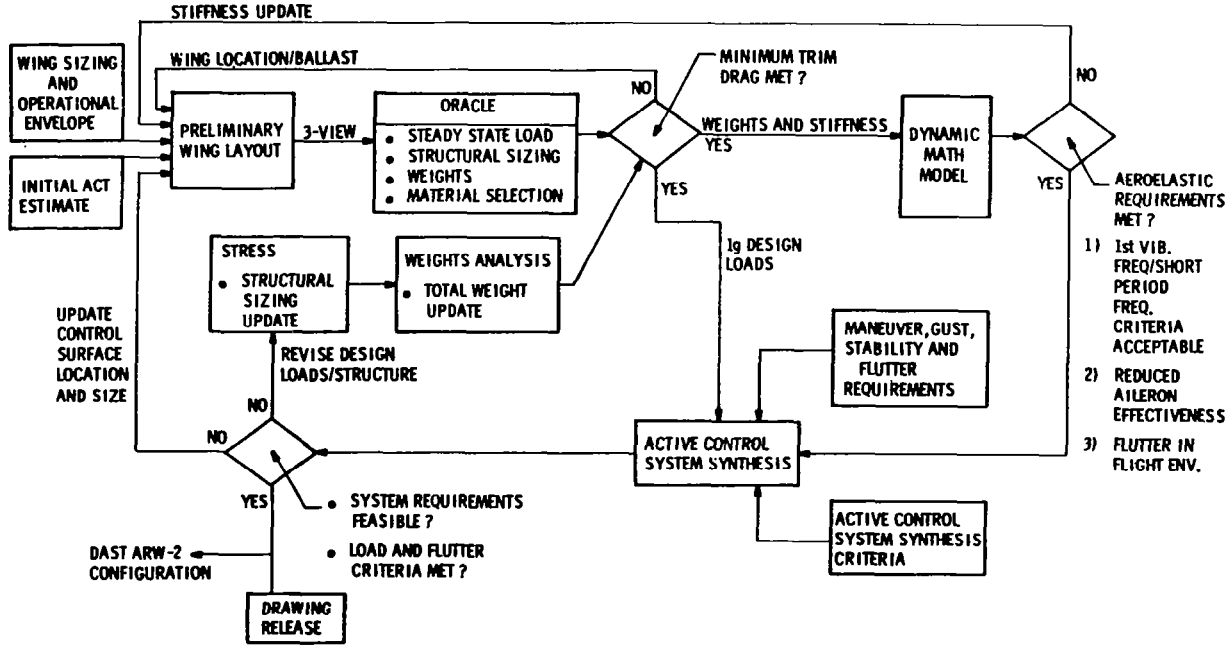

Figure 2.- DAST integrated ACT design.

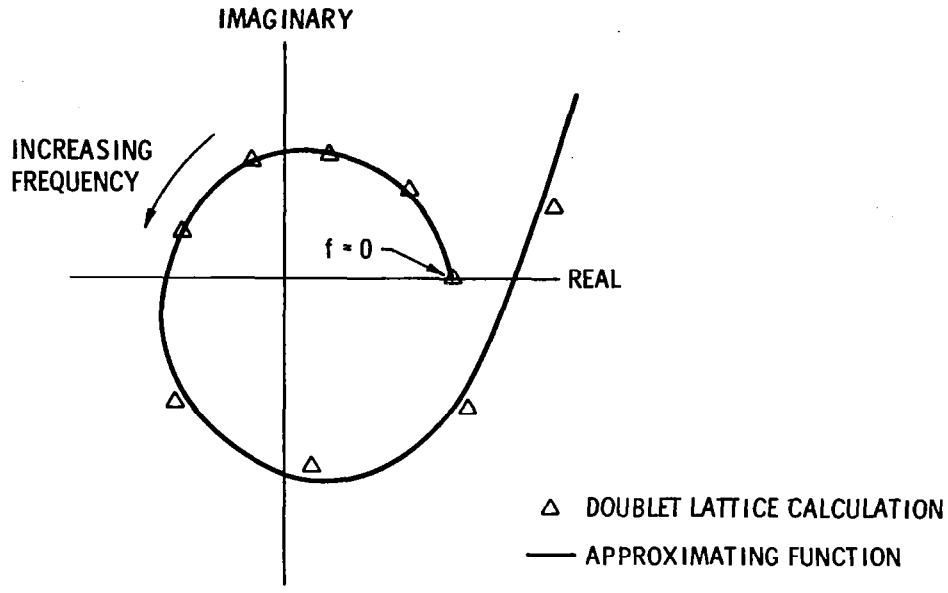

Figure 3.- Aerodynamic coefficient approximating function.

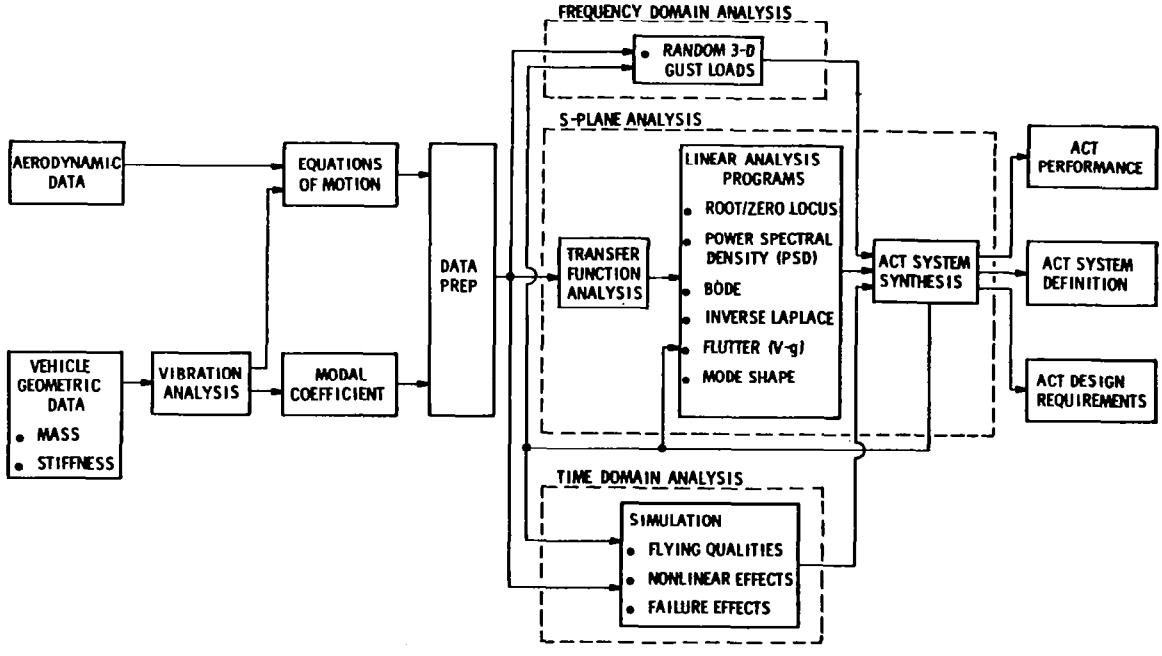

Figure 4.- ACT technology and analysis program integration.

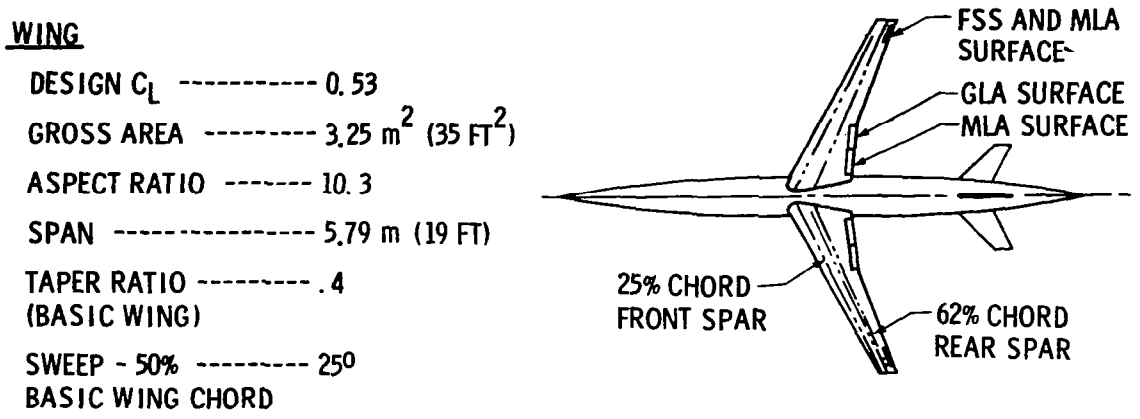

Figure 5.- DAST ARW-2 general arrangement.

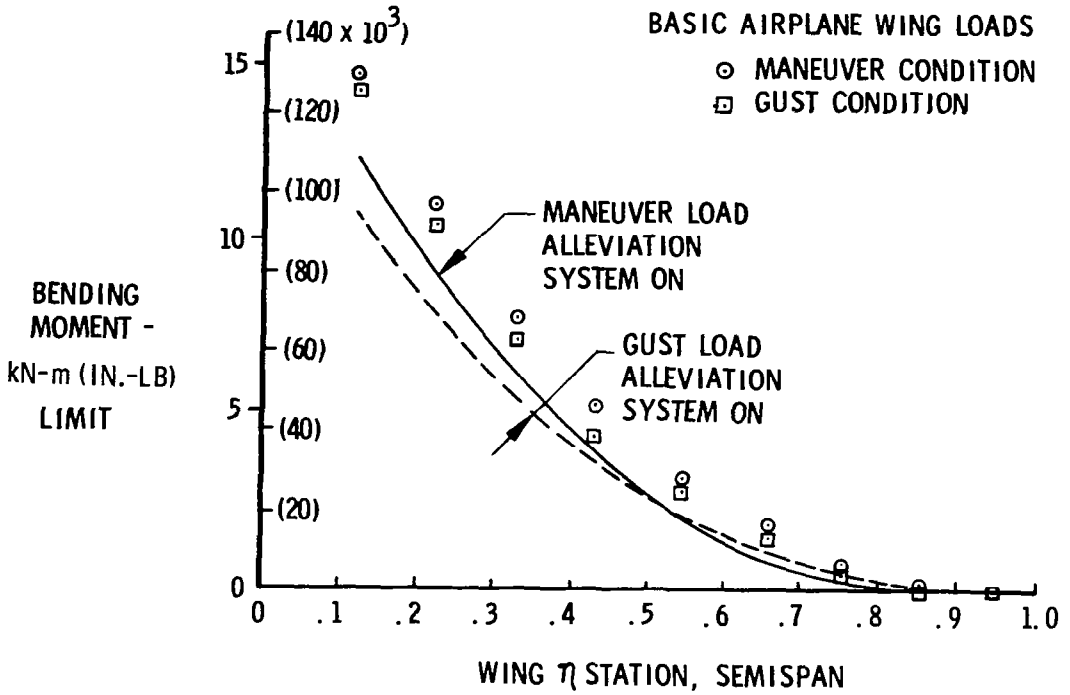

Figure 6.- DAST ARW-2 wing design loads.

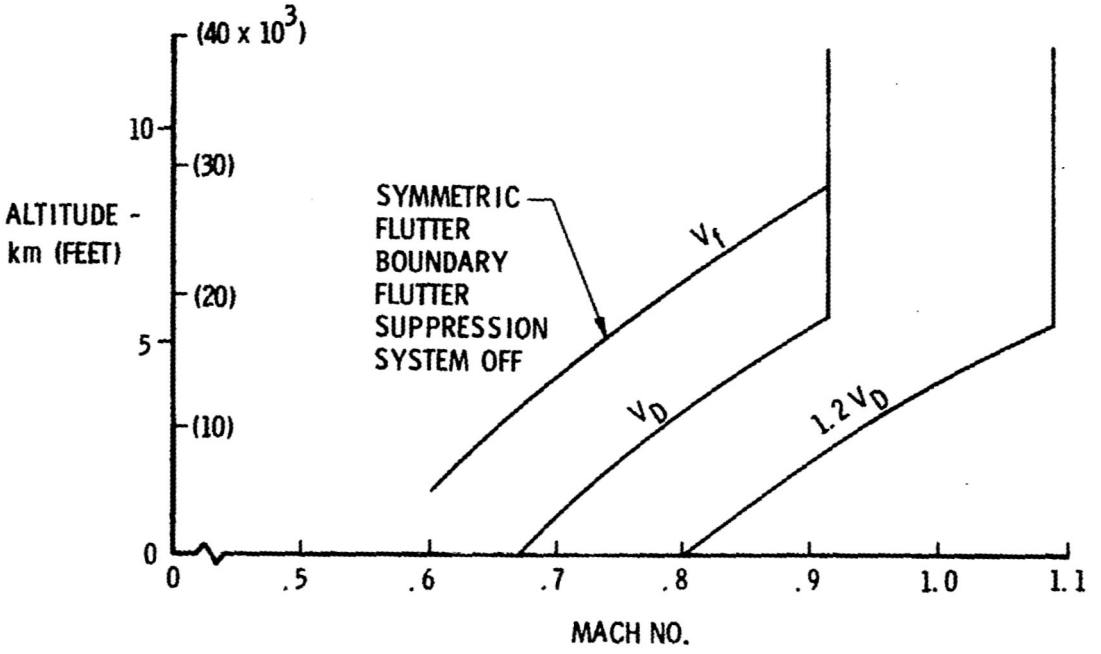

Figure 7.- DAST ARW-2 flutter boundary.

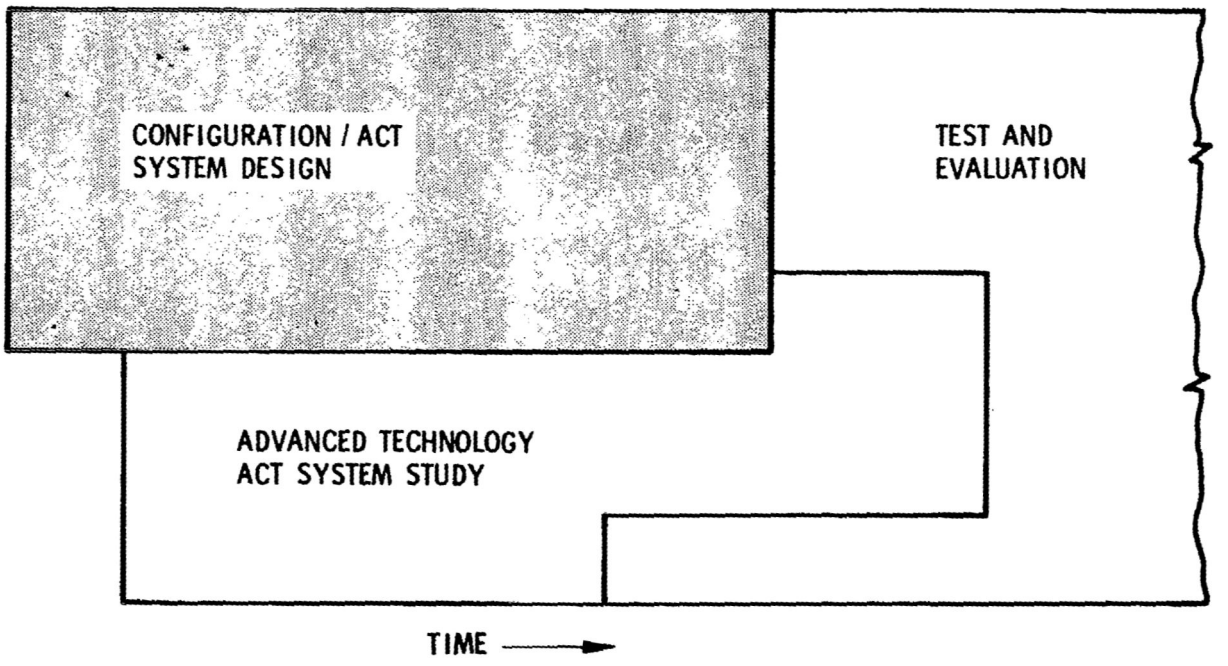

Figure 8.- Major elements of maximum benefit of ACT program plan.

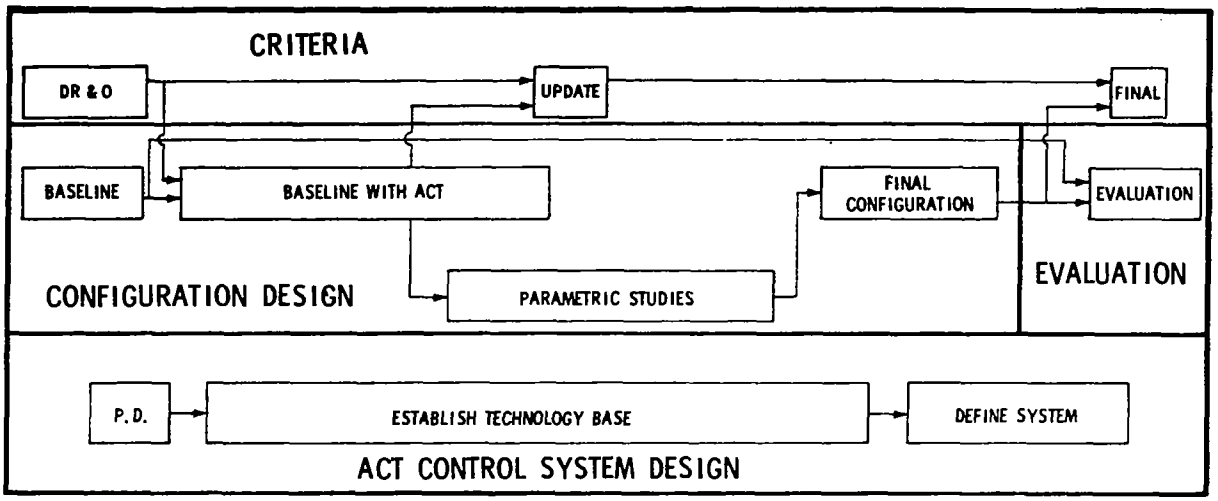

Figure 9.- Configuration/ACT system design task.

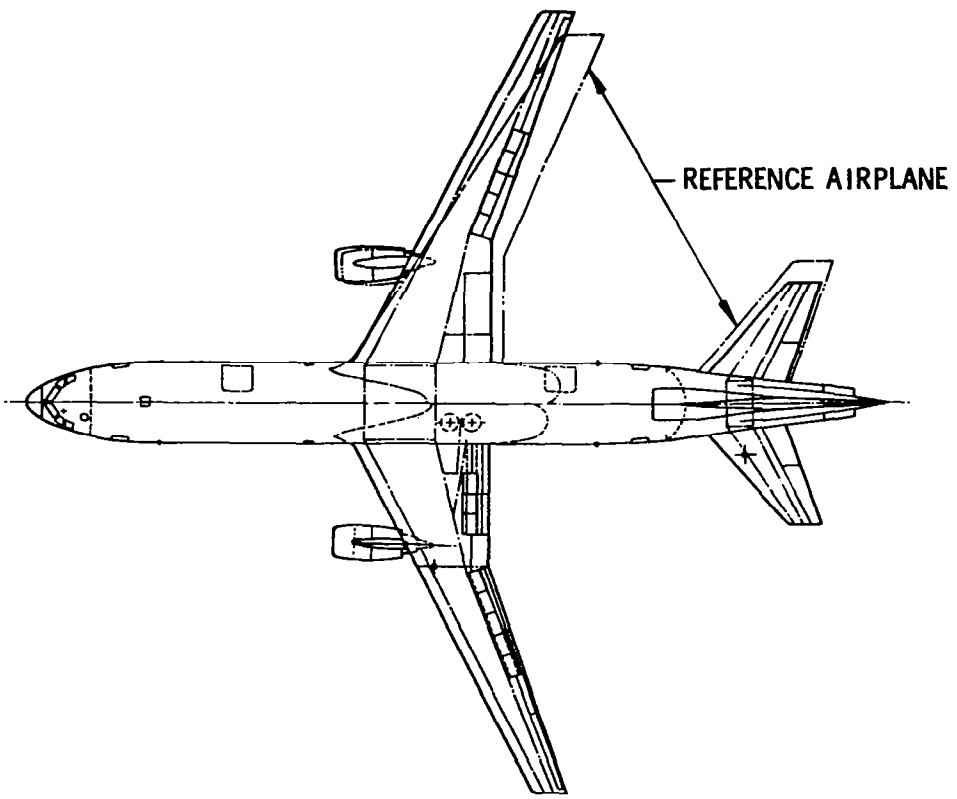

Figure 10.- Possible final ACT airplane.

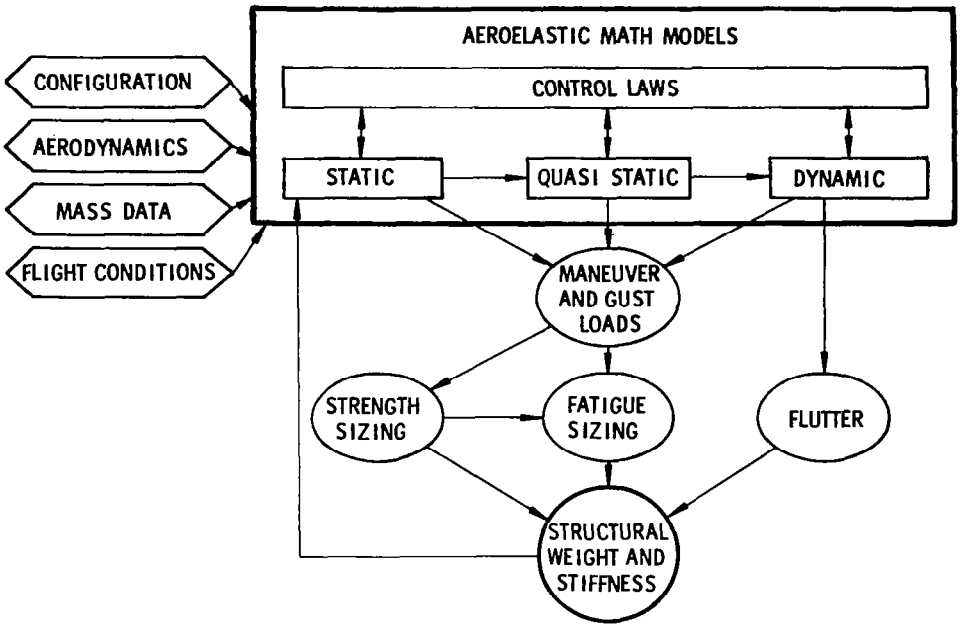

Figure 11.- Maximum benefits structural evaluation plan.

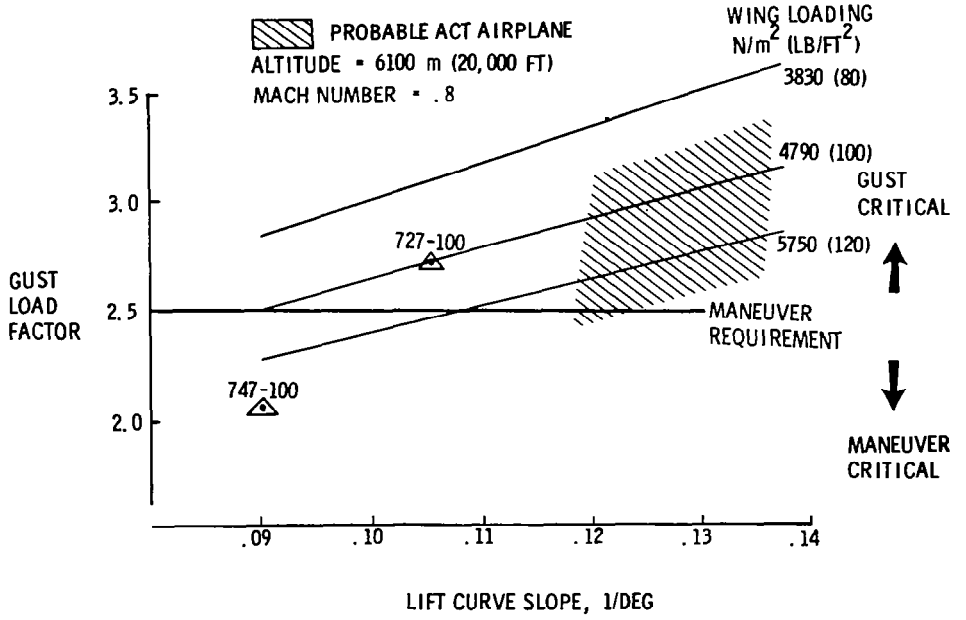

Figure 12.- Gust load factor sensitivity.

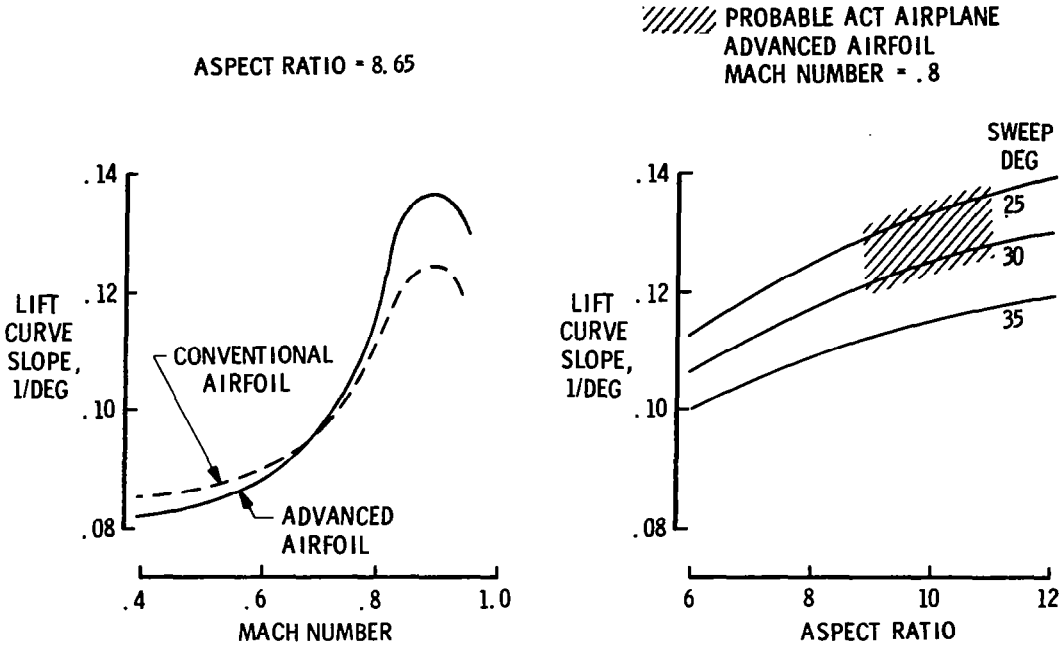

Figure 13.- Lift curve slope sensitivity.

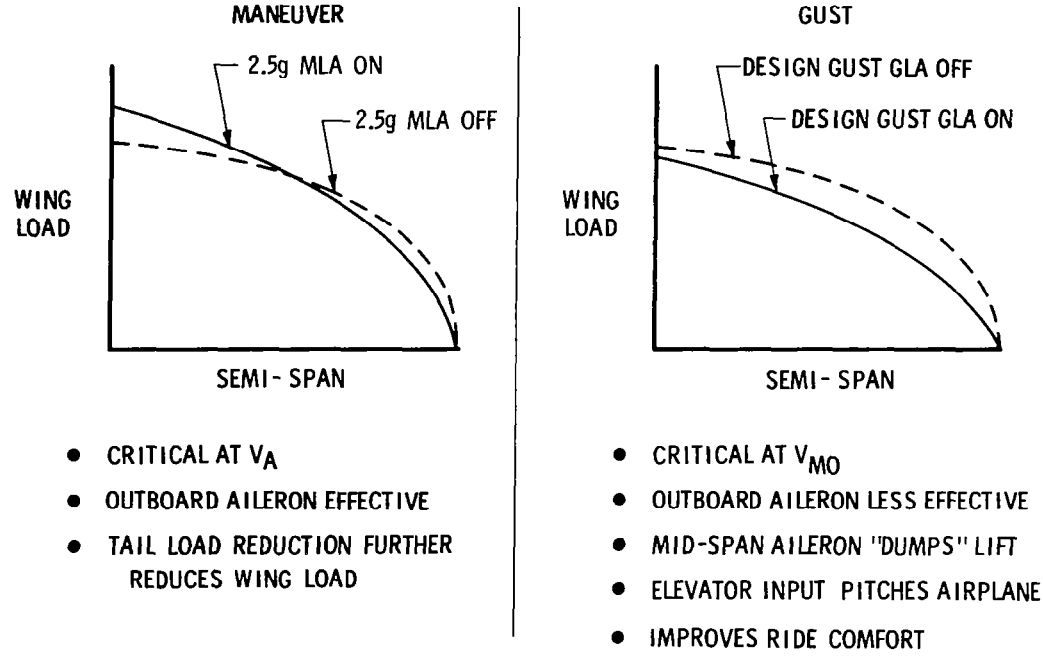

- CRITICAL AT V_A
- OUTBOARD AILERON EFFECTIVE
- TAIL LOAD REDUCTION FURTHER REDUCES WING LOAD

- CRITICAL AT V_{MO}
- OUTBOARD AILERON LESS EFFECTIVE
- MID-SPAN AILERON "DUMPS" LIFT
- ELEVATOR INPUT PITCHES AIRPLANE
- IMPROVES RIDE COMFORT

Figure 14.- Load alleviation.

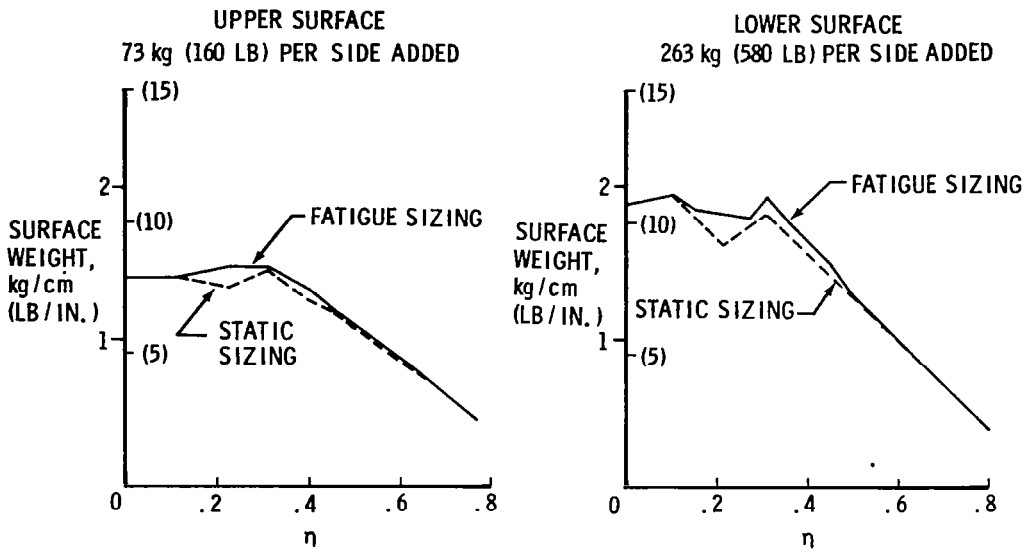

Figure 15.- 747 wing box surface areas.

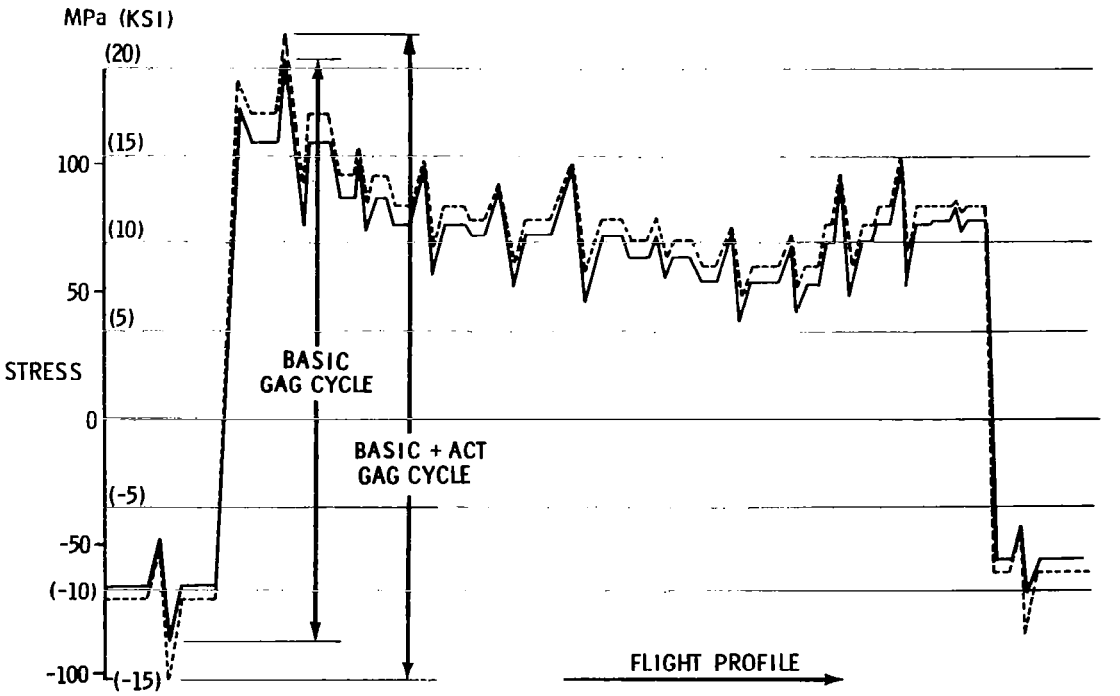

Figure 16.- Typical wing lower surface stress for fatigue analysis.

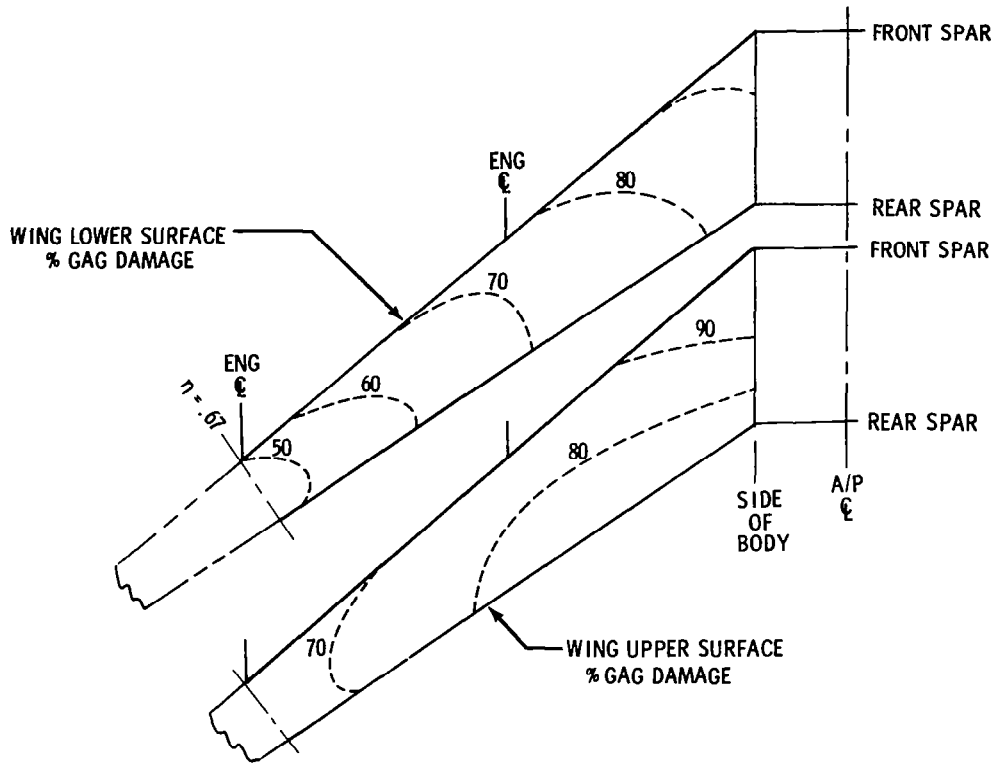

Figure 17.- Percent GAG damage.

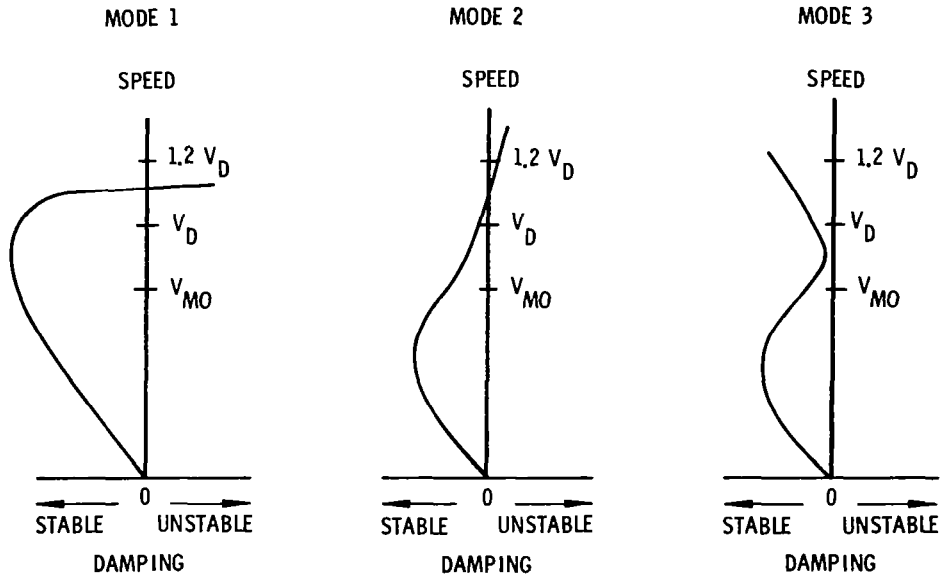

Figure 18.- Flutter stability.

OPERATIONS AND SAFETY INTRODUCTION

John H. Enders
NASA Headquarters

The technology addressed in the four previous sessions of this conference can generally be characterized both as pertaining to specific portions of the aircraft and as being capable of reasonable development without great dependence on actual flight operations. Technology development where such dependence does exist is the subject of this session entitled "Operations and Safety". The term "operations" is used in a broad sense to include deliberate, controlled operations as well as exposure and response to unscheduled events such as inputs due to natural phenomena. All these individually or collectively can affect the safety, economics, annoyance, trip time, and system capacity of the aircraft, the passengers, the airports, and/or the community. The ultimate goal is to achieve, through proper vehicle design and operations, high acceptance of air transport by all interest groups.

The first paper in the session provides an overview of safety as it pertains to the avoidance of, or safe response to, unscheduled events, including accidents, bad weather, and fire. The subjects of the remaining papers involve deliberate, controlled operations of aircraft. The second and third papers involve research on airplane subsystems which are sensitive to operations. The first such paper addresses the phenomena of aircraft-induced trailing-vortex atmospheric disturbances affecting following aircraft. The disturbances can be modified by changes in aircraft wing configuration. A paper on landing-gear technology discusses research toward improving system reliability and component life for conventional take-off and landing operations and for providing advanced systems capable of more versatile operations.

The fourth and fifth papers involve research in subject areas where terminal area flight operations are critically important. The first of these papers describes a method for accurately predicting the noise transmitted to the ground during aircraft landings and take-off. Not discussed is the effort underway within NASA to better predict and reduce aircraft interior noise. The fifth paper is on flight experiments to improve terminal area operations for achieving a more precise flight path than presently possible. By allowing closer spacing of aircraft, such improved precision has the potential for increasing system capacity, for minimizing fuel usage and operating costs, and for decreasing delays, all with no sacrifice in safety.

The sixth and seventh papers address two areas in economics associated with operations of complete air carrier systems. One of these papers reports the results of a study of the factors affecting airline operations, particularly in the airframe maintenance area, from which an improved cost model has been developed. In the seventh, and final, paper, airline operating costs are factored into the much bigger picture of airline ROI (return on investment), manufacturing ROI, and aircraft price to provide an approach for analyzing the benefits and costs for aeronautical research and technology.

OVERVIEW OF SAFETY RESEARCH

John H. Enders
NASA Headquarters

SUMMARY

Aircraft safety is reviewed by first establishing a perspective of air transportation accidents as a function of calendar year, geographic area, and phase of flight, and then by describing the threats to safety and NASA research underway in the three representative areas of engine operational problems, meteorological phenomena and fire.

The aircraft engine operational safety discussion addresses engine rotor burst protection, where both experimental and analytical efforts are underway, and aircraft nacelle fire extinguishment where experimental studies are being carried out to examine the effectiveness of various candidate remedies (for example, application of dry chemicals).

NASA meteorological research is focused on the aircraft-weather interface, both by fine-scale characterization of weather phenomena, and by providing warning or protection against weather hazards. Studies underway are described in the areas of severe weather wind shears and turbulence, clear air turbulence, and lightning.

The present NASA fire program emphasizes fire impact management through fire resistant materials technology development. A description is given of the ongoing five-year FIREMEN Project whose objectives are to identify better fire safety materials for the aircraft interior and to improve the understanding of fire dynamics, test methodologies, and toxicity reduction schemes.

INTRODUCTION

Safety is a subjective term, with many definitions. It includes concepts of risk exposure, risk taking, and risk management. It defies unique interpretation but can be thought of as the absence or control of factors which can cause injury, loss of life, or damage to or loss of property. The meaning of acceptable safety, on the other hand, varies with the situational and time frameworks, and with the individual's perception of risk coupled with his willingness to be exposed to risk and the degrees of exposure. Starr in reference 1 discusses the differences in acceptable risk levels, depending upon whether it is a "voluntary" or "involuntary" risk. These concepts hold high significance for those involved in improving safety and operational efficiency in air transportation. They explain, in part, the vast differences in air transport, general aviation, and auto fatal accident statistics, and suggest reasons for the intense public scrutiny of the typical air transport accident, whereas general aviation and auto accidents receive considerably less attention.

To establish a perspective, consider transportation fatalities for 1977. Of a total 50 856 transportation fatalities, air transport accounted for 654 or 1.3 percent. General aviation suffered 1395 fatalities or 2.7 percent of the total. Another view of air transport safety is given by the fact that in 1977, out of about 5 million U.S. Air Carrier take-offs and landings, only six fatal accidents occurred.

Figure 1 shows the cumulative picture of jet hours and hull losses. Between 1959 and 1977, 300 jet hulls have been lost, world-wide. U.S. carriers account for one-third of the total losses but log slightly more than one-half of the world-wide 142 million cumulative flight hours. Figure 2 shows the cumulative hull loss rate for the same period. As of the end of 1977, U.S. air carriers averaged 1 hull loss per 779 000 hours, slightly less than one-half the loss rate of the rest of the world. Table I shows hull loss rates by geographical area. The dramatic improvement in losses for Australia and South Pacific areas is evident, as is the steady improvement in U.S. operations. These regional figures are interesting, because they raise questions concerning the differences in operational facilities, training, maintenance, regional weather and operating environment, human factors, navigation, and communications. The common denominator is that the same U.S. equipment predominates in each region. Table II is an estimated cost of commercial jet accidents. Note that neither injury liability nor third party damage is included. Although aviation is a highly safe mode of transportation, operating problems, incidents, and accidents continually point the way for safety improvements.

Aviation Safety and Operating Problems Research is itself the subject of conferences similar to this one which are held about every 5 to 6 years. The most recent took place at NASA Langley Research Center in 1976 (ref. 2). This research is a broad topic, infused in disciplinary and project effort, as is evident from the safety considerations noted in many other papers presented during this Conference.

The NASA research program in Aviation Safety derives from identification of operating problems which erode safety margins and from lessons learned through accident analysis by National Transportation Safety Board (NTSB) and Federal Aviation Administration (FAA). The vast bulk of NASA aeronautics funds is spent on keeping aircraft flying efficiently and reliably, with improved performance. Accidents and incidents suggest research and development actions necessary for improving understanding and knowledge of the natural environment and the physical and the operational environments. About 5 percent of the budget is devoted to research on safety and operational problems. Of this segment, about three-fourths is oriented towards avoiding accident-enabling situations; this effort includes aviation meteorology, vehicle systems, operational systems, and human factors. The remaining one-fourth is directed at maximizing occupant survival in case an accident occurs and includes crashworthiness and crash fire research.

Figure 3 shows the distribution of fatalities by phase of jet transport operations. About 80 percent of fatalities occur in the terminal phases, either during approach and landing, during take-off or take-off aborts, or

because of loss of control while on the runway. In these cases, the aircraft speeds are lower than during en route operation, so chances for survival of an accident are correspondingly higher; the bulk of our safety effort is directed at preventing accidents and maximizing occupant survival in terminal operations phases.

The remainder of this paper will present a brief overview of three representative operating problems and safety research efforts:

(a) Aircraft engine operational safety
(b) Aviation meteorology research
(c) Fire technology

AIRCRAFT ENGINE OPERATIONAL SAFETY

The aircraft turbine engine and its associated fuel and control systems, contain considerable kinetic and chemical energy which must be controlled in order to preserve adequate safety margins. Engine structural failure and inflight fires are events which, although rare, demand preventive and survival attention.

Engine Rotor Burst Protection

NASA Lewis Research Center has been exploring engine rotor failure and fragment control since the late 1960's with the objective of providing a basis of understanding upon which engine rotor integrity can be improved and fragment control schemes can evolve.

Uncontained engine failures are rare events (fig. 4) and remain somewhat centered about 1 per million flight hours. However, the damage wrought by a fragment (fig. 5) is awesome, can reduce the operational margin of safety to near zero (fig. 6) or in the extreme case can be fatal. In U.S. air carrier service, uncontained rotor bursts vary about a mean of 20 to 25 occurrences per year (fig. 7), and not surprisingly, tend to occur more during the high power operation of take-off and climb (fig. 8).

In cooperation with the Naval Air Propulsion Test Center, NASA-built spin facilities (fig. 11) are used to obtain empirical information on rotor failure and fragment impact on containment rings of various high strength materials. Figure 10 is a typical high-speed photographic sequence of a T-58 rotor, scored to control fragment size, failing, and impacting a test containment ring. Analysis of this type of data permits evaluation and screening of various containment ring materials and designs.

Concurrent with this empirical effort is an analytical program at the MIT Aeroelastic and Structures Research Laboratory, designed to develop theoretical procedures for predicting large-deflection elastic-plastic transient structures to cope with rotor burst fragment attack. Earlier efforts have concentrated on containment/deflector (C/D) structures whose axial dimensions are comparable with those of the attacking fragments, and hence the associated structural

responses are essentially two-dimensional. Recent research efforts have concentrated on analysis of C/D structures whose axial dimensions are much larger than those of attacking fragments; hence, the associated structural response to be analyzed is essentially three-dimensional. A series of computer programs have been developed which can predict C/D ring response from an assumed fragment attack, or conversely yield loading parameters of a fragment attack from given ring deflections and behavior.

A NASA-sponsored workshop "An Assessment of Technology for Turbojet Engine Rotor Failures" was held at MIT (ref. 3) on March 29-31, 1977 where this NASA program was presented along with results of other foreign and domestic government and industry programs. As engines grow larger and fragment energies continually increase, the problem of insuring adequate safety margin remains with us.

Aircraft Nacelle Fire Extinguishment

Modern jet aircraft engine nacelles contain various piping, tubing, etc., carrying pressurized oil, fuel, and hydraulic fluids. Large volumes of air induced from outside the engine or bypassed from the compressor section ventilate the nacelle space to insulate the hot engine surfaces from the adjacent structure, manifolds, and fairings. Failures of piping due to various causes have occurred and sometimes result in sprays which contact the hot surface, ignite, and burn vigorously in the local air streams. Extinguishing such fires is difficult, and must be rapid and effective to prevent major structural damage or loss of the aircraft. An "effective" extinguishant should be able to initially reduce the fire and to continue to suppress reignition until the fuel flow can be stopped or the hot ignition surface is cooled.

Figure 11 shows an inflight nacelle fire, surrounded by pictures of a small nacelle fire research rig at Ames Research Center designed to examine methods of applying effective fire control. A stream of Jet A fuel is channelled via capillary tubes to a glowing hot surface located in the base of an open trough over which is flowing a stream of air. At the upper left, air flows at 20 m/sec over a stainless steel surface heated to 800° C while Jet A fuel flows onto the surface. At double the airspeed (center left), a very energetic and practically invisible blue flame exists over the test surface. A set of thin parallel rods welded to the surface retain the fuel in intimate contact with the surface while several metal projecting strips act as flame holders for globules of fuel that evaporate and burn on the hot surface.

At predetermined burning conditions for the particular flammable liquid (e.g., Jet A, Jet B, JP 4, etc.), a dry chemical extinguishant is injected in a single, 1-second burst typically knocking the flames down (bottom photograph) and continuing for several seconds or longer to suppress the reignition of the flowing air-fuel mixture contacting the heated surface that was initially capable of igniting the fuel. The dry extinguishant fuses on the hot metal surface, and insulates the fuel from it and thus prevents reignition. In the upper right photograph, the glowing thermocouple leads and red hot surface are still visible through the extinguishant cloud being thinned by the air flow.

The ongoing experiments conducted with Ames nacelle fire simulator are providing new insight into better techniques of controlling hot-surface-ignited fires.

AVIATION METEOROLOGY RESEARCH

Aircraft encounters with bad weather situations continue to produce accidents, incidents, and disruptions to schedules which are frequently surrounded by circumstances which prompt investigators and analysts to question the inevitability of the event.

Bromley of the FAA (ref. 4) reports that statistics for 1975 on delays for periods $\geq$30 minutes show that weather is a significant causal factor affecting the efficiency of air transportation. (See fig. 12.) These FAA data are representative of the past 5 years and show weather parameters as mutually exclusive categories. The percentage of weather-caused delays has varied from 65 percent to 90 percent, with the total number of these delays being >30 000 per year for each year of the 5-year period.

McLean of NTSB (unpublished) cites air carrier statistics showing unexpected encounters with clear air turbulence as the major cause of accident, characterized mostly by injuries to crew or passengers when seat belts have not been used. Factors associated with severe storms account for the most fatalities in air carrier operations, both en route and in the terminal area. Low visibility, due to fog on the ground, has caused fatal errors in judgment on landing and was a major factor in the Tenerife accident.

The Federal government alone spends about \$2/3 to \$3/4 billion annually on meteorological operations and supporting research, \$1/4 billion of this specifically on aviation. FAA, U.S. Coast Guard, NASA, and the military services support meteorology research specifically directed at aviation operations, while National Oceanic and Atmospheric Administration (NOAA) provides basic weather research, data collection, analysis, and dissemination services.

NASA aviation meteorology research centers around the aircraft-weather interface. It addresses both the need to provide sufficiently fine-scale characterization of weather phenomena such as wind fields at all flight levels, severe storms, lightning, icing, and turbulence; and the need for providing warning or protection against weather effects such as clear air turbulence (CAT), wind shear, lightning strikes, and icing. Three efforts illustrate this research

Severe Weather Conditions

The local gust front (fig. 13) created by the rain-cooled outflow from a severe thunderstorm is a familiar phenomenon. The downdraft impinges upon the surface of the earth and spreads radially outward and thus generates substantial wind speed variation and large wind shears near its leading edge as well as at its core. This developing gust front may extend beyond 15 to 20 km from

the storm and poses a serious danger to aircraft operating in its vicinity. Several accidents over recent years have been attributed to encounters with downdrafts or the outflowing gust front.

NASA has been interested in determining the feasibility of predicting conditions under which wind and turbulence environments dangerous to aircraft operations exist. Extensive ground measurements of atmospheric boundary-layer behavior using instrumented towers and laser Doppler systems have been made (ref. 5). Recently, Aeronautical Research Associates of Princeton (ARAP), under contract to NASA, have applied an axisymmetric atmospheric boundary-layer numerical turbulence model to the gust front situation. This model is used to reconstruct wind and turbulence profiles which may have existed at low altitudes at the time of aviation accidents. The predictions obtained are consistent with available flight recorder data, but neither the input boundaries nor the flight recorder observations are sufficiently precise for these case studies to be interpreted as verification tests of the model predictions. The results do provide a physically consistent set of wind and turbulence profiles which may be used to help understand those meteorological conditions which may lead to low-level wind shear and turbulence profiles, as well as providing a set of profiles for use in flight simulation studies which have proved hazardous in the past (ref. 6). The ARAP computer model solves the velocity, temperature, and turbulence distributions in the atmospheric boundary layer. It is based on using invariant modeling for closure of the dynamic equations of the ensemble-averaged single-point, second-order correlations of the fluctuating velocities and temperatures. The model appears to give a good representation of the physical dynamics associated with a local downdraft. Simulated trajectories flown through these model results demonstrate the types of problems that pilots could encounter.

Preliminary results indicate the most important variables to be the temperature decrement and the altitude from which the downdraft originates. Surface roughness and velocity of the storm cell may also be expected to have a strong influence on the winds close to the surface.

Clear Air Turbulence (CAT) Characterization and Warning

Unexpected encounters with turbulence in clear air continue to account for the majority of transport nonfatal accidents. Injuries to flight and cabin crew members as well as to passengers could be avoided or reduced if CAT could be reliably forecast or predicted as to extent and intensity.

CAT occurrence is associated with mountain waves, with shear layers attendant to the jet stream, and with instabilities in the atmosphere's temperature lapse rate. Under the guidance of the Federal Coordinator for Meteorology and Supporting Research, NASA and other agencies have worked for several years to characterize CAT in functional terms so that its occurrence and geographical extent could be understood and reliably forecast from analysis of measurable parameters (ref. 7). Forecasting accuracy has improved substantially in recent years, and has allowed more frequent warning of CAT areas; seat belt usage has also prevented many injuries. However, unexpected CAT encounters still occur so that in-flight detection and warning remains a highly

desired capability. As an adjunct of the CAT characterization program, NASA has also been engaged in exploring laser technology applications to the airborne CAT detection problem. This effort has been described at previous Langley Conferences on Aircraft Safety and Operating Problems in 1971 and 1976 (refs. 8 and 9). Since that time, additional system improvements have been made and airborne evaluation (fig. 14) of the upgraded system is scheduled to be completed during the next CAT season, January to March 1979.

A companion effort in airborne CAT detection was undertaken last year as a result of the discovery, during astronomical observation flights aboard the NASA C-141 Kuiper Airborne Observatory, of a correlation between atmospheric water vapor concentration variations and the existence of CAT. A simple prototype infrared radiometer and signal microprocessor detects these water vapor anomalies which seem to be associated with CAT presence. Figure 15 shows the system installation aboard the NASA Lear Jet where it is undergoing flight validation and concept validation. By mid-Spring, 1978, assessment of the promise of this concept as a practical candidate airborne CAT detection system should be possible.

Lightning Hazards Research

NACA and NASA research publications since the 1920's have included reports on various aspects of atmospheric electrical phenomena. Of these, the greatest concern to safe flight operations is undoubtedly lightning. Following the 1963 Elkton, Maryland, accident whose probable cause was determined to be ignition of fuel vapors by a lightning strike, NASA began a series of efforts to determine, in quantitative terms, the effects of lightning strikes on aircraft fuel systems, nonaluminum metals and nonmetallics, and induced effects within aircraft electrical systems which increasingly employed microcircuit elements. In addition, nonelectrical damage to aircraft structure from shock waves emanating from lightning strokes was assessed. Data, knowledge, and understanding from these and other efforts was summarized in a reference publication issued last November entitled "Lightning Protection for Aircraft." (See ref. 10.) NASA in partnership with USAF and other government agencies plans to continue its research on lightning and its effects in order to better characterize the air-to-aircraft strike, to assess effects on advanced control systems, and to explore means of protecting nonmetallic structural elements.

Other Recent Meteorology Efforts

Brief mention must be made of two other related efforts in meteorology operations supported by NASA's Manned Space Flight and Applications Offices.

The Kennedy Space Center, concerned about lightning strike hazards to ground and spacecraft launch operations, has developed a Lightning Detection and Ranging (LDAR) System (ref. 11). The system operates in the frequency band of 30 to 50 Mhz and uses a central receiving station with four outlaying receiving stations, each some 8 km from the central station. The LDAR system locates the position of electrical discharges in the atmosphere by processing the time of arrival of the pulsed radio frequency (RF) radiation emitted by the lightning discharge. LDAR is a near real-time system with a capability

of detecting ten data points per second and recording these on digital tape. It affords a means of providing lightning hazard information to aircraft flights within a radius of up to 160 km of the central station. In addition, refueling and other ramp operations could benefit from the safety assurance afforded by LDAR's precise tracking of lightning activity.

A system was developed by NASA for the NOAA to provide a low-cost prototype data handling system to transmit meteorological data gathered from wide-body jet aircraft flying remote routes to ground users via synchronous meteorological data relay satellites. The Aircraft to Satellite Data Relay (ASDAR) project, after successful intensive in-house and airline tests, will continue under evaluation for a year (ref. 12). The routine updating of en route weather over remote areas of the world is made possible by this system and safer operations should result.

FIRE TECHNOLOGY

Successful egress from a crashed airplane can be hindered or made impossible by fire, while in-flight fires must be dealt with directly and promptly to insure survival. Statistics and studies dealing with aircraft accidents present evidence of aircraft occupants surviving crash impact, only to succumb to the associated fire or its effects (fig. 16). Although three catastrophic in-flight interior fires have occurred in turbine-powered transport operations, by far the majority of in-flight interior fires have been of small magnitude, were detected early, and have generally been controlled with minimum damage to life or property. The potential for catastrophe remains, however, and it is essential that continuing attention be focused on preventing, detecting, and extinguishing the in-flight fire.

Because aircraft fires are complex phenomena, it is helpful to structure approaches to dealing with fire within the fire dynamics logic tree, shown in figure 17. Fire safety is insured by either preventing ignition in the first place or, failing that, to manage or control the impact of the fire. Preferably, it is desirable to prevent the fire from occurring, by isolating fuels from ignition energy sources, by making materials ignition resistant, or by modifying jet fuel so that ignition of spilled fuel does not take place during the critical crash period. The impact of fire, on the other hand, can be controlled by limiting burning rate responses of materials, by providing thermal barriers, by suppressing fire through extinguishing schemes, or delaying fire build-up until occupants can be evacuated (ref. 13).

NASA's present fire program emphasizes fire impact management through fire resistant materials technology development. The extensive use of organic materials in aircraft interiors (fig. 18) provides opportunities for material fire response rate modification, to either prevent the involvement of these materials or to limit their rate of reponse so that more time is available for occupants to evacuate a survivable crashed airplane. To this end, NASA is seeking fire safety improvements in materials used in ceiling panels, enclosure panels, sidewall panels and windows, thermoplastic moldings, seat fabrics and cushion materials, and floor panels (fig. 19). This materials technology

is being developed concurrently with improving our understanding of fire dynamics, test methodologies, and toxicity reduction schemes. The effort is closely coordinated with FAA and DOD fire research and development. This work is incorporated in a 5-year project designated as FIREMEN (FIre REsistant Materials ENgineering). Begun in 1976, FIREMEN will be completed in 1981 at which time it is expected that advanced, low-toxicity, low-smoking, fire-resistant material candidates will have been thoroughly evaluated not only from a fire safety point of view, but also from the very real aspects of basic materials availability, processability, long-term stability, and economics. The results will provide industry with hard data by which engineering judgments on design and selective employment of promising materials can be made.

The technical basis for the FIREMEN program lies in materials modification or synthesis (fig. 20). The flammability of materials can be decreased by post-manufacture treatment with fire retardant chemicals or by synthesis of new polymers with fire resistant behavior built into the material structure itself. Both methods are attractive for certain applications; however, the respective fire performance boundaries, weight and economic costs, must be clearly understood in order to extract the optimum benefits offered.

Additive treatments can be economically attractive and offer good protection from exposure to short duration, moderate heat flux level. However, it has been found that prolonged exposure to externally generated heat (as in a fuel-fed fire or electrical short, in itself not involving the treated materials) can pyrolize the flame treatment chemicals which in themselves become the source of smoke and incapacitating gases. In addition, when all the treatment chemical is pyrolyzed, the basic material is left unprotected and rapidly becomes involved in the fire (ref. 14).

Polymer synthesis, on the other hand, is based upon developing compounds with high char yields when exposed to external heat fluxes. For a given polymer class, the reduction of flammability is generally accompanied by a reduction of smoke and incapacitating gases. The cost and weight are somewhat higher than currently used organics, and both availability of basic monomers and processability of some of the polymers is somewhat limiting to a more vigorous application of these concepts.

Nevertheless, candidate wall panels (fig. 21), seat fabrics and cushion materials have been constructed and tested and show improved fireworthiness. Long-term stability, durability, and other practical design considerations are currently being evaluated.

CONCLUDING REMARKS

NASA aircraft operating problems and safety research effort continues to respond to needs of the aeronautical community. Expanding the basic understanding and knowledge of physical, chemical, environmental, and operating environments where safety margins are impacted is the key to safe, reliable, and efficient design and operation of transport aircraft.

REFERENCES

1. Perspectives on Benefit-Risk Decision Making: Report of a Colloquium Conducted by the Committee on Public Engineering Policy, National Academy of Engineering on April 26-27, 1971. Comm. on Public Eng. Policy, 1972. (Available from NTIS as PB-213 685/1.)

2. Aircraft Safety and Operating Problems. NASA SP-416, 1976.

3. An Assessment of Technology for Turbojet Engine Rotor Failures. NASA CP-2017, 1977.

4. Bromley, Edmund, Jr.: Aeronautical Meteorology: Progress and Challenges — Today and Tomorrow. Bulletin of the American Meteorological Society, vol. 58, no. 11, Nov. 1977, pp. 1156-1160.

5. Fichtl, George: Aeronautical Requirements for Wind Shear Data Produced for Eighth Air Navigation Conference. ICAO-WP/7, Int. Civil Aviat. Organ. (Montreal, Canada), 1974.

6. Lewellen, W. S.; Teske, M. E.; and Segur, H.: Turbulent Transport Model of Wind Shear in Thunderstorm Gust Fronts in Warm Fronts. ARAP Report No. 327 (Contract No. NAS 8-32037), 1978.

7. Scoggins, J. R.; Clark, T. L.; and Possiel, N. C.: Relationships Between Stratospheric Clear Air Turbulence and Synoptic Meteorological Parameters Over the Western United States Between 12-30 km Altitude. NASA CR 143837, 1975.

8. Aircraft Safety and Operating Problems. NASA SP-270, 1971.

9. Aircraft Safety and Operating Problems. NASA SP-416, 1976.

10. Fisher, F. A.; and Plumer, J. A.: Lightning Protection of Aircraft. NASA RP-1008, 1977.

11. Lennon, C. L.: The Performance of a Real-Time, Time-of-Arrival Lightning Location System (LDAR). NASA paper presented at the 1976 Annual Meeting, American Geophysical Union, December 6-10, 1976.

12. Steinberg, Robert: Automated Meteorological Data from Commercial Aircraft via Satellite — Present Experience and Future Implications. NASA TM-73750, 1978.

13. Parker, J. A.; Kourtides, D. A.; Fish, R. H.; and Gilwee, W. J.: Fire Dynamics of Modern Aircraft from a Materials Point of View. J. Fire & Flammability, vol. 6, Oct. 1975, pp. 534-553.

14. Hillenbrand, L. J.; and Wray, J. A.: A Full-Scale Fire Program To Evaluate New Furnishings and Textile Materials Developed by the National Aeronautics and Space Administration. NASA CR-2468, 1974.

TABLE I.- HULL LOSS RATE

[By geographical area; data obtained by M. W. Eastburn of American Airlines]

Area	1960	1965	1975	9 Mos. '77
World	1/144 000	1/265 000	1/ 410 000	1/ 464 000
Australia/South Pacific	--	1/335 000	1/2 360 000	1/3 110 000
U.S.	1/165 000	1/354 000	1/ 674 000	1/ 711 000
Europe	1/274 000	1/310 000	1/ 410 000	1/ 460 000
Canada	--	1/306 000	1/ 535 000	1/ 709 000
Africa	--	1/244 000	1/ 136 000	1/ 189 000
Asia	--	1/131 000	1/ 144 000	1/ 168 000
Central & South America	1/ 13 000	1/ 48 000	1/ 141 000	1/ 162 000
World excl. U.S.	1/125 000	1/203 000	1/ 286 000	1/ 339 000

TABLE II.- ESTIMATED ACCIDENT COSTS: COMMERCIAL JETS '52 — 9 MOS. '77

[In millions of U.S. dollars; data obtained from M. W. Eastburn of American Airlines]

	U.S.		World excluding U.S.		World	
	Number	Dollars	Number	Dollars	Number	Dollars
Hulls loss	98	599.6	194	977.6	292	1577.2
Est. partial damage	----	282.3	----	219.1	-- ---	501.4
Liability (fatals only)	2800	522.6	7514	232.9	10 314	755.5
Total		1404.5		1429.6		2834.1

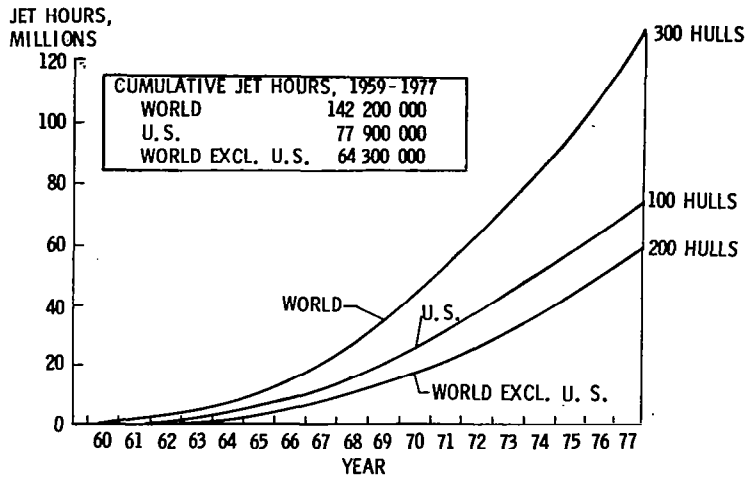

Figure 1.- Air carrier operations. Jet hours - hulls lost (includes 35 destroyed by sabotage and war-like action; 6 U.S.; 29 Non U.S.). Figure obtained from M. W. Eastburn of American Airlines.

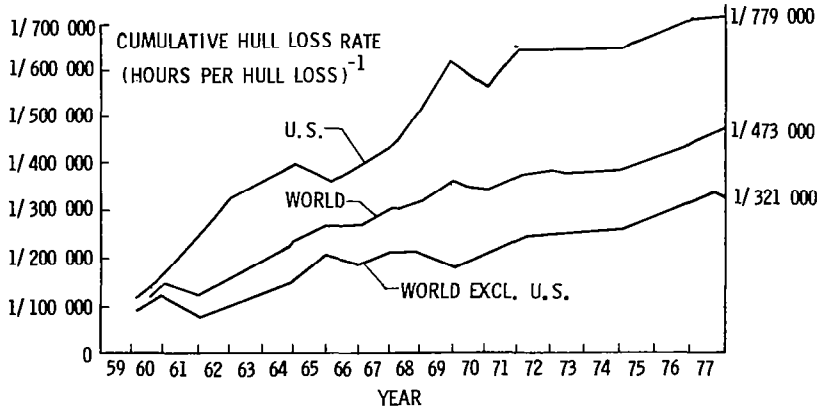

Figure 2.- Air carrier operations. Hull loss rate includes 35 hulls destroyed by sabotage and war-like action. Figure obtained from M. W. Eastburn of American Airlines.

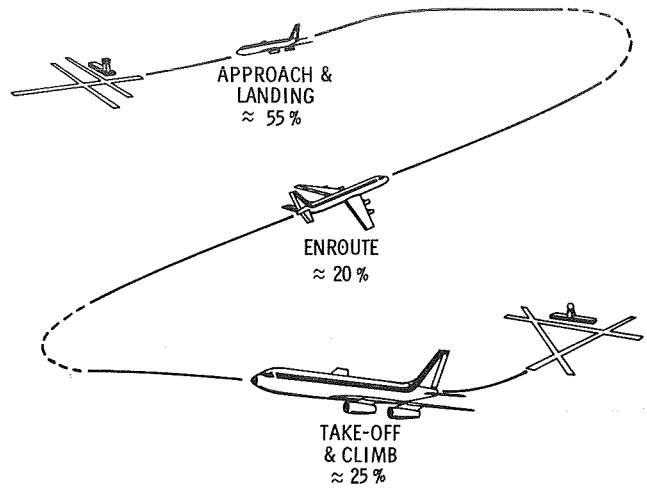

Figure 3.- Distribution of jet transport fatal accidents by phase of flight.

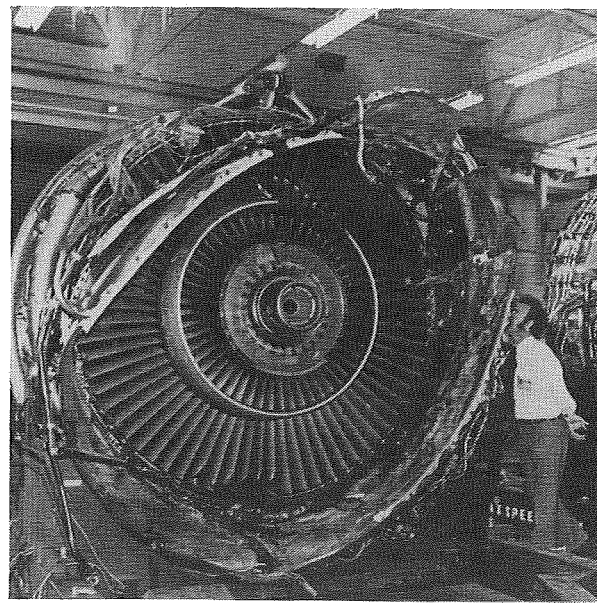

Figure 4.- Engine component failure.

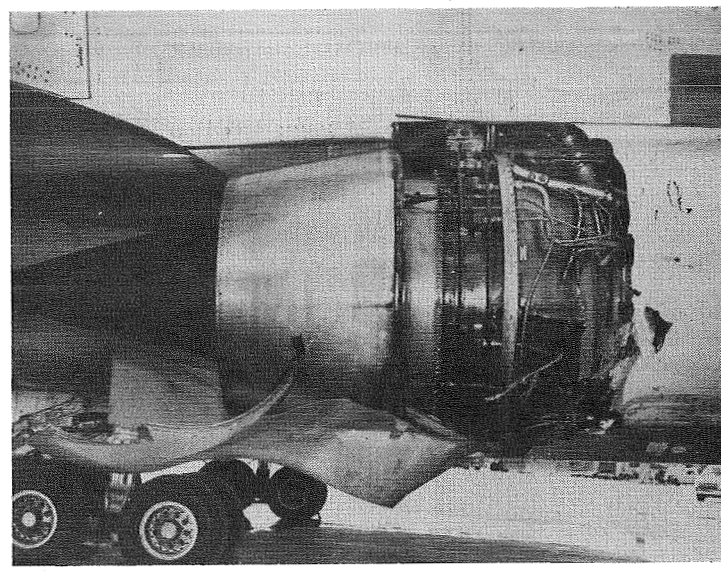

Figure 5.- Uncontained failure of jet engine.

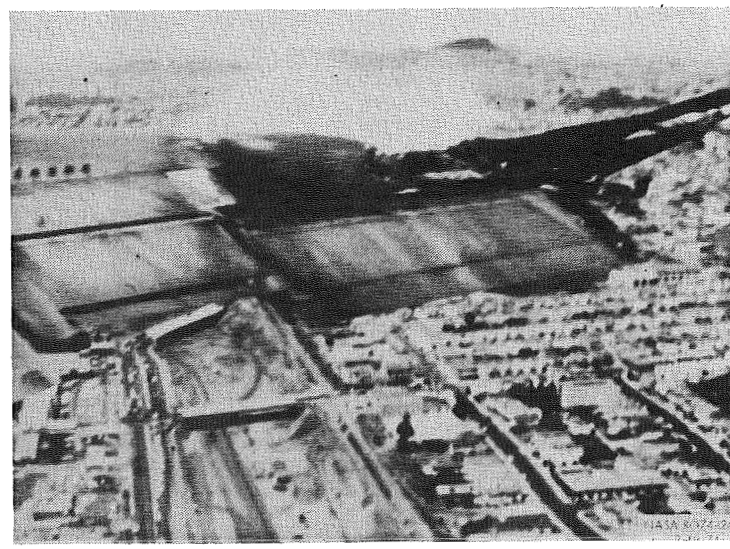

Figure 6.- In-flight engine component failure.

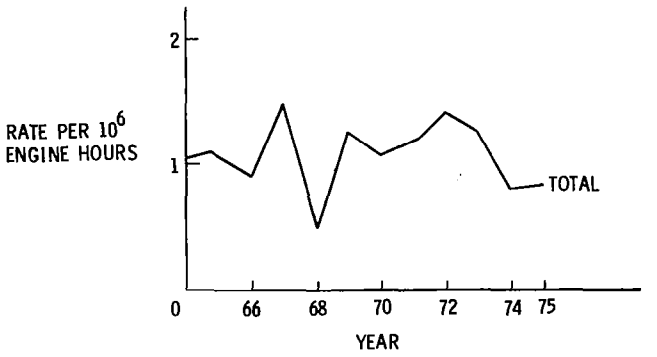

Figure 7.- World-wide noncontainment engine failure rate.

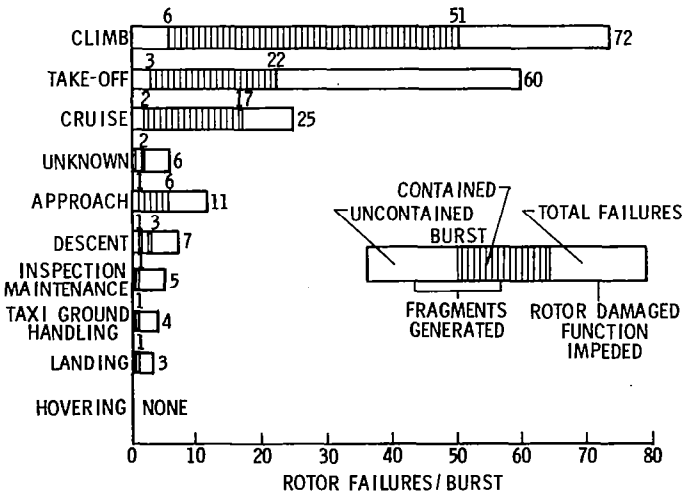

Figure 8.- Flight condition at rotor failure/burst - 1975.

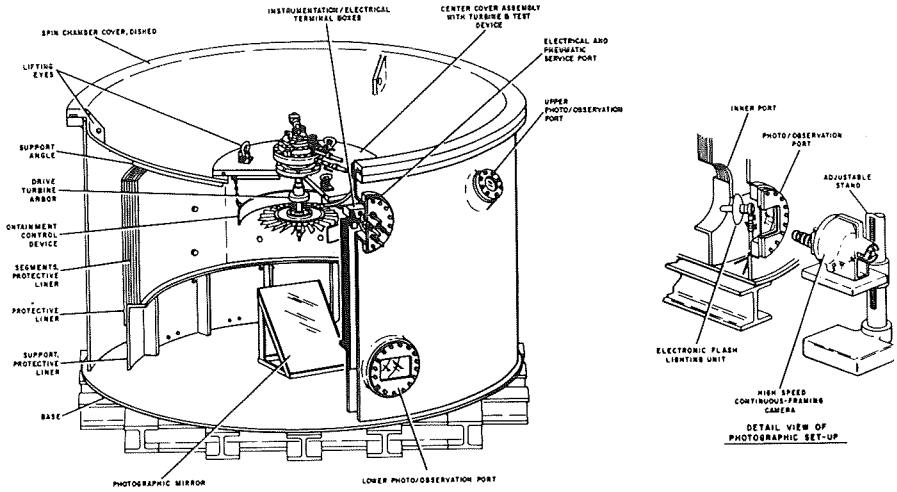

Figure 9.- Spin chamber facilities.

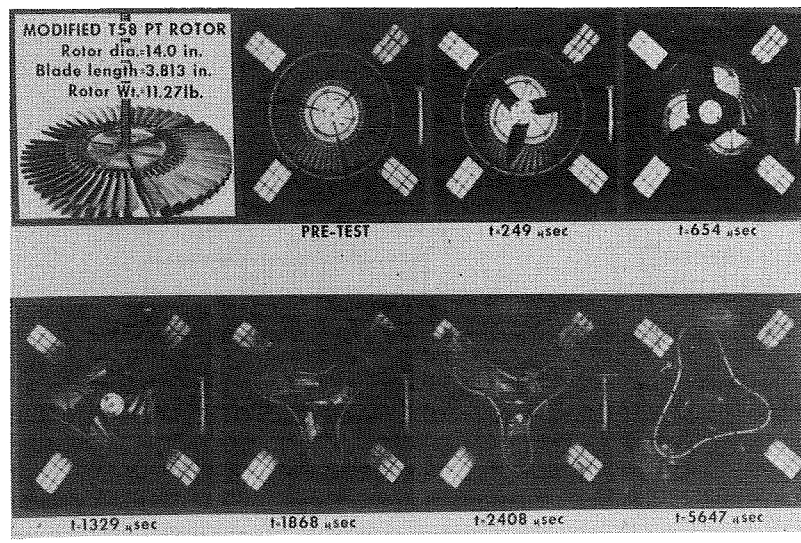

Figure 10.- Bladed rotor fragment generator and bladed rotor burst test results (1 in. = 2.54 cm; 1 lb = 4.448 N).

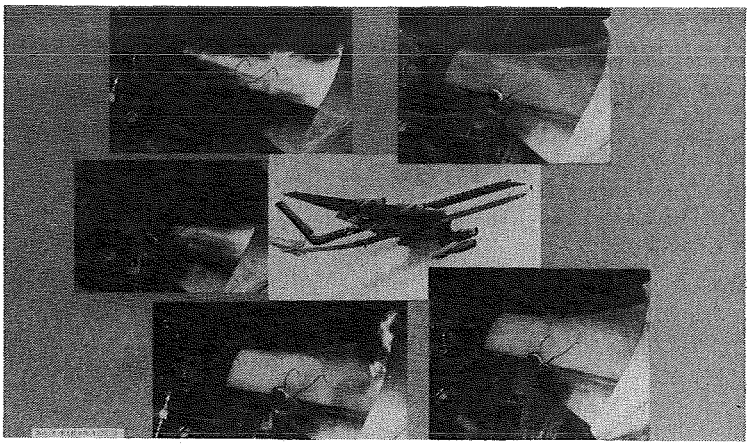

Figure 11.- Engine in-flight fire extinguishant research.

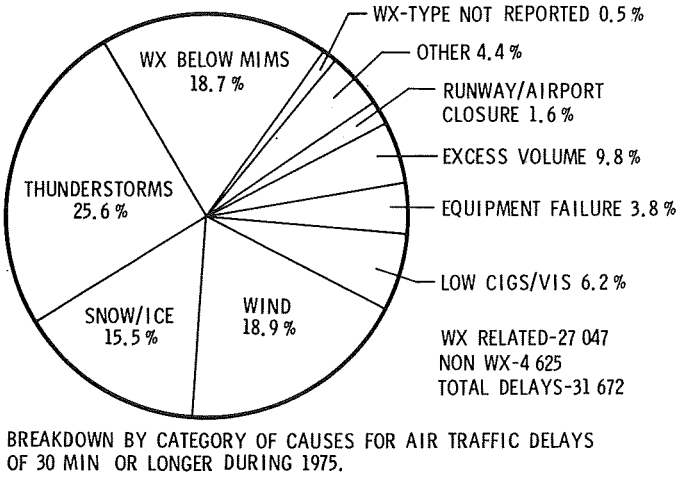

BREAKDOWN BY CATEGORY OF CAUSES FOR AIR TRAFFIC DELAYS OF 30 MIN OR LONGER DURING 1975.

Figure 12.- Impact of weather on safety and efficiency of air transportation. (Data from Bromley, Bulletin American Meteorological Soc., vol. 58, no. 11, Nov. 1977, pp. 1156 ff.)

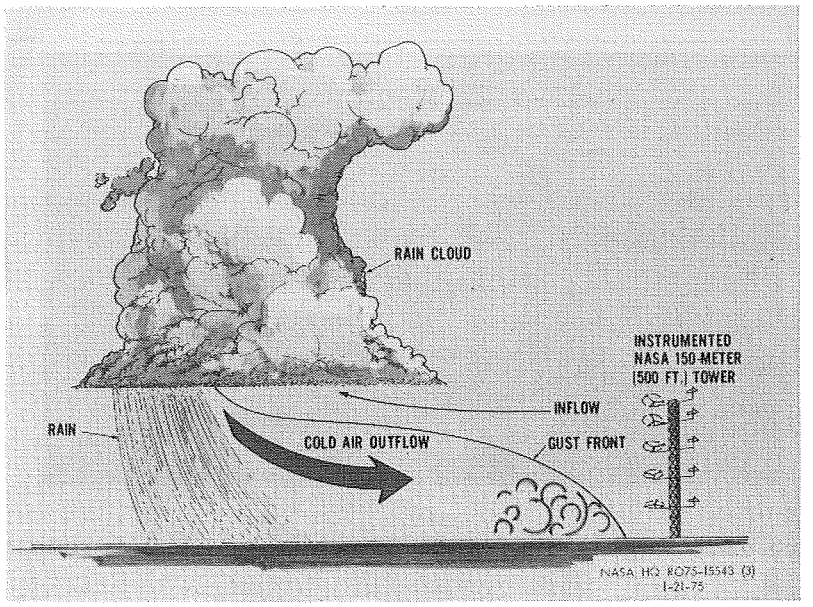

Figure 13.- Thunderstorm gust front technology development.

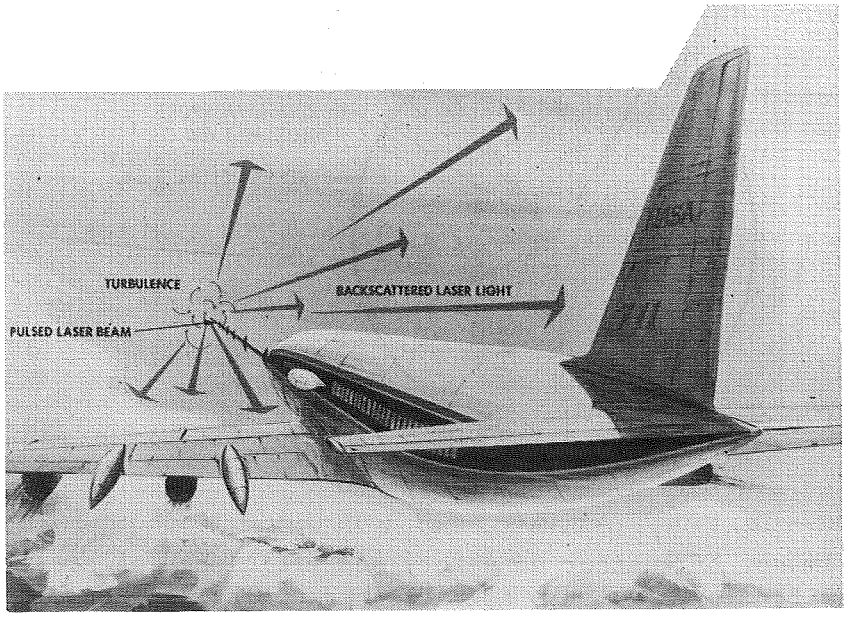

Figure 14.- CAT research instrumentation on CV990.

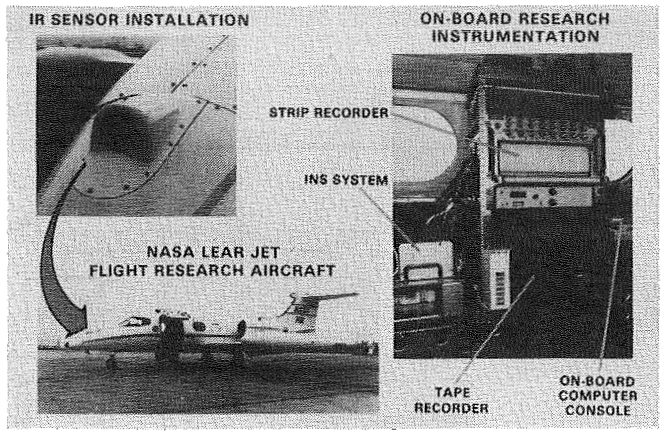

Figure 15.- Clear air turbulence research infrared radiometer detector system.

Figure 16.- Fireburned fuselage.

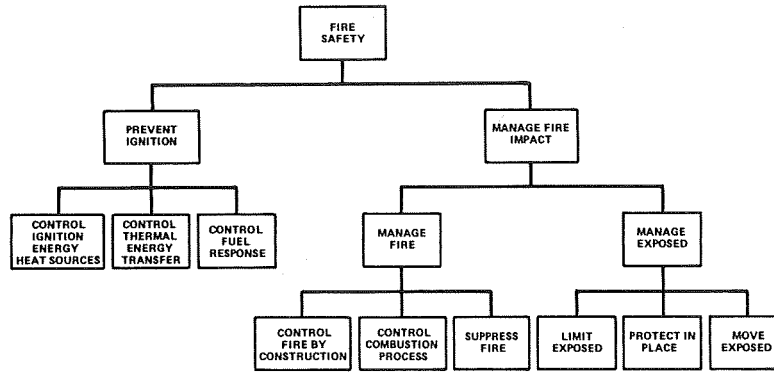

Figure 17.- Aircraft fire dynamics logic tree.

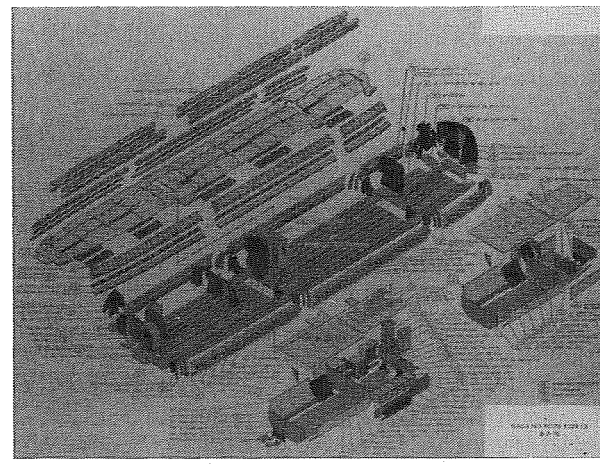

Figure 18.- Representative aircraft cabin interior trim assembly breakdown. Nonmetallic materials.

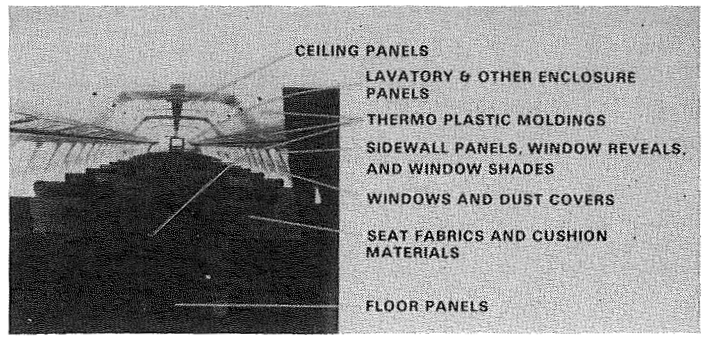

Figure 19.- Improved fire safety in aircraft interior materials.

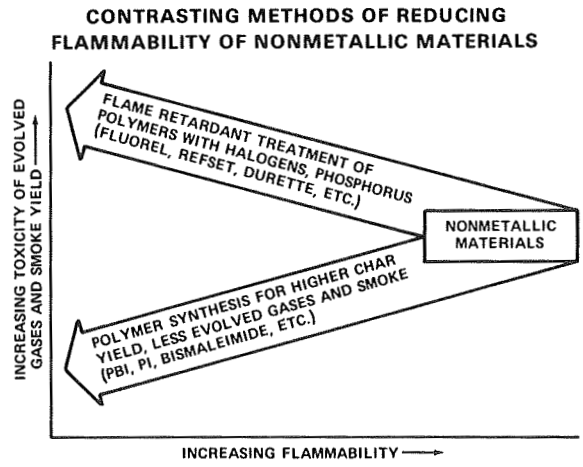

Figure 20.- Aircraft fire safety research.

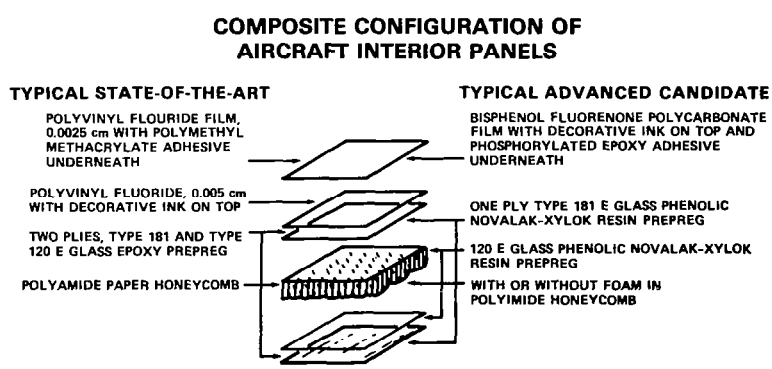

Figure 21.- FIREMEN program.

WAKE VORTEX TECHNOLOGY

R. Earl Dunham, Jr.
NASA Langley Research Center

Marvin R. Barber
NASA Dryden Flight Research Center

Delwin R. Croom
NASA Langley Research Center

INTRODUCTION

Aircraft trailing vortices are one of the principal factors affecting aircraft arrival and departure rates at airports. Minimization of the trailed vortex strength would allow reduction of the present spacing requirements. Such reductions would allow full utilization of advances in automatically aided landing systems as described in reference 1, while maintaining or improving safety within the terminal area. For several years, NASA has been conducting an intensive in-house and contractual research effort involving theoretical and experimental studies of various wake vortex minimization techniques, the results of which were reported in reference 2. NASA's work was done in conjunction with the Federal Aviation Administration investigation of various sensing devices for detecting the presence of vortices within the terminal area. The FAA's investigation is aimed at developing, for installation at major airports, a vortex avoidance system that would increase runway capacity by varying the separation distances to conform to the conditions present. A complete ground-based detecting system would involve the detection and prediction of the presence and strength of the vortices present at a given time. Both the NASA effort for vortex reduction and the FAA effort for detection aid the overall national air transportation goal to alleviate aircraft trailing vortices as an operational constraint. The purpose of this paper is to review the NASA effort.

EXPERIMENTAL METHODS

Shown in figure 1 are the experimental facilities that have been used to evaluate the various vortex minimization concepts. Pictured are the four primary model test facilities that have been used along with flight tests. For all tests, the basic operational problem of one airplane flying in trail behind another and encountering the vortex wake is recreated. The primary model test facilites employ the experimental method illustrated in figure 2. The vortex upset potential on the trailing aircraft is determined by measuring the vortex-induced rolling moment on a trailing airplane. For the vortex minimization tests, the vortex generator aircraft has generally been representative of a wide-body jet while the vortex penetrator has been either a small jet transport (DC-9) or a business jet size airplane (Learjet or T-37). The vortex minimization concepts are

implemented on the transport airplane while measurements are made to assess the performance degradation attributable to the vortex minimization scheme. Measurement of the vortex induced rolling moment on the trailing airplane provides a direct measurement of the effectiveness of the vortex minimization concept.

The wind tunnels used for the model tests are the 40- by 80-foot tunnel at Ames Research Center and the V/STOL tunnel at Langley Research Center. In addition to these two wind tunnels, two model towing facilities were used. In these facilities, both the vortex generator model and the trailing rolling moment model are towed through a quiescent fluid medium. In one of these facilities (vortex flow facility) located at Langley Research Center, the models are towed through the air, and in the other facility, the models are towed in a water basin. Tests in the water towing basin were conducted under contract to Hydronautics, Inc. The model facilities provide for downstream measurements of the vortex wake from very near field to as much as 2 scale miles behind the vortex generator aircraft. Additional details concerning these facilities can be found in reference 3.

EXPERIMENTAL RESULTS

Wake vortex minimization experiments have shown that significant reduction in the vortex-induced rolling moment on a trailing airplane can be achieved primarily by increasing the normal dissipation rate by using turbulence to rapidly diffuse the vorticity. The experiments have indicated several methods of increasing turbulent diffusion either directly by turbulence injection or indirectly through vortex interaction. The following sections briefly describe these methods.

Turbulence Injection

Shown in figure 3 is a device which was flight tested on a C-54 airplane to investigate the effect of turbulence injection on the vortex wake. The device, as illustrated, consisted of considerable flat-plate area normal to the free stream to produce turbulence near the wingtip. The device did not alter the wing lift characteristics but added an increment of drag. The device increased the basic airplane drag coefficient by about 0.05. The flight-test results of the device are reported in reference 4 and shown in figure 4. The flight test consisted of flying a PA-28 Cherokee airplane in the C-54 airplane vortex wake at various separation distances with and without the turbulence device on the C-54. As shown in figure 4, without the turbulence device on the C-54 airplane, the PA-28 airplane could penetrate no closer than 8 km before the roll-control capability of the PA-28 airplane was exceeded. However, the turbulence injection device caused a visible alteration of the vortex pattern which was marked with

smoke (reference 4) and significantly reduced the vortex-induced rolling moment. As shown in figure 4, the vortex-induced roll was always lower than the roll-control capability of the PA-28 airplane. These flight tests were the first quantitative indication that wake vortex effects could be significantly reduced. It is recognized that the implementation of such a concept has considerable operational penalties; however, the turbulence produced by equipment on airplanes, such as landing gear, engines, and engine pods, can be used to provide reduction in trailed vortex strength. Details concerning the development and tests of the turbulence device are given in references 4 to 6.

Vortex Interaction

Vortex interaction and control is a term used to describe the turbulence and shear stress produced during coalescence of several vortices into a single vortex. Some of the work described in reference 7 has shown that two vortices of the same sense considerably strain and distort each other during the merging process. The production of turbulence during the merging process is discussed in more detail in the analytical studies in references 8 and 9. The vortex wake behind a large jet transport is dominated by several vortices coming from the wingtip, flap end, wing-body junction, and other places where large changes in spanwise load distribution occur. Downstream, the vortices from one-half the airplane coalesce into a single vortex leaving behind the classical vortex pattern of a pair of aircraft trailing vortices. Numerous methods have been attempted to control the early wake development, two of which are described in this section.

The simple inviscid analytical techniques discussed in reference 10 indicated that the vortex wake development of a wide-body transport aircraft could be considerably altered by introducing an additional vortex pair into the wake. Model tests of such a method were conducted and described in reference 11. To produce an additional vortex pair in the wake of a wide-body jet model, fins were placed on the upper surface of the wing as shown in figure 5. The fins were canted with respect to the local free-stream so as to produce a vortex of the same sense as the wingtip vortex. The spanwise postion of the fin on a 747 model airplane was varied during tests in the 40- by 80-foot wind tunnel. The effect of the fin vortex on the model wake was measured 15 spans behind the 747 model using a Learjet size wing for rolling-moment measurement. The results of these tests are shown in figure 6. For these tests, the ratio of the fin height to wing span of the 747 model was about 0.08 and the fin cord was about 0.04 of the span. As indicated in figure 6, the vortex-induced rolling moment was reduced by about a factor of 4 with the fin at about the 50-percent-semispan position. The effect of fin spanwise location on the vortex-induced rolling moment is significant. The work on the fin concept is relatively new and, at this time, little has been done to address the operational problems that may be incurred with the implementation of this method.

Another method of controlling vortex interaction is to vary the spanwise position of the flap vortex and relative strengths of the flap and wingtip vortices. This is done by altering the spanwise load distribution. Analytical studies of such a method are discussed in reference 8. The results of reference 8 indicated that, if the wingtip and flap vortices were of nearly equal strength and the flap vortex was located at about the 40-percent-semispan position, the effect of vortex interaction was maximized. Numerous model tests and flight tests were conducted employing span load alteration for vortex interaction. A 747 airplane was used in which only the inboard flap section was deployed for the landing approach. Details concerning the model tests of this method are described in reference 7. Flight-test results of this configuration are indicated in figure 7 and 8.

In figure 7, the vortex pattern behind a 747 airplane in the normal landing approach flap configuration is made visible by smoke devices mounted under the wing. The wake is seen to develop quickly into a pair of trailing vortices. Flights with the 747 were conducted at a lift coefficient of 1.2. Vortex penetrations were conducted with Learjet and T-37 airplanes. During these tests, roll upsets greater than the control capability of the Learjet and T-37 airplanes were experienced at distances of from 6 to 8 n. mi. behind the 747 airplane (reference 12).

Figure 8 illustrates the vortex pattern behind the 747 airplane at a lift coefficient of 1.2 with only the inboard flap segment deployed. This configuration is seen to inhibit the merging of the wingtip and flap vortex into single vortex. The enhanced vortex interaction produces a significantly diffuse vortex wake. Model tests (reference 7) indicated that this configuration would reduce the vortex-induced rolling moment about 50 percent. Flight tests indicated that the T-37 airplane could approach as close as 3 n. mi. behind the 747 airplane before experiencing large roll upsets. This wake vortex minimization method has considerable performance penalties which prohibit its operational use; however, the method does illustrate the importance of vortex interaction for future aircraft design consideration.

Flight Spoilers

A concept was developed which employs both the principle of turbulence injection and vortex interaction through span load alteration. The method consists of deploying selected flight spoilers on the airplane. Considerable details concerning the development and implementation of this concept are described in references 13 to 17. Evaluation of the flight spoilers have been conducted on DC-10, L-1011, and 747 airplane models. Flight tests have also been conducted using the spoiler concept on 747 and L-1011 airplanes. Flight tests and model tests with the 747 airplane have shown that the use of the two outboard spoiler sections can reduce the vortex-induced rolling moment on a Learjet size airplane by about 50 percent.

Photographs of flight tests using the spoiler concept on a L-1011 airplane are shown in figures 9 and 10. The vortex pattern for the normal landing approach configuration of the L-1011 is shown in figure 9. Tests indicated that for a T-37 airplane, roll upsets exceeding the roll control power of the T-37 were experienced at about 6 n. mi. The use of the three outboard spoiler sections on the L-1011 airplane for vortex minimization and their effect on the vortex pattern is seen in figure 10. Comparison of smoke-marked vortex wake with and without the spoilers deployed (figs. 9 and 10) indicates that the vortex wake is quickly diffused. The spoiler both sheds turbulence into the wake and alters the span load distribution. The relative importance of turbulence and span load alteration on the spoilers ability to diffuse the vortex is unknown. Tests showed that a T-37 airplane could approach as close as 2 n. mi. without an uncontrollable upset.

Details concerning the performance decrement caused by the use of the spoilers are covered in references 13 to 17. The spoilers do appear to offer several advantages for vortex minimization use on existing airplanes, since they are effective and available for use. Certain operational problems, such as possible buffet and associated structural problems, approach speed increases, and climb requirements, are still unanswered. By comparison with the other methods discussed for vortex minimization, the spoilers offer the greatest chance for operational use on existing aircraft. The other vortex minimization techniques described can only be implemented in future aircraft design.

ANALYTICAL STUDIES

Under an NASA contract, a computer code was developed to solve the vortex equations of fluid motion including convection and turbulent diffusion. The objective of the theoretical work is to describe in detail the vortex wake for a given aircraft configuration. The computer code is capable of calculating the wake history including the effect of atmospheric conditions such as winds, wind shear, atmospheric turbulence, atmospheric stability, and the influence of the ground plane. The computer code is a two-dimensional, time marching, finite difference approximation to the Reynold's stress equation. Details concerning the computer code are reported in references 8 and 9. All of the vortex minimization methods described in the previous experimental sections have been investigated using the computer code. The analytical results generally agree with the experimental results.

Shown in figure 11 are the calculated results of a pair of vortices descending into a wind shear. These results of the computer code are taken from reference 18. Shown in the figure are vorticity contours in the cross-flow plane at increasing nondimensional time increments. Over the time steps shown, the left vortex is seen to decrease in maximum

vorticity from five nondimensional units to two units. The right vortex is seen to completely vanish because of its interaction with the opposite sensed vorticity in the wind shear.

A flight-test result of one vortex vanishing while the other vortex remains for a considerable time was reported in reference 19. For these tests a small single-engine airplane was flown over El Mirage dry lake bed under various atmospheric stability and turbulence conditions while the vortices were made visible by smoke and photographed. Although the exact wind conditions for which one vortex was seen to disappear and the other remain were not documented, it does appear that some wind shear was present. The calculations shown in figure 11 serve to illustrate the capability of computer code while offering an explanation of the solitary vortex observed during the tests of reference 19.

FUTURE EFFORT

Although the basic methods of vortex minimization have been identified, considerable effort is required to provide a comprehensive technology base for understanding the intricate interrelationship of direct turbulence effects and indirect turbulence effects through vortex interaction. To aid in achieving this understanding, extensive model tests are being conducted using the model shown in figure 12. This model has an aspect ratio of 7, an NACA 0012 airfoil, and a rectangular planform of 248.9 cm span, with 72 movable airfoil sections. The local angle of attack of each section can be independently set, thus allowing a wide range in span load variation. Detailed near-field and far-field flow measurements along with the measured wing load pressure distribution will be obtained to aid in validation of the analytical techniques presently developed. Work on the analytical techniques is continuing for improvement in the existing computer code. Flight tests and model tests are being continued to provide a better assessment of the operational feasibility of implementing wake vortex minimization concepts on existing aircraft.

CONCLUDING REMARKS

This paper has provided a brief overview of the highlights of NASA's wake vortex minimization program. The significant results of this program can be summarized as follows:

1. Tests have shown that it is technically feasible to reduce significantly the rolling upset created on a trailing aircraft. Prior to NASA's effort, there was considerable doubt as to the possibility of achieving a measurable reduction in the trailing vortex strength.

2. The basic principles or methods by which reduction in the trailing vortex strength can be achieved have been identified. At least one of these methods may have application to existing airplanes while all of the principles are suitable for implementation in future aircraft wing designs.

3. An analytical capability for investigating aircraft vortex wakes has been developed. The analytical techniques have been shown to agree generally with previous experimental test results. The analytical techniques will be useful in future aircraft designs.

REFERENCES

1. Salmirs, Seymour; and Morello, Samuel A.: Flight Experiments To Improve Terminal Area Operations. CTOL Transport Technology - 1978, NASA CP-2036, 1978, pp.

2. Wake Vortex Minimization. NASA SP-409, 1977.

3. Stickle, Joseph W.; and Kelly, Mark W.: Ground-Based Facilities for Evaluating Vortex Minimization Concepts. Wake Vortex Minimization, NASA SP-409, 1977, pp. 129-155.

4. Hastings, Earl C., Jr.; Patterson, J. C., Jr.; Shanks, Robert E.; Champine, Robert A.; Copeland, W. Latham; and Young, Douglas C.: Developlent and Flight Tests of Vortex-Attenuating Splines. NASA TN D-8083, 1975.

5. Patterson, James C., Jr.; Hastings, Earl C., Jr.; and Jordan, Frank L, Jr.: Ground Development and Flight Correlation of the Vortex Attenuating Spline Device. Wake Vortex Minimization, NASA SP-409, 1977, pp. 271-303.

6. Patterson, James C., Jr.: Lift-Induced Wing-Tip Vortex Attenuation. AIAA Paper No. 74-38, Jan.-Feb. 1974.

7. Corsiglia, Victor R.; and Dunham, R. Earl, Jr.: Aircraft Wake-Vortex Minimization by Use of Flaps. Wake Vortex Minimization, NASA SP-409, 1977, pp. 305-338.

8. Bilanin, Alan J.; Teske, Milton E.; Donaldson, Coleman duP.; and Williamson, Guy G.: Vortex Interactions and Decay in Aircraft Wakes. NASA CR-2870, 1977.

9. Bilanin, Alan J.; Teske, Milton E.; Donaldson, Coleman duP.; and Snedeker, Richard S.: Viscous Effects in Aircraft Trailing Vortices. Wake Vortex Minimization, NASA SP-409, 1977, pp. 61-128.

10. Rossow, Vernon J.: Convective Merging of Vortex Cores in Lift-Generated Wakes. AIAA Paper No. 76-415, July 1976.

11. Rossow, Vernon J.: Effect of Wing Fins on Lift-Generated Wakes. AIAA Paper No. 77-671, June 1977.

12. Barber, Marvin R.; Hastings, Earl C., Jr.; Champine, Robert A.; and Tymczyszyn, Joseph J.: Vortex Attenuation Flight Experiments. Wake Vortex Minimization, NASA SP-409, 1977, pp. 369-403.

13. Croom, Delwin R.: The Development and Use of Spoilers as Vortex Attenuators. Wake Vortex Minimization, NASA SP-409, 1977, pp. 339-368.

14. Croom, Delwin R.: Low-Speed Wind-Tunnel Investigation of Various Segments of Flight Spoilers as Trailing-Vortex-Alleviation Devices on a Transport Aircraft Model. NASA TN D-8162, 1976.

15. Croom, D. R.: Development of Spoilers as Trailing Vortex Hazard Alleviation Devices. Paper presented at Conference on Aircraft Wake Vortices (Cambridge, Mass.), Mar. 1977.

16. Croom, Delwin R.; Vogler, Raymond D.; and Williams, Geoffrey M.: Low-Speed Wind-Tunnel Investigation of Flight Spoilers as Trailing-Vortex-Alleviation Devices on a Medium-Range Wide-Body Tri-Jet Airplane Model. NASA TN D-8360, 1976.

17. Croom, Delwin R.; Vogler, Raymond D.; and Thelander, John W.: Low-speed Wind-Tunnel Investigation of Flight Spoilers as Trailing-Vortex-Alleviation Devices on an Extended-Range Wide-Body Tri-Jet Airplane Model. NASA TN D-8373, 1976.

18. Bilanin, A. J.; Teske, M. E.; and Hirsh, J. E.: The Role of Atmospheric Shear, Turbulence, and a Ground Plane on the Dissipation of Aircraft Vortex Wakes. Paper presented at 16th Aerospace Science Meeting (Huntsville, Ala.), Jan. 1973.

19. Tombach, Ivar: Observations of Atmospheric Effects on Vortex Wake Behavior. J. Aircr., vol. 10, no. 11, Nov. 1973, pp. 641-647.

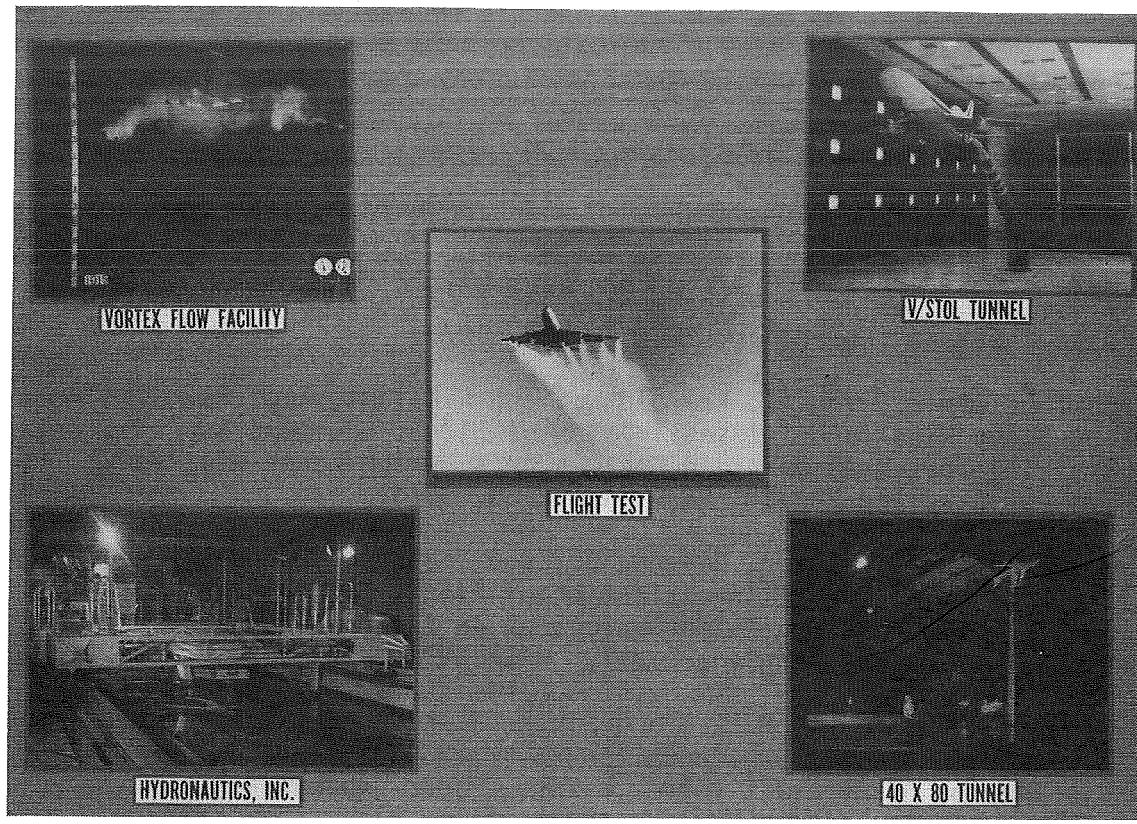

Figure 1.- Experimental facilities.

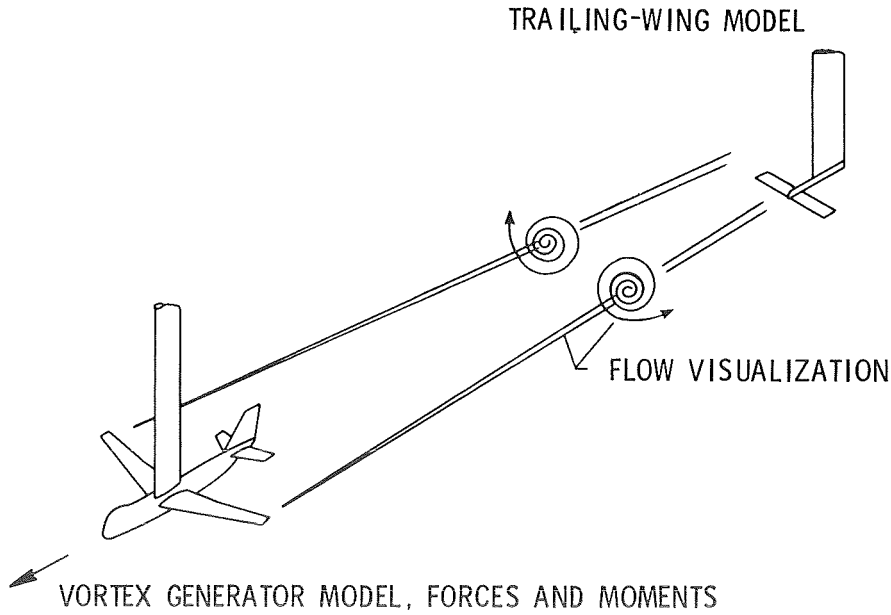

Figure 2.- Experimental test technique.

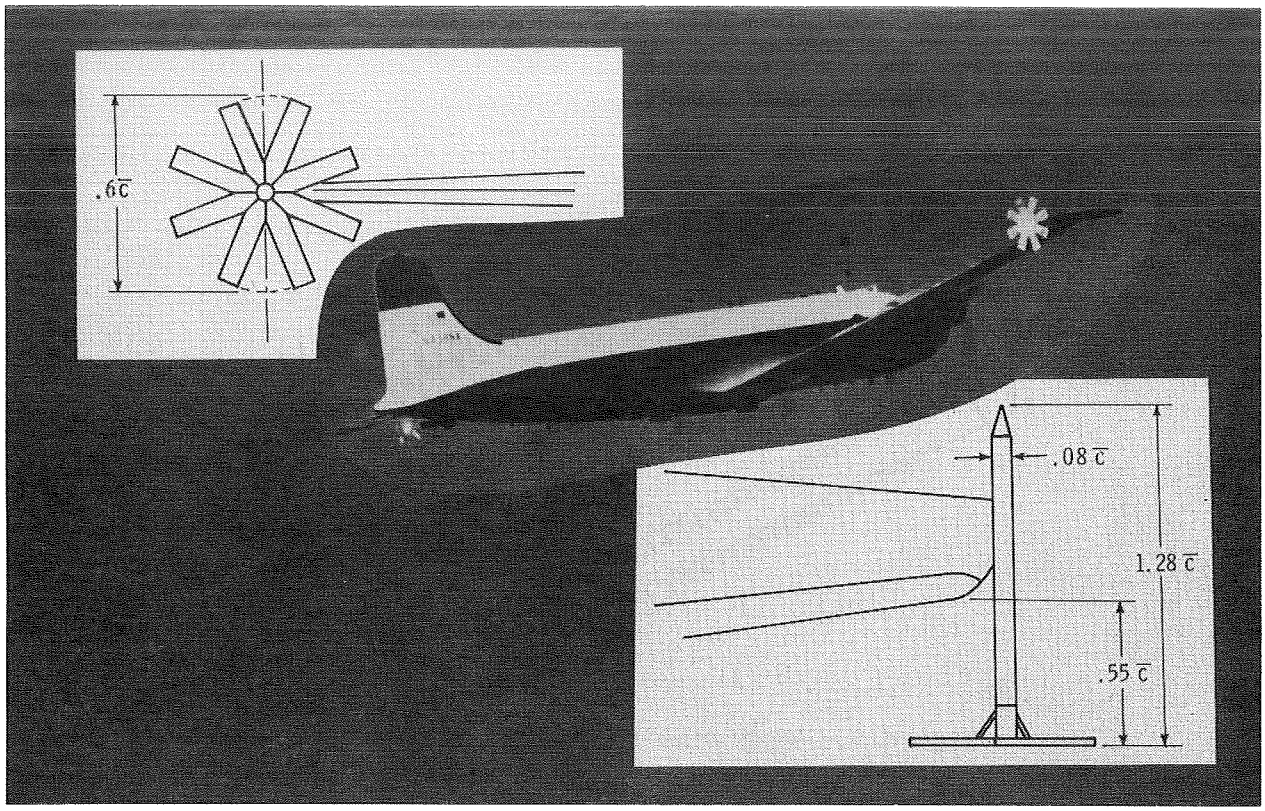

Figure 3.- Turbulence device installed on C-54 airplane for flight tests. ($\bar{c}$ is wing mean aerodynamic chord.)

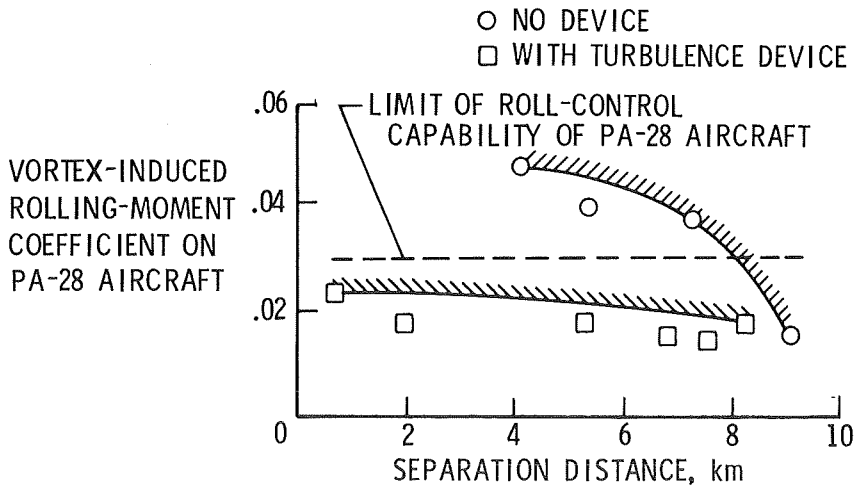

Figure 4.- Flight-test results of the turbulence device.

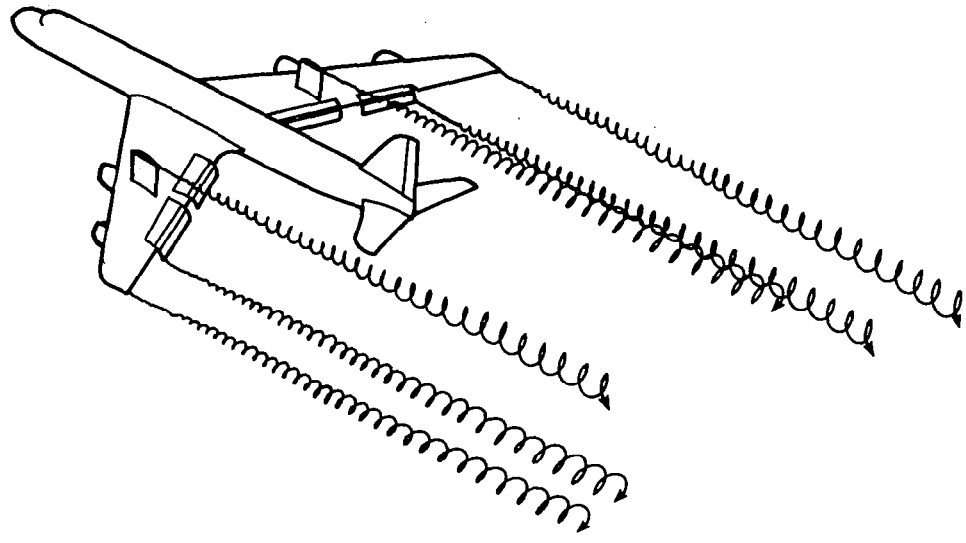

Figure 5.- Wing fins for vortex attenuation.

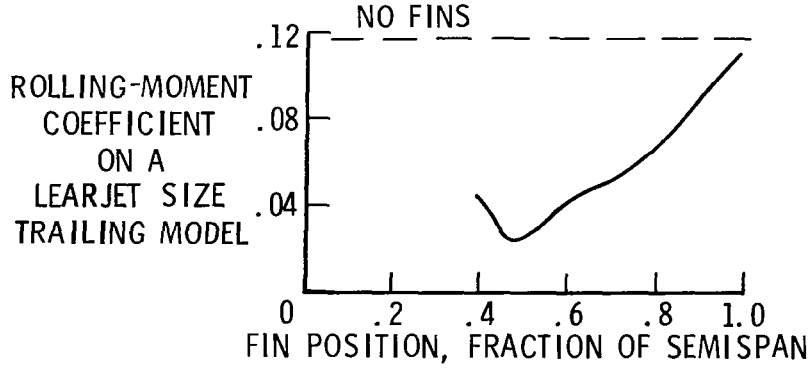

Figure 6.- Model-test results of wing fin.

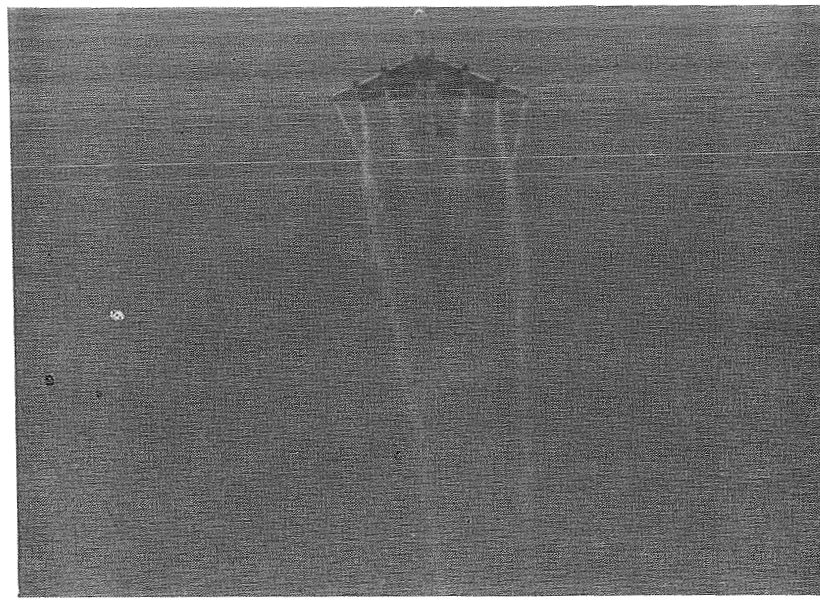

Figure 7.- 747 airplane with all flaps extended.

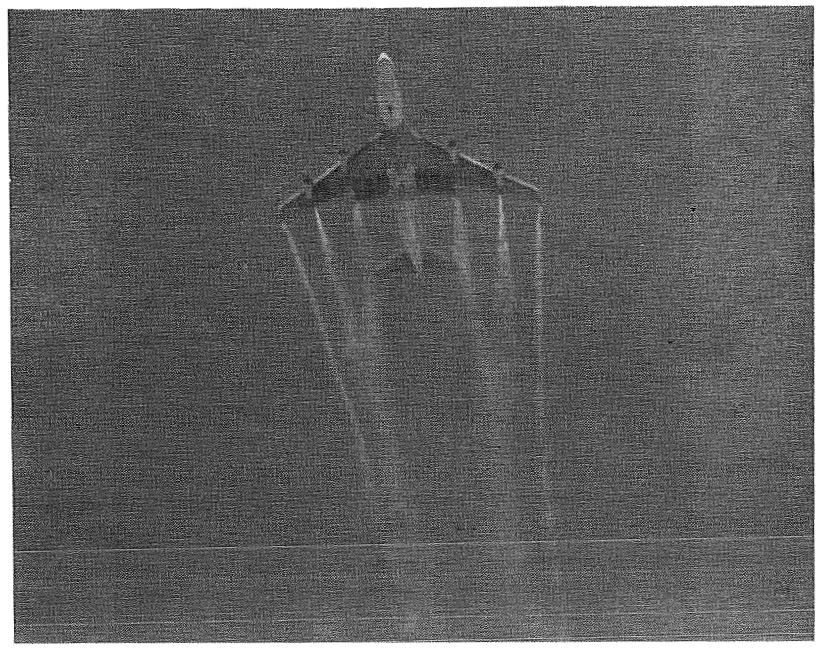

Figure 8.- 747 airplane with only inboard flap extended.

Figure 9.- L-1011 in normal landing approach configuration.

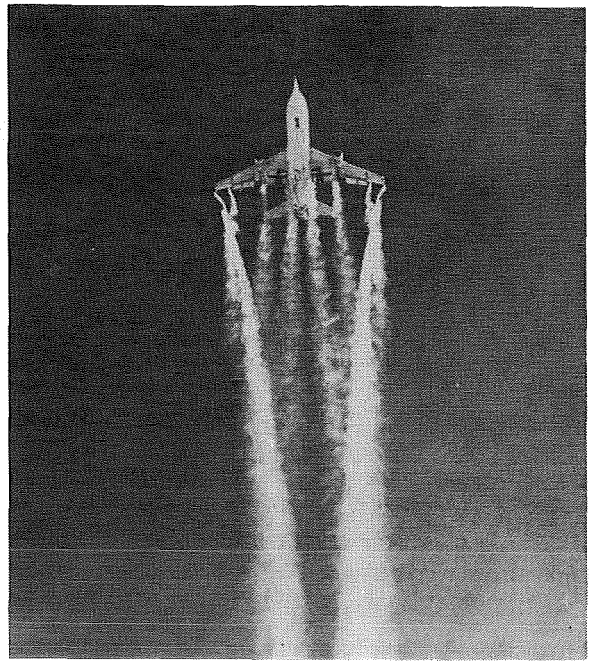

Figure 10.- L-1011 with spoilers deployed for vortex minimization.

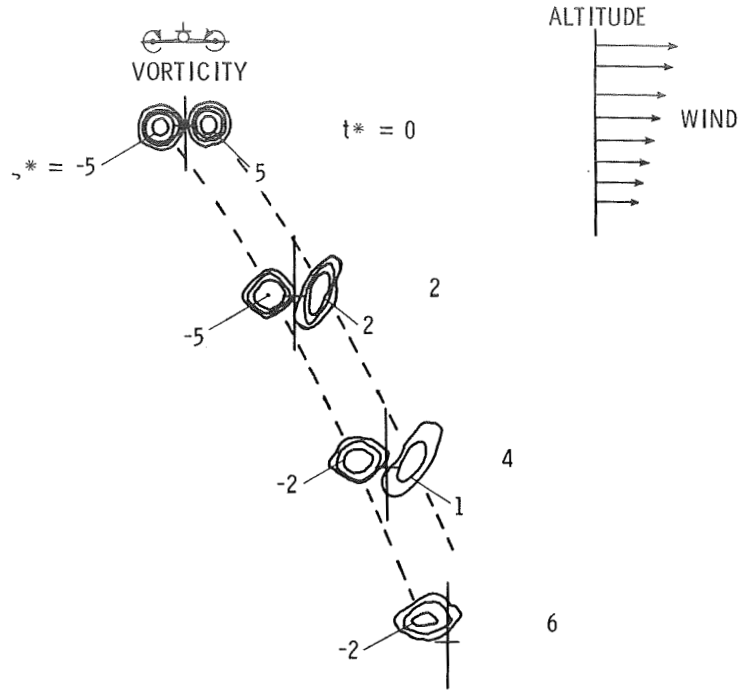

Figure 11.- Analytical results of pair of vortices descending into a wind shear. (t* is nondimensional time; ζ* is nondimensional vorticity.)

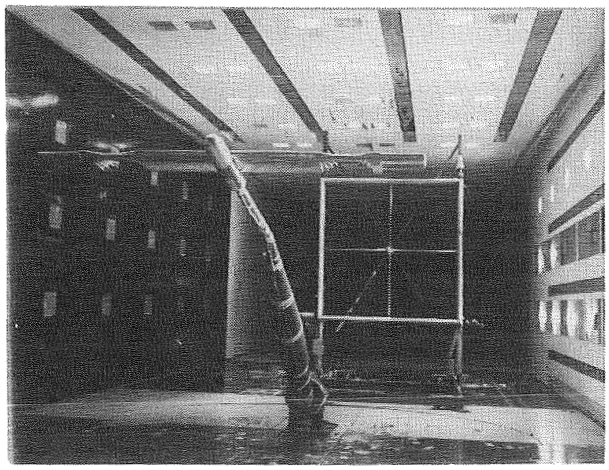

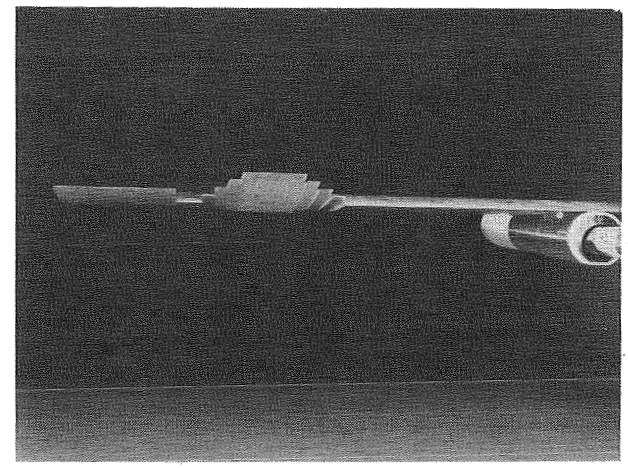

Figure 12.- Model used for variable span load investigation.

SUMMARY OF NASA LANDING-GEAR RESEARCH

Bruce D. Fisher, Robert K. Sleeper, and Sandy M. Stubbs
NASA Langley Research Center

SUMMARY

The landing gear research being conducted at NASA Langley Research Center is summarized in this report, and research relative to tire tread, powered-wheel taxiing, air cushion landing systems, and crosswind landing gear is discussed in some detail.

INTRODUCTION

The purpose of this paper is to present a brief summary of the airplane landing-gear research underway at NASA. The technology areas include:

Ground-handling simulator	Tire/surface friction characteristics
Antiskid braking systems	Tire mechanical properties
Space shuttle nose-gear shimmy	Tire-tread materials
Active control landing gear	Powered wheels for taxiing
Wire brush skid landing gear	Crosswind landing gear
Air cushion landing systems	

This paper will deal mainly with the programs on tire-tread materials, powered-wheel taxiing, air cushion landing systems, and crosswind landing-gear research with particular emphasis on previously unreported results of recently completed flight tests. Work in the remaining areas will only be mentioned briefly as follows.

An airplane ground-handling simulator is being developed to provide a research tool for investigating, in perfect safety, directional control and braking problems of airplanes on slippery runways in the presence of crosswinds. One excellent example of its application is to explore airplane control problems during high-speed turnoffs from main runways onto taxiways. The simulation development was performed under contract and is currently being adapted to the Langley visual-motion simulator. A discussion of some of the significant developments can be found in references 1 and 2.

An antiskid braking system research program is in progress at the Langley aircraft landing loads and traction facility (LLT) to determine ways to improve the performance of current antiskid systems on slippery runways and to obtain data for the development of more advanced systems. Test data from two different antiskid systems have been reported in references 3 and 4 although two antiskid systems in the program have yet to be tested.

Space shuttle nose-gear shimmy tests were performed at the LLT prior to the first landings of the shuttle on the dry lake bed at NASA Dryden Flight Research Center. These data have not yet been published, but no shimmy problems were encountered either in the track tests or in the actual landings.

Active control landing-gear research is underway in an attempt to attenuate landing-gear loads imposed on the structure of large flexible airplanes. The goal is to improve the structural dynamic response characteristics and to obtain an economically acceptable fatigue life of the airframe structure. Analytical results for landings of a supersonic airplane have shown that as a result of a cycle-by-cycle analysis of landing impact and roll-out for a passive and an active gear, the active gear was effective in significantly reducing the structural fatigue damage for the ground operational phase. Dynamic drop tests are currently underway using a light airplane landing gear modified to an active control configuration. References 5 to 8 present discussions of some of the active control landing-gear research.

A brake system using wire brush skids in conjunction with the wheels of the main landing gear offers the potential of superior braking characteristics on wet runways when compared with conventional airplane tire and brake systems. Wire brush skids are currently being investigated to determine their friction characteristics and wear rates. Reference 9 presents results of some early work on various potential wire materials for wire brush skids.

Tire/surface friction characteristics play a very important role in the ground-handling behavior of an airplane during take-off and landing. Much effort in the past has been spent on modifying the texture of the runway, such as by pavement grooving, and on developing new tire-tread patterns in attempts to delay the deleterious effects of tire hydroplaning during wet runway operations. A summary of runway slipperiness research is given in reference 10, and a recent report on the friction characteristics of tires with various tread patterns and rubber compounds is presented in reference 11.

Several efforts are underway at Langley Research Center in the general area of tire mechanical properties. An analytical time model is being developed to aid in the design of landing-gear systems and to assist in the solution of many airplane ground operational problems. In this development, a computer program is being formulated to describe the shape and stress of a free, pressurized elliptic toroidal shell where properties of the shell may be anisotropic and nonhomogeneous. In a related effort, experimental tests are being conducted to determine dynamic characteristics of nonrotating tires in contact with a surface. Further, tests are underway to obtain the mechanical properties of two sizes of airplane tires during operation over a wide range of test parameters, including forward speed. Data from these tests will be incorporated into a tire mechanical property data bank which is being compiled by The University of Michigan under a NASA grant.

TIRE-TREAD MATERIALS RESEARCH

Tire wear is of major economic concern to commercial and military aviation since tire replacement accounts for approximately half of the overall landing-gear maintenance cost of present-day jet airplanes. For example, it is estimated that for the worldwide fleet of Boeing 727 airplanes, the cost of tire replacement approaches $20 million annually. The Chemical Research Projects Office at the Ames Research Center recently instituted a program to develop new tread materials in an attempt to improve the overall lifetime and the cut and blowout resistance of airplane tires. Langley Research Center was requested to participate in the program by evaluating the wear characteristics and the friction behavior of tires retreaded with the newly developed rubber compounds.

In the initial effort, a number of size 49 x 17 airplane tires were retreaded with one of the experimental materials which, for small specimen laboratory tests, exhibited improved hysteresis and fatigue life. For comparison purposes, additional tires of this size were retreaded in the same mold but with a standard state-of-the-art material. To acquire friction data, a tire from each stock was installed on a test carriage at the aircraft landing loads and traction facility shown in figure 1 and was exposed to high-speed braking tests on dry and wet concrete surfaces. Wear data were obtained by enlisting the services of the Federal Aviation Administration, which flew a Boeing 727 airplane equipped with sets of tires made from both the experimental and standard stocks.

The initial tests were encouraging in that track tests showed the level of developed friction did not deteriorate for the experimental

stock, and the wear performance during flight tests proved to be equivalent to the standard stock. Since the formulation of the stock that was tested was only an initial attempt and was not considered the optimum blend of ingredients, it is likely that a blend could be perfected that would considerably improve tread longevity. Such an optimization, however, would best be accomplished by the tire industry.

In continuation of the tread material test program, the new ground test vehicle shown in figure 2 was developed to obtain for detailed study simultaneous measurements of tire friction and wear properties under closely controlled braking and cornering conditions. The first group of tires to be tested with the new vehicle were eighty 22 x 5.5 airplane tire carcasses obtained from the U.S. Navy. Twenty of these tires were retreaded with a state-of-the-art polyblend, twenty with natural rubber, and twenty each with two different experimental compounds.

Friction and wear tests were conducted during the past year in which these tires were exposed to a variety of braking and cornering operations on several typical runway surfaces, with a sample of the preliminary results presented in figure 3. The figure shows that during the slow speed tests at various amounts of slip (braking), all compounds develop approximately the same friction characteristics. The wear rate (rubber removed per unit distance) for the two experimental treads, however, does appear to be slightly greater than that of the state-of-the-art polyblend but much less than for natural rubber. As mentioned earlier, an optimized blend of the ingredients in one or both of these experimental treads could conceivably improve their wear performance.

In addition to these tests, more flight programs are being conducted to obtain wear data on these tread materials under flight operational conditions by using the B-727 airplane. A commercial airline is currently flying with sets of tires which include 50 experimental and 50 standard treads to determine comparative wear characteristics under realistic commercial fleet use. No wear data are yet available from this program.

POWERED WHEELS FOR AIRPLANE TAXIING

Another area of research is a powered-wheel concept for movements of airplanes around congested air terminals. Energy conservation and ecological considerations have caused the transportation industry to review systems and operational procedures in an effort to achieve

savings in energy and reductions in noise and air pollution. The aircraft industry in particular has conducted studies to achieve greater operational efficiency in terms of energy. A number of studies have centered around alternatives to the use of the jet engines as a means of providing the power for taxiing airplanes. A specific alternative using a secondary power source involves individually powered wheels in the main landing gear; thus, dependence on a ground-based power source such as a tow tractor would be eliminated.

The main objective of the powered-wheel program undertaken at Langley was the design, manufacture, and test of a suitable, full-scale, hydraulically powered motor that would be compatible with the outboard wheels of a large transport airplane and capable of providing suitable taxi performance. Compatibility included no interference with braking other than removal of three-fifths of the brake stack in the outboard wheels and essentially no change in the ground check-out or removal and replacement for tires, antiskid systems, and brakes.

Currently under NASA contract, The Bendix Corporation has applied their DYNAVECTOR concept to the motor actuator, gear box, and clutch mechanism shown in figure 4 that can be mounted in the outboard wheels of the B-737-100 landing gear, one of which is shown in figure 5. Hydraulic pressure from an auxiliary power unit would be used to power the motor, and it is anticipated that taxi speeds up to 24 km/hr (15 miles/hr) can be obtained on runway grades up to 4 percent, with an additional capability of reverse operation for backing away from terminal area parking. Currently, this unit is undergoing static stall torque tests and no-load high-speed tests. If current problems can be solved, dynamometer tests may be attempted to study the unit's characteristics under several typical simulated airplane taxi and landing-to-take-off cycles.

AIR CUSHION LANDING SYSTEMS

Ground loads transmitted through conventional landing gear play a major role in the design of the airframe since those loads are concentrated at discrete points on the airplane structure. Similarly, pavement design (runway, taxiway, ramps, etc.) is based upon loadings in the tire footprint. With the current trend of larger and heavier airplanes, efforts to maintain acceptable loadings both in the airframe and on the ground have resulted in a multiplicity of gears. The expense in volume and weight for such systems, which serve no useful purpose once the airplane is airborne, is high. Furthermore, the concentrated wheel loads are beginning to exceed the bearing strength of the runway. One approach to these problems that is currently under

consideration is to replace the conventional gear with an air cushion landing system (ACLS). In addition to reduced runway loads, the air cushion may offer improved crosswind performance, attractive amphibious capabilities, and simple retraction and storage mechanisms, all at a potential system weight saving. In view of these features, considerable attention has been given to establishing the feasibility of such a landing system, particularly in terms of its landing impact behavior and its ground-handling performance.

Figure 6 shows several photographs of air cushion testing at NASA Langley Research Center. In figure 6(a), a scale model ACLS representing a 1/4-scale C-8 transport is shown which was tested at the aircraft landing loads and traction facility for behavior at landing impact, vulnerability to obstacles, and ground stability at forward speeds up to scale landing speeds. The models were constrained only laterally and longitudinally, and model motions and accelerations, as well as ACLS trunk pressures and flows for a variety of test conditions, were measured. Also shown in the figure is the model as it approaches a ditch obstacle. Similar tests were made using a 0.3-scale model of a Navy fighter airplane (ref. 12).

Tests of a concept to provide all-terrain launch and recovery of Remotely Piloted Vehicles (RPV) using an ACLS were conducted at high forward speeds on a test carriage at the aircraft landing loads and traction facility as shown in figure 6(b). The concept featured separate launch and recovery trunks, the latter being ground stowed within a zippered cover while the launch trunk was attached over this assembly directly to the fuselage with Velcro strips and was jettisoned after take-off. The purpose of the tests was to observe any flutter of the inflated launch trunk, to initiate and monitor the jettison of that trunk, and to observe the inflation of the ground-stowed recovery trunk, all at speeds of 100 knots. These tests have resulted in a redesigned retention-release system for the launch trunk.

Figure 6(c) is a photograph of a free-body test vehicle designed to investigate the ground stability and ground-handling problems of a number of ACLS concepts to a larger scale than is presently possible with the existing test carriages. The vehicle is trailer transportable so that tests may be carried out on a wide variety of potential landing surfaces such as swamps, beaches, and plowed fields. This vehicle has been outfitted, and testing is imminent. Other experimental ACLS tests are reported in references 13 and 14.

An analytical model of an ACLS has been developed for NASA by Foster-Miller Associates, Inc. under contract. (See ref. 15.) The model includes a systematic and rational analysis of each of the four primary subsystems affecting ACLS behavior: the air supply fan, the air feeding or ducting system, the trunk, and the cushion. All pertinent pressures and flows are represented as is the trunk shape, the resulting cushion area, and pressure for both static and dynamic operation. The forces thus generated on the body are summed together with external forces due to aerodynamic and ground friction, and the resulting airplane motions in heave, pitch, and roll are computed. The program is constructed in modular form and has been written with sufficient generality such that a wide variety of practical ACLS designs may be investigated.

Figure 7 presents a comparison of a purely analytical dynamic analysis with an experiment using the small ACLS model shown in figure 6(d). Portrayed are trunk pressure and vertical motion resulting from a drop with the model restrained to pure heave motion only. The agreement between analysis and experiment is thought to be quite good, with model behavior and overall pressure and motion being quite accurately predicted by the analysis. Following impact, the first few cycles in trunk pressure are quite large owing to repetitive stalling of the fan. Hysteresis losses during the stall eventually dissipate enough of the drop energy so that fan stall no longer occurs and system damping is reduced to a low and marginally stable value.

In addition to this work, Bell Aerospace Textron under contract with NASA is studying seven different categories of future airplanes to determine the most attractive applications of air cushion landing systems and to quantify the benefits which could be expected using such a landing system. Another objective of the study is to identify the technical barriers that yet remain to applications of ACLS to the various categories of airplanes.

CROSSWIND LANDING GEAR

The landing and take-off operations of an airplane in the presence of a crosswind require special piloting techniques which can impose significant additional demands on the pilot. For instance, one landing technique used by pilots requires that an airplane approach the runway in a side-slipping attitude such that immediately before touchdown the airplane must be rolled to level the wings prior to touchdown. Another method utilizes a crabbed approach. Immediately before touchdown, the airplane must be decrabbed to aline the gears with the runway centerline. Special attention must be given in the former technique to

clearance for low-winged airplanes, and both techniques require considerable pilot skill and familiarity with the airplane flight response characteristics. A crosswind landing-gear system could permit an airplane to approach the runway in a manner similar to that of the crabbed landing technique and yet could eliminate the need for the critical decrabbing manuever before touchdown.

Landing-gear concepts intended to permit an airplane to touch down in the crabbed attitude have been designed, a few units have been installed on certain airplanes, and one type of crosswind landing gear has been incorporated on two large types of military airplanes. In an effort to investigate various landing-gear systems, the Langley Research Center engaged in a crosswind landing-gear program which included small-scale landing-gear model studies, development of ground-run equations of motion to describe the roll-out motion of an airplane subjected to lateral forces, and the installation of a research landing-gear system on an airplane capable of being adapted to different crosswind landing-gear modes of operation.

Model Studies

Four different crosswind landing-gear concepts for which the main gears were free to pivot, to be steered, or to be otherwise constrained, were evaluated in small-scale model tests in reference 16. For these tests the model, which was equipped with pneumatic tires, was launched onto the laterally sloped runway shown in figure 8, where the laterally sloped runway simulated a crosswind. Following launch the model was free, and subsequent to solenoid engagement, each gear could be individually steered by remote control. Subject to the limitations of the tests, the model operator preferred that the main gears be alined with the direction of motion prior to touchdown and that nose-gear steering be provided.

Ground-Run Equations of Motion

To supplement crosswind landing-gear studies, planar equations of motion were derived to describe the ground-run trajectory of an airplane. The equations were programed to compute the position and heading of an airplane subjected to disturbing forces and to the steering action of tires. The disturbing forces included aerodynamic forces and gravity forces due to runway tilt. The latter forces were included to permit correlation with the model studies. Furthermore, since for some crosswind landing-gear systems the gears may be momentarily without steering control, equations to describe freely swiveling

wheel motion were also provided. Tire forces were determined after considering the tire motions and the force equilibrium normal to the runway surface.

The equations were applied to a trial test of the model for which the gears were locked in the direction of the motion imposed at launch. The right side of figure 9 shows a spatial display of the trajectory, where the triangular symbol denotes the model. For this test the model is shown to drift slightly in the direction of the simulated crosswind (downhill) before ultimately heading into the wind (uphill). The brief initial downhill drift was attributed to slight misalinement conditions at launch, and the basic uphill motion occurred because the resultant lateral ground reaction force was forward of the vehicle center of gravity. The position and heading of the model as a function of time are displayed on the left side of the figure. The data points denote measured values obtained from time-correlated films of the tests by using the data reduction scheme of reference 17. The solid-line time histories of the figure depict the trajectory of the model as computed from the programed equations of motion. The figure shows good agreement between the computed results and the experimental results from a test having initial launch speed of 4.4 m/sec, an initial lateral velocity of 0.1 m/sec, an initial heading of 0.7°, and an initial heading rate of change of -5.4 deg/sec.

Other applications of the equations of motion to the test model and a derivation of the equations are being studied.

Flight Tests

A flight investigation was conducted to study piloting techniques and crosswind limitations for a light transport with a conventional tricycle gear. Among the results of that program reported in reference 19, it was indicated that control during ground roll-out was the most critical problem, and that aerodynamic control required for slip or decrab may be limiting. These results led to the conclusion that a crosswind landing gear should be beneficial in extending the crosswind landing limits.

The potential benefits of a crosswind landing-gear system can be illustrated by figure 10, which is a schematic of a crabbed approach. During the approach, the airplane is crabbed into the wind with controls essentially neutral so that its ground track is along the extended runway centerline. With a crosswind gear, the wheels can be alined with the airplane ground track for touchdown, which eliminates the need for the demanding pilot task and large control inputs to decrab

or slip the airplane prior to touchdown. By starting the roll-out with the aerodynamic controls near the neutral datum, the full control range is available for additional control.

The modes of operation chosen to investigate for the crosswind landing-gear flight research program discussed in this paper were based on the previously discussed model studies (ref. 16), and on the experiences gained in the study of reference 18. The test objectives of the crosswind landing-gear program were to extend the crosswind landing limits of the airplane and to evaluate and demonstrate the effectiveness of lift spoilers and various modes of crosswind landing-gear operation.

Description of system. - The test airplane (fig. 11) was a high-wing, twin turboprop light transport. A summary sketch of the changes made to the airplane is given in figure 12. Single main wheels were replaced by the dual wheel units from a military helicopter. The main gear legs of the transport were inverted and the right and left legs were interchanged. This lowered the airplane ground line by about 15.2 cm (6 in.). Appropriate modifications were also made to the nose gear to account for the lower ground line. The main gear units were physically connected by a metal tie rod to insure that the main gear units were tracking together and to facilitate the centering of the gear. The research crosswind landing-gear system was not optimized for weight, aerodynamics, or operational simplicity.

The wing-lift spoiler system, consisting of two hydraulically-actuated panels on the upper surface of each wing, was automatically limited to deployment at touchdown by means of main gear weight switches in series with an arming switch and a throttle position switch.

The main and nose gear could be pivoted as a unit $\pm 30^\circ$ for crosswind landings. The nose gear could be steered an additional $\pm 3^\circ$ about its prevailing position through the rudder pedals. For research purposes, the crosswind landing-gear system was designed to provide the capability of investigating three crosswind landing-gear concepts. The three modes of crosswind landing-gear operation are outlined in table I. In the castor mode, the gear were free to aline with the direction of travel at touchdown. However, to prevent the airplane from veering off the runway, steering must be initiated shortly after touchdown. In the preset mode, the pilot set the gear to the desired offset angle with a tiller bar in the cockpit. (See fig. 13.) (The tiller bar, which controls the pivot angle of the gear, was located on the control column behind the pilot's control wheel, and could also be used to steer the nose gear during low speed taxiing when the main gear were locked.) In the automatic mode, the radio compass system was used to generate an error signal proportional to the angle between a selected runway heading and the airplane heading. This signal, summed with a main-gear position feedback signal, was used to automatically keep the gear alined with the runway centerline while in flight.

In the castor and preset modes, the main gear could be locked in position by pressing a switch on the pilot's control wheel. (See fig. 13.) This switch activated a hydraulic castor lock on each main gear unit. In the castor mode, the castor locks would activate when the switch was depressed and the main gear weight switches were actuated. In the preset mode, the castor locks were actuated in the air in order to lock the gear in position prior to touchdown. In the automatic mode, the gear was locked in position after either of the two main gear weight switches was compressed without the pilot having to press the switch. It should be noted that the main gear must be locked or restrained in order to develop nose-wheel steering capability.

In any mode, after a weight switch on the nose gear had been activated, the pilot could select rudder pedal steering of the nose gear by depressing and holding a thumb switch on the pilot's control wheel. This switch was adjacent to the main gear castor lock switch, as shown in figure 13. The nose-wheel travel with rudder pedal steering was $\pm 3^{\circ}$. This feature was incorporated to allow the pilot to have limited authority nose-wheel steering for the high-speed part of the ground roll without having to release the control wheel or throttle to reach the tiller bar.

The pilot could also center the gear in any mode by pushing a single switch on the crosswind control panel shown in figure 13. The gear centering command overrode all other inputs or actions. The conventional aerodynamic (rudder and aileron) and low-speed nose-wheel steering controls were retained from the original airplane. Main gear braking effectiveness was greatly reduced because hard braking caused flat spots or blown tires. Apparently, with the airplane heeling, one of the dual wheels would not carry sufficient load to overcome brake torque and would be ground flat. Reverse thrust became the principal braking control although very little actual thrust was developed due to the slow engine response.

A crosswind landing-gear position indicator was developed for this program. The location of the indicator in the airplane instrument panel is shown in figure 13, and a schematic of the indicator is shown in figure 14. The gyro compass card was driven by a gyro slaved to the compass heading. The double-bar needle pointed to the landing runway magnetic heading, which was input to the system with the runway heading selector knob (part of the horizontal situation indicator on the test airplane). The angular difference between the centerline of the fixed airplane symbol and the runway heading (double-bar needle) was the crab angle of the airplane. The single-bar needle indicated the angle of the gear with respect to the airplane centerline. When the gear were properly alined with the runway centerline, the single-bar and double-bar

needles superimposed. In the example given in figure 14, the runway heading and gear position are purposely shown misalined. The airplane is shown flying to a heading of 350°, crabbed 15° to the right of runway centerline. The gear are shown offset 20° to the left of airplane centerline, which means that the gear have been rotated 5° too far. In the preset mode, the pilot would use the tiller bar in the cockpit to bring the gear into alinement with the runway. In the automatic mode, the misalinement would indicate a system malfunction. It is understood that some airplanes with crosswind landing gear have actually landed with the landing gear set in the wrong direction. The use of this indicator should prevent such an occurrence. The pilot can determine proper wheel alinement from a quick scan without mentally having to process information to relate heading and landing-gear deflection magnitude and direction. Details on the crosswind landing-gear position indicator may be found in reference 19.

Results. - A matrix of the test conditions for this investigation is given in table II. A total of 195 crosswind landings were made in the program by three test pilots who used the three modes of crosswind landing-gear operation. The crosswinds given in this paper are the direct crosswind components computed from the wind magnitude and direction recorded at the time of touchdown by a wind sensor at the 6.1-m (20-ft) elevation of a meteorological tower located near the test runways. All landings were made in Visual Flight Rules (VFR) conditions to a dry runway surface. The pilot's task was to land, roll out, and stop the airplane within the STOL runway markings that were painted on the existing runways. The STOL runways were 30.5 m (100 ft) wide and 457 m (1500 ft) long. The markings for these runways are given in reference 20. The three runways on which they were painted were 1524 to 2743 m (5000 to 9000 ft) long and 46 to 61 m (150 to 200 ft) wide. The landings were made using a 3° or 6° approach angle, which was indicated by the visual guidance system described in reference 18. All landings were made using full flap deflection and the wing-lift spoilers were used after touchdown for most of the tests.

The pilots have stated that with the crosswind gear "....it is possible to make crosswind landings in crosswind conditions that are far more severe than could be handled with the conventional gear." With the conventional gear (ref. 18), the crosswind limits were 15 to 20 knots. The largest crosswind encountered during that program was 22 knots, which caused the pilot to abort the landing just prior to touchdown. It can be seen in table II that, with the crosswind gear, 11 landings were made with crosswinds between 20 and 25 knots, and 5 landings were made with crosswinds between 25 and 30 knots. In three

tests, the main gear rotated to the right control limits at 30°. The crosswinds of 26 to 27 knots are about one-half the stall speed of the airplane.

The self-alining feature of the crosswind landing gear (castor mode or automatic mode) was found to be essential for landings in high crosswinds. For the airplane gear configuration tested, the preferred mode of crosswind landing-gear operations was the castor mode. The pilots found the crosswind landing gear to be particularly beneficial in crosswinds above 15 knots where the crab angle approached 20°. As can be seen in table II, the landings with the largest crosswinds were made using the castor mode. A schematic of a typical large crosswind landing, using actual values measured during one test, is given in figure 15. The airplane was crabbed 23.5° to the right of runway centerline at touchdown to compensate for the right crosswind of 26 knots. The touchdown speed of 58 knots was just over twice the crosswind magnitude. Time histories from a castor mode landing with an even greater crosswind (23.7 knots from the left) are given in figure 16(a). During the approach and landing, the sideslip oscillated about zero, until the airplane was nearly stopped on the ground, at which time the forward speed was so low the sideslip record was off scale. Bank, aileron, and rudder also oscillated about zero. At touchdown, the main and nose gear freely alined with the direction of travel, swiveling to the right (clockwise) to offset the left crab angle. The main gear castor locks were applied 2 sec after touchdown, and the pilot used tiller bar steering of the nose gear. Although the pilots preferred rudder pedal steering, the pilot felt it was necessary this time to use the tiller bar for steering in order to get additional nose wheel travel. (Rudder pedal steering was limited to $\pm 3°$.) At the end of the ground roll, the "center" switch was used to bring all gear back to the airplane centerline. Because of the self-alining feature of the gear at touchdown, the pilot did not have to monitor or operate the gear during the approach. As one pilot said of castor mode landings, "No precision is involved. I like them."

The pilots' second preference was for the automatic mode, saying the automatic mode "should be equally as good as the castor mode if we had a higher response rate in the gear." This comment is reasonable when one considers that the automatic mode is actively self-alining in so far as requiring no pilot adjustment. Time histories for an automatic mode landing with a right crosswind of 13.6 knots are given in figure 16(b). During the approach, the main and nose gear tracked the crab angle closely through some rather severe heading changes, with the gear offset to the left (counterclockwise) to compensate for the right crab angle. At touchdown, the castor locks were automatically applied, and the nose gear stopped tracking crab angle to make it

available for steering. In this landing, the pilot used rudder pedal steering of the nose gear for about 13 sec. The records were terminated before the gear were centered. If, as in the present case, the touchdown forces on the wheels are adequate to aline the gear without producing an objectionable reaction in the airplane, the castor mode would be preferable to the more complex and expensive automatic mode.

For the preset mode, the pilot is required to choose and set the crosswind landing gear to an appropriate offset angle for touchdown. Time histories for a 15.6 knot crosswind landing in the preset mode are given in figure 16(c). Early in the approach, the pilot selected an offset angle of 12° right, to match the average left airplane crab angle. During the approach, the pilot made several adjustments, eventually returning the crosswind landing gear to 12°, after which the castor locks were applied. During the flare, there was a sudden change in heading due to wind shear and the airplane landed with a crab angle of only 5.5° left, giving a 6.5° misalinement with direction of travel. The pilot used rudder pedal steering to compensate during the ground roll out, with the full 3° of nose-wheel travel available through the rudder pedal system. This approach illustrates the problem of coordinating crab angle and gear offset angle, especially in unsteady conditions, in which the crab angle is continually changing. This problem is particularly severe in the flare. Quoting one of the pilots, "In the flare, the pilot can't be looking at the cockpit instruments, so he finds it difficult to judge if the airplane crab angle is the same (i.e., same in magnitude, but opposite in direction) as the gear angle." The large crosswinds encountered in this program were always accompanied by considerable turbulence, gustiness, and wind shear. These unsteady conditions are reflected in the aileron, rudder, and crab angle time histories for all three approaches in figure 16. For the unsteady conditions experienced during the castor mode approach (fig. 16(a)) and the automatic mode approach (fig. 16(b)), it is doubtful if the pilots would have attempted a preset mode crosswind landing. The castor and automatic modes relieved the pilots of having to continually adjust and monitor the gear position. The pilots found the preset mode to be very undesirable in unsteady conditions. In fact, they stated that the preset mode was the "most undesirable of the three modes."

The maximum lateral dispersion during ground roll out was 18.3 m (60 ft), and the maximum airplane roll distance was less than 457.2 m (1500 ft) although very little main gear braking was used. The pilots believe that much smaller lateral dispersions and shorter roll distances would have been possible if the airplane had improved main gear braking, increased nose-gear steering travel through the rudder pedals, more effective wing-lift spoilers, and faster engine spool-up time for improved braking and steering (asymmetric thrust).

The pilots feel that greatly improved safety and comfort can be realized by developing an operational castor mode crosswind landing-gear system incorporating castor locks and rudder pedal steering. Side forces would be reduced at touchdown to produce a smooth landing for the passengers. The operation of a crosswind landing gear on slippery runways needs further study, analysis, and/or testing.

CONCLUDING REMARKS

The landing-gear research being conducted at NASA Langley Research Center is summarized and research relative to tire-tread developments, powered-wheel taxiing, air cushion landing systems, and crosswind landing gear is discussed in some detail. The status of these four programs are as follows:

Tire-tread wear - the preliminary ground tests are complete and flight tests to determine wear characteristics in fleet use are underway

Powered wheels - the prototype is under development

Air cushion landing gear - analysis and experimental tests are underway

Crosswind landing gear - model and flight tests are now complete and equations of motion describing the ground-run trajectory have been derived for a model test

The preliminary results of the crosswind landing-gear flight tests indicated:

1. Landings can be made with crosswinds up to 27 knots with a crosswind landing gear; the previous crosswind limits with the conventional tricycle landing gear were 15 to 20 knots.

2. For the light transport airplane tested, the self-alining feature of the crosswind landing gear was found to be essential for landing in severe crosswinds.

3. The castor mode (passive self-alinement) was preferred by the pilots; presetting the landing gear prior to touchdown was the least desirable of the three modes of operation that were investigated.

REFERENCES

1. Stubbs, Sandy M.; and Tanner, John A.: Status of Recent Aircraft Braking and Cornering Research. Aircraft Safety and Operating Problems, NASA SP-416, 1976, pp. 257-269.

2. McDonnell Aircraft Co.: Expansion of Flight Simulator Capability for Study and Solution of Aircraft Directional Control Problems on Runways. Phase II - Final Report. NASA CR-145044, 1976.

3. Stubbs, Sandy M.; and Tanner, John A.: Behavior of Aircraft Antiskid Braking Systems on Dry and Wet Runway Surfaces - A Velocity-Rate-Controlled, Pressure-Bias-Modulated System. NASA TN D-8332, 1976.

4. Tanner, John A.; and Stubbs, Sandy M.: Behavior of Aircraft Antiskid Braking Systems on Dry and Wet Runway Surfaces - A Slip-Ratio-Controlled System With Ground Speed Reference From Unbraked Nose Wheel. NASA TN D-8455, 1977.

5. Bender, E. K.; Berkman, E. F.; and Bieber, M.: A Feasibility Study of Active Landing Gear. AFFDL-TR-70-126, U.S. Air Force, July 1971. (Available from DDC as AD 887 451L).

6. Wignot, Jack E.; Durup, Paul C.; and Gamon, Max A.: Design Formulation and Analysis of an Active Landing Gear. Volume I. Analysis, AFFDL-TR-71-80, Vol. I, U.S. Air Force, Aug. 1971. (Available from DDC as AD 887 127L.)

7. McGehee, John R.; and Carden, Huey D.: A Mathematical Model of an Active Control Landing Gear for Load Control During Impact and Roll-Out. NASA TN D-8080, 1976.

8. Barrois, W.: Use of General Fatigue Data in the Interpretation of Full-Scale Fatigue Tests. AGARD-AG-228, Oct. 1977, pp. 62-64.

9. Dreher, Robert C.: Studies of Friction and Wear Characteristics of Various Wires for Wire-Brush Skids. NASA TN D-8517, 1977.

10. Horne, Walter B.: Status of Runway Slipperiness Research. Aircraft Safety and Operating Problems, NASA SP-416, 1976, pp. 191-245.

11. Yager, Thomas J.; and McCarty, John L.: Friction Characteristics of Three 30 x 11.5-14.5, Type VIII, Aircraft Tires With Various Tread Groove Patterns and Rubber Compounds. NASA TP-1080, 1977.

12. Leland, Trafford J. W.; and Thompson, William C.: Landing-Impact Studies of a 0.3-Scale Model Air Cushion Landing System for a Navy Fighter Airplane. NASA TN D-7875, 1975.

13. Thompson, William C.: Landing Performance of an Air-Cushion Landing System Installed on a 1/10-Scale Dynamic Model of the C-8 Buffalo Airplane. NASA TN D-7295, 1973.

14. Thompson, William C.; Boghani, Ashok B.; and Leland, Trafford J.W.: Experimental and Analytical Dynamic Flow Characteristics of an Axial-Flow Fan From an Air Cushion Landing System Model. NASA TN D-8413, 1977.

15. Boghani, A. B.; Captain, K. M.; and Wormley, D. N.: Heave-Pitch-Roll Analysis and Testing of Air Cushion Landing Systems. NASA CR-?917, 1978.

16. Stubbs, Sandy M.; Byrdsong, Thomas A.; and Sleeper, Robert K.: An Experimental Simulation Study of Four Crosswind Landing-Gear Concepts. NASA TN D-7864, 1975.

17. Sleeper, Robert K.; and Smith, Eunice G.: A Transformation Method for Deriving From a Photograph, Position and Heading of a Vehicle in a Plane. NASA TN D-8201, 1976.

18. Fisher, Bruce D.; Champine, Robert A.; Deal, Perry L.; Patton, James M., Jr.; and Hall, Albert W.: A Flight Investigation of Piloting Techniques and Crosswind Limitations During Visual STOL-Type Landing Operations. NASA TN D-8284, 1976.

19. Champine, Robert A.: Crosswind Landing-Gear Position Indicator. NASA Tech Brief LAR-11941, 1976.

20. Spangler, Roman M., Jr.: Simulated Ground-Level STOL Runway/ Aircraft Evaluation. FAA-RD-73-110, Federal Aviation Administration, Sept. 1973.

TABLE I. - MODES OF OPERATION FOR CROSSWIND RESEARCH

Mode	Crab set of gear	Ground control
Castor	Passively - by ground forces during touchdown	In addition to conventional aerodynamic, brake, and low-speed nose-wheel steering control, the pilot can select:
Preset	Pilot control during approach	1. Nose-wheel steering at high speed through rudder pedals 2. Wing-lift spoilers
Automatic	Servo driven by signals from aircraft heading and runway direction	3. Return gear to center 4. Preset crab angle for take-off

TABLE II. - MATRIX OF TEST CONDITIONS RECORDED FOR 195 LANDINGS

Approach angle, deg	Number of landings for each 5-knot crosswind interval						Crosswind mode
	0 to 5	5 to 10	10 to 15	15 to 20	20 to 25	25 to 30	
-3	4	20	37	45	11	5	Castor
-3	0	17	20	5	0	0	Automatic
-3	0	11	11	4	0	0	Preset
-6	1	3	0	0	0	0	Castor
-6	0	1	0	0	0	0	Automatic
-6	0	0	0	0	0	0	Preset

Figure 1.- Aircraft landing loads and traction facility.

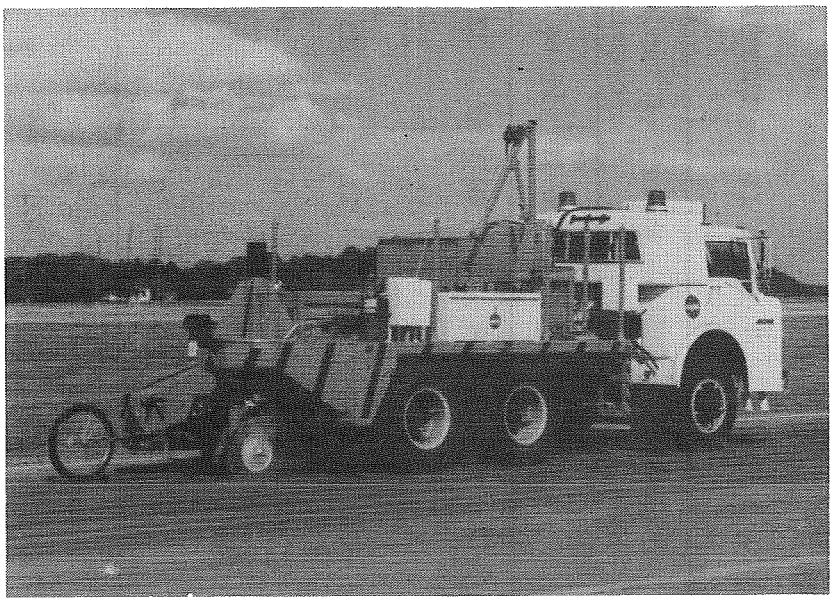

Figure 2.- Instrumented tire test vehicle.

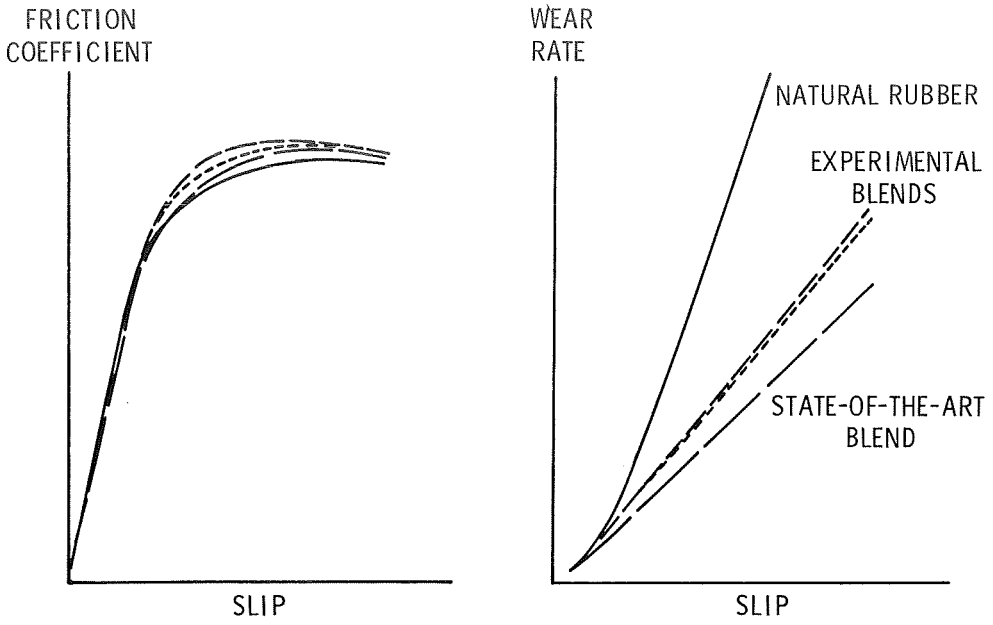

Figure 3.- Low-speed friction and wear characteristics of several tire-tread compositions.

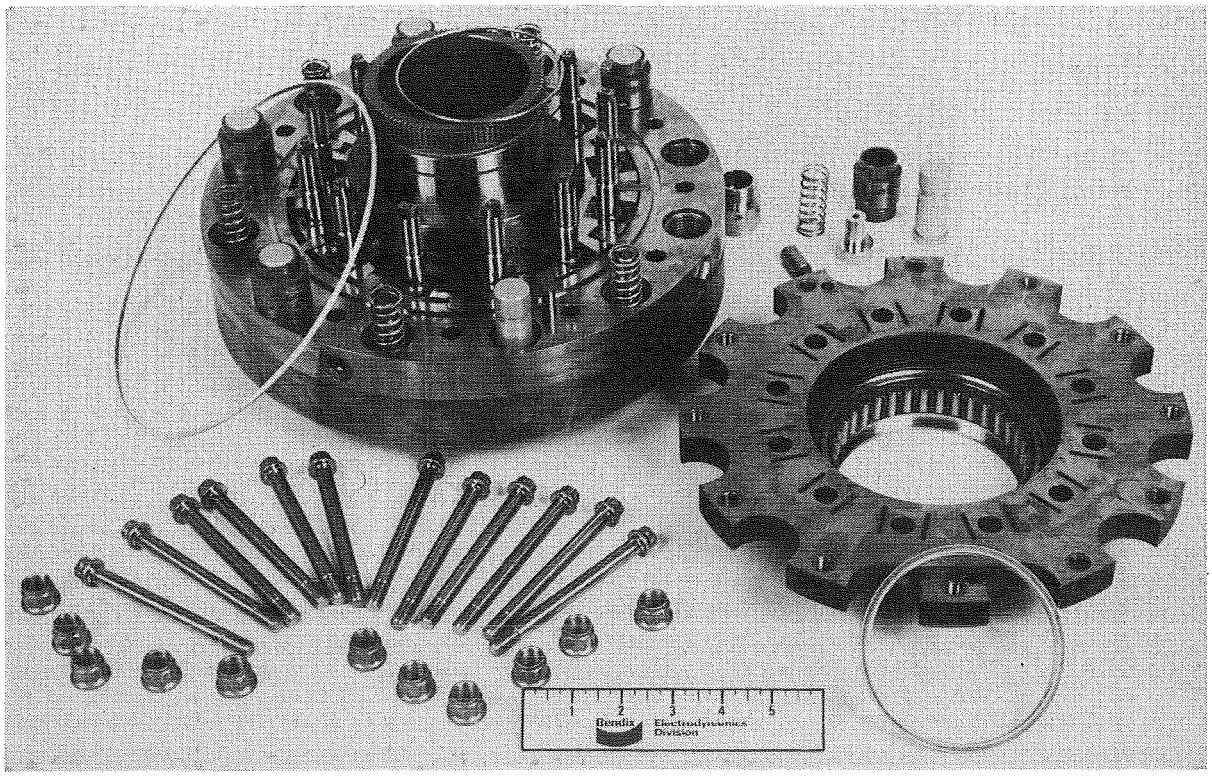

Figure 4.- Powered wheel hydraulic motor.

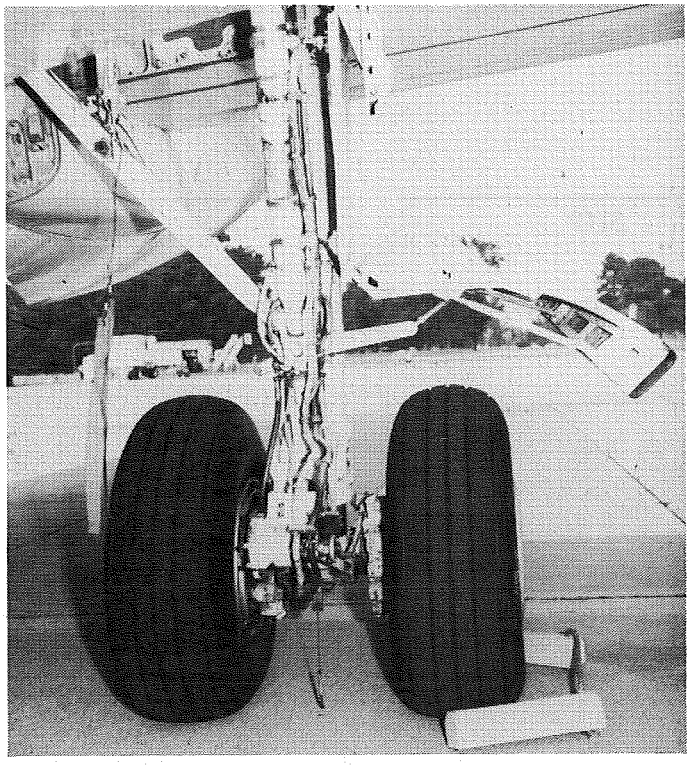

Figure 5.- B-737 main landing gear unit.

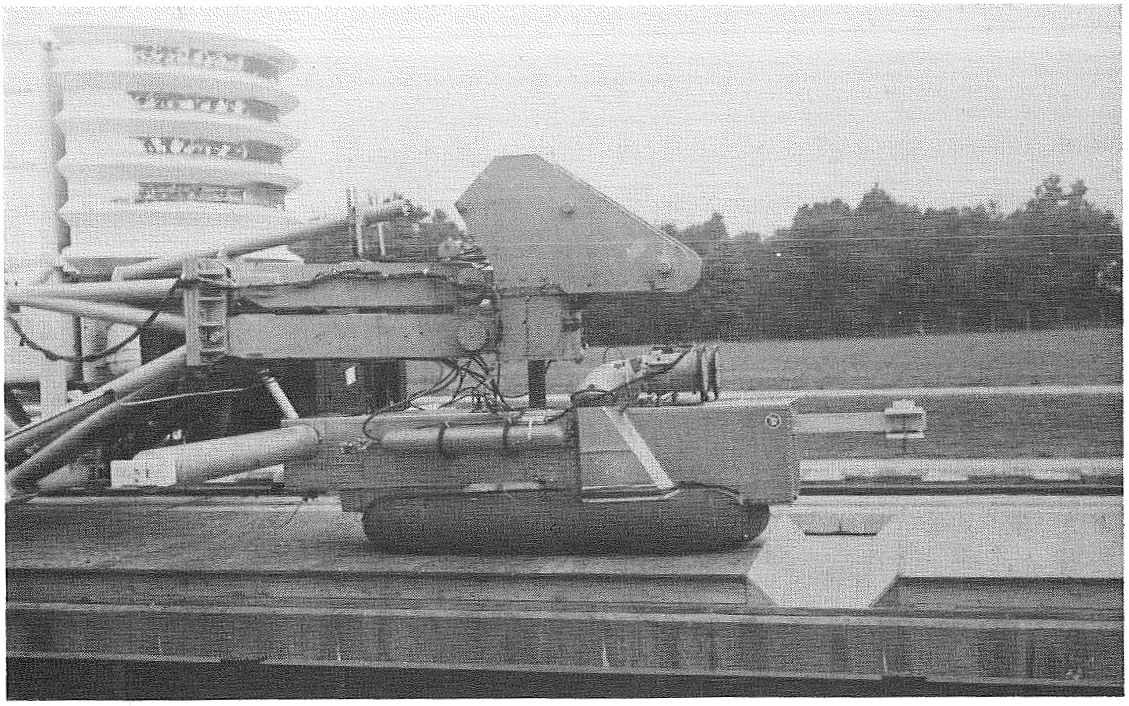

(a) Scale model testing: landing impact and ground handling.

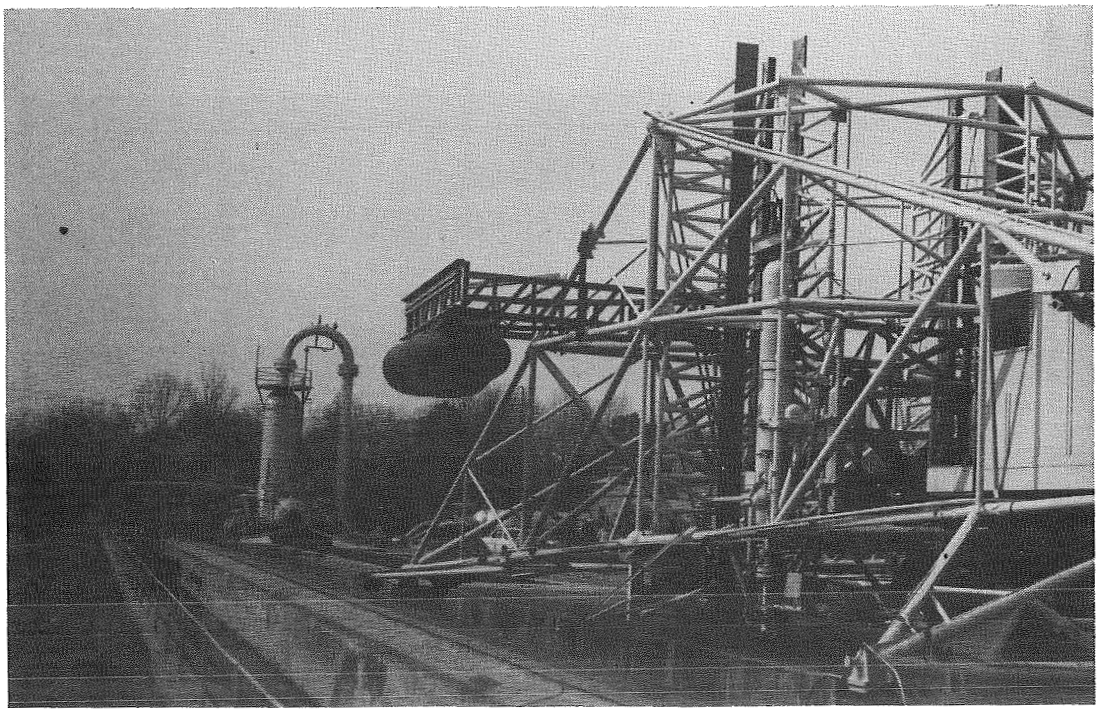

(b) RPV deployment tests at high forward speed.

Figure 6.- ACLS research.

(c) Free-body ground-handling tests: RPV and general ACLS.

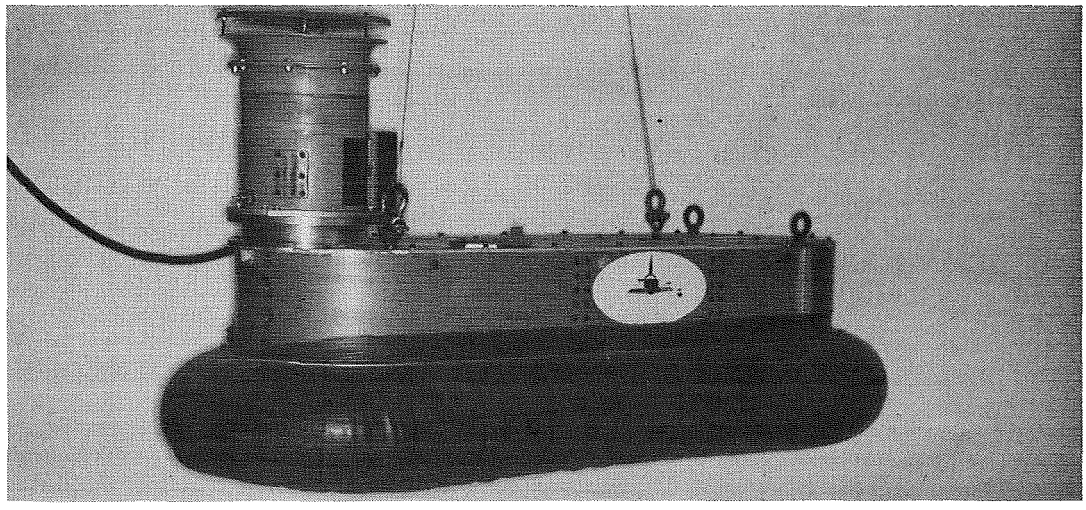

(d) Experimental corroboration of basic ACLS research. Interactive variables include fan air supply characteristics, trunk shape and kinematics, cushion flow and shape, and stability criteria.

Figure 6.- Concluded.

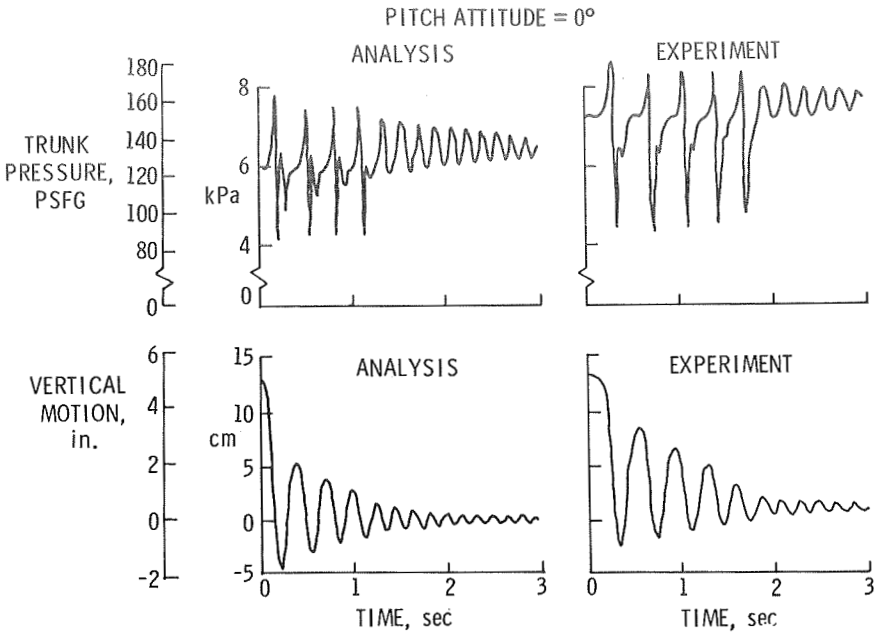

Figure 7.- Verification of dynamic ACLS model analysis; heave (vertical) motion only. Pitch attitude = 0°.

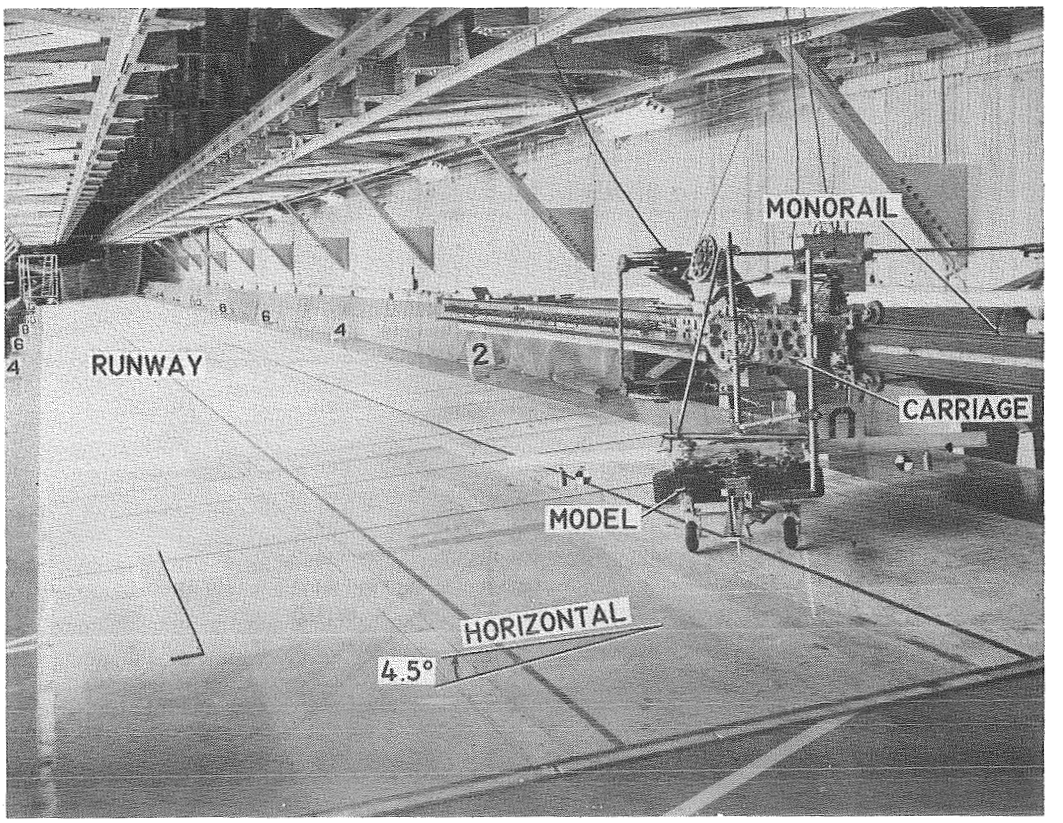

Figure 8.- Crosswind model test.

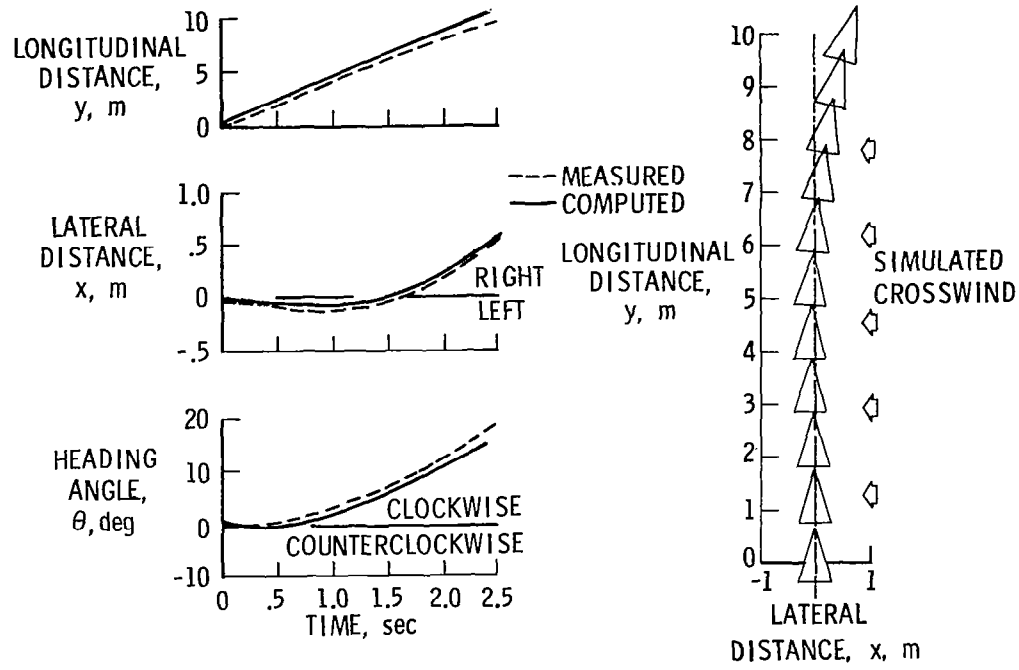

Figure 9.- Computed ground roll trajectory of landing-gear model.

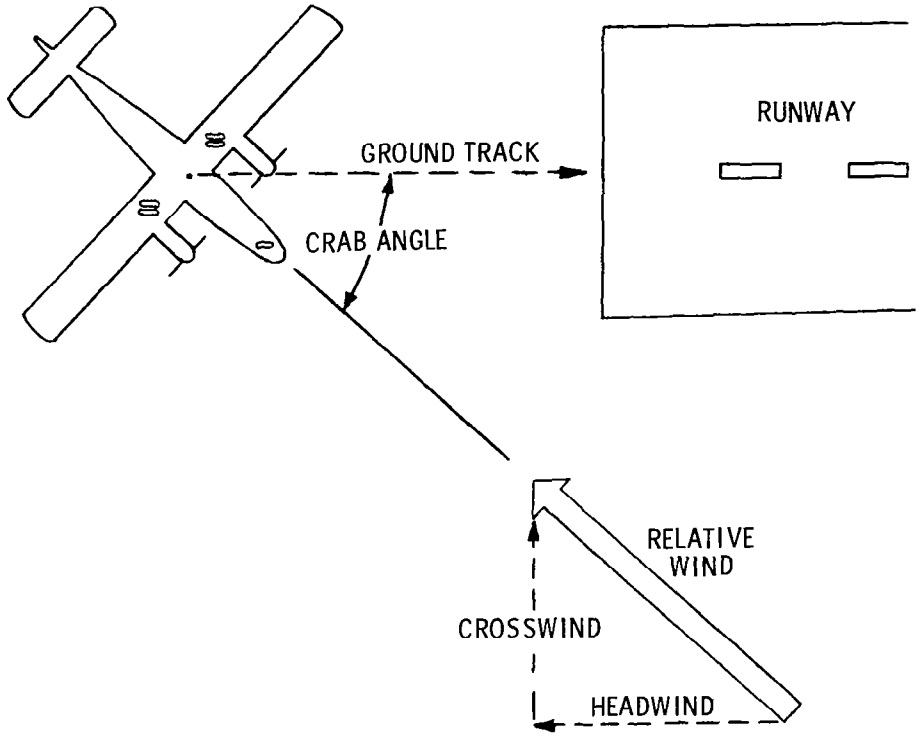

Figure 10.- Schematic of typical crosswind landing with crosswind gear.

Figure 11.- Crosswind landing-gear flight research airplane.

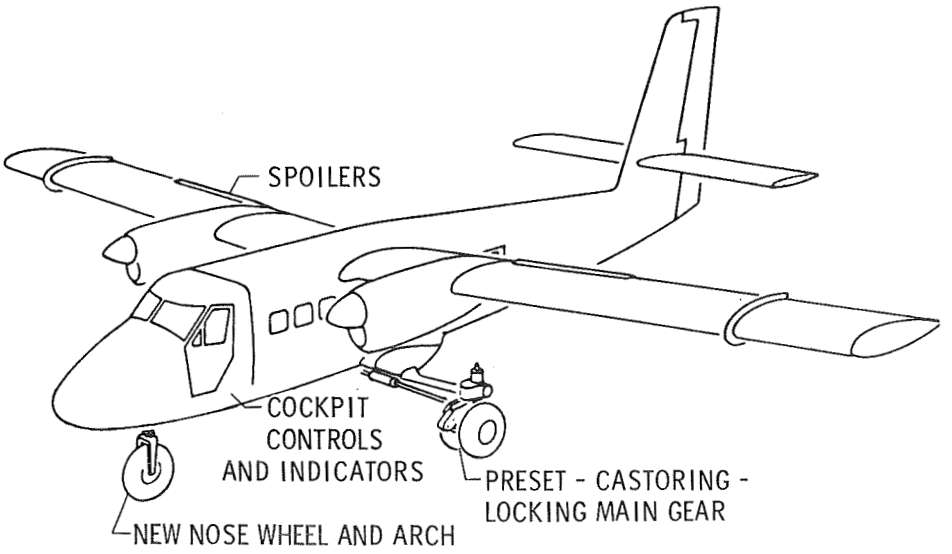

Figure 12.- Modification to NASA Twin Otter for crosswind landing.

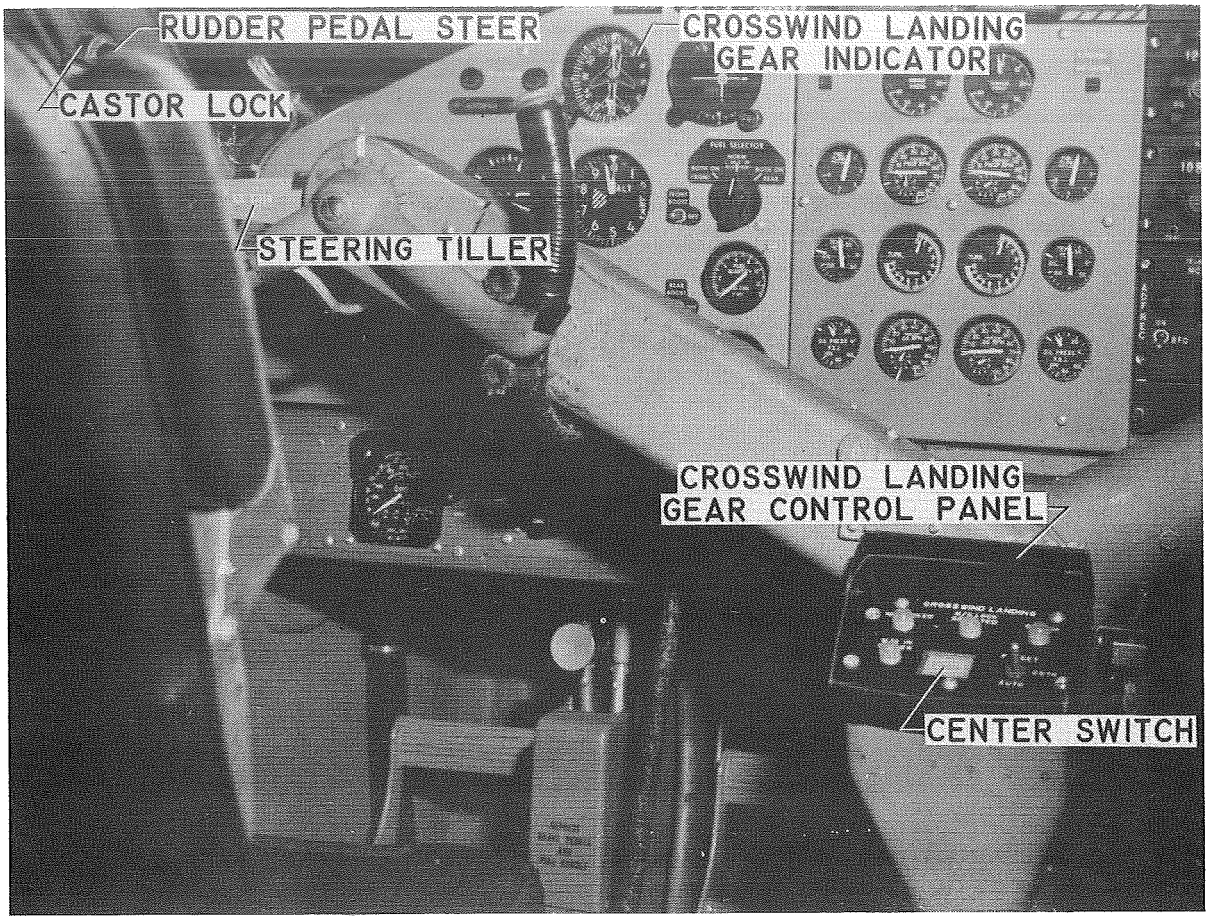

Figure 13.- Instrument panel for crosswind landing-gear test airplane.

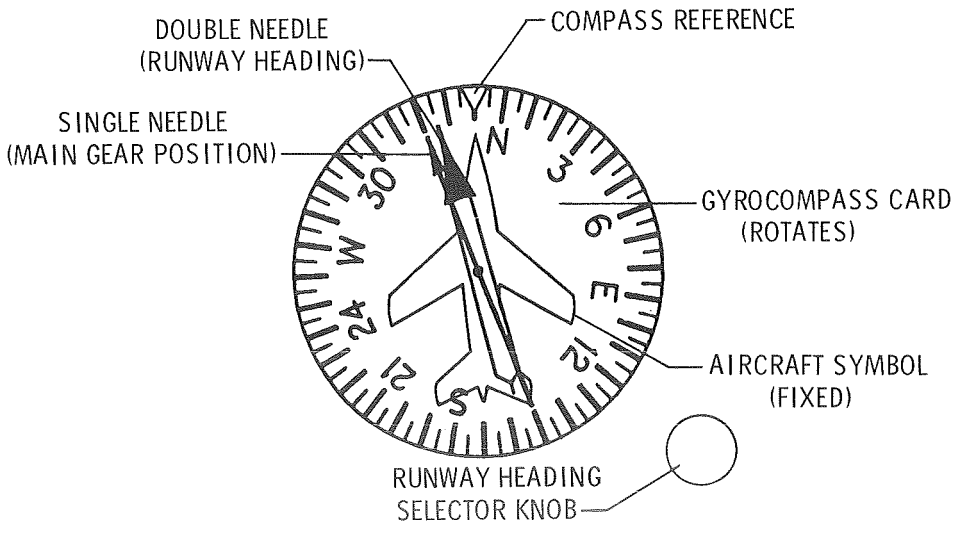

Figure 14.- Crosswind landing-gear position indicator.

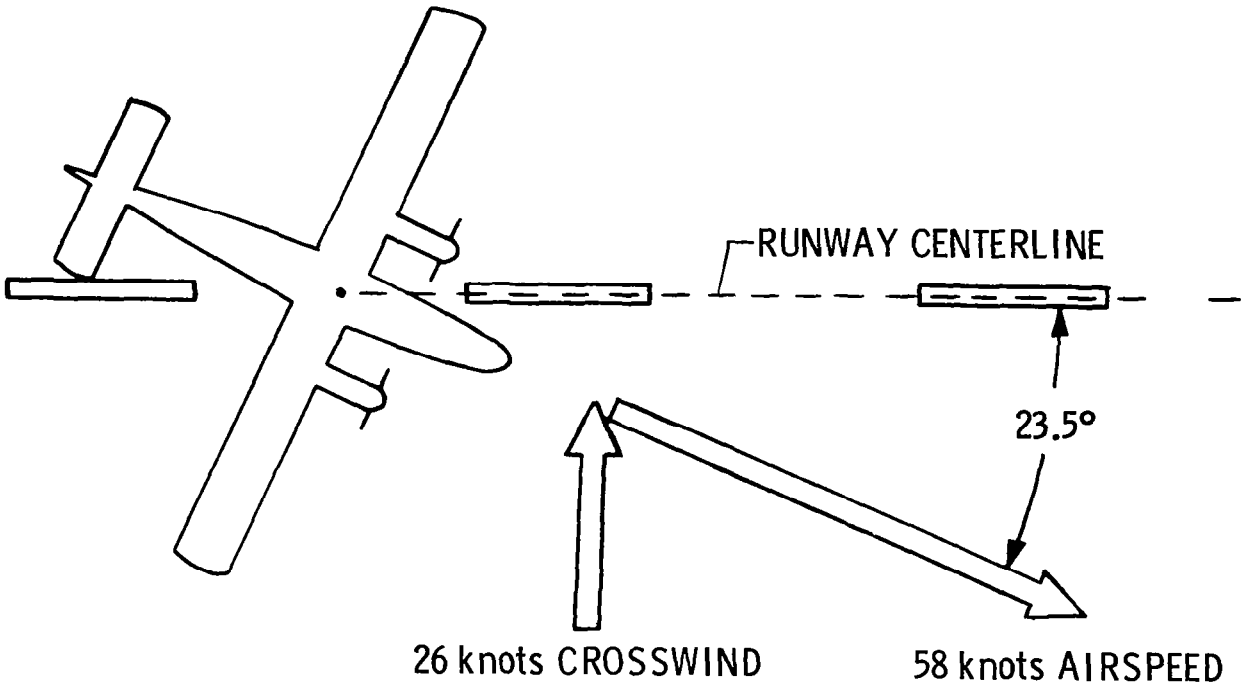

Figure 15.- A 26-knot crosswind landing with crosswind gear.

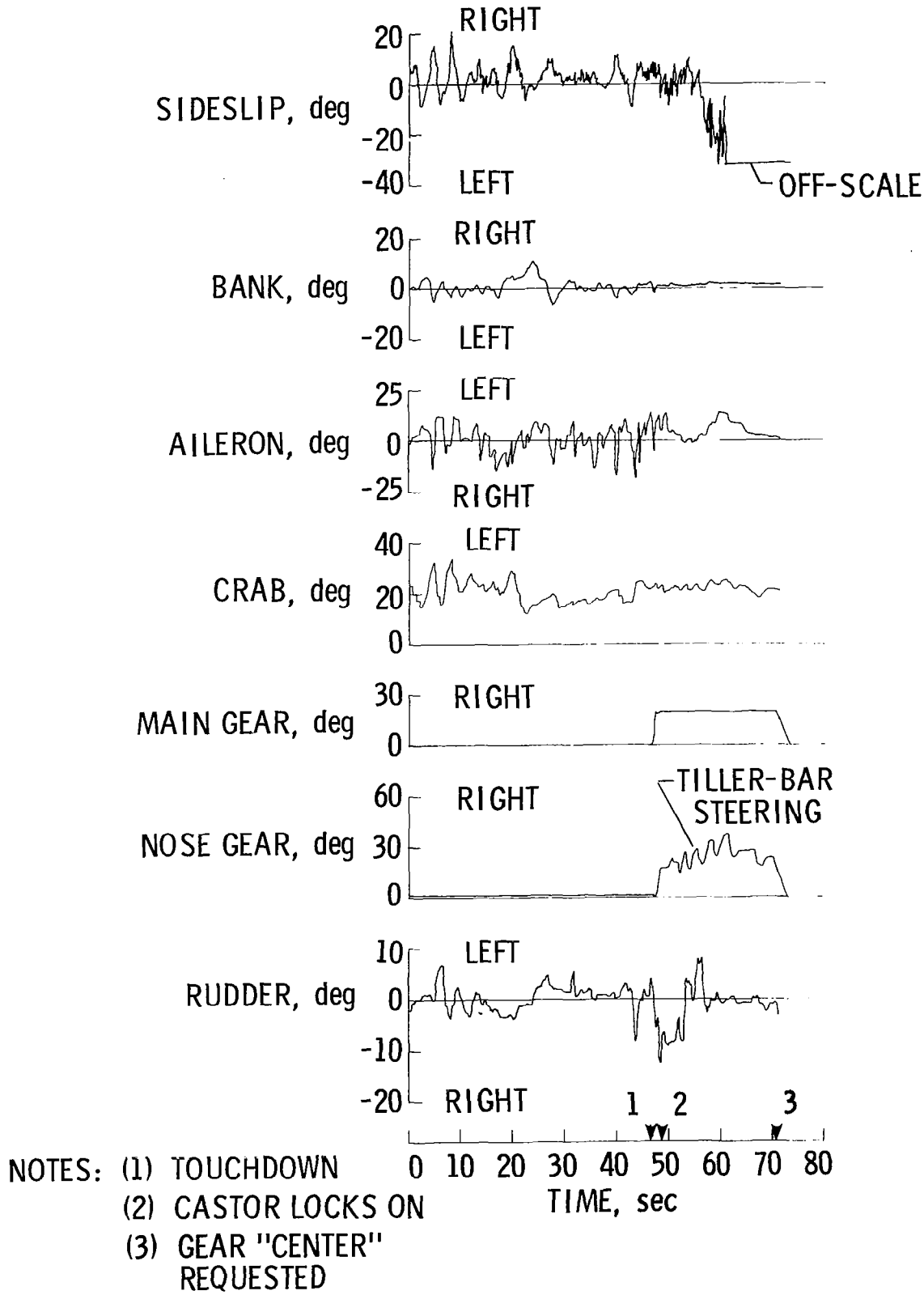

(a) Castor mode landing.

Figure 16.- Crosswind landing time histories.

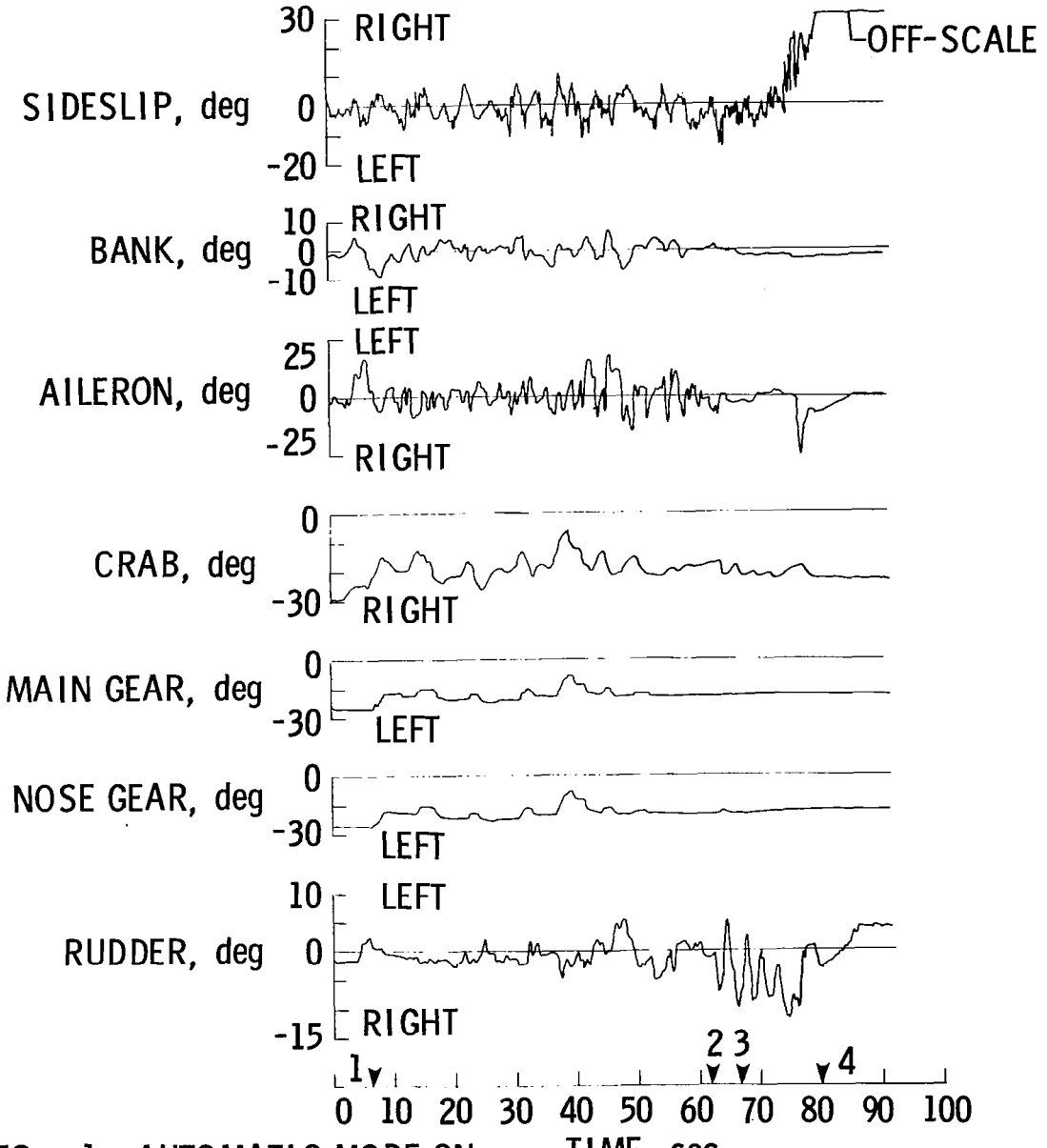

NOTES: 1 - AUTOMATIC MODE ON
2 - TOUCHDOWN
3 - BEGIN RUDDER PEDAL STEER
4 - END RUDDER PEDAL STEER

(b) Automatic mode landing.

Figure 16.- Continued.

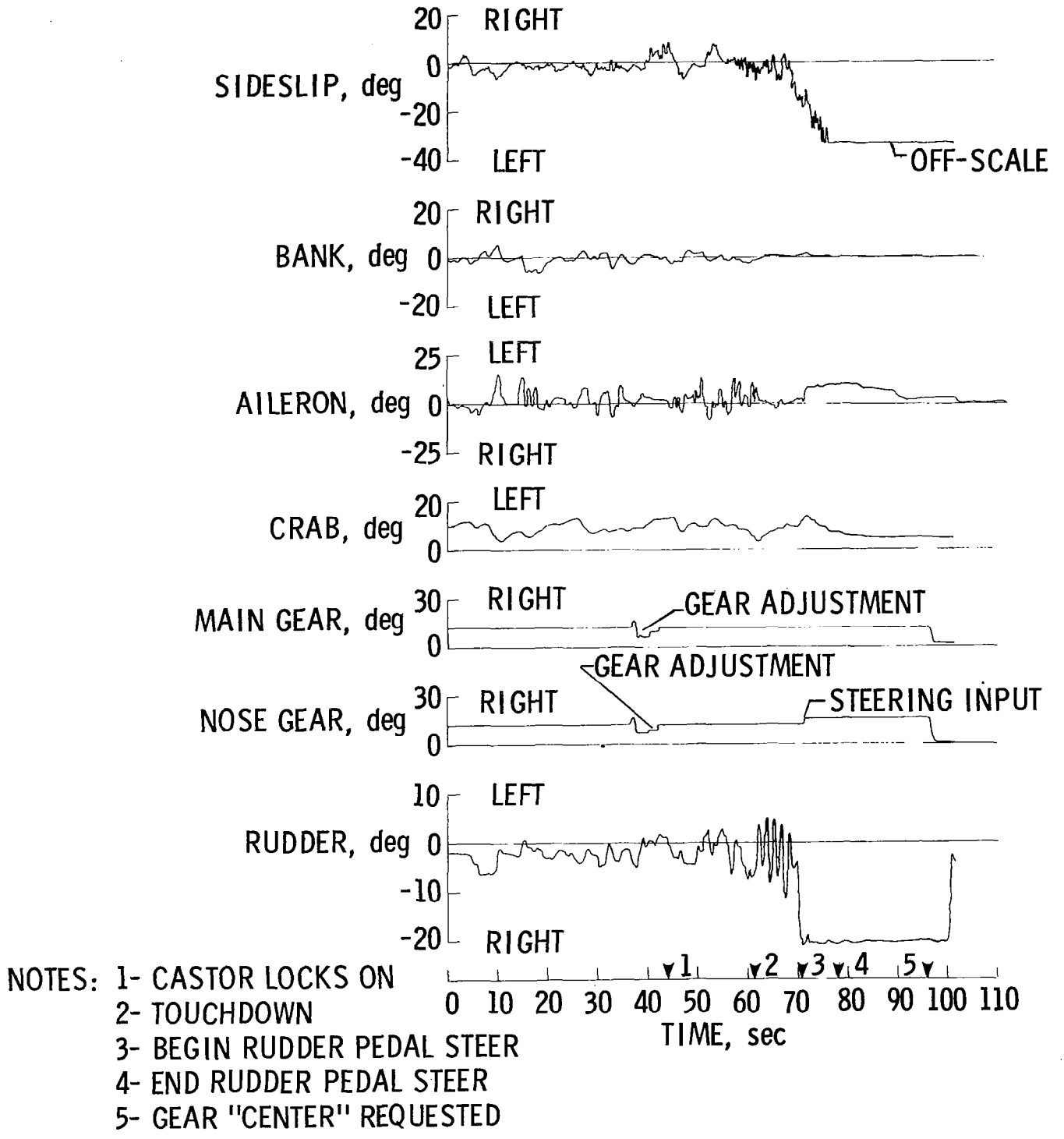

NOTES: 1- CASTOR LOCKS ON
2- TOUCHDOWN
3- BEGIN RUDDER PEDAL STEER
4- END RUDDER PEDAL STEER
5- GEAR "CENTER" REQUESTED

(c) Preset mode landing.

Figure 16.- Concluded.

NOISE PREDICTION TECHNOLOGY FOR CTOL AIRCRAFT

John P. Raney
NASA Langley Research Center

SUMMARY

The application of a new aircraft noise prediction program (ANOPP) to CTOL noise prediction is outlined. Noise prediction is based on semi-empirical methods for each of the propulsive system noise sources, such as the fan, the combustor, the turbine, and jet mixing, with noise-critical parameter values derived from the thermodynamic cycle of the engine. Comparisons of measured and predicted noise levels for existing CTOL aircraft indicate an acceptable level of accuracy.

INTRODUCTION

The noise produced by jet-powered aircraft has become an increasingly important consideration since their introduction to the commercial fleet in the late 1950's. The noise of aircraft operating near airports seriously affects over six million people in the United States alone. Aircraft noise has, therefore, become, as indicated in figure 1, an important consideration in the design of CTOL aircraft. Consequently, methods for calculating, with known accuracy, the environmental noise that a proposed new aircraft will produce are being developed. Although not indicated in figure 1, noise minimization is at odds with other design considerations such as weight minimization, propulsion plant efficiency, and direct operating cost minimization and thus increases the number of interactions to be juggled by the preliminary design team for a new aircraft.

In order to predict the noise that an aircraft will produce, the specifics of its aerodynamic and propulsion cycle characteristics must be known and values of the noise-critical parameters supplied as input data to the noise prediction algorithms. Furthermore, the computer implementation of the noise prediction algorithms must be compatible with the requirements mandated by the preliminary design activity; namely, it must be complete, responsive, and accurate.

The purpose of this paper is to describe a state-of-the-art aircraft noise prediction program (ANOPP) recently developed by NASA. This program is presently being used by NASA's supersonic cruise aircraft research (SCAR) project and by NASA in an international study to determine expected noise levels of future supersonic cruise aircraft.

SYMBOLS AND ABBREVIATIONS

A	atmospheric absorption factor
c_a	ambient speed of sound
D	drag
$D(\theta)$	directivity factor
f	frequency
G	ground effects factor
g	gravitational acceleration
h	altitude (see fig. 2)
I	source noise intensity
L	lift
M	aircraft Mach number
$\dot{m}$	mass flow rate
$m(\theta)$	forward speed exponent
$\overline{p_o^2}$	mean-squared pressure at observer
R	gas constant
$R(t)$	aircraft position vector
$r(t)$	observer position vector relative to aircraft
r_o	reference distance
S	entropy
$S(f)$	frequency factor
T	temperature
T_a	ambient temperature
$T(h,V,\Omega_c)$	engine thrust
t	time

U	universal power function for jet noise
V	aircraft velocity
$\dot{V}$	aircraft acceleration
W	aircraft weight
x,y	reference coordinates (see fig. 2)
α	coefficient of absorption
Γ	reflected wave factor
γ	thrust angle
θ,ϕ	aircraft orientation angles
Π	acoustic power
ρ	density
ρ_a	ambient air density
Ω_c	corrected engine rotor speed
ω	density exponent
EPNL	effective perceived noise level
PNL	perceived noise level
PNLT	tone-corrected perceived noise level
OASPL	overall sound pressure level
SPL	sound pressure level

NOISE PREDICTION METHODOLOGY: ANOPP

The essential ingredients to aircraft noise prediction (see fig. 2) are (1) the source intensity I, (2) the aircraft position given by the vector R(t), (3) the aircraft orientation given by θ and ϕ, and (4) the location of the observer given by the vector r(t). In addition, the atmospheric and ground-impedance characteristics indicated by A and G must be specified. The source intensity I is the sum of the individual

noise sources and their associated directivity $D_i(\theta,\phi)$ and spectral $S_i(f)$ factors:

$$I = \sum_{i=1}^{\text{All Sources}} \frac{\Pi_i}{4\pi r_o^2} D_i(\theta,\phi)\, S_i(f) \tag{1}$$

The mean-squared pressure at the observer is given by

$$\overline{p_o^2} = \rho_a c_a A|G|^2 \frac{I}{(r/r_o)^2} \tag{2}$$

where A accounts for atmospheric absorption and G accounts for ground effects. When the source intensity is specified as the mean-squared pressure in, say, 1/3-octave frequency bands, the resulting mean-squared pressure at an observer in these same frequency bands can then be calculated and converted to sound pressure level (SPL) in decibels. Subsequent computation of perceived noise level (PNL), tone-corrected perceived noise level (PNLT), effective perceived noise level (EPNL), or some other logarithmic noise scale may then be accomplished (ref. 1).

Generation of Noise-Critical Parameters

Aircraft flyover noise depends on the aircraft flight trajectory and on the throttle setting (thermodynamic state of the engine) during flight. The noise prediction algorithms implemented in ANOPP require as input data, values of specific propulsion cycle parameters together with the resulting flight trajectory of the aircraft.

Propulsion cycle. - The noise generated by aircraft engines is related to the thermodynamic state of the engine during the flight. For example, the combustion noise depends on pressures and temperatures at the combustor inlet and exit stations, and the fan noise is correlated with the total temperature rise across the fan. These variables are obtained from a temperature-entropy diagram for the engine cycle, as shown in figure 3 (ref. 2). This diagram represents the thermodynamic state of the engine and contains the information which is necessary for the prediction of propulsion noise. Presently, ANOPP accepts data from an externally generated T-S diagram as input; however, since the aircraft trajectory also depends on these data, a capability is being added for computing the engine cycle within the ANOPP system.

Flight dynamics and aircraft trajectory. - Noise prediction requires a knowledge of the position of both the aircraft and the observer. Since ANOPP accounts for directivity effects, the aircraft orientation must also be known. For the purpose of this paper, a simple two-degree-of-freedom analysis of the trajectory is adequate. Figure 4 shows typical flight-path segments for a take-off and for a landing maneuver. The take-off has a ground roll, a lift-off, an acceleration, and a pull-up segment; the landing has approach, flare, and roll-out segments.

The basic equations controlling the trajectory are the conditions of dynamic equilibrium tangent to and normal to the flight path. The tangential equation is

$$\frac{W}{g}\dot{V} = -W \sin \gamma + T - D \tag{3}$$

where W is the aircraft weight; T, the thrust, which is a function of altitude, aircraft velocity, and corrected rotor speed; D, the aerodynamic drag; V, the aircraft velocity; and γ, the thrust angle. The normal equation is

$$L = W \cos \gamma \tag{4}$$

where L is the aerodynamic lift. Combining these equations gives

$$\frac{\dot{V}}{g} = \frac{T}{W} - \frac{\cos \gamma}{(L/D)} - \sin \gamma \tag{5}$$

Note that different aircraft may have the same trajectories if the similarity parameters T/W and L/D in equation (5) are equal and if the aircraft are operated in the same fashion.

Component Noise Sources: Jet Noise

Typical noise-generating components of a fan jet engine are indicated in figure 5. The ANOPP library of prediction modules contains methods for computing the acoustic power Π for most of the significant component noise sources on modern jet-powered CTOL aircraft, including jet noise (refs. 3 and 4), fan and compressor noise (ref. 5), combustion noise (ref. 6), turbine noise (ref. 7), and airframe noise (refs. 8 and 9). The procedure for predicting the acoustic power of a propulsion noise source using parameter values from the engine cycle is outlined below for jet noise. The procedures for other propulsion noise sources are similar and are described by Zorumski (ref. 10).

The noise from a single circular jet (see fig. 6) is predicted by using the semiempirical formulae proposed by the Society of Automotive Engineers aircraft noise standards committee (ref. 3). The SAE procedure gives the total acoustic power from the jet as

$$\Pi_{JET} = 6.67 \times 10^{-5} \dot{m} c_a^2 \left(\frac{\rho_{JET}}{\rho_a}\right)^{\omega - 1} U\left(\frac{V_{JET}}{c_a}\right) \tag{6}$$

where $U\left(\frac{V_{JET}}{c_a}\right)$ is the universal power curve for jet noise, which follows approximately a V_{JET}^7 law in the velocity range up to $\frac{V_{JET}}{c_a} = 2$ and a lower exponential value at higher velocities. The density exponent ω varies from -1 at low jet velocities to +2 at high jet velocities. The intensity of a static jet noise source is given by

$$I_{STATIC} = \frac{\Pi_{JET}}{4\pi r_o^2} D(\theta)\, S(f) \tag{7}$$

where $D(\theta)$ and $S(f)$ are directivity and frequency factors peculiar to jet noise, and directivity dependence on the angle ϕ has been dropped. The intensity of a moving jet noise source is given by

$$I_{FLIGHT} = (1 - M \cos\theta)^{-1} \left[(V_{JET} - V)/V_{JET}\right]^{m(\theta)} I_{STATIC} \tag{8}$$

where the additional terms account for observed effects for an aircraft in forward flight.

Finally, the mean-squared pressure at an observer location is calculated using

$$\overline{p_o^2} = \rho_a c_a A|G|^2 I_{FLIGHT} \tag{9}$$

The jet noise prediction procedure is summarized in figure 7.

CTOL NOISE PREDICTION

The ANOPP flow chart for a typical CTOL noise prediction is given in figure 8. The aircraft performance section of the program consists of

subprograms for the engine cycle analysis and for the aircraft trajectory analysis. The engine cycle analysis is used to predict the thermodynamic state of the engine, that is, pressures, temperatures, and flows at points within the engine, from engine component data. These data are necessary inputs to the noise source prediction modules of ANOPP. The aircraft trajectory subprogram predicts the distance, altitude, and pitch of the aircraft as functions of time from an input of the thrust setting and angle-of-attack scheduling, the aerodynamic data, and the weight of the aircraft. Alternately, the cycle and trajectory data may be input as time-dependent tables. Once the cycle and trajectory computations are complete, the source noise power Π, directivity D, and spectrum S are evaluated for each noise source. Shielding effects may then be introduced by modifying the directivity. The noise from different sources is then added and the effects of spherical spreading and atmospheric attenuation are introduced to obtain the time history of the acoustic spectrum at a selected observer position. With this spectrum history, the subjective effects of the noise, such as perceived noise level (PNL) and effective perceived noise level (EPNL), may be computed.

ANOPP ARCHITECTURE

ANOPP architecture provides for the efficient generation, handling, and storage of the large quantities of data required by the aircraft noise prediction process through an extremely flexible data base management scheme. Noise prediction methodologies are implemented in independent functional modules that are scheduled by the executive system at execution time in accordance with simple control instructions provided by the user. Job progress may be inspected or protected from computer failure by a checkpoint-restart provision. A typical CTOL noise prediction including trajectory analysis, atmospheric modeling, propagation and ground effects, and calculation of component and total noise levels at selected observer positions can all be accomplished in one computer run with turnaround time on the order of an hour or two.

ANOPP VALIDATION STATUS

Validation of ANOPP commences at the module level. The circular jet noise module, for example, implements the equations of reference 2, which are the result of correlation with a data base of approximately 30 000 measurements. The inverted flow (coannular) jet noise equations implemented in a separate module have been correlated against nearly 200 000 measurements on subscale model jets. Prediction methodologies for other component noise sources are to a lesser degree also validated at the module level but far less high-quality data are available. In particular, much more data are required for turbomachinery noise sources, which can dominate or contribute significantly

to aircraft noise levels for certain operating conditions. Although ANOPP incorporates the best available prediction technology, much work is required in order to achieve the highest possible level of confidence in each component noise source prediction method.

Measured aircraft flyover data together with the required values of engine cycle parameters have recently become available which permit comparison with predicted noise levels. In figure 9 measured data for a Learjet airplane in level flight at an altitude of 122 m (400 ft) are compared with ANOPP predicted levels. The ANOPP computations were made using only jet, shock cell, and combustion noise, since contributions from other sources were judged to be negligible (see fig. 8). The predicted perceived noise level as a function of angle to engine inlet averaged about 3 dB low. The spectrum at $\theta = 120°$ was, however, well predicted.

In figure 10 measured data for a Concorde aircraft in level flight at an altitude of 300 m (1000 ft) are compared with ANOPP predicted levels, again using only the jet, shock cell, and combustion noise modules. The predicted perceived noise level agreement with data is good as is the spectrum agreement at $\theta = 130°$. The difference between measured and predicted levels for the spectrum at frequencies above 2000 Hz may be due to contributions of turbomachinery noise sources, which were not included in the ANOPP prediction. For both these examples the measured and predicted effective perceived noise levels (EPNL) were in excellent agreement.

In a recent informal study which involved measured data for several aircraft with each operating at power settings corresponding to both take-off and landing, the ANOPP results, which included predictions for turbomachinery and airframe noise, averaged 2 to 3 dB below the measured perceived noise levels. The accuracy of ANOPP predictions was generally good and indicated that ANOPP is a viable system and acceptable for use in the preliminary design process.

Present validation plans call for detailed comparison of measured and predicted noise levels for high-bypass-ratio, wide-body aircraft. Every attempt will be made to identify component noise sources through spectral analysis and other techniques. Data for low power settings for which jet noise is not the dominant source will be included in order to validate turbomachinery, combustion, and airframe noise prediction methods.

CONCLUDING REMARKS

A comprehensive, efficient, user-oriented aircraft noise prediction program (ANOPP) developed by NASA has been described. The program implements semiempirical methods for predicting aircraft noise from a knowledge of the

trajectory and the thermodynamic cycle of an existing or proposed aircraft. Comparisons of measured and predicted noise levels for existing CTOL aircraft indicate an acceptable level of accuracy. Other comparisons, not presented in this paper, also corroborate this conclusion. Further validation studies involving high-bypass-ratio propulsion systems together with continued improvements and application of the ANOPP system to NASA projects are anticipated.

REFERENCES

1. Noise Standards: Aircraft Type Certification. Federal Aviation Regulations, vol. III, pt. 36, FAA, Dec. 1969, as amended.

2. Cohen H.; Rogers, G. F. C.; and Saravanamutto, H. I. H.: Gas Turbine Theory, Second ed. Halsted Press, 1975.

3. Gas Turbine Jet Exhaust Noise Prediction. ARP 876, Soc. Automot. Eng., Inc., Mar. 1978.

4. Kozlowski, Hilary; and Packman, Allan B.: Aerodynamic and Acoustic Tests of Duct-Burning Turbofan Exhaust Nozzles. NASA CR-2628, 1976.

5. Heidman, M. F.: Interim Prediction Method for Fan and Compressor Source Noise. NASA TM X-71763, 1975.

6. Huff, Ronald G.; Clark, Bruce; and Dorsch, Robert G.: Interim Prediction Method for Low Frequency Core Engine Noise. NASA TM X-71627, 1974.

7. Krejsa, Eugene A.; and Valerino, Michael F.: Interim Prediction Method for Turbine Noise. NASA TM X-73566, 1976.

8. Fink, Martin R.: Airframe Noise Prediction Method. FAA-RD-77-29, Mar. 1977. (Available from DDC as AD A039 664.)

9. Heller, Hanno H.; and Dobrzynski, Werner M.: Sound Radiation From Aircraft Wheel-Well/Landing Gear Configurations. AIAA Paper No. 76-552, July 1976.

10. Zorumski, William E.: Aircraft Flyover Noise Prediction. NOISE-CON 77 Proceedings, George C. Maling, Jr., ed., Noise Control Found., c. 1977, pp. 205-222.

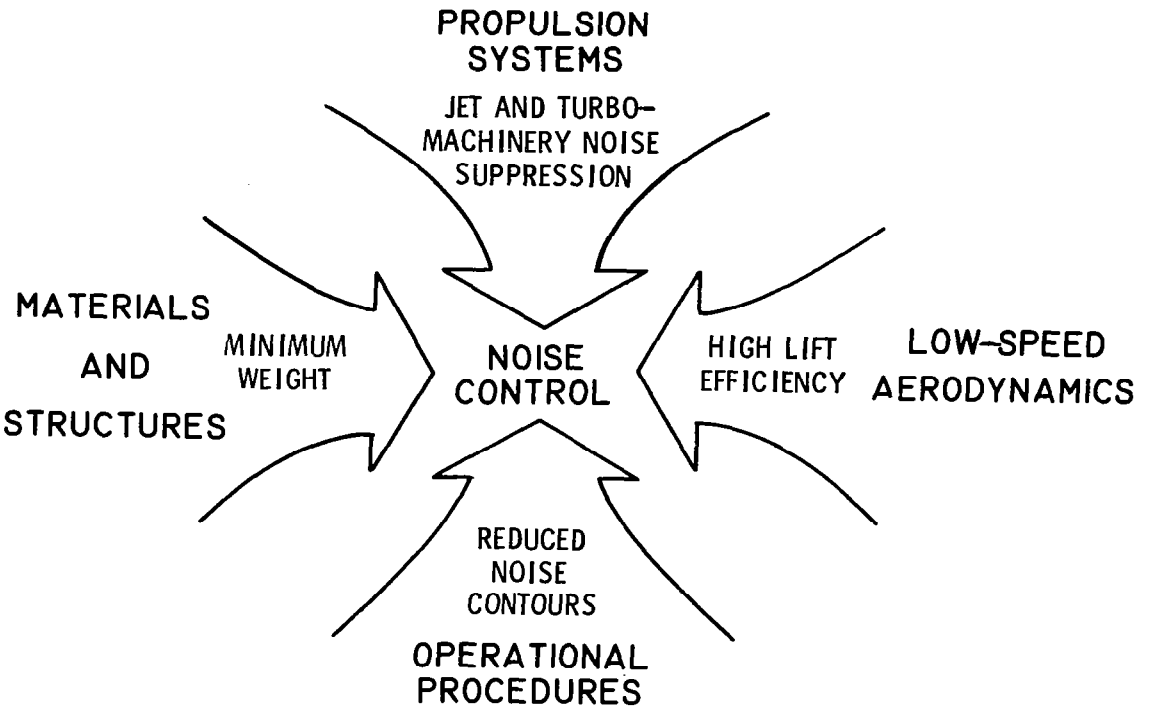

Figure 1.- Noise is an aircraft design constraint.

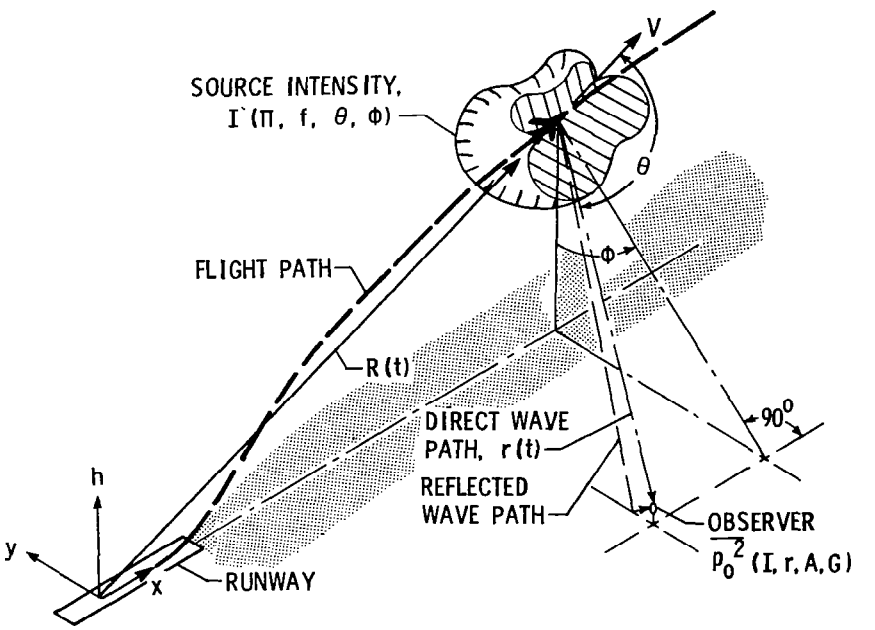

Figure 2.- Required ingredients for aircraft noise prediction.

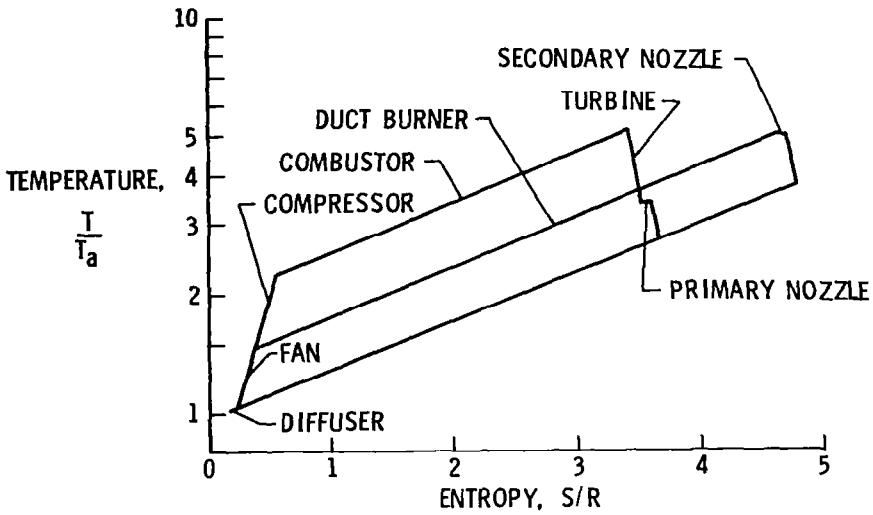

Figure 3.- Representative propulsion cycle.

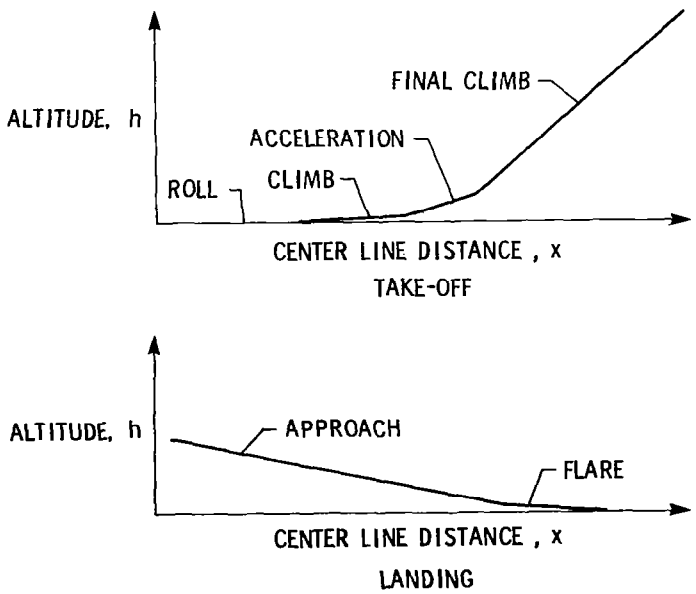

Figure 4.- Flight trajectories.

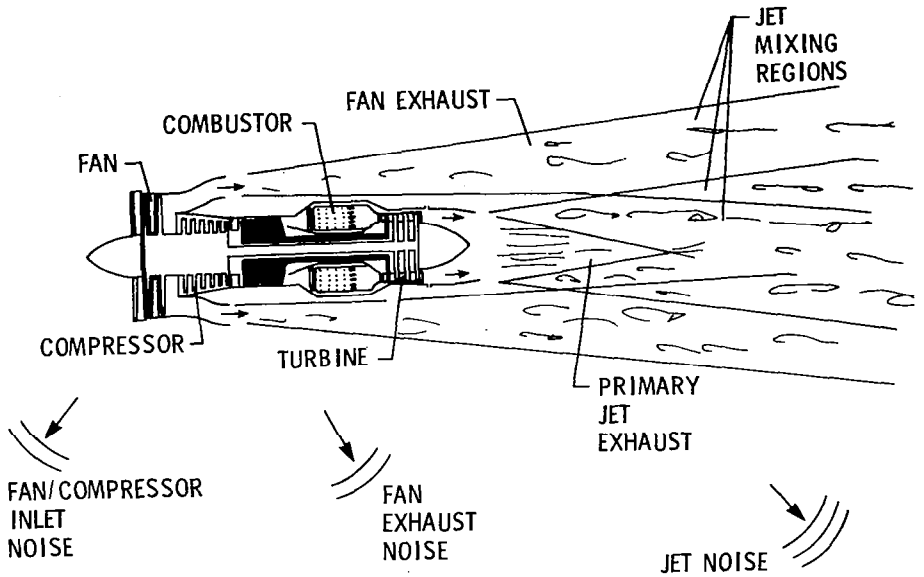

Figure 5.- Propulsion noise sources.

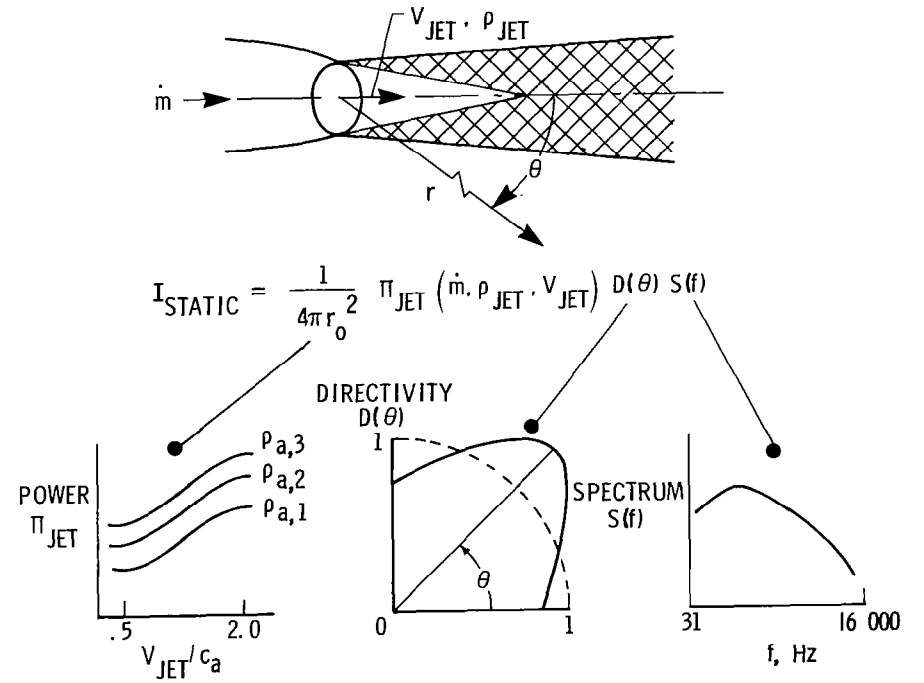

Figure 6.- Jet noise.

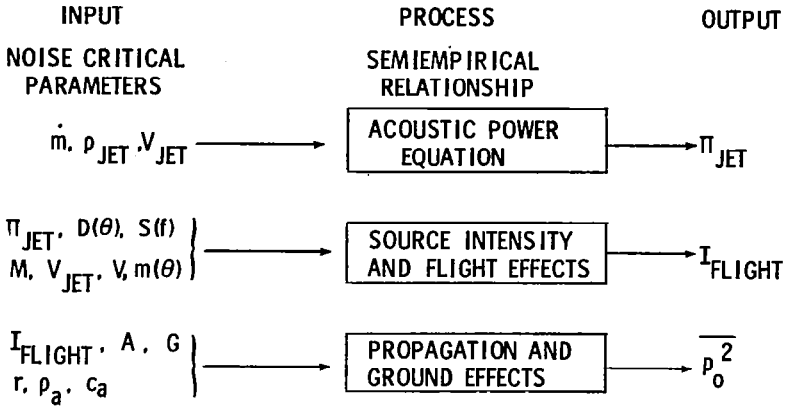

Figure 7.- Jet noise prediction procedure.

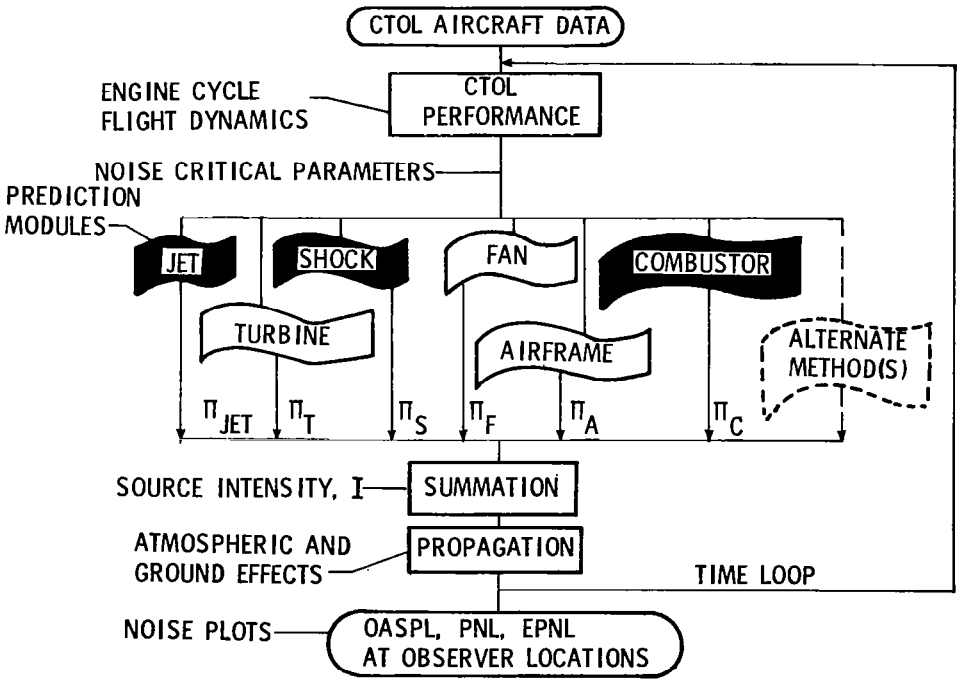

Figure 8.- CTOL noise prediction. (Highlighted prediction modules were used for calculations shown in figs. 9 and 10.)

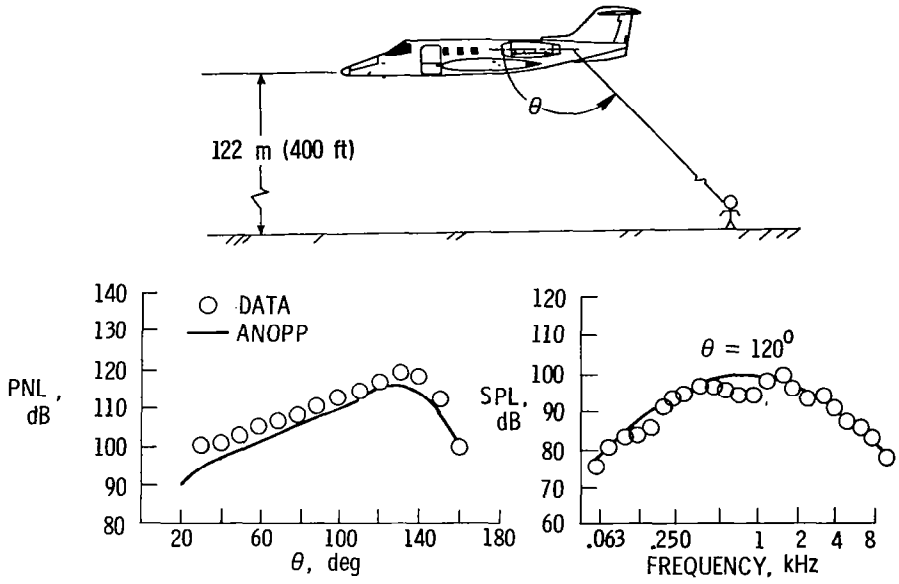

Figure 9.- ANOPP flyover noise validation — Learjet.

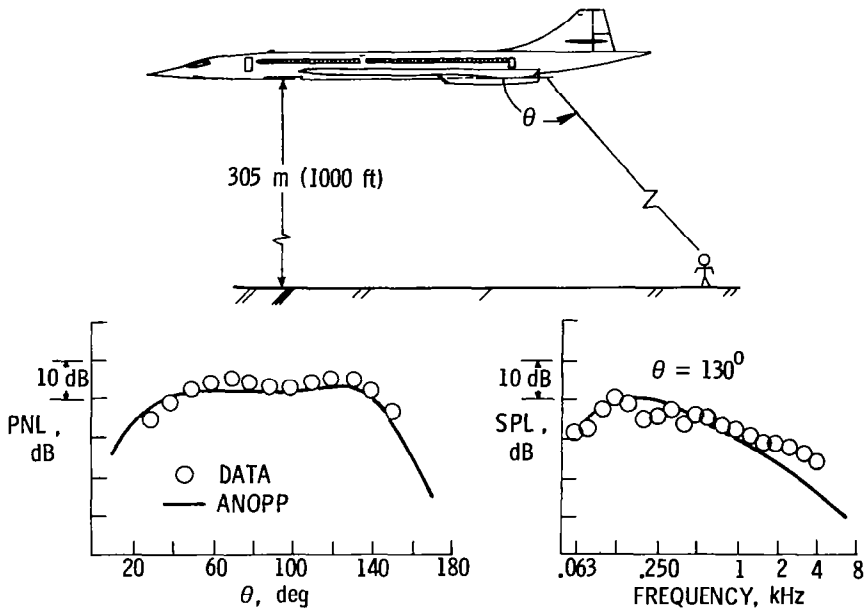

Figure 10.- ANOPP flyover noise validation — Concorde.

FLIGHT EXPERIMENTS TO IMPROVE TERMINAL AREA OPERATIONS

Seymour Salmirs and Samuel A. Morello
NASA Langley Research Center

SUMMARY

A brief description is given of the objectives and activities of the terminal configured vehicle (TCV) program and of some of the airborne facilities. A short analysis of some particular problems in CTOL operations in the terminal area is also presented to show how the program's technical objectives are related to the defined problems. The test aircraft was flown both manually and automatically with manual monitoring over paths including 130° intercepts and 2.0-km (1.1 n. mi.) and 0.8-km (0.44 n. mi.) finals. Some statistical data are presented from these and other flight profiles designed to address specific terminal area problems. An overview is presented of research studies receiving emphasis in the next biennium and their application to the terminal area. A description of work being undertaken to study the addition of adjacent traffic information to present map displays is also given.

INTRODUCTION

The terminal configured vehicle (TCV) program was conceived to address the problems of operation in the crowded terminal area airspace and the integration of the airborne avionics systems necessary to improve the efficiency of those operations. The airborne experimental systems necessary to do the research were first described in reference 1 and are illustrated in figures 1, the TCV B-737 airplane; 2, the interior of the airplane showing the locations of the computer systems and the all-electronic aft flight deck; and 3, a block diagram of the entire experimental system interconnections. The aircraft automatic controls, manual controls, and displays have been modified to incorporate advances which will be discussed in this paper. The changes needed for operations in the Microwave Landing System environment are illustrated in figure 4.

The program objectives were first presented in reference 2. These objectives have been reviewed by many in the aviation community who have a stake in the terminal area operation. The refined and restated objectives are shown in table I. The problems of the terminal area are complex and interrelated. The classification of table I serves to simplify discussion and does not imply the isolation of issues.

The attempts to solve these interrelated problems lead to the recognition of identifiable and desirable capabilities which contribute to the capacity

and efficiency of the airspace system. Some of the system requirements and specifications are illustrated in figure 5. The curved approach capability serves many of the problems stated in table I, as does the freedom to operate in lower minimums with greater regularity. Reduced interaircraft spacing, closer runway spacing, precise navigation in time as well as distance, and rapid runway clearance are also desirable factors which can be quantified.

The terminal configured vehicle program has been working on many aspects of the problems related to the curved descending flight profile. Both automatic and manually augmented modes have been flown using the electronic displays with the Time Referenced Scanning Beam (TRSB) Microwave Landing System (MLS) as the principal navigation aid. The achievements of these flight tests will be discussed.

Many research issues must still be resolved before improvements are realized in the capability of the commercial long-haul air transport system. Those related specifically to the aircrew tasks are shown in figure 6 which presents a breakdown of the approach path into its phases.

Generally, the program is pursuing its goals at a moderate pace by utilizing the research results obtained at the NASA Langley Research Center and at other centers of research. Cooperative research programs are being pursued with the NASA Ames Research Center and with the FAA. The most notable of the FAA cooperative programs which have already received extensive attention are the basic display system evaluation and, more recently, operations with the MLS. The latest advanced research program being considered in cooperation with the FAA and the NASA Ames Research Center will deal with the cockpit display of traffic information (CDTI).

ABBREVIATIONS

A/C	aircraft
AFD	aft flight deck
AGARD	Advisory Group for Aerospace Research and Development
AGCS	automatic guidance and control system
ARTS	automatic radar terminal system
ATC	air traffic control
Az	azimuth
BCAS	beacon collision avoidance system
CAB	Civil Aeronautics Board

CAT II	Category II; decision height less than 61.0 m (200 ft) but over 30.5 m (100 ft), runway visual range less than 610 m (2000 ft) but over 366 m (1200 ft)
CAT III	Category III; decision height less than 30.5 m (100 ft), runway visual range less than 366 m (1200 ft)
CDTI	cockpit display of traffic information
CRT	cathode ray tube
CWS	control wheel steering system
DABS	discrete address beacon system
DME	distance measuring equipment
DOT	U.S. Department of Transportation
EADI	electronic attitude director indicator (vertical situation display)
EHSI	electronic horizontal situation indicator (map display)
El	elevation
FAA	Federal Aviation Administration
ICAO	International Civil Aviation Organization
IFR	instrument flight rules
ILS	instrument landing system
INS	inertial navigation system
IVSI	instantaneous vertical speed indicator
MAG	magnetic ground track
MLS	microwave landing system
NAFEC	National Aviation Facilities Experimental Center
NASA	National Aeronautics and Space Administration
NAVAIDS	electronic ground navigation aids
NCDU	navigation control and display unit
RNAV	area navigation

Runway 13L	left hand runway with landing heading of 130°
TCV	terminal configured vehicle
TRSB	time referenced scanning beam
VFR	visual flight rules
VOR	visual omni range station
3-D	area navigation with altitude information
4-D	time controlled four dimensional navigation
σ	standard deviation

OPERATIONAL PROBLEM AREAS AND POTENTIAL BENEFITS

A discussion of some of the current problems in normal long-haul air transport operation will serve to illustrate the need for the extensive and advanced programs being pursued. A recent projection of air traffic growth is shown in figure 7. The growth projections illustrated are conservative, as indicated by the actual data on fleet size in 1976. Projections have consistently tended to be conservative. The boundaries projected by the DOT Transportation System Center (ref. 3) are an attempt to account for the unforseen demands.

The impact of such growth is illustrated in figure 8. The figure shows the number of airports which are expected to reach IFR capacity (delays in excess of 15 minutes over normal peak hour delay) in the next twenty years. It is expected that by 1984 twenty-one major hub airports will have reached IFR capacity by current standards. That date, incidently, is near the time when our next generation of aircraft is expected to be in the fleet. The number of airports which become IFR limited is projected to increase at a slower rate thereafter simply because the number of major hubs (the places where people want to go) are limited.

How does growth in the present system affect air travel? Figure 9 is a composite of the time intervals combined to construct a city to city flight as presently scheduled. Emphasize the work "scheduled." The times shown here are those published in the schedule. They include (as indicated by the cross hatching) a number of categories of delay. The time alloted to each is an average of the times actually experienced in each category. If the airplane leaves and arrives at the scheduled times, the passenger is unaware of any of these delays. When a passenger arrives late, that event is not a part of these schedule components. Note that the time, and indirectly the fuel, required to fly from Newport News to Washington National Airport is now 42 percent greater flying a B-727 under instrument rules than it was in

1965 flying a Lockheed Electra under visual rules. These increases occurred in spite of the increase in normal cruise speed and largely as a result of increased traffic and congestion. The flight from Newport News to Atlanta is particularly interesting because it takes place on a B-727, the most common aircraft in the trunk system today, and over a route of 468 n. mi. The average stage length for the B-727 fleet is about 430 n. mi. The illustration, therefore, has the connotation of the most common flight of the most common aircraft and is indicative of the whole fleet's fuel and time usage. The schedule buildup may be described in the following terms:

Gate departure -	Close doors.
Taxi out -	Engine start, check list, taxi to runway over minimum distance.
Taxi-out delay -	Waiting for other traffic clearance, nondirect routes to the runway.
Area maneuvering -	Vectoring by the air traffic controllers to get the airplane into route system.
Stage length -	Minimum distance to destination at optimum cruise altitude. Includes climb and descent.
Airway route increment -	Additional distance required to be flown to stay within the jet airways system.
Terminal area delay -	Average delay experienced because of other traffic.
Weather delay -	Average delay experienced because of extra distance flown to avoid weather.
ATC maneuvering -	Vectoring from air route to approaches because of traffic, wind changes, etc.
Taxi-in delay -	Delays after departing runway prior to gate arrival for gate assignment, other traffic, etc.
Taxi in -	Time to reach gate over minimum ground route.
Gate arrival -	Open doors for passenger departure.

In discussing delays, it is important to realize the different interpretations of "delay." The CAB concern with schedule adherence sees no delay per se in these schedules. The ATC system is concerned with delays other than normal and above the daily average (different than peak hour delay).

The passenger, however, is vitally concerned with the time to destination (the basic impetus for air traffic growth) and the reliability of his schedules. It is worth noting that the percentage of time related to the normal delays built into the flights represents almost a quarter of the scheduled flight time. This extra flying time is directly related to fuel consumption as well as to other direct costs.

Another aspect of the terminal area problem is illustrated in figure 10. This illustrates the New York terminal area with its four major airports and the instrument approach paths crossing control areas. The controller's communication problem in dealing with traffic across these zones can only be imagined. Further, note the overflights of high density residential areas. Also indicated on the figure is the Canarsie (CRI) approach into John F. Kennedy International Airport (JFK) runway 13L. This approach is designed for the alleviation of noise in the community, but it is only flown under visual flight rules. It is one of the approaches that has been flown with the TCV B-737 using MLS without visual reference from the AFD. These problems in traffic flow are not unique to New York. The Norfolk terminal area, for example, includes twenty-three airports operating in a rapidly growing noise-sensitive residential community.

In order to solve these problems and increase the flow of traffic, additional capability must be incorporated into the airplane. The automatic systems must operate more precisely over a greater volume of airspace, and the aircrew must have more information in easily understood forms. In order to make use of the information and perform necessary extended mission requirements, the flight controls must be better related to the displays and the mission. The interaction of the displays, pilot controls, and automatic controls constitute an inseparable aircraft system. Indeed, the system requirements are a vital part of the traffic flow requirements in the terminal area.

Some potential benefits for today's ATC systems are discussed in reference 4. If the ground aids are available, if the manual and automatic systems are properly designed, if the displays present the proper information, and if the trailing vortex problem can be alleviated, closer aircraft spacing throughout the system can result in an increase in capacity of 85 percent. That amounts to a change in the current separation standard capacity limit from about 30 to 55 aircraft landings per hour per runway. (See fig. 11.) Other built-in delay elements of the individual aircraft, such as taxi delays and RNAV, can be better addressed by more accurate scheduling into the terminal area. The need for accurate time delivery will impose a requirement on the aircraft and on the ground systems. Accurate 4-D navigation can then be made available and can be effectively used to achieve major benefits in air traffic flow.

The planned ATC system components which contribute to these benefits are the MLS and the increased analysis capability in the Automatic Radar Terminal System (ARTS). The addition of automated metering and spacing (M & S) and a digital data link (exemplified by the Discrete Address Beacon System (DABS)) are also expected to provide unique additions. Air derived data links (i.e., Beacon Collision Avoidance System (BCAS)), having more precision and higher

data rates than the radar system, may at times have a significant effect. The Global Positioning Satellite (GPS) system is also expected to contribute in all areas of the ATC system.

FLIGHT TEST RESULTS

The TCV program has recently addressed the problem of curved descending decelerating flight onto a short final leg. This program, pursued in analysis and simulation, was flight tested in the spring and summer of 1976. The data have been analyzed and presented at the AGARD symposium on guidance and control design considerations in references 5 and 6. A graphical summary of all the close-in-final flight profiles that have been flown during the past two years is shown in figure 12. This summary figure includes flights during the summer of 1976 and the most recent flights in December of 1977 where the Canarsie approach in New York was flown.

The tests at the FAA National Aviation Facilities Experimental Center (NAFEC) were flown with the two profiles shown in figure 13. The flight was manually controlled from the aft flight deck of the airplane. After takeoff, the pilots engaged the automatic 3-D navigation system which derived position data from the inertial system updated by dual DME's. After entry into the MLS coverage, the navigation solution was switched from the inertial system to the MLS signals. The automatic landing system was automatically engaged as the airplane turned onto the final approach. The two outstanding features of these flights were the short final which was reduced to as low as 1.5 n. mi. and the preceding 130^{o} turn during the descent onto the final. Keep in mind that a typical ILS approach in today's standards starts with 30^{o} to 45^{o} intercept of the final at distances of 8 to 12 n. mi. (See fig. 12.) Figure 14 is a statistical summary of all the automatic 3-n. mi. approaches flown during the NAFEC MLS tests. These data comprise some 200 flights in a wind environment with strong gusts and shears. Data in table II allow comparison of the NAFEC MLS flights with previous flights on the CAT III ILS at NAFEC and with manual flight performance on the MLS.

The profile for the series of display information comparison tests is shown in figure 15. The flight path designed for these tests required the pilot to turn onto final with a 183-m (600 ft) lateral error. This offset was introduced to challenge the pilot with a sufficiently difficult task to tax him in his use of the displays and controls without visual cues on final.

Figure 16 is the graphic representation of performance on the 3-n. mi. final approach with the pilot using a velocity-vector control mode and an integrated situation-display format. It is important to note that the lateral overshoots to the final approach for this unusually difficult approach path are almost within the runway width. The significance of these data on the need for closely spaced runways cannot be understated. Of equal importance are the pilot's favorable comments on the acceptance of these profiles with the displays available to him.

Some results from these manually controlled approaches (ref. 5) are shown in figure 17. Data are shown for both the integrated display and one in which only standard horizontal guidance information was available in the vertical situation display. The data are for the nominal 30.5-m (100 ft) altitude and are shown with the FAA performance requirement boundary for Category II flight director performance. The Category II criteria for performance with a flight director are based on a long stabilized approach and enclose the data and statistics which were obtained from the close 130° approach with the TCV system using MLS guidance. Figure 18 is also of interest in that it shows similar results on approaches of only 1.5 n. mi. under manual control. Even here the overshoots are quite small in relation to proposed requirements for more closely spaced runways. The pilots expressed confidence in the displays and controls on these flights as well.

Quantitative statistical data are not yet available from all the MLS related flights in Argentina and New York, but successful automatic flight performance has been demonstrated. Controlled flights were conducted in Argentina under conditions of reduced angular MLS coverage (40° azimuth) and limited navigation aid availability for the RNAV portion of the flight. The airplane made successful automatic and manual landings with straight finals of 2.0 km. However, the approach intercept angle was designed to 60° in a noise abatement maneuver to avoid a local community. Additional successful automatic landings were made at JFK with finals of 0.44 n. mi. using the Carnarsie approach to runway 13L.

Flight tests (ref. 7) have also been conducted on the operation of the 4-D RNAV system in the airplane with the inertial system updated by dual DME's (DME stations are automatically selected for optimal positioning accuracy). The flights were of about an hour and a half duration and started and ended in a tracking radar environment. They included climbs, descents, turns, and speed changes. The results had 1.4 seconds mean error with a 0.7 second standard deviation. These data represent another basic ingredient of necessary avionics systems to operate with fuel efficiency in the terminal area.

ADVANCED DISPLAY AND CONTROL SYSTEMS PROGRAM

The TCV program has research effort scheduled to address the full range of interrelated issues in the terminal area. The scope of these research programs are illustrated in figure 6.

Profile Descent

The boundary of the terminal area flight profile is envisioned as beginning with descent from cruise altitude. Altitude and speed information displayed on the electronic horizontal situation indicator (EHSI) are being studied to permit precise descent from cruise to a terminal area metering point with minimum fuel requirements. The objective is not merely to invoke the idle power

descent but to do so in a precise manner so that the airplane can readily fit into the ATC requirements. With sufficient control capability and adequate display of information including wind data, the flight crew should be able to make good their descent and, at the same time, relieve the traffic controller's workload. Specifically, precise path following is expected to remove controller uncertainty about target progress and reduce the variables he must consider.

Curved Path Guidance

Significant problems still remain in developing the ability to predetermine the precisely follow curved paths. The previously cited automatic and manual flight results were dependent on having adequate navigation information and the accuracy with which the airplane is flown prior to acquisition of the curved flight path. As the low altitude portion of the curved flight was extended and the final approach shortened, the precision, the guidance accuracy, and the information available to the pilots on their display became more critical. The displays were adequate, and acceptable to the pilot, for following the curved flight to the short final as long as his performance kept him nearly on track. The presence of the lateral guidance information in the horizontal situation display was inadequate. As indicated in reference 5, the pilots could perform a much better approach with the lateral guidance information in the vertical situation display. The pilots simply did not like to (could not?) divide their attention between the two displays while maneuvering at low altitudes. They are not generally able to manually control the approaches when the runway is initially at extreme look angles relative to the flight path or when very little maneuvering time is available. The critical nature of the display becomes exaggerated on very short finals.

Two requirements can be defined from these considerations, and both are being studied. First, some clearly defined path to the runway must be identified in the vertical situation display when close tracking is necessary or desired. The two most actively pursued concepts that are under investigation are a "path-in-the-sky," which is described in reference 8 and illustrated in figure 19(a), and a second display being studied at the University of Illinois, which is shown in simplified form in figure 19(b). In the second display, the path is defined by a sequence of "poles" fixed at particular ground locations related to the final approach path. The pole tops are at the 3° glide slope. The lines connecting the poles predict the path of the airplane at those locations.

The second major requirement is the apparent usefulness of predictive information so that the pilot can quickly correlate his controlling actions with his future path tracking requirements. Reference 9 provides an excellent discussion of the state-of-the-art of predictive displays in general. The TCV B-737 displays already include predictive position and altitude information on the electronic horizontal situation indicator (EHSI), or map display. The flight path and track angle symbols on the electronic altitude director indicator (EADI) indicate the instantaneous ground referenced predicted intercept at the runway. Both the "path" and "poles" displays are

developing expanded predictive capability. A report on this activity is expected to become available during the summer of 1978.

The pathway displays and tighter path tracking can be expected to have additional advantages outside the scope of the pilots' approach requirements. That capability will contribute to improved traffic flow by permitting more closely spaced (more numerous) runways, more aircraft in trail and more paths in the terminal area. The more predictable and accurate the target airplane performance is the more effectively the controller can handle his sector traffic.

RNAV-MLS Transition

Automatically controlled curved approaches, while performed more accurately than the manual ones, are still very dependent on the delivery of the airplane to the boundaries of the precision navigation aid (MLS) and on the wind environment. The TCV program has planned for the analysis and design of algorithms and control laws for transition from the normal navaids position derivation, and consequent delivery errors, to the more precise data and paths of the microwave landing system. Further work is necessary to anticipate and assure the successful close-in final path achievement of runway alignment, with the associated increase in control gains under an expanded wind envelope.

The automatic control problems are being treated as a compatible whole, as are the display programs. The control laws are being designed using advanced parameter estimation techniques. The laws will then be implemented directly, based on digital computer architecture. They are designed to use a low data sampling rate to reduce computations and to incorporate the basic cross coupling in the aircraft dynamics to enhance system performance.

The advanced estimation algorithms will make use of the discrete data to be available from the MLS and will not require inertial platform quality signals to provide adequate filters for position, rates, and altitudes. The algorithms will also estimate the wind environment for use in the control laws.

Wind Shear

A preliminary set of simulation tests have been started which are aimed at understanding the benefits of presenting flight path angle, runway aim point, and thrust management information to the pilot on a final appraoch in various wind shear environments. Additional tests are planned and will be reported at a later date. These planned studies will cover a wide variety of shears including those the FAA has identified for study. Pilots (in simulator tests) have been able to recognize the effects of the shear on flight path and air speed and have successfully negotiated a variety of shears (but not those associated with thunderstorms as yet) with the displayed information (particularly thrust command). A second program is involved in the flight evaluation of a potential wind (total energy change) sensor. The displays are, of course, dependent upon the sensing of the wind parameters.

A parallel program to improve automatic aircraft control in severe wind shear is now in simulation. Some of the results of the analytical work have been reported in reference 10. The wind shear portion of this optimal control is implemented by estimating winds and using the estimate in the control law. The wind estimate is modified continually on the approach.

Landing and Turnoff

The progress of the airplane to touchdown upon and departure from the runway in reduced visibility has been a concern of the TCV program. High capacity operations cannot be achieved unless airplanes exit the runway quickly, allowing the following closely spaced airplane to land without potential interference. To accomplish this, the aircraft must land in a precise spot, slow, and turn off the runway on carefully designed runway exits. Such exits will, in reduced visibility, include some form of guidance sensor system.

The aircraft automatic landing system is being modified and will be flown in a mode where the distance dispersion resulting from wind variations can be reduced. Modifications to present control laws, including an automatic throttle response loop during flare, will be tested soon. The most promising concept that has evolved in simulation so far is to automatically initiate flare at a constant altitude and to modulate the descent in order to follow an exponential curve to achieve a nearly fixed touchdown distance. Simulation results show the difference in touchdown statistics between a 15-knot tail wind and a 15-knot head wind to be less than 1.5 meters (5 feet) with a maximum touchdown rate of descent of 0.9 meter per seconds (3 feet per second).

A design study has been conducted to incorporate a direct lift control function as a part of the TCV B-737 spoiler operation. The devices are being planned for flight tests in combination with appropriate control law design studies to evaluate precision tracking and touchdown criteria. Simultaneously, a series of display studies are being initiated to permit the pilot to use these powerful flight path control devices. Results from some tests of displays of flight path information have received initial in-flight evaluation in the piloted operations on short finals described earlier. They will be reported on this summer.

Low Visibility Landing Displays

Application of the cockpit CRT displays to the landing situation as both a monitor and as a control device is also being undertaken for low visibility operations. Studies have been inaugurated to see what texture patterns can be added to the outlined computer-drawn runway on the EADI to aid the pilot. It is desirable that the runway represent a surface which provides the pilot with enough information to enable him to make proper judgements on the initiation of flare and on his subsequent control of velocity and altitude. A related issue dealing with the magnification factor (the ratio of apparent displayed runway size to the actual observed runway size) is also being examined in relation to the TCV B-737 display size.

Cockpit Display of Traffic Information (CDTI)

Figure 11 and reference 4 indicate that significant potential benefit to an airplane in a high density traffic situation (routine for long-haul operations) could be realized from better control of spacing and timing in both enroute and terminal air traffic.

A concept for achieving this benefit by providing the aircrew with traffic information has been suggested and studied for a number of years by the Massachusetts Institute of Technology (ref. 11) and by the NASA Ames Research Center.

This concept purports to ease the controller problem by allowing the pilot to have local tactical control and by having him assume his traditional responsibility for continuous navigation. The controller would no longer be required to operate a very slow response control loop with poor data accuracy. He would, however, sequence traffic as always. In addition, two groups (the air and ground crews) can be monitoring the system for blunders. One aspect of a blunder is that it is a gross error that remains undetected by the person that acts. At present only one group (ground controllers) has the capability to detect such errors before they become hazardous. The pilots, of course, do not now have that ability. Further, CDTI might help to relieve the controllers of continuous monitoring functions because of an acceptable level of target behavior; that is, it is hoped that the aircrews would have sufficient information and control capability to achieve and maintain their own separation after being advised of the situation.

The basic TCV display and control work, when supplemented by surrounding traffic information, will be examined to determine whether there is a material improvement in flight performance and terminal area efficiency. When more rapid execution of desired maneuvers and closer spacing is attempted in order to provide increased runway handling and increased airspace occupancy, the issue of workload for all the personnel in the system will be a crucial one to be resolved. The ability to plan and cross check the traffic situation is expected to relieve concerns about safety.

The issues inherent in this concept relate to the means of providing sufficiently accurate and frequent data to the cockpit; the aircrew monitoring functions and the controllers' problems and functions; the potential for unwarranted action; the means for providing for controller awareness; and the determination of specific roles and responsibilities. Determination of additional ground information for controllers and development of methods for presenting this information are necessary to allow optimal use of CDTI in the ATC system. This type of study is a necessary part of the overall program.

NASA is developing a program in cooperation with the FAA to address these and other issues. Both the Langley Research Center and the Ames Research Center are participating in the definition of a plan to resolve these pertinent airborne system issues and to implement the necessary research programs over the next 2 to 5 years.

At Langley, the TCV program is conducting simulation and flight programs on the addition of traffic to the present map (EHSI) display. Experiments will be conducted considering the full range of display and control capability available in the airplane. Simulation and flight test systems are being implemented and some preliminary flight tests will be conducted this spring.

One possible application of traffic information to the present TCV map display is illustrated in figure 20. The basic map display includes our own aircraft and its predicted path; NAVAIDS; area boundaries; magnetic track; present ground speed, wind speed, and direction; identification of current navigation data sources being used; and map scale. It is planned to add ground tracks as shown for two other aircraft, their identification, altitude in hundreds of feet, ground speed in tens of knots, and their positions now, four and eight seconds ago. An alternative display will use a prediction of the future position of other traffic rather than the past position. That symbolism is expected to relieve the aircrew of the need to make that extrapolation.

CONCLUDING REMARKS

The TCV program is vitally concerned with the aircraft's operational capability in the air traffic system. This program involves the capability of the aircraft, its system, and flight crew to imprcve the efficiency and safety of the terminal area in a more demanding weather environment than present. It also includes the capability of the airborne system to work synergistically with the air traffic control system to improve the traffic flow with reduced problems for both the aircrew and ground controller.

So far, the simulation and flight test program has demonstrated that major elements can be responsibly addressed, and in some areas, with considerable success.

The studies conducted to date represent only a small but well defined portion of the system problems. The current programs described in this paper are planned steps in the overall solution of the problem.

REFERENCES

1. Salmirs, Seymour; and Tobie, Harold N.: Electronic Displays and Digital Automatic Control in Advanced Terminal Area Operations. AIAA Paper No. 74-27, Jan.-Feb. 1974.

2. Reeder, John P.; Taylor, Robert T.; and Walsh, Thomas M.: New Design and Operating Techniques and Requirements for Improved Aircraft Terminal Area Operations. NASA TM X-72006, 1974.

3. AATMS Programs Office: Advanced Air Traffic Management System Study - Technical Summary. DOT-TSC-OST-75-6, U.S. Dep. Transp., Mar. 1975.

4. Credeur, Leonard: Basic Analysis of Terminal Operation Benefits Resulting From Reduced Vortex Separation Minima. NASA TM-78624, 1977.

5. Morello, Samuel A.: Recent Flight Test Results Using an Electronic Display Format on the NASA B-737. NASA Paper presented at AGARD 25th GCP Symposium on Guidance and Control Design Considerations for Low Altitude and Terminal Area Flight (Dayton, Ohio), Oct. 1977.

6. Walsh, Thomas M.; and Weener, Earl F.: Automatic Flight Performance of a Transport Airplane on Complex Microwave Landing System Paths. NASA Paper presented at AGARD 25th GCP Symposium on Guidance and Control Design Considerations for Low Altitude and Terminal Area Flight (Dayton, Ohio), Oct. 1977.

7. Knox, Charles E.: Experimental Determination of the Navigation Error of the 4-D Navigation, Guidance, and Control Systems on the NASA B-737 Airplane. NASA Paper presented at AGARD 25th GCP Symposium on Guidance and Control Design Considerations for Low Altitude and Terminal Area Flight (Dayton, Ohio), Oct. 1977.

8. Knox, Charles E.; and Leavitt, John: Description of Path-in-the-Sky Contact Analog Piloting Display. NASA TM-74057, 1977.

9. Smith, R. L.; and Kennedy, R. S.: Predictor Displays: A Human Engineering Technology in Search of a Manual Control Problem. TP-76-05, U.S. Navy, June 30, 1976.

10. Halyo, Nesim: Development of a Digital Automatic Control Law for Steep Glideslope Capture and Flare. NASA CR-2834, 1977.

11. Connelly, Mark E.: Simulation Studies of Airborne Traffic Situation Display Applications - Final Report. Rep. ESL-R-751 (Contract FA71-WAI-242 (Task F)), Massachusetts Inst. Technol., May 1977.

Table I. - TCV GOAL: IDENTIFY AIRPLANE AND FLIGHT MANAGEMENT TECHNOLOGY THAT WILL BENEFIT CTOL TERMINAL AREA OPERATIONS

OBJECTIVES	ELEMENTS
1. IMPROVE TERMINAL AREA CAPACITY AND EFFICIENCY	a. SYSTEMS AND PROCEDURES FOR ATC EVOLUTION b. SYSTEMS AND PROCEDURES FOR RUNWAY CAPACITY c. PROFILES AND PROCEDURES FOR FUEL CONSERVATION
2. IMPROVE APPROACH AND LANDING CAPABILITY IN ADVERSE WEATHER	a. HUMAN FACTOR ELEMENTS FOR EFFECTIVE FLT MANAGEMENT b. SYSTEMS AND INFORMATION TO MINIMIZE WIND-SHEAR HAZARD c. AIRBORNE SENSORS FOR WEATHER-PENETRATION
3. REDUCE NOISE IMPACT	PROFILES AND CONFIGURATIONS FOR NOISE REDUCTION

Table II. - PERFORMANCE RESULTS FOR TCV B-737 WITH ILS AND MLS GUIDANCE

Approaches		Reference altitude, m (ft)	Vertical position		Lateral position	
Type	Number		Mean, m (ft)	1σ, m (ft)	Mean, m (ft)	1σ, m (ft)
CAT III ILS	45	61.0 (200)	58.8 (193)	± 0.6 (2.1)	0.6 (2)-R	± 2.4 (7.8)
(40°, 10 n. mi.)		30.5 (100)	28.3 (93)	± 1.1 (3.7)	0 (0)	± 2.3 (7.7)
MLS, automatic	56	61.0 (200)	58.8 (193)	±1.5 (5)	0.9 (3)-R	± 1.2 (4)
(130°, 3 n. mi.)		30.5 (100)	29.0 (95)	±1.5 (5)	0.9 (3)-L	± 1.2 (4)
		Overshoot on final	----------	----------	9.1 (30)-R	± 18.3 (60)
MLS, manual	27	61.0 (200)	59.4 (195)	± 3.0 (10)	1.5 (5)-R	± 7.9 (26)
(130°, 3 n. mi.)		30.5 (100)	29.6 (97)	± 1.2 (4)	0.3 (1)-R	± 4.6 (15)

Figure 1.- TCV B-737 airplane.

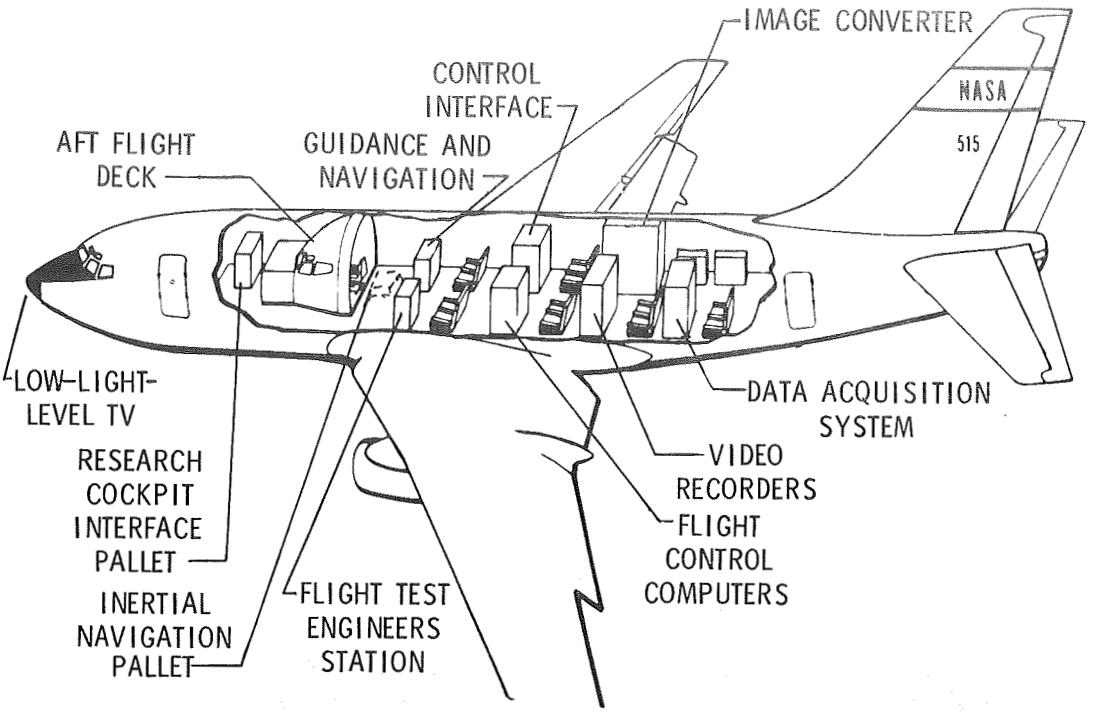

(a) Location of system components.

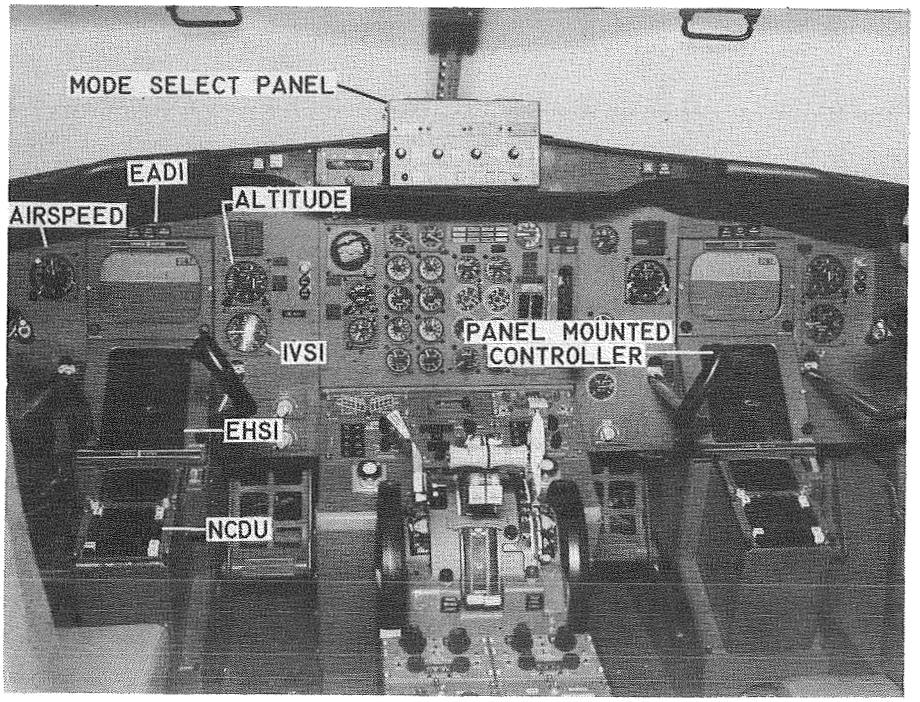

(b) Aft flight deck control and display layout.

Figure 2.- TCV B-737 interior arrangement.

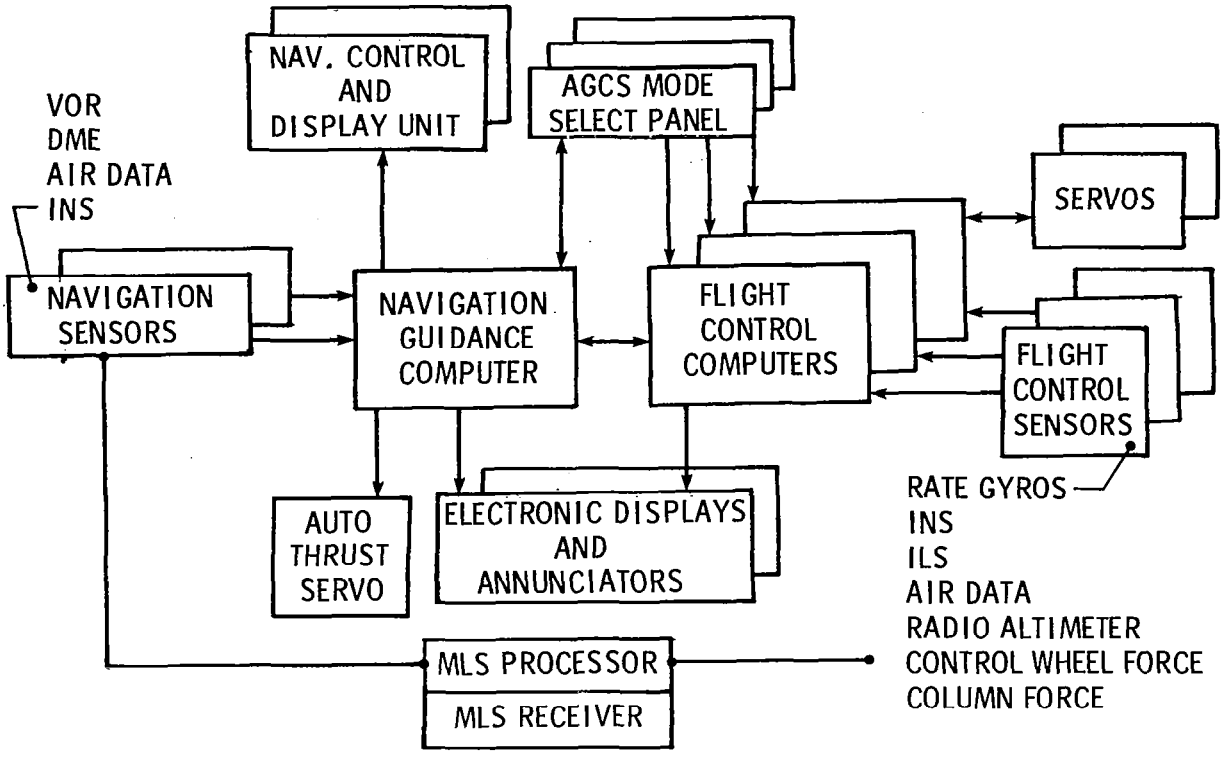

Figure 3.- TCV B-737 experimental system interconnections.

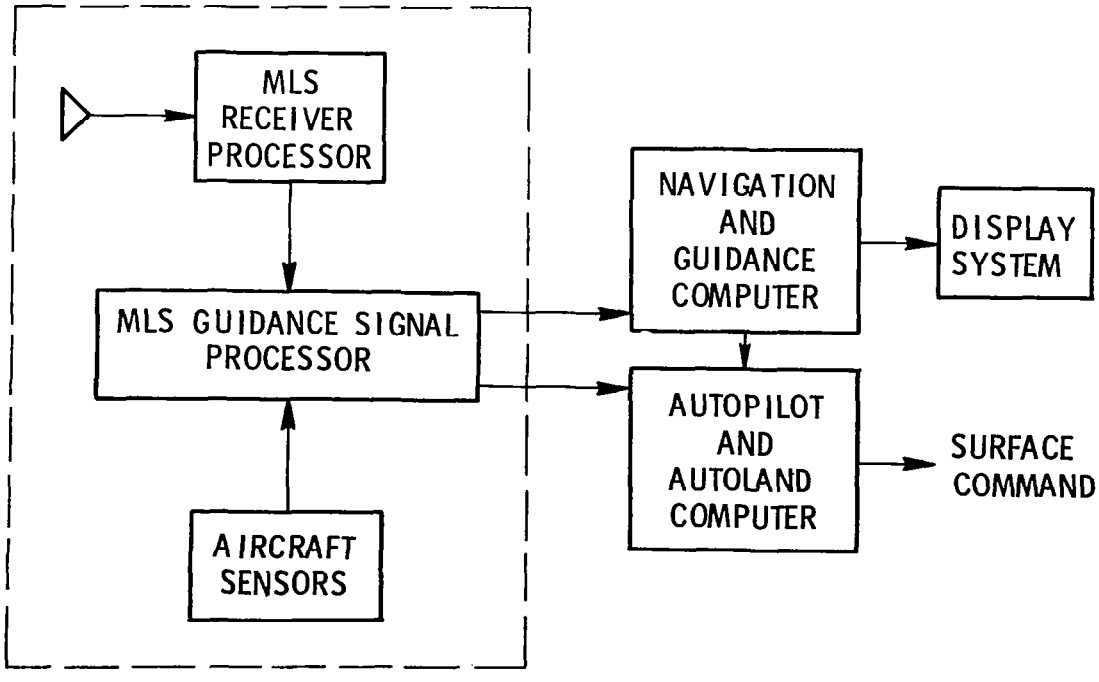

Figure 4.- MLS integration with TCV aircraft.

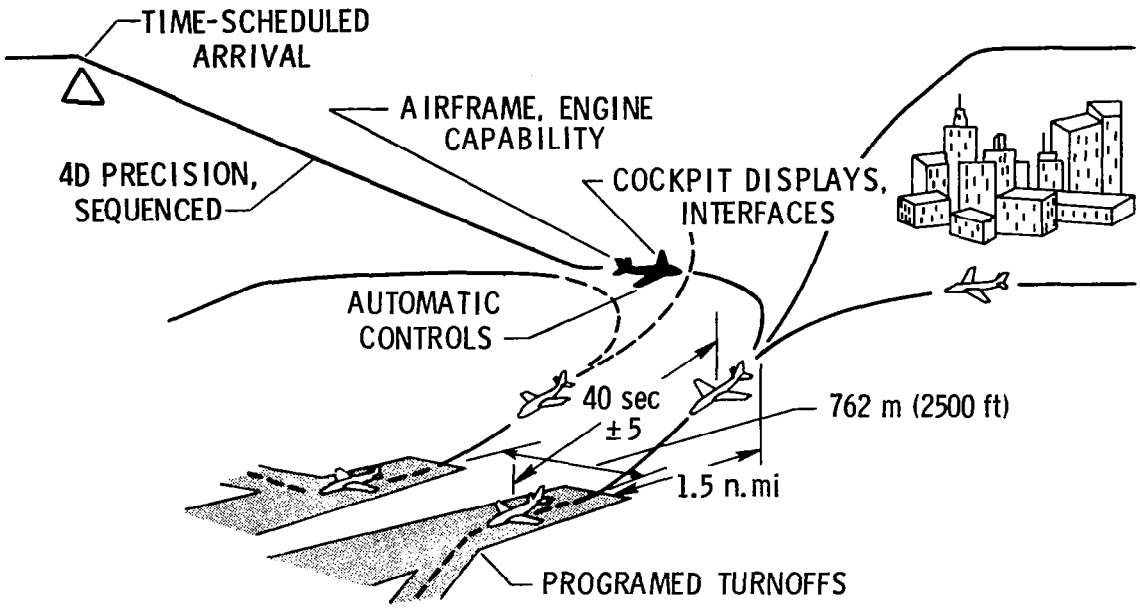

Figure 5.- High capacity terminal area operations in low visibility.

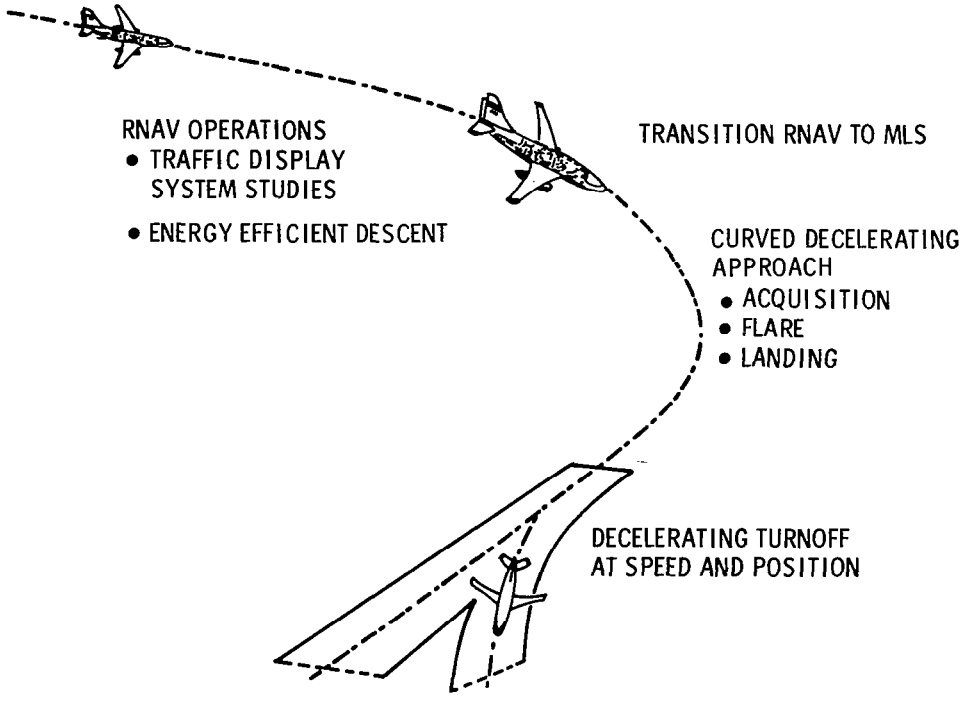

Figure 6.- TCV terminal area efforts.

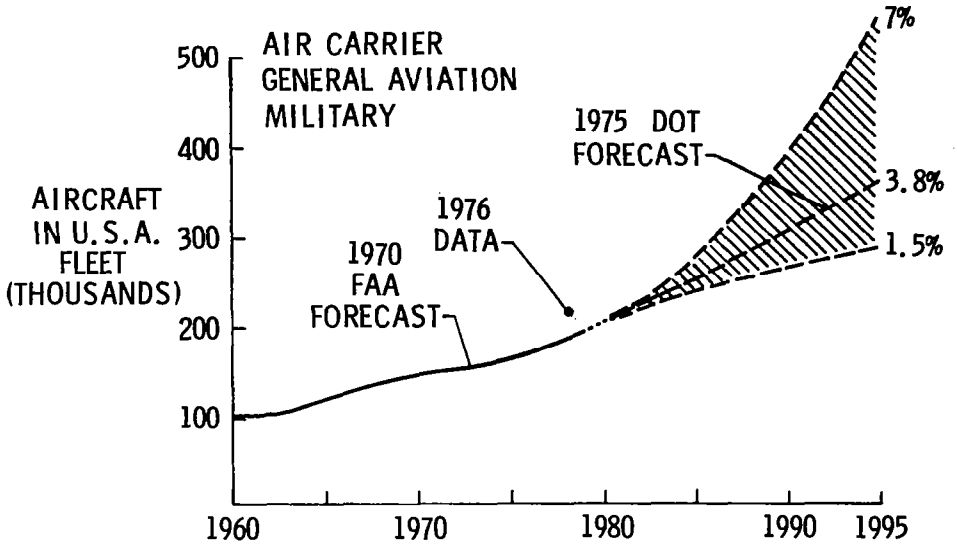

Figure 7.- Airfleet growth projections.

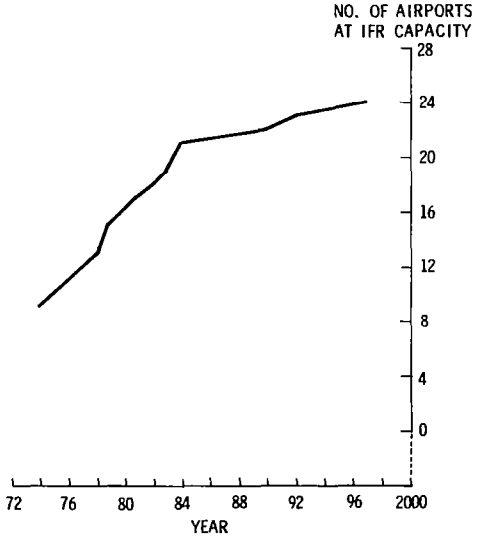

Figure 8.- Number of airports having reached IFR capacity with present ATC.

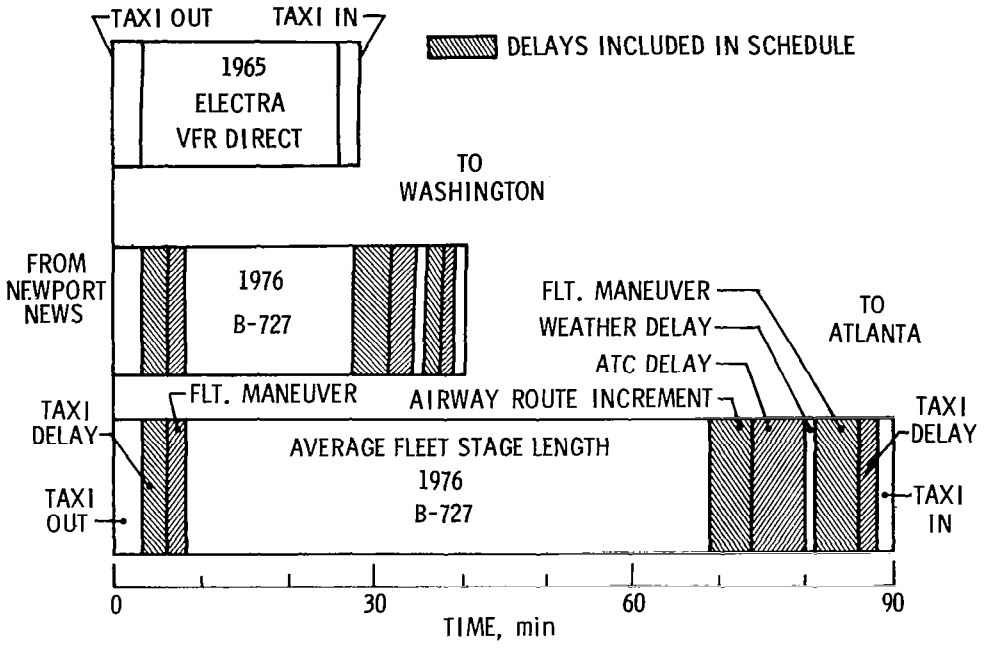

Figure 9.- Airline schedule components (nonstop).

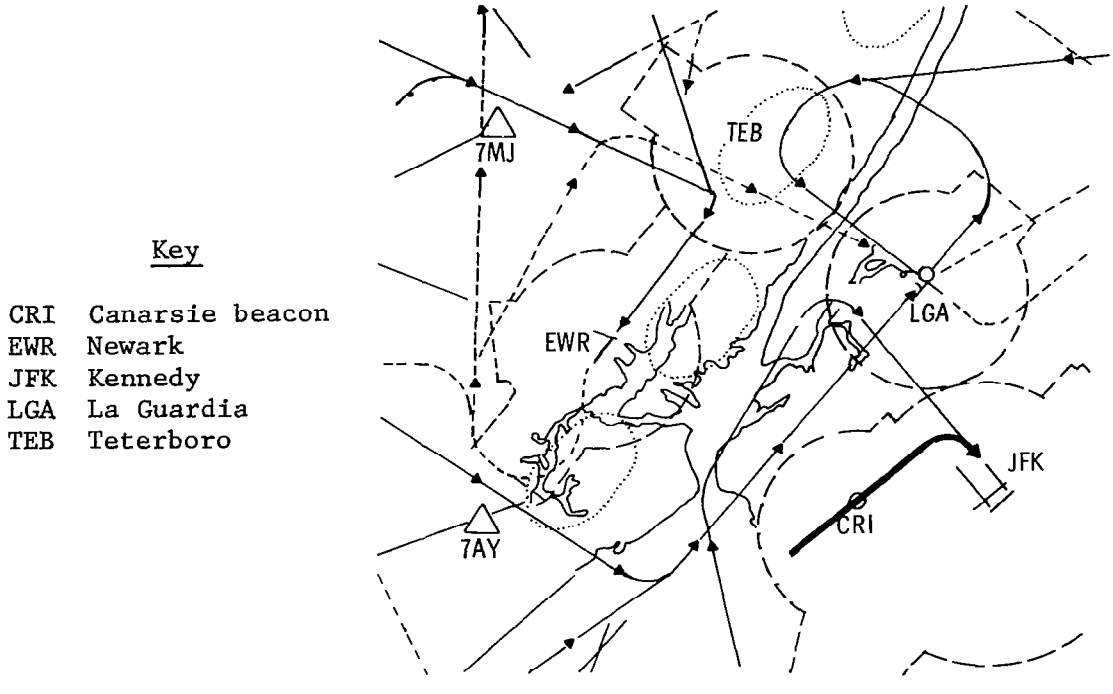

Figure 10.- New York terminal area.

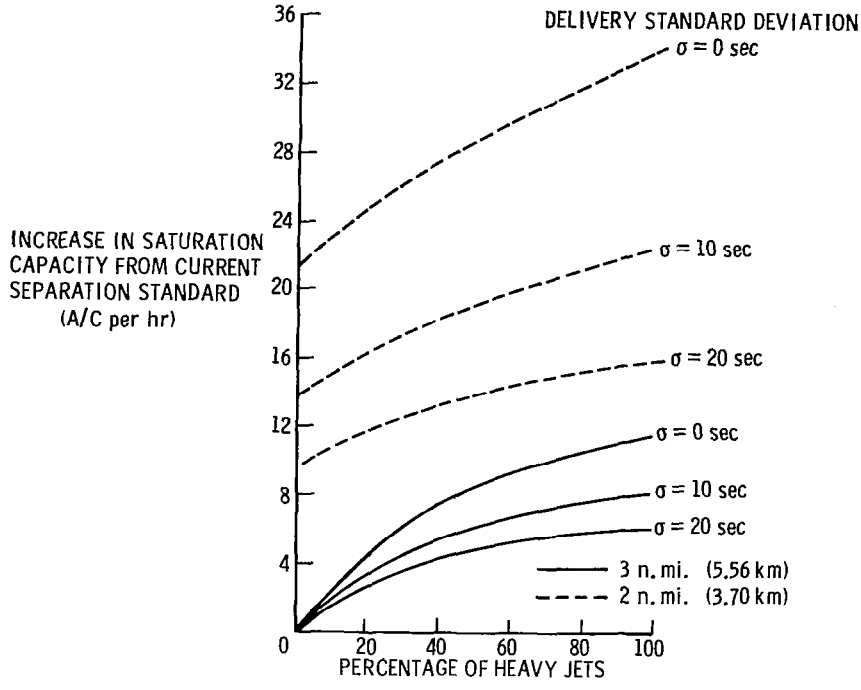

Figure 11.- Effect of delivery accuracy and spacing on capacity.

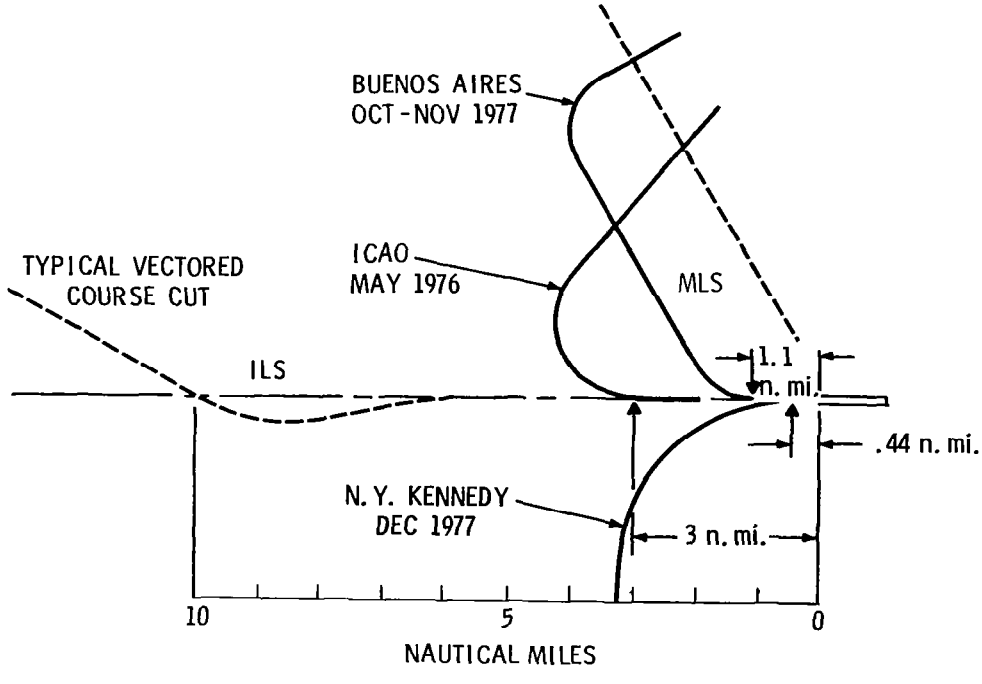

Figure 12.- Landings from close-in finals.

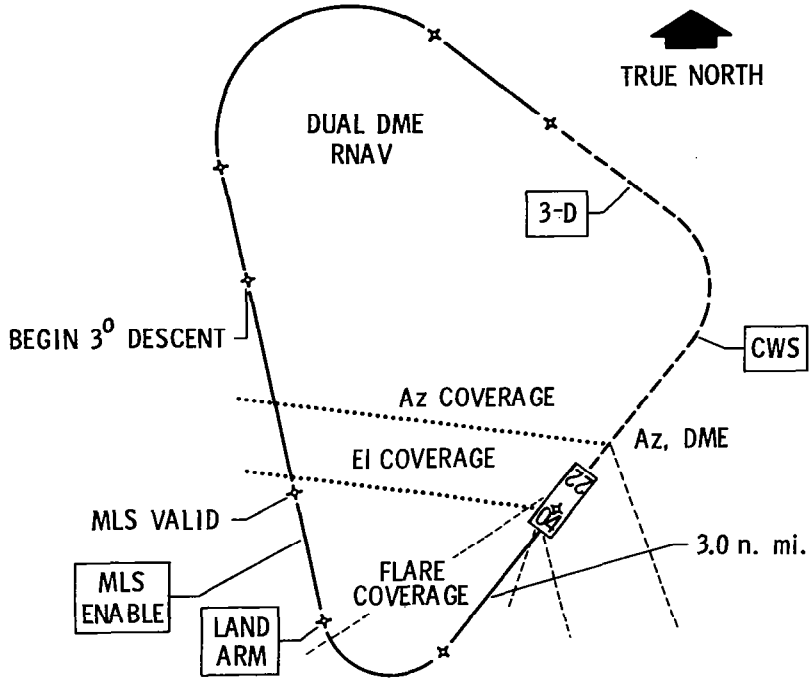

(a) Capture from 130° azimuth.

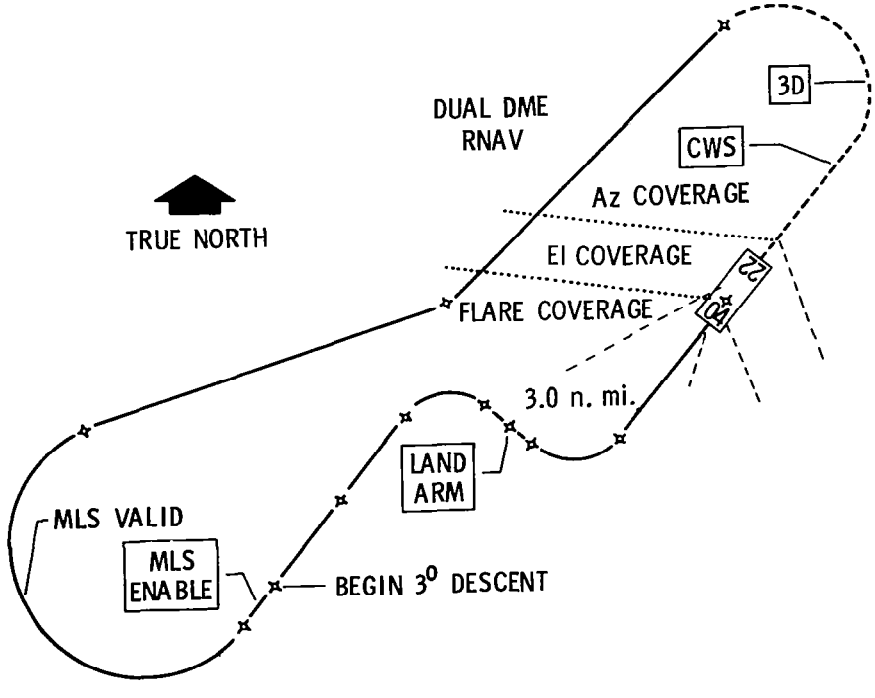

(b) Capture from S-turn azimuth.

Figure 13.- MLS NAFEC approach paths.

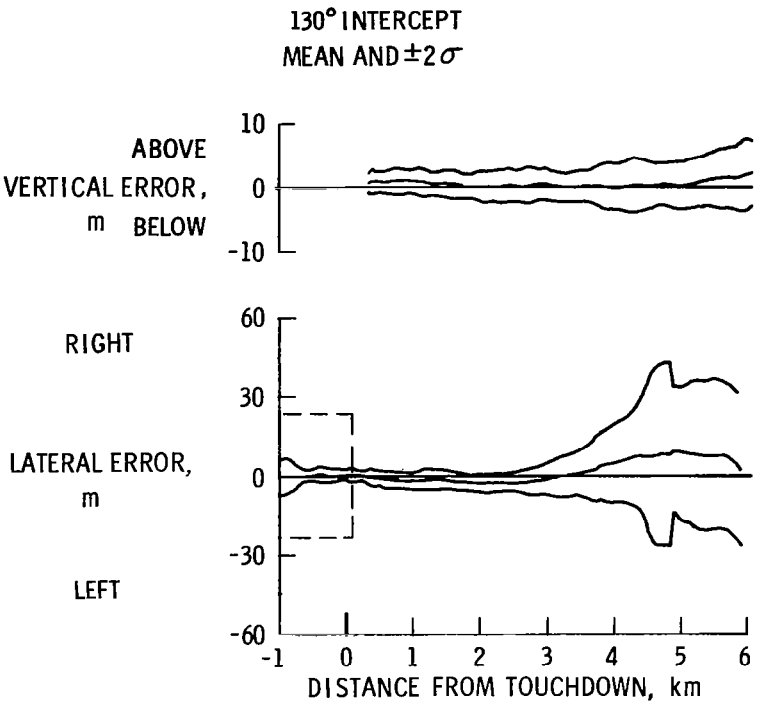

Figure 14.- Automatic tracking results on 3-n. mi. approach path.

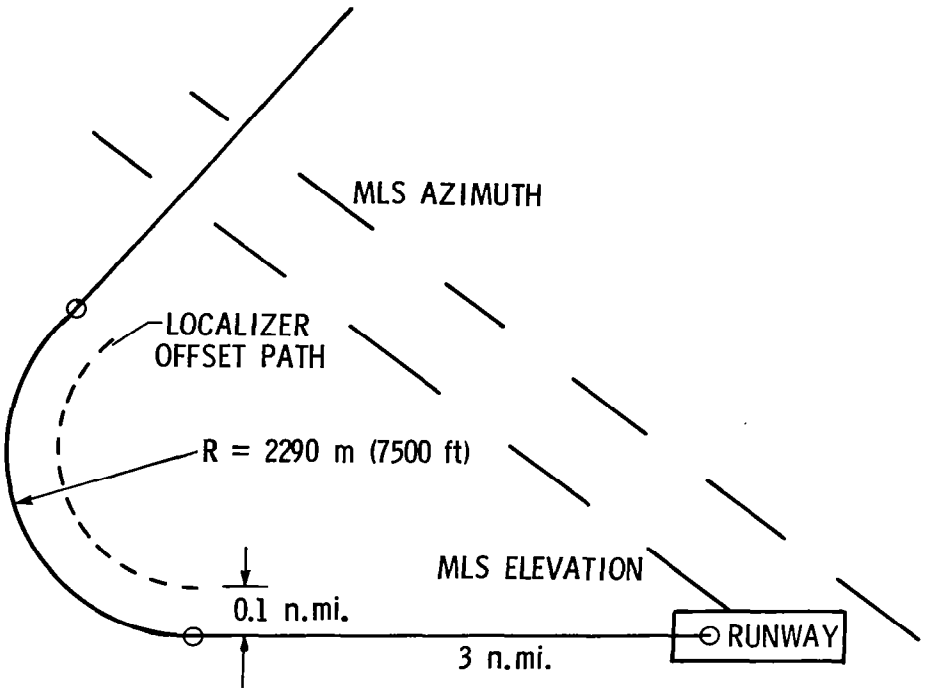

Figure 15.- Plan view of approach path to runway 04 at NAFEC.

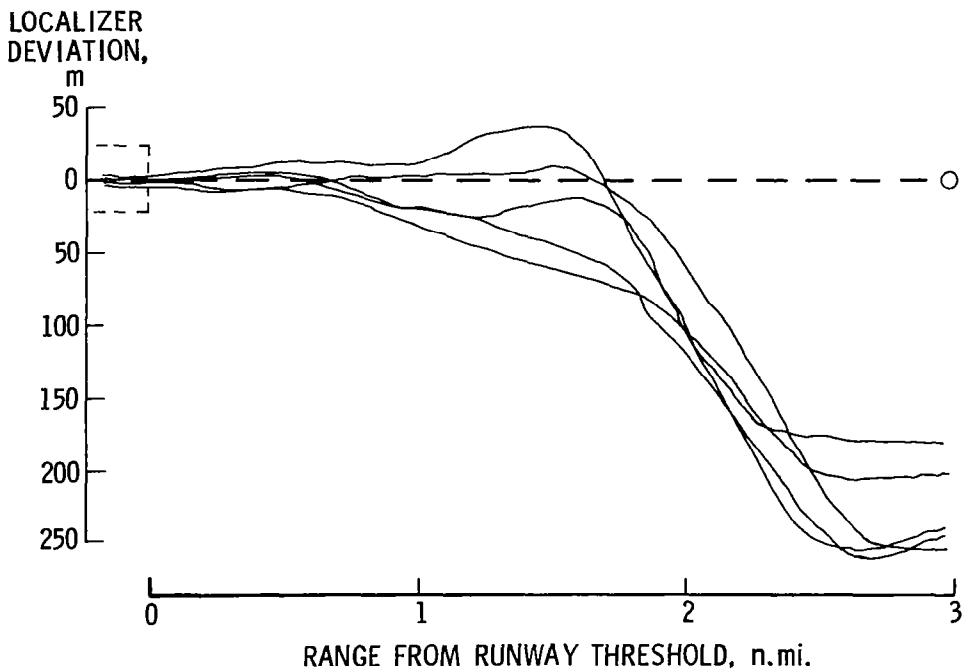

Figure 16.- Localizer tracking using integrated situation display format.

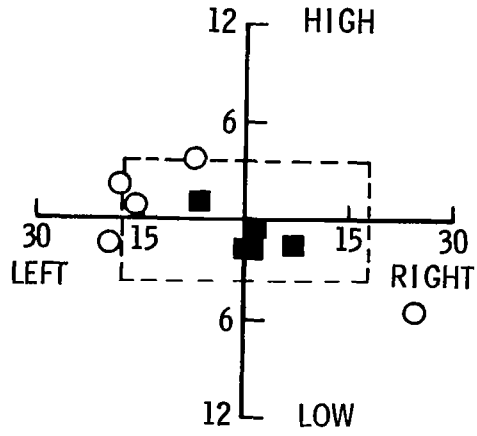

○ BASELINE DISPLAY

■ INTEGRATED DISPLAY

– – – – – CATEGORY II FLIGHT DIRECTOR CRITERIA

NOTE: ALL SCALES IN METERS

Figure 17.- Manual approach display data comparison.

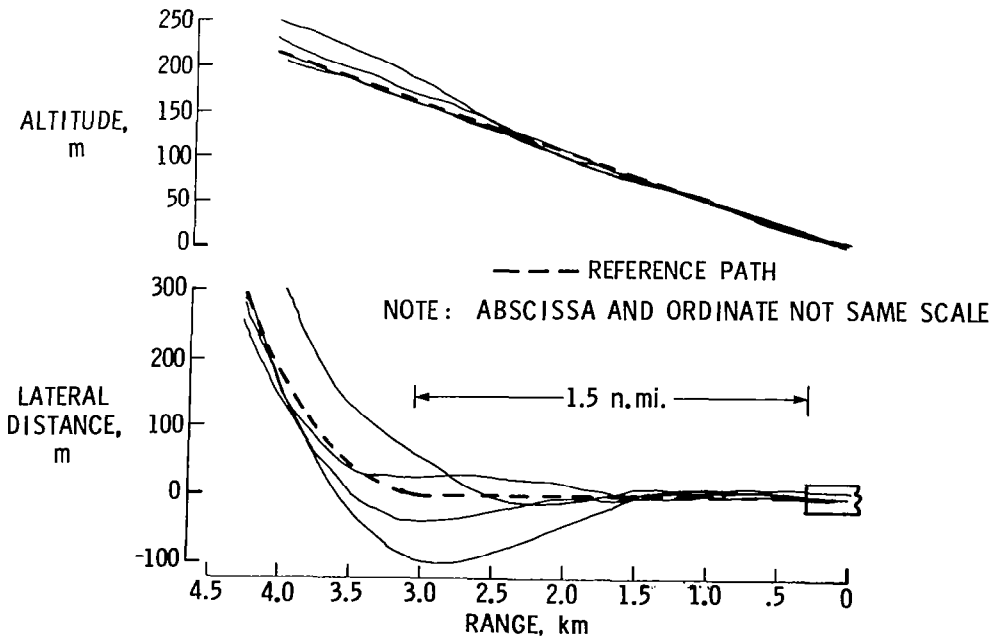

Figure 18.- Manual tracking results on 2.78-km (1.5 n.mi.) approach path.

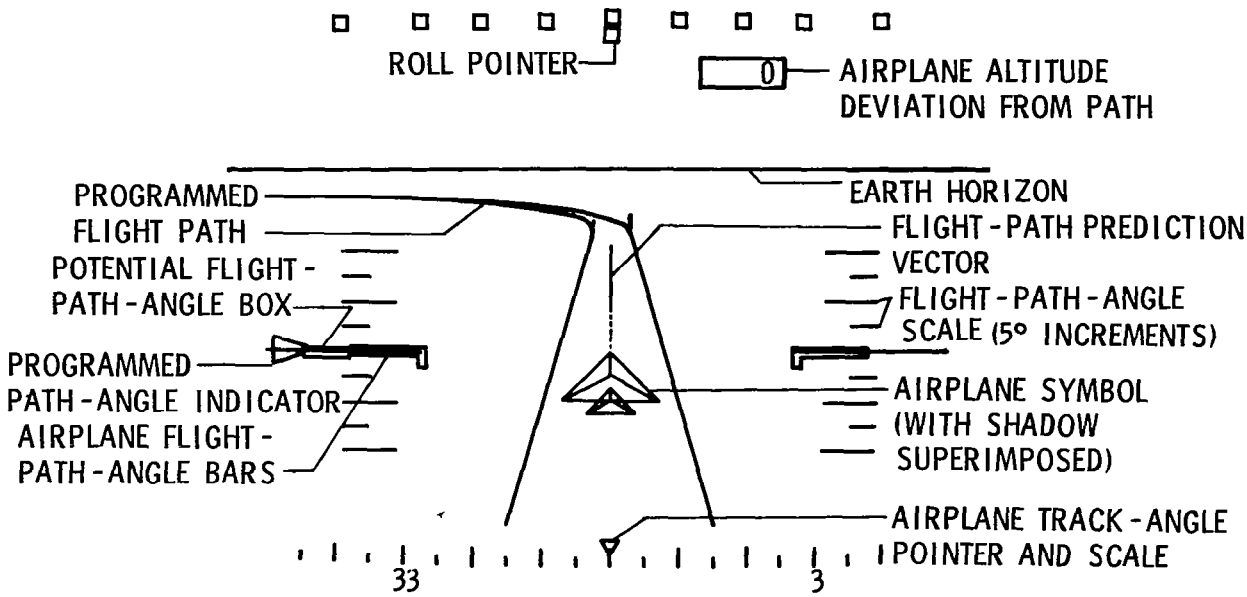

(a) Path-in-the-sky.

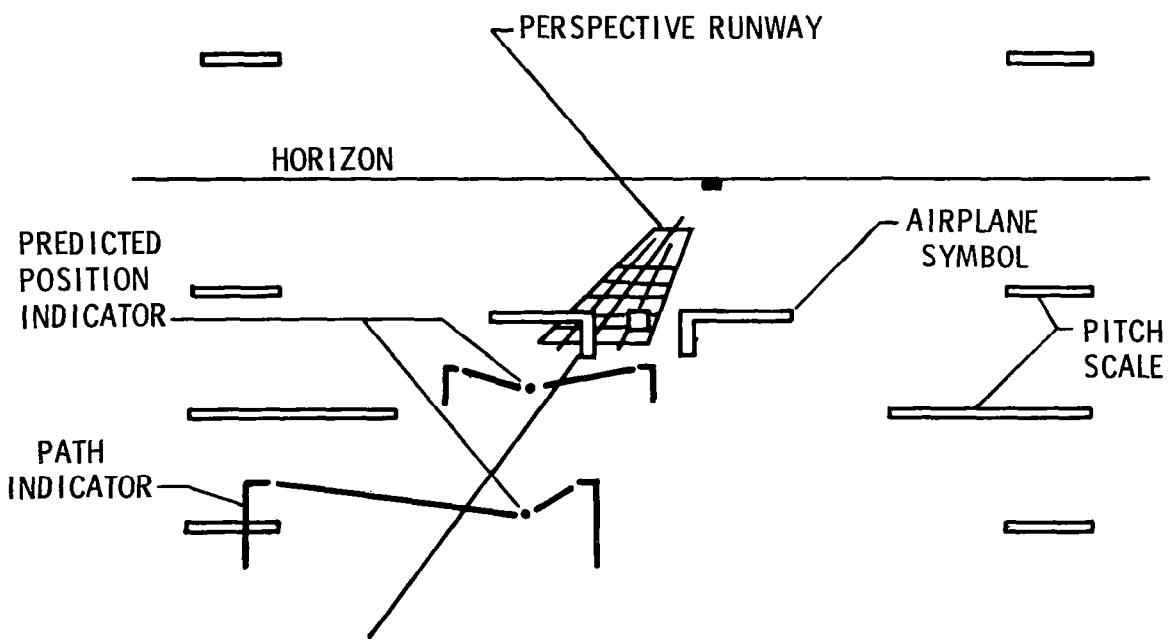

(b) Predictive position and vectors.

Figure 19.- Curved approach vertical situation display.

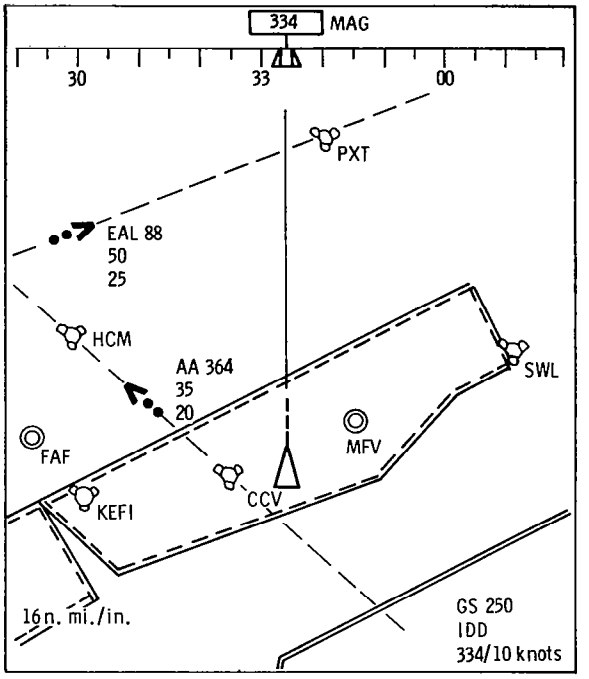

Figure 20.- Proposed CDTI and map display (sample NAVAIDS and other aircraft). Note: Map scale is 1.17 km/mm.

ESTIMATING AIRLINE OPERATING COSTS

Dal V. Maddalon
NASA Langley Research Center

SUMMARY

A review has been made of the factors affecting commercial aircraft operating and delay costs. From this work, an airline operating cost model was developed which includes a method for estimating the labor and material costs of individual airframe maintenance systems. The model, similar in some respects to the standard Air Transport Association of America (ATA) Direct Operating Cost model, permits estimates of aircraft-related costs not now included in the standard ATA model (e.g., aircraft service, landing fees, flight attendants, and control fees). A study of the cost of aircraft delay was also made and a method for estimating the cost of certain types of airline delay is described. All costs are in 1976 dollars.

INTRODUCTION

In 1976, Americans spent over $17 billion to obtain air transportation services (ref. 1). Of this amount, the airlines used roughly $8 billion to purchase and operate their aircraft fleet. The introduction of aircraft which incorporate new technology to reduce these costs is fundamental to the long-term health of the U.S. civil aviation industry. The National Aeronautics and Space Administration (NASA) has the primary governmental role in developing new civil aircraft technology and is therefore concerned with the cost of applying this technology to future airline fleets. Examples of such NASA work include studies of supercritical aerodynamics, composite materials, active controls, terminal configured vehicles, very large cargo transports, supersonic airplanes, and hydrogen-fueled aircraft.

A prime means of determining the payoff from specific examples of innovative research is to incorporate the technological advance into a specific airplane configuration study and economically compete the advanced design against a conventional aircraft (e.g., ref. 2). Langley Research Center, in cooperation with industry designers, has followed this procedure for many years to help guide the nation's basic aeronautical research and technology development effort. Some past airplane studies of this type are illustrated in figure 1, along with the companion studies of airplane economics.

In doing the economic work, NASA has used the basic cost model (ref. 3) developed by the Air Transport Association of America (ATA) to calculate the direct operating cost (DOC) associated with the study aircraft. The ATA last revised this model in 1967. It is updated annually by the aircraft manufacturers but such work is not publicly available.

Reviews of the aircraft configuration studies (by airline personnel intimately familiar with operating costs) indicated a concern about the adequacy of these cost comparisons and particularly about the calculation of maintenance costs. Close examination of the assumptions made in using the ATA model (and an appreciation for its inherent limitations) led to the conclusion that a comprehensive review of this entire subject was needed.

Lewis Research Center first acted on this problem by sponsoring a study of propulsion-system maintenance costs. The results of that work, done under contract to American Airlines, Inc. (with United Technologies Corporation/Pratt & Whitney Aircraft Group and the Boeing Commercial Aircraft Company as subcontractors), were published in reference 4. The experience gained during this engine study helped lead to the present work which includes a review of all aircraft-related operating costs encountered with commercial airplanes (except for engine maintenance).

Inputs to the present study are illustrated in figure 2. The objectives of the work were to obtain a better understanding of airline operating costs and thereby develop a more complete and detailed cost model and to look at the costs associated with airline delays.

AIRLINE COST STUDIES

Approach

The study was done under contract by American Airlines, Inc. (AA), who subcontracted a significant part of the work to the Boeing Commercial Airplane Company (fig. 3). AA was responsible for the management of the overall effort, for providing very detailed data for Boeing analysis, and for studying cost components not inherently associated with the aircraft (e.g., stewardess pay and landing fees). The Boeing Company organized the basic data, developed and exercised the necessary computer programs, utilized their less detailed but broader data base, and carried out much of the analytical work. Study airplanes chosen for analysis were the Boeing 747, 737, 727, 707, and the McDonnell Douglas DC-10. The data base generally consisted of 1974 and 1975 airline experience.

Initially, much time was spent in putting the large amount of collected data into a proper format and in revising software programs so that rapid data correlations and analyses could be developed. A complete description of the techniques used and the work done is given in reference 5 since space limitations here do not allow coverage of all topics studied.

The individual costs that were examined and their relative importance for a typical aircraft (Boeing 727-200) are shown in figure 4. These include airframe maintenance, flight crew, spares investment, flight attendants, aircraft service, landing fees, insurance, depreciation, and fuel. For comparison with the standard ATA model, the costs studied here include all of the ATA costs plus flight attendants, aircraft service, landing fees, and control fees. Most of the effort, however, was concentrated in looking at the detailed costs of airframe maintenance systems.

Airframe Maintenance Costs

Model development.- The ATA model breaks maintenance system costs only into labor and material costs (fig. 4) for the entire airframe and the entire engine (plus an allowance for overhead burden which includes supervision and inspection costs). Like some other cost-estimating relationships in the ATA model, airframe maintenance cost is expressed essentially as a function of airframe weight, first cost, and labor rate. In contrast, the present model computes labor and material maintenance costs for each of the 26 airframe systems (propulsion system cost estimates are provided in ref. 4) as a function of the characteristics of the maintenance system. Individual system costs are identified from airline data by using the ATA-100 maintenance coding system. (See table I.) Using the present model, therefore, the relative importance of various system maintenance costs can be determined if certain design specifications of the study aircraft are known.

Figure 5 illustrates a problem which arose during the course of the study. This chart compares AA airframe maintenance costs to those of the entire domestic industry fleet for three different aircraft. Although fairly close agreement between airlines was obtained for the DC-10 and B-707, poor agreement was obtained for the B-747. Extra care was thus taken in using and analyzing American Airlines data to ensure that any conclusions drawn were representative of the industry as a whole rather than of a single airline. Industry-wide data obtained from the Civil Aeronautics Board Form 41 were often used during the study for this and other purposes. There are many reasons why one airline's maintenance cost experience can depart significantly from the fleet average. Often it is due to the route structure being flown, but other factors which can cause differences include utilization, union contract provisions, airline efficiency and size, management and maintenance philosophy, degree of government regulation, and climate.

An example of the data correlations made for each of the 26 airframe systems is given in figure 6 for the landing-gear system. The labor and material cost per trip is given for the entire domestic fleet (2.5-hr average flight length). Good correlation between cost and maximum gross weight is obtained both for the entire landing-gear system (consisting of the gear, tire, and brake subsystems) and also for only the gear and tires. In addition to maximum gross weight, other correlation parameters were also tried (e.g., kinetic energy and approach speed), and these met with varying degrees of success. Since good correlation was obtained with this simple weight parameter, it was selected for use in the final cost model. The equations developed from such correlations for each of the 26 airframe maintenance systems are summarized in table II and provide trip costs in 1976 dollars for a standard 2.5-hr flight length. A shorter form of these equations is given in reference 5. Table III shows how many individual aircraft system specifications must be known in order to use these cost relationships as compared with the ATA model. Correlating parameters used are based on the physical characteristics of the airplane whenever possible.

Cost ranking.- The data showing the relative importance of various airframe costs for different aircraft (fig. 7) indicate that landing gear is the

single most important airframe maintenance cost for the first-generation jets such as the B-707 and B-727. This cost was reduced to only the fourth most important cost on the second-generation DC-10 and B-747 wide-body jets. This is probably because of improved tire and brake technology and also better airline maintenance techniques. Major improvements in maintenance cost come from the very dramatic increases in the time interval between major inspections as airlines and regulatory agencies gain additional confidence in specific aircraft and as airlines develop improved repair methods over a long period of time. Nevertheless, inspections and miscellaneous costs remain very high for the original narrow-body jets (as they also do for the newer wide-body aircraft). Equipment and furnishings is also a leading airframe maintenance cost as is the auxiliary power system (which was not used on all of the first-generation jets). These four systems, together with the navigation system, generally account for over 50 percent of the total airframe maintenance cost (fig. 7). The high costs of the auxiliary power unit (together with reliability problems sometimes associated with this equipment) often lead airlines to urge designers to consider this system as another engine which should ideally meet the performance and reliability standards demanded of the basic engine.

Learning-curve effects.- Just as an airplane manufacturer experiences a production-cost learning curve as more and more copies of a new airplane are fabricated, an airline experiences a maintenance-cost learning curve when introducing a new technology aircraft. To a large extent, this is a result of learning how to do many individual tasks better, quicker, and therefore cheaper. This trend is illustrated in figure 8 over a 17-yr period for the B-707. When it was first introduced, this aircraft represented a radical change in technology level. In the first year or two of ownership, maintenance costs were relatively low because of the newness of the equipment. However, a peak cost level occurred in the third year of ownership (707-123 data), after which costs steadily declined until a mature cost level was finally reached about 12 yr after introduction. This mature cost occurred at a magnitude less than half that of the peak cost and was even lower than the cost encountered when the airplane was new. Derivative aircraft, such as the B-707-323, benefited from this previous experience. This aircraft, introduced 8 yr later, shows the same general trend of low initial cost, a peak several years later, and finally a mature cost at about the same level as that of the original high-time B-707-123 fleet. Other data for the B-727, B-747, and DC-10 indicate that these later aircraft experienced airframe maintenance trends similar to that of the derivative B-707 aircraft. This is not surprising since airframe technology did not greatly change with the introduction of the wide-body aircraft. Designers of new technology aircraft (e.g., composite primary structure and laminar-flow control), however, must guard against the possibility of high introductory maintenance costs by a technique such as "design for maintenance" or some other control measure which insures the maintenance reliability of the new technology. Figure 8 also illustrates why airlines become apprehensive when researchers talk of introducing a radical new technology aircraft.

Model validation.- Figure 9 compares the present cost model (see data points) predictions for airframe maintenance with the actual costs (shown by solid lines) for various aircraft in 1976. Reasonable agreement is obtained across this broad grouping of transport aircraft. Maintenance results for the

present model are compared with the ATA model (adjusted for inflation) in figure 10. The original 1967 form is, of course, inadequate and considerably overstates maintenance cost because of the learning-curve effect.

Flight-Crew Costs

In addition to airframe maintenance, numerous other costs affecting airline operation were reviewed. One example is the flight crew's pay. Flight-crew pay increases with increasing flight length and maximum take-off gross weight (fig. 11(b)) because these two parameters are generally defined in union contracts as the prime determinants of a pilot's pay. Because of the weight-pay relation, the highest flight-crew pay in the American Airline system was attained by pilots flying heavily loaded freighter aircraft rather than by those flying lighter weight passenger aircraft. Technology which reduces maximum aircraft weight while accomplishing the same mission (e.g., composite materials) therefore provides some hope of reducing flight-crew costs, provided that this basic rule of pay determination is not altered in future union contracts.

Improved flight-control technology may eventually eliminate the need for the third crew member. Figure 11(a) shows that reducing the crew from three to two reduces crew costs about 15 to 20 percent rather than causing a proportionate cost reduction (since union-company seniority agreements insure that it is the functions of the lowest paid crew member that are merged or eliminated). Indirect flight-crew costs (e.g., fringe benefits, overnight charges, and local transportation) are not included in these data correlations and add another 25 to 30 percent to the total flight-crew cost. Copilot pay is roughly 66 percent of the captain's pay, and the third crew member is paid roughly 60 percent of the captain's pay.

Airframe Spares

The introduction of a new aircraft can cause a significant "spares" start-up expense. In the example given in figure 12, American Airlines' investment in airframe spares as a ratio of its total airframe investment is initially very high because the airline has only a few copies of the model in its fleet and has overstocked many parts as a precautionary measure. The rapid fleet buildup which occurs after purchase of the initial aircraft dramatically reduces this cost ratio in the first 2 yr of the fleet's life. A much smaller cost reduction then occurs in later years as the airline uses up its excess part inventory and better manages its purchase of replacement parts, concentrating on those parts which have demonstrated a high likelihood of early failure. Introduction of a mature aircraft to an airline fleet usually results in a lower introductory cost than is shown here since the airline is able to benefit from the start-up experience of other airlines. The cost of spares is included in the depreciation cost calculation.

Fleet Utilization

To prorate certain fixed costs such as depreciation and spares, it is also necessary to estimate aircraft utilization. Therefore, variations in the use of individual airplanes were reviewed. This work indicates that the main factors affecting aircraft utilization were individual airline route structure and the degree of passenger demand. Using this and other trip information, trips made per unit time was analyzed. Figure 13 shows how the number of trips vary as a function of stage length and flight length. Data correlations were obtained from this information and were used in calculating costs which are dependent on aircraft utilization.

Delay Cost

Increasing demand for air transportation service has brought congestion to many of the country's busiest airports despite technological improvements. Air travel demand is expected to grow significantly far into the future, yet new airports are just not being built (ref. 6). These events indicate that the airline delay problem, already significant, could become far more serious in the future and perhaps cause large-scale waste of resources and major changes in airline operations. Because of the potential importance of this problem and the nature of this study, the cost and sources of airline delay were also examined.

Airlines regularly monitor their delays and track their associated cost in order to make reductions in delays that are caused by factors over which they exercise some control. It is this airline information that provided the base for the delay work reviewed here. Examples of direct delay costs include flight crew, fuel, maintenance, passenger handling, and lost revenue. In 1976, the cost of delay to American Airlines was $38.8 million (fig. 14), a cost which does not include lost revenue or air-side delay costs.

Although technology can do little to eliminate occurrences such as last-minute passenger cancellations and late arrivals, there are other delay sources which may be more amenable to improvement through technological advance. Examples include delays caused by unscheduled mechanical maintenance and weather conditions. Maintenance-related delays now cost American Airlines about $4.9 million in station hold costs and about $1.9 million in cancellation losses (fig. 14). These costs represent about 4 percent of the total (both airframe and engine) 1976 maintenance costs. Identification of problem and high-cost mechanical delays can lead to better design of maintenance systems which would improve reliability and reduce the probability of part and component failure. Weather-related losses can be alleviated, for example, by flight-control technology which permits operations in poor visibility conditions. In 1976, weather delays cost American Airlines $3.2 million in station hold costs and another $1.7 million in cancellation costs (fig. 14).

The impact of maintenance delays on dispatch reliability for various aircraft is shown in figure 15. Start-up problems typically occurring with the introduction of a new aircraft fleet keep dispatch reliability at the relatively

low 90 to 93 percent level during the first year of use. Since this can have a disastrous impact on airline profitability, intensified trouble-shooting efforts by both airlines and manufacturers are aimed toward cleaning up problem areas. The figure also illustrates the rapid improvement in dispatch reliability which occurs in the first few years of use as a result of such efforts. In the mature state, a reliability level between 96 to 98 percent is reached.

The cost of delay as a function of time for various aircraft is included in figure 16, which shows that such costs may range from $120 for a delay lasting less than 30 min on a B-727-200 to $2,154 for a delay lasting over 1 hr on a B-747 (American Airlines data). However, the figure also shows that most delays are well under a 1-hr duration, with the average being about 35 min long. Maintenance delay and cancellation costs by the ATA system code are summarized in table IV for the AA fleet, assuming an average 2.5-hr flight length. Correlating equations for different types of airline delays are given in table V as a function of airplane size for the AA fleet.

CONCLUDING REMARKS

A detailed study of airframe maintenance costs has been made which permits a better understanding of the factors that cause such costs. High airframe maintenance cost areas were identified for various aircraft. The data and techniques described here and in the basic contractor report should prove useful to airlines and manufacturers who are interested in analyzing and controlling airframe maintenance costs. A new approach to airline cost modeling was developed and exercised. This approach may be useful to those interested in estimating airline operating costs on both existing and advanced technology aircraft. The work described here may serve as a first effort toward determining many of the underlying factors which impact airline operating costs.

REFERENCES

1. Kloster, Linda, ed.: Air Transport 1977. Air Transport Assoc. of America, [1977].

2. Maddalon, Dal V.; and Wagner, Richard D.: Energy and Economic Trade Offs for Advanced Technology Subsonic Aircraft. Proceedings of the Fourth Intersociety Conference on Transportation, American Soc. Mech. Eng. c.1976, Paper No. E&F-5. (Also available as NASA TM X -72833, 1976.)

3. Standard Method of Estimating Comparative Direct Operating Costs of Turbine Powered Transport Airplanes. Air Transport Assoc. of America, Dec. 1967.

4. Sallee, G. Philip: Economic Effects of Propulsion System Technology on Existing & Future Aircraft. NASA CR-134645, 1974.

5. American Airlines: A New Method for Estimating Current and Future Transport Aircraft Operating Economics. NASA CR-145190, 1978.

6. Joint DOT-NASA Civil Aviation Research and Development Policy Study — Supporting Papers. DOT-TST-10-5, NASA SP-266, 1971.

TABLE I.- ATA MAINTENANCE SYSTEMS

Air conditioning (21)
Autopilot (22)
Communications (23)
Electrical power (24)
Equipment and furnishings (25)
Fire protection (26)
Flight controls (27)
Fuel (28)
Hydraulic power (29)
Ice and rain protection (30)
Instruments (31)
Landing gear (32)
Lighting (33)
Navigation (34)
Oxygen (35)
Pneumatics (36)
Water/waste (38)
Airborne auxiliary power (49)

Structures – general (50)
Doors (52)
Fuselage (53)
Nacelles/pylons (54)
Stabilizers (55)
Windows (56)
Wings (57)
Powerplants – general, including cowling (71)
Engine (72)
Engine fuel and control (73)
Ignition (74)
Engine air (75)
Engine controls (76)
Engine indicating (77)
Exhaust (78)
Oil (79)
Starting (80)
Airframe – inspection and miscellaneous (99)

( ) ATA code number

TABLE II.- AIRFRAME MAINTENANCE SYSTEM COST EQUATIONS

ATA System	Labor	Material
Inspection and miscellaneous	$7.66 + 0.377 \times AFW/10^3$	$1.21 + 0.062 \times AFW/10^3$
Air conditioning	$2.0386 + 0.01532 \times AC$	$2.32 + 0.011 \times AC$
Autopilot	$2.238 \times (N)CHANN$	$0.631 + 0.398 \times (N)CHANN$
Communications	$0.01772 \times$ Seats (w/o MUX) $0.0276 \times$ Seats (w/MUX)	$0.00693 \times$ Seats (w/o MUX) $0.0118 \times$ Seats (w/MUX)
Electrical	$1.336 + 0.00396 \times (N)GEN \times KVA$	$1.42 + 0.00577 \times (N)GEN \times KVA$
Equipment and furnishings	$9.11 + 0.0531 \times$ Seats $\times$ CF	$2.38 + 0.0361 \times$ Seats $\times$ CF
Fire protection	$0.0726 \times [(N)ENG + (N)APU]$* $0.213 + 10^{.359} \times [(N)ENG + (N)APU]$**	$0.082 + 0.0552 \times [(N)ENG + (N)APU]$* $0.365 \times [(N)ENG + (N)APU]$**
Flight controls	$6.84 + 0.0035 \times MGW/10^3$	$3.876 + 0.00655 \times MGW/10^3$
Fuel	$1.114 + 0.0262 \times Fuel/10^3$	$0.595 + 0.0123 \times Fuel/10^3$
Hydraulic power	$2.31 + 0.0034 \times HYD$	$1.55 + 0.0080 \times HYD$
Ice and rain	$0.5089 + 0.0013 \times MGW/10^3$	$0.0847 + 0.0037 \times MGW/10^3$
Instruments	$0.509 + 0.009 \times AFW/10^3$	$0.235 + 0.0031 \times AFW/10^3$
Landing gear	$4.58 + 0.0710 \times MGW/10^3$	$4.961 + 0.1810 \times MGW/10^3$
Lighting	$1.51 + 0.0072 \times$ Seats $\times$ CF	$0.047 + 0.0087 \times$ Seats $\times$ CF
Navigation	$2.94 + 2.1 \times (N)INS + 3.58 \times CF$	$0.086 + 1.2 \times (N)INS + 3.675 \times CF$
Oxygen	$0.515 + 0.00265 \times$ Seats	$0.00458 \times$ Seats (Conventional) $0.00752 \times$ Seats (OXY GEN)
Pneumatics	$0.181 + 0.0003 \times AC \times Thrust/10^4$	$0.0019 \times AC \times Thrust/10^4$
Water/waste	$0.339 + 0.0023 \times$ Seats $\times$ CF	$0.00485 \times$ Seats $\times$ CF
Airborne auxiliary power	$0.7185 + 0.0003 \times [APU\text{-}SHP \times APU\text{-}FR]^{\frac{1}{2}}$ (× 1.8 for double spool, variable vanes)	$1.466 + 0.0007 \times [APU\text{-}SHP \times APU\text{-}FR]^{\frac{1}{2}}$ (Labor and material cost per APU operating hour)
Structures	$3 + 0.0099 \times AFW/10^3$	
Doors	$1.147 + 0.006 \times$ Seats	$0.387 + 0.00785 \times$ Seats
Fuselage	$1.5 + 0.046 \times AFW/10^3$	0.5833
Nacelles/pylons	$0.3366 \times$ Pod NAC	$0.1391 \times$ Pod NAC
Stabilizers	0.834	0.3737
Windows	$0.763 + 0.00043 \times$ Seats	$0.0284 \times$ Seats (Flat windshield) $0.0362 \times$ Seats (Curved windshield)
Wings	2.9475	$0.126 + 0.00506 \times$ Wing Area

* Single circuit
** Dual circuit

ABBREVIATIONS

AC	air conditioning total pack air flow, kg/min
AFW	airframe weight, kg
APU	airborne auxiliary power unit
CF	defined complexity factor = {short range operations 0.6; medium range 1.0; long range 1.6}
CHANN	channels
ENG	engines
Fuel	fuel used, kg
FR	air conditioning flow rate output, kg/min
GEN	electrical generators
HYD	flow of hydraulic pumps, ℓ/min
INS	inertial navigation system
KVA	kilovolt amperes
MGW	maximum certified gross weight, kg
MUX	multiplex unit
N	number of
NAC	nacelle
OXY GEN	oxygen generator
SHP	shaft horsepower, watts
Thrust	thrust, N
Wing area	wing area, m^2

TABLE III.- AIRFRAME MAINTENANCE COST-DEPENDENT VARIABLES

ATA	Present
Airframe weight	Airframe weight
Labor rate	Labor rate
First cost	Take-off gross weight
	Air conditioning flow rate
	Autopilot channels
	Seats
	Multiplex unit
	Electrical generators number/capacity
	Auxiliary power unit
	Single/dual circuit
	Fuel
	Hydraulic pump flow
	Inertial navigation system
	Oxygen generator
	Thrust
	Shaft horsepower
	Nacelle number
	Windshield type
	Complexity factor

TABLE IV.- DELAY AND CANCELLATION COSTS (MAINTENANCE)

[American Airlines fleet — 2.5-hr flight length]

System	Cost, dollars/flight hr
Landing gear	1.183
Hydraulic	1.108
Flight controls	.915
Engine (basic)	.541
Navigation	.506
Engine starting	.352
Air conditioning	.333
Engine oil	.305
Fuel	.287
Fire protection	.279
Engine fuel and control	.255
Thrust reverser	.248
Electrical	.234
Pneumatics	.217
Doors	.204
Other	1.433
Total	8.400

TABLE V.- CORRELATION OF DELAY DATA FOR AA FLEET

Delay category	Equation	Coefficient of determination*
Late arrivals from another station	Y = 12.374 - 0.0232X	0.76
Maintenance	Y = 2.134 + 0.011X	0.69
Passenger service	Y = 2.763 + 0.014X	0.94
Ground equipment	Y = 0.486 + 0.013X	0.91
Stores and parts shortages	Y = -0.020 + 0.002X	0.79
Late crew and crew caused delays	Y = 0.420 + 0.001X	0.69
Airplane late from hangars	Y = 1.002 + 0.010X	0.95
Other	Y = 0.555 + 0.019X	0.90
All causes	Y = 31.258 + 0.053X	0.88

Y = Delays and cancellations per 100 departures
X = Seats (for X between 100 and 450)
*1.0 is perfect data fit; $\leq$.6 is poor data fit

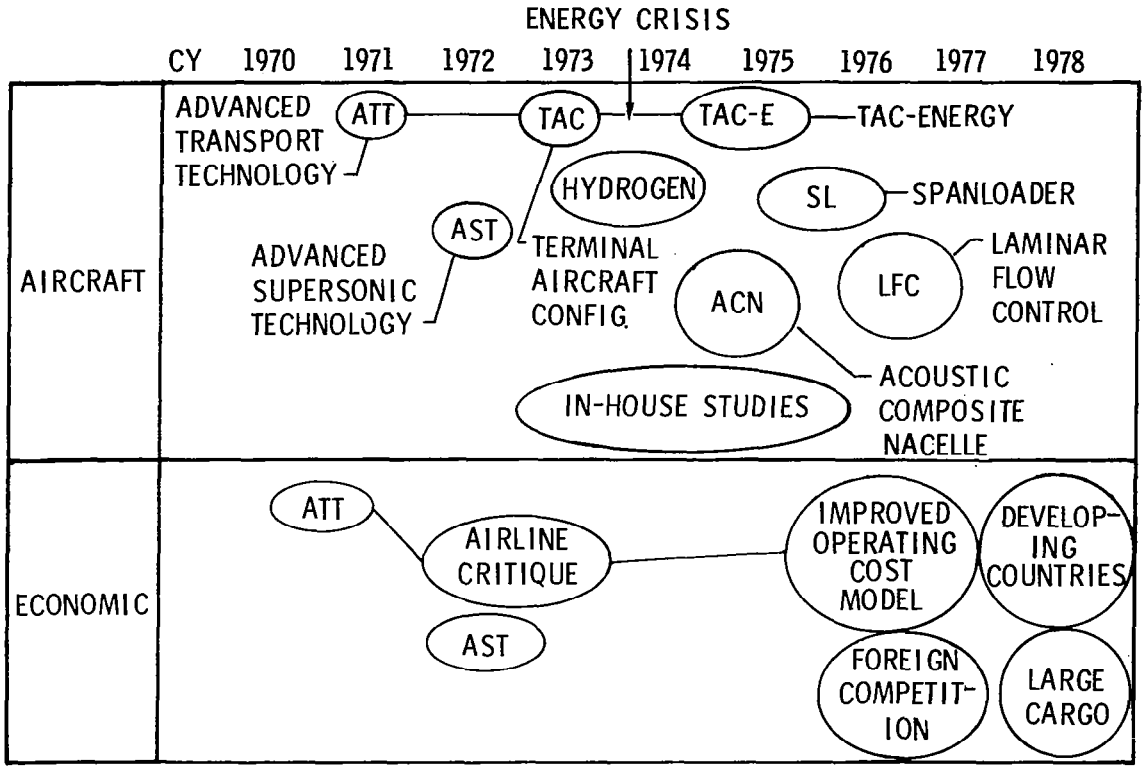

Figure 1.- Aeronautical Systems Division system studies.

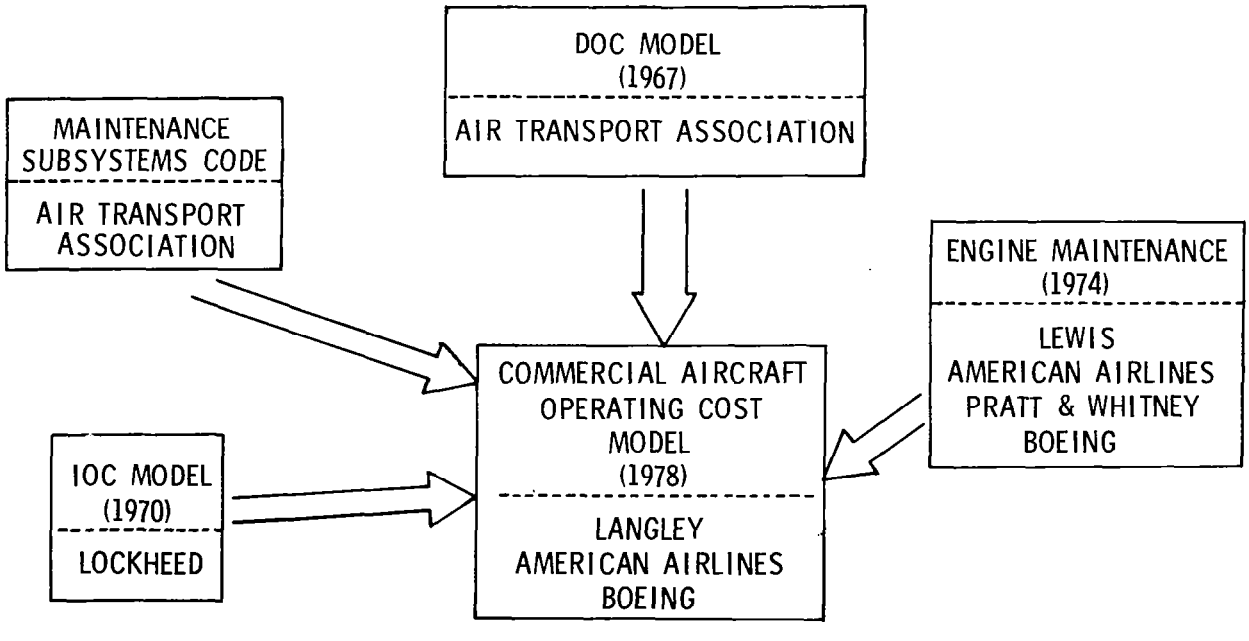

Figure 2.- Cost model evolution.

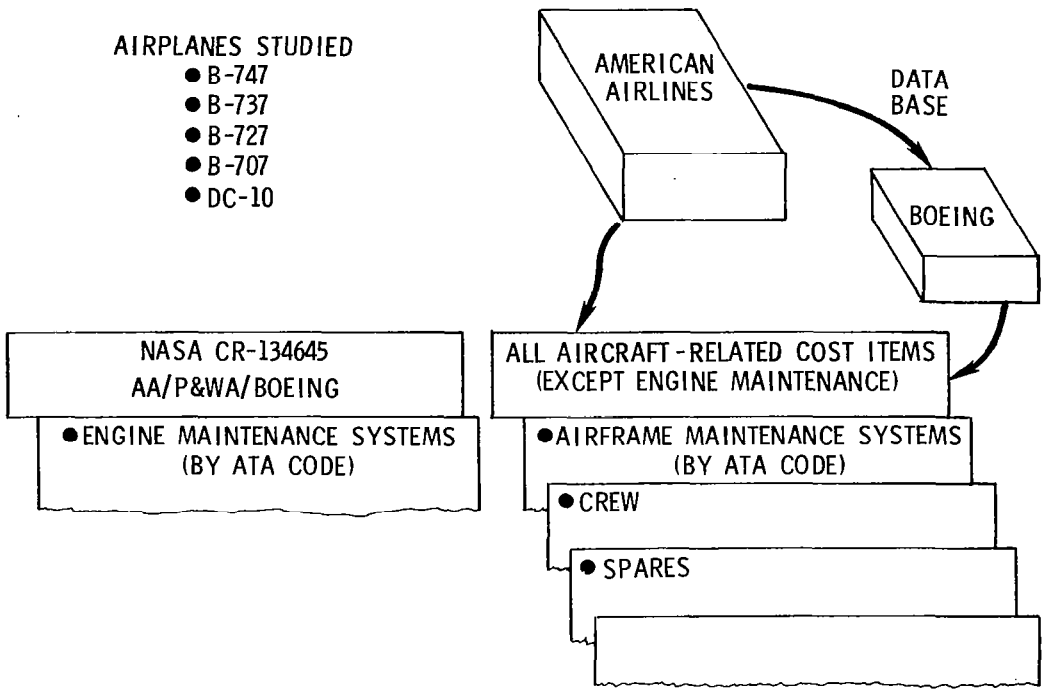

Figure 3.- Data analysis approach. Costs given in 1976 dollars.

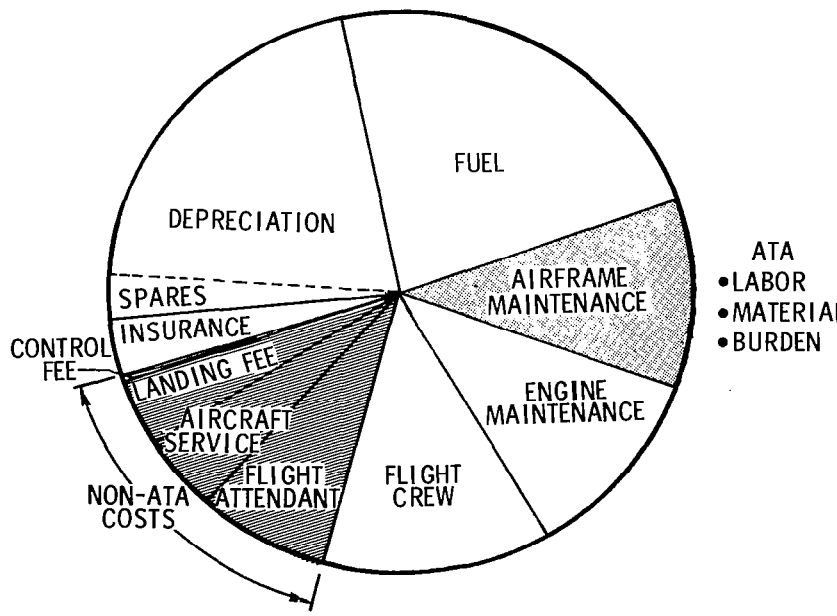

Figure 4.- Aircraft-related operating expenses (within scheduled flight time).

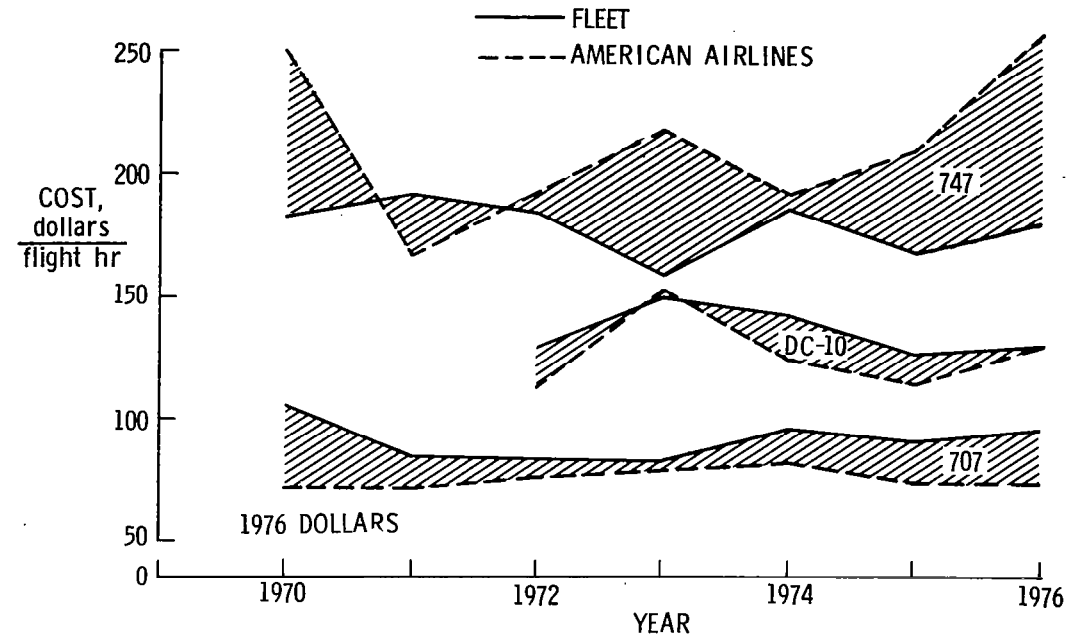

Figure 5.- Actual airframe maintenance costs for both U.S. domestic fleet and American Airlines.

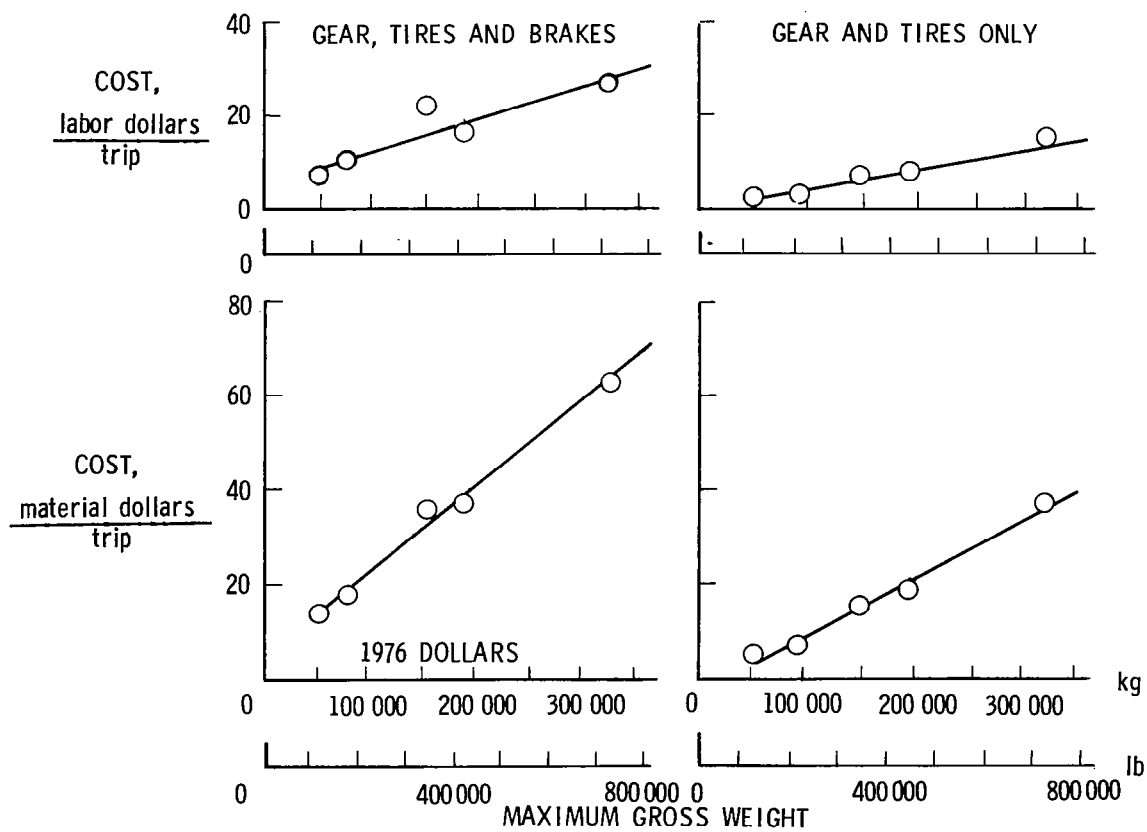

Figure 6.- Landing-gear operating expense for U.S. domestic fleet.

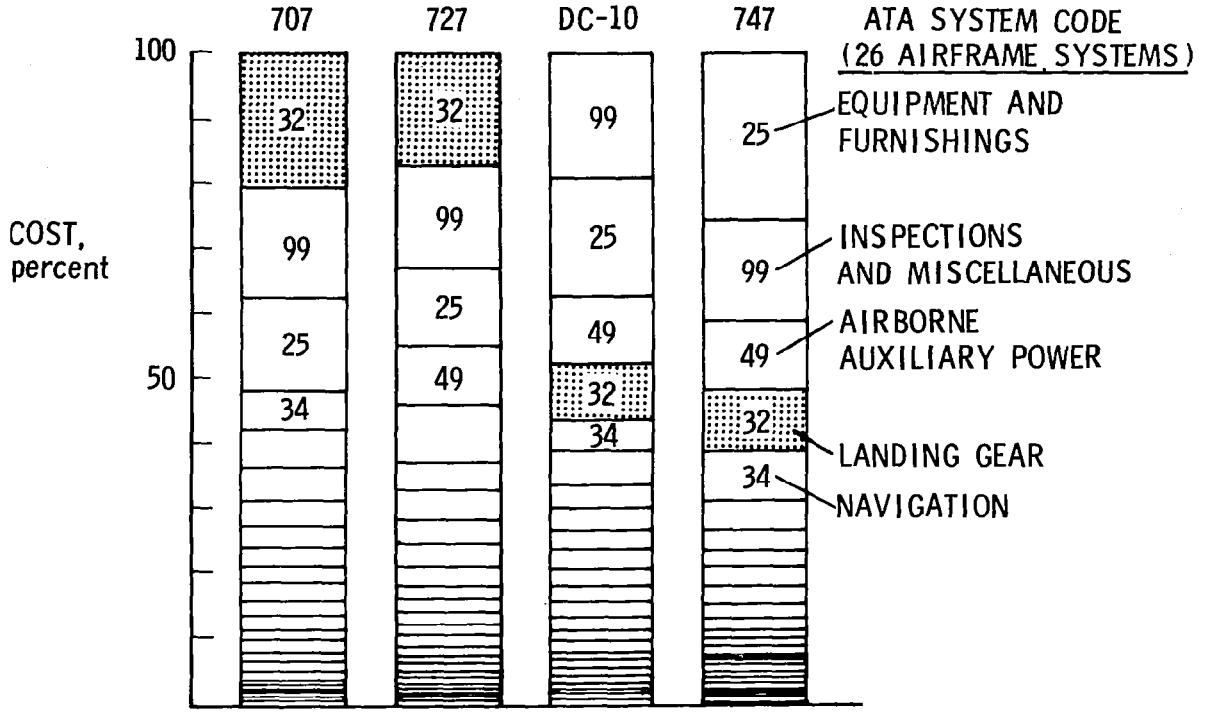

Figure 7.- Maintenance cost of airframe systems for B-707, B-727, DC-10, and B-747 (American Airlines data).

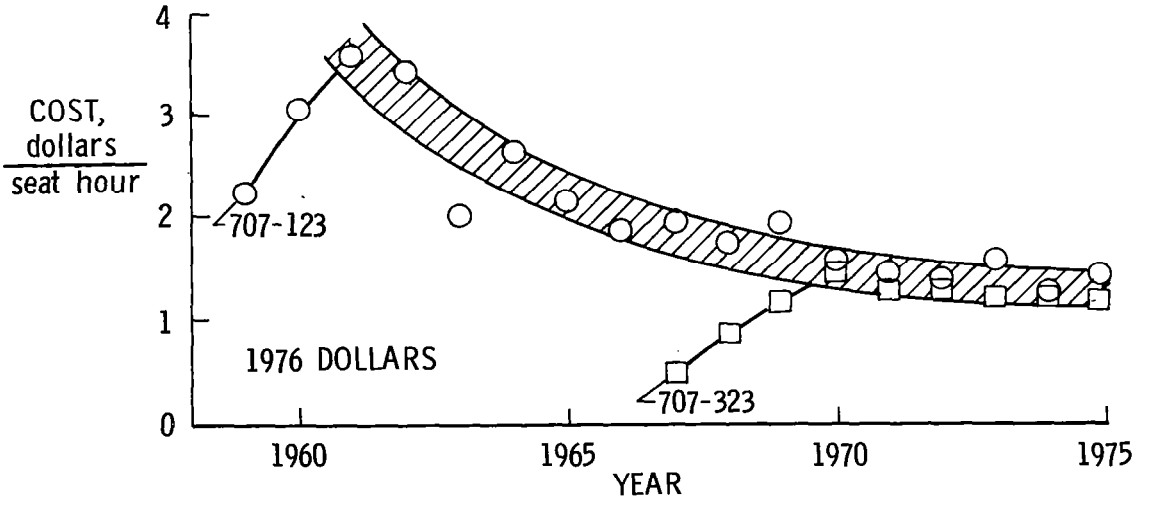

Figure 8.- Airframe maintenance learning curve for B-707 (American Airlines data).

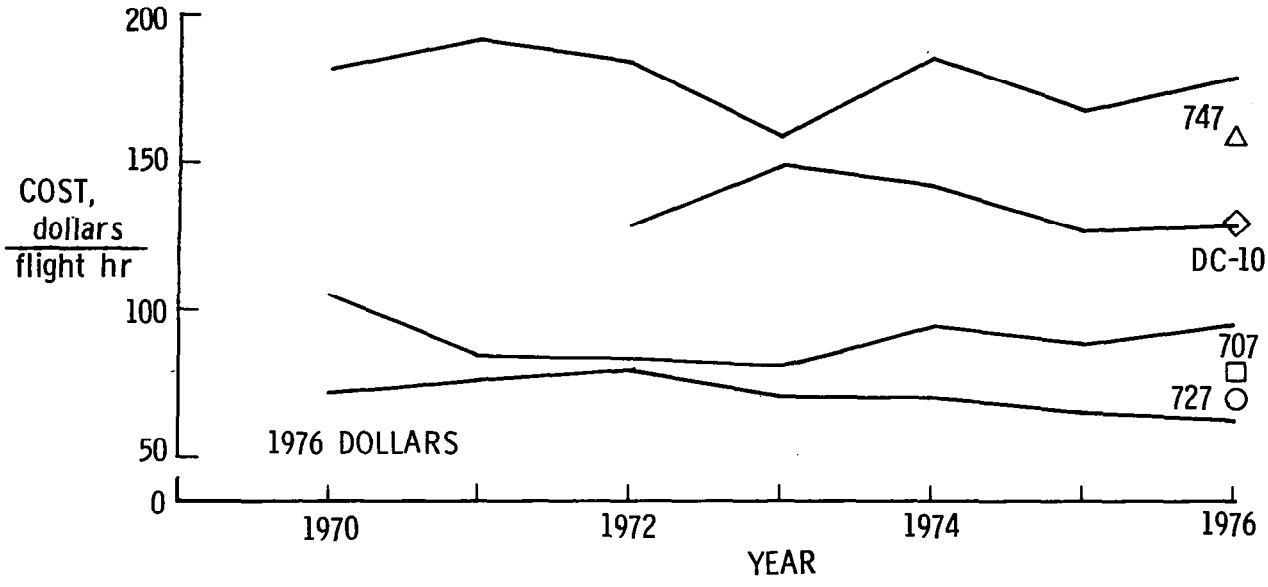

Figure 9.- Actual U.S. domestic fleet airframe maintenance costs compared with model prediction for B-747, DC-10, B-707, and B-727. Symbols indicate cost model result.

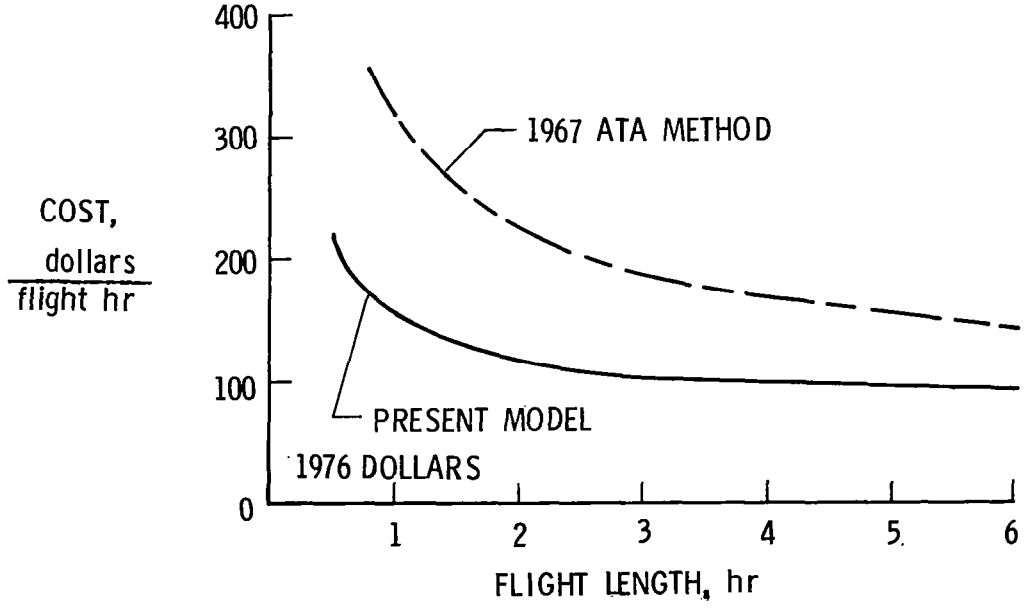

Figure 10.- Airframe maintenance cost model results for wide-body type aircraft (about 200 passengers).

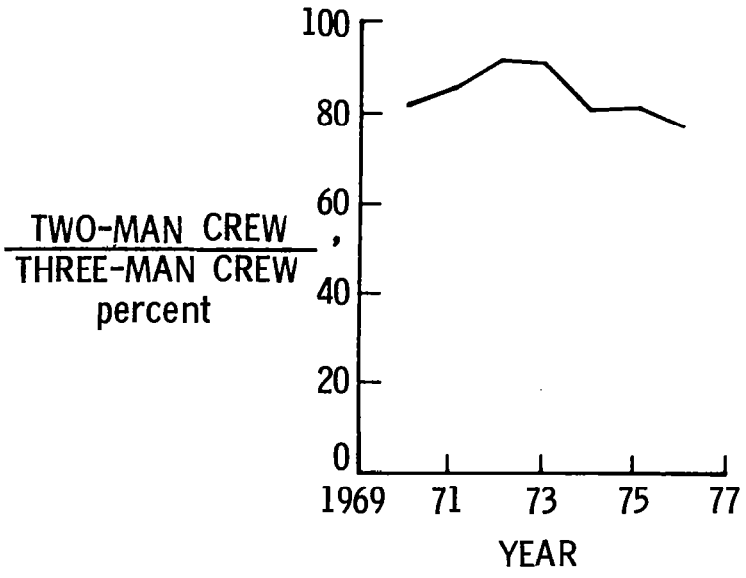

(a) Ratio of two-man crew cost to three-man crew cost for B-737-200 U.S. domestic fleet.

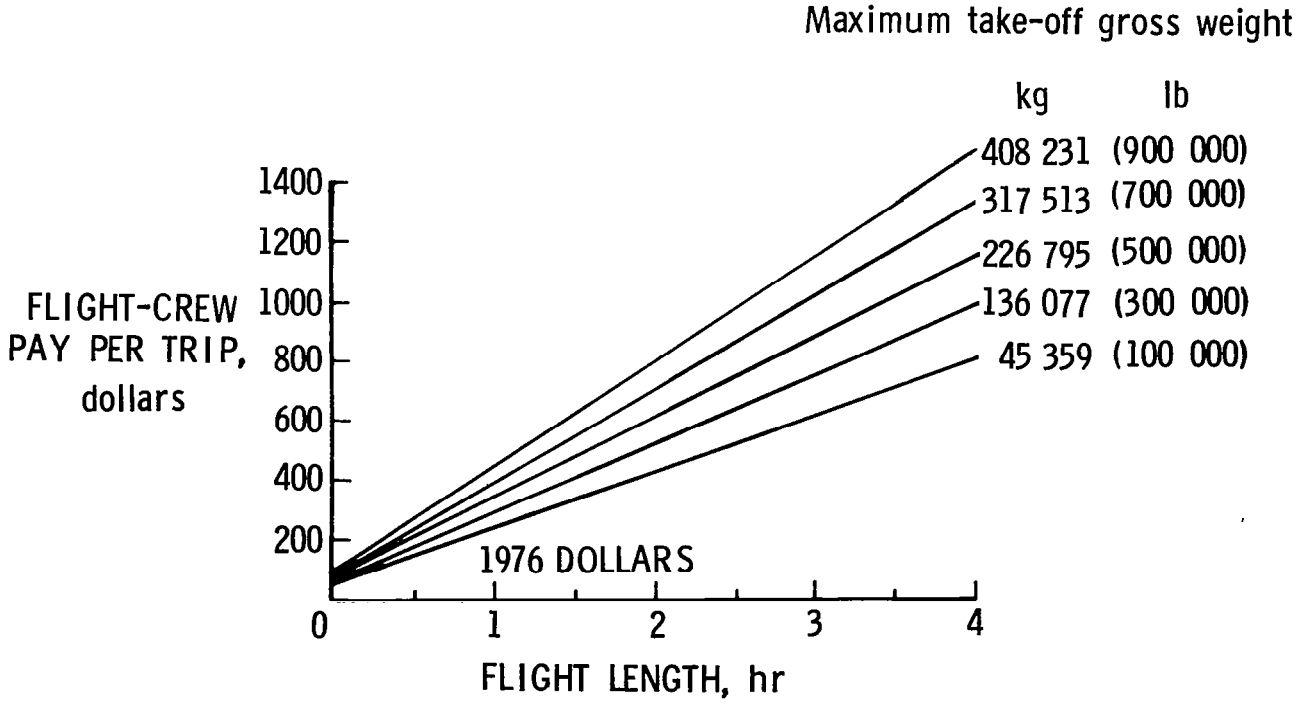

(b) Pay versus flight time and take-off gross weight for a three-man crew.

Figure 11. Flight-crew pay.

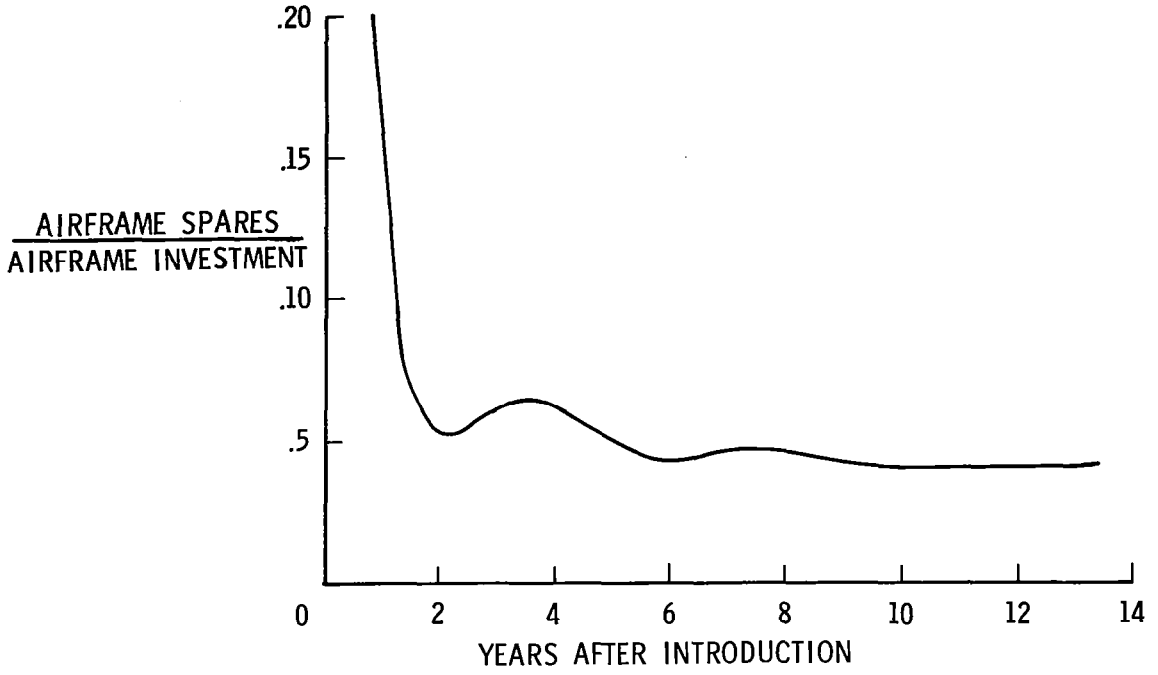

Figure 12.- Airframe spares cost as a ratio of airframe investment cost for B-727 (American Airlines data).

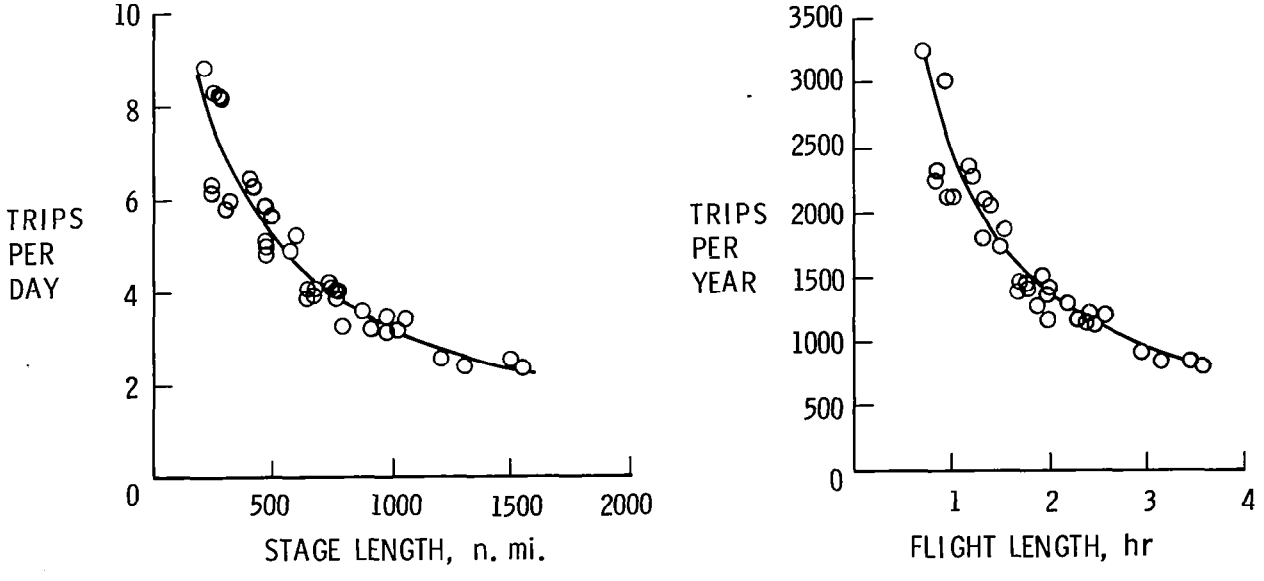

Figure 13.- Average U.S. domestic fleet utilization for 1974 and 1975.

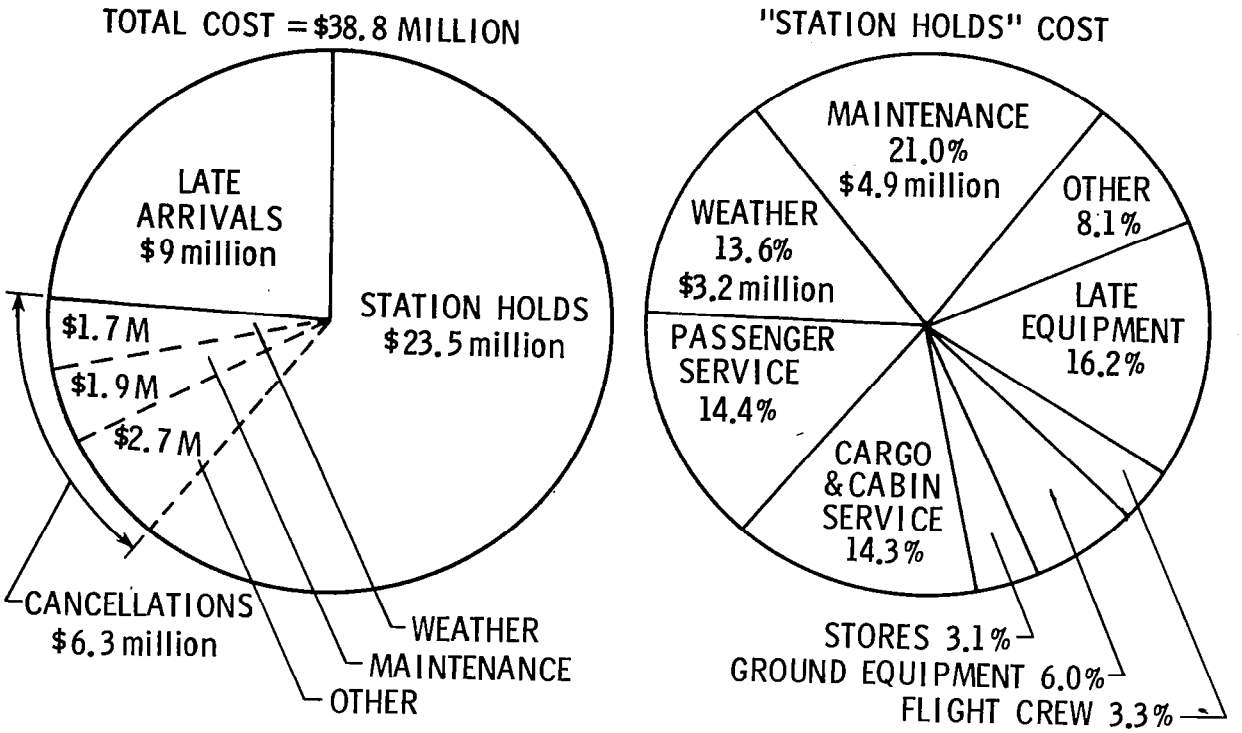

Figure 14.- Annual cost of delay to American Airlines (1976 data).

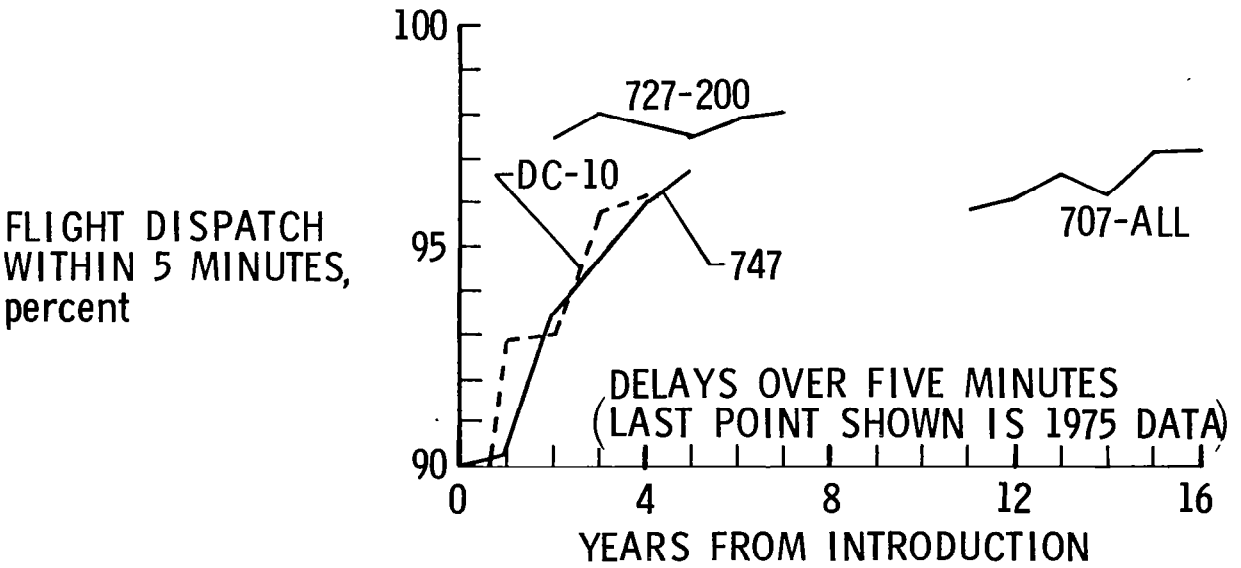

Figure 15.- Impact of maintenance delays on dispatch reliability for B-707, B-727-200, B-747, and DC-10 (American Airlines data).

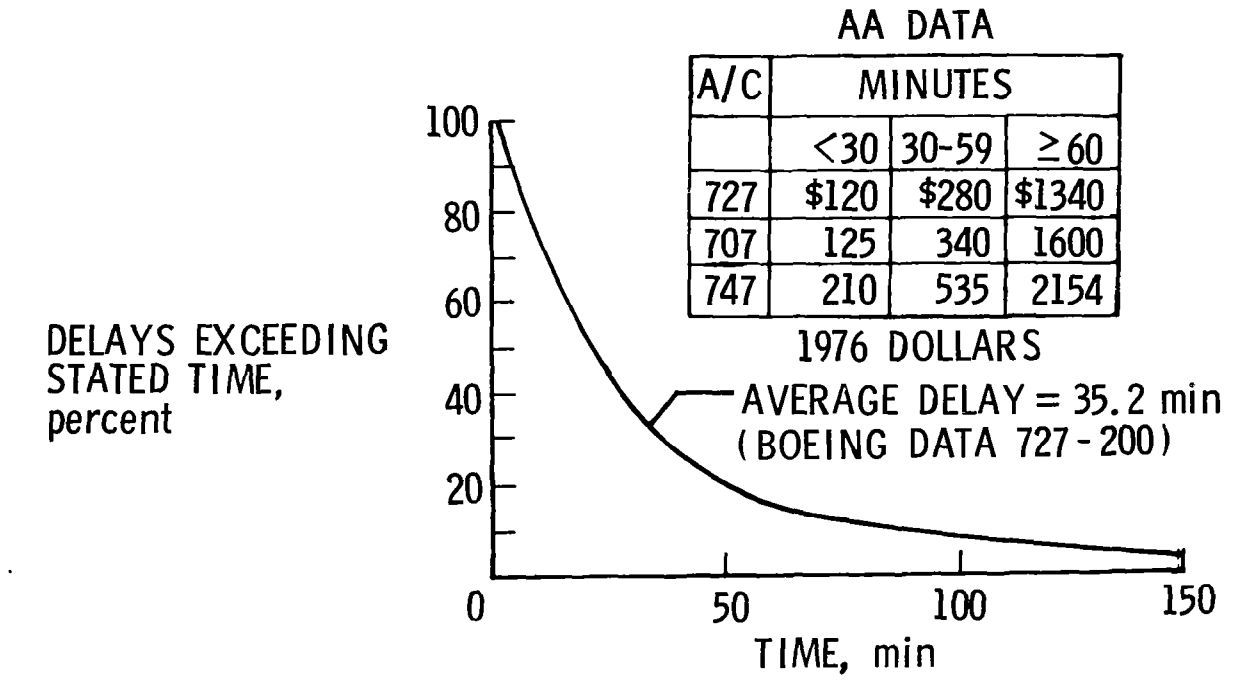

Figure 16.- Length and cost of maintenance delays for B-727, B-707, and B-747.

A METHOD FOR THE ANALYSIS OF THE BENEFITS AND COSTS FOR AERONAUTICAL RESEARCH AND TECHNOLOGY

Louis J. Williams, Herbert H. Hoy, and Joseph L. Anderson
Ames Research Center

ABSTRACT

This paper presents a relatively simple, consistent, and reasonable methodology for performing cost-benefit analyses which can be used to guide, justify, and explain investments in aeronautical research and technology. The elements of this methodology (labeled ABC-ART for the Analysis of the Benefits and Costs of Aeronautical Research and Technology) include estimation of aircraft markets; manufacturer costs and return on investment versus aircraft price; airline costs and return on investment versus aircraft price and passenger yield; and potential system benefits--fuel savings, cost savings, and noise reduction. The application of this methodology is explained using the introduction of an advanced turboprop powered transport aircraft in the medium range market in 1987 as an example.

INTRODUCTION

As part of the NASA Aircraft Energy Efficiency (ACEE) program formulation, a benefit analysis was performed to estimate the potential fuel savings which could be obtained by applying the advanced technologies in the ACEE program (ref. 1). At the time this analysis was performed the only benefit that was estimated was fuel savings and the economic consequences could not be determined. However, it was recognized that even with very large potential benefits it is also desirable to determine whether the technology, if developed, would be economically attractive to the potential users. In order to provide the capability for investigating these tradeoffs between the benefits of advanced technology and the economics of the air transportation system, a cost benefit methodology with the acronym ABC-ART has been developed. ABC-ART is an abbreviation for the Analysis of the Benefits and Costs of Aeronautical Research and Technology. The name also is meant to imply that the intention is to develop a methodology that is as simple as ABC. The objective of ABC-ART is to provide a consistent, simple, and reasonable methodology for performing cost-benefit analyses which can be used to guide, justify and explain investments in aeronautical research and technology. The elements of ABC-ART include aircraft market projection, manufacturer research, development, test and evaluation (RDT&E) and production cost estimation, manufacturer return on investment (ROI) versus price estimation, airline ROI versus price estimation, required passenger yield calculations, and the tabulation of the potential system benefits--fuel savings, cost savings, noise reduction, etc.

As a means of illustrating the application of the ABC-ART, an example using the introduction of a 1987 Propfan Transport into the U.S. trunk and local service carrier medium range aircraft market will be used. This example also assumes a revenue-passenger-mile growth rate of 6% per year, a constant passenger load factor of 55%, a 16-year aircraft retirement age, and that the 1987 Propfan Transport is the only medium range transport aircraft produced from 1987 to 1995. The Propfan Transport used for this example is the Boeing wing-mounted propfan study aircraft shown in figure 1. This aircraft was designed to carry 180 passengers for 1800 n.mi. at a cruise speed of Mach 0.8. The aircraft has a take-off gross weight (TOGW) of 122 062 kg (269 100 lb) and an operating empty weight (OEW) of 83 710 kg (184 550 lb). The aircraft has 2 Pratt & Whitney study turboshaft engines (STS476) with 22 721 kW (30 470 shaft horsepower (SHP)) each. Based on the airline recommendations received on the aircraft examined in the RECAT studies, the manufacturer specification of 180 seats was reduced to 171 seats to allow for garment stowage areas.

AIRCRAFT MARKET PROJECTION AND FUEL SAVING BENEFITS

In order to develop the aircraft market projection, data are required on the current fleet and its history. These data include (figure 4) information on the current fleet aircraft years of introduction; aircraft productivity data in terms of average aircraft seating capacity, block speed, and utilization; aircraft retirement age; fuel consumption rates; revenue-passenger-mile (RPM) growth rates; load factors; and projected retrofit, derivative, or new aircraft data:

Inputs:

(a) Current and historical fleet data by aircraft type

  (1) Aircraft year of introduction
  (2) Aircraft productivity data (seats, block speed, utilization)
  (3) Retirement age
  (4) Fuel Consumption

(b) Growth Rates

(c) Load Factors

(d) Projected retrofit, derivative, or new aircraft data

Outputs:

(a) Projected future fleet information

  (1) RPM's by year and aircraft type
  (2) Fuel usage by year and aircraft type
  (3) Aircraft requirements

For this example, the aircraft data used are shown in table I. These data are the average for the U.S. trunk carriers as reported to the Civil Aeronautics Board in 1975 (ref. 2). It is grouped into the aircraft type categories for the two-engine narrow-body turbofan aircraft (2ENBTF), three-engine narrow-body turbofan aircraft (3ENBTF), four-engine narrow-body turbofan aircraft (4ENBTF), four-engine narrow-body turbojet aircraft (4ENBTJ), three-engine wide-body turbofan aircraft (3EWBTF), and four-engine wide-body turbofan aircraft (4EWBTF). For the purposes of this analysis these aircraft are further grouped into the short, medium, and long range market categories on the basis of aircraft range capability. Because it appears that about one-half of the 4ENBTJ and 4ENBTF aircraft are being used on route segments where they could be replaced by an aircraft with medium range capability, these aircraft were split into both markets equally. The new aircraft being evaluated is the new two-engine wide-body propfan aircraft (N2EWBPF) with the same operating characteristics as the 3ENBTF it is intended to replace, except for a larger passenger capacity and lower fuel consumption.

These data are input to a computer program (BET) and information on RPM's and fuel usage by year and aircraft type are computed. The projected information on the medium range aircraft market share by aircraft type (fig. 2) shows the RPM's carried by the four-engine narrow-body turbojet aircraft (4ENBTJ), four-engine narrow-body turbofan aircraft (4ENBTF), three-engine narrow-body turbofan aircraft (3ENBTF), new two-engine wide-body propfan aircraft (N2EWBPF), and new 1995 aircraft(N1995AC). The N1995AC has the same characteristics as the N2EWBPF, but it is included in order to finish the production run of the N2EWBPF in 1995.

The only medium range aircraft available from 1975 to 1987 is the 3ENBTF. During this period new buys of this aircraft are used to accommodate the RPM growth and the retirement of the 4ENBTJ and 4ENBTF aircraft. The N2EWBPF is introduced in 1987 and production of the 3ENBTF is stopped. The N2EWBPF is produced until 1995 when the N1995AC production takes over for the remainder of the case through 2005. The demand for the N2EWBPF results in a required production run of 872 aircraft. The fuel usage for these medium range aircraft, corresponding to the RPM's carried, is shown in figure 3. The fuel savings for the N2EWBPF relative to continued use of the 3ENBTF is indicated by the cross-hatched area. This fuel savings is 38×10^9 liters (240 million barrels) from 1987 to 1995 alone.

MANUFACTURING ROI VERSUS PRICE

The manufacturing ROI versus price estimation procedure is illustrated in figure 4. From the fleet projection information obtained previously (RPM's versus year by aircraft type), a production schedule is developed to closely approximate the required demand while maintaining the production rate fixed as much as possible. This production schedule is input to a computer program

which estimates the aircraft manufacturing costs as a function of the aircraft component weights, labor rates, and learning curves. This program (ACCOST) has been developed at Ames Research Center over the past several years. It was first based on some original work on total airframe costs by Planning Research Corporation in 1964 (ref. 3) and subsequently has been continually improved by The Rand Corporation. The current version of ACCOST determines the production cost for each system and the assembly and delivery costs for the complete aircraft using cost estimating equations developed in reference 4. This current version of ACCOST is described in detail in reference 5. The resulting estimated RDT&E costs, first-unit costs, learning curves, and assumed airline prepayment schedule are input to a manufacturing cash-flow ROI calculation which computes the manufacturer ROI versus price. The manufacturing cost breakdown is shown in table II. The RDT&E is the sum of the airframe design and engineering development, subsystem development, propulsion development, and development support. The first unit manufacturing cost includes the airframe, avionics procurement, propulsion procurement, and final assembly and checkout.

The manufacturing costs and revenues per month are illustrated in figure 5. For this example, the propulsion RDT&E costs were assumed to be uniformly incurred over a period from 4-1/2 years prior to first delivery until first delivery. The airframe and subsystem RDT&E costs were assumed to be uniformly incurred from 3-1/2 years prior to first delivery until first delivery. And the development support was assumed to be uniformly incurred from 2-1/2 years prior to first delivery until one year after first delivery. The manufacturing costs begin one year prior to first delivery and reflect a one year "pipeline." The influence of an initial production rate of 7 per month increasing to 11 per month and the manufacturing learning curves can clearly be seen on the manufacturing cost curve. The airline payments shown on figure 5 are for an aircraft price of $20 million per aircraft with a prepayment schedule of 5% down on order (assumed two years before delivery), 25% in payments from order to delivery, and 70% on delivery. The notches in the airline payment curve reflect a production adjustment at the end of the 7 per month production period and end of the production run to match the required demand.

The cumulative manufacturer cash flows (without any discounting) are illustrated in figure 6. The net cash flow curve indicates a bucket of about $1.5 billion just after first delivery and a breakeven point 2-1/2 years after first delivery. The manufacturer internal rate of ROI (corresponding to the discount rate which makes the sum of the discounted cash flows equal to zero) is shown as a function of aircraft price and total production quantity in figure 7. For an ROI of zero (corresponding to constant dollars), the required aircraft price is a little over $11 million for a production run of 872 aircraft or $15.7 million for a production run of 436 aircraft. The ROI for 436 aircraft corresponds to the case when two manufacturers compete for the same market and make the same RDT&E investments or when a manufacturer estimates a price based on that production quantity. For a more reasonable

ROI of 15%, the required prices are $14 million for 872 aircraft or $20.5 million for 436 aircraft.

AIRLINE ROI VERSUS PRICE

The airline ROI versus price estimation procedure is illustrated in figure 8. The first step in this procedure involves the calculation of the aircraft direct and indirect operating costs using a computer program called OPLIFE. This calculation requires input information on the aircraft weights and performance characteristics; aircraft price, prepayment schedule, and depreciation schedule; and airline labor and overhead rates. The DOC relationships were developed by the Massachusetts Institute of Technology (refs. 6 and 7) and represent a modification of the 1967 Air Transport Association (ATA) formulae updated to agree with the actual operating expenses reported by the U.S. domestic trunks to the CAB in 1975. The IOC relationships were also developed by MIT (ref. 8) using the CAB Version 6 costing methodology (ref. 9) developed to meet the costing needs of the Domestic Fare Structure Study which the CAB initiated in 1966 (ref. 10). These IOC costs reflect the 1973 operational experience for the U.S. domestic trunk airlines.

The DOC and IOC as well as the assumed aircraft price and prepayment and depreciation schedules are input to an airline ROI calculation. This program uses the discounted cash flow method to calculate the aircraft internal rate of ROI over a specified operational period. This computer program was developed by MIT (ref. 11) around a basic methodology developed in 1971 by Eric Anderson of NASA Ames Research Center. This ROI calculation can be tailored for a variety of considerations including yearly variations in revenues per year, operating costs per year, different prepayment or depreciation schedules, interest rates for external financing, as well as different corporate tax rates and capital gains tax rates. Although the ROI in this example is for a single aircraft operated at an average stage length over its entire operational period, the ROI calculation procedure can handle up to 100 aircraft in a fleet purchased by an airline over a planning horizon of 25 years. For this example the revenue per year is input to the ROI calculation, but it could also be made a function of the traffic volume, as indicated in figure 8. The assumptions used for this example are:

(a) DOC & IOC - MIT Mod. of ATA & CAB

(b) Annual revenue input

(c) Investment--5% down two years before delivery - 25% payments until delivery - 70% balance financed @ 10% on delivery

(d) Depreciation--double declining for 8 years - (ECLIFE/2)-straight line for next 8 years - 15% residual value - recovered at 16 years

(e) 48% corporate income tax rate.

The tax computation reflects normal corporate practices and takes into account the carrying backwards and forwards of normal operating losses as well as of capital gains and losses.

The resulting airline ROI is shown as a function of aircraft price and revenues per year in Figure 9. In this case, the ROI calculation after taxes already includes interest of 10% on the 70% of the aircraft price which is financed on delivery. The $8.0 million revenue per year level corresponds to the revenue which would occur if the fares resulted in a yield per RPM equal to the 1975 average yield for the U.S. domestic airlines. If the airline required a 15% ROI and the fares resulted in revenues of $8.0 million per year, the airline could pay up to $17.5 million for the new propfan transport. If the aircraft price is higher, the fare levels would have to be raised to achieve the same ROI. Or if the aircraft price were lower, the fares could be reduced for the same ROI level.

ABC-ART EXAMPLE CONCLUSIONS

If we overlay the manufacturer ROI versus price and airline ROI versus price relationships we can see the tradeoffs that result (fig. 10). If we assume that a 15% ROI is a reasonable target for both the manufacturer and the airline there are several values of aircraft price that may be acceptable depending on the manufacturer production quantity or airline fare levels. If the manufacturer price is $14 million, based on the full 872 aircraft production quantity, the airline could also achieve a 15% ROI at a fare level 6.25% lower than the 1975 levels. If the manufacturer price of $20 million is based on one-half of the projected market or 436 aircraft, the airline fare levels would have to be raised by 6.25% to achieve a 15% airline ROI.

In summary, the example conclusions from this cost-benefit methodology are:

(a) U.S. airline medium range market requires 872 new propfan aircraft from 1987-1995

(b) 1987 propfan could save 38×10^9 liters (240 million barrels) of fuel from 1987-1995

(c) Fuel savings equal $4.0 billion @ 10.6¢ per liter (40¢ per gallon)

(d) Manufacturer price for 15% ROI must be at least -- $14M for 872 aircraft production - $20M for 436 aircraft

(e) Airline cost for 15% ROI must be less than -- $17.5M for 1975 fare levels - $20.5M for 1975 fare levels plus 6%

(f) At 15% ROI the 1987 propfan appears economically feasible.

Based on the assumptions in this example, the U.S. airline medium range aircraft market would require 872 new propfan transports from 1987 to 1995. During this period alone, the 1987 propfan could save 38×10^9 liters (240 million barrels) of fuel. This fuel saving equals $4 billion at a fuel price of 10.6¢/liter (40¢/gallon). The manufacturer price for a 15% ROI must be at least $14 million for an 872 aircraft production run or $20 million for a production run of 436 aircraft. The airline cost for a 15% ROI must be less than $17.5 million at 1975 fare levels or $20.5 million at 1975 fare levels plus 6.25%. It appears that a reasonable aircraft price could be found where the 1987 propfan would be economically feasible.

POTENTIAL ABC-ART APPLICATIONS

This example has only indicated one potential application of the ABC-ART methodology. This tool can also be applied to examine many air transportation system interactions. These interactions should include the examination of a general airline route network and aircraft mix. This would insure that the overall system benefits for a new aircraft are obtained. Otherwise it is possible to miss some of the benefits that can occur when an aircraft improves the total system operation by allowing the other aircraft in the fleet to be used more efficiently. The examination of the economic feasibility of a new aircraft should also include the examination of other alternatives, particularly the continued production of the existing aircraft. The potential ABC-ART applications are:

(a) Examine system interactions

  (1) General airline route network and aircraft mix
  (2) Compare aircraft alternatives
  (3) Fare-demand elasticity

(b) Develop technology goals

  (1) Operating cost improvements versus aircraft cost
  (2) Evaluate technology scenarios under economic constraints
  (3) Noise, emission, congestion benefits
  (4) Subsidy -- fare surcharge questions

Questions involving fare-demand elasticity can be addressed by adding another interactive feedback loop to the entire process to take the required fare levels, compute the resulting demand, and recompute the projected fleet requirements. The ABC-ART methodology can also be used to develop technology goals. It can examine the tradeoffs in operating cost reductions versus aircraft cost increases. It can be used to evaluate technology scenarios under economic constraints to insure that the assumptions on new aircraft appear reasonable. Other benefits of technology can also be calculated. The capability to examine aircraft noise has been added to the ABC-ART under a NASA contract with the Stanford Research Institute. This capability is currently being used to examine future noise reduction scenarios in cooperation with the FAA.

Because the ABC-ART fleet projection estimates numbers of aircraft of each type in the future years, this information can also be used to indicate potential emission and congestion effects. The ABC-ART methodology can also examine subsidy and fare surcharge requirements and the impact of new technology on these requirements.

In conclusion, the ABC-ART methodology is not capable of predicting the future, but it can be a useful tool for examining many air transportation system alternatives and provide guidance on what is required to move in the preferred direction.

REFERENCES

1. Staff, NASA Office of Aeronautics and Space Technology: Aircraft Fuel Conservation Technology. Task Force Report, Sept. 10, 1975.

2. Staff, Civil Aeronautics Board: Aircraft Operating Cost and Performance Report. 1975.

3. Staff, Planning Research Corporation: Methodology for Estimating Development, Production, and Operating Costs of Transport Aircraft, PRC R-634, Dec. 1964.

4. Beltramo, M. N.; Trapp, D. L.; Komoto, B. W.; and Marsh, D. P.: Parametric Study of Transport Aircraft Systems Cost and Weight, Science Applications, Inc., Economic Analysis Division, NASA CR-151970, 1977.

5. Anderson, Joseph L., and Beltramo, Michael N.: Development of Transport Aircraft Systems Cost and Weight, NASA TM X-73186, 1976.

6. Evani, Sunder: 1975 Update of U.S. Airline Operating Costs, FTL 77-1, Flight Transportation Laboratory, Massachusetts Institute of Technology, Jan. 1977.

7. Ausrotas, Ray, and Evani, Sunder: FTL75 Method of Estimating Comparative Direct Operating Costs of Turbojet/Turbofan Powered Transport Airplanes, Flight Transportation Laboratory, Massachusetts Institute of Technology, 1977.

8. Evani, Sunder: FTL73 Method of Estimating Comparative Indirect Operating Costs of Turbine Powered Transport Airplanes and Computer Program INDIR (IOC 73). Flight Transportation Laboratory, Massachusetts Institute of Technology, May 1977.

9. Staff, Civil Aeronautics Board: Costing Methodology, Version 6 Updated, Domestic Fare Structure, CAB Report, June 1976.

10. Staff, Civil Aeronautics Board: Domestic Passenger Fare Investigation, January 1970 to December 1974 (Appendix B, Phase 9) CAB Report, U.S. GPO-003-006-00071-9, 1975.

11. Evani, Sunder: User's Memo for RICAF, A Computer Program for Estimating the Operating Costs and Return on Investment for the Life of a Commercial Aircraft Fleet, Flight Transportation Laboratory, Massachusetts Institute of Technology, Nov. 1977.

TABLE I.- BASELINE AIRCRAFT DATA U.S. TRUNKS 1975.

AIRCRAFT TYPE	MARKET (RANGE)	INTRO. YEAR	NO. OF SEATS	FUEL CONSUMP. kg/SEAT km	FUEL CONSUMP. lb/SEAT mi	BLOCK SPEED km/hr (mph)	UTILIZATION hrs/yr	RETIREMENT AGE years
2ENBTF	SHORT	HIST.	89.7	0.0608	(0.2157)	501 (311)	2849	16
3ENBTF	MED	HIST.	112.2	0.0603	(0.2140)	576 (358)	3079	16
4ENBTJ	MED & LONG	HIST.	134.0	0.0711	(0.2523)	657 (408)	2509	16
4ENBTF	MED & LONG	HIST.	144.3	0.0552	(0.1959)	650 (404)	3102	16
3EWBTF	LONG	HIST.	236.3	0.0438	(0.1553)	663 (412)	3042	16
4EWBTF	LONG	HIST.	352.6	0.0394	(0.1398)	731 (454)	3259	16
N2EWBPF	MED	1987	171.0	0.0321	(0.1140)	576 (358)	3079	16

REF: AIRCRAFT OPERATING COST AND PERFORMANCE REPORT – CAB JULY 1976

TABLE II.- 1987 PROPFAN AIRCRAFT COST ESTIMATION (MILLIONS OF DOLLARS).

RESEARCH, DEVELOPMENT, TEST, AND EVALUATION			
AIRFRAME DESIGN AND ENGINEERING DEVELOPMENT			223.73
SUBSYSTEMS DEVELOPMENT			130.27
PROPULSION DEVELOPMENT			466.32
DEVELOPMENT SUPPORT			445.44
GROUND TEST VEHICLES (1.0)		26.49	
GROUND TEST SPARES		2.65	
FLIGHT TEST SPARES		22.57	
TOOLING AND SPECIAL TEST EQUIPMENT		330.45	
FLIGHT TEST OPERATIONS		32.92	
GROUND SUPPORT EQUIPMENT		28.11	
TECHNICAL DATA		2.26	
			(1265.76)
(MANUFACTURING – FIRST UNIT)		(34.74)	
AIRFRAME	(26.49)		
AVIONICS PROCUREMENT	(.62)		
PROPULSION PROCUREMENT	(5.98)		
FINAL ASSEMBLY AND CHECKOUT	(1.65)		
AIRCRAFT PRODUCTION,			
OPERATIONAL VEHICLES (872.0)			5111.83
SPARES			918.51
FACILITIES			0.00
SUSTAINING ENGINEERING			642.89
SUSTAINING TOOLING			522.21
GROUND SUPPORT EQUIPMENT			766.77
TECHNICAL DATA			102.24
MISCELLANEOUS EQUIPMENT			10.46
TRAINING EQUIPMENT			34.43
INITIAL TRAINING			261.60
INITIAL TRANSPORTATION			34.21
			(8405.16)
TOTAL COST			9670.92
TOTAL NUMBER OF FLIGHT VEHICLES PRODUCED			872
AVERAGE UNIT AIRPLANE COST			$11.09M

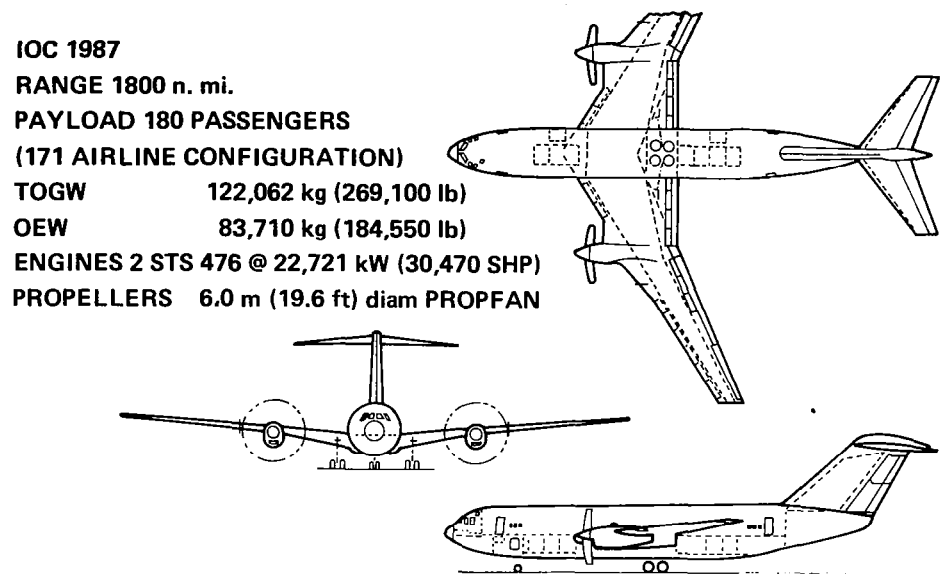

Figure 1.- Candidate new propfan aircraft - Boeing propfan study aircraft (767-762).

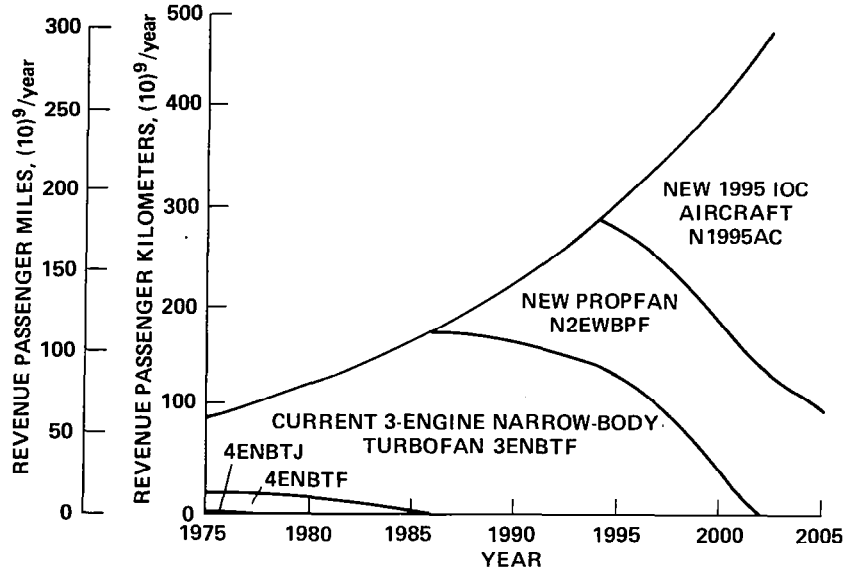

Figure 2.- Medium range aircraft market share by aircraft type. 6%/yr RPM growth.

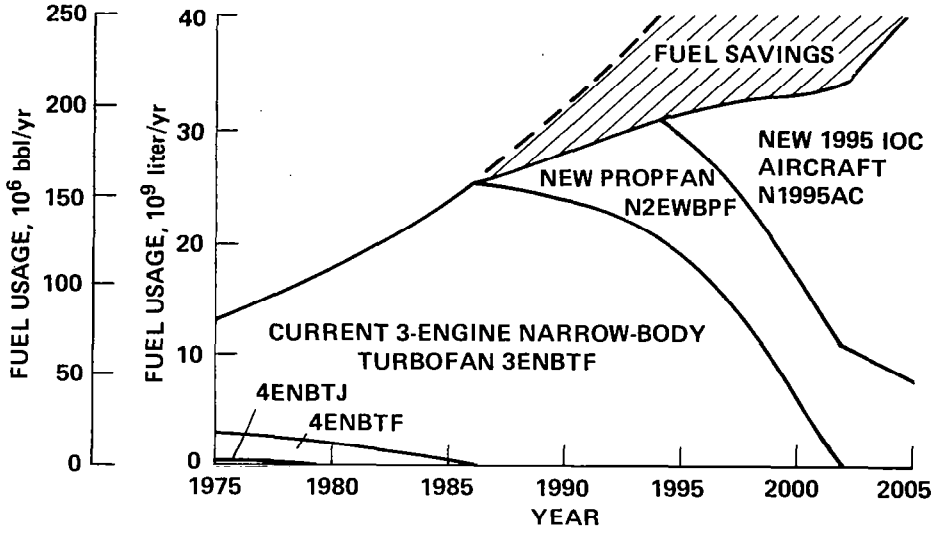

Figure 3.- Medium range aircraft fuel usage by aircraft type. 6%/yr RPM growth.

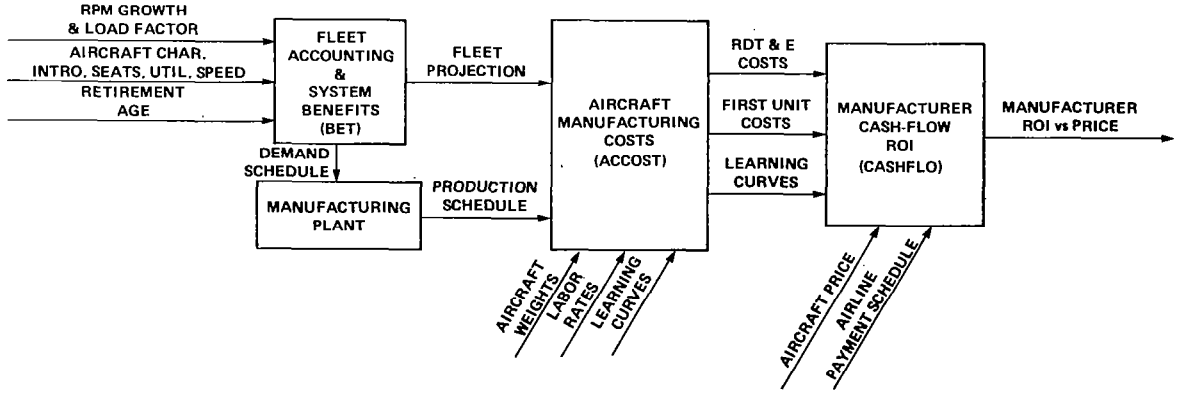

Figure 4.- Manufacturing ROI versus price estimation procedure.

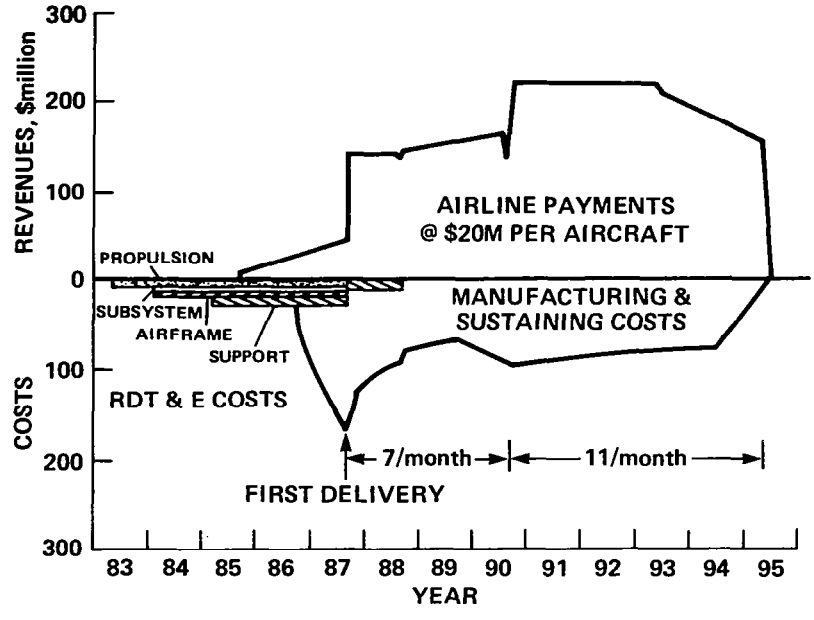

Figure 5.- Manufacturer cash flows per month.

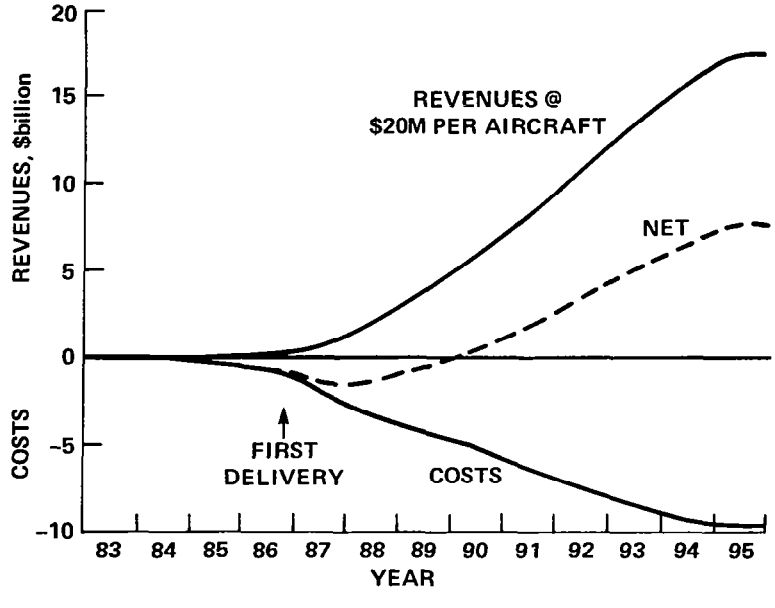

Figure 6.- Manufacturer cumulative cash flows.

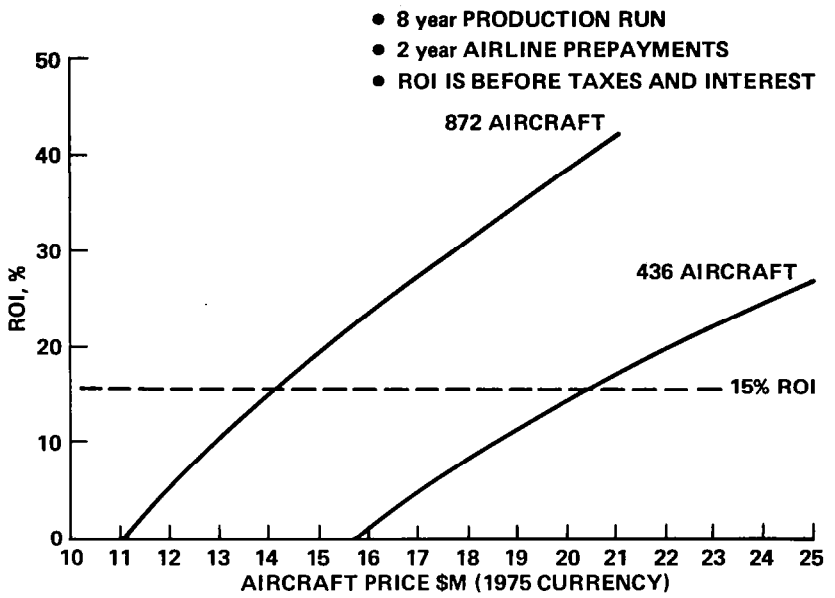

Figure 7.- Manufacturer ROI versus price.
1987 propfan aircraft.

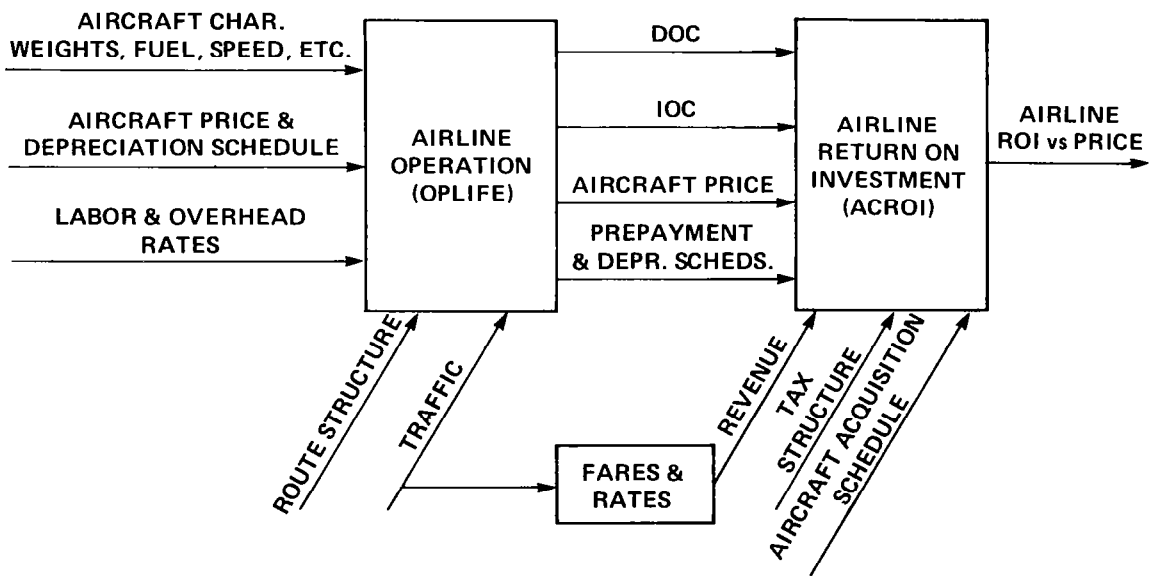

Figure 8.- Airline ROI versus price estimation procedure.

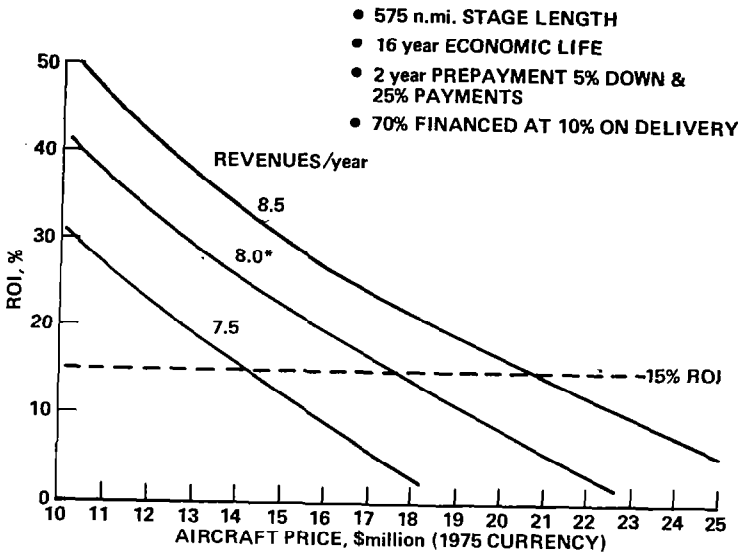

*CORRESPONDS TO REVENUES BASED ON 1975 U.S. DOMESTIC AVERAGE YIELD = 7.68¢/RPM

Figure 9.- Airline ROI versus price.
1987 propfan aircraft.

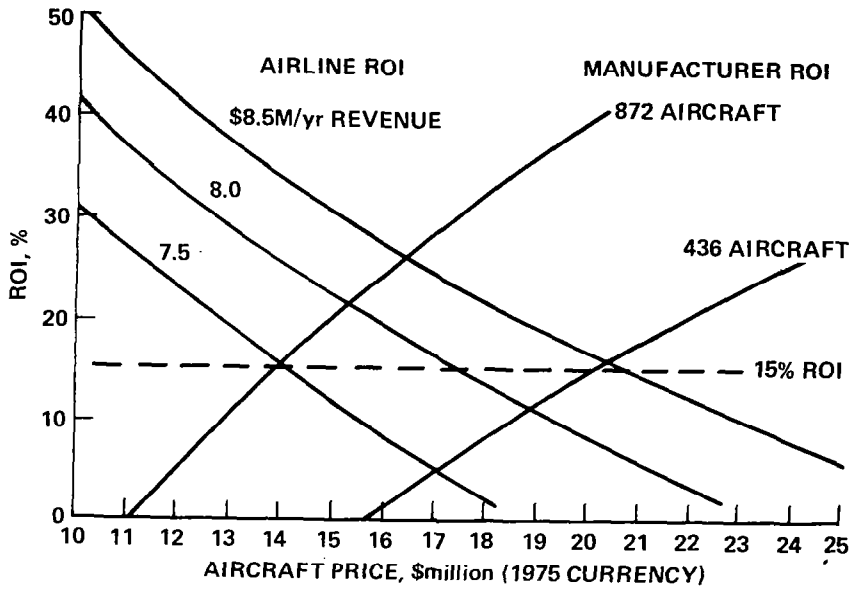

Figure 10.- Industry ROI'S versus price.
1987 propfan aircraft.

ADVANCED SYSTEMS OVERVIEW

William S. Aiken, Jr.
NASA Headquarters

The previous sessions of this conference on CTOL transport technology have covered in great detail technological progress for what we might call conventional CTOL aircraft and their related systems problems. In this final session, we are going to take a brief look at some of the problems, possibilities, and progress for somewhat less conventional forms of air transportation which may be needed in the future and for which the technology data base is, for the most part, quite incomplete. To be discussed are short-haul aircraft, supersonic cruise aircraft, air systems using coal-derived fuels, and unconventional vehicles. In the final paper on unconventional vehicles, we will hear about long-range aircraft incorporating special laminar-flow concepts and a continuously flying aerial relay transportation system utilizing cruise liners and feeder aircraft.

From my point of view, there are several major goals for passenger air transportation systems of the future. They are

Get there
Get there cheaper using less energy
Get there faster

all with today's levels of convenience and comfort to the passengers. In addition, the possibilities for increased cargo movement by air raise some interesting technical, economic, and logistics problems.

As shown in figure 1, these goals can be related to the themes of the papers to be presented in this session. Getting there and getting there using less energy are primary goals of future aircraft to be used in short-haul passenger transportation. By short haul, I mean the operations at flight stage lengths up to about 800 kilometers (500 miles) by the U.S. trunk airlines, local service carriers, and commuter airlines. As shown in figure 2, the FAA forecast to 1989 indicates almost a doubling of passenger enplanements for U.S. certificated route air carriers. In addition, as shown in figure 3, the FAA forecasts more than a doubling of passenger enplanements on U.S. commuter airlines. The importance of the short-haul market becomes more apparent when you learn, for example, that in August 1974 the U.S. scheduled carriers used 28 percent of their fuel in flights with stage lengths up to 800 kilometers. In that year, 1974, the average overall flight stage length of all U.S. certificated route air carriers was about 800 kilometers, with the local service airlines averaging less than 320 kilometers (200 miles). It would appear that a fairly large number of advanced, fuel-conservative, short-haul aircraft will be needed in the future to handle the forecasted passenger demand.

In the supersonic cruise area, the major goal is, of course, to get there faster. It is of interest to speculate on the potential market which speed could bring to international travel, by looking back to see what happened when we made the transition from propeller-driven aircraft to jets. Figure 4 shows

the dramatic growth in international air travel from 1958 to 1975: across the Atlantic, a 10-to-1 increase and in the Pacific, a 20-to-1 increase. In the future supersonic age, similar, almost step-function increases appear possible. Getting there faster will also mean more people getting there, because supersonic operations can be scheduled at times other than those used by subsonic aircraft.

With respect to energy use, the projections shown in figure 5 for the year 2000 indicate that U.S. demands for energy will exceed our domestic production by over 20 percent, with transportation demands alone exceeding our domestic petroleum production. Thus it is important to consider now how coal-derived fuels for aircraft might be used to shift some of the demand burden from petroleum.

Before getting into the papers in this session, I would like to show you a third FAA forecast — namely air cargo, because this subject will be discussed in the last paper today. Figure 6 shows an almost tripling of U.S. domestic air cargo traffic. With this projected increase, it is appropriate to begin serious study of the possibilities which might be offered by unconventional aircraft using less energy and becoming part of the air cargo system of the future.

The first paper in this session, by Lou Williams of Ames Research Center, will address some of the problems and potential solutions for aircraft operations in the high-density part of the short-haul market. The paper will not cover the low- to medium-density part served by smaller aircraft, an aspect we are now just beginning to look at with the objective of identifying what really needs to be done from a technology standpoint.

The next paper, by Neil Driver of Langley Research Center, is a progress report on the status of the technology base deemed vital to any expanded effort, up to the point of technology readiness, for future supersonic transports.

Coal-drived fuels and their application to aircraft systems are the subject of Bob Witcofski's paper. In the paper presented earlier in this conference by Jack Grobman of Lewis Research Center, titled "Impact of Broad Specification Fuels on Future Jet Aircraft," The characteristics of fuels required by jet engines were covered. These same characteristics apply to the synthetic jet-type fuels which will be covered in Witcofski's paper.

The last paper in this session on advanced transport aircraft is, it seems to me, an appropriate one with which to close this conference. In this paper by Del Nagel of Langley Research Center you will see that considerable imagination has been applied and the aircraft systems to be discussed are, to say the least, unconventional and certainly for the future.

THEME OF SESSION PAPERS	GOAL		
	GET THERE	GET THERE CHEAPER USING LESS ENERGY	GET THERE FASTER
SHORT HAUL	✓✓	✓✓	
SUPERSONIC CRUISE	✓		✓✓
COAL-DERIVED FUEL	✓	✓✓	
UNCONVENTIONAL AIRCRAFT	✓	✓✓	

✓✓ PRIME RELATIONSHIP ✓ SECONDARY

Figure 1.- Air transportation system goals as related to themes of session papers.

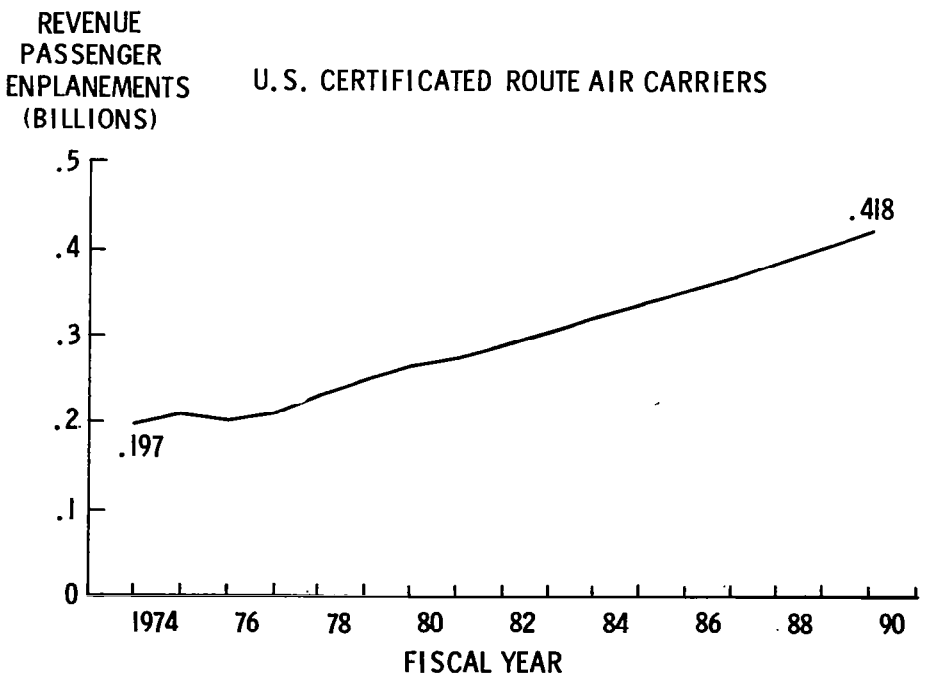

Figure 2.- FAA forecast - 1978 to 1989 - for U.S. certificated route air carriers.

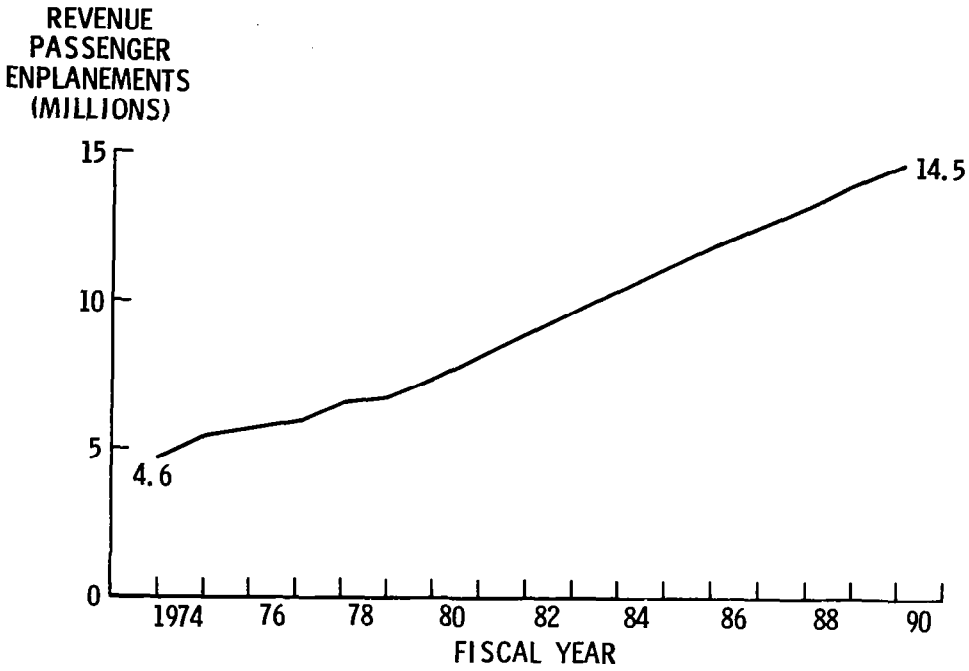

Figure 3.- FAA forecast - 1978 to 1989 - for U.S. commuter airlines.

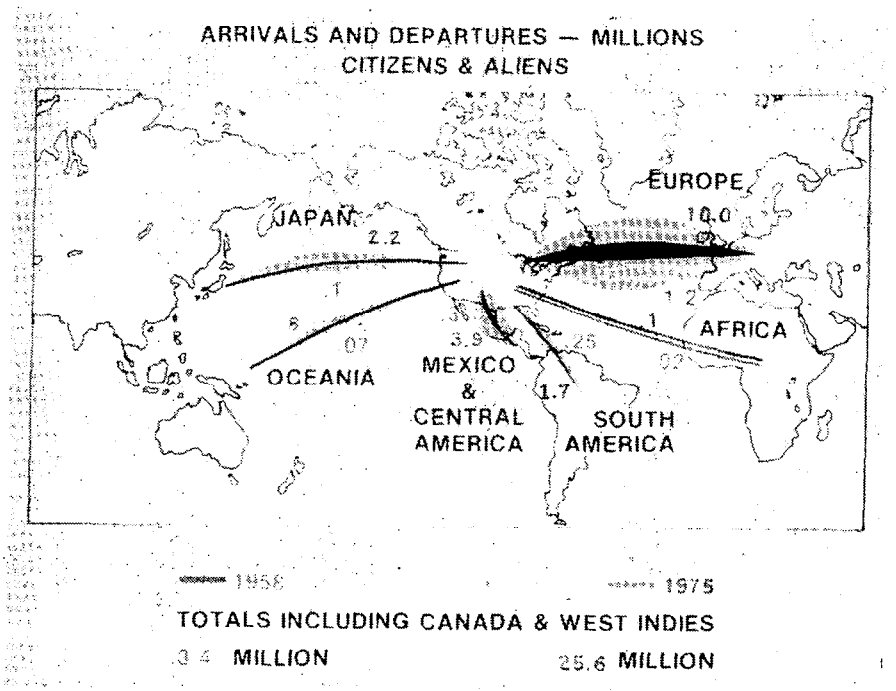

Figure 4.- Growth of international air travel with jet transports.

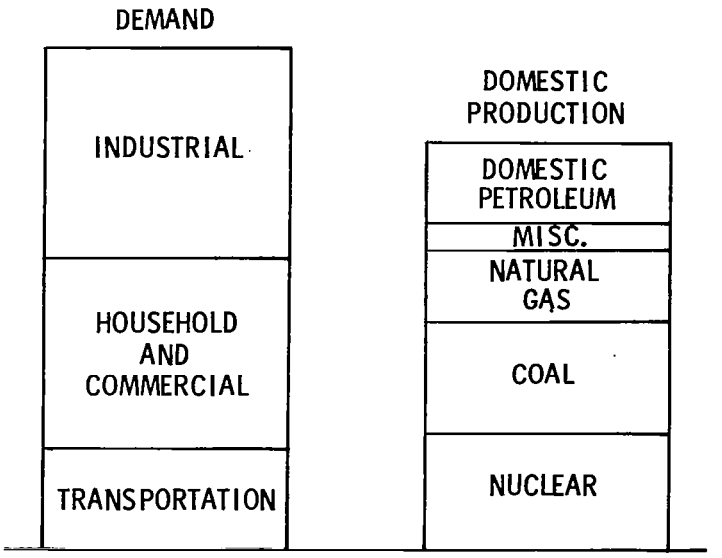

Figure 5.- U.S. energy balance projection for year 2000.

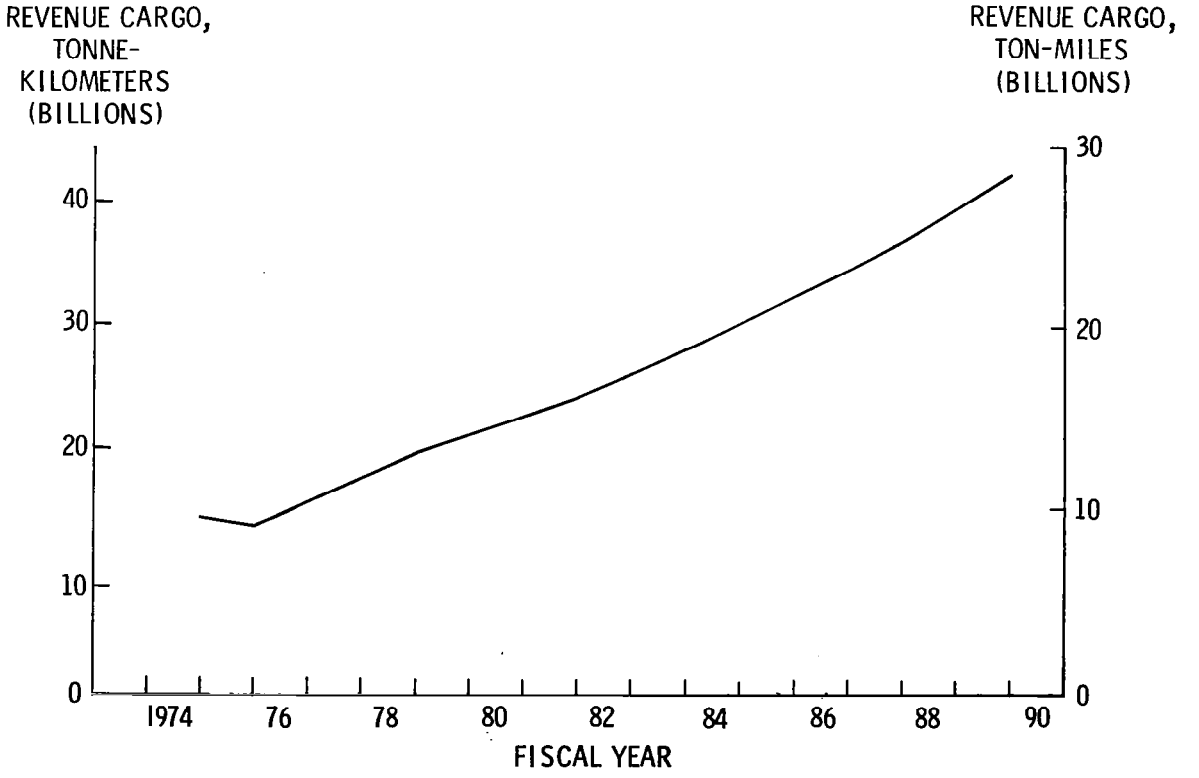

Figure 6.- FAA forecast - 1978 to 1989 - for U.S. air cargo traffic at U.S. airports.

SHORT-HAUL CTOL AIRCRAFT RESEARCH

Louis J. Williams
NASA Ames Research Center

SUMMARY

This summary paper reviews the results of the reduced energy for commercial air transportation (RECAT) studies on air transportation energy efficiency improvement alternatives, reviews subsequent design studies of advanced turboprop powered transport aircraft, and discusses the application of this research to short-haul air transportation. Although much has already been published on the RECAT studies, the results of these studies are far from obsolete, and it is important to briefly review these results because of their importance to the ongoing ACEE program. Although most of the ACEE program technology will be applicable to advanced short-haul transport aircraft to some degree, the advanced turboprop is particularly attractive. This will be demonstrated by reviewing the results of several recent turboprop aircraft design studies. The potential fuel savings and cost savings for advanced turboprop aircraft appear substantial, particularly at shorter ranges.

INTRODUCTION

Currently, civil air transportaion consumes about 38 billion liters (ten billion gallons) of fuel annually. While this amounts to less than 2 percent of the total U.S. energy consumption and only 4 percent of the total U.S. petroleum consumption (ref. 1), air transportation is currently 100 percent dependent on petroleum fuels and strongly influenced by the availability and cost of these fuels. Maintaining a healthy air transportation system is important. At present, for any trip greater than a few hundred kilometers, there is no other transportation alternative that can compare in terms of speed, passenger comfort, and reliability. Until such a substitute can be found, we must examine ways to improve air transportation's energy efficiency. Even when alternative fuels are developed, they will undoubtedly be high priced and energy efficiency will still be very important.

Increasing aircraft energy efficiency is not a new objective. It has always been important in terms of performance and operating cost, even at pre-embargo prices. The energy efficiency of the newer, stretched narrow-body jet aircraft is better than the initial smaller jet aircraft and the newest wide-body aircraft are the most energy efficient (fig. 1). From 1965 to 1975, these more efficient aircraft have been added to the airline fleet and the older turbojet aircraft have been replaced (fig. 2). As a result, the average energy efficiency, measured in seat-kilometers per liter (seat-miles per gallon), of the U.S. trunk airlines has increased by 33 percent (fig. 3) over this ten-year period.

An examination of the current U.S. scheduled air carrier fuel usage by stage length and equipment type (fig. 4, refs. 2 and 3) reveals the dominance of the short/medium range operations by the Boeing 727 aircraft. Because of the large number of B727's in service, this single aircraft type currently accounts for 35 percent of the total airline fuel usage (fig. 5). It is also important to note that 53 percent of the airline fuel is used for stage lengths of less than 1600 kilometers (1000 miles) and over 30 percent is used for stage lengths of less than 800 kilometers (500 miles).

While fuel efficiency was important when these aircraft were designed in the 1960's, it has now become one of the major design goals. Until the middle of 1973, the price that the airlines were paying for jet fuel had remained constant for many years. However, since that time, these fuel prices have tripled (fig. 6). Even though labor costs have also increased substantially over this period, these fuel price increases have resulted in fuel cost accounting for a much larger fraction of direct operating cost. In 1973, fuel cost amounted to 25 percent of the direct operating cost for average operation of a Boeing 727; by 1975 it had risen to 38 percent. At the current level of U.S. airline fuel use of 38 billion liters (10 billion gallons) per year, each 0.3-cent per liter (one-cent per gallon) increase in the price of fuel costs the airlines 100 million dollars. Even ignoring the desire to increase airline energy efficiency from a conservation viewpoint, these price increases provide considerable incentive.

RECAT STUDY

From 1974 to 1976 a study examining the "Cost/Benefit Tradeoffs for Reducing the Energy Consumption of the Commercial Air Transportation System," referred to as RECAT, was conducted under NASA sponsorship. This study involved the coordinated efforts of the Douglas Aircraft Company (ref. 4), Lockheed-California Company (ref. 5), United Air Lines, Inc. (ref. 6), and United Technologies Research Center (ref. 7). The purpose of this study was to examine, on a common basis, many of the alternatives for increasing the energy efficiency of air transportation in order to identify the most promising areas for research and technology emphasis. The alternatives considered included operational procedures (higher density seating, higher load factors, and flight procedures), aircraft modifications, derivatives of current production types, and new aircraft exploiting advanced technology in aerodynamics, composite structure, active control, and advanced propulsion.

Aircraft Operation

One of the quickest methods of increasing aircraft energy efficiency, as measured on a seat-kilometer per liter (seat-mile per gallon) basis, is to increase the number of seats on the aircraft. This can be done by eliminating lounges and garment bag storage areas, reducing the first class/coach seating ratio, increasing the number of seats abreast, and by reducing the seat pitch. Since 1973, the airlines (as indicated by data from United Air Lines) have increased the seating density considerably by these methods. To serve as a

basis of comparison in the RECAT studies, a baseline increased density seating configuration was specified. This seating configuration represents a 10 percent first class/90 percent coach arrangement with 965-mm (38 in.) first class/ 864-mm (34 in.) coach seat pitch and seats in place of garment bag storage on the Boeing 727 and 737 aircraft. These seating density increases result in aircraft energy efficiency increases ranging from 5 to 22 percent relative to 1973 (fig. 7).

While these increases in seating density look very favorable in terms of energy efficiency measured in seat-kilometers per liter (seat-miles per gallon), they really represent a ficticious improvement unless the number of passengers per flight increases also. The increase in passengers per flight can be obtained by increasing the seating density and holding the passenger load factor constant or just increasing the load factor. An increase in load factor from 50 to 60 percent is equivalent (in terms of passengers carried) to a 20 percent increase in seating density with a constant load factor of 50 percent. When frequency of service, load factor, and seating density are considered, the most efficient aircraft for transporting passengers over a given route network is not necessarily the aircraft with the highest energy efficiency in seat-kilometers per liter (seat-miles per gallon). For example, over a 1000 n. mi. stage length (fig. 8), even though a Boeing 737 (17 seat-kilometers per liter (39 seat-miles per gallon)) is some 26 percent less energy efficient in seat-kilometers per liter (seat-miles per gallon) than a DC10 (23 seat-kilometers per liter (53 seat-miles per gallon)), the B737 is the most energy efficient aircraft in terms of passenger-kilometers per liter (passenger-miles per gallon) for carrying less than 97 passengers.

In addition to passenger capacity, another factor which must be considered when comparing aircraft energy efficiency is the aircraft's range capability. For example (fig. 9), at short stage lengths the Boeing 737-200 is more energy efficient in seat-kilometers per liter (seat-miles per gallon) than the Boeing 727-200 or Douglas DC8-61. However, at medium stage lengths, the B727-200 is more energy efficient than the B737-200 or DC8-61. And at longer stage lengths, beyond the capability of the B737-200, the DC8-61 is more energy efficient than the B727-200. In order to provide the long range capability of the DC8-62 or the B747-100, some penalty in shorter range energy efficiency is incurred. In order to maximize aircraft energy efficiency, it is very important to critically examine the desire for extra range capability for scheduling flexibility against the actual range required for the stage lengths on which the aircraft will be flown.

Although the energy efficiency improvements possible with increased seating density and higher load factors are large initially, they are limited in extent and are obtained at the expense of passenger comfort and convenience. Another means of increasing aircraft energy efficiency is with fuel conservative flight procedures and increased aircraft maintenance. In the RECAT studies these operational alternatives were grouped into those that could be implemented within the current air traffic control (ATC) system and those that could be obtained with ATC advances (fig. 10). Within the current ATC system small percentage improvements in energy efficiency can be obtained by reducing cruise speed to long range cruise (maximum n.mi. per kg of fuel) levels,

reducing the current step climb increment from 1.2 to 0.6 km (4000 to 2000 ft) to allow closer adherence to optimum cruise altitudes, loading the aircraft closer to the aft c.g. to reduce trim drag, increasing airframe maintenance to reduce excrescence drag, reducing the operating empty weight slightly by removing any accumulated unnecessary equipment, and increasing engine maintenance to reduce the engine specific fuel consumption deterioration with time. Additional operational energy efficiency improvements that require ATC system advances include cruise climb to maintain the optimum cruise altitude, reducing holding delays by an average of one minute, and reducing terminal area delays by an average of four minutes. While the individual fuel savings that are obtainable with improved flight procedures and increased aircraft maintenance attention are small, the summation is significant and worthy of attention.

Aircraft Modification

Another means of improving aircraft energy efficiency, without sacrificing passenger comfort and convenience, is by modification of the current aircraft types. In the RECAT study, the modifications that were examined ranged from adding improved aerodynamic fairings to retrofitting with new engines (fig. 11). The effect of the most promising modifications on the respective aircraft energy efficiency ranged from 4 to 39 percent. The largest aircraft energy efficiency increase was obtained by replacing the existing turbojet engines on the DC8-20 with new refan JT8D engines. However, this modification was estimated to cost about $5 million per aircraft and appeared economically unattractive unless required for some other reason, such as noise abatement. While the aerodynamic modifications offered smaller percentage improvements on the order of 4 to 8 percent, the estimated modification costs were also considerably smaller and appeared economically reasonable. This was particularly true for those aircraft that are expected to remain in service for many years.

Derivatives and New Turbofan Powered Aircraft

Some of the more extensive design modifications are only feasible for new production versions or derivatives of the current aircraft. Derivatives are of interest because they allow the manufacturer and the airlines to capitalize on the experience that has been obtained on that aircraft type and to minimize the development expense that is required. In the past, the most common derivatives have involved a fuselage stretch to increase the aircraft capacity in response to increasing passenger demand. Now, in addition to this desire and with much higher fuel costs, these derivatives must also be designed to operate more efficiently. The effect of increased fuel price on aircraft design is reflected, of course, in increased emphasis on aerodynamics, structures, and propulsion efficiency. Externally, this is most evident in the wing design. At yesterday's fuel prices, the optimum aircraft for minimum direct operating cost (DOC) was designed to cruise at Mach 0.85 and had a wing aspect ratio of about 8 and a wing sweep of about 35°. At a fuel price of 16¢/liter (60¢/gallon), the optimum turbofan powered aircraft for minimum DOC would cruise at Mach 0.78 and have a wing aspect ratio of about 11 and a wing sweep of 28°. If the aircraft was designed for minimum fuel usage, regardless of the economics,

the optimum cruise speed drops to Mach 0.7 with a straight wing and a wing aspect ratio over 15.

New Turboprop Powered Aircraft

In the 1950's, the seemingly unlimited supplies of cheap jet fuel coupled with the speed and altitude advantages of the turbojet resulted in its being favored over the 1950's turboprop. Today's environment of higher fuel prices and energy conservation have necessitated a re-examination of the turboprop--not the 1950's version, but a new, highly loaded, multibladed turboprop using advanced blade structure and aerodynamics technology for efficient, high-speed operation. Because this concept lies between the conventional turboprop and an unshrouded, high bypass ratio turbofan, the Hamilton-Standard Division of United Technologies refers to it as the propfan. Based on analysis and wind-tunnel tests (ref. 8), the propulsive efficiency of the advanced turboprop or propfan is about 20 percent better at Mach 0.8 than a high bypass ratio turbofan (fig. 12). This efficiency advantage is even greater at lower speeds, increasing to 35 to 40 percent at Mach 0.7. In order to evaluate the overall impact on complete configurations and to identify the critical technology areas, three design studies of propfan powered aircraft have been completed to date.

Because of different study ground rules and assumptions, the propfan aircraft fuel savings identified in these three studies ranged from 8 to 28 percent in comparison with their turbofan counterparts for a 1000 n.mi. stage length (fig. 13). In all cases, the efficiency advantages of the propfan compared to the turbofan are greater at lower altitudes and speeds, and this results in larger fuel savings at shorter stage lengths. This is one reason why the propfan looks particularly attractive for the short- and medium-haul markets currently being served by the short-medium range DC9, B737, and B727 aircraft.

The largest fuel savings identified in these studies were for a propfan derivative DC9-30 investigated by the Douglas Aircraft Company. For this comparison, the derivative was not resized to the same design range as the baseline DC9-30. Instead, the gross takeoff weight and payload were held constant. The takeoff, approach, and cruise performance of the propfan derivative were chosen to match the baseline DC9-30 performance and the propfan was sized for Mach 0.8 cruise at 9-km (30 000 ft) altitude. Two levels of porpfan performance were examined. One propfan design was based on performance levels corresponding to an eight-blade propfan with a rotational tip speed restricted to 67 meters/sec (720 fps), corresponding to the Lockheed Electra Propeller, and current technology turboshaft engine performance. This resulted in a propeller efficiency of 0.73 and an installed cruise thrust specific fuel consumption (TSFC) of 0.066 kg/hr/N (0.65 lb/hr/lb). The other propfan design was based on an eight-bladed propfan with a 74-meters/sec (800 fps) tip speed and turboshaft engine performance corresponding to JT10D/CFM56 turbofan core engine technology. This resulted in a propeller efficiency of 0.80 and an installed TSFC of 0.054 kg/hr/N (0.53 lb/hr/lb). Depending on the assumed propulsion system efficiency, the derivative propfan would use from 27 to

33 percent less fuel than the current DC9-30 at its average operational stage length of 290 n.mi. For the same takeoff gross weight with a passenger load factor of 58 percent, this fuel savings would also translate into a maximum range capability improvement of 41 to 73 percent, depending on the propulsion system efficiency assumed.

The fuel savings shown for the DC9 propfan derivative are larger because the comparison is with an older technology, low bypass ratio, JT8D turbofan rather than a comparable technology turbofan. However, the DC9 propfan derivative does not include the application of any of the other advanced aerodynamics, structures, or active controls technologies that could improve the efficiency still further. Also, the low bypass ratio JT8D engines are the ones that are currently in service and being sold in large quantities on this airplane type.

Another advanced turboprop design study was conducted with the Boeing Commercial Airplane Company (ref. 9). In this study, two propfan powered configurations were compared with an equivalent technology level advanced turbofan powered aircraft. These aircraft were designed to carry 180 passengers in equal comfort for a maximum range of 1800 n.mi. at a cruise speed of Mach 0.8. All three configurations were twin-engine, wide-body aircraft using 1976 design airframe technology and engine technology corresponding to 1980-1985 certification. One propfan design had the engines mounted on the wings, the other had the engines mounted on struts attached to the fuselage aft body. The fuel savings identified in this study were more modest, amounting to 13.5 percent for the wing-mounted propfan configuration at a 500 n.mi. stage length and 13 percent for the aft-mounted configuration. These smaller fuel savings reflect the Boeing study assumptions of a propfan noise level in cruise 10 db higher than the Hamilton-Standard noise goal, resulting in a larger acoustic treatment weight penalty, and an increase in drag due to the effect of the propeller slipstream on the wing aerodynamics. These are two of the critical technology areas that are currently being investigated experimentally.

The most recent advanced turboprop design study was a follow-on to the Lockheed-California Company RECAT study (ref. 10). In the original RECAT study, Lockheed examined a four-engine propfan powered aircraft in comparison with an equivalent technology level advanced turbofan (JT10D) powered aircraft. These aircraft were both designed to carry 200 passengers in equal comfort for a maximum range of 1500 n.mi. at Mach 0.8 cruise speed. The technology levels reflect 1985 service introduction and include a supercritical airfoil, aspect ratio 10 wing, active controls for longitudinal stability augmentation, and composite secondary structure. The most recent Lockheed-California study also used these design groundrules for the baseline turbofan and propfan aircraft but expanded the original study to include a comparison at Mach 0.75 cruise speed, 2000 n.mi. design range, and an investigation of alternative advanced engines. The data shown on figure 13 reflects the latest study results for the 1500 n.mi. design range and the propfan powered by a Pratt & Whitney study turboshaft engine (STS 476) based on the JT10D engine core. The resulting fuel saving for the Mach 0.8 cruise speed propfan aircraft compared to a JT10D technology turbofan at Mach 0.8 cruise speed was 19.6 percent for a typical in-service stage length of 475 n.mi. and a 58 percent passenger load factor. This fuel saving increased to 22.9 percent when the cruise speed was reduced to Mach 0.75 for both of these aircraft.

These fuel savings translate into the DOC savings shown in figure 14. These cost savings are for the average in-service stage length assumed for the three studies and are shown as a function of fuel price. The largest savings in operating cost are indicated for the Lockheed propfan aircraft at a cruise speed of Mach 0.75.

Fuel Savings Potential

The RECAT study examined many alternatives for increasing air transportation energy efficiency. In comparing the energy efficiency of current aircraft, modified versions of these aircraft, new near-term aircraft using current technology, and the 0.8 M Lockheed propfan aircraft (CL-1320), the improvement potential is very encouraging (fig. 15). Compared with the DC8-61 for a 1000 n.mi. stage length, a short-body DC10 derivative could save 26 percent in fuel and provide an energy efficiency improvement of 35 percent in seat-kilometers per liter (seat-miles per gallon); a new near-term aircraft using current technology but designed for minimum DOC with 16¢/liter (60¢/gallon) fuel could save 39 percent in fuel and provide a 64 percent improvement in seat-kilometers per liter (seat-miles per gallon); a new advanced technology propfan aircraft could save 52 percent in fuel and provide a 108 percent improvement in seat-kilometers per liter (seat-miles per gallon).

The relative attractiveness of these alternatives is a question of timing and economics. The potential improvement over time is very high (fig. 16). In the near term, extending from 1972 to 1980, energy efficiency improvements will require strenuous attention to the individually small improvements possible with increased load factor, increased seating density, fuel conservative flight procedures, and the gradual replacement of older aircraft with current production types. The airlines have already accomplished a lot in this direction (ref. 11). As a result, the energy efficiency of the U.S. scheduled airlines has risen from 7.4 passenger-kilometers per liter (17.5 passenger-miles per gallon) in 1973 to 8.8 (20.7) in 1976. The airlines actually used 3 billion liters (800 million gallons) less fuel in 1976 than in 1973, while carrying 21 million more passengers. From 1980 to 1985, the introduction of modifications and derivatives of current aircraft can provide continuing increases in efficiency. And, beyond 1985, sufficient advanced technology should be available to justify the development costs of completely new aircraft. By the end of the century, the energy efficiency of air transportation may be twice what it is today. Regardless of whether petroleum derived fuels are still being used, the fuel will undoubtedly be high priced and precious, and these efficiency improvements will be required.

SHORT-HAUL CTOL RESEARCH

As evidenced by the fact that over half of the fuel used by air transportation is used on stage lengths of less than 1600 kilometers (1000 miles), increasing the energy efficiency of short-haul CTOL transports is extremely important. It appears that most of the research in the ACEE program is equally as applicable to the large short-haul CTOL aircraft as it is to long-haul

CTOL aircraft (with the possible exception of laminar flow control). The problem is just more difficult. The aircraft total operating costs per seat-kilometer are higher at the shorter stage lengths and the IOC's become more important. The aircraft spends a larger fraction of its time at the gate loading and unloading passengers and cargo, taxiing in and out, waiting in line for takeoff, climbing and descending, and being routed around in the terminal area. Because this emphasis on performance in the terminal area was recognized many years ago, NASA embarked on research programs oriented toward short-haul powered lift transports for high density markets. Example programs are the Quiet Short-Haul Research Aircraft (QSRA) and the Quiet Clean Short-Haul Experimental Engine (QCSEE). In addition, NASA will conduct flight experiments with the prototype aircraft developed in the Air Force AMST program (YC14 and YC15). These are technology programs oriented toward a thorough understanding of powered lift aerodynamics combined with high bypass turbofan propulsion technology for transport aircraft with short field length capability. Because the advanced turboprop offers efficiency advantages over the turbofan, particularly at the lower altitudes and speeds encountered more frequently on short-haul flights, it looks particularly attractive for advanced short-haul RTOL and CTOL transport aircraft. In support of advanced turboprop research, Ames Research Center has research underway emphasizing advanced turboprop engine-airframe integration technology. The tradeoffs on aircraft design to improve the efficiency and economics for advanced large short-haul CTOL transport aircraft will continue to be examined as the ACEE program research proceeds.

More recently, a modest program has been initiated which is oriented toward the small short-haul CTOL transport aircraft used by the local service and commuter carriers. This is the area where the lack of modern aircraft technology is most apparent. There are many aircraft used today in short-haul air transportation which represent relatively "old" technology, and there are many others which are being operated very inefficiently at short stage lengths. Development of the appropriate technologies for a new, small short-haul aircraft can only come from a better understanding of the diverse nature of the short-haul market and a clear definition of aircraft requirements both in terms of aircraft characteristics (size, speed, etc.) and possible technology improvements. For civil systems, this can only be done through a continuing interchange of ideas with the aircraft-manufacturing and airline industries and an understanding of possible government regulatory and policy actions. As part of this process, the NASA Ames Research Center sponsored a two-day symposium in November 1977, on small community air service, with emphasis on interregional service. The objective of the symposium was to provide a forum for the discussion of the markets for short-haul air transports, aircraft definition, and technology status and future requirements. Because of the diverse market requirements it is obvious that no one aircraft can be defined in terms of size, cruise speed, and field length to satisfy all short-haul markets in an optimum way. However, it is apparent that the potential exists for advanced technology specifically designed for short haul that will have a positive effect on any new aircraft that is developed.

The appropriate research program for small CTOL transport aircraft is still in the early stages of definition. However, the emphasis to date is

being placed on modern wing technology for cruise at Mach 0.7 to 0.75 with improved aerodynamics, on the application of new materials and structural design techniques for reduced weight and cost, on the development of advanced aircraft systems, on advanced turboprop propulsion systems, on low cost avionic systems, and on improved high-lift devices. With emphasis on potential near-term developments, reduced aircraft initial and operating cost becomes a major criterion for all aspects of this program.

REFERENCES

1. Mascy, Alfred C. and Williams, Louis J.: "Air Transportation Energy Consumption - Yesterday, Today, and Tomorrow," AIAA Paper 75-319, 1975.

2. "Official Airline Guide," published by the Reuben H. Donnelley Corporation, August 1, 1976.

3. Staff, Civil Aeronautics Board: "Aircraft Operating Cost and Performance Report," Report for 1965 through 1975.

4. Kraus, E. F. and Van Abkoude, J. C.: "Cost Benefit Tradeoffs for Reducing the Energy Consumption of the Commercial Air Transportation System," Douglas Aircraft Company; June 1976. Volume I: Technical Analysis, NASA CR-137923; Volume II: Market and Economic Analysis, NASA CR-137924; Summary Report, NASA CR-137925.

5. Hopkins, J. P. and Wharton, H. E.: "Study of the Cost/Benefit Tradeoffs for Reducing the Energy Consumption of the Commercial Air Transportation System." Lockheed-California Company; August 1976. Final Report, NASA CR-137926; Summary Report, NASA CR-137927.

6. Coykendall, Richard E.; Curry, John K.; Domke, Albert E.; and Madsen, Sven E.: "Study of the Cost/Benefit Tradeoffs for Reducing the Energy Consumption of the Commercial Air Transportation System." United Air Lines, Inc.; June 1976; NASA CR-137891.

7. Gobetz, F. W.; LeShane, A. A.; and Dubin, A. P.: "Cost/Benefit Tradeoffs for Reducing the Energy Consumption of Commercial Air Transportation;" United Technologies Research Center, June 1976; Final Report, NASA CR-137878.

8. Staff, Hamilton Standard Division of United Technologies Corporation: "Prop-Fan, Fuel Conservative Propulsion for the 1980's High Speed Air Transports," January 1977; Status Summary, Hamilton Standard SP 02A77.

9. Staff, Boeing Commercial Airplane Company, Preliminary Design Department: "Energy Consumption Characteristics of Transports Using the Prop-Fan Concept." Final Report, NASA CR-137937, October 1976; Summary Report, NASA CR-137938, November 1976.

10. Tullis, R. H. and Revell, J. D.: "Fuel Conservation Merits of Advanced Turboprop Transport Aircraft," Lockheed-California Company, August 1977, NASA CR-152096.

11. Staff, Air Transport Association of America: "Airlines and Fuel Conservation: Doing More with Less," February 1977.

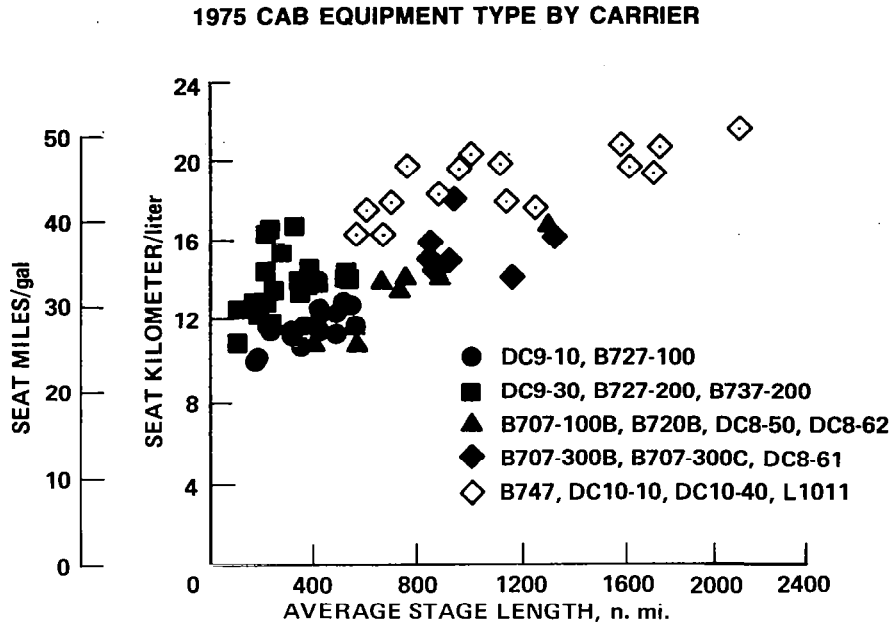

Figure 1.- Airline aircraft energy efficiency.

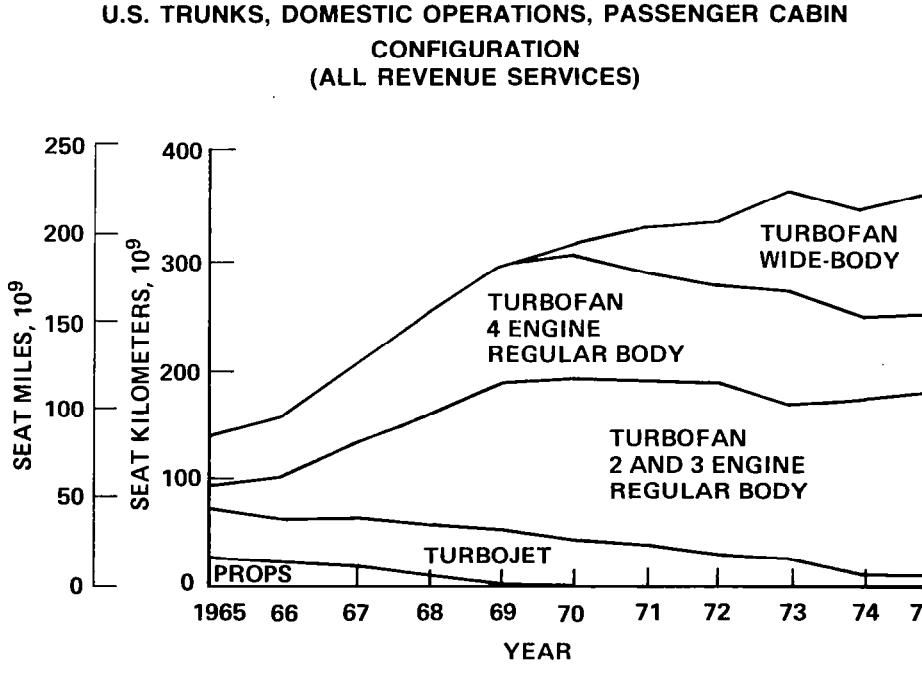

Figure 2.- Airline capacity by equipment group.

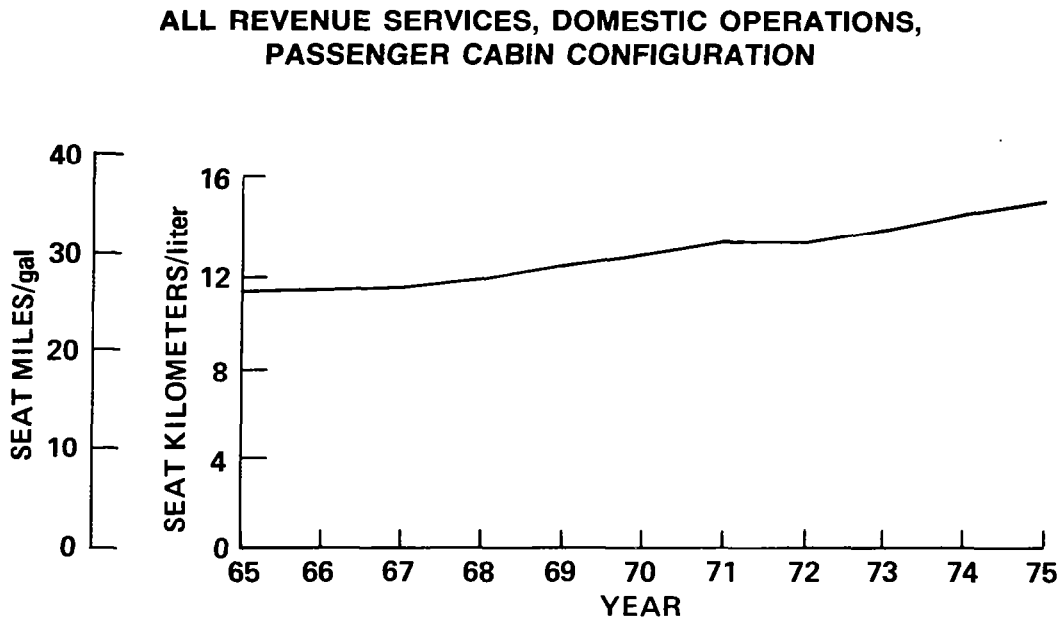

Figure 3.- Average U.S. trunk airline energy efficiency.

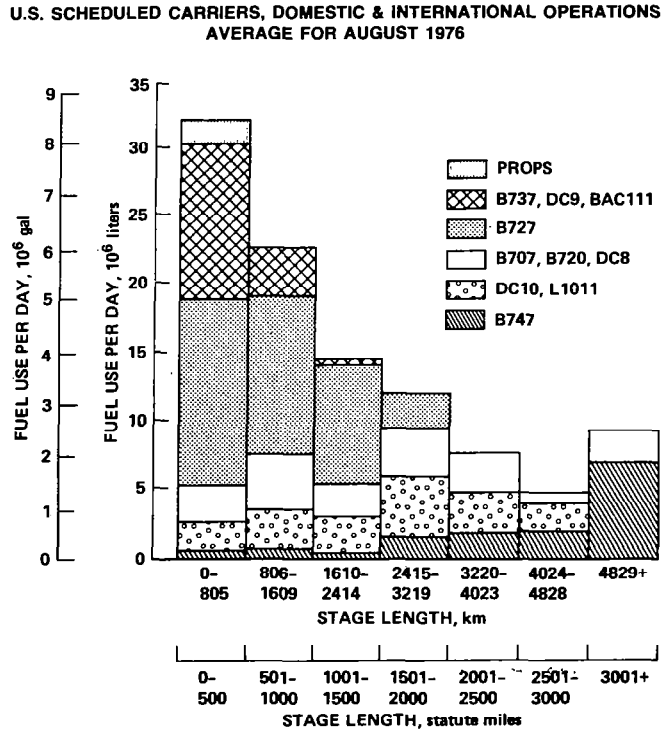

Figure 4.- Aircraft fuel usage.

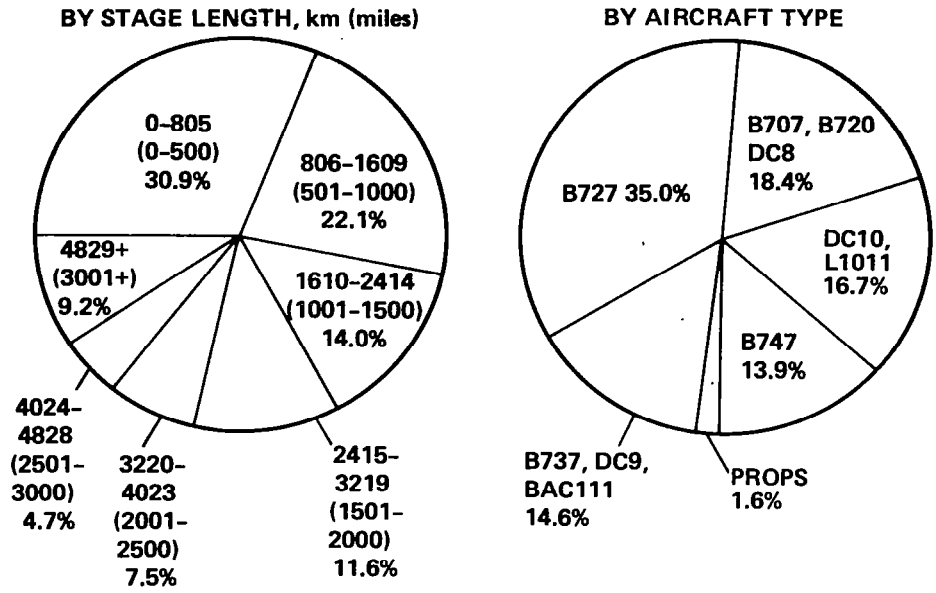

Figure 5.- Aircraft fuel use distribution.

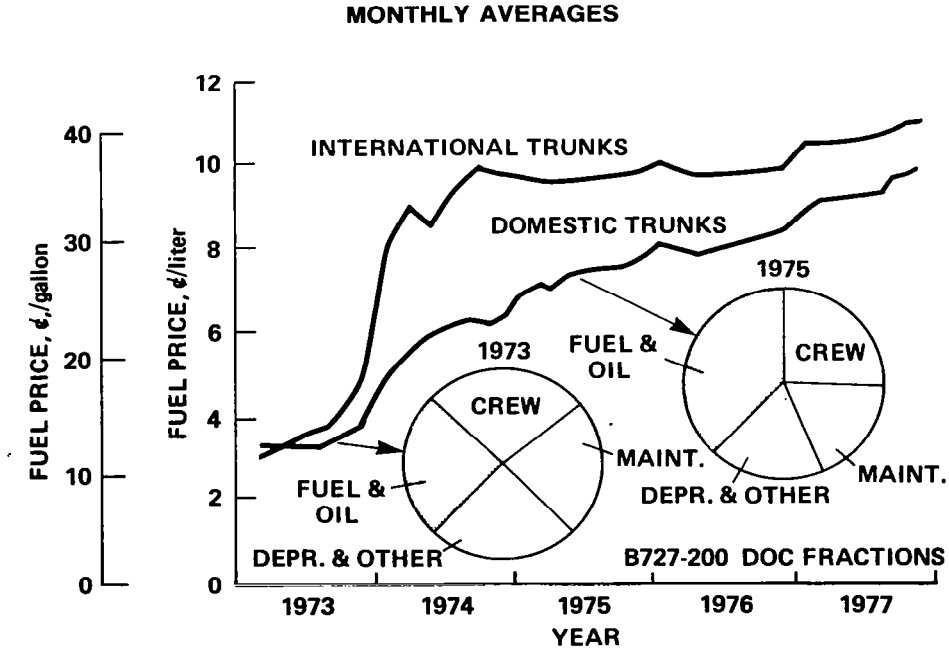

Figure 6.- U.S. airline jet fuel price.

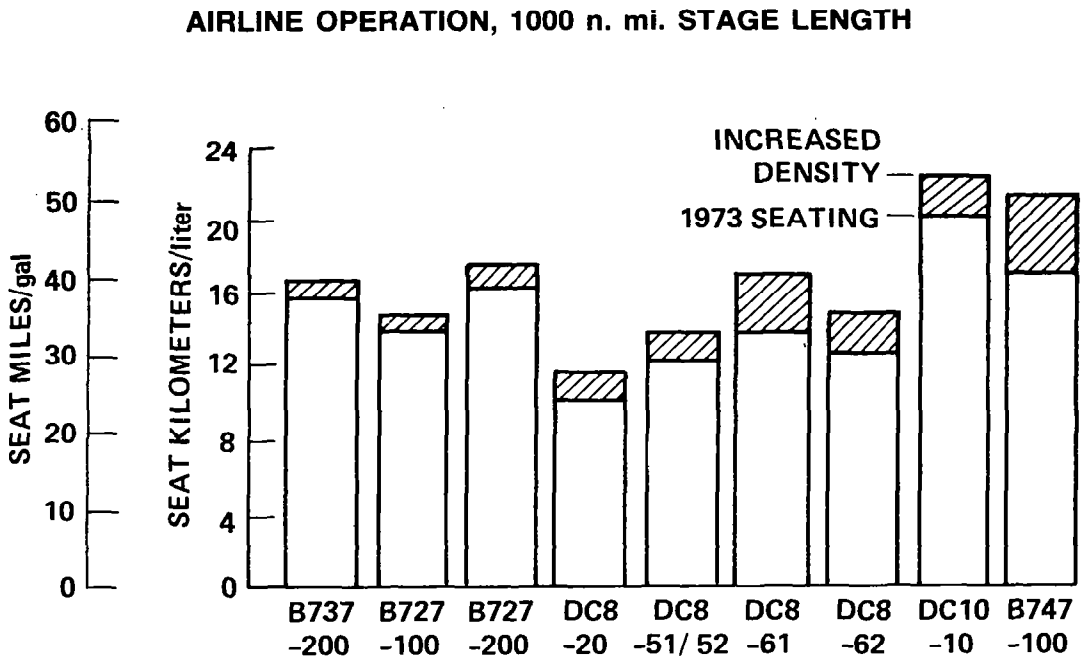

Figure 7.- Effect of seating density on aircraft energy efficiency.

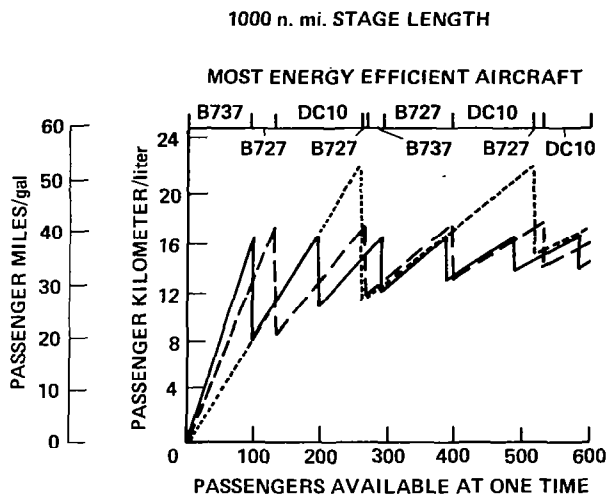

	AIRCRAFT	SEATS	SEAT KILOMETER / liter	(SEAT MILES / gal)
———	B737-200	97	16.5	(38.8)
·-·-·-·-	B727-200	132	17.7	(41.6)
— — —	DC 10-10	258	22.4	(52.7)

Figure 8.- Aircraft energy efficiency versus passengers carried.

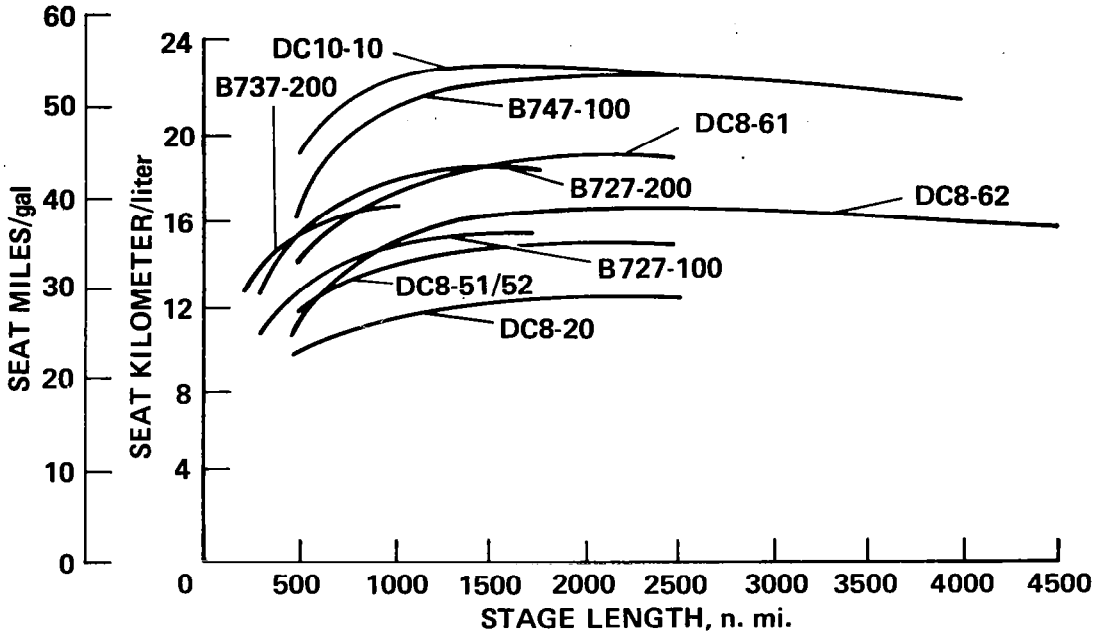

Figure 9.- Aircraft energy efficiency versus stage length for airline operation with increased density seating.

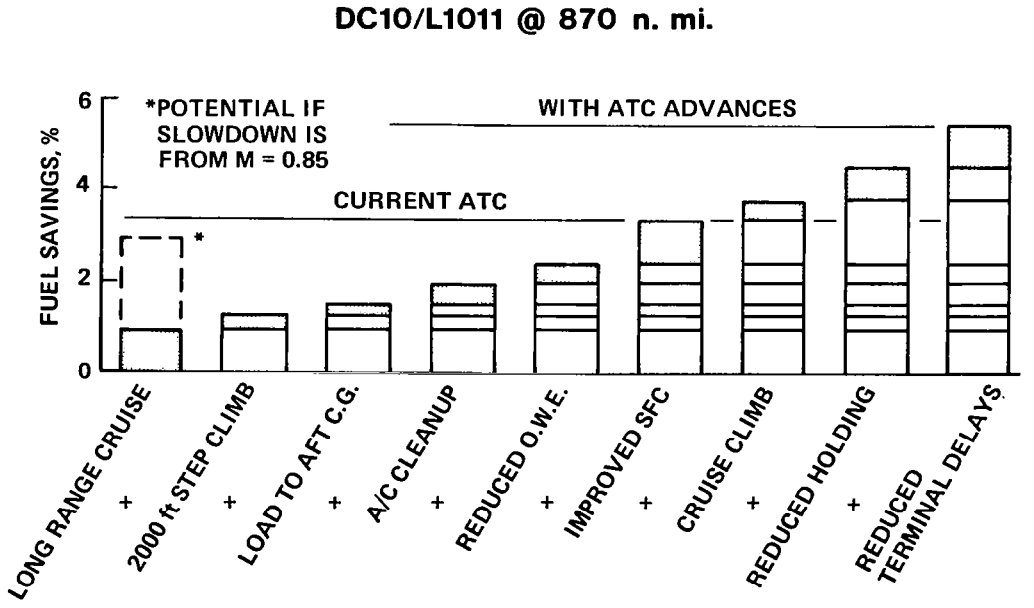

Figure 10.- Effect of flight procedures and aircraft maintenance.

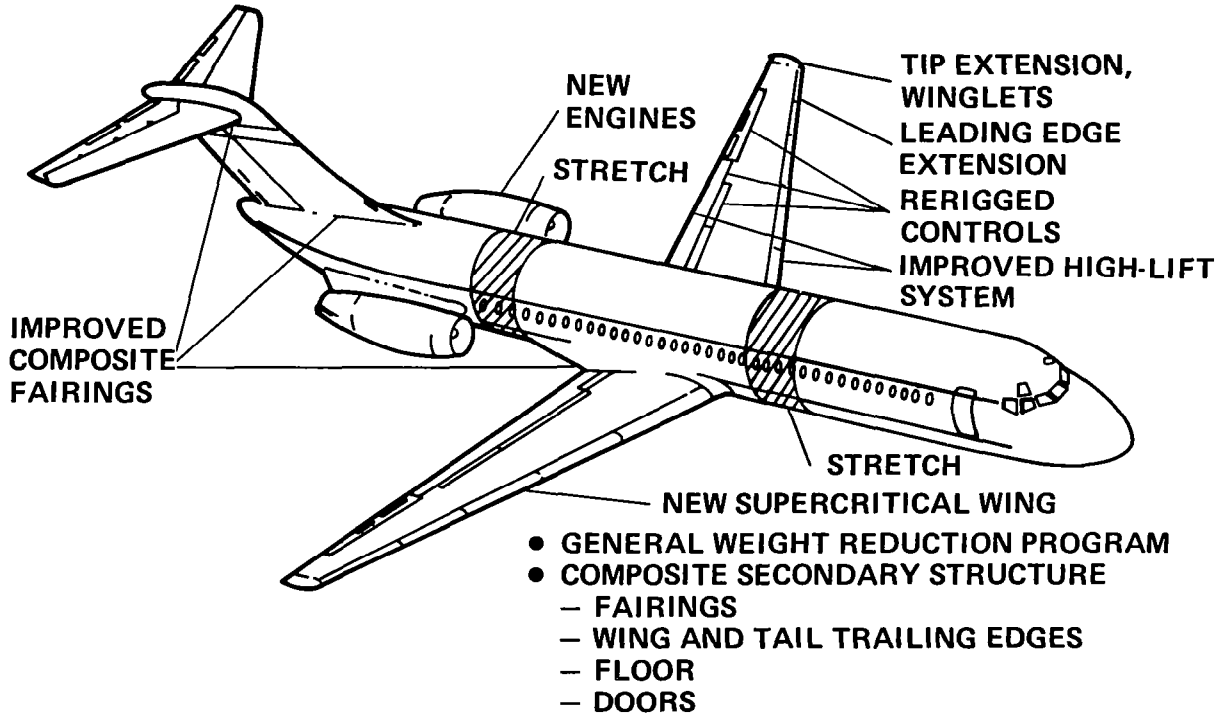

Figure 11.- DC-9 modification and derivative considerations.

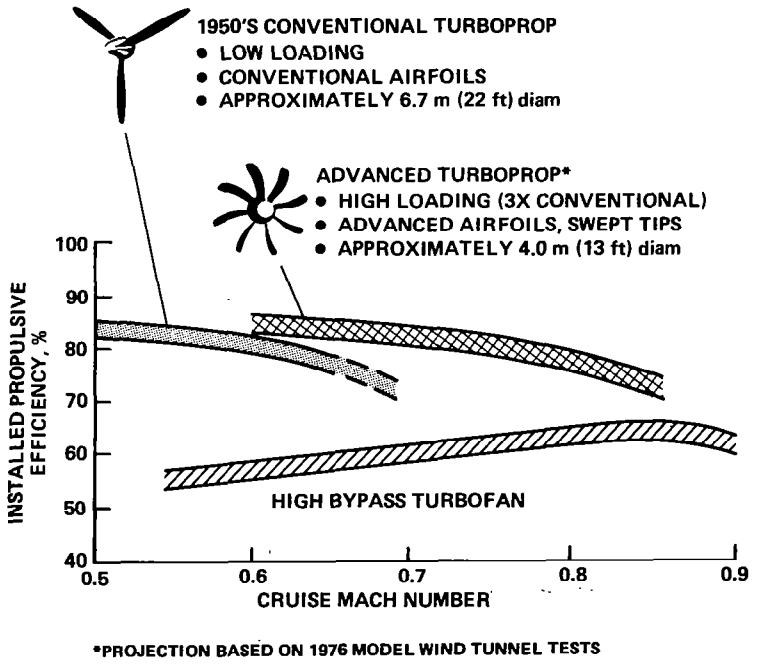

Figure 12.- Propulsive efficiency.

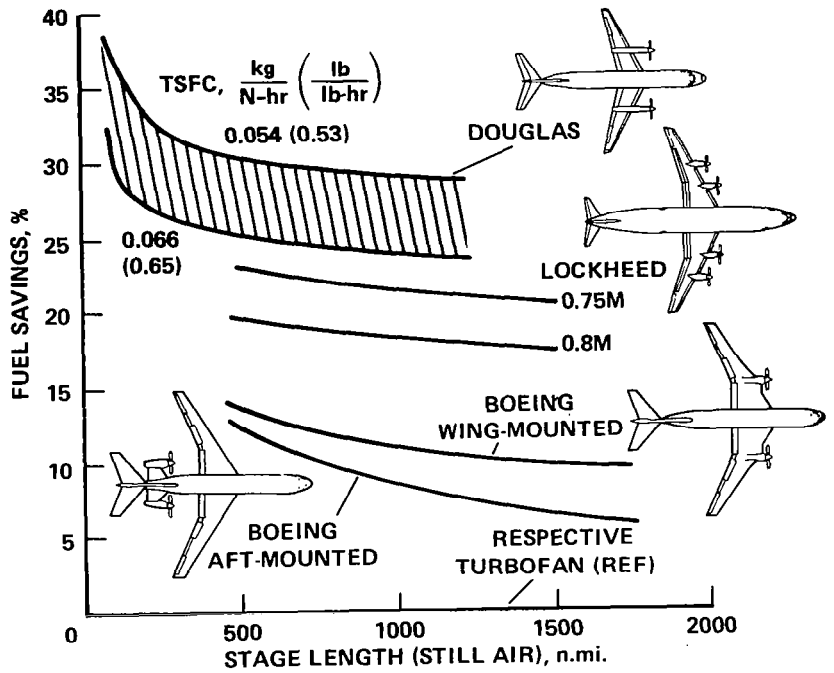

Figure 13.- Propfan aircraft fuel savings.

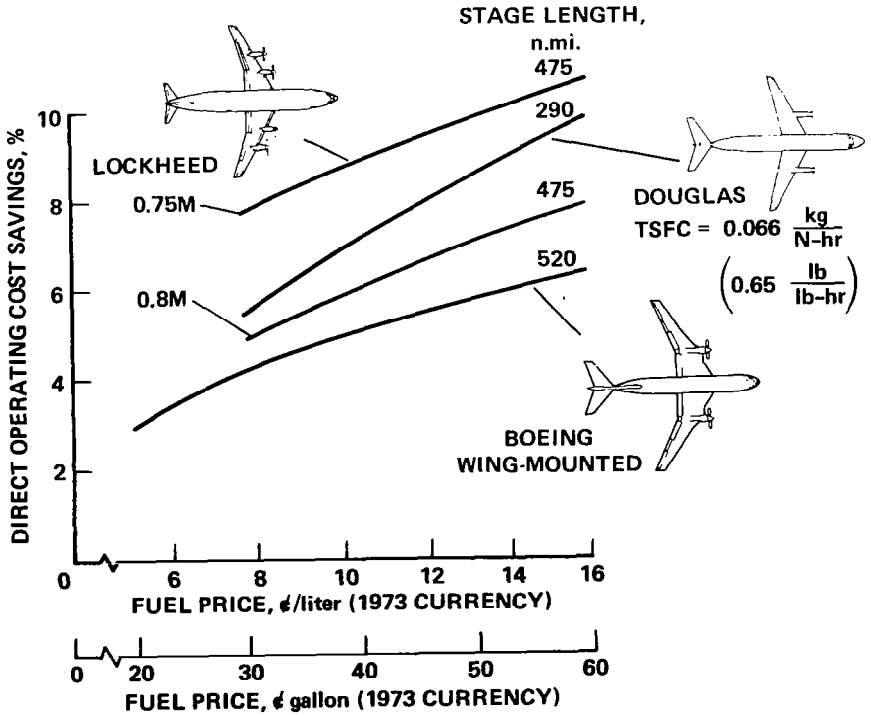

Figure 14.- Propfan aircraft cost savings.

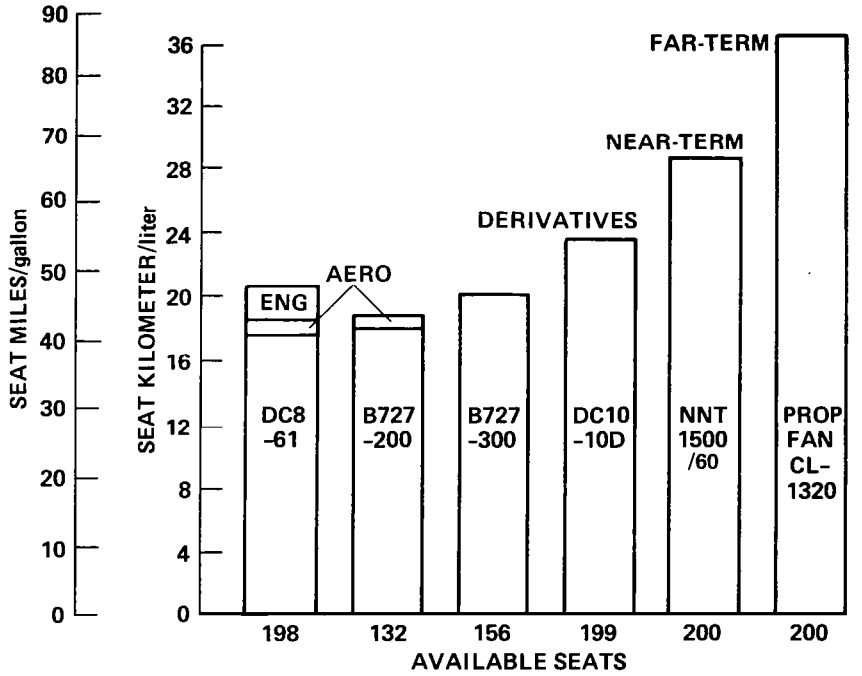

Figure 15.- Aircraft energy efficiency — modifications, derivatives, and new aircraft for airline operation over 1000 n.mi. stage length.

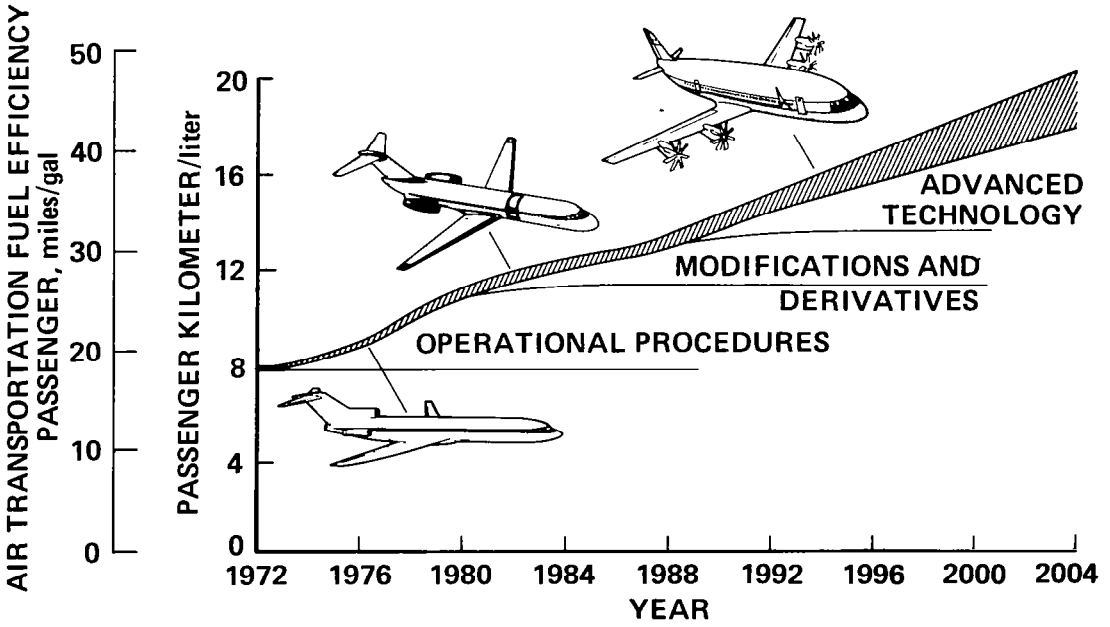

Figure 16.- Air transportation energy efficiency.

PROGRESS IN SUPERSONIC CRUISE AIRCRAFT TECHNOLOGY

Cornelius Driver
NASA Langley Research Center

SUMMARY

The Supersonic Cruise Aircraft Research (SCAR) program has identified significant improvements in the technology areas of propulsion, aerodynamics, structures, take-off and landing procedures, and advanced configuration concepts. These technology areas require significant further development before they are ready for application to a commercial aircraft. However, they may answer the adverse factors that were instrumental in the cancellation of the National Supersonic Transport (SST) program. They offer the promise of an advanced SST family of aircraft which may be environmentally acceptable, have flexible range-payload capability, and be economically viable. Further development requires an augmented SCAR technology program.

INTRODUCTION

This paper is a brief overview of the highlights of the NASA Supersonic Technology program. This program was generated about a year after Congress cancelled the National Supersonic Transport (SST) program in 1971. The Advanced Supersonic Technology program was conceived to preserve the base of knowledge developed during the SST program and to build on this technical base in an orderly way, thus preserving the capability to respond to the commercial supersonic challenge in the future. The present name of this advanced Supersonic Technology program is Supersonic Cruise Aircraft Research (SCAR). The results of the first four years of effort were reported in November 1976 at the SCAR conference at Langley Research Center, where 50 technical papers were presented (ref. 1).

Two areas are not discussed in this paper - sonic boom and upper atmosphere pollution. The large long-range airplanes being considered would be primarily used on over-water routes where very low boom levels are not required. In general, modest subsonic legs to avoid over-land booms can be accommodated without significant economic penalty. The upper atmosphere pollution area has been addressed by the Climatic Impact Assessment Program (CIAP) study (ref. 2) and the High Altitude Pollution Program (HAPP) study (ref. 3). The most recent results (ref. 4) indicate that the NO_x impact on the ozone problem is much better understood than in 1971. The impact of the supersonic transport is very small. Indeed, it may even increase the ozone level.

One of the problems inherent in a technology program is a method for quantifying progress. The method being used by the contractors and in-house at Langley is the development of reference airplane configurations (fig. 1).

These show the improvement obtained in range, payload, or gross take-off weight, or economics through better engines, structures, or aerodynamics. This reference concept is also utilized to study airframe-propulsion integration problems, to measure take-off and landing noise improvements, and even to develop new flight procedures for areas like noise reduction. It should be clearly recognized, however, what these reference airplanes are not. They are not preliminary designs for an airplane program. They are not the configurations that anyone would build or offer to the world airlines. Airplane designs for those purposes require depth of development and substantiation several orders of magnitude greater than that required for realistic technology measurement purposes. When airplanes are referred to in this paper, recognize that they are for reference purposes, for measurement of improvements, and for increased understanding of the problem areas.

Problems such as marginal range/payload capability, marginally acceptable take-off and landing noise, flutter, and unknown high altitude pollution effects are a serious detriment to any airplane program. These problems existed at the end of the SST program and provided focal points for the implementation of the technology program to be described in abbreviated fashion in this paper. The technology areas to be reviewed are propulsion, aerodynamics, structures, operating procedures, and advanced concepts.

Measurements and calculations were made in the U.S. Customary Units. They are presented herein in the International System of Units (SI) with the equivalent values given parenthetically in the U. S. Customary Units.

PROPULSION

The heart of any advanced airplane is the propulsion system. Both the U.S. SST and the Concorde used an afterburning turbojet propulsion system. The Rolls-Royce Olympus engine in the Concorde is a very advanced engine with an overall efficiency approximately 7 percent higher than the latest high-bypass-ratio turbofan engine in use (ref. 5). Unfortunately, the afterburning turbojet produces a level of jet noise on take-off that is of questionable acceptability for airplanes of the 1990's and beyond.

The responsibility for the engine and inlet portions of the SCAR program are assigned to the Lewis Research Center. Both the General Electric Company and Pratt and Whitney Aircraft Group - United Technologies Corporation work under coordinated contracts with Lewis and the Langley system study contractors. The specific propulsion areas discussed are as follows:

Variable-cycle engine
Better performance
Higher temperatures
Reduced emissions
Coannular noise effect
Advanced suppressor
Advanced materials and structures

Both General Electric and Pratt and Whitney have developed concepts for advanced engines with higher airflows to help solve the noise problem. These engines can vary the airflow capability of the engine to match the varying requirements with Mach number - thus, the generic term variable-cycle engine (fig. 2). These engines act much like a turbojet at cruise and more like a turbofan for take-off and subsonic operation. The variable flow capability of these engines has provided important gains in the subsonic flight regime, particularly for subsonic missions and reserve flight conditions where the values of specific fuel consumption have been reduced by as much as 35 percent compared with a turbojet engine (fig. 3). These gains have resulted primarily from the reduction in spillage and boattail losses provided by the varying airflow capability of the variable-cycle engine.

These engines employ advanced technology in their temperature and cooling levels, their combustor technology, noise reduction, subsonic performance and, of course, in their weights. Improved efficiency combustors have provided important gains in the NO_x emissions index (fig. 4). More than a 50-percent reduction from present NO_x levels has been demonstrated in rig tests. Conceptual combustors which provide even further reductions (ref. 6) are being studied.

Both Pratt and Whitney and General Electric have determined that an inverted exhaust velocity profile can provide a 3 to 5 dB noise reduction compared with a fully mixed exhaust flow having the same airflow and thrust (fig. 5). This "coannular" effect results from having the hotter, higher velocity exhaust flow on the outside of the jet and the slower, cooler flow near the center. It has been demonstrated experimentally with both dual-flow and plug nozzles. These effects have been identified statically with small test nozzles. A significant part of the variable-cycle-engine program is directed to proving these effects with larger nozzles and with the correct temperatures and airflows representative of an actual turbine engine. Tests to confirm the noise reductions with forward velocity effects are under way. In addition, the McDonnell Douglas Corporation has developed an advanced suppressor system to provide an alternate method of noise reduction (fig. 6). They have had favorable small-scale static tests and favorable whirl-rig tests conducted in conjunction with Rolls-Royce Limited in England. They have also recently completed forward velocity tests in the Ames 40- by 80-foot wind tunnel.

These engines also use advanced material and structural techniques to achieve the projected weight levels. One of these, a titanium-fan duct is shown in figure 7. Significant reductions in cost are being demonstrated.

In total, these propulsion advances result in a range gain of about 500 n. mi. over a conventional turbojet engine.

ADVANCED AERODYNAMICS

The airplanes being studied in the SCAR program utilize wings with subsonic leading edges and optimized camber and twist for reduction in drag due to lift (fig. 8), optimum area ruling, and favorable interference effects (fig. 9) to attain supersonic cruise lift-drag ratios (L/D) between 9 and 10. The Boeing Company has applied wing-body blending (fig. 10) to their airplane which, with small planform improvements, has resulted in a 20 percent improvement in L/D. In 1977, Boeing proposed the blended wing-body "family" concept (fig. 11), which offers a solution to the airplane payload/size problem with little or no effect on the aerodynamics of the airplane. A base 270-passenger, 5-abreast airplane can be laterally stretched up to a 6-abreast configuration or down to a 4-abreast configuration with important advantages in terms of meeting customer desires without significantly affecting the aerodynamics. This concept is discussed further in the section "Advanced Concepts."

Langley in-house effort has concentrated on the low-speed area (fig. 12) to improve take-off and landing aerodynamics. Important gains have been made in keeping the flow attached on these highly swept planforms. Improved flap lift increments and near-linear pitching moments have resulted. A new problem has surfaced which indicates that the low-speed shape of these highly swept, flexible airplanes is substantially different than the cruise shape (fig. 13). The differences (5° anhedral, for instance) result in less critical rolling moments and more linear pitching moments. Tests are in progress to identify these incremental effects.

If all the aerodynamic improvements are combined, a range increase of about 500 n. mi. is obtained.

ADVANCED STRUCTURES

The most exciting advance in the structural area is probably the application of finite-element modeling (fig. 14) and advanced computational methods to these large flexible wings. Computational modules have been developed and combined to provide detailed analysis of very complex systems. An airplane structural model typically consists of over 4000 elements with 2000 degrees of freedom. This computer technology has resulted in a reduction in the structural design turn-around time from 3 months to less than a week. This means fast evaluation of innovative ideas and approaches that could not have been considered in the past. These strength-design models can be evaluated for flutter (fig. 15) in an equally fast turn-around time. Thus, the impact on flutter of items like engine mass and location, engine support beam stiffness, or presence of wing fuel can be determined quickly and reliably.

A spin-off of the Rockwell International B-1 program - superplastic forming and concurrent diffusion bonding of titanium (SPF-DB) - is another

promising new structural area (ref. 1). Figure 16 shows two types of titanium structure. One began as two flat titanium sheets which were bonded together and formed into skin, ribs, and stringers, concurrently. The other was a four-sheet complex-core sandwich somewhat similar to honeycomb. These techniques promise large weight and cost reductions - studies for application in specific areas have resulted in 10- to 30-percent weight reductions with cost savings of over 50 percent.

Significant effort has gone into studying the various forms of high-temperature polyimide composite structures (fig. 16). Initial studies indicate even larger weight savings than the SPF-DB titanium.

Langley, Boeing, and McDonnell Douglas have all studied active-control landing gears (fig. 17). Each used different approaches and had different degrees of success. The studies have progressed to the point, however, that active gears are almost a certainty on the long-fuselage supersonic cruise type airplane because of significant payoffs in terms of sensitivity to runway roughness, horizontal tail size required for rotation, and even aft center-of-gravity limits.

It is believed that the incorporation of the structure technology gains could result in an 8- to 10-percent reduction in operating empty weight or a gain in range of about 300 n. mi.

ADVANCED PROCEDURES FOR NOISE REDUCTION

Some of the most exciting work coming out of the SCAR program involves an understanding that an SST does not want to take off and land with the same rules as its subsonic counterpart; the SST wants to behave differently (fig. 18). First, recognize that in contrast to a subsonic aircraft, where they are all fixed, the engine, inlet, and nozzle on an SST have a significant degree of variability. It follows naturally that if this variability is utilized, important noise reductions may occur.

During take-off from brake release until approximately wheels-up, sideline noise is favorably affected by forward velocity effects and ground attenuation. For a constant throttle setting, maximum noise normally occurs as the airplane climbs out of ground attenuation at an altitude of about 213 m (700 ft) (fig. 19). With an auto-throttle procedure, increasing the throttle about 15 percent from brake release until the altitude was reached where the maximum sideline noise would normally occur would result in the aircraft reaching that point at a higher velocity and/or altitude with no increase in sideline noise. Furthermore, flap settings may also be automated, since they are simple plain flaps. The combination of reduced flap settings and increased velocity results in a cut-back L/D that has increased to more than 10 compared with a normal value of around 7. Present results indicate noise over the community may be reduced 5 to 7 dB by these different procedures. Significantly, in these deeper cut-back cases jet noise may no

longer dominate; other sources such as compressor, fan, or shock noise become important.

On the approach end of the runway, equally exciting things are possible by use of decelerating approaches and increased glide slopes. On a 3^{o} glide slope, for instance, the decelerating approach reduces noise by 4 or 5 dB. Further, each 1^{o} increase in glide slope reduces noise about 2 dB. Increases in glide slopes may be possible for an SST because of the large favorable ground effect produced by the low-aspect-ratio wing. During landing, jet noise is small. Inlet choking and duct treatment are required to quiet the other engine noise sources. Airframe noise itself becomes a significant factor.

The most important result of these studies is that important gains in noise reduction are possible when we understand the airplane and how it can be operated safely to reduce noise. Another important feature is the decrease in noise as the airplanes are operated at reduced payloads and/or reduced gross weights. Because the SST has such a large fuel fraction, reduced weight operations become particularly important. Perhaps the best proof lies in the Concorde experience at John F. Kennedy International Airport, where the Concorde operates at a take-off gross weight approximately 10 433 kg (23 000 lb) less than the take-off gross weight from Dulles International Airport. During the first three months, the flight measurements have indicated an average noise level at the monitor stations of 96.5 EPNdB (refs. 7 to 9) which is well below the 108-dB FAR 36 requirements (ref. 10) and far below the 117-dB levels demonstrated at Dulles.

CONCLUDING REMARKS

Based on the technologies just reviewed, it is reasonable to project some of the characteristics of advanced supersonic systems. There will be families of supersonic aircraft just as there have been families of subsonic aircraft. For supersonic aircraft, however, the stretch or shrink will be lateral instead of longitudinal. This will enable a variety of payloads and ranges to be obtained with most of the expensive parts of the aircraft remaining constant between the various models. This stretch capability will make possible greater market penetration, longer and larger production runs, and reduced cost. The variable-cycle engine, the reduced structural weight, and improved aerodynamics will provide large payload range capability. For the first time, supersonic ranges in excess of 5000 n. mi. can be considered. If the coannular noise effect and the automated take-off and landing procedures identified in the SCAR program can be substantiated at full-scale operating conditions, the airplane will be capable of attaining stringent noise goals. These advanced airplanes will utilize hardened stability augmentation systems which will allow the center of gravity to be aft of the neutral point and still provide superior pilot handling characteristics. If necessary, it will be feasible to implement an active flutter suppression system. The economics of such an airplane would make it very competitive with the subsonic wide bodies of a similar size.

REFERENCES

1. Proceedings of the SCAR Conference - Parts 1 and 2. NASA CP-001, [1977].

2. Grobecker, A. J.; Coroniti, S. C.; and Cannon, R. H., Jr.: Report of Findings - The Effects of Stratospheric Pollution by Aircraft. TST-75-50, U.S. Dep. Transp., Dec. 1974. (Available from DDC as AD A005 458.)

3. Oliver, R. C.; Bauer, E.; Hidalgo, H.; Gardner, K. A.; and Wasylkiwskyj, W.: Aircraft Emissions: Potential Effects on Ozone and Climate - A Review. FAA-EQ-77-3, Mar. 1977. (Available from DDC as AD A040 638.)

4. Broderick, Anthony J.: Stratospheric Effects From Aviation. [Paper] 77-799, American Inst. Aeronaut. & Astronaut., July 1977.

5. Calder, P. H.; and Gupta, P. C.: The Application of New Technology for Performance Improvement and Noise Reduction of Supersonic Transport Aircraft. [Paper] 77-830, American Inst. Aeronaut. & Astronaut., July 1977.

6. Aircraft Engine Emissions. NASA CP-2021, 1977.

7. Monitoring of Concorde Operations at John F. Kennedy International Airport During October 1977. FAA, U.S. Dep. Transp., Nov., 3, 1977.

8. Monitoring of Concorde Operations at John F. Kennedy International Airport During November 1977. FAA, U.S. Dep. Transp., Dec. 13, 1977.

9. Monitoring of Concorde Operations at John F. Kennedy International Airport During December 1977. FAA, U.S. Dep. Transp., Jan. 12, 1978.

10. Noise Standards: Aircraft Type Certification. Federal Aviation Regulations, vol. III, pt. 36, FAA, Dec. 1969.

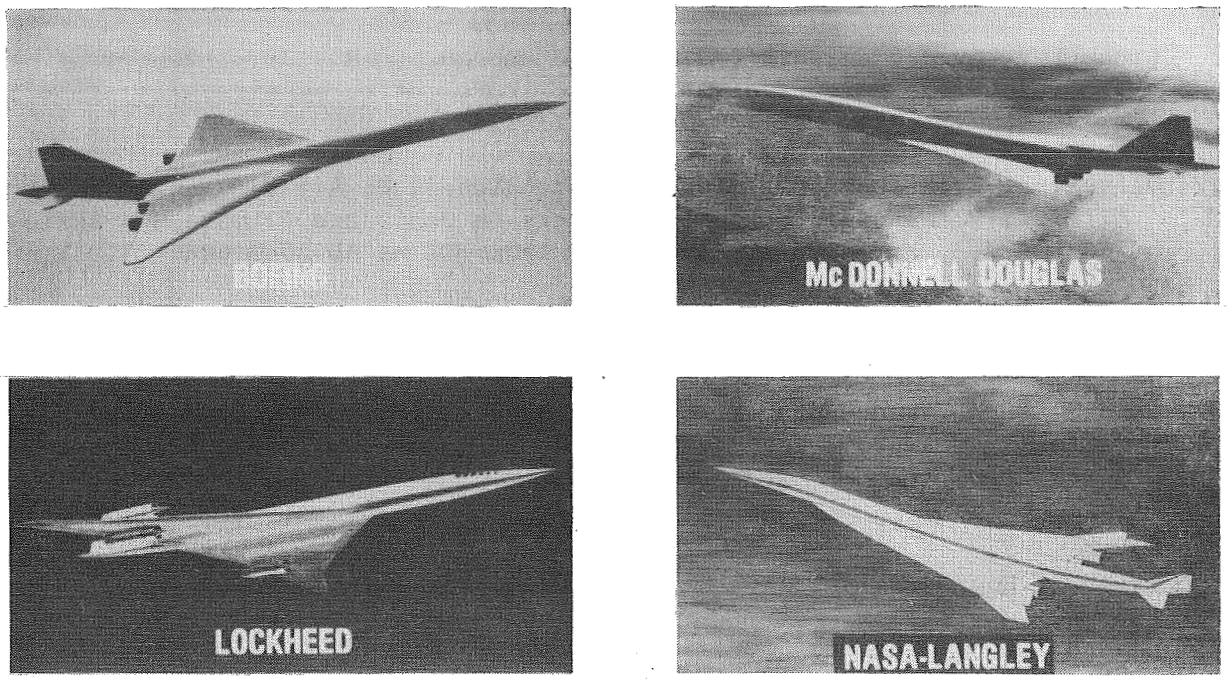

Figure 1.- Advanced supersonic cruise aircraft configurations.

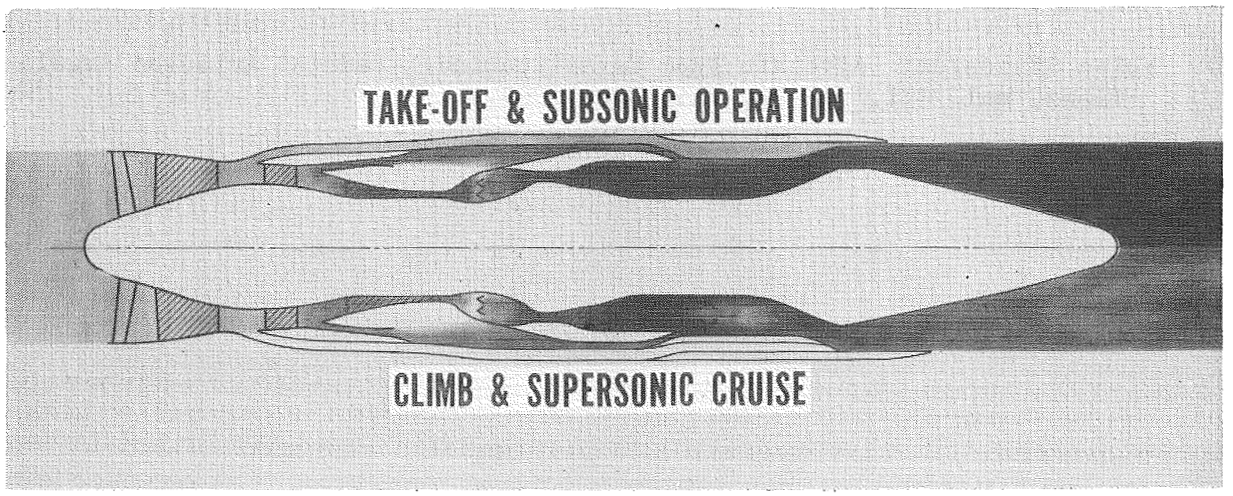

Figure 2.- Variable-cycle engine.

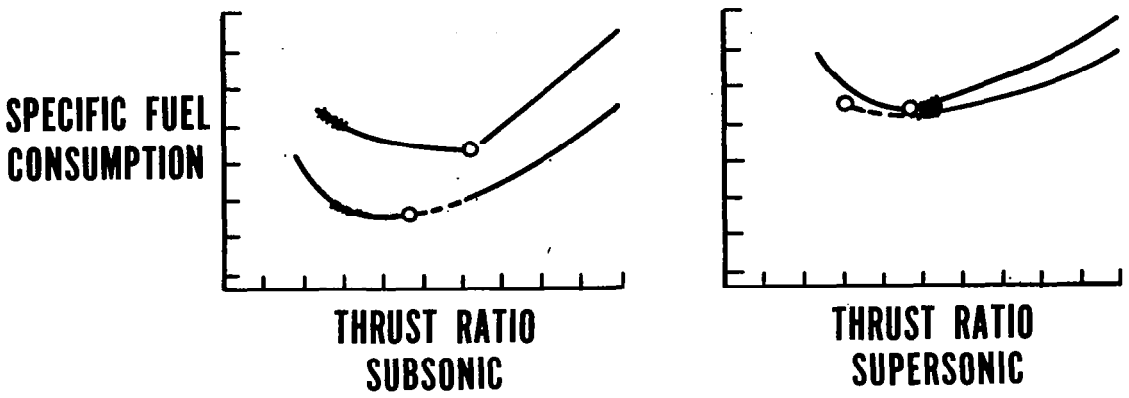

Figure 3.- Better engine performance.

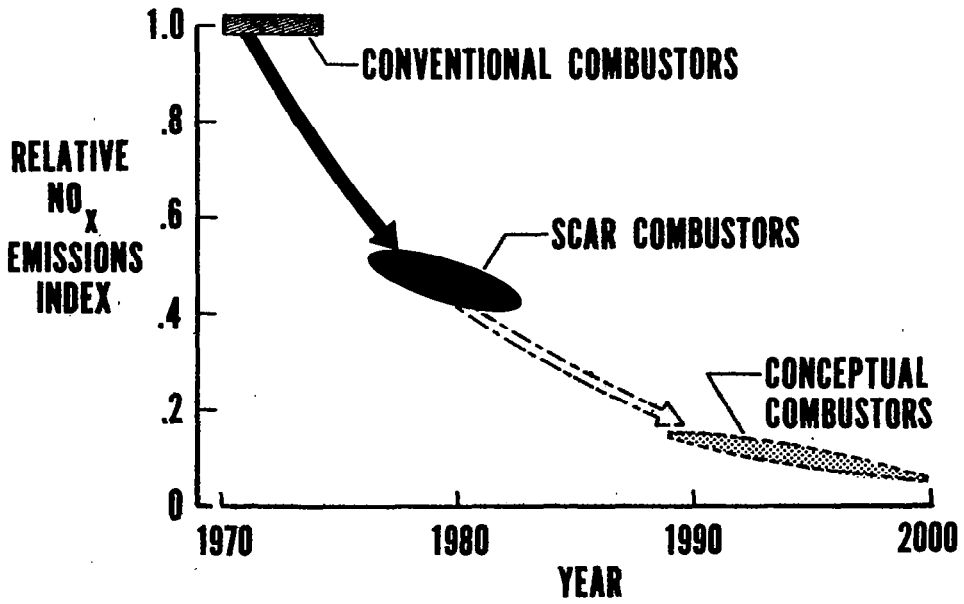

Figure 4.- Emission progress.

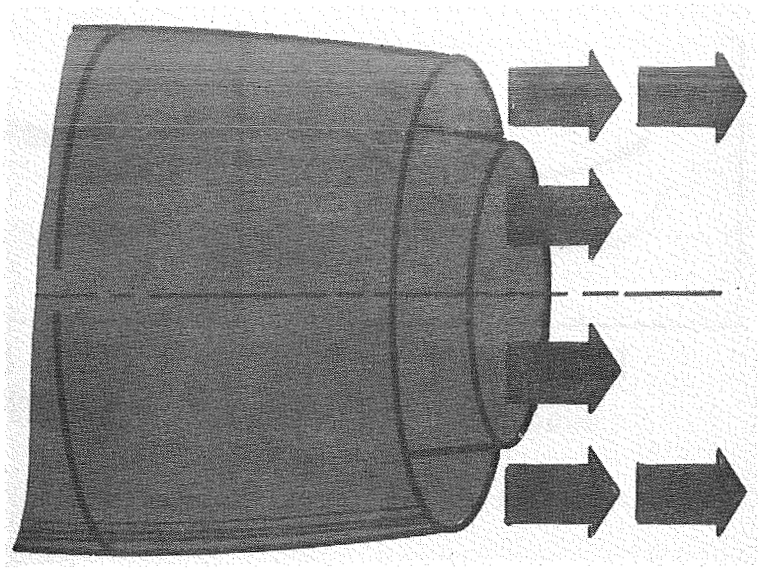

Figure 5.- Coannular noise effect.

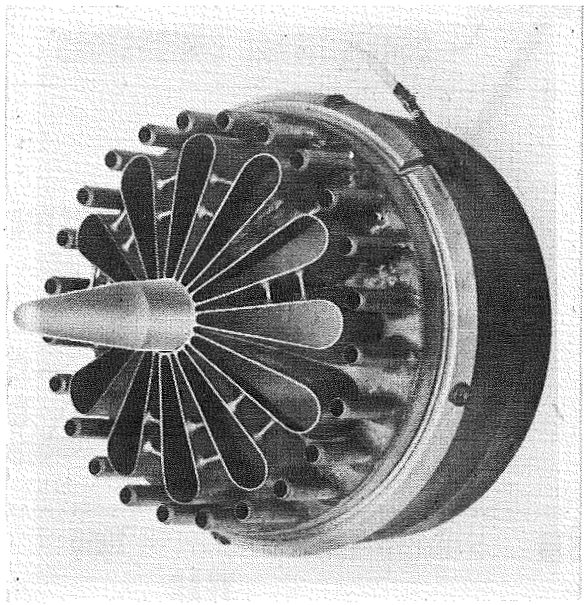

Figure 6.- Advanced suppressor.

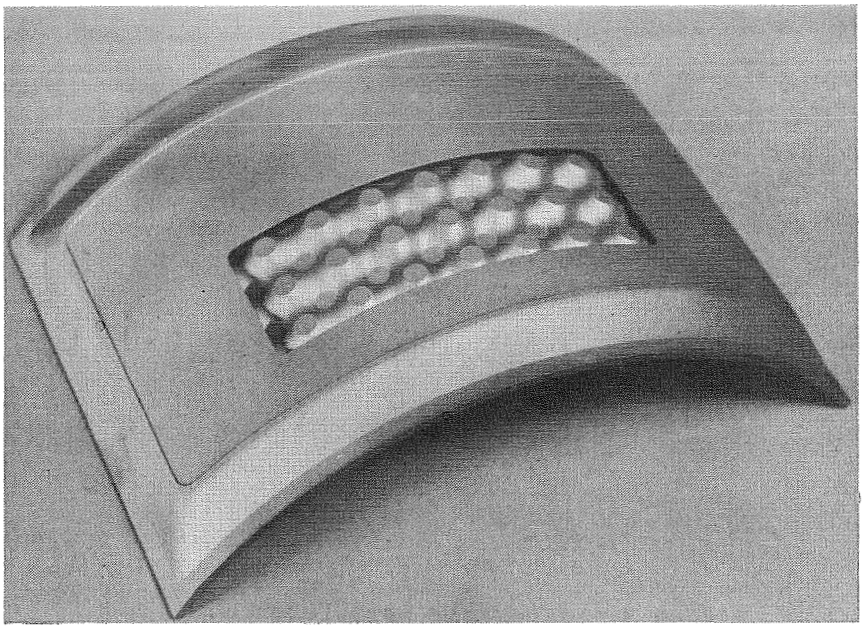

Figure 7.- Advanced structures.

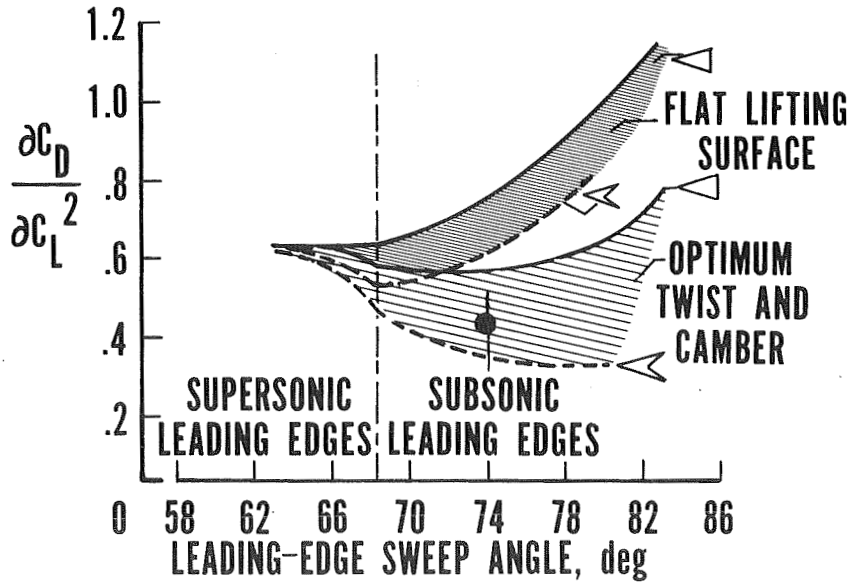

Figure 8.- Wing design considerations at a Mach number of 2.7. (Variation of drag-due-to-lift parameter with sweep angle.)

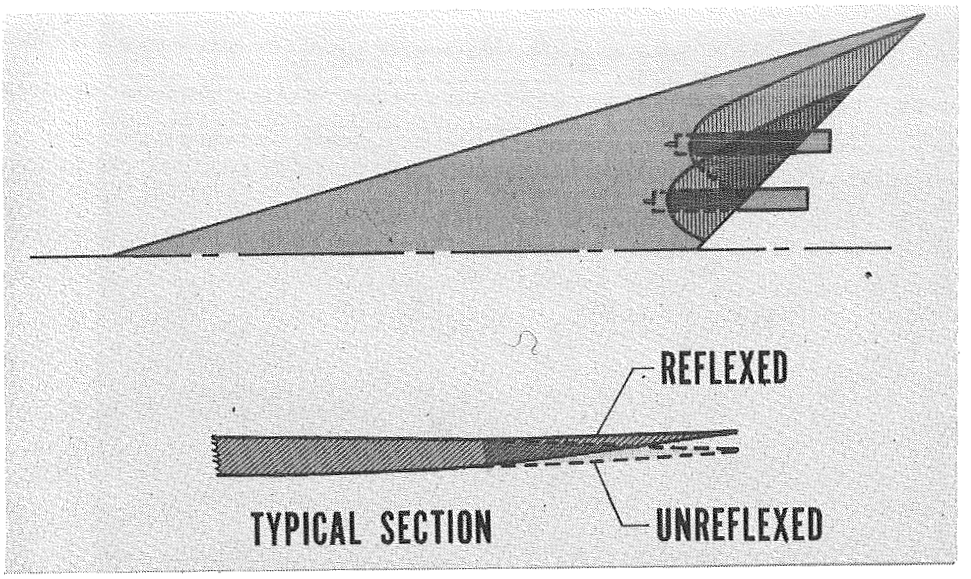

Figure 9.- Favorable interference.

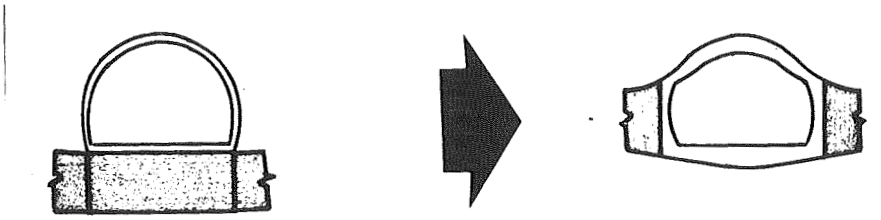

BENEFITS:

- REDUCED DRAG
- SMALLER ENGINE
- BETTER FUEL EFFICIENCY
- INCREASED AIRPLANE RANGE

Figure 10.- Wing-body blending.

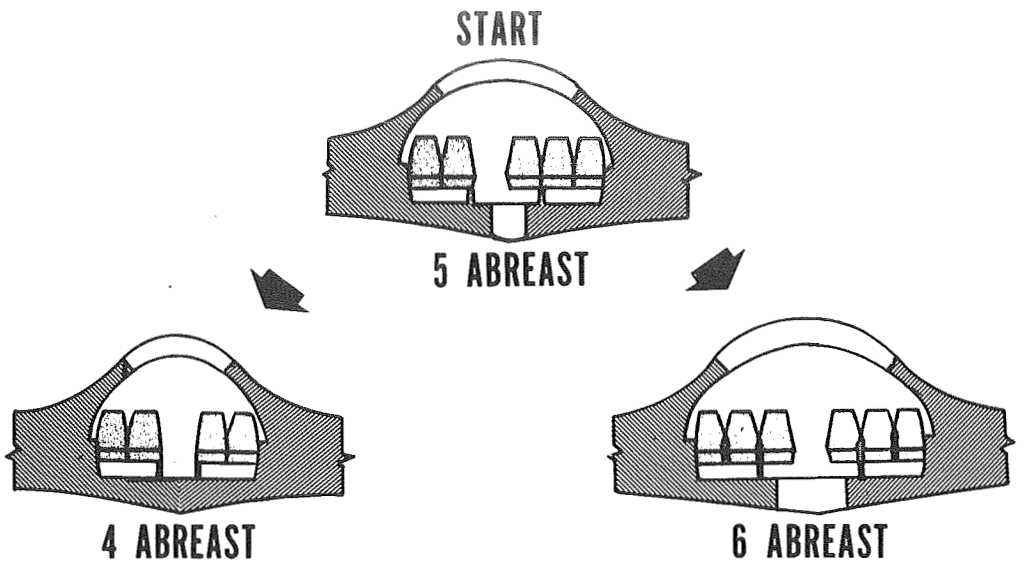

Figure 11.- Family concept.

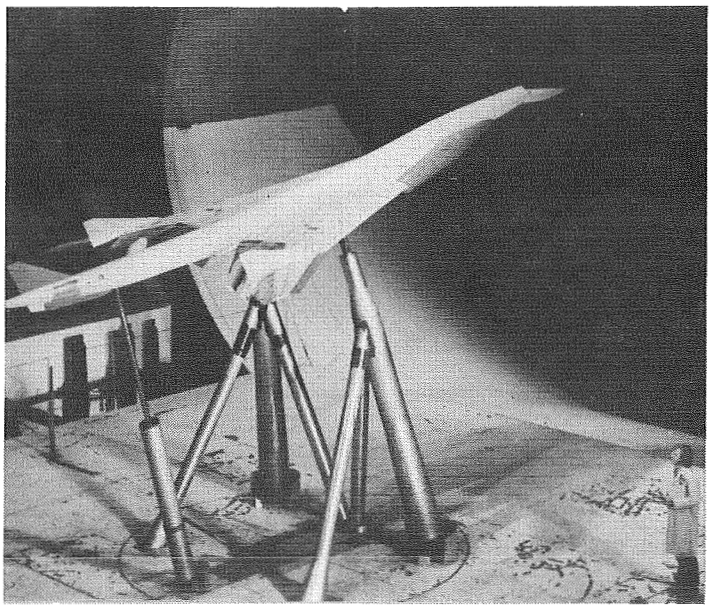

Figure 12.- Low-speed wind-tunnel model.

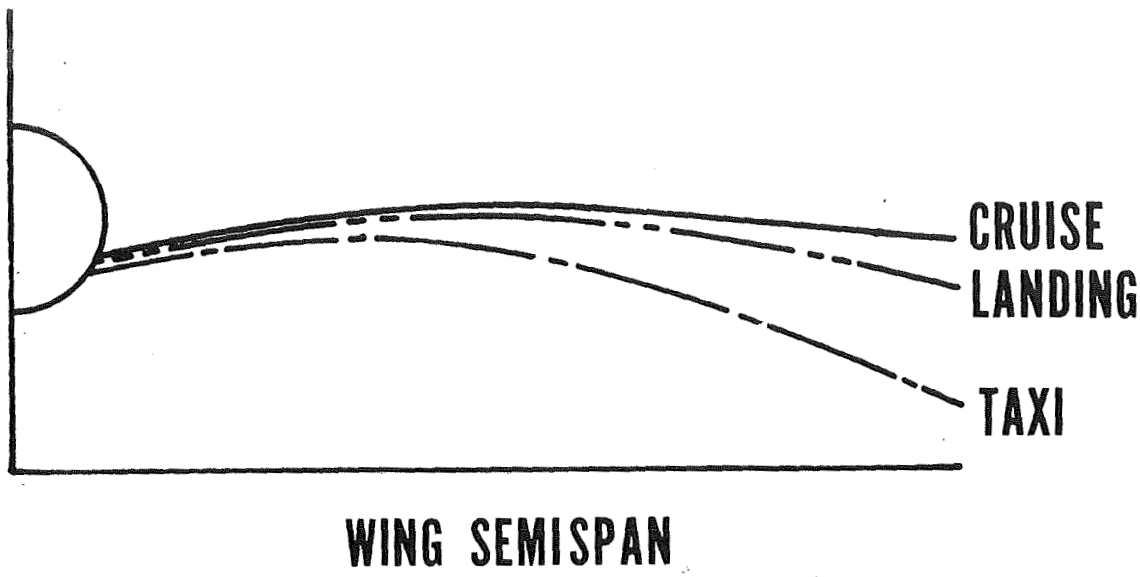

Figure 13.- Wing semispan shape.

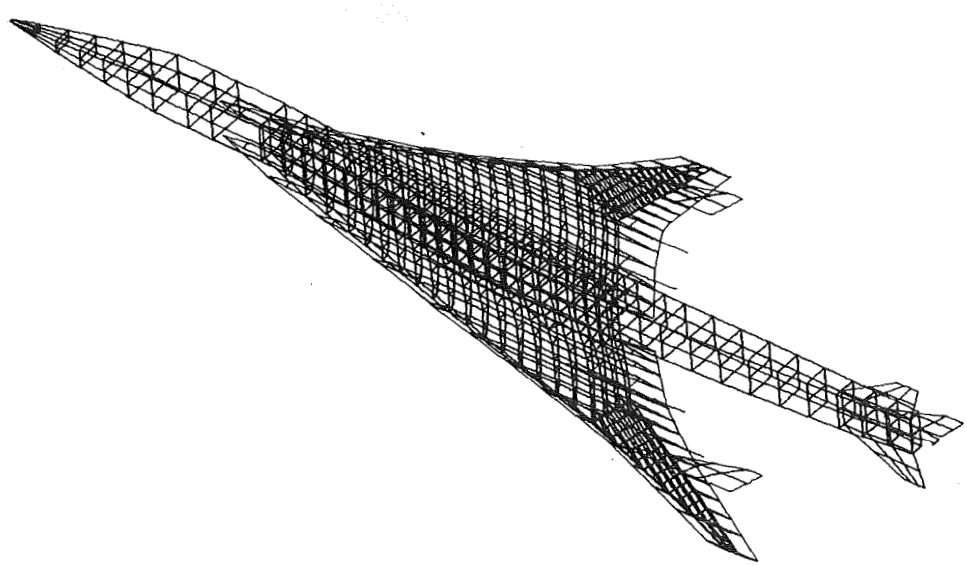

Figure 14.- Finite-element model.

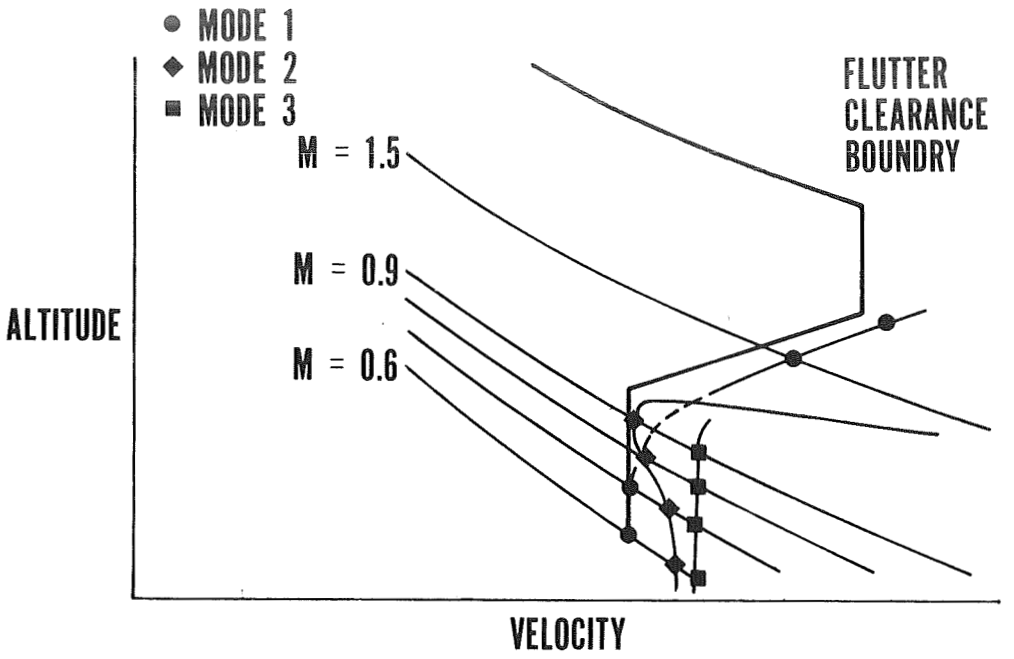

Figure 15.- SCAR arrow wing flutter results at various Mach numbers M.

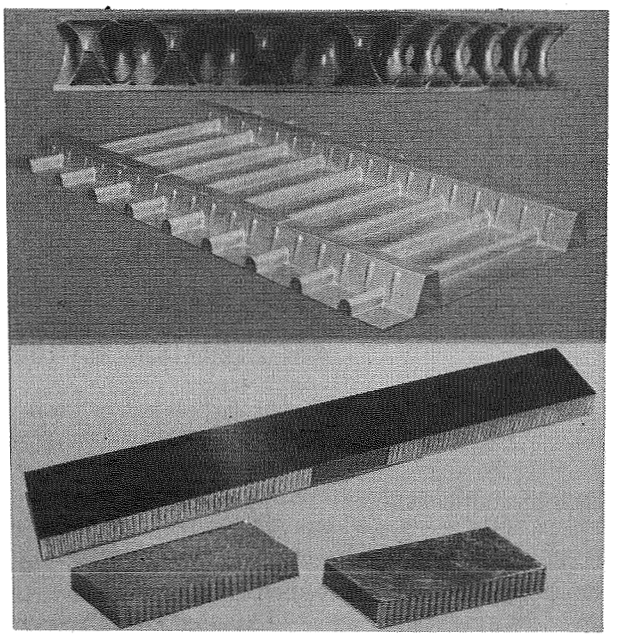

Figure 16.- Advanced materials.

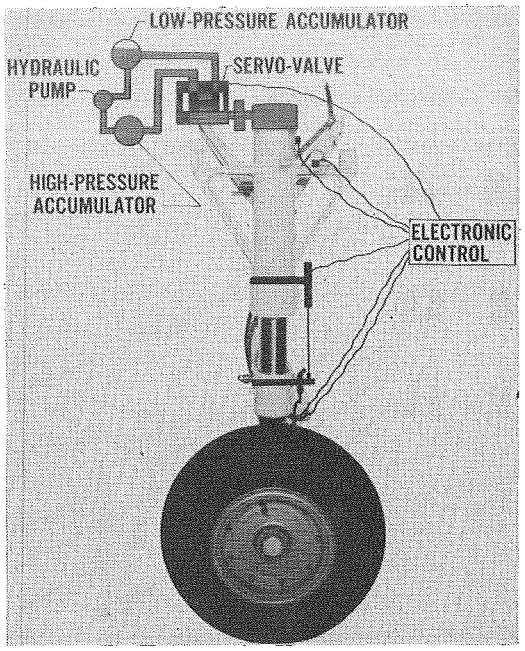

Figure 17.- Active-control landing gear.

LANDING

- DECELERATING APPROACH
- INCREASED GLIDE SLOPE
- INLET CHOKING

TAKE-OFF

- INCREASED THRUST DURING GROUND ROLL (GROUND ATTENUATION)
- AUTO THROTTLE
- AUTO FLAPS
- ACCELERATION/ALTITUDE

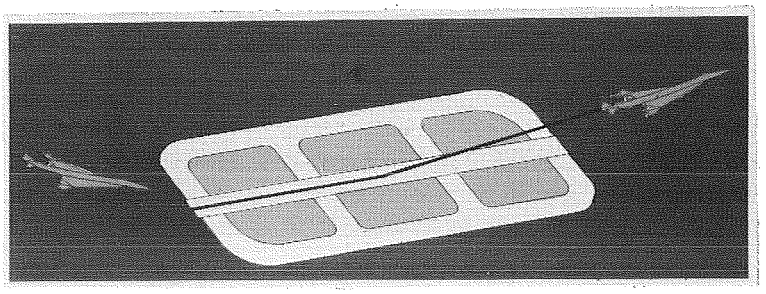

Figure 18.- Advanced procedures for noise reduction.

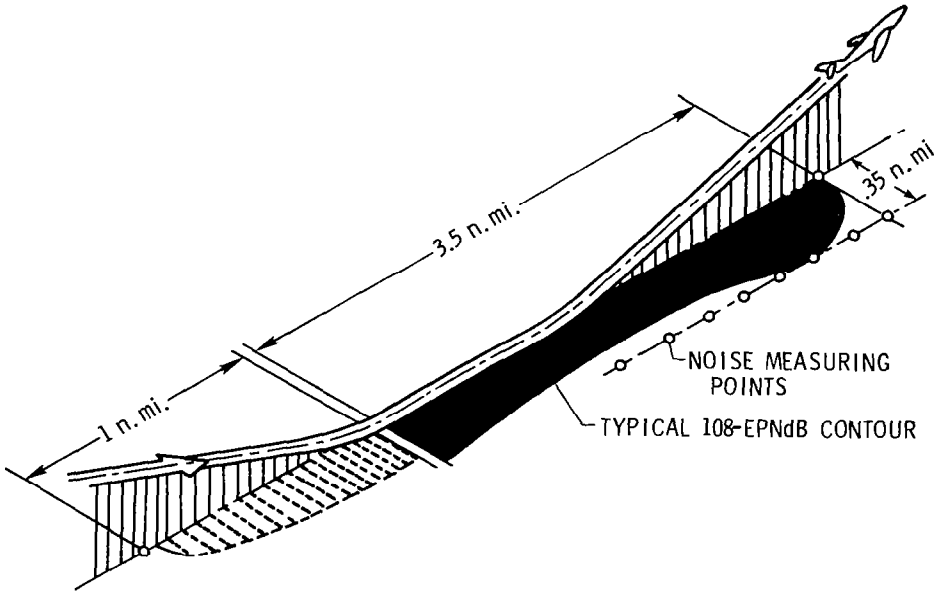

Figure 19.- Airport and community noise contours.

PROGRESS ON COAL-DERIVED FUELS FOR AVIATION SYSTEMS

Robert D. Witcofski
NASA Langley Research Center

SUMMARY

The results of engineering studies of coal-derived aviation fuels and their potential application to the air transportation system are presented. Synthetic aviation kerosene (SYN. JET-A), liquid methane (LCH_4) and liquid hydrogen (LH_2) appear to be the most promising coal-derived fuels. Aircraft configurations fueled with LH_2, their fuel systems, and their ground requirements at the airport have been identified. These LH_2-fueled aircraft appear viable, particularly for long-haul use, where aircraft fueled with coal-derived LH_2 would consume 9 percent less coal resources than would aircraft fueled with coal-derived SYN. JET-A. Distribution of hydrogen from the point of manufacture to airports may pose problems. Synthetic JET-A would appear to cause fewer concerns to the air transportation industry. The ticket price associated with coal-derived LH_2-fueled aircraft appears competitive with that of aircraft fueled with coal-derived SYN. JET-A. Of the three candidate fuels, LCH_4 is the most energy efficient to produce, and an aircraft fueled with coal-derived LCH_4 may provide both the most efficient utilization of coal resources and the least expensive ticket as well. The safety aspects associated with the use of cryogenic fuels such as LCH_4 and LH_2 in the air transportation system are yet to be determined.

INTRODUCTION

This paper addresses the use of alternate fuels in the air transportation system and relates the use of such fuels to concerns of the general public, the air transportation industry, and the air traveler. The bulk of the material presented herein is the product of a program sponsored by the NASA Langley Research Center. The program is directed at providing answers to some of the many technical questions which decision makers will face when deciding which alternate fuels will be most advantageous to use and which sectors of the nation's energy consumers should use them.

ABBREVIATIONS AND SYMBOLS

APU	auxiliary power unit
DCF	discounted cash flow
DOC	direct operating cost
GH_2	gaseous hydrogen

IOC	indirect operating cost
LCH_4	liquid methane
LH_2	liquid hydrogen
L/D	lift-drag ratio
M	Mach number
MISC.	miscellaneous
OEM	operating empty mass
PL	payload
SYN. JET-A	synthetic aviation kerosene

PUBLIC CONCERNS

Although civil air transportation accounts for only 2 percent of the total United States energy consumption and about 4 percent of the petroleum energy consumed, the utilization of alternate fuels in the air transportation system would affect the general public to varying extents, depending upon the alternate fuel selected. The areas of national needs, candidate fuel selection, and community impact are addressed.

National Needs

Oil provides 47 percent of the total energy consumed by the United States (ref. 1) and transportation requires 54 percent of this oil consumption. Figure 1 shows the historical and projected production and consumption of oil in the United States. The projection of domestic oil production was taken from the ERDA document of reference 2. The projected oil consumption represents a relatively modest 2 percent per annum growth rate when compared with the 3.7 percent growth rate which has occurred over the past decade. The United States currently imports about 46 percent of its oil, compared with 41 percent 1 year ago. These imports require an expenditure of $30 billion per year. The potential role which synthetic fuels, produced from oil shale and coal, might play in filling this gap is shown in figure 2. Figure 2, taken from the Project Independence Report (ref. 3), shows the projected decline of domestic oil and natural gas production after 1985 and the projected demand based on a growth rate of 2.5 percent per annum. The demand model assumed that oil and natural gas would not be used for electricity generation after 1985. As shown in the figure, the report also indicated that a major portion of the gap might be filled by rapid development of synthetic fuels from coal and oil shale.

Thus, a national need for synthetic fuels exists at the present time. However, for reasons which are beyond the scope of this paper, the United States has only an embryonic synthetic fuels industry.

What Fuels?

There are a number of synthetic fuels which can be produced from United States energy resources. This paper deals only with those which appear suitable for application to aviation. A number of synthetic fuels were judged not to be viable for aviation use and are listed in figure 3 together with their masses and volumes (for equal energy content) relative to JET-A fuel (conventional aviation kerosene) and with the criteria for rejection. JET-A is presented only as a reference. All the synthetic fuels listed in figure 3 were rejected basically because of their higher masses, although toxicity and corrosion were also contributing factors. For a long-range airplane, fuel mass can be 40 to 50 percent of the airplane gross take-off mass. Doubling the mass of the fuel has an adverse domino effect by increasing structural weight and decreasing aircraft performance.

The candidate synthetic fuels judged viable for aviation use are listed in figure 4, where their mass and volume characteristics are compared with those of JET-A fuel. Liquid methane and liquid hydrogen are, of course, cryogenic fuels and must be stored at temperatures of -162° C and -253° C, respectively. Both LCH_4 and LH_2 have higher relative volumes than JET-A but, more importantly, have lower relative masses. Consideration must also be given to the energy resources (other than conventional oil and natural gas) from which they can be produced. These are as listed in the following table:

Synthetic fuel	Energy source for fuel	Program study area
SYN. JET-A	Coal Oil shale	Fuel production from coal ✓ Aircraft ✓ Air terminal requirements ✓
Liquid methane (LCH_4)	Coal	Aircraft and fuel systems Air terminal requirements Fuel production from coal ✓
Liquid hydrogen (LH_2)	Coal Nuclear Thermal Organic	Aircraft and fuel systems ✓ Air terminal requirements ✓ Fuel production from coal ✓

The scope of the alternate fuels program being sponsored by the Langley Research Center is also given in the table on the previous page. Synthetic JET-A (SYN. JET-A), liquid methane (LCH_4), and liquid hydrogen (LH_2) are being studied in the program. The study areas for the three fuels include the aircraft and the aircraft fuel systems, ground requirements at the air terminal and airport, and fuel production. The check marks indicate studies which have been completed. Most of the Langley-sponsored effort has been in the areas of liquid hydrogen fuel and the production of all three fuels. Fuel production studies were included in the program in order to obtain a better overall picture of the synthetic fuels options. Fuel production study results are discussed first, since they are most germane to the area of public concerns. Aircraft and airport study results are discussed in later sections.

The Langley-sponsored fuel production studies have been limited to production from coal. Coal was selected as the energy source for the studies because it is the largest fossil fuel resource in the United States (ref. 2) and because all three candidate fuels can be produced from coal, thus providing a common basis for comparison.

Although there are many variations to the many methods for producing fuels from coal, all the processes have one basically common ingredient (fig. 5), which is the production of a synthesis gas. In these processes, coal, steam, and either air or oxygen are combined in a coal gasification vessel to produce a synthesis gas (a gas rich in CO, H_2, and CH_4). Part of the coal is reacted with the air or oxygen to provide the heat for the production of the synthesis gas. The constituency of this synthesis gas can be controlled to a great extent by varying the pressure and temperature in the basic coal gasification vessel (ref. 4). What happens to the synthesis gas after it leaves the coal gasifier depends upon the desired end product.

If the end product is to be hydrogen, the synthesis gas production is tailored (high temperature) to produce a gas rich in H_2. The CO is combined with steam, over the proper catalyst, to produce more H_2 (labeled as the water-gas shift process in fig. 5).

If the end product is to be methane, the synthesis gas production is tailored (high pressure) to produce a gas rich in CH_4. Proper amounts of CO and H_2 are produced to provide for the methanation reaction (a reaction of CO and H_2 over a catalyst), which produces CH_4.

If the desired end product is to be SYN. JET-A, there are two basic processes which may be employed. One process is that of coal liquefaction, in which the basic role of the synthesis gas is to provide H_2, which is added to the coal to produce a mixture of gases and liquids. There are a number of methods by which the hydrogen can be added to the coal, and the method of hydrogen addition is the major feature which distinguishes one coal liquefaction process from another. (See ref. 5 for details.) The second basic process is known by the generic term as the Fischer-Tropsch process. This process was utilized by Germany in World War II to produce gasoline from coal and is currently being used in South Africa for the production of a variety of fuels

from coal. In the Fischer-Tropsch process, the synthesis gas is reacted over the proper catalyst to produce a mixture of gases and liquids. The proper selection of the catalysts, reaction pressure, and reaction temperature can control the nature of the gases and liquids produced. Portions of the gas - product (basically H_2) from the coal liquefaction and Fischer-Tropsch processes are utilized to upgrade the liquid products to SYN. JET-A and other liquid fuels.

The processes just described are but general descriptions of how the three fuels may be produced from coal. There are many modifications of these processes, which are more exotic and are aimed at reducing coal consumption, decreasing oxygen requirements, and decreasing production cost. Some of these processes are described in reference 5.

The principal findings of the Langley-sponsored fuel study for three key factors are summarized as follows:

	SYN. JET-A	LCH_4	LH_2
Efficiency, coal to fuel, percent . . .	54	64	49
Price for 127 MJ, the energy in 3.79 ℓ (1 gal) of JET-A, cents . . .	67	51	82
Other potential product uses	Diesel fuel	Substitute natural gas	Production of chemicals and food

The first factor is the efficiency with which the fuels may be produced from coal. This factor is important from the standpoint of efficient utilization of the remaining United States coal resources and from the cost standpoint as well, since coal cost can be a large contributor to coal-derived fuel costs. Herein, efficiency is defined as the ratio of the heating value of the fuels produced by a process to the heating value of the coal required to produce the fuels. Liquid methane was determined to be the most thermally efficient fuel producible from coal, followed by SYN. JET-A and LH_2. Also shown is the price of 127 MJ of energy (the energy content of 3.79 ℓ (1 gal) of JET-A fuel) for each fuel. The prices are based on a coal cost of \$22/tonne (\$20/ton) and 1974 dollars. A private-investor financing method was used to determine the return on investment. The basic features of this method are summarized as follows:

Project life	25 years
Depreciation	16-year sum of the digits on total plant investment
Capital	100 percent equity

DCF return rate	12 percent
Federal income tax	48 percent
Return on investment during construction	DCF return rate × 1.878* years × Total plant investment
Plant stream factor	90 percent

*10 percent for 3 years, 90 percent for 1.75 years.

Liquid methane was determined to be the least expensive fuel, followed by SYN. JET-A and LH_2. It was also determined (ref. 5) that because of the higher efficiency associated with the production of LCH_4, the price of LCH_4 was the least sensitive to increases in the cost of the coal used in its production.

The table on the previous page also lists other potential product uses for each fuel. When synthetic fuel plants are built, there will be competition for their outputs from sectors other than air transportation. For instance, there will be competition for synthetic diesel fuel, a distillation fraction similar to SYN. JET-A. There will also be competition for methane for use as substitute natural gas and competition for hydrogen for production of chemicals (such as fertilizer) and for food processing. Reference 6 documents the potential future demand for hydrogen for a variety of uses.

Community Impact

Consideration must be given to potential concerns of the community at larg which the implementation of the candidate alternate fuels might create. The following table summarizes how two of these concerns - the distribution system and its safety and aircraft emissions - differ, depending upon the fuel selecte

Community concern	SYN. JET-A	CH_4	H_2
Distribution system and safety	No change (JET-A lines)	No change (natural gas lines)	High pressure or large lines
Aircraft emissions (relative to JET-A)	Same or worse	Improved	Greatly improved

Fuel distribution.- It is likely that the plants which will produce coal-derived synthetic fuels will be located where the coal is located. The locations of the major coal deposits in the United States are shown in figure 6. The fuels, once they have been produced, must then be transported to the points at which they will be used - the nation's airports. Figure 7 shows the

existing major liquid petroleum pipeline network as well as the coal deposits in the United States. This extensive existing network could be used to transport coal-derived synthetic JET-A to its ultimate point of use. Figure 8 shows the existing major natural gas pipeline network as well as the coal deposits. These lines could be used to distribute coal-derived methane across the nation, since natural gas is more than 90 percent methane. No such national pipeline network exists for carrying hydrogen.

For equal volumes of gas, the heating value of hydrogen is about 1/3 that of natural gas. Reference 7 has indicated that for fully turbulent pipeline flow and the same pipeline diameter and pressure, the velocity of hydrogen flow in the line is nearly 3 times that of natural gas. Therefore, the major gas lines leading from gas wells, which are generally fully turbulent, could deliver about 90 percent as much energy throughput for hydrogen as for natural gas.

Reference 7 also indicated that although the volume of leakage through cracks and holes would be about 2-1/2 to 3 times greater for hydrogen than for natural gas, the lower energy density of hydrogen (again 1/3 that of natural gas) may more than compensate for its higher leak rate and thus the energy loss would be about the same.

The entire question of the compatibility of natural gas pipelines with hydrogen is being addressed at the present time in experiments sponsored by the U.S. Department of Energy and the gas industry. At the Institute of Gas Technology (IGT) in Chicago, three closed pipeline loops have been assembled to circulate hydrogen gas through natural gas lines, valves, and pumps, which have been donated by the gas industry. The goals of the work at IGT are to determine the energy throughput, pumping requirements, leak rates, and safety aspects associated with the use of the natural gas pipeline system for gaseous hydrogen transportation. Work is underway at the Sandia Laboratories, Livermore, California, to determine the potential problems and solutions associated with hydrogen embrittlement of natural gas pipeline materials. Results of these studies will go far in establishing whether new pipelines will be required for gaseous hydrogen transportation and, if so, how they should be designed and operated to provide safety to the public equal to at least that which exists for natural gas pipelines. Should new pipelines be required for hydrogen transportation, the communities in the path of these pipelines would be disrupted by their installation.

Aircraft emissions.- The emissions characteristics of the alternate fuels relative to JET-A fuel are summarized in a previous table. When SYN. JET-A is referred to in this paper, it is assumed that the quality and physical characteristics of the fuel are the same as current-day JET-A specifications. There are, however, trade-offs which might be made between fuel specifications, fuel costs, and efficiency of production. Synthetic JET-A of lesser quality could be produced at a somewhat lower cost and at a greater efficiency, but the emissions from an aircraft utilizing the fuel would increase as would engine maintenance. The problem is basically that of increasing or decreasing the hydrogen content of the fuel. The higher the hydrogen content of the fuel, the better the emissions characteristics and engine maintenance requirements. Adding hydrogen to the fuel costs money and energy, however.

Use of either LCH_4 or LH_2 compared with SYN. JET-A should result in improved emissions characteristics. Hydrogen is considered to be an environmentally superior fuel, its only combustion products being water and oxides of nitrogen. Lean burning (ref. 5) offers the potential for drastic reduction of oxides of nitrogen.

INDUSTRY CONCERNS

The introduction of alternate fuels into the air transportation system will have a maximum impact on the air transportation industry. Industry concerns are addressed in this section from the standpoint of the air transport manufacturers, the operational aspects, and the airport itself.

Air Transport Manufacturers' Concerns

The following table summarizes how synthetic fuel selection may cause concerns to the engine and airframe manufacturers, if and when such fuels are utilized:

<table>
<tr><th>System</th><th>SYN. JET-A</th><th>LCH_4</th><th>LH_2</th></tr>
<tr><td>Engines</td><td rowspan="3">Present aircraft compatible</td><td colspan="2">Present engines compatible but R & D could improve efficiencies over JET-A</td></tr>
<tr><td>Aircraft fuel system</td><td rowspan="2">Presently unidentified, work underway</td><td>System identified
R & D needs
Cryoinsulation
Pumps</td></tr>
<tr><td>Aircraft configuration</td><td>Defined
Best with fuselage tanks
Certification?</td></tr>
</table>

Synthetic JET-A would (again if the fuel specifications are unchanged) be completely compatible with the present aircraft and their systems. A study of the characteristics of methane-fueled aircraft has just been initiated by Langley with the Lockheed-California Company (CaLAC), and the results of this study should help to define what demands LCH_4 would place upon the air transport manufacturers.

Considerable information has been obtained on the characteristics of aircraft fueled with liquid hydrogen. The study of reference 8 was carried on in 1974 by the Lockheed-California Company (CaLAC) to determine how an LH_2-fueled aircraft should be configured, where the fuel should be stored onboard the aircraft, and how well the aircraft would perform in relation to aircraft

fueled with JET-A. The results of this study are summarized in figure 9 for subsonic aircraft designed to carry 400 passengers 10 000 km. The empty masses of the two aircraft were about the same. The big difference was in the mass of the fuel required by the Jet-A aircraft, which amounted to about 3 times that required by the LH_2 aircraft. This difference resulted in a gross take-off mass 25 percent lower and a wing area 20 percent less for the LH_2 aircraft, as shown in the plan view to the left of the figure. The smaller wing of the LH_2 aircraft, combined with an 11 percent longer and 13 percent wider fuselage, resulted in a cruise lift-drag ratio of 16, compared with 18 for the JET-A aircraft; but this decrease in aerodynamic efficiency was overriden by the lower gross take-off mass of the LH_2 aircraft. The energy consumption (on-board energy only, exclusive of fuel production energy) was 10 percent less for the LH_2 aircraft than for the JET-A aircraft (706 kJ/seat-km for LH_2 versus 786 kJ/seat-km for JET-A).

The initial CaLAC study (ref. 8) also determined that the best place to locate the low-density LH_2 fuel was in tanks within the fuselage, both fore and aft of the double-decker passenger compartment, as shown in the illustration of figure 10. External wing tank configurations were also studied, but the drag caused by the tanks resulted in excessive fuel consumption. The major difference identified (but not detailed) between an LH_2 aircraft and one fueled with conventional JET-A would be in the fuel systems.[2] A follow-on effort by CaLAC (under Contract NAS1-14614) is nearly completed and addresses the conceptual design of the total fuel system of an LH_2 aircraft, optimized for total fuel system and aircraft performance. The study considers all aspects of the fuel system, (e.g., fuel containment, fuel delivery, fuel flow control, and engine), as illustrated in figure 11. Identified highlights of the study, summarized in figure 12, include the design of a workable, light-weight, integrated fuel system; an 18-percent onboard energy savings for the LH_2 aircraft over JET-A aircraft (compared with 10 percent identified in the earlier 1974 effort); and a 9-percent savings in coal resources, compared with the coal resources required to power SYN. JET-A aircraft. The coal resources considered include the energy content of the coal required to produce the synthetic fuels.

The study also pointed out that the performance (based on the thrust per megajoule of fuel) of engines designed to use LH_2 may be superior to that of engines fueled with JET-A (about 5 percent, which contributes to the 18-percent onboard energy savings). Research and development effort was identified as needed in this area as well as in the areas of insulation and pumps.

The certification of an LH_2 aircraft and its fuel system was only partially addressed in the study and remains a moot question. Testing will be required to provide the development of new components, the qualification of components and subsystems, and the demonstrations of complete systems performance, safety, and reliability prior to flight testing. In carrying out the design study of the LH_2 aircraft fuel system, consideration was given to the Federal Airworthiness Regulations. For instance, each of the two fuel tanks was subdivided into two tanks in order to provide compliance with Section 953 of FAR 36 (ref. 9), which requires an independent fuel supply system for each engine. The study

also identified portions of the Federal Airworthiness Regulations which had been developed specifically for JET-A fuel but which would not be directly applicable to LH_2 aircraft. Specific revisions to the regulations, consistent with the intent of the regulations but tailored specifically for LH_2, were also defined.

Operational Concerns

Use of synthetic fuels will have varying effects on the operational aspects of the air transportation system, as shown in the following table:

Operational aspect	SYN. JET-A	LCH_4	LH_2
Aircraft size*	Present aircraft compatible	Presently undefined	More viable for large aircraft and long haul
Introduction to fleet*		Phase-in problems: All new aircraft Fuel availability	
Engine maintenance*		20 to 30% less (2.5% less DOC)	
Turnaround time*		Presently undefined	Compatible
Safety*		?	?

*Relative to JET-A.

SYN. JET-A is seen to be compatible with present aircraft in all operational aspects. With regard to the cryogenic fuels, a point-design long-haul LCH_4 aircraft is currently under study by CaLAC, as mentioned previously. Turnaround times for the LCH_4 aircraft are to be determined in the study, but the performance of LCH_4 aircraft sized for different range-payload missions will not be addressed. The performance of LCH_4 aircraft should not be as sensitive to changes in design mission as is the performance of LH_2 aircraft, since LCH_4 requires 60 percent more fuel volume than JET-A, compared with 300 percent more fuel volume required for LH_2. The CaLAC LH_2 aircraft studies (refs. 8 and 10), which addressed a number of range-payload combinations, determined that LH_2 aircraft were more viable for large aircraft and long-haul missions, both of which require use of a large amount of energy.

The introduction of cryogenic fuels to the fleet may cause phase-in problems. New aircraft designed specifically for cryogenic fuels will certainly be required for LH_2 and most probably for LCH_4 as well. Fuel availability, both nationwide and worldwide, could also be a problem with cryogenic fuels.

Regarding engine maintenance, the CaLAC LH_2 fuel system study determined that from experience obtained by pumping natural gas and utilizing natural gas as a pump fuel (essentially CH_4), 20 percent less maintenance can be expected from turbine engines burning methane. On the basis of these data, expected engine maintenance is estimated to be 30 percent less from the use of hydrogen. This lower engine maintenance translates into a 2.5-percent decrease in direct operating cost for LH_2 aircraft.

Turnaround times for LCH_4 aircraft are presently undefined but are to be determined in the CaLAC LCH_4 study. The studies of references 11 and 12, which analyzed the ground requirements for LH_2 aircraft at the airport, determined that LH_2 aircraft fueling, servicing, and passenger movements could be accomplished within conventional turnaround times.

The safety aspects associated with the use of either LCH_4 or LH_2 as an aircraft fuel have not been determined. However, safety was a prime consideration in the studies of LH_2 aircraft and their ground requirements at the airport.

In the CaLAC LH_2 aircraft fuel system study, the design of the system included failure mode analyses. For instance, in screening the various fuel tank insulation concepts, a design criterion was that no single or probable combination of failures would lead to loss of life or aircraft.

Airport Concerns.

The introduction of synthetic fuels into the air transportation system may cause new concerns regarding operations at the airport. Some of these concerns are listed in the following table:

<table>
<tr><th>Airport concern</th><th>SYN. JET-A</th><th>LCH_4</th><th>LH_2</th></tr>
<tr><td>Fuel supply</td><td rowspan="6">Present systems compatible</td><td>Proximity to natural gas distribution</td><td>Proximity to H_2 manufacturer</td></tr>
<tr><td>Fuel processing and storage</td><td colspan="2">On-site liquefaction and storage land area generally available</td></tr>
<tr><td>Fuel delivery to aircraft</td><td rowspan="3">Presently undefined, work underway</td><td>Safe system defined</td></tr>
<tr><td>Aircraft maintenance area</td><td>New facilities required</td></tr>
<tr><td>Passenger enplanement</td><td>Double-deck aircraft accommodations</td></tr>
</table>

With SYN. JET-A, all systems and operations will be compatible with those presently in use. With methane, the proximity of the fuel supply would be as close as the nearest natural gas pipeline. Whether or not the existing natural gas pipelines could be used for the transport of gaseous hydrogen is a moot question. As discussed in the section entitled "Fuel Distribution," tests are currently being conducted to determine the compatibility between natural gas lines and gaseous hydrogen. Should new lines be required for hydrogen, the proximity of the airport to the H_2 manufacturer may be a concern.

The ground requirements for LCH_4 aircraft at the airport are presently undefined but are being addressed in the CaLAC LCH_4 study which is currently underway.

Dual studies of the requirements for hydrogen-fueled aircraft at the airport were conducted by Boeing (ref. 11) and CaLAC (ref. 12). The studies assumed that all wide-body jets at two major airports (Chicago-O'Hare International Airport and San Francisco International Airport) would be fueled with LH_2. It was determined that sufficient land area was available at both airports for the required on-site hydrogen liquefaction and storage facilities. Although methane liquefaction and LCH_4 storage facilities were not addressed in these studies, it appears reasonable that sufficient land area would exist for methane liquefaction and storage facilities, since methane liquefaction is less complex than hydrogen liquefaction and LCH_4 requires less storage volume than LH_2. Closed-loop systems were defined for delivering the LH_2 from storage to the aircraft. It was also determined that to prevent accumulation of hydrogen vapors in aircraft maintenance buildings, new defueling and maintenance facilities would be required for LH_2 aircraft. The earlier LH_2 aircraft configuration studies determined that the LH_2 fuel should be stored in large-diameter tanks fore and aft of a double-deck passenger compartment. Therefore, for ease of passenger emplanement, double-deck passenger loading facilities at the air terminal would be required.

A schematic view of the LH_2 fuel facilities at the airport is shown in figure 13. Gaseous hydrogen is delivered to the airport via pipeline and thence to a liquefaction plant, where the hydrogen is liquefied and stored in large cryogenic vessels. The LH_2 is pumped through two pipelines (vacuum jacketed) and is continuously circulated around the perimeter of the air terminal and returned to the storage vessels. Two LH_2 lines are utilized to provide system redundancy. Despite the fact that the LH_2 fuel tanks onboard the aircraft will never be completely empty during normal use, the temperature of a large portion of the tank will be significantly higher than that of the LH_2. About 15 percent of the LH_2 placed in the aircraft will be vaporized as a result of H_2 vapors created during tank cool down, resaturation of the LH_2 in the aircraft fuel tank, boil-off prior to fueling, and displaced ullage gas. The studies showed that it is desirable from the standpoints of cost and energy conservation to collect the cold H_2 vapors and reliquefy them. To this end, the third pipeline shown in figure 13 is used to capture the H_2 vapors and return them to the liquefaction plant for reliquefaction. Hydrogen vapor created by boil-off in the storage vessels and by the flashing of the LH_2 returning to the storage vessels is also reliquefied. The LH_2 distribution lines and H_2 vapor collection lines are located in either open trenches with

steel grates covering the trenches or are buried in positively ventilated tunnels. Tunnels could be made under the runways without interrupting airport operations.

Figure 14 illustrates in more detail the process at each hydrant whereby the aircraft are fueled. Each airline is provided with an appropriate number of fueling hydrants. A hydrant truck is used to connect the hydrant to the aircraft. Two lines are connected to the aircraft, one for delivering the LH_2 fuel to the aircraft and one for returning the cold H_2 vapors produced during aircraft fueling to the liquefaction plant for subsequent reliquefaction. After the aircraft has been fueled, the line which connects the hydrant to the aircraft is purged with helium (carried in pressurized bottles on the truck), and the mixture of helium and hydrogen is transferred via a small third line to the return vapor line to the liquefaction plant. This process permits the recovery of the H_2 in the line and, more importantly, the recovery of the purge helium.

The ground systems defined by Boeing and CaLAC are completely enclosed and permit essentially no H_2 to escape. Estimates of the capital investments required to provide LH_2 facilities at Chicago-O'Hare International Airport and San Francisco International Airport were $469 million and $340 million, respectively. In an earlier section of this paper ("What Fuels?") the price of coal-derived alternate fuels was discussed. The fuel prices shown for LCH_4 and LH_2 include the amortized capital investment required for liquefaction plants. The hydrogen liquefaction plants represent a major portion (60 to 85 percent) of the capital investment required for the LH_2 airport facilities.

Although safety was a prime consideration in the LH_2 airport studies, the safety aspects associated with the use of LH_2 and LCH_4 at the airport are yet to be fully determined. Overall, SYN. JET-A would appear to cause fewer concerns to the air transportation industry than would either LCH_4 or LH_2.

AIR TRAVELER'S CONCERNS

Three major concerns to the air traveler are safety, service, and cost. Synthetic JET-A would effect no change to safety and service. The safety aspects, as they concern the air traveler, have not been determined for LCH_4 or LH_2. However, if a fuel release occurs during an aircraft crash, the more volatile the fuel, the greater the likelihood of a fire. Liquid methane and liquid hydrogen are more volatile than SYN. JET-A. In addition, the minimum energy for ignition of H_2 in air is 1/10 that of CH_4 and SYN. JET-A; thus an even greater possibility of fuel ignition exists for H_2. However, mitigating factors may be the characteristics of an H_2 fire - mainly its short duration and lower thermal radiation and the fact that no asphyxiating smoke occurs.

With regard to service and delays, the Boeing and CaLAC LH_2 airport studies indicated that the use of LH_2 should not cause ground delays and that the required modifications to the airport should not cause an interruption in services. As mentioned previously, an insufficient nationwide and worldwide availability of LCH_4 or LH_2 could introduce inconveniences to the air traveler,

particularly during the early phases of implementation of such fuels. Obviously, the aircraft using these fuels could fly only to and from locations where the fuels were available. Not all countries have coal resources (or oil shale for that matter) from which to produce synthetic fuels. Insight into these potential problems will be obtained as the synthetic fuels industry develops in the United States and abroad.

Regardless of which synthetic fuel is selected, the air traveler will pay a higher price for an airline ticket. The bar graph shown in figure 15 illustrates the passenger ticket price for transport aircraft which utilize synthetic coal-derived aviation fuels, and JET-A fuel at 9.5¢/ℓ (36¢/gal). Each bar is divided to show amounts associated with direct operating cost (DOC), indirect operating cost (IOC), and miscellaneous costs (MISC.). The shaded area of DOC indicates that portion of the ticket price associated with fuel cost. Two ticket prices are shown for the coal-derived fuels, one for which the coal used to produce the fuels costs $11/tonne ($10/ton) and one for which the coal costs $33/tonne ($30/ton). The ticket cost bar for the LCH_4 is dashed, as it is based on a "best guess" performance of LCH_4 aircraft. More definitive performance figures will be obtained from studies by CaLAC now underway. The synthetic fuel costs do not include the costs associated with storing and distributing the fuels at the airport. The major portion of the LH_2, and most likely of the LCH_4, fuel costs is however represented here, since the fuel costs include the liquefaction plant - which (from refs. 11 and 12) is the major airport facility cost for LH_2 (again, 60 to 85 percent). The principal point to be made from figure 15 is that the ticket cost associated with LH_2 is competitive with that of SYN. JET-A if coal costs $11/tonne ($10/ton) and is slightly lower if coal costs $33/tonne ($30/ton). Liquid methane may provide the least expensive ticket of the three coal-derived fuels. It must be mentioned that the fuel costs shown in figure 15 are based on 1974 dollars. Should the fuel costs be updated to current year dollars, the ticket cost associated with all the synthetic fuels would increase.

CONCLUDING REMARKS

The results of engineering studies of coal-derived aviation fuels and their potential application to the air transportation system have been presented. Synthetic aviation kerosene (SYN. JET-A), liquid methane (LCH_4), and liquid hydrogen (LH_2) appear to be the most promising coal-derived fuels.

To date, most of the aviation systems studies have centered on LH_2 as a fuel. Liquid-hydrogen-fueled aircraft configurations, their fuel systems, and their ground requirements at the airport have been identified. From these studies, LH_2 aircraft appear viable, particularly for long-haul use, where aircraft fueled with coal-derived LH_2 would consume 9 percent less coal resources than would aircraft fueled with coal-derived SYN. JET-A. Distribution of hydrogen from the point of manufacture to airports may pose problems. Synthetic JET-A would appear to cause fewer concerns to the air transportation industry than would either LCH_4 or LH_2. The ticket price associated with coal-derived LH_2-fueled aircraft appears competitive with that of aircraft fueled with coal-derived SYN. JET-A.

Of the three candidate fuels, LCH_4 is the most energy efficient to produce, and an aircraft fueled with coal-derived LCH_4 may provide both the most efficient utilization of coal resources and the least expensive ticket as well. Ongoing studies will provide a better assessment of the potential for LCH_4 as an aircraft fuel.

Although safety was given prime consideration in the systems studies reported, the safety aspects associated with the use of cryogenic fuels, such as LCH_4 and LH_2, in the air transportation system are yet to be determined.

REFERENCES

1. LeGassie, Robert W.; and Ordway, Frederick I.: A Quick Look at the National Energy Plan. Astronaut. & Aeronaut., vol. 15, no. 11, Nov. 1977, pp. 28-35.

2. A National Plan for Energy Research, Development & Demonstration: Creating Energy Choices for the Future, Volume I. ERDA-48, June 28, 1975.

3. Project Independence. Project Independence Rep., Fed. Energy Adm., Nov. 1974.

4. Hottel, H. C.; and Howard, J. B.: New Energy Technology - Some Facts and Assessments. Massachusetts Inst. Technol., c.1971.

5. Witcofski, Robert D.: Alternate Aircraft Fuels - Prospects and Operational Implications. NASA TM X-74030, 1977.

6. Hydrogen Tomorrow - Demands & Technology Requirements. JPL 5040-1 (Contract No. NAS 7-100), Jet Propul. Lab., California Inst. Technol., Dec. 1975.

7. Pangborn, J.; Scott, M.; and Sharer, J.: Technical Prospects for Commercial and Residential Distribution and Utilization of Hydrogen. Int. J. Hydrogen Energy, vol. 2, no. 4, Dec. 23, 1977, pp. 431-446.

8. Brewer, G. D.; Morris, R. E.; Lange, R. H.; and Moore, J. W.: Volume II - Final Report: Study of the Application of Hydrogen Fuel to Long-Range Subsonic Transport Aircraft. NASA CR-132559, 1975.

9. Airworthiness Standards: Transport Category Airplanes. FAR Pt. 25, FAA, Feb. 1, 1965.

10. Brewer, G. D.; and Morris, R. E.: Final Report: Study of LH_2 Fueled Subsonic Transport Aircraft. NASA CR-144935, 1975.

11. Preliminary Design Department, Boeing Commercial Airplane Co.: An Exploratory Study To Determine the Integrated Technological Air Transportation System Ground Requirements of Liquid-Hydrogen-Fueled Subsonic, Long-Haul Civil Air Transports. NASA CR-2699, 1976.

12. Brewer, G. D., ed.: Final Report: LH_2 Airport Requirements Study. NASA CR-2700, 1976.

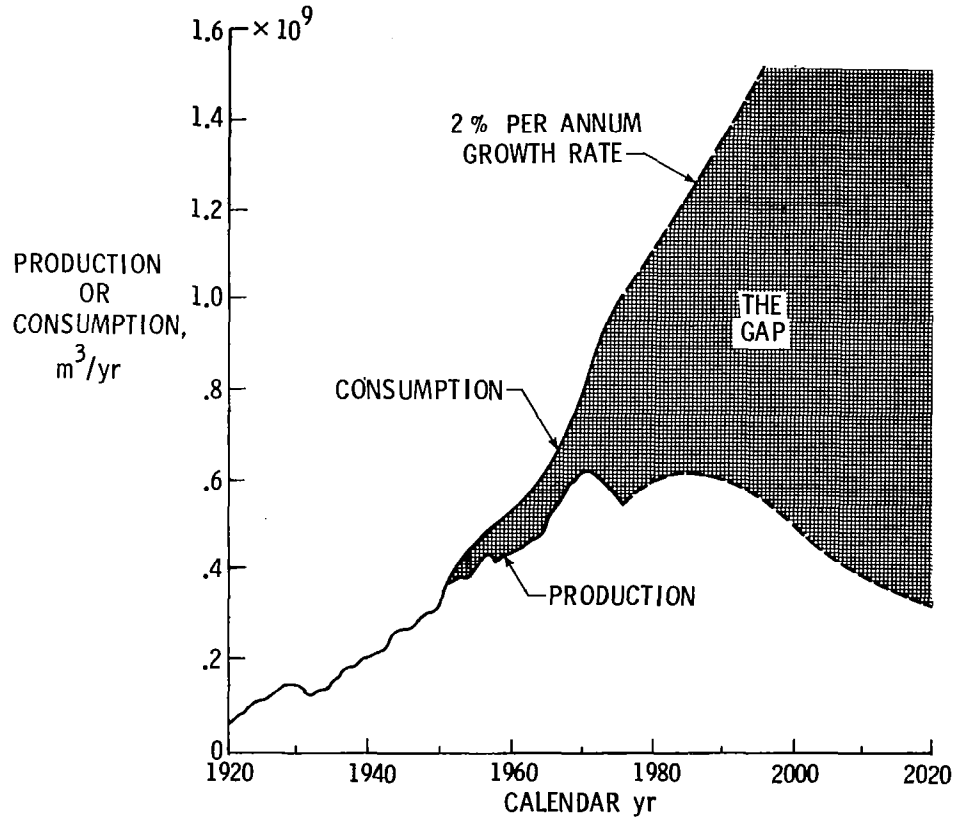

Figure 1.- Historical and projected production and consumption of oil in the United States.

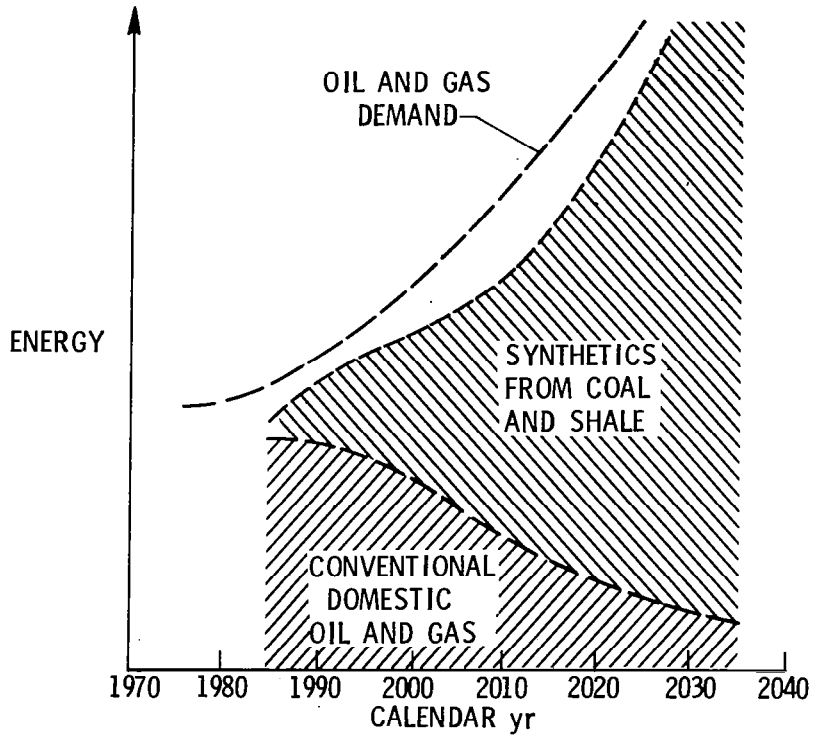

Figure 2.- Potential role of synthetic fuels in the United States, as posed by Project Independence (ref. 3).

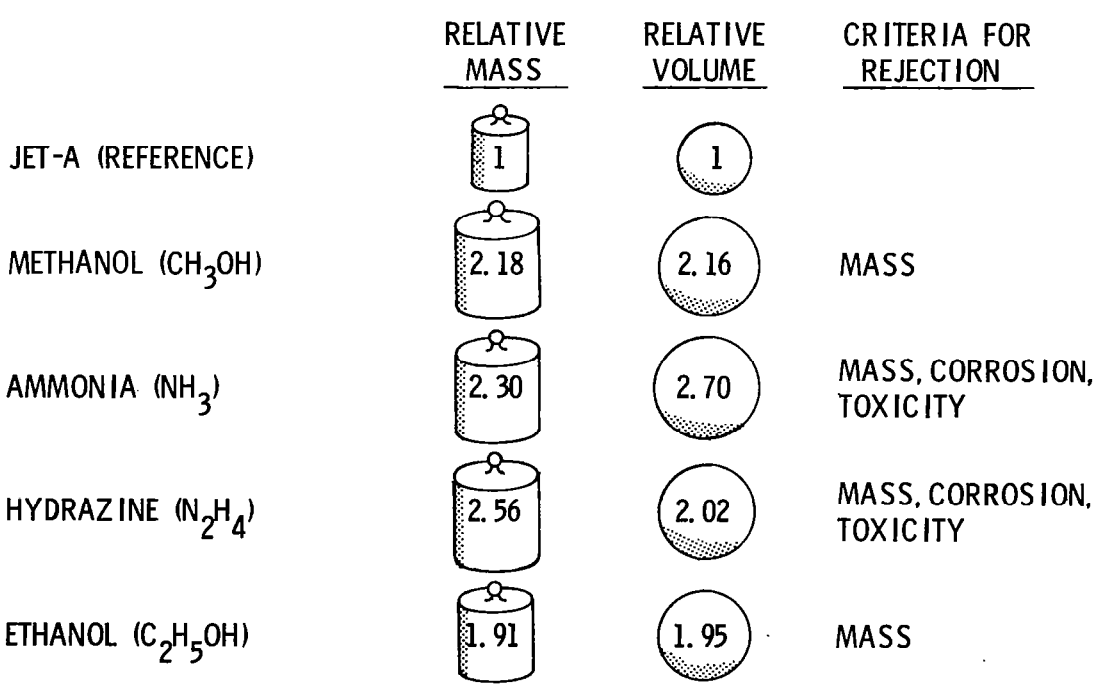

Figure 3.- Candidate synthetic liquid fuels judged not to be viable for aviation use.

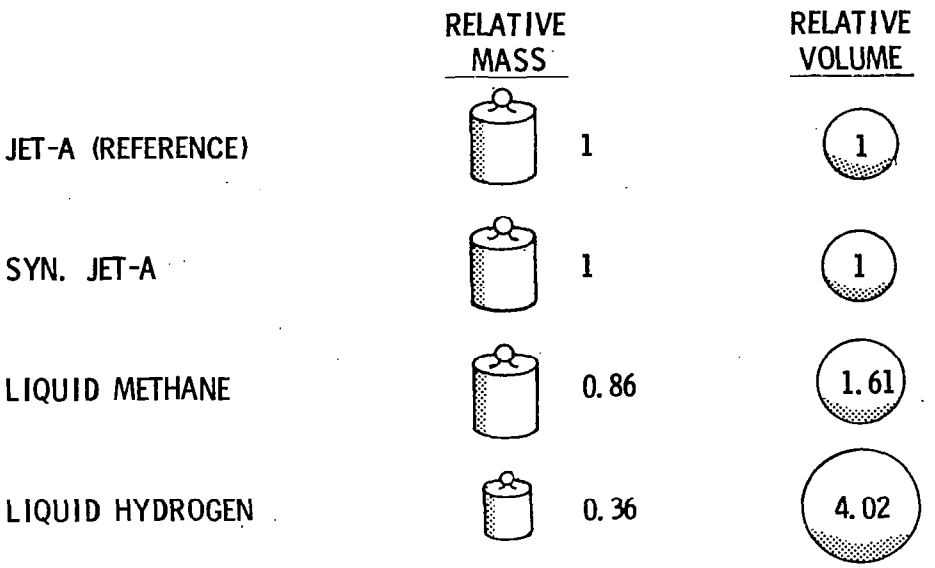

Figure 4.- Candidate synthetic liquid fuels judged viable for aviation use.

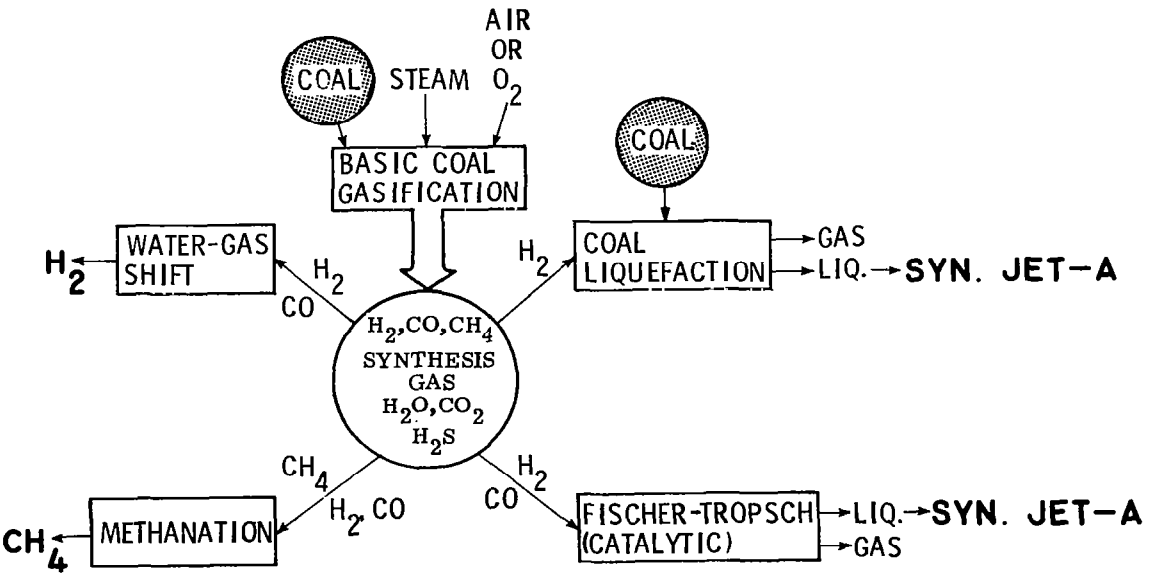

Figure 5.- Production processes for coal-based synthetic fuels.

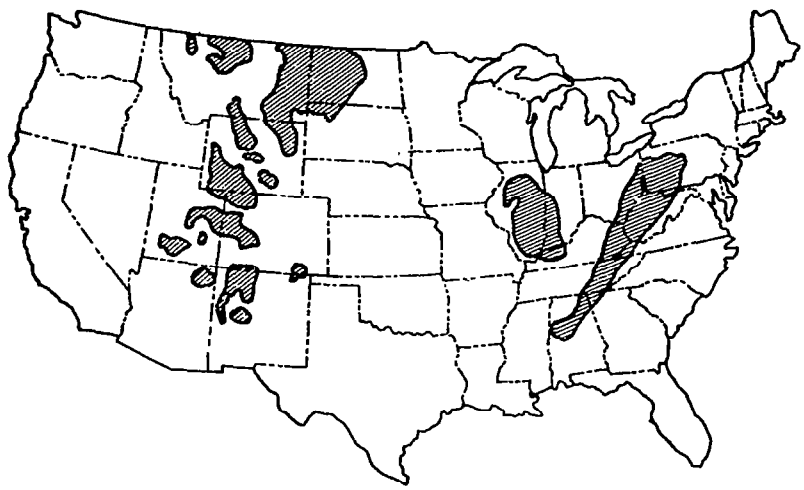

Figure 6.- Locations of major coal deposits in the United States.

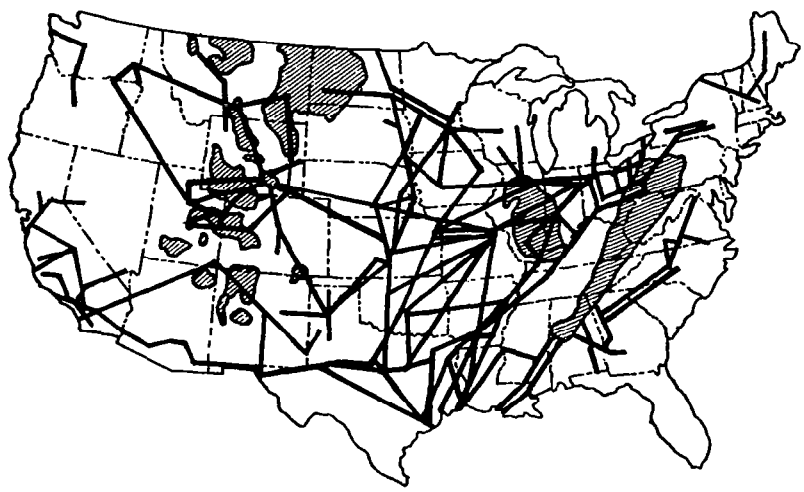

Figure 7.- Locations of major coal deposits in the United States with respect to existing major liquid petroleum pipeline network.

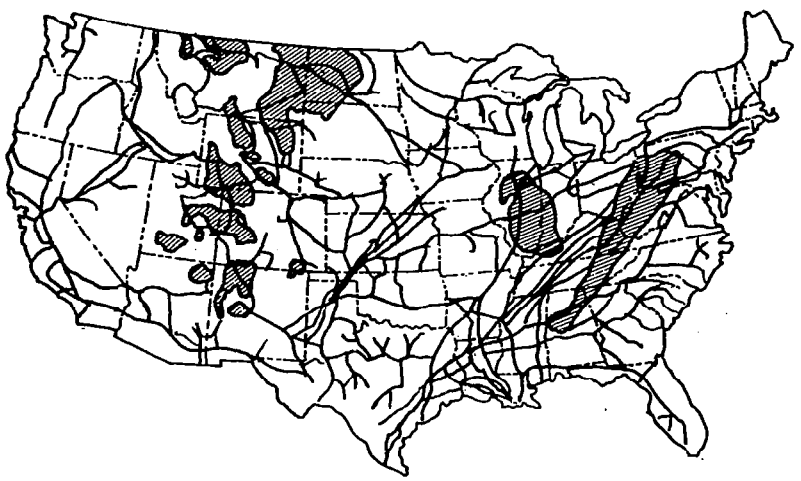

—— MAJOR NATURAL GAS LINES

Figure 8.- Locations of major coal deposits in the United States with respect to existing major natural gas pipeline network.

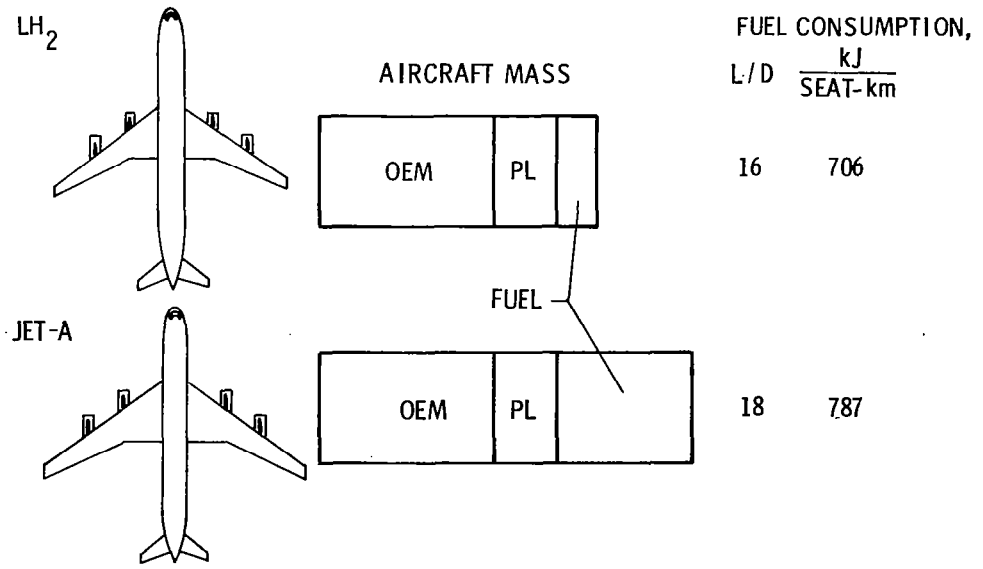

Figure 9.- Comparison of transport aircraft fueled with JET-A and with LH_2. M = 0.85; 400 passengers; range, 10 000 km.

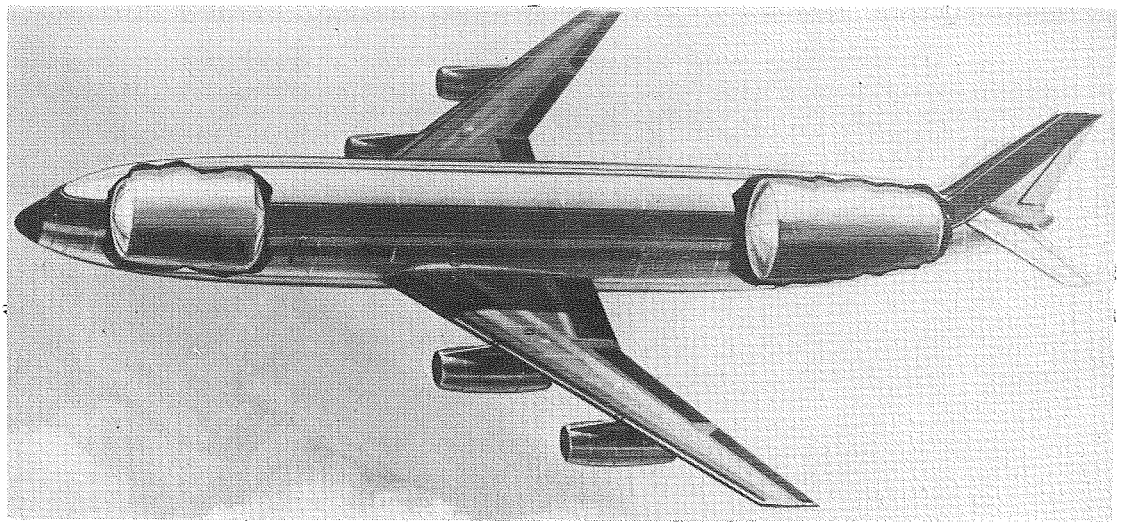

Figure 10.- Cutaway drawing of a subsonic LH_2-fueled transport aircraft.

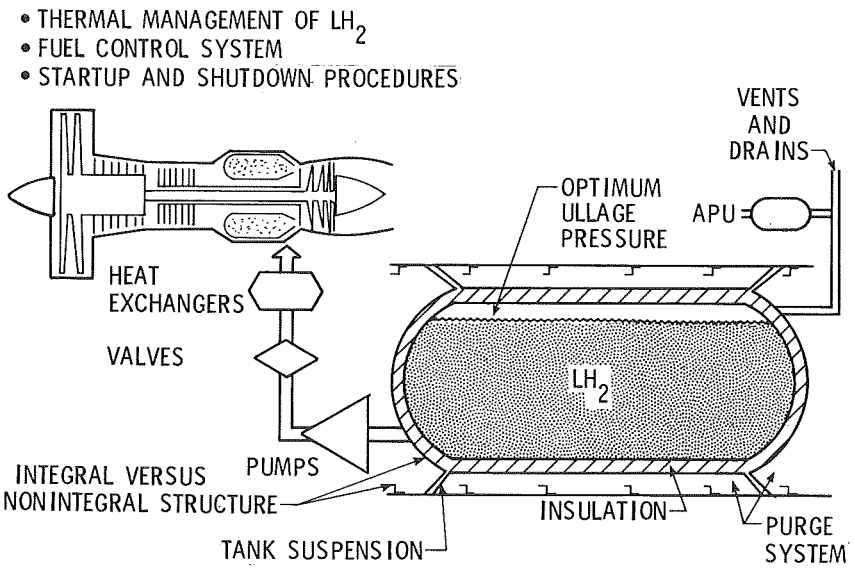

Figure 11.- Aspects considered during conceptual design of the fuel system for an LH_2-fueled aircraft.

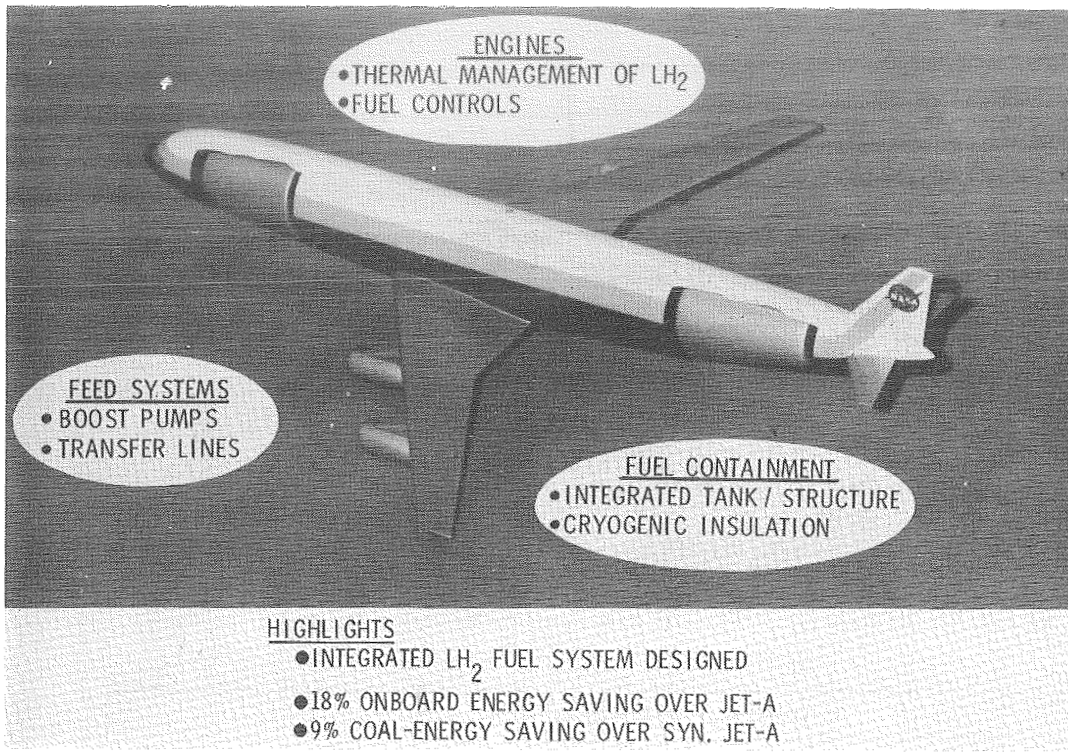

Figure 12.- Overview and highlights of fuel system study for LH_2-fueled aircraft.

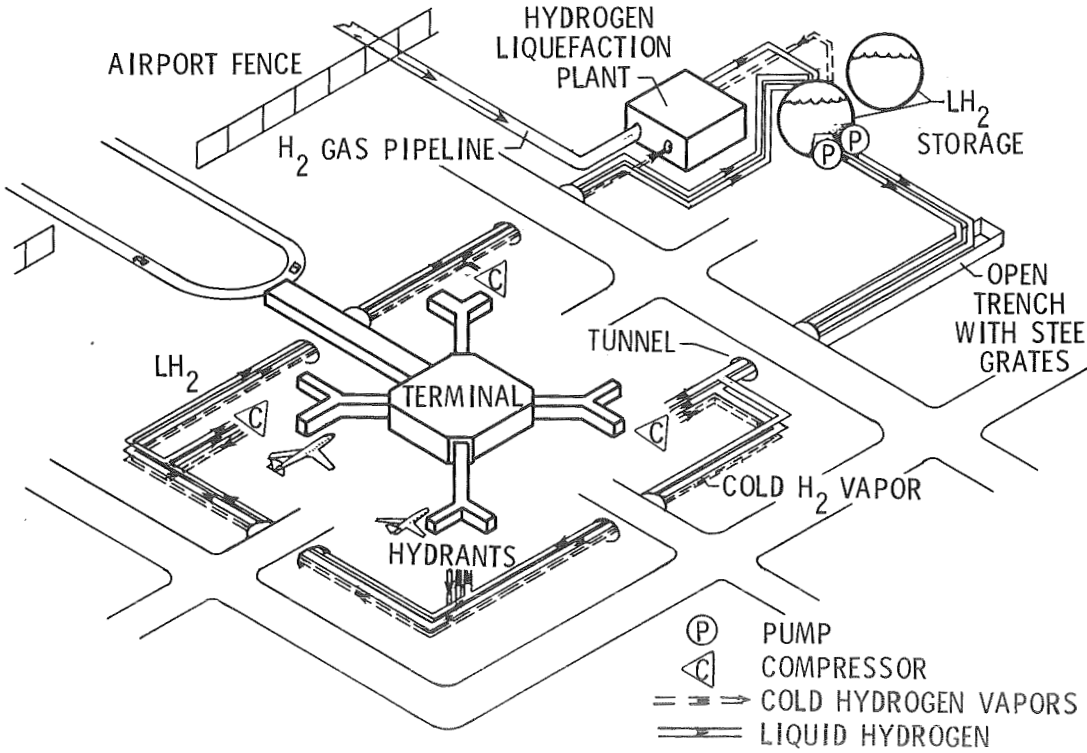

Figure 13.- Schematic of hydrogen liquefaction, storage, and distribution system at an airport.

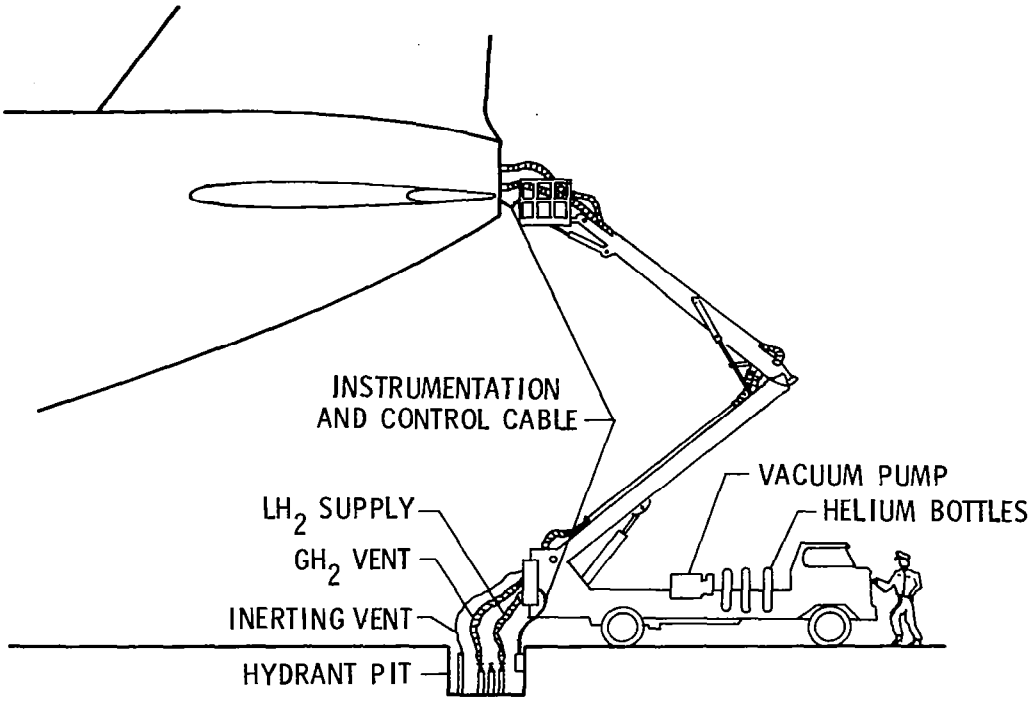

Figure 14.- Fueling of an aircraft with LH_2 via a hydrant truck.

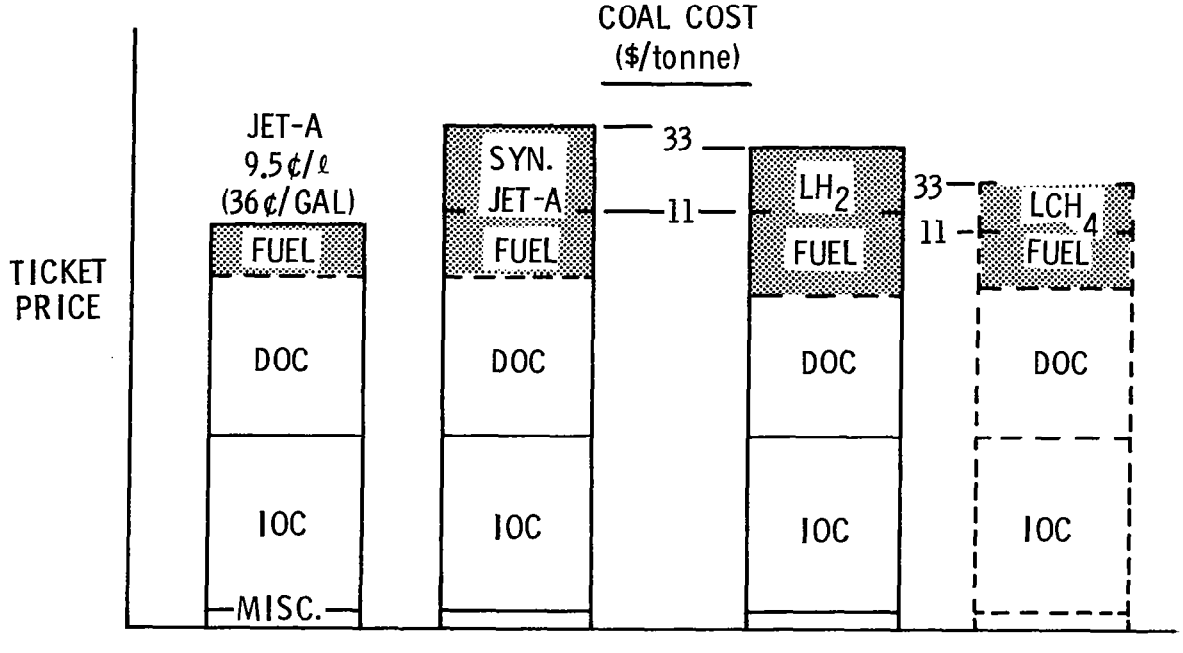

Figure 15.- Effect of coal-derived fuels on airline passenger ticket price, compared with JET-A at 9.5¢/ℓ (36¢/gal) for coal costs of $33/tonne and $11/tonne ($30/ton and $10/ton).

STUDIES OF ADVANCED TRANSPORT AIRCRAFT

A. L. Nagel
NASA Langley Research Center

SUMMARY

Studies have been made of several concepts for possible future airplanes, including all-wing distributed-load airplanes, multi-body airplanes, a long-range laminar flow control airplane, a nuclear-powered airplane designed for towing conventionally powered airplanes during long-range cruise, and an aerial transportation system comprised of continuously flying "liner" airplanes operated in conjunction with short-range "feeder" airplanes. The studies indicate that each of these concepts has the potential for important performance and economic advantages, provided certain suggested research tasks are successfully accomplished. Indicated research areas include all-wing airplane aerodynamics, aerial rendezvous, nuclear aircraft engines, air-cushion landing systems, and laminar flow control, as well as the basic research discipline areas of aerodynamics, structures, propulsion, avionics, and computer applications.

INTRODUCTION

Studies of concepts for future aircraft are a continuing activity at Langley Research Center. This paper reports on studies of advanced cargo airplanes, long-range laminar flow control airplanes, a nuclear tug, and a transportation system comprised of a continuously flying airliner that is loaded and sustained with the aid of feeder airplanes.

Motivations for these airplane studies include the hope of identifying promising areas for research or evaluating various applications of new technologies, and uncovering voids that may exist in related technologies. An example of the latter might be a need for aerodynamic data for implementation of active control systems.

In the examples that follow, the discussion centers around the airplane concepts, potential performance, and research that would be required if the concepts were to be considered more seriously. Energy comparisons are given. However, while energy considerations are obviously very important, the most difficult challenge to continued growth of air transportation may well be terminal-area congestion and related problems. It is not the purpose of this paper to discuss this aspect of new airplanes, but it should be kept in mind that large size and long range are features that tend to reduce the number of terminal-area operations.

SYMBOLS

Values are given in both SI and U.S. Customary Units. Calculations were made in U.S. Customary Units.

A	area
AR	aspect ratio
c_d	section drag coefficient
c_l	section lift coefficient
L/D	lift-drag ratio
M	Mach number
M_{CR}	cruise Mach number
M_{DD}	drag divergence Mach number
R_e	Reynolds number
W_G	gross weight
W_P	payload weight

DISTRIBUTED-LOAD AIRPLANES

Historically, the gross weight of new airplanes entering service has doubled every eight years. The driving force behind this trend is the "economy of scale"; that is, the fact that generally it is more efficient to do things on a large scale. Although there have been important improvements in technology throughout the history of aviation, much of the outstanding efficiency of current jet transports is due to their large size. Hence, the trend to ever larger aircraft can be expected to continue.

However, there may be changes in configuration with very large airplanes as a result of trends illustrated in figure 1. The figure shows that the available volume within the wing increases more rapidly than the volume required for fuel and payload. As indicated on the figure, there is a size below which a fuselage is required to provide adequate volume. Above that size, the wing volume alone is sufficient and no fuselage is required, at least on the basis of volume.

This trend arises from the aerodynamic requirement for approximately constant wing loading, a condition set by landing and take-off considerations. The wing area then must grow in proportion to the gross weight. For geometrically similar wings, the volume increases as the three-halves power of wing area and hence as the three-halves power of the gross weight. The fuel and

payload, on the other hand, are roughly proportional to gross weight, so their required volume is approximately linear in figure 1. In the scaling study from which figure 1 is taken the fuel and payload fractions were found to decrease slightly with increasing gross weight; therefore, the "volume-required" curve is actually slightly concave downward and must fall below the wing volume curve at some point.

The trend shown is very general and is not likely to be reversed by technological advances, although any specific numerical results are dependent on technology level. For example, the allowable wing loading has increased from 1200 Pa (25 lb/ft^2) for the DC-3 to well over 4800 Pa (100 lb/ft^2) for current wide-body transports, changing wing volume by approximately 8 times for an airplane with a given gross weight. There are other factors that complicate the trade-offs, but the figure is correct in indicating that for very large airplanes there should be sufficient volume in the wings to meet all requirements.

Carrying payload in the wings provides another potential advantage illustrated in figure 2. In a conventional wing-body configuration, the payload weight is concentrated in the fuselage and must be supported by the wing acting as a beam. If the payload is distributed along the wing span, its weight is largely balanced by the local lift. The result is much smaller bending moments, which permits a lighter structure. Of course, the cruise equilibrium condition illustrated here is only one of many structural design conditions, so even the complete elimination of bending moments in flight would not eliminate all the structural weight. However, design studies have shown important weight savings for large airplanes loaded in this fashion, as indicated in the figure.

With these thoughts in mind, large payload-in-the-wing airplanes, called distributed-load freighters (DLF), have been studied for about four years now, both in-house and under contract. Industry has also conducted studies of similar airplanes, some of them preceding the NASA studies. Figure 3 is an NASA DLF concept devised by Thomas A. Toll of Langley Research Center several years ago. It is about 794 000 kg (1 750 000 lb) all-up weight, and has a wing span of about 107 m (350 ft). It may or may not be desirable to add cargo pods as shown in this figure, depending on the density of the payload. Such pods make it easier to achieve a proper wing loading for best performance, and also make it possible to arrange a landing gear in a way that permits rotation for take-off. Most DLF studies have assumed take-off without rotation because of constraints imposed by the landing gear arrangement.

Figure 4 shows a series of DLF's studied by the indicated firms. The configurations of The Boeing Company and McDonnell Douglas Corporation were developed in NASA-funded studies. The airplanes shown in figure 4 are all approximately twice the gross weight of current wide-body airplanes. Some specific data are given in table I. Each of these airplanes carries its payload in the wing, which tends to drive the configurations toward low aspect ratios and wing loadings. Although the Douglas configuration looks more conventional than the others, its fuselage exists primarily to provide a support for the tail.

Lockheed-Georgia Company, which conducted its study without NASA funding, coordinated its study in timing and ground rules with the NASA studies, and so provided an additional comparison. Lockheed began with an all-wing configuration, but added a fuselage and canard as a means of accommodating outsize cargo and to improve balance and control.

In this first series of NASA studies, it became evident that DLF configuration trade-offs, particularly wing design, are much different than for conventional airplanes. One aspect of the new considerations is illustrated in figure 5 (based on information in ref. 1). A series of wing cross sections is presented showing the internal arrangement of the cargo, which would be carried in standardized 2.4- by 2.4-m (8- by 8-ft) containers of either 3.05- or 6.10-m (10- or 20-ft) length. The figure shows the cargo containers with shading, and the cargo bays are shown in dotted lines. The cargo bays are somewhat higher than the container height in order to accommodate occasional outsize cargo or military equipment. As shown, the airfoil thickness ratio depends on the number of rows of cargo containers. For three rows of containers, the airfoil has a very high thickness ratio, 0.24, which is accompanied by a low drag divergence Mach number. This indicates the speed beyond which drag becomes unacceptably large, and so (for a given sweep) determines the speed of the airplane. As the number of rows of containers is increased, the airfoil thickness ratio is reduced and drag divergence Mach number increases, which permits higher flight speeds. Also shown in the figure is the cross-section utilization; that is, the ratio of payload (not payload bay) cross section to total wing cross section. This ratio increases from 36 percent for the 3-row wing to 41 percent for the 7-row wing, which indicates a significant improvement in volumetric efficiency. Hence, on the basis of figure 5, one expects that a large number of rows is advantageous.

However, if one considers the best overall design for a given payload, it is obvious that the span of the airplane must also be considered. For a given payload, the span tends to vary linearly with payload and inversely with the number of container rows (assuming the payload extends to the wing tip). This aspect of DLF configuration selection is illustrated in figure 6. This figure illustrates two possible configurations for the case of 340 000-kg (750 000-lb) payload, one with three rows of containers and the other with five rows. The 3-bay configuration is seen to have a high aspect ratio, which should give a high L/D at speeds well below M_{DD}. At some speed, however, the advantage of high aspect ratio will be more than offset by the aerodynamic penalty of its high thickness ratio. The DLF studies highlighted the fact that there is relatively little applicable wind-tunnel data for properly trading off the opposing trends of span and thickness ratio.

The most recent of the DLF's studied under NASA contracts is shown in figure 7, along with a Boeing 747 to illustrate the scale. It is a very large airplane, with a wing span of 153 m (503 ft) and a gross weight of about 1 361 000 kg (3 000 000 lb). This airplane has swept wings, which permits increased cruise speed and provides sufficient overall length to eliminate the need for a separate tail. The figure also shows how the DLF span compares with a 61-m (200-ft) wide runway, which is the width of the runways at JFK International Airport and several other large airports, although most current airports have 46-m (150-ft) wide runways. In order to distribute landing and

taxi loads, this DLF has a 7.32-m (24-ft) landing gear with a tread of about 122 m (400 ft). This airplane would therefore require special runways, but the cost of runway widening is not large in the overall cost equation if the airplane is presumed to operate out of only a small number of major airports. Hence, this airplane is visualized as operating in a hub-spoke fashion from a small number of dedicated airports, with smaller airfreighters bringing cargo to it from conventional airports. It may be that with further development, an air-cushion landing gear would offer a significant advantage by making it easier to operate out of more airports.

Figure 8 illustrates the method of loading.

An economic comparison is shown in figure 9. The economic parameter chosen is the direct operating cost (DOC) normalized by the DOC of a current wide-body airplane. An advanced technology conventionally configured airplane is shown for comparison with two DLF's of the same technology level. The swept wing DLF of figure 7 is about 27 percent lower in DOC than the advanced conventional airplane, and less than half that of a current airplane.

The smaller unswept DLF is only marginally better than the advanced conventional airplane at the size shown. This is partially due to the reduced cruising speed imposed by its unswept wing.

The enormous productivity of such a large and fast airplane as the swept-wing DLF raises the question of market growth. The current cargo market would not support development of such an airplane.

A smaller airplane that retains much of the structural benefit of span loading, without the extreme runway width requirements, could be attractive. Curve (b) of figure 10 suggests that a double fuselage airplane, such as that shown on figure 11, has these features. Although its cost per available tonne kilometer (ton mile) is expected to be higher than that of the DLF, it may save enough in handling costs to be competitive because of its compatibility with existing runways. Only very limited studies of this airplane have been made to date; however, there have been several quite successful twin-body airplanes in the past.

The DLF studies indicate that the concept is promising and offers advantages for very large airplanes. A number of areas for technology research have been identified. These are discussed in references 1 to 7 and include thick airfoils, low-aspect-ratio untapered wings, wing-tip devices, control schemes (aerodynamic and electronic aspects), propulsion integration, structures, aeroelastics, and handling qualities. Possible advanced technologies include LFC (see section entitled "Laminar Flow Control Airplanes") boundary layer control on thick airfoils (see ref. 8, ch. VI), jet flaps, and the various propulsive lift concepts (see ref. 9, e.g.). The application of these advanced technologies to DLF's obviously involves all the airplane design and economic trade-offs, but basic disciplinary research is needed before the design trade-offs can be addressed.

Considerations of the size and productivity of DLF's show a need for better market information than is now available. At present growth rates, it

would be several decades before there would be sufficient cargo traffic to make such airplanes economical. NASA is therefore conducting a number of studies aimed at providing a better understanding of possible future conditions. Among these studies are

CLASS (Cargo logistics and systems study) - a worldwide survey of users, airports, and carriers to determine the current outlook, the possible role of advanced technology for stimulating the growth of air cargo, and indications of desirable airplane characteristics.

Developing countries - a study of the potential use of advanced airplanes (including cargo) in countries that have no well-developed transportation infrastructure. A preliminary survey of all such countries has been made. A study of Brazil and Indonesia in greater depth is now under way.

Civil/military relations - NASA cooperates with USAF in searching for civil airplane concepts that could be used directly or with minimal modification for military airlift.

LAMINAR FLOW CONTROL AIRPLANES

Laminar Flow Control (LFC) is the subject of references 10 to 15. Briefly, however, LFC is a technology for reducing airplane drag by maintaining laminar boundary layers. The laminarization is accomplished by sucking a small amount of the external boundary layer flow through the skin. As shown schematically in figure 12, an LFC system requires a perforated or slotted skin and a compressor to expel the sucked air. Figure 12 is highly simplified; there must also be a system of internal ducting so that suction air from various regions of the airfoil (which will have a wide range of pressures) can all be processed efficiently.

The motivation for adding all this complexity is shown in figure 13. As shown, the drag of a fully laminarized airfoil is almost ten times smaller than that of a modern turbulent flow airfoil. The LFC curve of this figure includes the equivalent drag of the suction power.

The basic trade-off involved in LFC is then between the large drag reduction in the laminarized areas, and the weight and complexity of the suction system. LFC also requires closer tolerances on surface smoothness than current practice, which implies additional care in manufacture and additional care to keep the laminarized surfaces clean. Additional maintenance is therefore to be expected.

Studies show that the overall trade-offs are very favorable as far as fuel consumption is concerned. For fairly conventional long-range passenger airplanes, fuel consumption reductions of up to 29 percent have been reported (ref. 16). The economic benefits are smaller and are subject to great uncertainty because there is no applicable experience with maintenance costs. It is an objective of the LFC element of the Aircraft Energy Efficiency (ACEE) project to provide better information about maintenance costs.

In this section, examples are given of advanced configurations designed to maximize the benefits of LFC. Some of the important considerations involved in configuring with LFC are as follows:

(1) Laminarization becomes increasingly difficult as the length Reynolds number is increased. LFC has been achieved in wind tunnels with Reynolds numbers up to about 60 million and in flight up to about 47 million. Additional experiments are needed to show that laminarization can be obtained at higher Reynolds numbers.

(2) Smoothness constraints became more severe with increasing unit Reynolds number.

(3) Other forms of disturbance, such as engine noise, must be minimized.

(4) Wing sweep increases the difficulty of laminarization. On swept wings, both positive and negative pressure gradients are usually destabilizing because an unstable cross flow is produced within the boundary layer.

(5) Benefits of LFC increase with range because the basic saving is in fuel, which is a larger fraction of total airplane weight and operating cost for long ranges than for short ranges.

(6) Aerodynamic disturbances originating from ice crystal clouds can cause temporary loss of LFC. The probability of encountering such clouds decreases with altitude, and is essentially zero above 12.2 km (40 000 ft) in the U.S. latitudes.

These considerations are discussed in more detail in reference 17.

From the foregoing discussion, it would be expected that a potentially attractive LFC airplane is therefore one that operates at long ranges and high altitudes (low unit Reynolds number), has LFC applied to wings and tail (maximum possible area), has high aspect ratio (short chord and low length Reynolds number), and has comparatively low sweep. Such an airplane is shown in figures 14 and 15. This type of airplane concept has been evolved over a period of many years by Werner Pfenninger, currently at Langley Research Center, who is well known for his work in LFC.

Among the unusual features of this configuration are struts, external fuel nacelles, split wing tips, and a rearward location for the wing-mounted engines. The calculated performance is much better than that of conventional airplanes, 30 percent payload fraction at a range of 11 000 n. mi. With laminarization applied to the wings, struts, empennage, engine nacelles, and wing-tip fuel nacelles, the lift-drag ratio is 48. With the struts, the optimum aspect ratio is very high, 16.3 for this particular configuration.

The use of struts may seem like a step backward since this once-common feature has almost entirely disappeared. The reason for their disappearance is that, although for a given wing span weight can be saved through the use of struts, a penalty is incurred in the form of strut drag. The minimum drag

of a well-designed strut is comparable to that of a wing of the same area, and at high speeds great care is needed to avoid premature drag rise due to flow interferences. These trade-offs are such that, for turbulent flow, struts have not been shown to "pay their way," although there has not been much research on modern strut-braced configurations.

With laminarized struts, the weight-drag trade-off is much different. Figure 13 indicates that the drag of well-designed laminarized struts could be reduced to almost negligible levels. The theory and some limited experimental data (unpublished) indicate that strut bracing offers a significant performance advantage for LFC airplanes (a comparison is given later).

The chord of the struts is large, about one-half of the wing chord, in order to provide torsional stiffness. Structurally, it is important that the struts provide torsional stiffness as well as bending strength, otherwise the weight penalties required to provide flutter margins could be excessive.

The laminarized tip tanks contain the reserve fuel. Under all normal conditions, these tanks will be full and provide appreciable bending moment relief. Flutter analyses have been made showing that the tip tanks significantly increase the flutter speed to well above the airplane cruise speed without considering any active controls. With additional fins on the nose of the tip tanks, active control technology could be applied to reduce both bending and torsional loads, as from gusts, on the wing.

The split wing tips were analyzed by Werner Pfenninger some thirty years ago. He was stimulated to do so by observations that some kinds of birds have similar features. The results of analysis of induced drag for such configurations are presented in figure 16. According to these theoretical results, the split tip configuration is almost as effective as vertical end surfaces in reducing induced drag. The total wing drag is calculated to be less than that for a wing with vertical surfaces, because the wetted area is smaller. The dot on the curve of figure 16 indicates that for the dimensions chosen for the airplane shown in figures 14 and 15, the induced drag is about 14 percent less than the minimum for an ideally loaded planar wing. Since, at optimum cruise conditions, the induced drag is nearly one-half of the total drag, the split tips increase the airplane lift-drag ratio by about six percent.

The wing-mounted engines are placed to the rear to reduce noise disturbances to the boundary layer. This location is undesirable from structural considerations, but the penalties are minimized by the design of the strut.

With the wing drag reduced by laminarization, and the wing weight reduced by external bracing, the optimum performance LFC airplane will tend to have higher aspect ratios and lower wing loadings than all-turbulent airplanes. These trends are also favorable for LFC because they lead to lower chord Reynolds numbers, lower unit Reynolds numbers, and higher cruise altitude. The various parameters are compared in table II.

Strut bracing permits thinner inboard wing sections and hence less wing sweep is needed, which makes laminarization easier. The unit Reynolds number

is seen to be much lower for the LFC airplane, increasing tolerances of roughness and waviness, and increasing the allowable slot size and spacing.

Many variations of the configuration in figure 14 have also been analyzed. A range performance comparison at a constant gross weight of 454 000 kg (1 000 000 lb) is given in figure 17. The symbols on the figure are front view sketches of the configurations actually studied. The "partial fuselage" laminarization points are calculated assuming LFC can be maintained to a length Reynolds number of 120×10^6. This is about twice what has actually been demonstrated experimentally, but is thought to be attainable.

Numerous research areas are suggested by this series of configurations, including

Wing-body strut aerodynamics and structures; various truss arrangements

Flutter, considering struts and tip tanks

Tip devices

Active control applications

High Reynolds number laminarization

NUCLEAR TUG

The success of composite vehicles assembled from specialized modules, such as the tractor-trailer truck and the railway train, has stimulated a number of investigations of the potential of airplane-glider combinations. Reference 18 reports some recent NASA efforts.

To date, NASA studies have not shown a performance advantage for a tug-glider system as compared with an airplane designed for the same mission and ground rules (technology level, field length, safety and noise regulations, etc.). Reference 18 actually finds a significant gain in overall energy efficiency by adding engines to the glider. However, tug-glider systems may offer advantages in other ways, such as extending the capability of an existing airplane at less cost than acquiring an all-new airplane, or by making use of a technology that is otherwise not applicable. An example of the latter is the nuclear tug.

The unique potential of nuclear powered airplanes is for almost unlimited range and endurance, a capability of little interest for commercial applications but of considerable importance to the military for missions such as station keeping or a missile launch platform. A traditional difficulty with nuclear powered airplanes has been in providing adequate take-off power. For this reason, many nuclear airplane concepts have assumed that the engines would use JP fuel for all or part of the power in portions of the mission other than cruise. This suggests using the nuclear airplane as a towing airplane for the cruise portion of a long-range flight, with the towed airplanes

operating independently in all other portions of the mission. The towed airplanes would carry the payload and only enough fuel for take-off, climb, descent and landing, plus reserves. Sizing of the nuclear propulsion system for towing in cruise would give adequate power for the tug alone to take off and climb, eliminating the need for an auxiliary power system.

A system of this type is illustrated in figure 18. The nuclear tug, shown in the foreground, has a gross weight of about 900 000 kg (2 000 000 lb), of which the reactor constitutes approximately 40 percent. Characteristics of the complete nuclear propulsion system are obtained from references 19 and 20.

The general arrangement of the tug is shown in figure 19. It is configured as a seaplane and would be constrained to always operate over water. A significant saving in reactor crash protection weight is possible if it need not be designed to survive a crash on dry land.

In the studies conducted so far, the towed airplanes are assumed to be C-5's, and the tug is sized for towing two airplanes. With the long-range military resupply mission in mind, the cruise Mach number has been selected as 0.70.

An energy comparison is presented in figure 20, using information on the C-5 from reference 21. The nuclear tug is seen to use much less jet fuel at all ranges, which is probably the most important comparison. The existence of a nuclear airplane implies an advanced nuclear technology such that nuclear fuel should be much less critical than petroleum. At very long ranges, the tug system uses less total energy (per unit weight of payload) as well. This is partly because energy is used in carrying the fuel in a conventional airplane, and that penalty increases with range. The largest effect, however, is a reduction in payload capacity for the conventional system at long ranges due to the large fuel weight that must be carried. There is, therefore, an added plus for the nuclear system; the total payload capability of a specified number of C-5's is maintained undiminished at all ranges.

Possible commercial applications of the nuclear tug would be transoceanic missions, either passenger or cargo. The economics of commercial operations are such that it would probably be desirable for the tug to remain aloft for extended periods, shuttling back and forth continuously for as long as maintenance or crew replacement requirements would permit. While modifications of existing airplanes could be used with the nuclear tug, it is probable that a better system could be obtained with an all-new design for the towed airplanes.

From the preliminary studies so far conducted, the concept of a nuclear tug appears to merit further study. The primary new technology need is for the nuclear power plant, but eventually an entire technology of large-scale tug-and-glider systems would have to be developed. Studies of fuel requirements, including reserves, for towed airplanes having points of origin and destination at various distances from the limits of the towed course would be useful. For maximum utilization in a commercial environment essentially continuous operation of the tug is desirable. Eventually, it may be desirable to develop a technique of rendezvous for crew replacement.

AERIAL RELAY

If, in the previous example, the payload could be transferred in flight to the nuclear tug, a better overall system might be obtained, since only the tug would be needed for the cruise leg. Preliminary studies of a system that makes use of in-flight transfer of payload, fuel, and crews have been made by Albert C. Kyser of Langley Research Center. The system is called the aerial relay transportation system (ARTS).

The motivations for the study are to explore the potential benefits of using specialized airplanes for the two distinct phases of any airplane trip: the terminal-area operations of take-off, climb, descent and landing, and the cruise portion. The possible benefits foreseen were superior performance, comfort, service, and reduced congestion. Studies to date indicate possible gains in all these areas, but extensive research will be required to confirm these benefits and preclude serious obstacles.

The basic features of ARTS are illustrated in figure 21. The system consists of large continuously flying "liners" that operate in conjunction with smaller "feeders." The function of the feeders is to carry passengers or other payload, fuel, and replacement crews to and from the liners. The function of the liners is to carry the payload from the vicinity of the trip origin to the vicinity of the destination. The liners would operate continuously along prescribed paths.

Several versions of the liner have been studied. In most of the versions, including that shown here, the liner itself is a system of airplanes that may be regarded as modules. The modules would take off and climb as individual airplanes and link up once they reach cruising conditions. In this way, extremely large wing-span liners could be built-up without requiring runways of equal width. The modular approach has other potentially useful features, as discussed later. The manner in which the feeder rendezvous with the liner is indicated on the third module in figure 21. This module has been shown in phantom to indicate that there is no prescribed number of modules in the liner. The wing-tip mechanism for holding the modules together is also an air lock designed to permit passengers to move from one module to another.

The general arrangement of an 800-passenger liner module is shown in figure 22. The configuration has been chosen with laminar flow control in mind. With turbulent flow, the large wetted area and low wing loading of this all-wing configuration would not be desirable, and a more conventional arrangement would probably be chosen. The liner modules are unswept because, to date, no satisfactory swept-wing modular configuration has been identified. The wing thickness is established largely on the basis of internal space and height required for the passengers, with considerations much like those discussed in the section entitled "Distributed-Load Aircraft." This type of configuration tends to have a large amount of floor space when adequate height is provided for the passengers. The configuration shown has approximately 1.4 m^2 (15 ft^2) per passenger, rather than 2.1 or 2.4 m^2 (7 or 8 ft^2) as with current wide-body airplanes, and therefore could have greatly enhanced passenger comfort.

The resulting configuration has a large thickness ratio (0.15) that restricts its cruise speed to a Mach number of around 0.75, considerably less than for current airplanes. However, as discussed later, the capability for in-flight transfer between modules would often avoid layovers on the ground, in which case the overall travel time could be less than with the current system.

The rudimentary fuselage contains the flight deck and accommodations for feeder docking and in-flight transfer of passengers, cargo, fuel, and crews.

The structural weight of the liner module shown in figure 22 is partially based on the results of DLF studies (refs. 1 to 5), with allowances for docking and tip coupling equipment, and passenger accommodations. The module would not be required to take off or climb fully loaded. Rather, it is assumed that the modules would take off only when nearly empty - no passengers and minimal fuel - in order not to compromise cruise efficiency, add weight, or increase cost. For example, it should not be necessary to provide high-lift devices on the modules.

Powering the liner poses a number of interesting design problems. The modules must be capable of flight alone, perhaps with the LFC system inoperative. The difference in thrust required between sustained flight as a single, turbulent airplane, and as part of a multimodule LFC liner is a factor of 5 to 10. Even if it is assumed that sustained loss of LFC is a rarely occurring emergency condition (similar to loss of thrust for current airplane) under which the module would be permitted to descend, the thrust required for individual flight may still be more than twice that required when joined to several other modules. In order to accommodate the large variation in required thrust without incurring very large drag penalties from engines which have been shut down, the configuration shown in figure 22 has buried engines and retractable "sugar scoop" inlets (visible in the front view).

The feeder characteristics (fig. 23) are based on study airplanes from reference 22. The nose and flight deck arrangement have been modified to permit docking with the liner and transferring passengers through the nose.

In order to get some assessment of the numbers of airplanes ARTS might involve, a simple initial route was assumed (fig. 24) and an examination made of the potential ARTS traffic. The feeders are expected to fly about 240 to 400 km (150 to 250 miles) in climbing to rendezvous with the liner, so that a single ARTS liner could serve a region about 500 km (300 miles) wide without requiring additional cruise distance for the feeders. The region served by the assumed liner route is indicated by the hatched band in figure 24. Counting only the applicable city-pair traffic among the major cities in this band, the traffic for which ARTS would be appropriate amounts to about 65 000 seats per day. If the ARTS has the same load factors as current airplanes, this indicates a minimum fleet of about 42 liner modules and 130 feeders. Such a fleet could provide hourly round-the-clock service within the 500-km (300-mile) band if operated as 3-module liners. Since the bulk of the existing traffic occurs during the daylight hours, a larger fleet would be needed. A reasonable projection might be 200 to 300 liners from 1990 to 2000 for this

one initial route. The existing traffic is remarkably uniform along the route (fig. 25), so the liners could be well utilized.

As the route network develops, the service could improve in both frequency and flexibility. After a number of major routes have developed, so that major intersections occur in the route network, it may be desirable to carry the in-flight transfer concept another step by having the multimodule liners exchange modules en route, as shown in figures 26 and 27.

Figure 26 indicates schematically that in the case of three routes meeting at a point, three liners could be scheduled to arrive simultaneously, separate and recombine in such a way as to comprise three new liners leaving that point. The value of such a maneuver is that passengers could be transferred from one route to another. For example, figure 27 shows the path of a passenger who leaves Houston, transfers in flight to another module and eventually arrives in New York, even though no single module makes that particular trip.

The significance of this in-flight transfer is that some of the airport function is accomplished aloft. For the passenger, this means reduced total travel time by avoiding layovers on the ground. It also means reduced airport congestion. On the average, today's passenger must now make two landings and take-offs per flight. With ARTS, only one take-off and landing per trip is needed. Ideally, then, this should lead to a reduction of roughly 50 percent in total airport traffic. The travel time and airport congestion aspects of ARTS seem to justify further study, independently of any cost or efficiency considerations.

Our studies of ARTS have been encouraging. Performance analyses indicate considerable improvement in terms of fuel efficiency and weight fractions over current airplanes. In order to substantiate these conclusions, research is needed in the basic disciplines of aerodynamics, propulsion, and structures (table III). However, the principle research needed relates to the operation of such a system, including routine rendezvous, tip coupling maneuvers, response of the multimodule liner to gusts, weather effects in general, fuel reserves, emergency conditions (e.g., inadvertent separation of liner modules), and automatic control of the entire liner fleet as a system.

CONCLUDING REMARKS

In this paper, a number of unconventional aircraft concepts have been presented. Each has attractive features according to the preliminary analyses that have been made.

The depth of the analysis varies. For the distributed-load freighters (DLF), there have been several design studies over a period of several years by several companies, plus NASA in-house and contract studies, with a samll amount of wind-tunnel testing. The laminar flow control (LFC) configurations have had several years of study, but there has been no wind-tunnel testing. The nuclear tug and aerial relay transportation system concepts are in very early stages of study.

Much further analysis and disciplinary research would be needed to determine if these concepts actually have merit. However, since the NASA purpose of these and similar studies is to identify potentially productive areas of research, they are considered to have served their purpose.

REFERENCES

1. Whitlow, David H.; and Whitener, P. C.: Technical and Economic Assessment of Span-Distributed Loading Cargo Aircraft Concepts. NASA CR-144963, 1976.

2. Technical and Economic Assessment of Span-Loaded Cargo Aircraft Concepts. NASA CR-144962, 1976.

3. Johnston, William M.; Muehlbauer, John C.; Eudaily, Roy R.; Farmer, Ben T.; Honrath, John F.; and Thompson, Sterling G.: Technical and Economic Assessment of Span-Distributed Loading Cargo Aircraft Concepts. NASA CR-145034, 1976.

4. Jernell, Lloyd S.; and Quartero, C. Baptiste: Design of a Large Span-Distributed Load Flying-Wing Cargo Airplane. NASA TM X-74031, 1977.

5. Whitehead, Allen H., Jr.: The Promise of Air Cargo - System Aspects and Vehicle Design. Acta Astronaut., vol. 4, no. 1/2, Jan./Feb. 1977, pp. 77-98.

6. Preliminary Design Dept., Boeing Commercial Airplane Co.: Technical and Economic Assessment of Swept-Wing Span-Distributed Load Concepts for Civil and Military Air Cargo Transports. NASA CR-145229, 1977.

7. Whitehead, Allen H., Jr.: Technical and Economic Evaluation of Advanced Air Cargo Systems. NASA TM-78672, 1978.

8. Thwaites, Bryan, ed.: Incompressible Aerodynamics. Oxford Univ. Press, Inc., 1960.

9. Powered-Lift Aerodynamics and Acoustics. NASA SP-406, 1976.

10. Srokowski, Andrew J.: Development of Advanced Stability Theory Suction Prediction Techniques for Laminar Flow Control. CTOL Transport Technology - 1978, NASA CP-2036, Pt. I, 1978, pp. 375-394.

11. Peterson, John B., Jr.; and Fisher, David F.: Flight Investigation of Insect Contamination and Its Alleviation. CTOL Transport Technology - 1978, NASA CP-2036, Pt. I, 1978, pp. 357-373.

12. Allison, Dennis O.; and Dagenhart, John R.: Design of a Laminar-Flow-Control Supercritical Airfoil for a Swept Wing. CTOL Transport Technology - 1978, NASA CP-2036, Pt. I, 1978, pp. 395-408.

13. Gratzer, Lewis B.; and George-Falvy, D.: Application of Laminar Flow Control Technology to Long-Range Transport Design. CTOL Transport Technology - 1978, NASA CP-2036, Pt. I, 1978, pp. 409-447.

14. Sturgeon, R. F.: Toward a Laminar-Flow-Control Transport for the 1990's. CTOL Transport Technology - 1978, NASA CP-2036, Pt. I, 1978, pp. 449-495.

15. Pearce, Wilfred E.: Application of Porous Materials for Laminar Flow Control. CTOL Transport Technology - 1978, NASA CP-2036, Pt. I, 1978, pp. 497-522.

16. Sturgeon, R. F.; Bennett, J. A.; Etchberger, F. R.; Ferrill, R. S.; and Meade, L. E.: Study of the Application of Advanced Technologies to Laminar-Flow Control Systems for Subsonic Transports. Volume I: Summary. NASA CR-144975, 1976.

17. Pfenninger, Werner: USAF and Navy Sponsored Northrop LFC Research Between 1949 and 1967 and Design Considerations of Large Global Range High Subsonic Speed LFC Transport Airplanes. Presented at the AGARD/VKI Special Course on "Concepts for Drag Reduction" (Rhode-St-Genese, Belgium), Mar. 28-Apr. 1, 1977.

18. Heyson, Harry H.; and Foss, Willard E., Jr.: Preliminary Study of Tug-Glider Freight Systems Utilizing a Boeing 747 as the Tug. NASA TM X-74006, 1977.

19. Muehlbauer, John C.; Byrne, David N.; Craven, Eugene P.; Randall, Charles C.; Thompson, Sterling G.: Thompson, Robert E.; Pierce Bill L.; Ravets, Jack M.; and Steffan, Richard J.: Innovative Aircraft Design Study, Task II - Nuclear Aircraft Concepts. LG77ER0008 (Contract F33615-76-C-0112), Lockheed-Georgia Co., Apr. 1977.

20. Thompson, Robert E.: Lightweight Nuclear Powerplant Applications of a Very High Temperature Reactor (VHTR). IECEC '75 Record, 1975, pp. 1089-1097.

21. Taylor, John W. R., ed.: Jane's All the World's Aircraft. McGraw-Hill Book Co., c.1970.

22. Morris, R. L.; Hanke, C. R.; Pasley, L. H.; and Rohling, W. J.: The Influence of Wing Loading on Turbofan Powered STOL Transports With and Without Externally Blown Flaps. NASA CR-2320, 1973.

TABLE I.- COMPARISON DLF CHARACTERISTICS

Agency	Range, n. mi.	W_P		W_G		Span	
		kg	lb	kg	lb	m	ft
Boeing	3000	320 000	700 000	760 000	1 670 000	95.7	314
Douglas	3000	287 000	618 000	610 000	1 350 000	86.9	285
Lockheed	3000	270 000	600 000	700 000	1 540 000	100.9	331
NASA	3200	270 000	600 000	620 000	1 360 000	88.4	290

TABLE II.- FLIGHT PARAMETER COMPARISON

	Turbulent Airplane	LFC Airplane
Wing loading, $\frac{kg}{m^2}$ $\frac{lb}{ft^2}$	683.5 (140)	415.0 (85)
Aspect ratio	7.0	16.3
Cruise lift coefficient	0.50	0.55 to 0.60
Altitude, km (ft)	10.36 (34 000)	13.72 to 14.02 (45 000 to 46 000)
Mean aerodynamic chord, m (ft)	8.32 (27.3)	7.32 (24)
Chord Reynolds number	57.4×10^6	30×10^6
Unit Reynolds number, per meter (per foot)	6.89×10^6 (2.10×10^6)	3.65×10^6 (1.11×10^6)

TABLE III.- DISCIPLINARY RESEARCH NEEDED FOR ARTS

Aerodynamics

Wing/airfoil:

- Low aspect ratio
- High thickness ratio
- Low design lift coefficient

Interference effects for vehicles in proximity:

- Liner-module
- Liner-feeder

Induced drag of modular configurations:

- Lift constraints on each module
- Moment constraints on each module

Control concepts

Structures and mechanisms

- Pressurized noncircular passenger compartment
- Low-weight LFC suction surfaces
- Tip-coupling mechanism and air lock
- Docking mechanism
- Mechanism for in-flight transfer

Propulsion

- Cruise-specialized engines
- Retractable inlet design
- Air starting
- Long run times between inspection

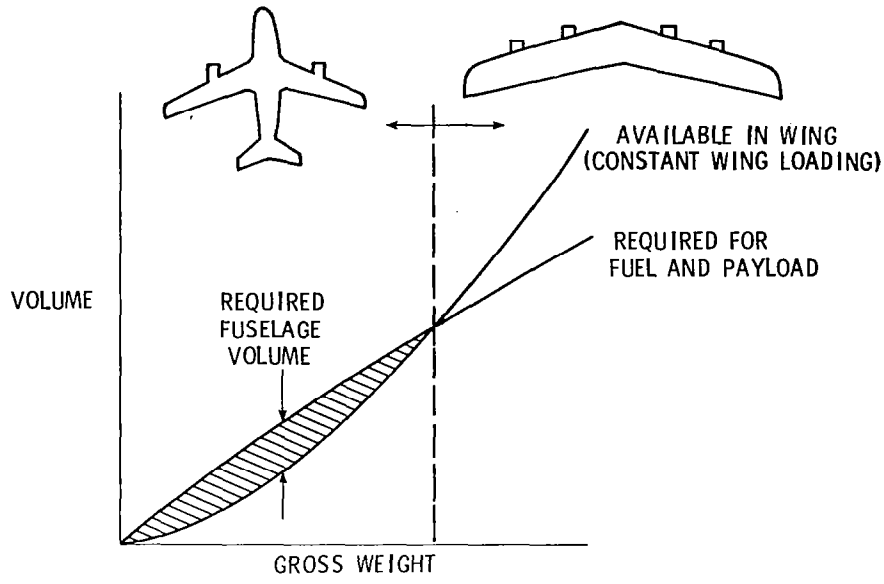

Figure 1.- Airplane size-volume trends.

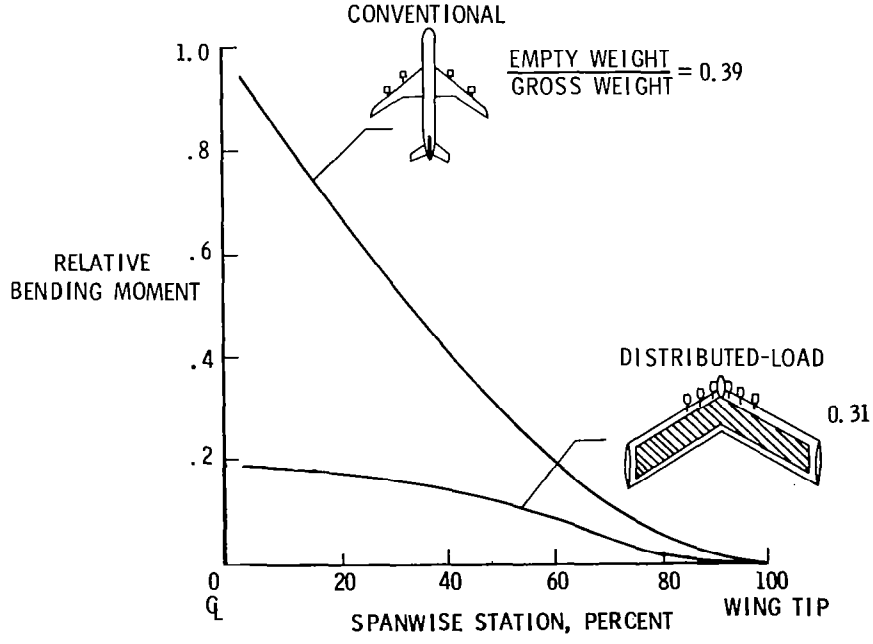

Figure 2.- Wing bending moments.

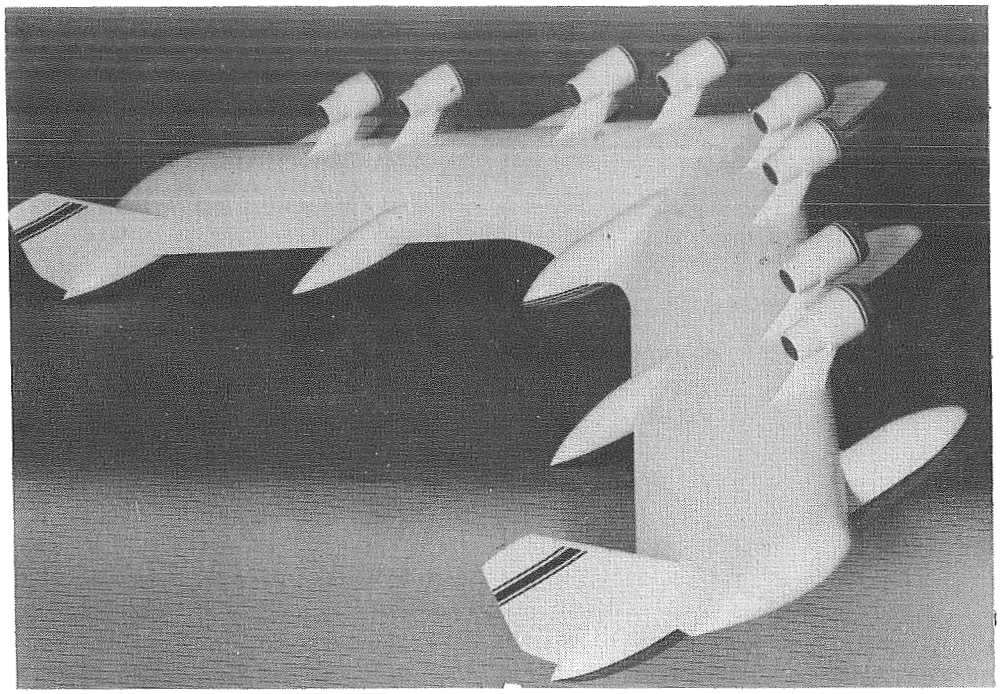

Figure 3.- Early NASA distributed-load airplane.

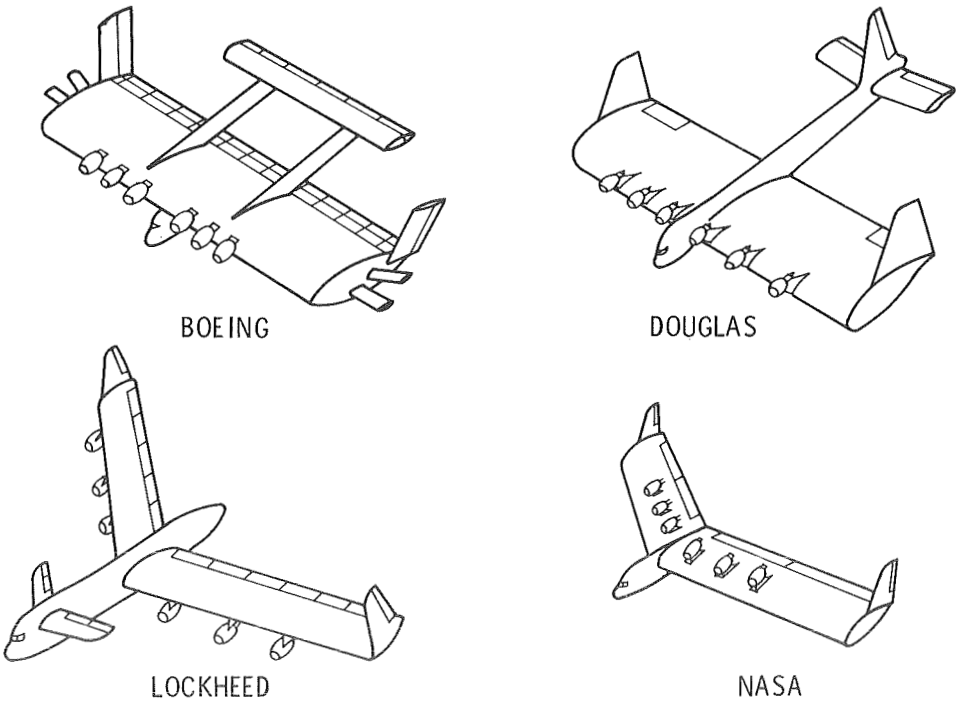

Figure 4.- DLF's studied by organization indicated.

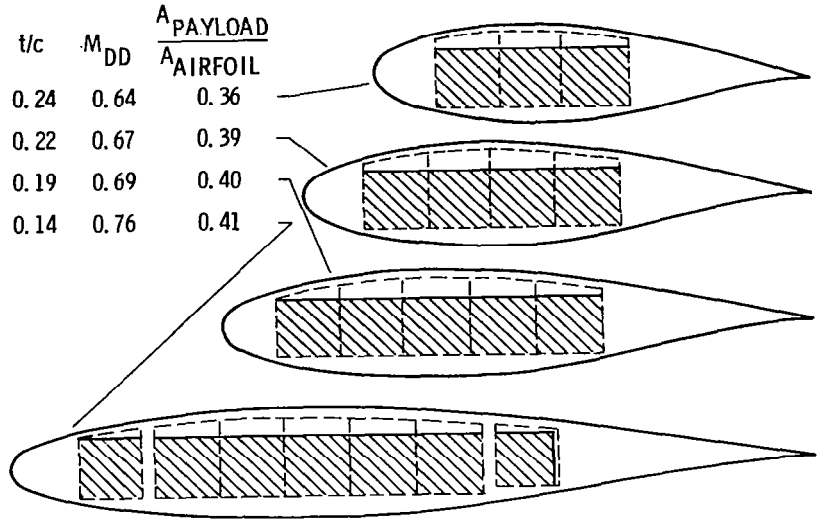

Figure 5.- DLF airfoil trade-offs.

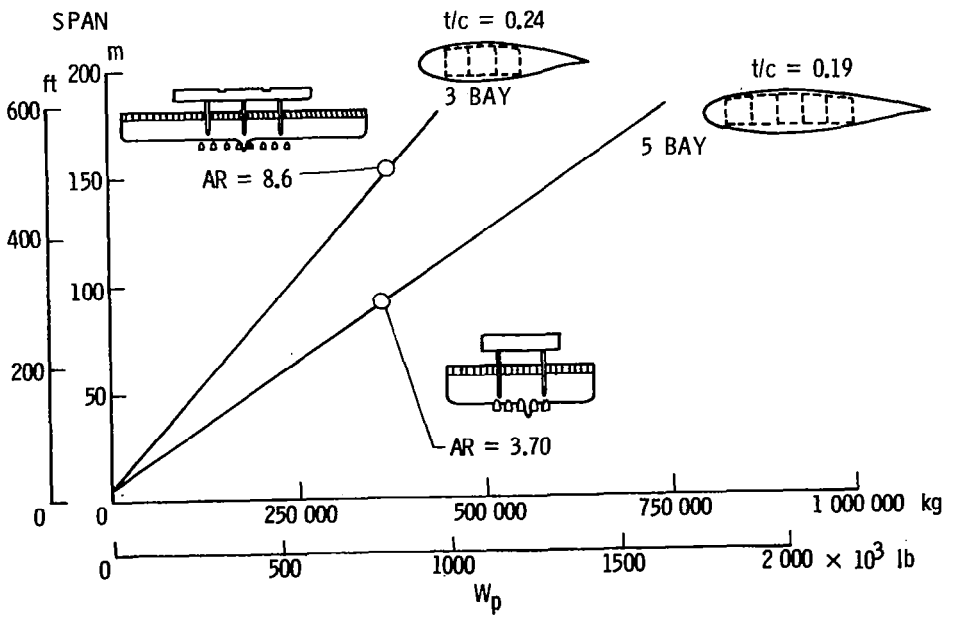

Figure 6.- Distributed-load airplane geometry constraints.

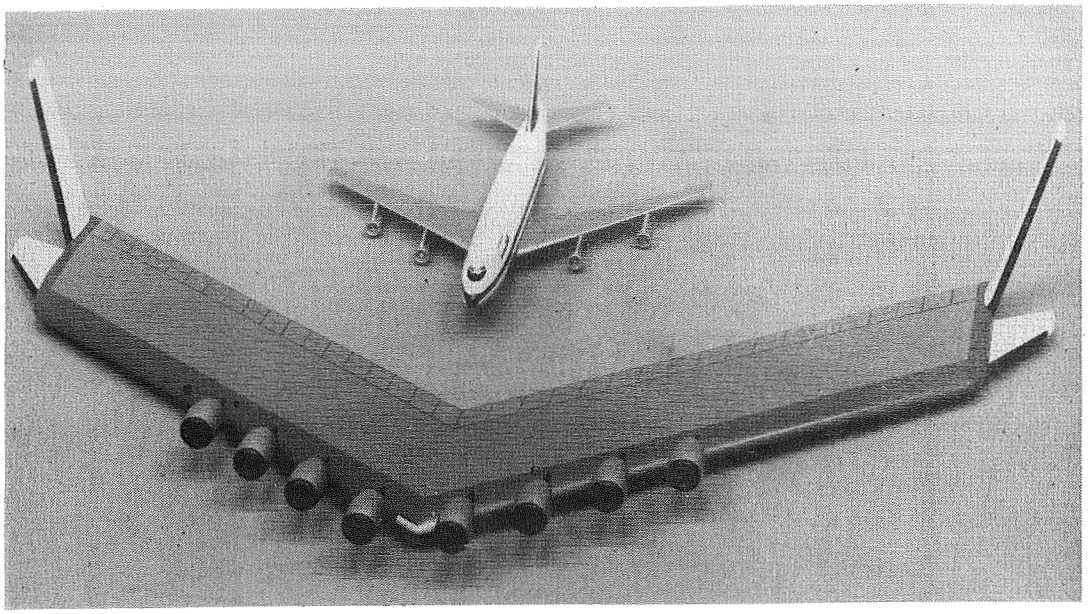

Figure 7.- Distributed-load freighter (NASA-Boeing study).

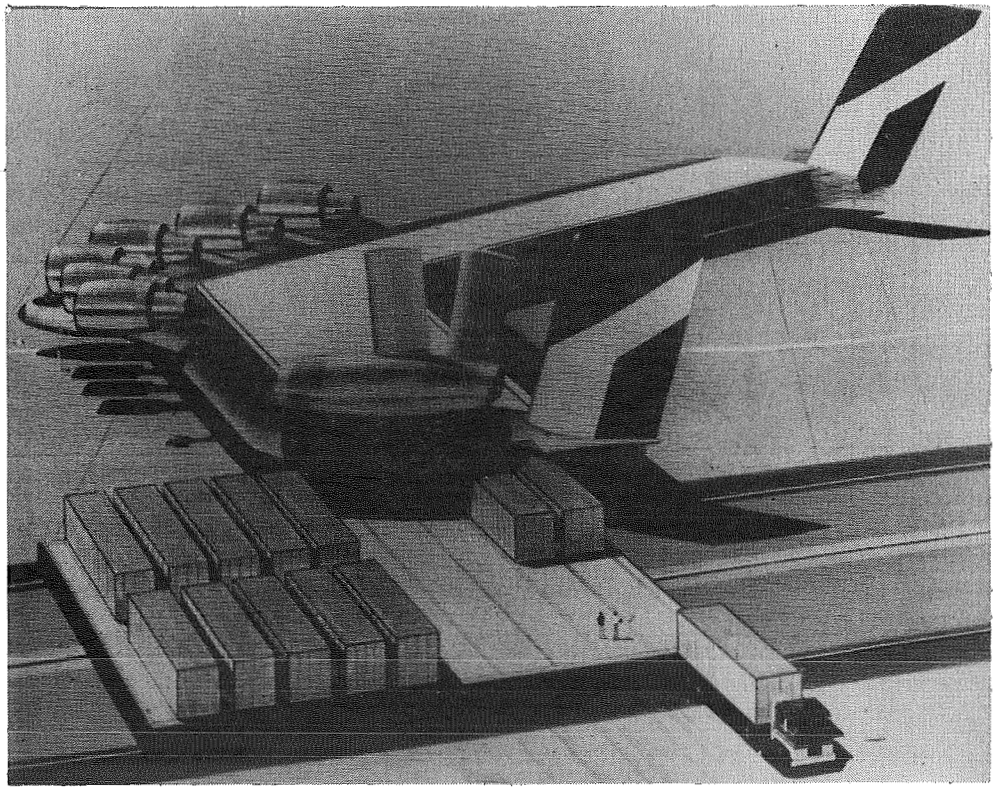

Figure 8.- Loading a distributed-load airplane.

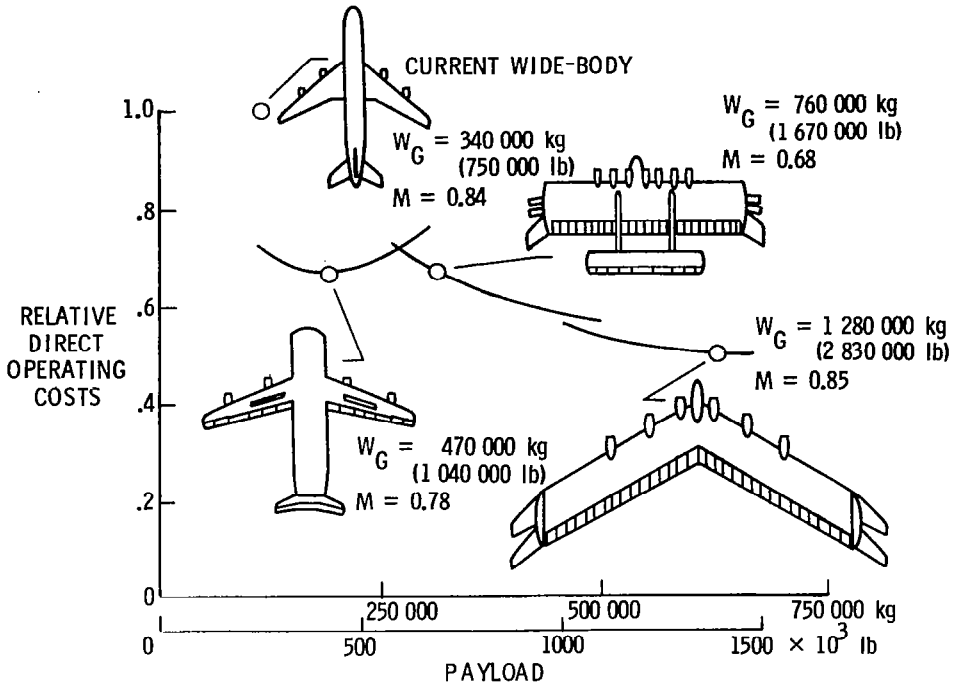

Figure 9.- Economic comparison of advanced cargo airplanes.

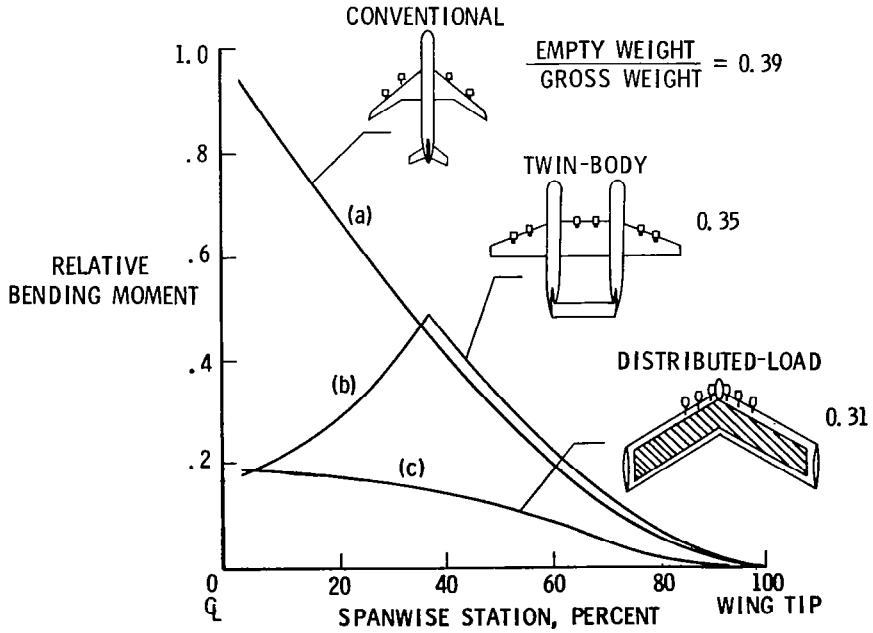

Figure 10.- Wing bending moment comparison.

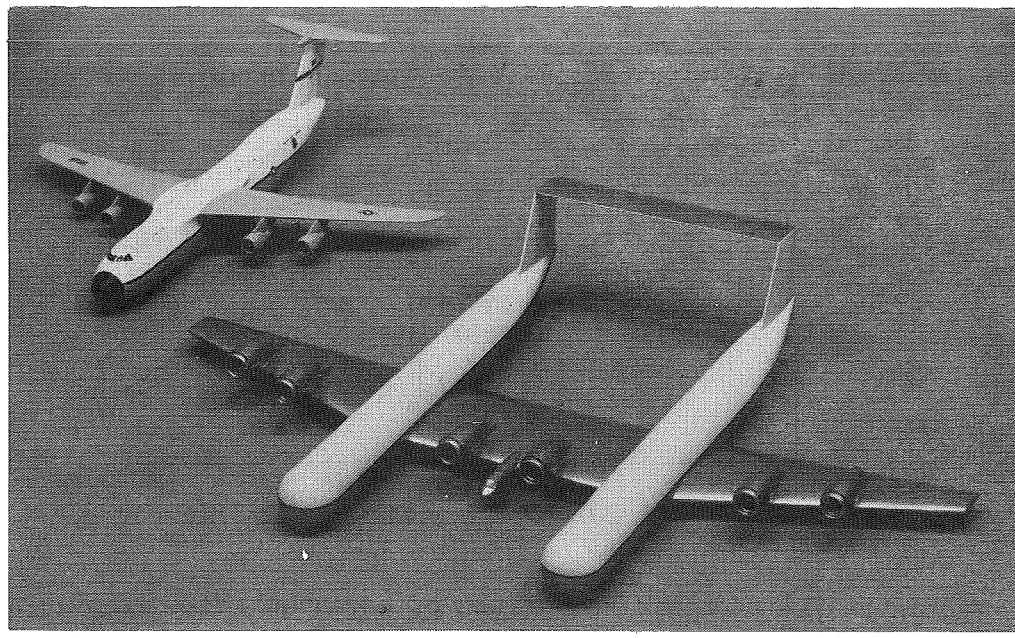

Figure 11.- Twin-body cargo airplane.

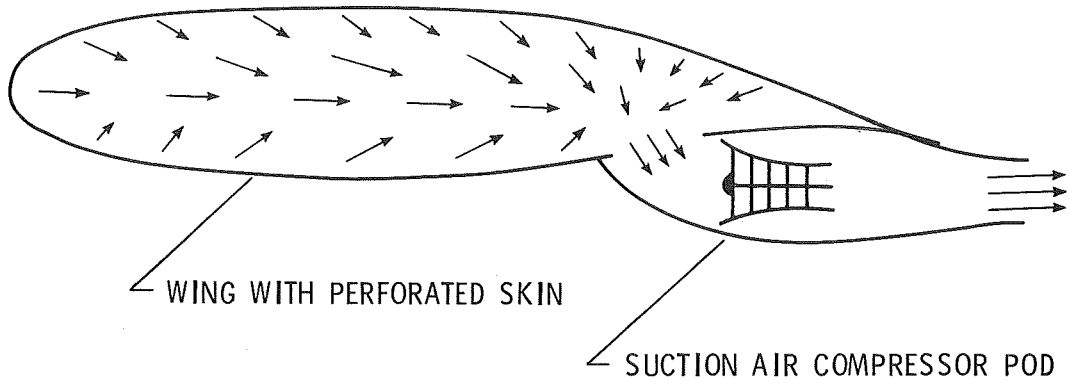

Figure 12.- Laminar flow control system.

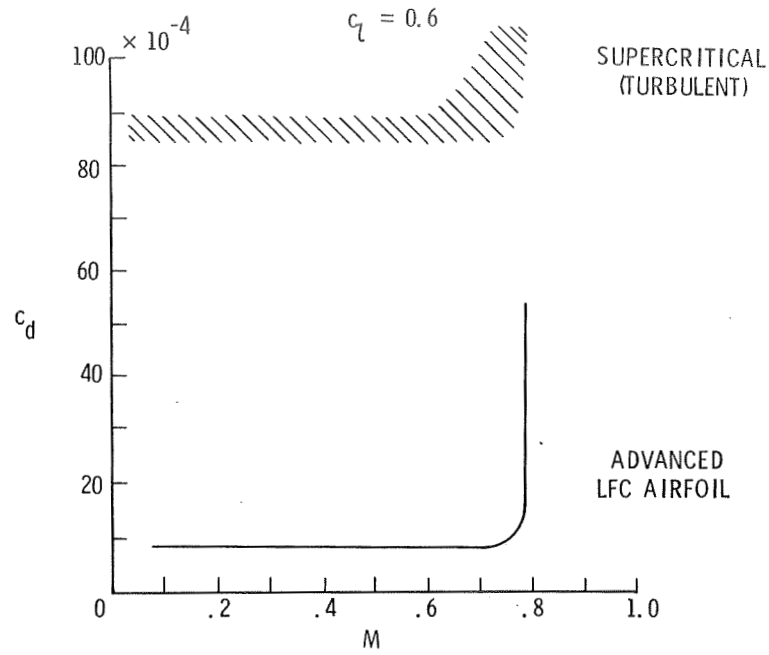

Figure 13.- Airfoil drag comparison.

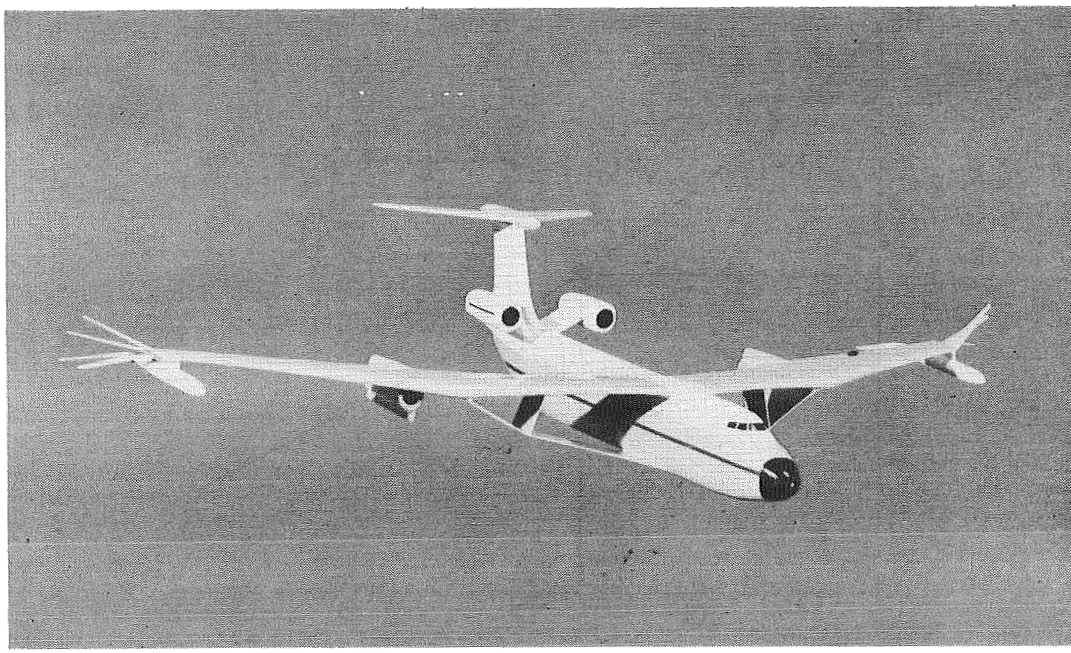

Figure 14.- Long-range LFC airplane.

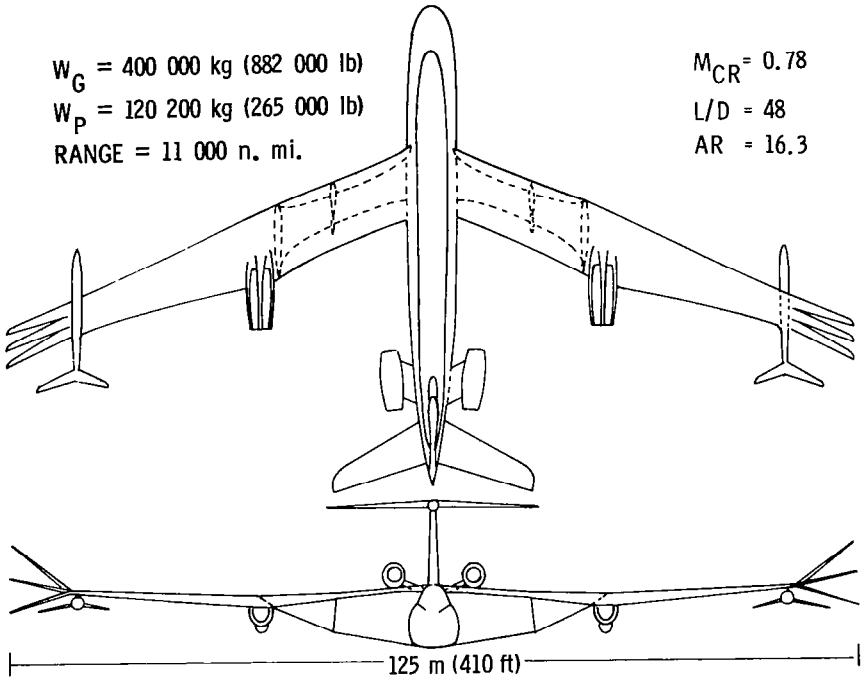

Figure 15.- Long-range LFC airplane general arrangement.

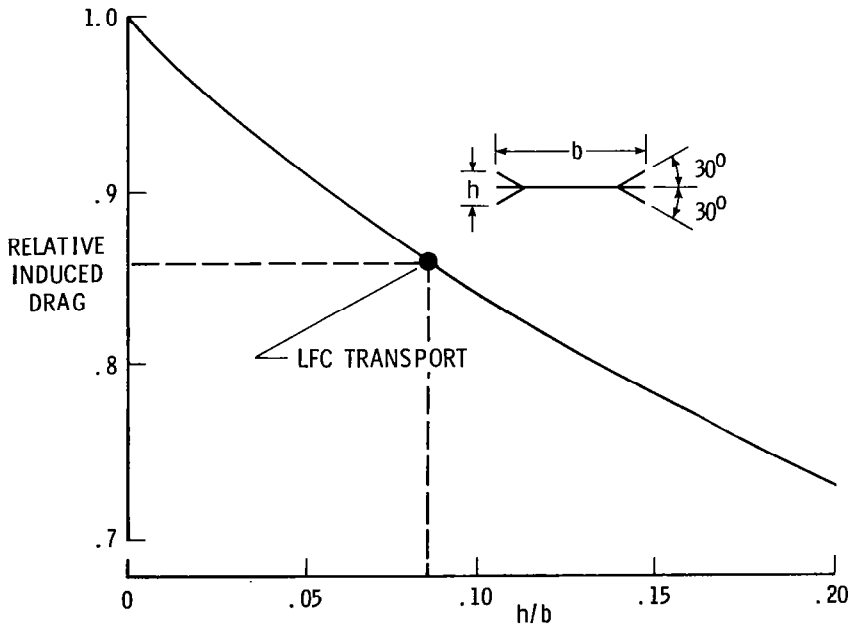

Figure 16.- Induced drag factor of wing with tip devices.

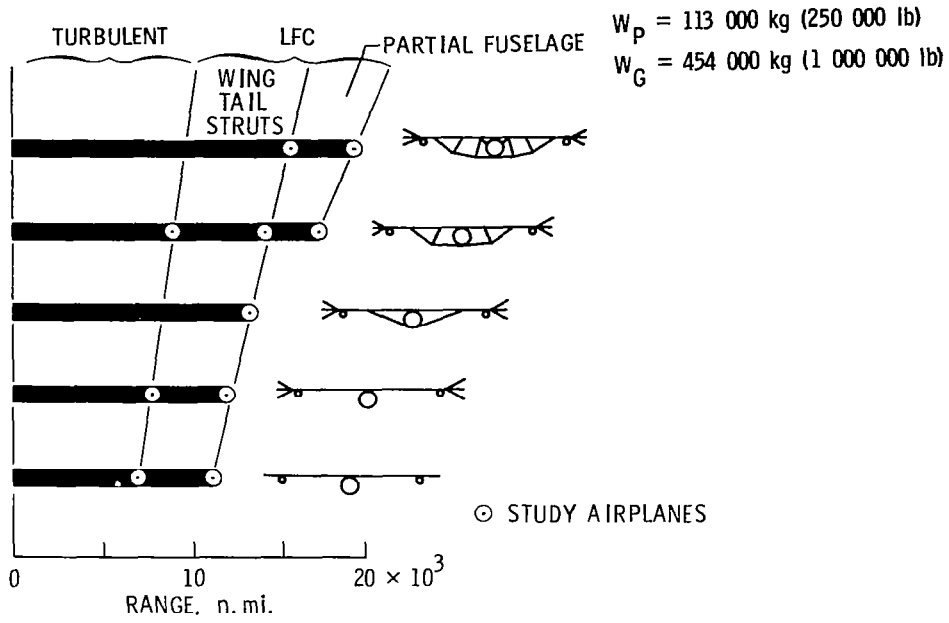

Figure 17.- Range comparison.

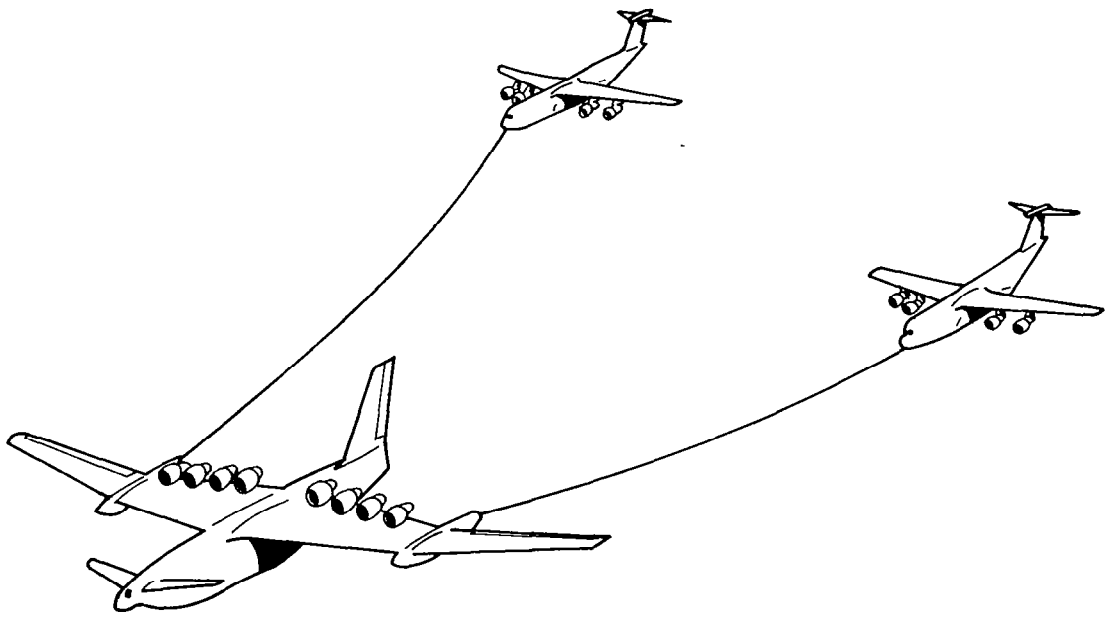

Figure 18.- Nuclear tug.

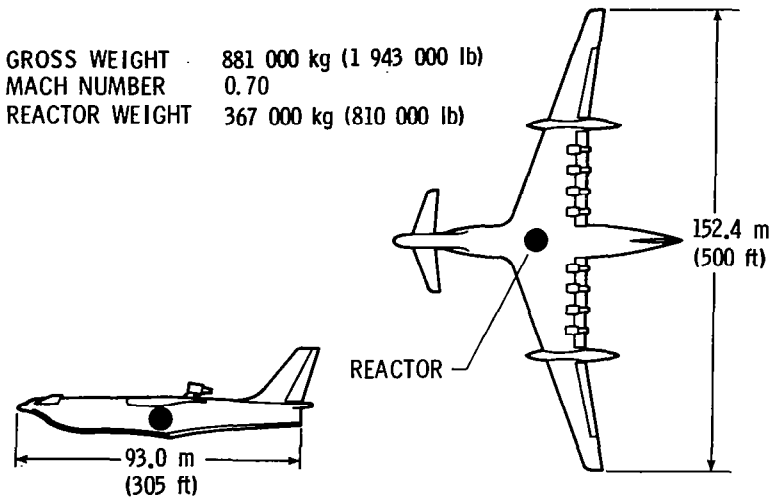

Figure 19.- Nuclear tug airplane general arrangement.

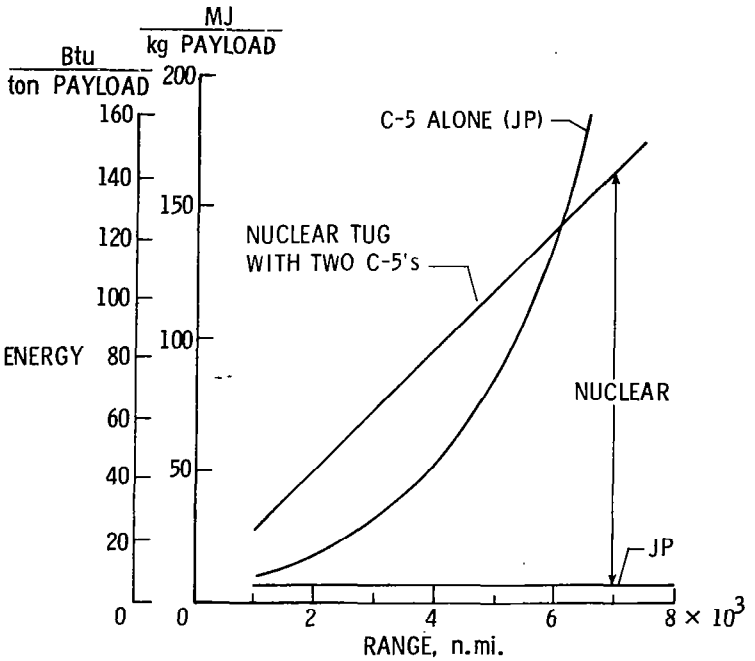

Figure 20.- Nuclear tug system energy comparison.

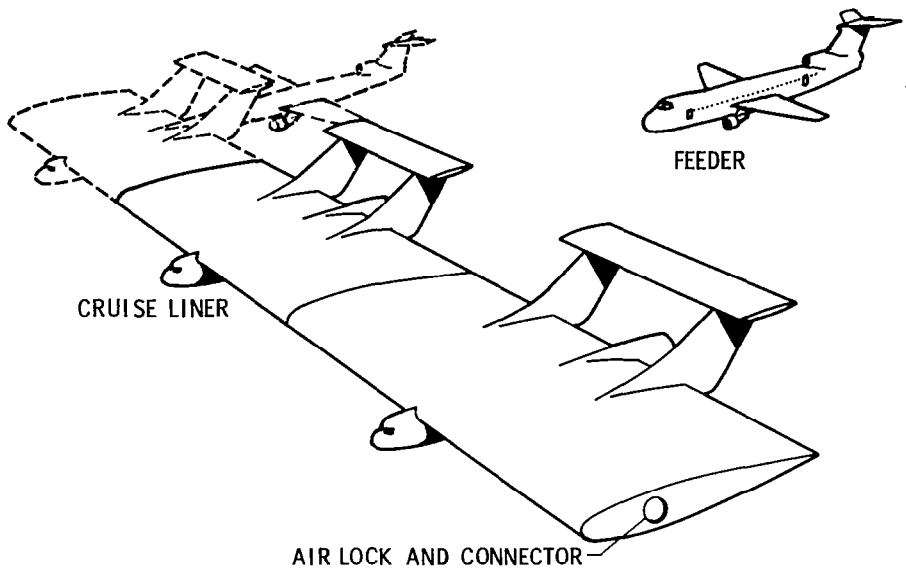

Figure 21.- Aerial relay transportation system.

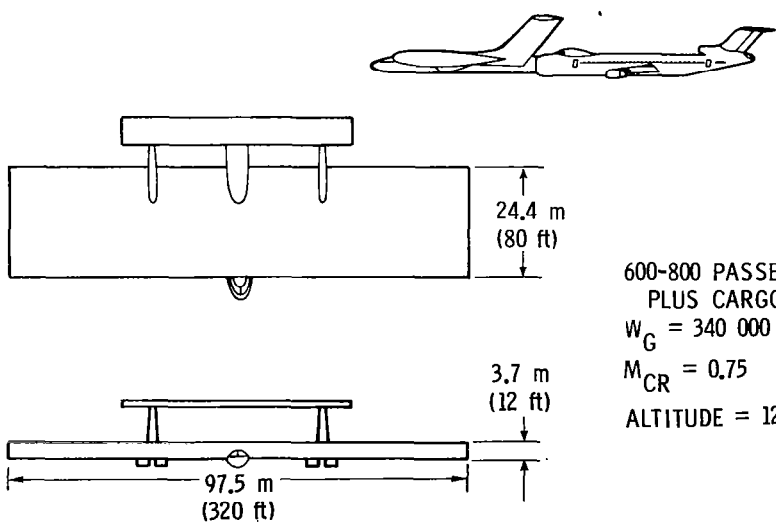

Figure 22.- ARTS LFC liner module.

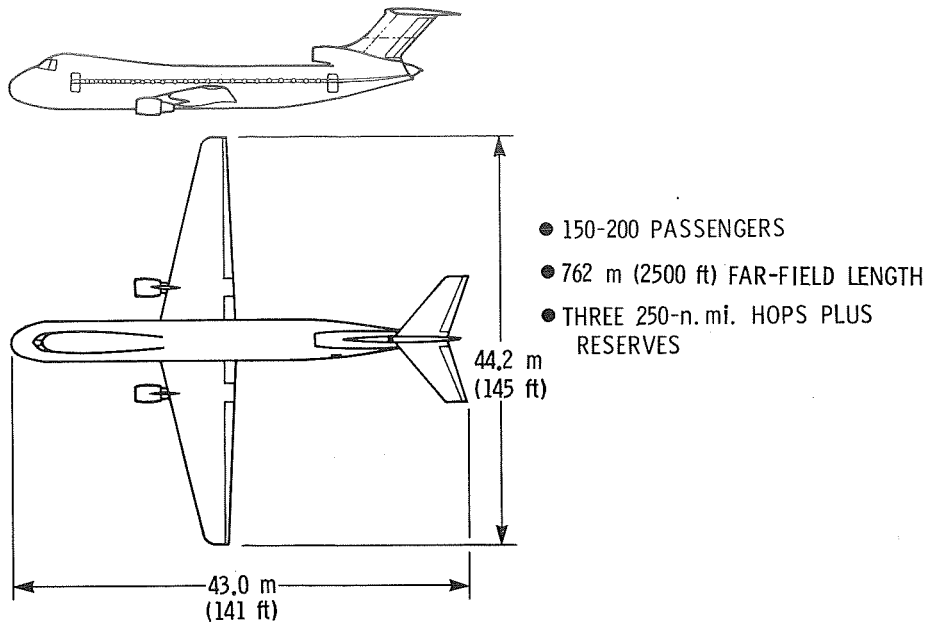

Figure 23.- ARTS feeder.

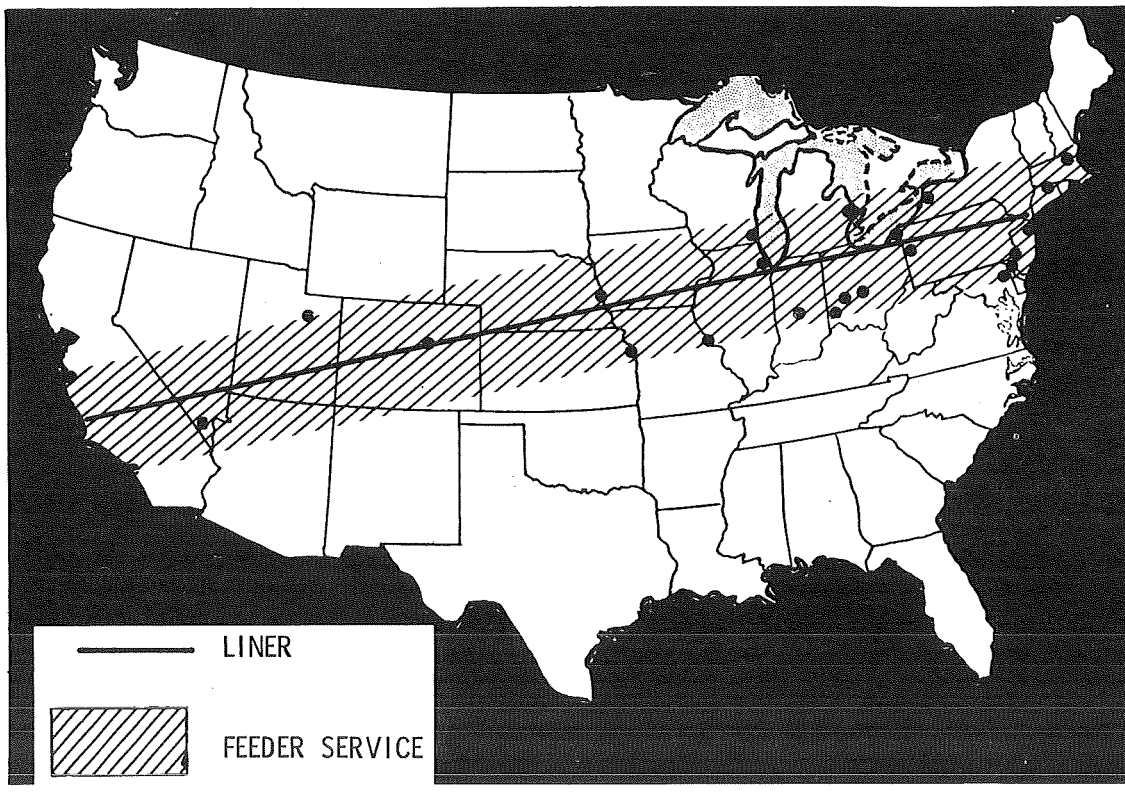

Figure 24.- Possible initial relay system route.

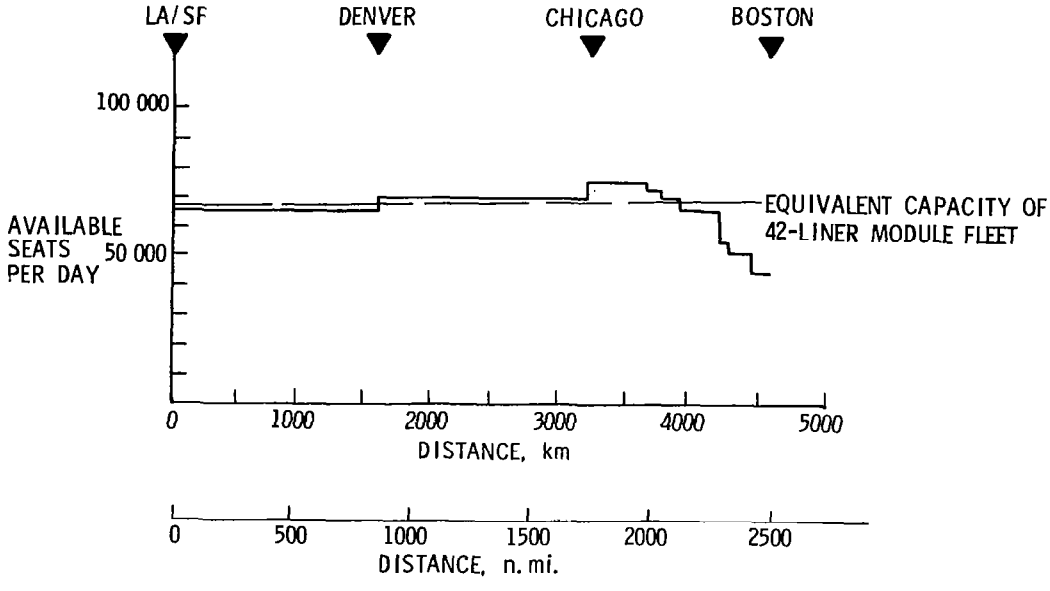

Figure 25.- Current scheduled airline traffic west to east.

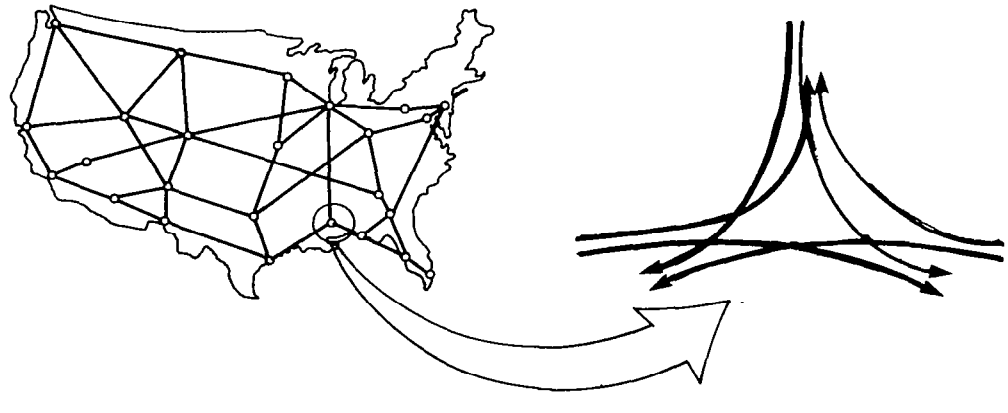

Figure 26.- Aerial relay transportation system enroute mixing at route intersection.

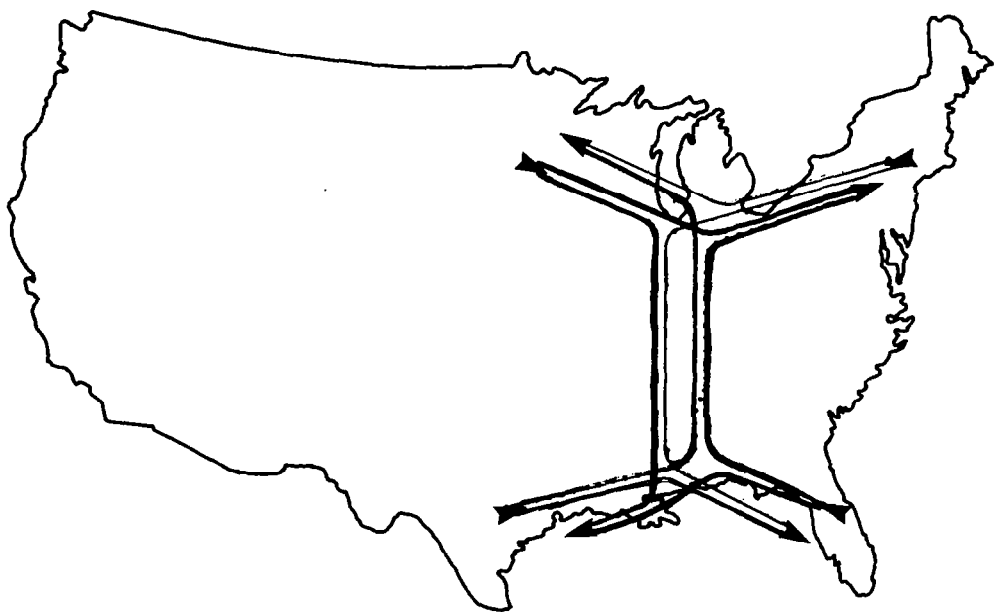

Figure 27.- Aerial relay transportation system enroute mixing of trip paths.

1. Report No. NASA CP–2036, Part II	2. Government Accession No.	3. Recipient's Catalog No.
4. Title and Subtitle CTOL Transport Technology – 1978		5. Report Date June 1978 6. Performing Organization Code
7. Author(s)		8. Performing Organization Report No. L–12178
9. Performing Organization Name and Address NASA Langley Research Center Hampton, VA 23665		10. Work Unit No. 516–50–23–01 11. Contract or Grant No.
12. Sponsoring Agency Name and Address National Aeronautics and Space Administration Washington, DC 20546		13. Type of Report and Period Covered Conference Publication 14. Sponsoring Agency Code

15. Supplementary Notes

16. Abstract

The proceedings of the NASA CTOL Transport Technology Conference held at Langley Research Center February 28 – March 3, 1978, are presented in this compilation. New technology generated by NASA in-house and contract efforts, including the ongoing Aircraft Energy Efficiency (ACEE) program, in the various disciplinary areas specifically associated with advanced conventional take-off and landing (CTOL) transport aircraft are presented. The conference was divided into six sessions:

1. A session on propulsion addressed jet engine performance deterioration and improvement; energy efficient engine design and integration; advanced turboprops, engine materials, noise, and emissions; and broad specification fuels.

2. A session on structures and materials addressed structural sizing methodology; environmental effects of composites; and applications of advanced composite materials.

3. A session on laminar flow control addressed insect contamination and alleviation; suction prediction techniques; porous materials; and laminar flow applications.

4. A session on advanced aerodynamics and active controls technology addressed advanced wings, winglets, and nacelles; aerodynamic flow calculation techniques; fault-tolerant computers; and active control applications.

5. A session on operations and safety addressed safety research; wake vortex phenomena; advanced landing-gear research; noise prediction; improved terminal area operations; airline operating costs; and a method for cost/benefit analysis for aeronautical research and technology.

6. A session on advanced systems addressed developments in short-haul and supersonic transport research; coal-derived fuels and aircraft systems; and advanced transport concepts.

17. Key Words (Suggested by Author(s))	18. Distribution Statement
Engines, Turboprops, Noise, Emissions, Fuels, Structures, Composite materials, Laminar flow control, Aerodynamics, Winglets, Active controls, Safety, Wake vortices, Landing gear, Aircraft economics, Aircraft concepts	Distribution – Unlimited Subject Category 01

19. Security Classif. (of this report)	20. Security Classif. (of this page)	21. No. of Pages	22. Price*
Unclassified	Unclassified	468	$14.50

* For sale by the National Technical Information Service, Springfield, Virginia 22161

NASA-Langley, 1978